NOTICE: When government or other drawings, specifications or other data are used for any purpose other than in connection with a definitely related government procurement operation, the U. S. Government thereby incurs no responsibility, nor any obligation whatsoever; and the fact that the Government may have formulated, furnished, or in any way supplied the said drawings, specifications, or other data is not to be regarded by implication or otherwise as in any manner licensing the holder or any other person or corporation, or conveying any rights or permission to manufacture, use or sell any patented invention that may in any way be related thereto.

AD 401161

DRL-A-202 September, 1962

GUIDE TO THE SELECTION OF ACOUSTIC FILTERS FOR LIQUID-FILLED SYSTEMS

by

E. L. Hixson, J. V. Kahlbau, and D. G. Galloway

Copy No. 68

Prepared under
U. S. Navy Bureau of Ships
Contract NObs-86165
RDTEE Subproject SF013-11-01, Task 1359

Defense Research Laboratory Acoustical Report No. 202

DEFENSE RESEARCH LABORATORY
THE UNIVERSITY OF TEXAS
AUSTIN 12, TEXAS

ABSTRACT

This manual gives design methods and presents a summary of experimental test data for four basic types of passive, dissipationless acoustic filters for attenuating noise in liquid piping. Filters of the (1) side branch, (2) expansion chamber, (3) combination, and (4) Quincke tube types are considered. Analytical methods applicable to lumped parameter acoustical systems, transmission lines, and combinations of these are developed. Several different filter performance criteria are defined. One of these, transmission loss, is adopted for comparing filters independently of source and load characteristics. Chapters I and II are devoted to introductory material--discussing the problem, covering certain relevant fundamentals of acoustics, and specifying filter elements in acoustical terms. Chapter III on filter design gives transmission loss curves versus dimensionless frequency for several different filters of each of the four types.

For all types of filters except expansion chambers, infinities of transmission loss are predicted at one or more discrete frequencies. Expansion chambers show zeros of loss at harmonically related frequencies with regions of broadband loss between. For side-branch filter elements there is defined a parameter q. T. L. curves for side-branch filters with one element or multiple identical elements indicate increases in loss with increases in q, but retain their general shape. For values of q above 10, increasing q by a factor of 10 results in approximately 20 dB increases in loss. For a branch filter with two identical elements and q = 100, loss of over 40 dB is indicated over almost all of the band, $0.25\ f_0 \leqq f \leqq 3.75\ f_0$, where f_0 is the resonant frequency of the branch elements. The maximum values of transmission loss for expansion chamber filters depend on a parameter m, the ratio of characteristic admittances of the chamber and connecting pipes. Ten dB increases in m result in about 10 dB increases in maximum transmission loss. Values of m of 3.16, 10, 31.6, and 100 for a single chamber filter correspond to transmission loss maxima of 4, 14, 24, and 34 dB, respectively. Combination filters show the broadband loss feature of expansion chambers and also the infinities of side-branch filters for a particular relationship between resonant frequency f_0 of the branch element and the frequency at which the chamber length is a half wavelength, f_ℓ. This filter gives over 25 dB loss from $0.1 \leqq f/f_\ell \leqq 1.3$. Loss curves for Quincke tube filters have repeating infinities at harmonically related frequencies which depend on the sums and differences of two acoustic path lengths. Broadband characteristics of Quincke tubes are not particularly attractive unless the tubes are larger than connecting pipes.

Graphical aids for determining parameters for particular types of elements are given, and worked examples illustrating the use of both the transmission loss curves and the graphical aids are included in Chapter III. Chapter IV summarizes results of acoustic filter tests. Data on one or more of each of the types of filters covered in Chapter III are given for various conditions of water flow, sound source character, and filter termination characteristics. Either output and input sound pressures or the ratio of these is plotted versus frequency or for frequency bands for each test. The acoustical circuit of the test filter with parameter values specified is shown on all sheets of plotted test data. Test results indicate many of the filter characteristics predicted by computation with somewhat less spectacular actual attenuations than the corresponding transmission losses.

PREFACE

This manual is intended for use as an aid in designing or selecting passive, dissipationless, acoustic filters for attenuating noise in liquid-filled piping systems. Four different types of filters are treated in it. They are (1) side-branch filters, (2) expansion chamber filters, (3) combination side-branch and expansion chamber filters, and (4) Quincke tube filters.

The manual has five chapters. Introductory material of Chapter I includes a brief historical sketch of the filter investigation program which preceded the writing of this manual and some general remarks concerning noise in liquid-filled piping systems. The second chapter, devoted to background material, reviews relevant fundamentals of acoustics and discusses filter performance criteria, mechanical forms of filter elements, and specification of filters in acoustical terms. The portion of Chapter II devoted to acoustical fundamentals can be skipped over by those readers who are already familiar with these aspects of acoustics. It should be noted, however, that use of the adopted system of units is also demonstrated in this section. Chapter III contains families of transmission loss curves for a variety of filters of each basic type. These curves reflect theoretical filter responses calculated on the basis of irregular acoustic transmission line ideas explained in Chapter II. The curves are plotted against dimensionless frequency scales. Chapter III also explains use of the curves, gives additional graphical aids for determining or adjusting filter parameters, and presents several worked examples of filter design problems. Chapter IV gives a summary of measured filter performance characteristics. In all cases the test filter is specified in terms of its acoustical parameters, the noise source is characterized, and the filter termination is described as completely as possible. Chapter V contains a few closing remarks concerning applicability of the methods presented in the manual.

The authors hope that this material will be useful to designers concerned with reduction of liquid-borne noise in piping, particularly those designing shipboard systems.

The authors wish to acknowledge the contributions of Drs. J. D. Gavenda and A. E. Sobey who were responsible for early theoretical studies of flow-through type filters for acoustic noise in liquid systems at DRL and of Mr. E. E. Mikeska who supervised the filter investigation program for a number of years. Guidance and valuable suggestions by Dr. C. M. McKinney of Defense Research Laboratory and by Dr. R. M. Sherwood and Mr. F. R. Lewis of the U. S. Navy Bureau of Ships, Code 345, both during the filter investigation program and in the preparation of this manual, are greatfully acknowledged. Thanks are also due to Mr. F. O. Bohls and Mr. E. L. Cousins of DRL who made many of the filter tests and assisted in reducing the test data.

Of the references cited in Appendix C some are especially helpful. The book by P. M. Morse, Ref. 29, and the handbook edited by C. M. Harris, Ref. 25, were consulted frequently. The published work of Don D. Davis and his co-workers, Ref. 8 and Ref. 25, Chapter 21, has guided us in work on expansion chamber and combination filters, particularly in selection of certain parameters.

TABLE OF CONTENTS

TABLE OF CONTENTS (CONT'D)

TABLE OF CONTENTS (CONT'D)

September 1962
JVK:vh

CHAPTER I: INTRODUCTION

A. BRIEF HISTORY

From May, 1955, to October, 1961, the U. S. Navy Bureau of Ships, Ship Silencing Branch, sponsored a technical program at Defense Research Laboratory (DRL), The University of Texas, in the design and development of passive acoustic filters to attenuate noise in liquid-filled piping systems. The work was performed under Contracts NObs-66932 and NObs-77033. During the program principal efforts were devoted to studying, designing, building, and testing passive, nondissipative filters of types that appeared adaptable for shipboard use.

Passive dissipationless filters of types that appeared promising on the basis of such practical considerations as safety, cost, size, weight, and acceptably low frictional flow resistance were treated.

Four types of filters were investigated both analytically and experimentally in the course of the program. These were (1) side-branch filters, (2) expansion chamber filters, (3) combination side-branch and expansion chamber filters, and (4) Quincke tube filters.

Various analytical approaches to filter design were used. The well known analogy--between linear acoustic, mechanical, and electrical systems--has been used extensively. Many experimental filters were designed by devising acoustical systems approximately analogous to lumped-parameter electrical filters. Refinements and extension of this approach led to the adoption of acoustic transmission line methods for specifying and analyzing filters.

Most of the experimental work was done in the Laboratory where developmental filter models were built and tested in water-filled systems.

Two different field tests of filters were carried out. One series of tests was made aboard the submarine USS GROUPER (AGSS-214) at New London, Connecticut, in May and June, 1959. In these tests noise measurements were made inside the trim pump suction and discharge lines and overside near the boat before and after installation of acoustic filters in both of the trim pump lines. The filters used in the trim lines were of the side-branch type, and each filter had three spring-piston branch elements. It was the purpose of these tests to determine whether use of filters in the trim lines would reduce overside noise, just noise inside the lines, or both. The measurements were made with the boat at dockside with all auxiliary machinery except the trim pump secured. Using the filters resulted in significant noise reductions at some overside hydrophone locations. Results of measurements of noise inside the trim lines were difficult to interpret, because during the test air was present inside the system.

Another field test of acoustic filters was conducted aboard a floating pontoon barge on Lake Travis near Austin, Texas, in July, August, and September, 1961. In these tests a three-element, side-branch filter with metal bellows elements and an expansion chamber filter with two, five foot long chambers 56 inches apart were individually tested in a pumping system aboard the test barge. Noise measurements were made overside and in the pump lines with and without the filters in the system. These tests are described and the test results presented and discussed in a formal report [Ref. 6]*.

Details of the analytical and experimental work performed under Contracts NObs-66912 and NObs-77055 are given in progress reports issued quarterly during the program. These, along with various other summary and technical reports covering particular phases and aspects of the filter program, are listed in Appendix C. Although these reports give a fairly complete account of the technical work performed during the filter program, they do not present the information in a form convenient for use in solving filter design problems.

This manual (1) gives an explanation of acoustical fundamentals most important in filter analysis, (2) describes certain basic types of filters that appear promising on the basis of practical considerations, (3) presents families of curves intended to simplify greatly the determination of filter proportions for given ideal performance, and (4) summarizes results of laboratory performance

*References are listed in Appendix C.

September 1962
JVK:vh

measurements made on experimental acoustic filters during the filter investigation program at DRL.

In preparing this manual the attempt has been made to keep in mind the special needs of naval architects who may use it. Terms more or less peculiar to the fields of acoustics and acoustical engineering have not been used without definition. Engineering units have been used; lengths are expressed in inches, weights in pounds, and time in seconds. A glossary of symbols is given in Appendix B.

September 1962
JVK:vh

B. GENERAL REMARKS CONCERNING NOISE IN LIQUID-FILLED PIPING SYSTEMS

For tactical reasons it is desirable for naval ships to be capable of operating quietly. Considerable effort has been devoted to reducing the amount of undesired sound, particularly machinery noise, radiated into surrounding water by ships and submarines. Rotating machine elements such as electric motor and generator armatures are carefully balanced, and vibration isolation mountings are extensively used. However, because of the nature of the primary functions of certain auxiliary machines it is difficult to isolate them vibrationally and acoustically from surrounding structure. This is true of liquid-handling pumps in particular. Pumps can be supported on conventional vibration isolation mountings, but they must also be attached to hoses, pipes, or other ducts for confining and conveying the pumped liquid. The necessary attachments provide both solid and liquid transmission paths for noise. In some low and medium pressure systems flexible pipe couplings or hoses can be used to alter sound transmission characteristics of the solid structure, but even if the flexible coupling is effective in interrupting the solid path, noise can still be propagated in the liquid column. It is, of course, the liquid borne sound aspect of the piping noise problem that we wish to eliminate or reduce by use of acoustic filters.

In operation, liquid-handling pumps ordinarily generate noise at several different internal sources. Noise in the pumped liquid is a combination of contributions from all of them. Unbalanced rotating elements of pumps excite surrounding liquid directly and also apply varying loads to support bearings which in turn excite the pump casing. The vibrating casing radiates to the liquid inside. Another source of noise in pumps of certain types is that associated with rapid passage of impeller vanes or blades by ports in the pump casing. In positive displacement pumps, valve action produces pressure pulsations in the pumped liquid. Cavitation and turbulence, as well as bearing and drive-motor noise, are common to pumps of many types. Construction details of the types of liquid pumps described in Ref. 28 suggest the noise generating mechanisms that are probably significant for each type. Centrifugal pumps are extensively used. Impeller blades and unbalanced rotors are the most important contributors to noise in liquids transferred by centrifugal pumps.

September 1962
JVK:vh

Generation and distribution of noise in a pumping system is ordinarily very complicated; a complete mathematical description of it is neither possible, nor for present purposes, necessary. The noise source characteristics of liquid pumps are often sufficiently described by the sound pressure amplitude-frequency spectrum obtained from a representative sample of the noise and the overall sound pressure level in the pumped liquid. Large amplitude components corresponding to centrifugal pump rotational and blade frequencies are found in the noise spectra of these pumps.

Noise in liquid media inside pump lines is also produced by pipe wall vibration, fluid turbulence, and flow excited mechanical vibration. Pipe wall vibration can be either a cause or a consequence of liquid-borne sound inside pipe. Thus, it is possible for liquid-borne sound indirectly to excite structural vibrations at points at which the containing pipe contacts or is supported by structural members. Therefore, use of acoustic filters to confine noise inside pump lines to the neighborhood of the source could be expected to reduce acoustic pressure levels and pipe-excited structural vibration at a considerable distance from the pump.

Since acoustic filters as herein considered affect only the liquid-borne noise, it is convenient to consider a system model comprising a single localized noise source, a sound transmission path, and an acoustic load. Figure 1(a) shows a simplified sketch of a shipboard pumping system; some of the paths by which sound from the pump may be transmitted to overside radiating surfaces are indicated. Figure 1(b) shows a model of the system which results from applying to the system the following simplifying assumptions:

(1) There is only one noise source.
(2) The noise source is localized.
(3) There is only one sound transmission path between the pump and its surroundings (the liquid path).
(4) The sound transmission path is uniform.
(5) The one sound transmission path terminates in an acoustic load of arbitrary character.

It is seen that these assumptions lead to an oversimplified representation of a pumping system, but even with this chosen model performance of a completely

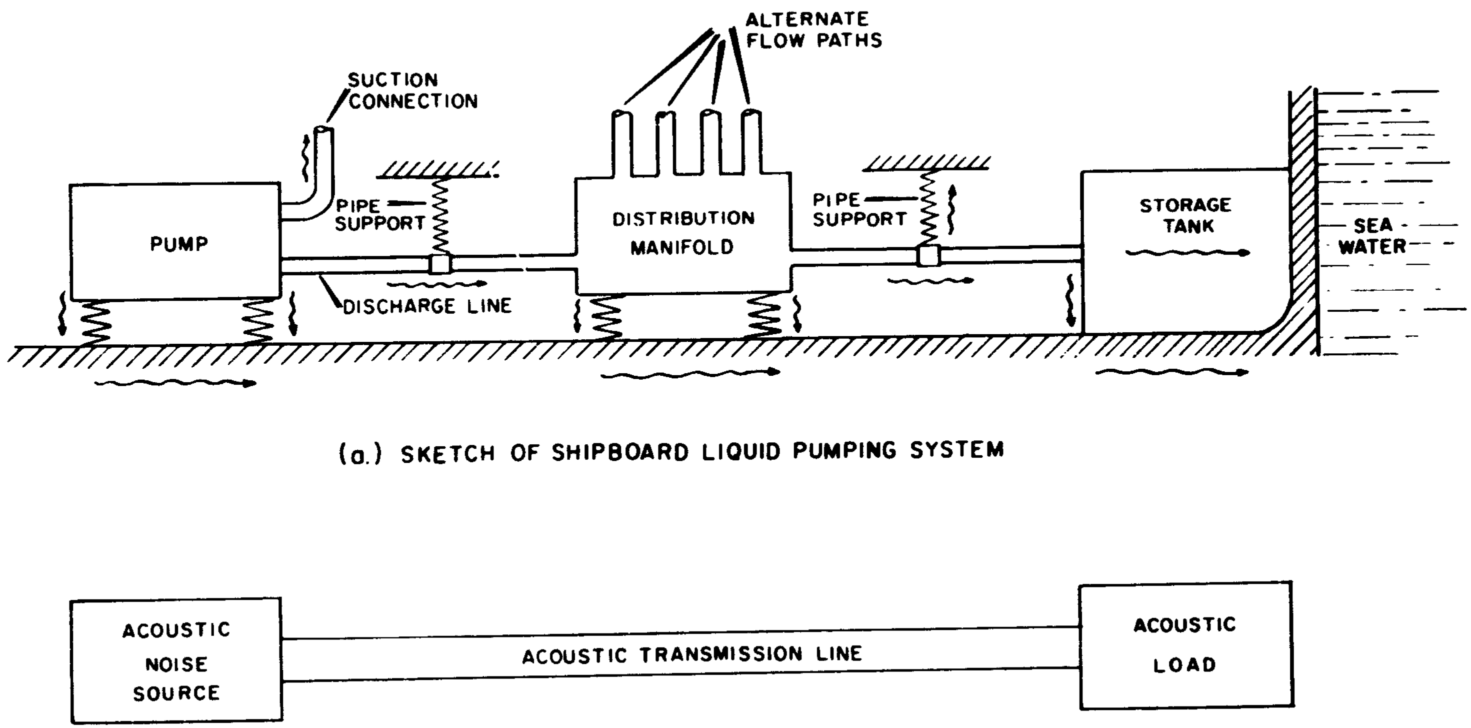

(a.) SKETCH OF SHIPBOARD LIQUID PUMPING SYSTEM

(b.) ACOUSTICAL MODEL OF LIQUID PUMPING SYSTEM

FIGURE 1
LIQUID PUMPING SYSTEM AND ITS ACOUSTICAL MODEL

DRL - UT
DWG AS 7104
JVK - BEE
9 - 10 - 62

specified filter in the system cannot be precisely predicted. The transmission line part of the system model is taken to be uniform, although the liquid-filled pipe of the actual installation may include bends, elbows, and other irregularities. If an acoustic filter is added to the system, any irregularities not included in the filter are considered either as a part of the source or of the load, depending upon where they are with respect to the filter.

September 1962
JVK:vh

CHAPTER II: BACKGROUND INFORMATION

A. SOME FUNDAMENTALS OF ACOUSTICS

1. Introduction

Fundamentally, sound waves are propagated, elastic disturbances of a substance. The substance can be in solid, liquid, or gaseous state. The only requirements are that the material must have mass and be able to store potential energy of compression or deformation, i.e., be resilient. Plane sinusoidal sound waves traveling in a homogeneous liquid or gas are in general partially reflected and partially transmitted when they encounter the surface of an obstacle of different material. The interactions of a sound wave in one medium with an obstacle of a different material are governed in part by the size of the obstacle in relation to the wavelength in the original medium. If the largest dimension of the obstacle in the direction of propagation is much smaller than a wavelength, then the obstacle can be characterized for purposes of determining its acoustical effects by specifying its so-called lumped acoustical parameters. If on the other hand the largest dimension of the obstacle in the direction of propagation is not small compared to a wavelength, then the obstacle behaves like a length of transmission line with characteristics in general different from those of the adjacent medium. It is apparent that since, for a given material, wavelength is inversely proportional to frequency, an object that is small in relation to a wavelength at one frequency is large compared to a wavelength at some sufficiently high frequency.

In this manual, acoustic filters are regarded as irregular acoustic transmission lines. The character of the line irregularities determines the type of acoustic filter. The special character, number, and distribution of irregularities determine the filter characteristics. In order to understand the methods of analysis to be employed, it is necessary to be familiar with certain fundamental concepts and relationships applicable to acoustic transmission line problems. In this section ideal lumped-parameter acoustical elements are described and methods for calculating their parameter values are given. The terms "analogous acoustic impedance" and "admittance" are defined; expressions for these quantities corresponding to combinations of ideal acoustical elements are given in terms of the lumped acoustical parameters of the elements. Acoustic transmission lines are described with particular reference to liquid-filled, rigid-walled pipes. The notions of distributed acoustical parameters and characteristic acoustic impedance and admittance are introduced, impedance/admittance transformation equations are given, and numerical examples illustrating applications of the equations to typical problems are shown.

These same ideas are common to passive linear systems generally; entirely analogous treatments can be given for mechanical and electrical systems. These analogies are not developed here, but electric circuit symbols are used to represent analogous acoustical elements. These symbols were adopted primarily because their use tends to simplify sketching acoustical circuits.

2. Ideal Acoustical Elements

The ideal acoustical elements can be understood by considering the response of a piston in a rigid wall to sinusoidal pressure variations in an acoustic medium in contact with the piston face. Such a piston can be considered subject to certain sets of restrictions on the friction, inertia, and elastic forces applied to it so that it becomes an acoustic resistance, inertance, or compliance depending upon the hypotheses. A piston of diameter d and area S idealized according to sets of hypotheses corresponding to acoustic resistance, inertance, and compliance is shown in Fig. 2. Static equilibrium between the piston and acoustic medium is assumed.

First we consider the piston to be massless, but subject to a drag force proportional to the first power of piston velocity through a proportionality constant r. Under these conditions the piston would be an ideal, lumped-parameter, acoustic resistor. Resistance is represented in acoustical circuits by the same graphical symbol ordinarily used for electrical resistance, a zig-zag line. The acoustic resistance parameter is represented by the literal symbol R. For the piston described, the numerical value of R can be calculated from the relationship

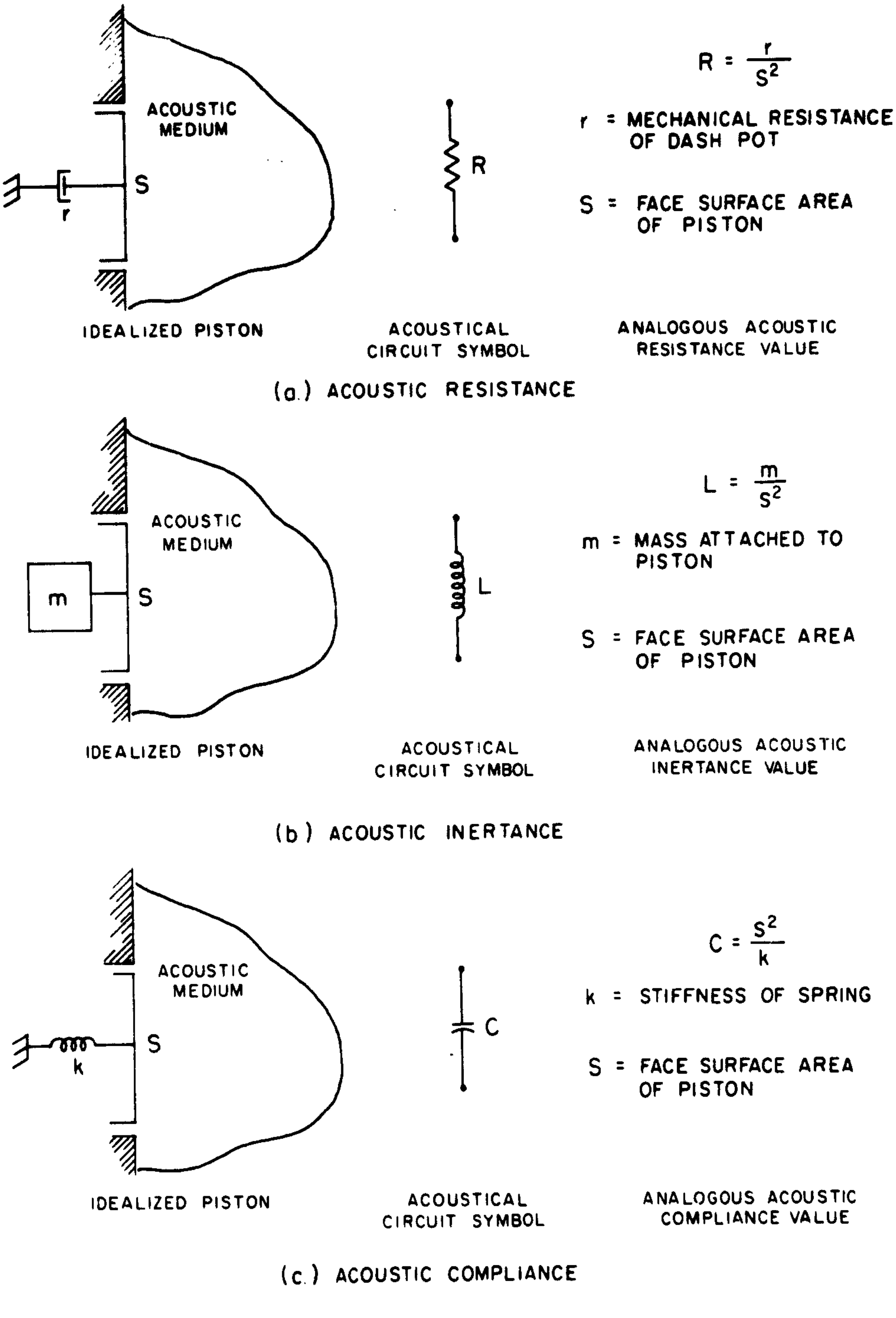

FIGURE 2
IDEAL ACOUSTICAL ELEMENTS

DRL – UT
DWG AS 7105
JVK · BEE
8 - 21 - 62

$$R = \frac{r}{S^2} \quad \frac{\text{lb sec}}{\text{in.}^5} \ .$$

Figure 2(a) is a sketch representing the piston; the acoustical circuit representation of resistance and the equation for calculating the value of the parameter R are also shown.

Next we consider the case in which the piston is taken to be frictionless and is attached to a weight of mass m, but is otherwise the same as before, Fig. 2(b). In this case the piston would offer an acoustic inertance to sinusoidal pressure variations at its face. Inertance is represented in acoustical circuits by the graphical symbol normally used to represent inductance in electrical circuits. The literal symbol for the inertance parameter is L. The value of L for this idealized piston, expressed in terms of the piston areas and the attached mass m, is

$$L = \frac{m}{S^2} \quad \frac{\text{lb sec}^2}{\text{in.}^5} \ .$$

Finally, we consider the case of Fig. 2(c), in which the piston is massless and frictionless, but is subject to an elastic restoring force proportional to its displacement from some equilibrium position. Let the proportionality constant, k, relate the restoring force to displacement. The effect of the piston in this case would be that of an ideal, lumped-parameter, acoustic compliance. Compliance is represented by the graphical symbol for electrical capacitance. The compliance parameter is represented by the literal symbol C. The value of C for the piston in terms of the area S and the constant k is expressed

$$C = \frac{S^2}{k} \quad \frac{\text{in.}^5}{\text{lb}} \ .$$

These idealized acoustical elements behave as lumped elements for waves striking the piston face at normal incidence or for any angle of incidence so long as $\lambda >> d$, say $\lambda = 10\ d$ or more, where λ is wavelength and d is piston diameter.

September 1962
JVK:vh

The ideal acoustical elements as given by these representations are not physically realizable. In fact, it is not possible to construct passive devices to offer pure acoustic resistance, inertance, or compliance over a broad band of frequencies. Physical elements, even in their linear behavior range always have mass, have either stiffness or compressibility, and produce energy losses due to internal friction while being deformed. In particular physical arrangements, however, certain ones of these characteristics may dominate. Physically realizable devices to approximate ideal acoustical element behavior over limited frequency ranges are possible.

It is of practical importance to consider the ways in which the ideal elements can be combined and their responses to sinusoidal sound waves calculated as functions of frequency both singly and in combination. In this connection we introduce the concept of analogous acoustic impedance. A sinusoidal sound pressure variation of angular frequency ω and amplitude p_{max} referred to an arbitrary time reference can be expressed

$$p(t) = p_{max} \cos(\omega t + \phi_p) \quad \frac{\text{lb}}{\text{in.}^2} \ ,$$

in which ϕ_p is a phase angle referring $p(t)$ to the chosen time reference. In phasor notation this pressure is expressed

$$P = \frac{p_{max}}{\sqrt{2}} e^{j(\varphi_p)} \quad \frac{\text{lb}}{\text{in.}^2} \ .$$

When such a pressure acts on an area S, there is in general an associated and resultant motion of velocity $v(t)$, of angular frequency ω, and amplitude v_{max} which can be written

$$v(t) = v_{max} \cos(\omega t + \varphi_v) \quad \frac{\text{in.}}{\text{sec}} \ ,$$

where φ_v is the phase angle relating $v(t)$ to the time reference. In phasor notation this velocity is expressed

$$V = \frac{v_{max}}{\sqrt{2}} e^{j(\varphi_v)} \quad \frac{\text{in.}}{\text{sec}} \quad .$$

The area S moving at velocity V represents a flow which is said to have volume velocity $\overline{V} = SV \quad \left(\frac{\text{in.}^3}{\text{sec}}\right)$. Analogous acoustic impedance Z is defined as the complex ratio of pressure P to volume velocity $\overline{V}$,

$$Z = \frac{P}{\overline{V}} \quad \frac{\text{lb sec}}{\text{in.}^5} \quad .$$

Analogous acoustic admittance Y is the reciprocal of impedance. Thus

$$Y = \frac{\overline{V}}{P} = \frac{1}{Z} \quad \frac{\text{in.}^5}{\text{lb sec}} \quad .$$

We now consider the acoustic impedances of the ideal acoustical elements of Fig. 2. In the case of the acoustic resistance, Fig. 2(a), a pressure P, acting on the face of the piston of area S, exerts a force PS and produces a velocity V. The dashpot plunger being moved at velocity V by the piston exerts a force on the piston of magnitude rV. So we have

$$PS = rV \quad \text{lb} \quad .$$

But, also

$$V = \frac{\overline{V}}{S} \quad \frac{\text{in.}}{\text{sec}} \quad ,$$

so

$$PS = r\frac{\overline{V}}{S} \quad \text{lb} \quad , \qquad \text{or} \qquad \frac{P}{\overline{V}} = \frac{r}{S^2} = R \quad \frac{\text{lb sec}}{\text{in.}^5} \quad .$$

Since the analogous acoustic impedance Z is defined as $\frac{P}{\overline{V}}$, Z for this ideal acoustic resistance is just the value of the resistance R.

Similar reasoning applied to the ideal acoustic inertance, Fig. 2(b), gives

$$PS = m \frac{d}{dt} V \quad \text{lb} \quad .$$

Differentiation of a phasor quantity with respect to time results in the quantity multiplied by $j\omega$.

$$\frac{d}{dt} V = j\omega V \quad \frac{\text{in.}}{\text{sec}^2} \quad .$$

So we have

$$PS = j\omega m V \quad \text{lb} \quad .$$

Replacing V by $\frac{\bar{V}}{S}$ gives

$$PS = j\omega m \frac{\bar{V}}{S} \quad \text{lb} \quad ,$$

so

$$\frac{P}{\bar{V}} = j\omega \frac{m}{S^2} \quad \frac{\text{lb sec}}{\text{in.}^5} \quad .$$

Thus the analogous acoustic impedance for this pure inertance is expressed

$$Z = j\omega \frac{m}{S^2} \quad \frac{\text{lb sec}}{\text{in.}^5} \quad ,$$

or in terms of the value of the inertance L,

$$Z = j\omega L \quad \frac{\text{lb sec}}{\text{in.}^5} \quad .$$

Finally we consider the compliance, Fig. 2(c). In this case, force of the pressure at the piston face is equated to the product of the spring stiffness k and the piston phasor displacement from equilibrium X.

$$PS = kX \quad \text{lb} \quad .$$

The displacement, however, is the time integral of velocity. Integration with respect to time of a sinusoidal function of time gives its phasor representation divided by $j\omega$.

$$X = \frac{V}{j\omega} \quad \text{in.} \quad .$$

Then

$$PS = \frac{kV}{j\omega} \quad \text{lb} \quad .$$

But as before, $V = \frac{\overline{V}}{S}$ so

$$PS = \frac{k\overline{V}}{j\omega S} \quad \text{lb} \quad , \qquad \text{and} \qquad \frac{P}{\overline{V}} = \frac{1}{j\omega}\frac{k}{S^2} \quad \frac{\text{lb sec}}{\text{in.}^5} \quad .$$

So in terms of the compliance C the acoustic impedance Z is

$$Z = \frac{1}{j\omega C} = \frac{-j}{\omega C} \quad \frac{\text{lb sec}}{\text{in.}^5} \quad .$$

Unless it is expressly stated to the contrary or implied by the context to be otherwise, the term <u>impedance</u> should be taken to mean analogous acoustic impedance as derived above. Adoption of this convention will avoid needless repetition.

It is of interest to consider the calculation of impedance of acoustical elements in combination. The elements can be arranged in series, parallel, or series-parallel combinations. If two or more of the elements of Fig. 2 are grouped together side by side in a wall within an area sufficiently small for lumped parameter considerations to be valid, they are combined in parallel. For example, consider the calculation of the impedance of two acoustic resistances of areas S_1 and S_2 and proportionality constants r_1 and r_2, Fig. 3(a) Each resistor is subjected to the same pressure, but impedance must be cal ulated on the basis of the total volume velocity, so $\bar{V}$ in the expression

$$Z = \frac{P}{\bar{V}} \quad \frac{\text{lb sec}}{\text{in.}^5} \quad \text{should be} \quad \bar{V}_1 + \bar{V}_2 = \bar{V} \quad \frac{\text{in.}^3}{\text{sec}} \ .$$

Since

$$Z_1 = \frac{P}{\bar{V}_1} = R_1 = \frac{r_1}{S_1^{\,2}} \quad \frac{\text{lb sec}}{\text{in.}^5} \quad \text{and} \quad Z_2 = \frac{P}{\bar{V}_2} = R_2 = \frac{r_2}{S_2^{\,2}} \quad \frac{\text{lb sec}}{\text{in.}^5} \ ,$$

we have

$$\bar{V}_1 = \frac{P}{Z_1} \quad \frac{\text{in.}^3}{\text{sec}} \quad \text{and} \quad \bar{V}_2 = \frac{P}{Z_2} \quad \frac{\text{in.}^3}{\text{sec}} \ ,$$

but

$$Z_1 = R_1 \quad \frac{\text{lb sec}}{\text{in.}^5} \quad \text{and} \quad Z_2 = R_2 \quad \frac{\text{lb sec}}{\text{in.}^5} \ ,$$

so

$$\bar{V}_1 = \frac{P}{R_1} \quad \frac{\text{in.}^3}{\text{sec}} \quad \text{and} \quad \bar{V}_2 = \frac{P}{R_2} \quad \frac{\text{in.}^3}{\text{sec}} \ .$$

Substituting $\bar{V} = (\bar{V}_1 + \bar{V}_2) = \left(\frac{P}{R_1} + \frac{P}{R_2}\right) \quad \frac{\text{in.}^3}{\text{sec}}$ into the expression for Z,

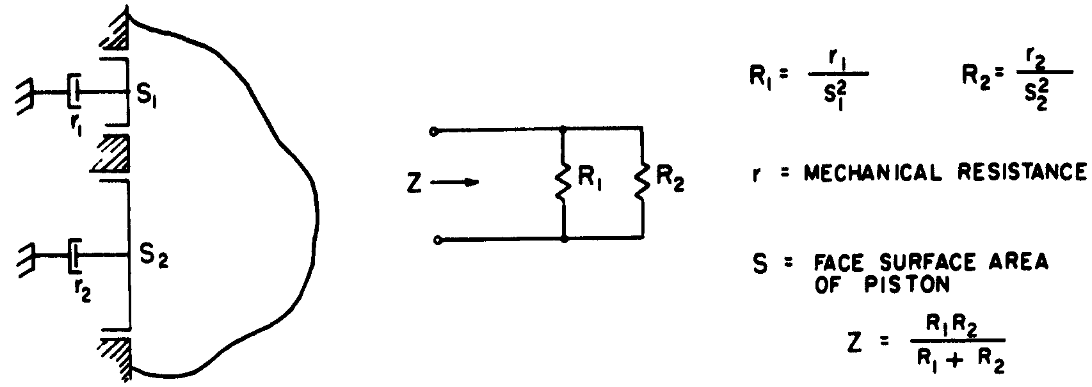

(a.) ACOUSTIC RESISTANCES IN PARALLEL

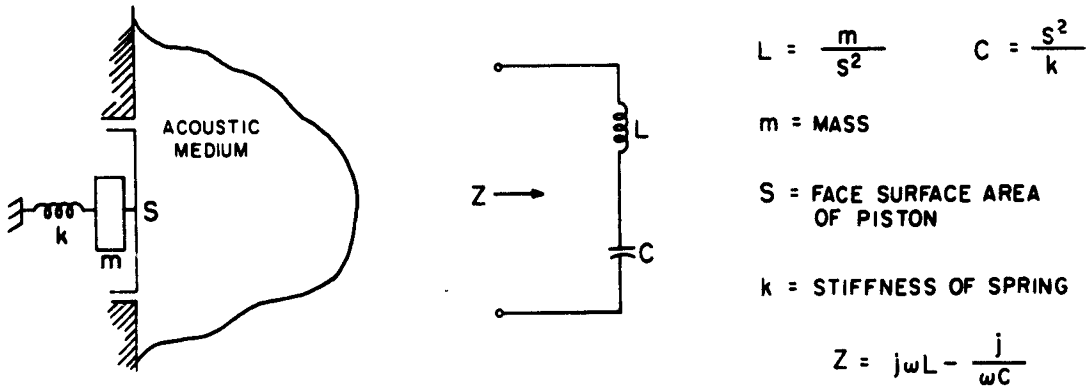

(b.) ACOUSTIC INERTANCE AND COMPLIANCE IN SERIES

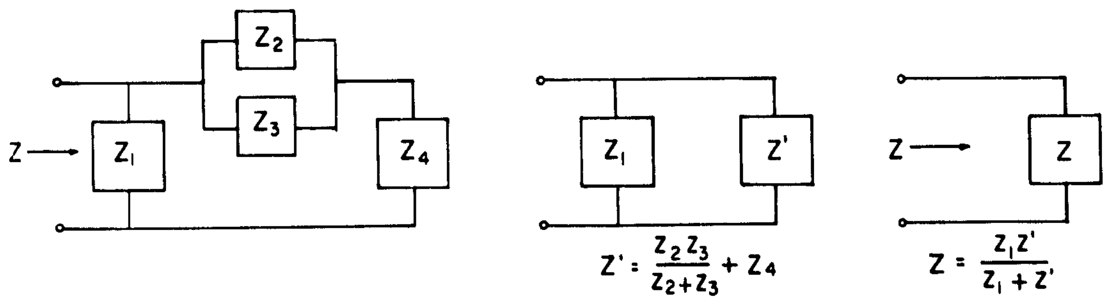

(c) FINDING IMPEDANCE OF SERIES-PARALLEL ACOUSTICAL CIRCUIT BY NETWORK REDUCTION

FIGURE 3
COMBINATION OF ACOUSTICAL ELEMENTS

DRL – UT
DWG AS 7106
JVK – BEE
8 – 22 – 62

$$Z = \frac{P}{\bar{V}_1 + \bar{V}_2}, \qquad \text{gives} \qquad Z = \frac{R_1 R_2}{R_1 + R_2} \quad \frac{\text{lb sec}}{\text{in.}^5} .$$

For more than two resistances, say n of them, combined in parallel

$$Z = \frac{1}{\frac{1}{R_1} + \frac{1}{R_2} + \ldots + \frac{1}{R_n}} \quad \frac{\text{lb sec}}{\text{in.}^5} .$$

Applying similar reasoning it is easy to show that in general the impedance of parallel combinations of ideal elements can be calculated by the formula

$$Z = \frac{1}{\frac{1}{Z_1} + \frac{1}{Z_2} + \ldots + \frac{1}{Z_n}} \quad \frac{\text{lb sec}}{\text{in.}^5} ,$$

where Z_n is the impedance of the nth element as already defined, irrespective of which kinds and how many of the elements are combined.

Figure 3(b) shows an element representable by ideal acoustical elements, an inertance L in series with a compliance C. Let the impedance of the inertance be Z_1,

$$Z_1 = j\omega \frac{m}{S^2} = j\omega L \quad \frac{\text{lb sec}}{\text{in.}^5} ,$$

and let the impedance of the compliance be Z_2,

$$Z_2 = \frac{-jk}{\omega S^2} = \frac{-j}{\omega C} \quad \frac{\text{lb sec}}{\text{in.}^5} .$$

Note that both of these impedances are frequency dependent. The ame volume velocity is common to both elements. Equating the pressure for e and the sum of mechanical reaction forces

$$PS = \left(j\omega m \frac{\overline{V}}{S} - \frac{jk\overline{V}}{\omega S} \right) \quad \text{lb} \quad .$$

Then

$$Z = \frac{P}{\overline{V}} = \frac{j\omega m}{S^2} - \frac{jk}{\omega S^2} = j\omega L - \frac{j}{\omega C} \quad \frac{\text{lb sec}}{\text{in.}^5} \quad .$$

Thus for this series combination the total impedance is the sum of the impedances of the ideal acoustical elements. It can be shown that in general if ideal acoustical elements with impedances Z_1, Z_2, ... Z_n are combined in parallel, the impedance of the combination is the reciprocal of the sum of the reciprocals of the individual element impedances; if they are combined in series, the total impedance is the sum of the element impedances. Impedances of series-parallel combinations can be found by using the rules already given to simplify the acoustical circuit by methods of network reduction as suggested by the sequence of acoustical circuit sketches of Fig. 3(c).

Examples

Fig. 4(a) shows three acoustical elements communicating to the inside of a liquid-filled tube. Calculate the input impedance $Z(\omega)$ of the combination for the following set of values:

$$S_R = 20 \text{ in.}^2 \qquad r = 0.40 \quad \frac{\text{lb sec}}{\text{in.}}$$

$$S_L = 25 \text{ in.}^2 \qquad m = 1.25 \times 10^{-2} \quad \frac{\text{lb sec}^2}{\text{in.}}$$

$$S_C = 30 \text{ in.}^2 \qquad k = 300 \quad \frac{\text{lb}}{\text{in.}}$$

It is assumed that the walls of the tube are rigid; that the tube is much shorter than the shortest wavelength of interest; and that the mass, compressibility, and internal resistance of the liquid itself are negligible.

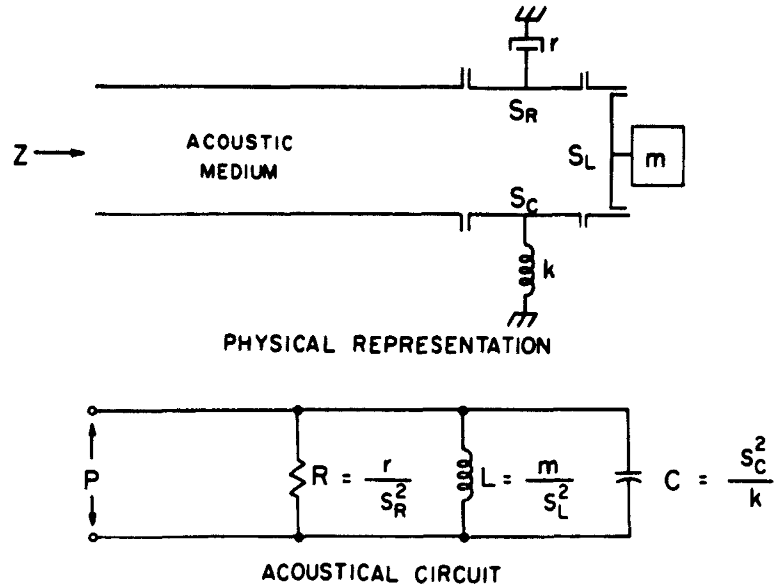

(a.) PARALLEL ACOUSTICAL ELEMENTS

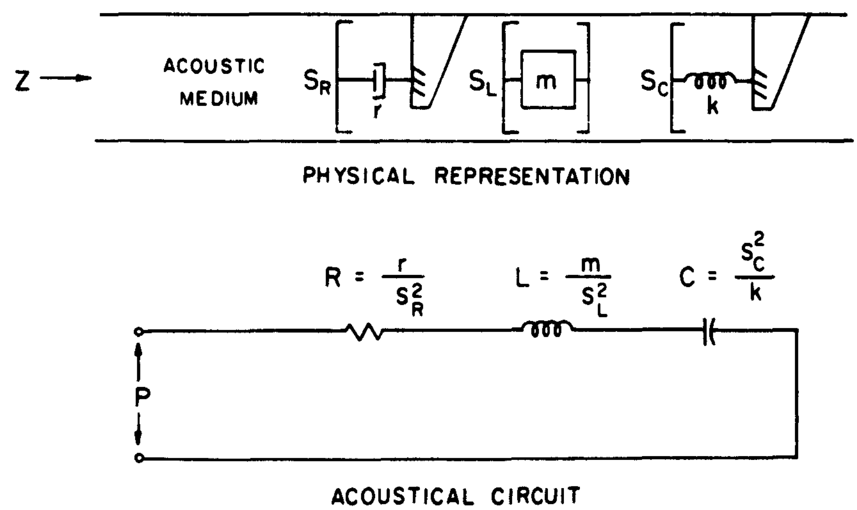

(b.) SERIES ACOUSTICAL ELEMENTS

FIGURE 4
SERIES AND PARALLEL COMBINATION OF ACOUSTICAL ELEMENTS

DRL - UT
DWG AS 7107
JVK - BEE
8 - 20 - 62

First we calculate the values of the parameters R, L, and C by the formulas

$$R = \frac{r}{S_R^{\ 2}} \quad \frac{\text{lb sec}}{\text{in.}^5}\ , \qquad L = \frac{m}{S_L^{\ 2}} \quad \frac{\text{lb sec}^2}{\text{in.}^5} \quad \text{and}$$

$$C = \frac{S_c^{\ 2}}{k} \quad \frac{\text{in.}^5}{\text{lb}}\ :$$

$$R = \frac{0.4}{400} = 10^{-3} \quad \frac{\text{lb sec}}{\text{in.}^5}\ ,$$

$$L = \frac{1.25 \times 10^{-2}}{625} = 2 \times 10^{-5} \quad \frac{\text{lb sec}^2}{\text{in.}^5}\ ,$$

$$C = \frac{30^2}{300} = 3 \quad \frac{\text{in.}^5}{\text{lb}}\ .$$

Then the impedances of these elements are

$$Z_R = R = 10^{-3} \quad \frac{\text{lb sec}}{\text{in.}^5}\ ,$$

$$Z_L = j\omega L = j\omega\, 2 \times 10^{-5} \quad \frac{\text{lb sec}}{\text{in.}^5}\ ,$$

$$Z_C = \frac{-j}{\omega C} = \frac{-j}{\omega(3)} \quad \frac{\text{lb sec}}{\text{in.}^5}\ .$$

Since the elements are combined in parallel,

$$Z = \frac{Z_R\, Z_L\, Z_C}{Z_R\, Z_L + Z_R\, Z_C + Z_L\, Z_C} \quad \frac{\text{lb sec}}{\text{in.}^5}\ ,$$

$$Z = \frac{(10^{-3})\,(j\omega)\,(2 \times 10^{-5})\left(\frac{-j}{3\omega}\right)}{(10^{-3})\,(j\omega)\,(2 \times 10^{-5}) - (10^{-3})\left(\frac{j}{3\omega}\right) + j\omega(2 \times 10^{-5})\left(\frac{-j}{3\omega}\right)} \quad \frac{\text{lb sec}}{\text{in.}^5},$$

$$Z = \frac{(0.66)\,(10^{-8})}{(0.66)\,(10^{-5}) + j\left(\omega \times 2 \times 10^{-8} - \frac{0.33 \times 10^{-3}}{\omega}\right)} \quad \frac{\text{lb sec}}{\text{in.}^5}.$$

Note that there is some frequency ω_o for which the imaginary term in the denominator of Z vanishes.

$$\left[\omega_o \times 2 \times 10^{-8} - \frac{(0.33)\,(10^{-3})}{\omega_o}\right] = 0$$

$$\omega_o{}^2 = \frac{(0.33)\,(10^{-3})}{(2)\,(10^{-8})} = (1.65)\,(10^4) \quad \frac{\text{rad}^2}{\text{sec}^2}$$

$$\omega_o = 128.4 \quad \frac{\text{rad}}{\text{sec}}.$$

Thus at a frequency of $f = \frac{\omega_o}{2\pi} = \frac{128.4}{6.28} = 20.4$ cps, the given elements are in parallel resonance and the impedance Z has the real value.

$$Z = \frac{(0.66)\,(10^{-8})}{(0.66)\,(10^{-5})} = 10^{-3} \quad \frac{\text{lb sec}}{\text{in.}^5}.$$

Note that this is just the value of the impedance of the resistive branch of the acoustical circuit. At the resonant frequency, f = 20.4 cps, the impedance magnitude is maximum; at other frequencies the impedance is of smaller magnitude and complex.

2. Calculate the impedance Z for the acoustical elements cf the foregoing example combined as shown in Fig. 4(b).

$$Z_R = 10^{-3} \quad \frac{\text{lb sec}}{\text{in.}^5} ,$$

$$Z_L = j\omega 2 \times 10^{-5} \quad \frac{\text{lb sec}}{\text{in.}^5} ,$$

$$Z_C = \frac{-j}{\omega \times 3} \quad \frac{\text{lb sec}}{\text{in.}^5} .$$

Combining these impedances in series

$$Z = Z_R + Z_L + Z_C$$

$$= 10^{-3} + j\left(\omega \times 2 \times 10^{-5} - \frac{0.33}{\omega}\right) .$$

Setting the imaginary part of Z equal to zero and solving for ω_o gives again

$$\omega_o = 128.4 \quad \frac{\text{rad}}{\text{sec}} \quad \text{and} \quad f = 20.4 \text{ cps} .$$

This is the frequency at which the impedance of the elements in series is real and has minimum magnitude.

3. Lossless Acoustic Transmission Lines

a. Smooth, Infinite Line

The preceding discussion dealt with systems of lumped-parameter acoustical elements. We now consider systems with distributed acoustical parameters. For these systems, acoustical circuits with only lumped-parameter elements are not adequate representations. Both fluid columns and solid rods behave as acoustic transmission lines if they are of sufficient length. Longitudinal waves are propagated on any of these lines; torsion and bending waves, however, are possible only in solids. Inasmuch as we are concerned with sound waves in liquid-filled pipes, transmission lines of the liquid column type will be considered.

The following distributed parameters apply to acoustic transmission lines generally:

(1) Series inertance per unit length,
(2) Shunt compliance per unit length,
(3) Series resistance per unit length,
(4) Shunt conductance per unit length.

There is some dissipation in any actual line, but in many cases of practical interest the losses are small and can be neglected. Analysis of lossless lines is simpler than that of lines with dissipation. Since in most cases the series resistance and shunt conductance per unit length for liquids confined in metal pipes are sufficiently small to justify the assumption of losslessness, only lossless lines will be considered here.

Figure 5(a) shows a portion of a rigid-walled, liquid-filled tube. The tube is thought of as extending to infinity on the right. At the left end it is fitted with a piston which radiates sound of single frequency ω into the liquid. Sinusoidal sound waves moving toward the right are propagated in the liquid column. Any volume element of the liquid has mass and is compressible. The mass gives rise to a distributed series inertance and the compressibility to a distributed shunt compliance. Figure 5(b) shows a representation of the infinite line in which the series inertances and shunt compliances per unit length of line are associated with lumped parameter elements. Such a line only approximates a smooth line. Figure 5(c) is the schematic representation of the smooth line of Fig. 5(a).

If the normal section area of the liquid column of Fig 5(a) is S, and the mass density and compressibility of the liquid are respectively $\rho \ \frac{\text{lb sec}^2}{\text{in.}^4}$ and $\kappa \ \frac{\text{in.}^2}{\text{lb}}$ then the series inertance of the line per unit length is

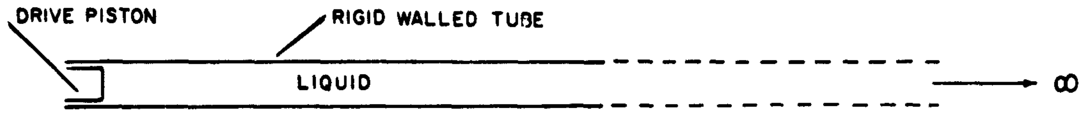

(a.) CONFINED LIQUID COLUMN ACOUSTIC TRANSMISSION LINE

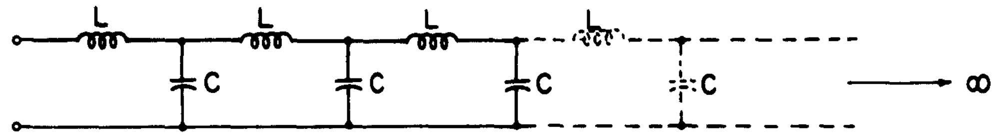

(b.) LUMPED PARAMETER ELEMENT APPROXIMATION OF SMOOTH INFINITE LINE

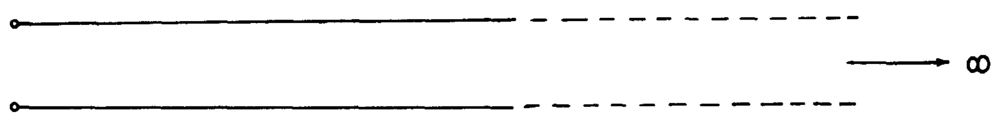

(c.) SCHEMATIC REPRESENTATION OF SMOOTH INFINITE LINE

FIGURE 5
LOSSLESS ACOUSTIC TRANSMISSION LINE OF INFINITE LENGTH

DRL - UT
DWG AS7108
JVK - BEE
8 - 7 - 62

$$L = \frac{\rho}{S} \quad \frac{\text{lb sec}^2}{\text{in.}^6} \ ,$$

and the shunt compliance per unit length is

$$C = S\kappa \quad \frac{\text{in.}^4}{\text{lb}} \ .$$

Series impedance of a unit length of the line is

$$Z = (0 + j\omega L) = \left(0 + j\omega \frac{\rho}{S} \right) \quad \frac{\text{lb sec}}{\text{in.}^6} \ ,$$

and the shunt admittance per unit length is

$$Y = (0 + j\omega C) = (0 + j\omega S\kappa) \quad \frac{\text{in.}^4}{\text{lb sec}} \ .$$

The characteristic acoustic impedance of the line is

$$Z_0 = \sqrt{\frac{Z}{Y}} = \sqrt{\frac{L}{C}} = \sqrt{\frac{\rho}{S^2\kappa}} \quad \frac{\text{lb sec}}{\text{in.}^5} \ .$$

The propagation constant is

$$\gamma = \alpha + j\beta = \sqrt{ZY} = j\omega\sqrt{LC} \ .$$

Then

$$\beta = \omega\sqrt{LC} \ .$$

The velocity of wave propagation on the line v is then ω/β, or

$$v = \frac{1}{\sqrt{LC}} = \frac{1}{\sqrt{\rho\kappa}} \quad \frac{\text{in.}}{\text{sec}} \ .$$

Then, in terms of this velocity,

$$Z_o = \frac{\rho v}{S} \quad \frac{\text{lb sec}}{\text{in.}^5} \ .$$

It is important to notice that the same symbols have been used for distributed and lumped inertance and compliance. However, this should not be confusing since the correct interpretation will be clear from context.

b. Smooth, Finite Lines

Figure 6 shows liquid columns, each of length ℓ, contained in uniform diameter tubes. Three different acoustic terminations are represented. They are

(1) Closed-end,
(2) Open-end,
(3) Impedance Z_L.

Acoustical circuit representations are given for each case. The input analogous impedances or admittances of these lines are expressible in terms of the line parameters, the line geometry or length, and the characteristics of the load.

Impedance at the input of the acoustic lines can be calculated in the same way as for the analogous electrical lines.

The input impedance, Z_i, of any uniform lossless line of length ℓ, terminated in some impedance Z_L is

$$Z_i = Z_o \left(\frac{1 + Ke^{-j2\beta\ell}}{1 - Ke^{-j2\beta\ell}} \right) \ ,$$

where β is the phase constant and K is the reflection coefficient.

$$\beta = \frac{\omega}{v} = \omega\sqrt{\rho\kappa} \quad \frac{\text{rad}}{\text{in.}} \ ; \qquad K = \frac{Z_L - Z_o}{Z_L + Z_o} \ .$$

Note that K is dimensionless and in general complex.

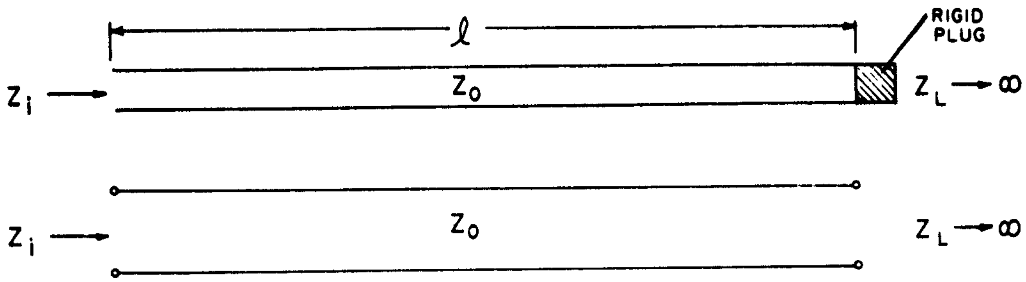

(a.) CLOSED-END ACOUSTIC TRANSMISSION LINE AND ITS ACOUSTICAL CIRCUIT REPRESENTATION

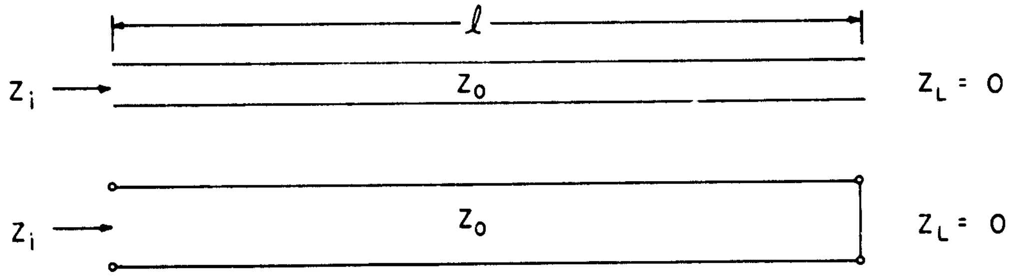

(b) OPEN-END ACOUSTIC TRANSMISSION LINE AND ITS ACOUSTICAL CIRCUIT REPRESENTATION

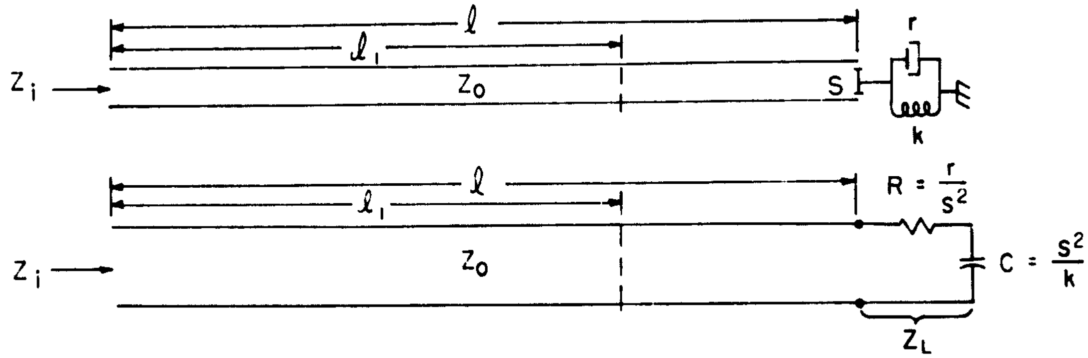

(c.) ACOUSTIC TRANSMISSION LINE TERMINATED IN A LOAD HAVING COMPLEX IMPEDANCE Z_L

FIGURE 6
LOSSLESS ACOUSTIC TRANSMISSION LINE OF FINITE LENGTH

DRL - UT
DWG AS7109
JVK - BEE
8 - 14 - 62

For a liquid column confined in a closed-end tube, Fig. 6(a), the load impedance is infinite. No matter what the liquid pressure is at the closed end of the tube, the volume velocity there is zero. Thus, the reflection coefficient is of unity magnitude and zero argument.

$$K = 1\underline{/0 \text{ rad}} \quad .$$

Another extreme limiting case is shown in Fig. 6(b). Here the end of the tube is open so there is a free surface at the end of the liquid column. The corresponding load impedance is zero and the reflection coefficient is again of unit magnitude but the argument is π radians.

$$K = 1\underline{/\pi \text{ rad}} \quad .$$

Figure 6(c) shows a general case; here the load impedance is taken to be representable by an ideal acoustic resistance and compliance in series.

$$Z_L = \left(R - \frac{j}{\omega C}\right) \quad \frac{\text{lb sec}}{\text{in.}^5} \quad .$$

Then the reflection coefficient is

$$K = \left(\frac{Z_L - Z_o}{Z_L + Z_o}\right) = \left(\frac{R - \frac{j}{\omega C} - Z_o}{R - \frac{j}{\omega C} + Z_o}\right) \quad .$$

Now both the magnitude and angle of K depend on the frequency ω.

<u>Examples</u>

1. Calculate the input impedance of 40 ft of water-filled, 3 in. i.d. pipe terminated by a rigid plug. Assume the walls of the pipe are rigid.

Characteristic impedance can be calculated from the equation,

$$Z_o = \frac{1}{S}\sqrt{\frac{\rho}{\kappa}} \quad \frac{\text{lb sec}}{\text{in.}^5} .$$

Area: $$S = \left(\frac{\pi}{4}\right)(3^2) = 7.06 \quad \text{in.}^2$$

Mass Density: $$\rho = (9.35)(10^{-5}) \quad \frac{\text{lb sec}^2}{\text{in.}^4}$$

Compressibility: $$\kappa = (3.34)(10^{-6}) \quad \frac{\text{in.}^2}{\text{lb}}$$

$$Z_o = \left(\frac{1}{7.06}\right)\sqrt{\frac{(9.35)(10^{-5})}{(3.34)(10^{-6})}}$$

$$Z_o = 0.75 \quad \frac{\text{lb sec}}{\text{in.}^5}$$

The phase constant β can be found from the relation

$$\beta = \omega\sqrt{\rho\kappa}$$

$$= \omega\sqrt{(9.35)(10^{-5})(3.34)(10^{-6})}$$

$$= \omega\sqrt{(3.12)(10^{-10})} = (\omega)(1.77)(10^{-5}) \quad \frac{\text{rad}}{\text{in.}} .$$

To be consistent with the length units in terms of which the phase constant is expressed, the length of the pipe must be expressed in inches.

$$\ell = (40)(12) = 480 \quad \text{in.}$$

Since $K = e^{j0}$,

$$Z_i = Z_o \left(\frac{1 + Ke^{-j2\beta\ell}}{1 - Ke^{-j2\beta\ell}} \right)$$

can be written

$$Z_i = Z_o \left(\frac{e^{j\beta\ell} + e^{-j\beta\ell}}{e^{j\beta\ell} - e^{-j\beta\ell}} \right) = Z_o \coth j\beta\ell$$

$$= -j\, Z_o \cot\beta\ell \quad .$$

$$Z_i = -j(0.75) \cot (\omega)\, (1.77)\, (10^{-5})\, (4.8)\, (10^2)$$

$$= -j(0.75) \cot \left[(8.50)\, (10^{-3})\, (\omega) \right] \quad \frac{\text{lb sec}}{\text{in.}^5} \quad .$$

Note that at all frequencies the real part of the input impedance is zero. This indicates that no energy is dissipated in either the line or the load.

2. Consider now a line terminated as shown in Fig. 6(b). If the length, characteristic impedance, and phase constant of the line are the same as in Example 1, what is the input impedance Z_i?

$$Z_o = 0.75 \quad \frac{\text{lb sec}}{\text{in.}^5} \quad ,$$

$$\beta = (1.77)\, (10^{-5})\, \omega \quad \frac{\text{rad}}{\text{in.}} \quad ,$$

$$\ell = 480 \quad \text{in.} \quad , \text{ and}$$

$$K = e^{j\pi} \quad .$$

$$Z_i = Z_o \left(\frac{1 + e^{j\pi} e^{-j2\beta \ell}}{1 - e^{j\pi} e^{-j2\beta \ell}} \right) = Z_o \left(\frac{1 - e^{-j2\beta \ell}}{1 + e^{-j2\beta \ell}} \right) .$$

$$Z_i = j\, Z_o \tan\beta\ell = j(0.75) \tan \left[(8.50)\ (10^{-3})\ (\omega)\right] \quad \frac{\text{lb sec}}{\text{in.}^5} .$$

Again the imput impedance of the line is imaginary, so no energy is dissipated in either the line or the load.

3. Consider the line and termination of Fig. 6(c). As in Examples 1 and 2, the line is lossless and of finite length. The load, however, is such that it can be represented by a complex acoustic impedance, that of an acoustic resistance and compliance in series.

Let the length and characteristics of the line be the same as in Examples 1 and 2.

$$Z_o = 0.75 \quad \frac{\text{lb sec}}{\text{in.}^5} ,$$

$$\ell = 480 \quad \text{in.} \quad , \text{and}$$

$$\beta = (1.77)\ (10^{-5})\ (\omega) \quad \frac{\text{rad}}{\text{in.}} .$$

Let the terminating acoustic resistance R be 1.0 $\frac{\text{lb sec}}{\text{in.}^5}$; let the acoustic compliance C be 0.16 in.^{5}/lb. Find the input impedance of the line at a frequency of 10 cps.

The load impedance Z_L is the sum of the impedance Z_R of the acoustic resistance and the impedance Z_C of the compliance.

$$Z_L = Z_R + Z_C \quad , \text{ where}$$

$$Z_R = R + j0 \text{ and } Z_C = 0 - \frac{j}{\omega C} \quad .$$

$$Z_L = R - j\frac{1}{\omega C} = (1.0 - j6.25\ \omega^{-1}) \quad \frac{\text{lb sec}}{\text{in.}^5} \quad .$$

Now the reflection coefficient K can be calculated.

$$K = \frac{Z_L - Z_o}{Z_L + Z_o} = \frac{1.0 - j6.25\ \omega^{-1} - 0.75}{1.0 - j6.25\ \omega^{-1} + 0.75} \quad .$$

$$K = \frac{0.25 - j6.25\ \omega^{-1}}{1.75 - j6.25\ \omega^{-1}} \quad .$$

Note that the reflection coefficient is now frequency dependent and is not in general of unity magnitude. At the given frequency of 10 cps, $\omega = 62.8\ \frac{\text{rad}}{\text{sec}}$.

$$K(62.8) = \frac{0.25 - j0.1}{1.75 - j0.1} = \frac{0.27e^{-j0.38}}{1.75e^{-j0.06}}$$

$$= 0.154e^{-j0.32} \quad .$$

The input impedance at a frequency of 10 cps is then

$$Z_i = Z_o \frac{1 + Ke^{-j2\beta \ell}}{1 - Ke^{-j2\beta \ell}} = 0.75 \left(\frac{1 + 0.154\ e^{-j0.32}\ e^{-j2\beta \ell}}{1 - 0.154\ e^{-j0.32}\ e^{-j2\beta \ell}} \right) \quad .$$

At 10 cps

$$\beta \ell = (1.77)\ (10^{-5})\ (62.8)\ (480) = 0.53 \quad \text{rad} \quad .$$

So

$$Z_i = Z_o \left(\frac{1 + 0.154\, e^{-j1.38}}{1 - 0.154\, e^{-j1.38}} \right)$$

$$= 0.75 \left(\frac{1 + 0.029 - j0.151}{1 - 0.029 + j0.151} \right)$$

$$= 0.795\, e^{-j(0.305)} = 0.795 \underline{|-17.4°} \quad .$$

In acoustical systems like those of the three previous examples the division between line and load can be made at any point along the line. For example, the division could have been made at a distance ℓ_1 from the input end of the line, Fig. 6(c). The load impedance on the line of length ℓ_1 could be calculated from

$$Z_{L_1} = Z_o \left[\frac{1 + Ke^{-j2\beta(\ell - \ell_1)}}{1 - Ke^{-j2\beta(\ell - \ell_1)}} \right] \quad ,$$

$$K = \frac{Z_L - Z_o}{Z_L + Z_o} \quad .$$

Then the input impedance of the line Z_i in terms of the impedance of this differently chosen load and the shorter length of line is

$$Z_i = Z_o \left(\frac{1 + K_1 e^{-j2\beta \ell_1}}{1 - K_1 e^{-j2\beta \ell_1}} \right) \quad ,$$

where

$$K_1 = \frac{Z_{L_1} - Z_o}{Z_{L_1} + Z_o} \quad .$$

Calculations of this kind can also be carried out for finding the input admittance Y_i of a finite lossless line terminated in a load admittance Y_L. The appropriate formula is

$$Y_i = Y_o\left(\frac{1 - Ke^{-j2\beta \ell}}{1 + Ke^{-j2\beta \ell}}\right)$$

$$K = \frac{Y_o - Y_L}{Y_o + Y_L} \quad .$$

c. Finite Line with Changes in Z_o

For purposes of calculating the input impedance of acoustic transmission lines, the division of the system into source and load can be made arbitrarily. This suggests extension of the methods used for smooth or uniform lines to nonuniform lines. The nonuniform lines of interest here are those having abrupt changes of characteristic impedance, branch impedances, or both.

Consider the line and load of Fig. 7(a). The line comprises three sections of lengths ℓ_1, ℓ_2, and ℓ_3 with characteristic impedances Z_{o_1}, Z_{o_2}, and Z_{o_3}, respectively. To find the input impedance Z_i at the left end, first calculate the impedance at the input to section 1, Z_{i_1}, in the usual way.

$$Z_{i_1} = Z_{o_1}\left(\frac{1 + K_1 e^{-j2\beta_1 \ell_1}}{1 - K_1 e^{-j2\beta_1 \ell_1}}\right) \quad .$$

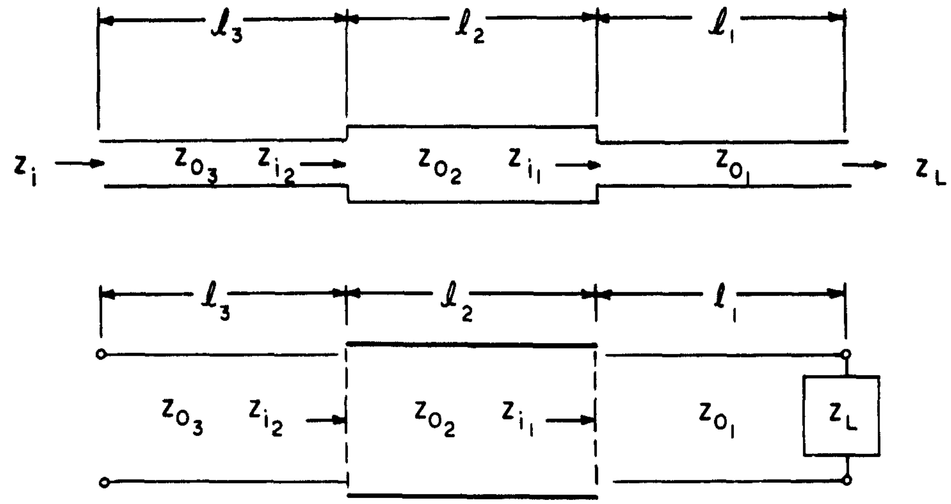

(a.) ACOUSTIC TRANSMISSION LINE WITH CHANGES IN Z_O AND ITS ACOUSTIC CIRCUIT REPRESENTATION

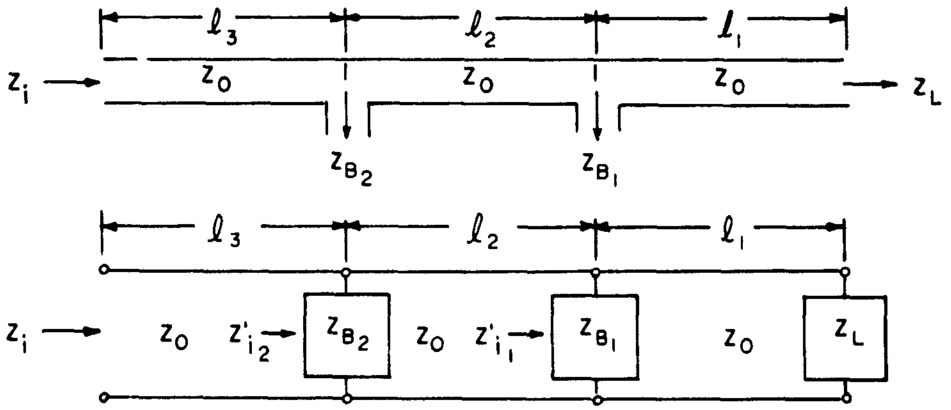

(b.) ACOUSTIC TRANSMISSION LINE WITH BRANCH IMPEDANCES AND ITS ACOUSTIC CIRCUIT REPRESENTATION

FIGURE 7

NON-UNIFORM AND BRANCHED ACOUSTIC TRANSMISSION LINES

DRL - UT
DWG AS 7110
JVK - BEE
8 - 13 - 62

$$K_1 = \frac{Z_L - Z_{o_1}}{Z_L + Z_{o_1}} \text{ , and } \beta_1 = \frac{\omega}{v_1} \text{ .}$$

The wave velocity calculated according to the equation $v = \frac{1}{\sqrt{\rho K}}$ is the free field velocity and is independent of the pipe characteristics. Certain refinements in the calculation of the wave velocity in liquids confined in pipes, Appendix A, show that in actual cases the velocity depends on normal area of the liquid column and the material and thickness of the pipe wall. For the sake of generality then, v and β are given subscripts to indicate that they may change from section to section on nonuniform lines.

Now that Z_{i_1} is known, it can be regarded as the load on section 2 of the line. Then Z_{i_2}, the input impedance of the second section, can be calculated.

$$Z_{i_2} = Z_{o_2}\left(\frac{1 + K_2 e^{-j2\beta_2 \ell_2}}{1 - K_2 e^{-j2\beta_2 \ell_2}}\right) \text{ , where}$$

$$K_2 = \frac{Z_{i_1} - Z_{o_2}}{Z_{i_1} + Z_{o_2}} \text{ , and } \beta_2 = \frac{\omega}{v_2} \text{ .}$$

Finally, still using the same reasoning,

$$Z_i = Z_{i_3} = Z_{o_3}\left(\frac{1 + K_3 e^{-j2\beta_3 \ell_3}}{1 - K_3 e^{-j2\beta_3 \ell_3}}\right) \text{ ,}$$

$$K_3 = \frac{Z_{i_2} - Z_{o_3}}{Z_{i_2} + Z_{o_3}} \text{ , and } \beta_3 = \frac{\omega}{v_3} \text{ .}$$

d. Finite Lines with Shunts

Figure 7(b) shows a line made up of three sections of lengths ℓ_1, ℓ_2, and ℓ_3, each having the same characteristic impedance Z_o. In addition there are branches with purely reactive impedances Z_{B_1} and Z_{B_2} at the ends of the center section. To calculate Z_i for this line, first calculate the input impedance Z_{i_1} of a length of line ℓ_1 of characteristic impedance Z_o loaded by an impedance Z_L. Then calculate Z'_{i_1} by parallel combination of Z_{i_1} and Z_{B_1}.

$$Z_{i_1} = Z_o\left(\frac{1 + K_1 e^{-j2\beta_1 \ell_1}}{1 - K_1 e^{-j2\beta_1 \ell_1}}\right) \text{, where}$$

$$K_1 = \frac{Z_L - Z_o}{Z_L + Z_o} \text{, and } \beta_1 = \frac{\omega}{v_1} \text{ .}$$

$$Z'_{i_1} = \frac{Z_{i_1} Z_{B_1}}{Z_{i_1} + Z_{B_1}} \text{ .}$$

Continuing according to this same scheme,

$$Z_{i_2} = Z_o\left(\frac{1 + K_2 e^{-j2\beta_2 \ell_2}}{1 - K_2 e^{-j2\beta_2 \ell_2}}\right) \text{, where}$$

$$K_2 = \frac{Z'_{i_1} - Z_o}{Z'_{i_1} + Z_o} \text{, and } \beta_2 = \frac{\omega}{v_2} \text{ .}$$

$$Z'_{i_2} = \frac{Z_{i_2} Z_{B_2}}{Z_{i_2} + Z_{B_2}} \quad .$$

And finally,

$$Z_i = Z_{i_3} = Z_o \left(\frac{1 + K_3 e^{-j2\beta_3 \ell_3}}{1 - K_3 e^{-j2\beta_3 \ell_3}} \right) \quad , \text{ where}$$

$$K_3 = \frac{Z'_{i_2} - Z_o}{Z'_{i_2} + Z_o} \quad , \text{ and } \beta_3 = \frac{\omega}{v_3} \quad .$$

These calculations would have been simplified by carrying them out in terms of admittance, because at the branch points the admittance Y_{i_n} and Y_{B_n} combine by direct addition.

e. Finite Lines with Shunts and Changes in Z_o

For lines having both nonuniformities and branch impedances as shown in Fig. 8, the input impedance can be found by combining the methods used for the lines of Fig. 7. The relationships to be used are the same as those for the line of Fig. 7(b) except that care must be taken to use values of Z_{o_n} peculiar to each section of the line.

With reference to Fig. 8 then, the impedance at the left end of section 1 is found as follows:

$$Z_{i_1} = Z_{o_1} \left(\frac{1 + K_1 e^{-j2\beta_1 \ell_1}}{1 - K_1 e^{-j2\beta_1 \ell_1}} \right) \quad .$$

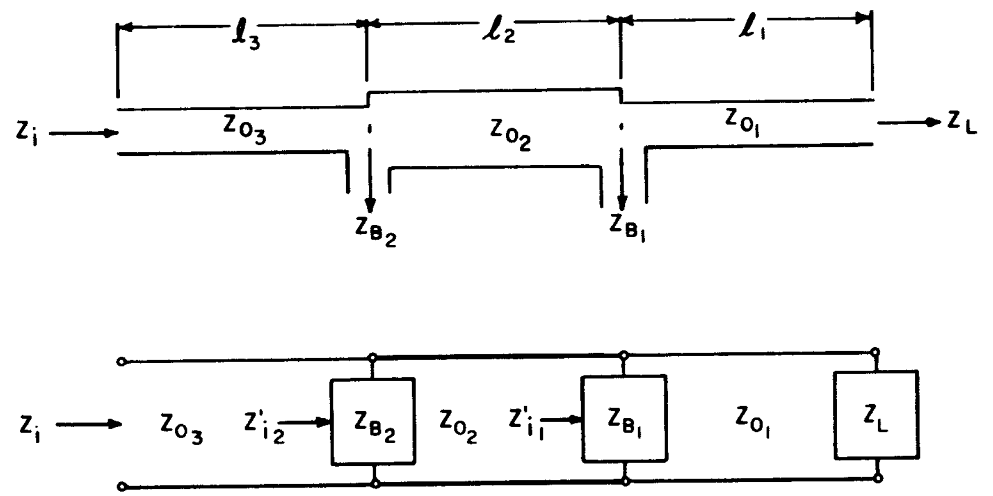

FIGURE 8

PHYSICAL LAYOUT AND SCHEMATIC REPRESENTATION OF ACOUSTIC TRANSMISSION LINE WITH BOTH BRANCHES AND CHANGES OF Z_O

DRL - UT
DWG AS7111
JVK - BEE
8 - 8 - 62

$$K_1 = \frac{Z_L - Z_{o_1}}{Z_L + Z_{o_1}} \text{ , and } \beta_1 = \frac{\omega}{v_1} \text{ .}$$

$$Z'_{i_1} = \frac{Z_{i_1} Z_{B_1}}{Z_{i_1} + Z_{B_1}} \text{ .}$$

At the left end of section 2

$$Z_{i_2} = Z_{o_2}\left(\frac{1 + K_2 e^{-j2\beta_2 \ell_2}}{1 - K_2 e^{-j2\beta_2 \ell_2}}\right) \text{ ,}$$

$$K_2 = \frac{Z'_{i_1} - Z_{o_2}}{Z'_{i_1} + Z_{o_2}} \text{ , and } \beta_2 = \frac{\omega}{v_2} \text{ .}$$

$$Z'_{i_2} = \frac{Z_{i_2} Z_{B_2}}{Z_{i_2} + Z_{B_2}} \text{ .}$$

And at the input

$$Z_i = Z_{i_3} = Z_{o_3}\left(\frac{1 + K_3 e^{-j2\beta_3 \ell_3}}{1 - K_3 e^{-j2\beta_3 \ell_3}}\right) \text{ .}$$

$$K_3 = \frac{Z'_{i_2} - Z_{o_3}}{Z'_{i_2} + Z_{o_3}} \text{ , and } \beta_3 = \frac{\omega}{v_3} \text{ .}$$

September 1962
JVK:vh

f. Branched Lines

Input admittances to branched lines, as shown in Fig. 9(a) are also of interest. An expression for the input admittance at the first branch point 1, Fig. 9(a), can be derived by making use of the so-called admittance parameters for the combination of branches between points 1 and 2. This admittance expression will be in terms of the load admittance Y_L and the lengths and characteristic admittances of the line A between the load and point 2 and both of the branches B and C.

For two points of an acoustic system there are defined four admittance parameters which characterize the system with respect to the chosen points:

$$Y_{11} = \frac{\bar{V}_1}{P_1}\bigg|_{P_2 = 0} \; ; \qquad Y_{12} = \frac{\bar{V}_1}{P_2}\bigg|_{P_1 = 0} \; ;$$

$$Y_{21} = \frac{\bar{V}_2}{P_1}\bigg|_{P_2 = 0} \; ; \qquad \text{and } Y_{22} = \frac{\bar{V}_2}{P_2}\bigg|_{P_1 = 0} \; .$$

Here $\bar{V}$ is volume velocity and P is sound pressure; subscripts on $\bar{V}$ and P refer to points 1 and 2. The particular systems considered here are uniform and bilateral; thus $Y_{11} = Y_{22}$, and $Y_{12} = Y_{21}$.

First consider a section of liquid column acoustic transmission line of length ℓ, characteristic admittance Y_0, and phase constant β, Fig. 9(b). Designate the left end of this line as point 1 and the right end as point 2. The parameter Y_{11} for this section of line is the ratio of volume velocity at point 1 to sound pressure at point 1 under the imposed condition that sound pressure at point 2 is zero. For the purpose of calculating Y_{11} it can be assumed that there is a free surface at point 2 of the liquid column. Recall that the input impedance of a uniform, open-end line is

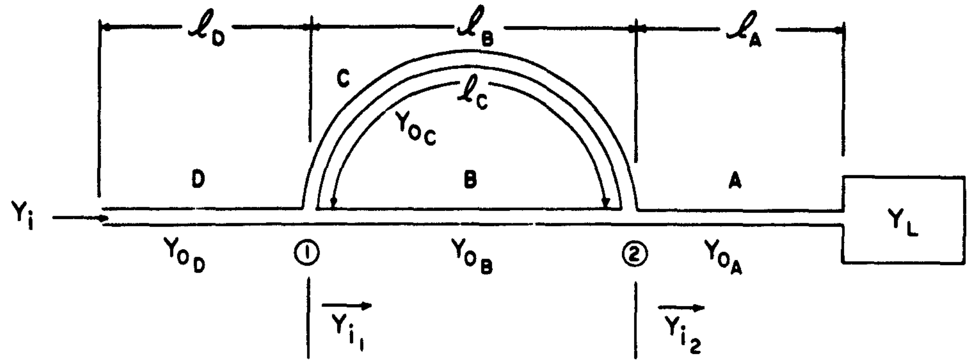

(a.) BRANCHED ACOUSTIC TRANSMISSION LINE

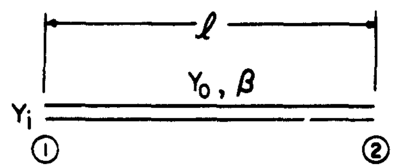

(b.) SINGLE LINE

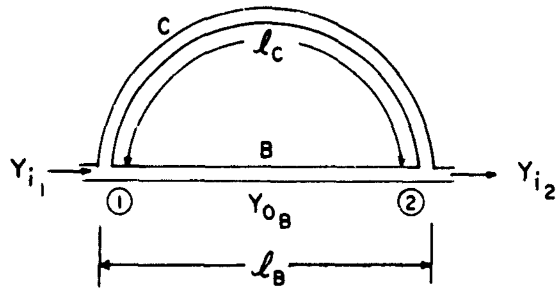

(c.) COMBINATION OF TWO LINES BETWEEN TWO POINTS

FIGURE 9
BRANCHED ACOUSTIC TRANSMISSION LINES

DRL - UT
DWG AS 7112
JVK - BEE
9 - 13 - 62

$$Z_i = Z_o \left(\frac{1 + Ke^{-j2\beta \ell}}{1 - Ke^{-j2\beta \ell}} \right) \quad \text{with } K = -1$$

or

$$Z_i = Z_o \tanh j\beta \ell = jZ_o \tan\beta \ell \quad .$$

Then

$$Y_{11} = \frac{1}{Z_i} = \frac{-jY_o}{\tan\beta \ell} = Y_{22} \quad .$$

To find parameters Y_{21}, consider incident and reflected waves on the line with pressures $P_{(+)}$ and $P_{(-)}$ and volume velocities $V_{(+)}$ and $V_{(-)}$, respectively. Equations for total pressure and volume velocity at a point on the line x units of length from point 2 can be written

$$P = P_{(+)} \left(e^{j\beta x} + Ke^{-j\beta x}\right) \quad ,$$

$$\overline{V} = V_{(+)} \left(e^{-j\beta x} - Ke^{-j\beta x}\right) \quad .$$

At x = 0

$$P = P_2 \quad \text{and} \quad \overline{V} = \overline{V}_2 \quad .$$

So,

$$P_2 = P_{(+)} (1 + K) \quad \text{and} \quad \overline{V}_2 = \overline{V}_{(+)} (1 - K) \quad .$$

$$\overline{V} = \frac{\overline{V}_2}{1 - K} \left(e^{j\beta x} - Ke^{-j\beta x}\right) \quad ,$$

$$P = P_{(+)}\left(e^{j\beta x} + Ke^{-j\beta x}\right)$$

$$= \frac{P_2}{1 + K}\left(e^{j\beta x} + Ke^{-j\beta x}\right) \quad .$$

Substituting $P_2 = \overline{V}_2 Z_2$ and $K = \dfrac{Z_2 - Z_o}{Z_2 + Z_o}$ in the expression for P gives

$$P = \frac{\overline{V}_2\, Z_2}{1 + \dfrac{Z_2 - Z_o}{Z_2 + Z_o}}\left(e^{j\beta x} + Ke^{-j\beta x}\right) \quad ,$$

or

$$P = \frac{\overline{V}_2}{2}\left(Z_o + Z_2\right)\left(e^{j\beta x} + Ke^{-j\beta x}\right) \quad .$$

Now recall the defining equation for Y_{21}:

$$Y_{21} = \frac{\overline{V}_2}{P_1}\bigg|_{P_2 = 0} \quad .$$

The condition $P_2 = 0$ implies $Z_2 = 0$. Letting $Z_2 = 0$ in the derived expression for P and letting $x = \ell$, the full length of the line between points 1 and 2, gives

$$\frac{P_1}{\overline{V}_2} = Z_o \sinh j\beta\ell = jZ_o \sin \beta\ell \quad .$$

Finally,

$$Y_{21} = \frac{\overline{V}_2}{P_1}\bigg|_{P_2 = 0} = \frac{1}{j\, Z_o \sin \beta\ell} = \frac{-j\, Y_o}{\sin \beta\ell} \quad ,$$

and

$$Y_{12} = Y_{21} \quad .$$

We can now write the admittance parameters for two lines of different lengths and characteristics connecting the same two points as lines B and C of Fig. 9(c). The admittance parameters for this combination are the sums of the corresponding parameters for the individual lines.

$$Y_{11} = Y_{22} = Y_{11}(B) + Y_{11}(C) = -j \left(\frac{Y_{o_B}}{\tan\beta_B \ell_B} + \frac{Y_{o_C}}{\tan\beta_C \ell_C} \right) \quad ,$$

and

$$Y_{12} = Y_{21} = Y_{12}(B) + Y_{12}(C) = -j \left(\frac{Y_{o_B}}{\sin\beta_B \ell_B} + \frac{Y_{o_C}}{\sin\beta_C \ell_C} \right) \quad .$$

Now equations expressing volume velocities at points 1 and 2 in terms of the sound pressure at these points and the admittance parameters can be written:

$$\overline{V}_1 = Y_{11} P_1 + Y_{12} P_2 \quad ,$$

$$\overline{V}_2 = Y_{21} P_1 + Y_{22} P_2 \quad .$$

If it is assumed that the branched lines are terminated in an admittance Y_{i_2} as shown in Fig. 9(c), the volume velocity at 2 is

$$\overline{V}_2 = -Y_{i_2} P_2 \quad .$$

The negative sign is required because $\overline{V}_2$ as it has been used in the definition of admittance parameters is volume velocity into point 2; whereas, for calculating the input admittance of the load at point 2, volume velocity into the load is used. Substituting this into the pair of volume velocity equations and transposing the left-hand side of the second equation gives

$$\overline{V}_1 = Y_{11} P_1 + Y_{12} P_2 \quad ,$$

$$0 = Y_{21} P_1 + (Y_{22} + Y_{i_2}) P_2 \quad .$$

Input admittance at point 1 is defined:

$$Y_{i_1} \equiv \frac{\overline{V}_1}{P_1} \quad .$$

Solving for this ratio from the last pair of equations and expressing the product $Y_{12}\, Y_{21}$ as $Y_{12}^{\;2}$ gives

$$Y_{i_1} = Y_{11} - \frac{Y_{12}^{\;2}}{(Y_{i_2} + Y_{22})} \quad .$$

In terms of the characteristics and lengths of individual branches B and C,

$$Y_{i_1} = -j\left(\frac{Y_{o_B}}{\tan\beta_B \ell_B} + \frac{Y_{o_C}}{\tan\beta_C \ell_C}\right) + \frac{\left(\dfrac{Y_{o_B}}{\sin\beta_B \ell_B} + \dfrac{Y_{o_C}}{\sin\beta_C \ell_C}\right)^2}{Y_{i_2} - j\left(\dfrac{Y_{o_B}}{\tan\beta_B \ell_B} + \dfrac{Y_{o_C}}{\tan\beta_C \ell_C}\right)} \quad .$$

Now the input admittance for the configuration of Fig. 9(a) can be written by use of this expression and the rules for admittance transformation along transmission lines as developed in previous paragraphs.

$$Y_{i_2} = Y_{o_A}\left(\frac{1 - Ke^{-j2\beta_A \ell_A}}{1 + Ke^{-j2\beta_A \ell_A}}\right) \quad ; \qquad \beta_A = \frac{\omega}{v_A} \quad ; \qquad K = \frac{Y_{o_A} - Y_L}{Y_{o_A} + Y_L} \quad .$$

$$Y_i = Y_{o_D}\left(\frac{1 - K_1 e^{-j2\beta_D \ell_D}}{1 + K_1 e^{-j2\beta_D \ell_D}}\right) \; ; \qquad \beta_D = \frac{\omega}{v_D} \; ; \qquad K_1 = \frac{Y_{o_D} - Y_{i_1}}{Y_{o_D} + Y_{i_1}} \; .$$

4. Wave Filtering Action of Irregular Lines

It can be seen in each of the transmission line cases considered except that of the smooth, infinite line, the input impedance and admittance of the line is frequency dependent. Thus, in general, for a given input sound pressure, a line accepts acoustic energy selectively with respect to frequency. That is, either improperly terminated or nonuniform lines exhibit acoustic filtering action.

The magnitude of sound pressure that a given acoustic source produces at the input to its load is governed by the strength of the source, its internal impedance or admittance, and the input impedance or admittance of the load. If the load on a source is provided by the input to a nonuniform, loaded transmission line like those considered in this section, it can be argued that since the line is without losses, all the acoustic energy accepted by the input admittance of the line is dissipated in the load. Considering this problem from the admittance standpoint, the source and load can be represented as shown in Fig. 10(a). Here the strength of the source is $\overline{V}_s$, a volume velocity, and the source internal admittance is Y_s. A load on this source comprising a loaded, nondissipative filter is applied at A. The input admittance Y_i at A can be found by whatever method is appropriate for the filter between A and B. Then the simplified circuit, Fig. 10(b), can be considered; here the filter and its load Y_L have been replaced by the input admittance Y_i. The sound pressure at point A can be written

$$P_A = \frac{\overline{V}_s}{Y_s + Y_i} \; .$$

But

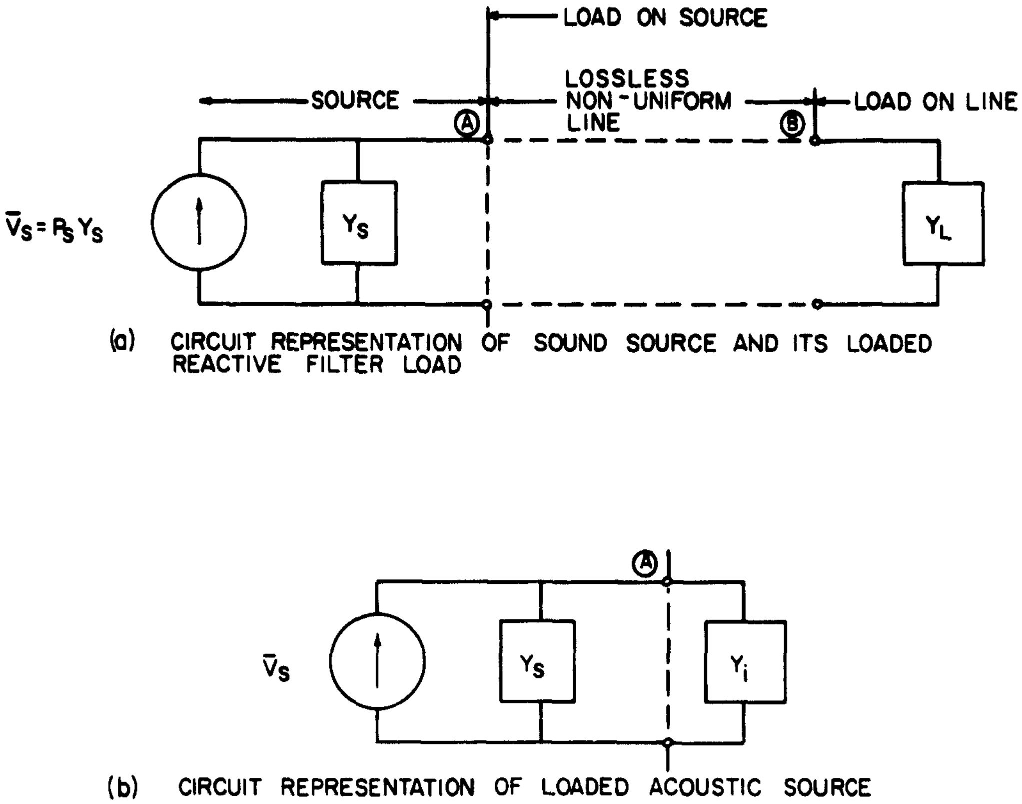

FIGURE 10
CIRCUIT REPRESENTATIONS OF ACOUSTIC SOURCE, FILTER, AND LOAD

DRL - UT
DWG AS 7115
JVK - PVW
8 - 15 - 62

September 1962
JVK:vh

$$\bar{V}_s = P_s Y_s \quad .$$

So

$$P_A = \frac{P_s Y_s}{Y_s + Y_i} = \frac{P_s}{1 + Y_i/Y_s} \quad .$$

Then the sound power W_L delivered to the load is

$$W_L = P_A^2 \, \mathrm{Re}(Y_i) = \left(\frac{P_s}{1 + Y_i/Y_s} \right)^2 \mathrm{Re}(Y_i) \quad .$$

Obviously this power cannot be calculated unless P_s and Y_s are known and unless Y_i is known for the particular load Y_L on the filter. In cases of practical interest these characteristics are not known. They are neither easy to calculate nor simple to measure. Therefore, the power transmitted by a filter cannot be found from a specification of the filter alone. That is, a given filter may perform differently in different systems.

B. FILTER PERFORMANCE CRITERIA

When designing filters it would be desirable to have a common basis for comparing them. Analytical predictions of their performance capability in particular systems would also be useful. Since such predictions cannot ordinarily be made, a basis for comparing filters independently of source and load characteristics must suffice. In comparing acoustic filters, it is natural to consider using performance criteria analogous to those customarily applied to electric wave filters.

Figure 11(a) shows a filter inserted between a source and load. The ratio of the magnitudes of sound pressure at point o, the filter output port, to sound pressure at point i, the filter input port, can be expressed in terms of the input and load admittances. Since there cannot be losses in the line, the power into point i must be the power delivered to the load admittance Y_L at point o. Expressed in equation form,

$$P_o^2 \, \mathrm{Re}(Y_L) = P_i^2 \, \mathrm{Re}(Y_i) \quad .$$

Or,

$$\frac{|P_o|}{|P_i|} = \left[\frac{\mathrm{Re}\ (Y_i)}{\mathrm{Re}\ (Y_L)}\right]^{1/2} \quad .$$

Although this ratio can be measured in an actual system, usually it cannot be analytically predicted for a given filter because Y_L, and hence Y_i, are not known.

Another pressure magnitude ratio is that of output pressure $|P_o|$ to blocked source pressure $|P_s|$. With reference to Fig. 11(a) it can be noted that the input pressure is applied across a parallel combination of admittances Y_s and Y_i. Thus, in terms of volume velocity of the source,

$$P_i = \frac{\overline{V}_s}{Y_s + Y_i} \quad ; \qquad P_i = \frac{P_s \, Y_s}{Y_s + Y_i} \quad ; \text{ or}$$

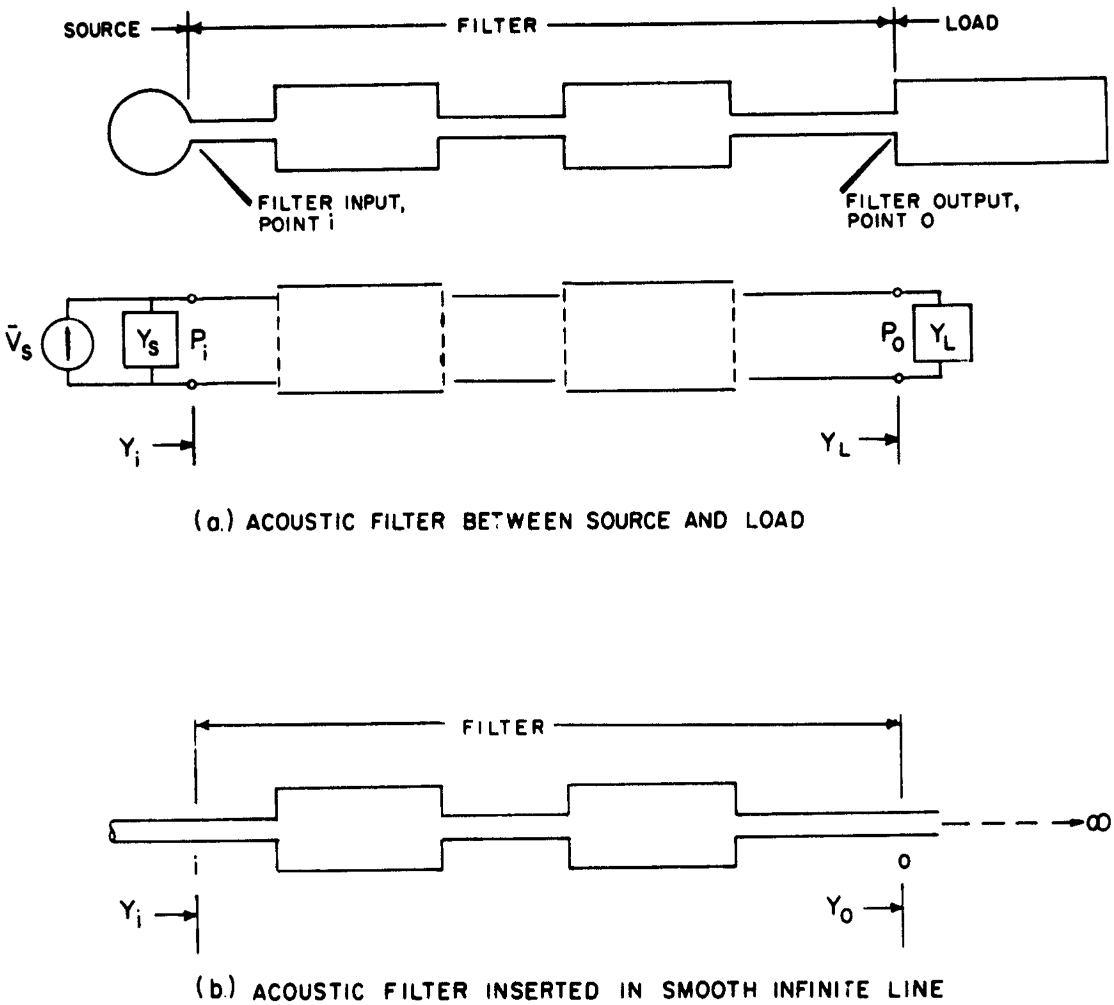

FIGURE 11
HYPOTHETICAL OPERATING CONDITIONS FOR AN ACOUSTIC FILTER

DRL - UT
DWG AS 7116
JVK - BEE
8 - 9 - 62

$$P_i = \frac{1}{1 + \frac{Y_i}{Y_s}} P_s \quad .$$

Substituting in the expression for the ratio of output to input pressure gives

$$\frac{|P_o|}{|P_s|} = \frac{1}{\left|1 + \frac{Y_i}{Y_s}\right|} \left(\frac{\text{Re } Y_i}{\text{Re } Y_L}\right)^{1/2} \quad .$$

This ratio cannot be calculated for the same reason that the output to input sound pressure ratio cannot; Y_L is not known.

Another ratio of interest is one that gives an indication of the influence on output pressure of replacing a smooth, uniform line between a source and its load by a filter. If the pressure at the point o with a filter in the line is P_{o_f} and pressure at the same point without a filter is $P_{o_{nf}}$, then their ratio can be expressed

$$\frac{|P_{o_f}|}{|P_{o_{nf}}|} = \frac{|Y_s + Y_{i_{nf}}|}{|Y_s + Y_{i_f}|} \left[\frac{\text{Re } (Y_{i_f})}{\text{Re } (Y_{i_{nf}})}\right]^{1/2} \quad .$$

The subscripts f and nf refer to conditions with and without filter, respectively, throughout. But, again Y_L must be known, or neither Y_{i_f} nor $Y_{i_{nf}}$ can be found. In electric wave filter theory the concept corresponding to this ratio $|P_{o_f}|/|P_{o_{nf}}|$ is called <u>insertion loss</u>.

Lack of knowledge of Y_L prevents practical use of any of the ratios discussed thus far. We seek a basis for filter comparison independent of Y_L. We assume that a filter is placed in an infinite line which has characteristic admittance Y_o, Fig. 11(b). Sinusoidal sound waves incident at point i are in general partially transmitted and partially reflected. Thus the total pressure at point i is the sum of pressures of incident and reflected waves.

$$P_i = P_{i+} + P_{i-} \quad .$$

The magnitude ratio of sound pressure at point o to incident wave sound pressure at point i expressed in terms of admittances is

$$\frac{|P_o|}{|P_{i+}|} = \frac{2}{\left|1 + \frac{Y_i}{Y_o}\right|} \left[\frac{\mathrm{Re}\,(Y_i)}{Y_o}\right]^{1/2} \quad .$$

This ratio can be calculated if details of the filter and characteristic admittance Y_o of the infinite line are known. If a filter for a specific application is being considered, the liquid it is to contain and the size of connecting pipes will likely be known. A reasonable choice for Y_o of the hypothetical infinite line is that of a column of the liquid contained in the connecting pipes. In this manual the ratio $\frac{|P_o|}{|P_{i+}|}$ for the described conditions is used extensively. From it we define a filter transmission loss, abbreviated T.L. It is expressed in decibels and defined,

$$\mathrm{T.L.(dB)} = -10 \log_{10} \left(\frac{|P_o|}{|P_{i+}|} \right)^2 = -20 \log_{10} \frac{|P_o|}{|P_{i+}|} \; .$$

The ratio $\frac{|P_o|}{|P_{i+}|}$ is less than or equal to one, so

$$\mathrm{T.L.(dB)} \geqq 0 \quad .$$

The four sound pressure magnitude ratios that have been discussed are listed below:

(1) Output-input pressure ratio

$$\frac{|P_o|}{|P_i|} = \left[\frac{\mathrm{Re}\ (Y_i)}{\mathrm{Re}\ (Y_L)}\right]^{1/2}$$

(2) Output-source sound pressure ratio

$$\frac{|P_o|}{|P_s|} = \frac{1}{\left|1 + \frac{Y_i}{Y_s}\right|} \left[\frac{\mathrm{Re}\ (Y_i)}{\mathrm{Re}\ (Y_L)}\right]^{1/2}$$

(3) Ratio of output sound pressures with and without filters

$$\frac{|P_{o_f}|}{|P_{o_{nf}}|} = \frac{|Y_s + Y_{i_{nf}}|}{|Y_s + Y_{i_f}|} \left[\frac{\mathrm{Re}\ (Y_{i_f})}{\mathrm{Re}\ (Y_{i_{nf}})}\right]^{1/2}$$

(4) Output-incident sound pressure ratio

$$\frac{|P_o|}{|P_{i+}|} = \frac{2}{\left|1 + \frac{Y_i}{Y_o}\right|} \left[\frac{\mathrm{Re}\ (Y_i)}{Y_o}\right]^{1/2}$$

$$\text{T.L. (dB)} = -20 \log_{10} \frac{|P_o|}{|P_{i+}|}$$

The forms of these expressions are unchanged if the sound pressure ratios are expressed in terms of impedances rather than admittances.

September 1962
JVK:vh

C. MECHANICAL FORMS OF FILTER ELEMENTS

It has been seen that a liquid column confined inside a uniform pipe constitutes a smooth, acoustic transmission line and that a nonuniform line in general constitutes an acoustic filter. In this section, consideration is given to the form and arrangement of mechanical elements that can be inserted in a pipe-run or tee-connected into a system to render the lines nonuniform. From the transmission line acoustical circuit viewpoint, lines can be made nonuniform in many different ways. Those considered here are (1) shunting admittances across the line at one or more points, (2) introducing abrupt changes in characteristic admittance along the line, (3) shunting admittances across the line and introducing abrupt changes in Y_0, and (4) dividing the line into two branches.

In actual liquid lines, shunt admittances which differ considerably from the admittance of an equivalent area of pipe wall can be introduced by tee-connecting so-called side-branch elements into the system. Only branch elements through which no net fluid flow is possible are of practical interest. Resistive elements should not intentionally be used as part of a side-branch element if the methods presented here are to be applied in the analysis of the resultant filter; these methods are restricted to purely reactive filters. There are two broad classes of side-branch elements: (1) those which behave very nearly like an acoustic system made up of lumped parameter reactive elements, and (2) those to which lossless transmission line acoustical circuit representations apply.

Filters with lumped parameter side-branch elements have received considerably more attention in the experimental program at Defense Research Laboratory than those with distributed parameter branch elements.

Lumped parameter branch elements of interest are those that can be adequately represented by an acoustic inertance and compliance in series. Many different mechanical assemblies can be used to approximate this series combination. Those discussed here are (1) spring-piston assemblies, (2) disk spring assemblies, (3) metal bellows, and (4) confined gases. Sketches of these are shown in

Figs. 12 and 13. The acoustical circuit and sample calculations for approximating shunt admittances of these branch elements are also given.

In all cases, m is the effective mass of mechanical elements that move in response to applied sound pressure, S is the effective area of the compliant acoustical element, and k is the effective stiffness of the compliant element.

The spring-piston, side-branch element of Fig. 12(a) comprises a piston exposed to the acoustic medium on one side and backed by a spring on the other. It is sealed against leakage by flexible diaphragm seals. The spring-piston assembly is housed in an enclosure suitable for adapting it to the system piping. The piston, the medium in front of the piston, and part of the spring all contribute to the effective mass m. If the space immediately in front of the piston communicates to the main liquid column inside the flow line by narrow passages or tubes, then there is an inertance contribution from such constrictions. The effective stiffness k is that of the spring.

The disk spring assembly, Fig. 12(b) is an assembly of bellville spring washers stacked in series, held together by formed metal ferrules, capped at one end, and coated with rubber to form a liquid seal. The effective mass is that of the cap and a part of that of the spring assembly. The mass of the liquid which moves with the assembly is also a part of the total effective mass and any tubes or constrictions present contribute to the total inertance. The stiffness is that of the spring assembly. Bellville washers are nonlinear; their stiffness decreases with deflection until they become flat. At one deflection they may have zero stiffness. Thus, the compliance of a disk spring branch element increases with system static pressure.

Metal bellows type branch elements are much like the disk spring elements except that a corrugated metal bellows is used for a compliant element. Because of their complicated shape, metal bellows not carefully engineered to have constant stiffness may be nonlinear and may show marked changes in stiffness with changes in deflection.

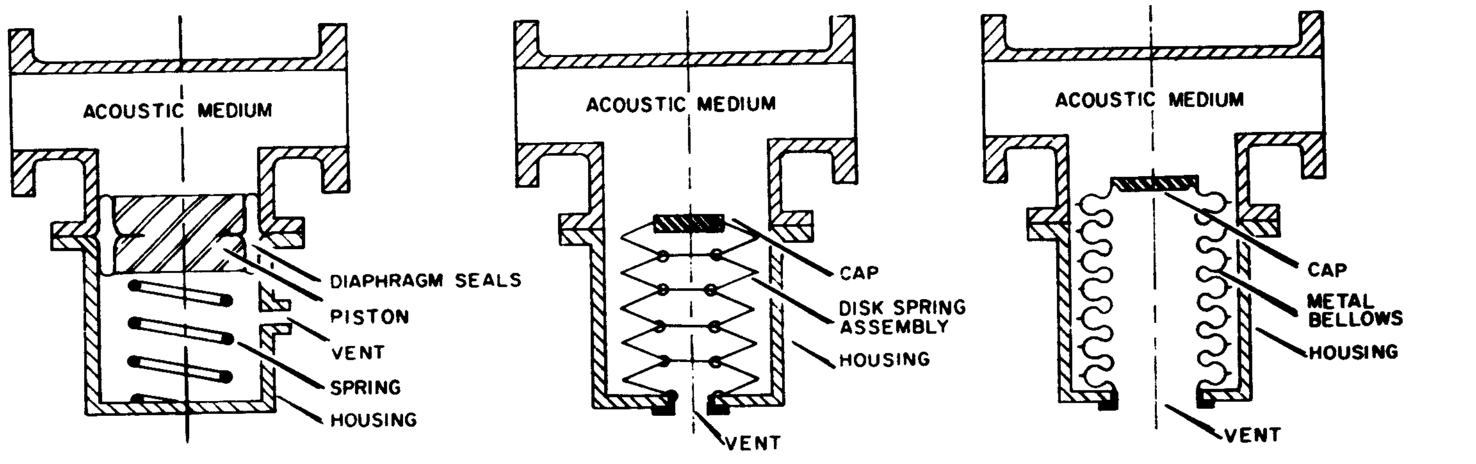

(a.) SPRING – PISTON BRANCH ELEMENT

(b.) DISK SPRING BRANCH ELEMENT

(c.) METAL BELLOWS BRANCH ELEMENT

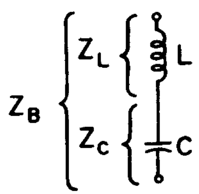

$$L = \frac{m}{S^2} \qquad C = \frac{S^2}{k}$$

$$Z_L = j\omega \frac{m}{S^2}$$

$$Z_C = \frac{-jk}{\omega S^2}$$

$$Y_B = \frac{1}{Z_B}$$

$$Z_B = j\left[\omega \frac{m}{S^2} - \frac{k}{\omega S^2}\right]$$

FIGURE 12
LUMPED-PARAMETER SIDE-BRANCH FILTER ELEMENTS

DRL - UT
DWG AS 7117
JVK - BEE
8 - 27 - 62

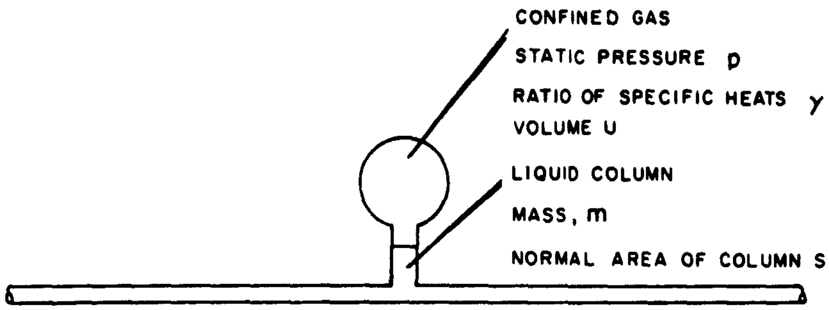

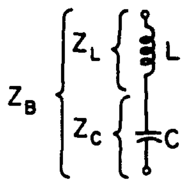

$$L = \frac{m}{S^2} \qquad Z_L = j\omega \frac{m}{S^2}$$

$$C = \frac{U}{\gamma p} \qquad Z_C = \frac{-j\gamma p}{\omega U}$$

$$Z_B = j\left[\omega \frac{m}{S^2} - \frac{\gamma p}{\omega U}\right], \quad Y_B = \frac{1}{Z_B}$$

FIGURE 13
CONFINED GAS, LUMPED-PARAMETER SIDE-BRANCH FILTER ELEMENT

DRL - UT
DWG AS 7118
JVK - BEE
8 - 27 - 62

Other series resonant side-branch elements can be devised. Confined volumes of gas (Fig. 13) can be used to provide compliance; the mass of some of the acoustic medium in a branch tube will supply inertance.

Calculations appropriate for finding the shunt admittances of combinations of various types of lumped parameter branch elements are given in detail in Chapter III.

The only type of distributed-parameter, side-branch element that has been investigated experimentally in the filter work at DRL is the closed-end, liquid-filled stub, Fig. 14. The shunt impedance for such an element can be calculated by use of the transmission line equations used for finding the input admittance of a smooth, finite line terminated by an infinite impedance. Figure 14(a) shows a straight stub tee-connected to the flow line and running perpendicular to it. The stub can also be run along the pipe or can even be formed around it, as in Fig. 14(b). Flow fairings of rubber or some similar material may be used in stubs.

It is possible to intermix the types of branch elements used in a single filter, but such filters will not be explicitly discussed here. However, the analytical methods developed are sufficiently general to handle filters with different types and any finite number of branch elements. It must be remembered that actual filter elements depart considerably from the idealized cases considered in deriving the equations for input admittance and transmission loss; it is not recommended that the methods given be applied to filters with a large number of elements. The calculations required for finding the transmission loss as a function of frequency for filters become quite burdensome for complicated configurations. Side-branch filters treated here have been limited to three or fewer branch elements of the same type. The shunt admittances of the elements of a single filter are not equal in all instances.

Nonuniformity on a transmission line can also be that due to abrupt changes in characteristic admittance. Since Y_o for a liquid column inside a pipe depends on the normal area of the column, $Y_o = \frac{S}{\rho v}$, an abrupt enlargement or reduction in the line introduces a change in characteristic admittance.

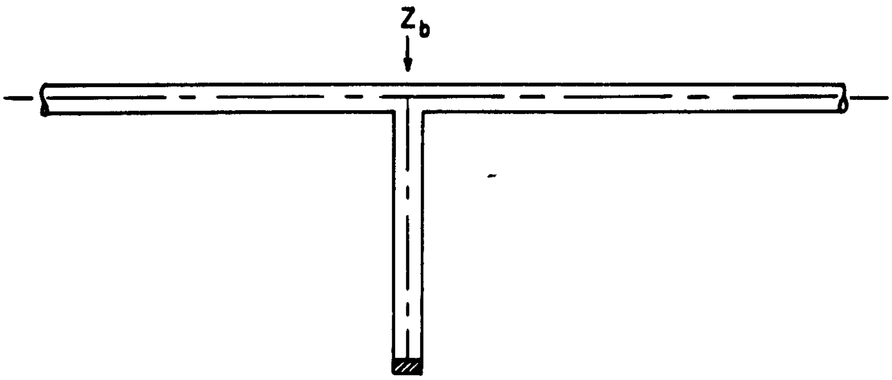

(a.) CLOSED-END BRANCH TUBE

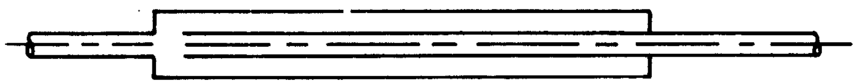

(b.) CLOSED-END BRANCH TUBE FORMED AROUND PIPE

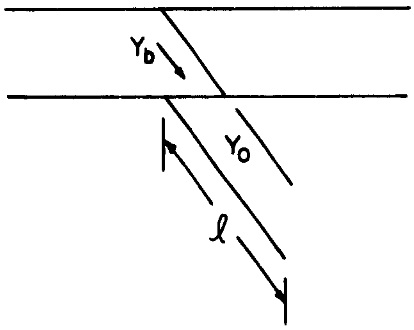

$$Y_b = j\,Y_0 \tan \beta \ell$$

$$\beta = \frac{\omega}{V} = 2\pi f \sqrt{\rho \kappa}$$

f = FREQUENCY

ρ = MASS DENSITY

κ = LIQUID COMPRESSIBILITY

FIGURE 14

DISTRIBUTED-PARAMETER SIDE-BRANCH FILTER ELEMENTS

DRL - UT
DWG AS 7119
JVK - BEE
8 - 27 - 62

Enlargements of the pipe are considered more attractive than reductions, since reductions increase flow resistance. Such enlargements have come to be called expansion chambers, although the term is somewhat misleading. Sudden enlargements in flow lines also increase flow resistance, but it is likely that expansion chambers could be faired with bushings of solid rubber or some other material without seriously impairing their effectiveness as filter parts. Figures 15(a) and (b) show, respectively, single and double expansion chambers in a flow line. Figure 15(c) shows an expansion chamber with a bushing of rubber or other suitable solid material to reduce turbulence. The material of such a fairing should have the same specific acoustic impedance (ρv) as the liquid in the system.

Combination filters which make use of both shunt admittances and changes in characteristic admittance are made by using both expansion chambers and side-branch elements in the same line. The mechanical forms of several different combination filters are shown in Fig. 16. Figure 16(a) shows combination filters with single, lumped parameter, side-branch elements; whereas Fig. 16(b) shows a combination filter with two chambers and two closed-end stub, distributed parameter, branch elements. The dotted lines indicate how the stubs can be placed around the pipe between the chambers for compactness.

A physical counterpart of the branched acoustic transmission line is shown in Fig. 17. Two tee-connections are made at separated points on a flow line, and a second line of different acoustic length connects them. This configuration is known as a Quincke tube, Fig. 17(a).

Fairing sleeves can be used with the Quincke tube since only one of the two parallel lines is required for the steady flow of liquid. Figure 17(b) shows a Quincke tube with fairing plugs at both tee-connections.

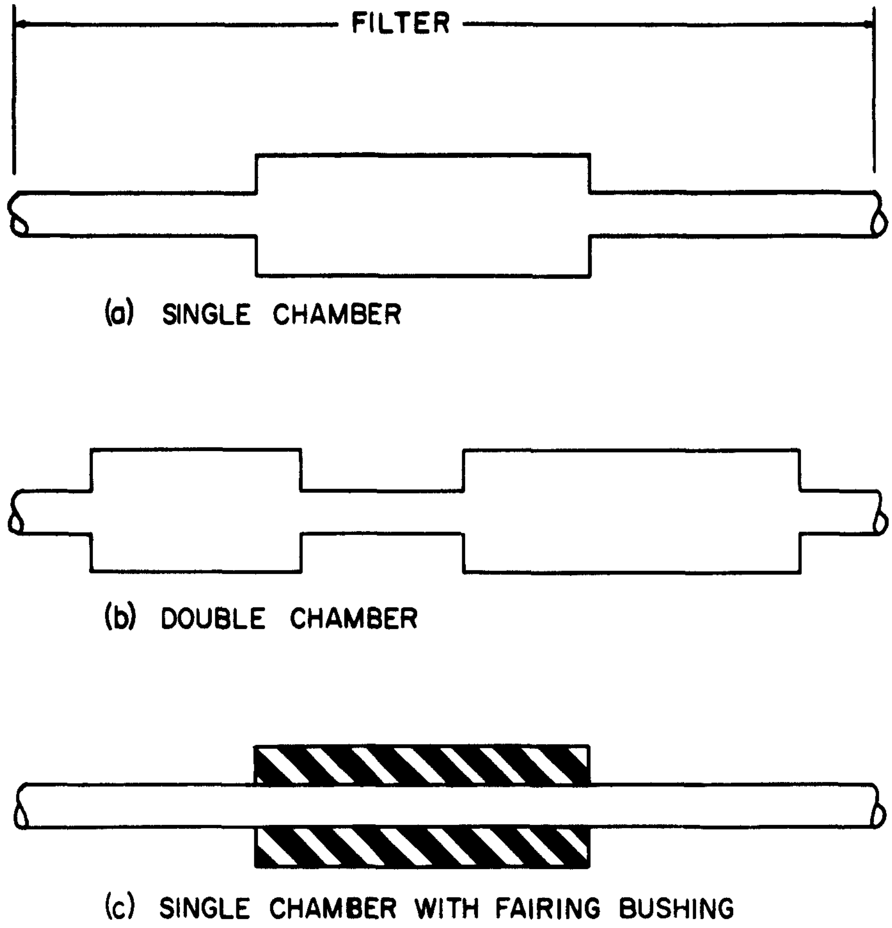

FIGURE 15
EXPANSION CHAMBER FILTERS

ORL - UT
DWG AS 7120
JVK - PVW
9 - 27 - 62

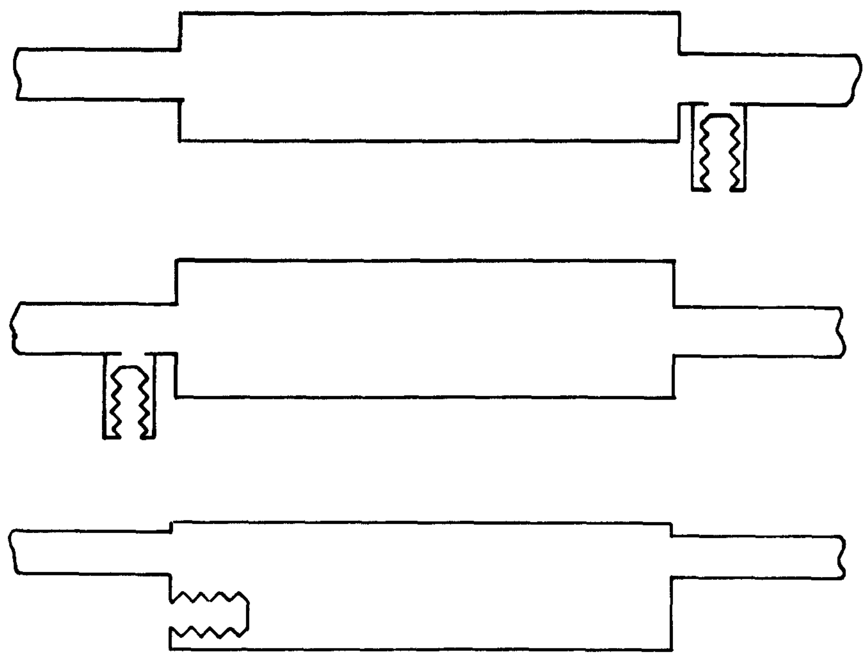

(a.) COMBINATION FILTERS WITH LUMPED-PARAMETER BRANCH ELEMENTS

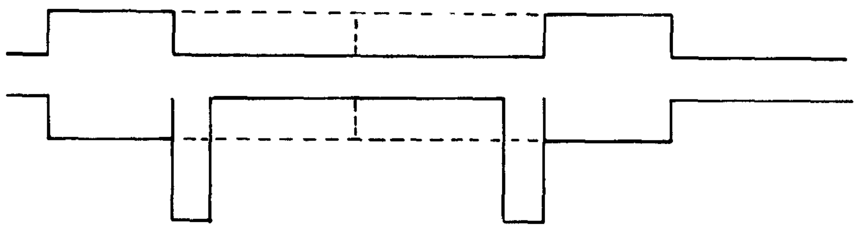

(b.) COMBINATION FILTER WITH DISTRIBUTED PARAMETER BRANCH ELEMENT

FIGURE 16
COMBINATION FILTERS

DRL - UT
DWG AS 7121
JVK - BEE
9 - 5 - 62

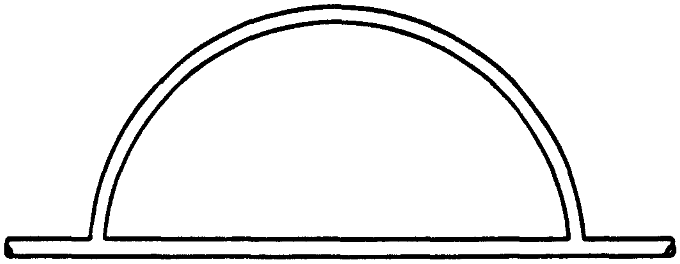

(a) BRANCHED LINE OR QUINCKE TUBE

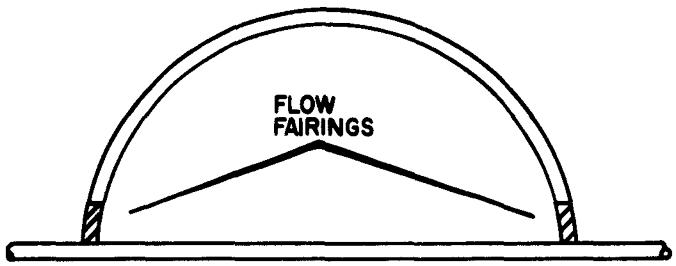

(b) QUINCKE TUBE WITH FLOW FAIRINGS

FIGURE 17
QUINCKE TUBE FILTERS

DRL - UT
DWG A57122
JVK - PVW
9-27-62

D. SPECIFICATION OF FILTERS IN ACOUSTICAL TERMS

To calculate the transmission loss of a filter, one must have sufficient information to be able to draw the transmission line acoustical circuit and specify it fully in terms of numerical values. There may be a tendency for those experienced in the mechanical design of piping systems to regard elements inserted in a system as having input and output ports at their points of connection to the system piping. It must be emphasized that acoustic filters may include some of the piping. It is important, therefore, to specify carefully the points taken as the input and output ports of a filter. Parts of the system between the noise source and the filter input port must be regarded as part of the source; similarly, parts of the system beyond the filter output port are taken as part of the load.

Consider the side-branch filter of Fig. 18. Figure 18(a) shows a representation of the mechanical layout of the filter. The end points are specified, and the distances between adjacent branch elements and filter ports are given. Figure 18(b) is a sketch of the filter transmission line acoustical circuit with the ideal acoustic element representation of each branch shown. Figure 18(c) shows the transmission line acoustical circuit for the filter with branch elements represented by their shunt admittances. If numerical values of all the quantities symbolized in Fig. 18(c) are known, the filter is completely specified; otherwise it is not. Remember that the branch admittances are in general frequency dependent.

Similar data are given to specify an expansion chamber filter except that in this case the characteristic admittance along the line changes, and localized shunt admittances are not present. Figure 19(a) shows a generalized expansion chamber filter, and Fig. 19(b) gives the appropriate acoustical circuit with the information required to specify it completely.

Similar sketches are given for a combination filter in Fig. 20 and for a Quincke tube filter in Fig. 21.

In all cases, the lengths, characteristic acoustic admittances, and wave velocities of all pipes and chambers that are part of the filter must be specified. If in addition the filter has side-branch elements, their admittances must also be given.

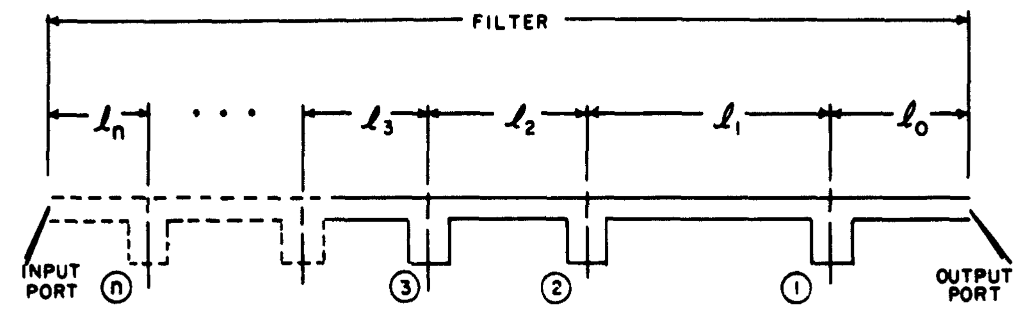

(a.) MECHANICAL ARRANGEMENT N-ELEMENT SIDE-BRANCH FILTER

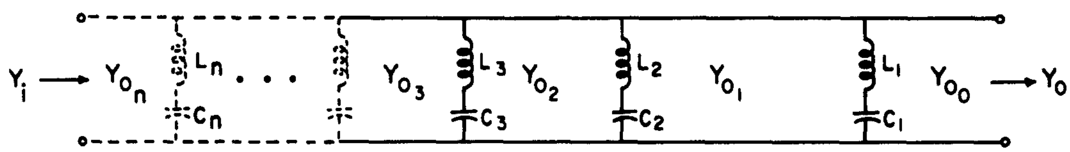

(b.) TRANSMISSION LINE ACOUSTICAL CIRCUIT SHOWING BRANCH CIRCUIT ELEMENTS

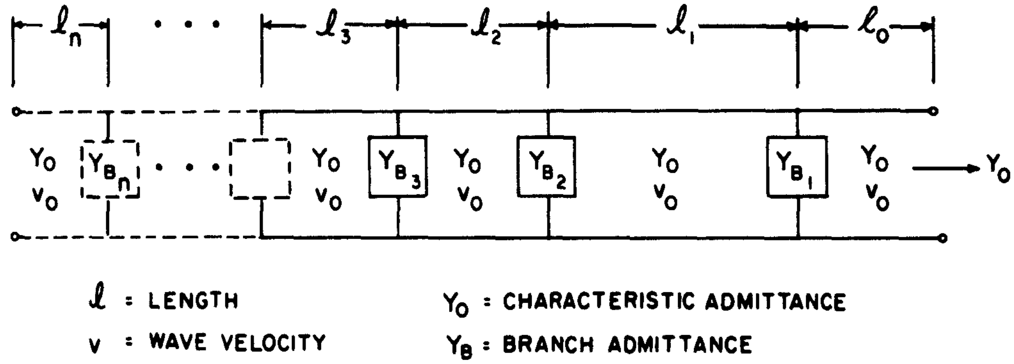

(c.) TRANSMISSION LINE ACOUSTICAL CIRCUIT SHOWING SHUNT ADMITTANCE OF BRANCH ELEMENTS

FIGURE 18
SPECIFICATION OF SIDE-BRANCH FILTERS IN ACOUSTICAL TERMS

DRL - UT
DWG AS 7388
JVK - BEE
9 - 7 - 62

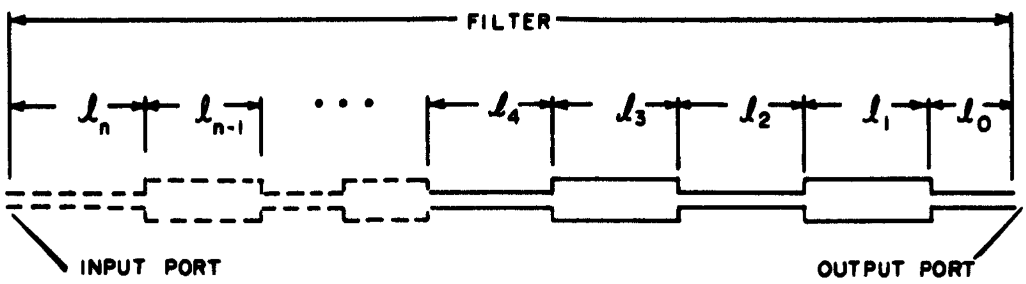

(a.) MECHANICAL ARRANGEMENT OF GENERALIZED EXPANSION CHAMBER FILTER

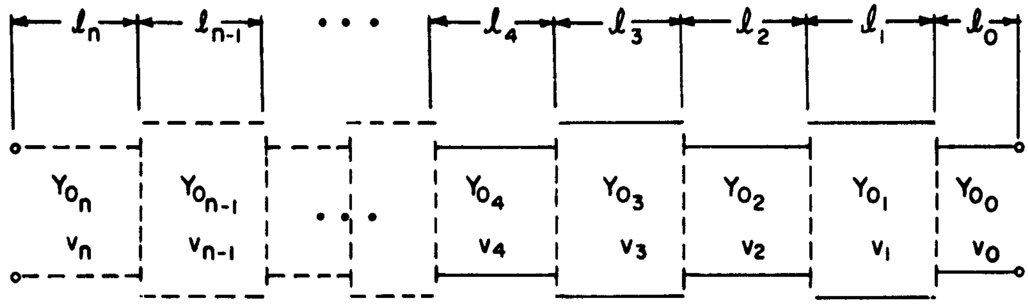

ℓ = LENGTH

v = WAVE VELOCITY

Y_O = CHARACTERISTIC ADMITTANCE

(b.) TRANSMISSION LINE ACOUSTICAL CIRCUIT OF EXPANSION CHAMBER FILTER

FIGURE 19
SPECIFICATION OF EXPANSION CHAMBER FILTERS IN ACOUSTICAL TERMS

DRL - UT
DWG AS 7389
JVK - BEE
8 - 10 - 62

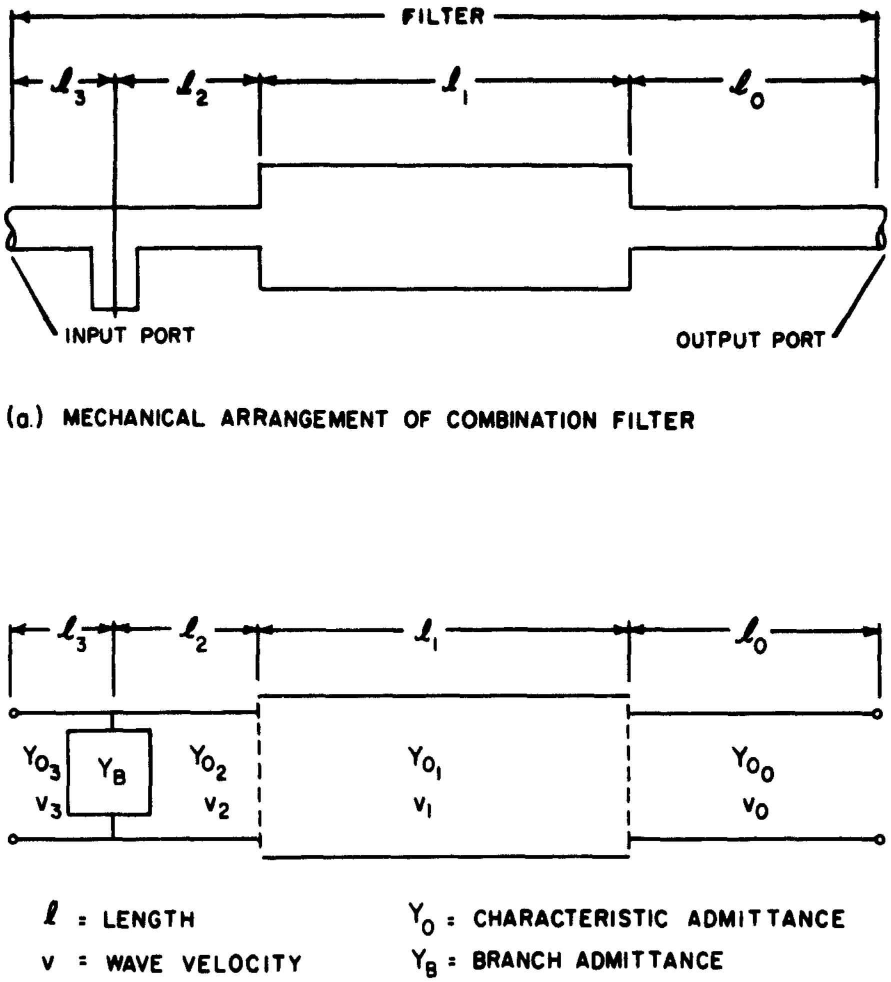

(a.) MECHANICAL ARRANGEMENT OF COMBINATION FILTER

(b.) TRANSMISSION LINE ACOUSTICAL CIRCUIT OF COMBINATION FILTER

FIGURE 20
SPECIFICATION OF COMBINATION FILTERS IN ACOUSTICAL TERMS

DRL - UT
DWG AS 7390
JVK - BEE
8 - 10 - 62

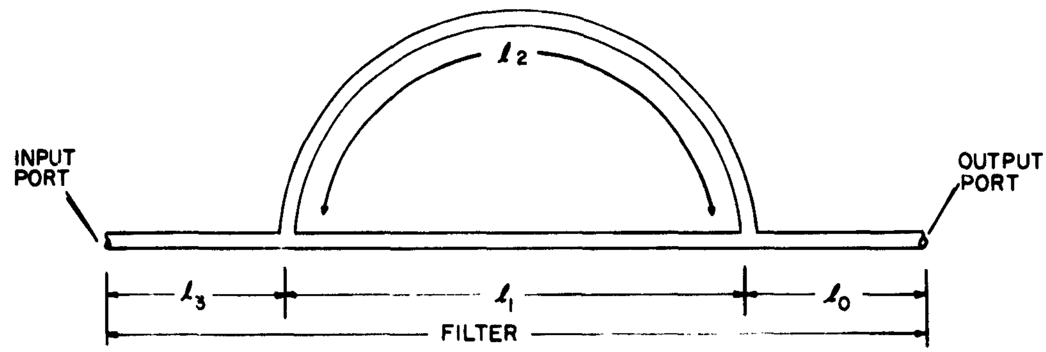

(a) MECHANICAL ARRANGEMENT OF QUINCKE TUBE FILTER

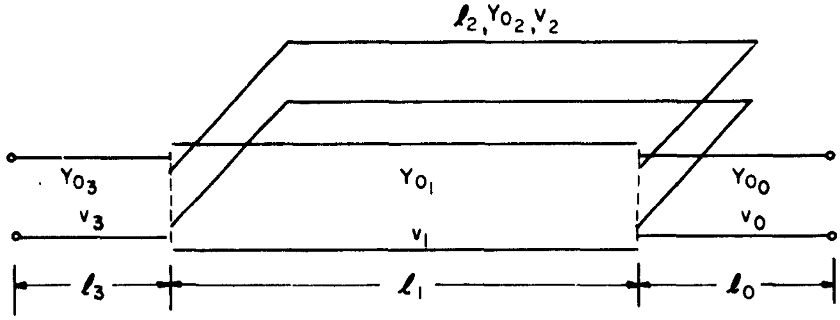

(b) TRANSMISSION LINE ACOUSTICAL CIRCUIT REPRESENTATION OF QUINCKE TUBE FILTER

FIGURE 21
SPECIFICATION OF QUINCKE TUBE FILTER IN ACOUSTICAL TERMS

DRL - UT
DWG AS 7391
JVK - PVW
8 - 10 - 62

September 1962
ELH:vh

CHAPTER III: FILTER DESIGN

A. INTRODUCTION

The predicted transmission loss curves for several acoustic filters are presented in this chapter. There are an infinite number of variations and combinations of these filters, but curves for only a selected few were calculated. They are the simpler configurations and probably the most practical. Wherever possible, the relationships between frequencies, transmission loss, and physical quantities are normalized so that the results can apply to many different physical situations. The transmission loss of other configurations can be calculated by using the expressions in Chapter II or the computer program presented in Appendix B.

The first class of filter considered is the side-branch filter with resonant elements that present an infinite shunt admittance at only one frequency. The transmission loss for a single element filter does not depend on the position of the element with respect to the noise source. But it does depend on a parameter, q, that relates the element compliance and resonant frequency to the piping system characteristic admittance.

When two or three identical sections are cascaded, a greatly increased transmission loss is predicted. Effectiveness now depends upon element spacing as well as upon q. Transmission loss curves are presented for two- and three-section side-branch filters. These filters provide wider attenuation bands and characteristics that are well suited to noise sources with large single frequency components at a fundamental and its harmonics. One side-branch element is resonated at the fundamental and the others at one or two of the harmonics.

The second class of filter presented uses a side-branch element that resonates at several frequencies. This element is a closed-end tube that resonates at frequencies for which its length is an odd multiple of a quarter wavelength in the tube. If the length is made a quarter wavelength at the fundamental frequency of a noise source, an infinite transmission loss occurs there and at odd harmonics. The effectiveness of such a filter does not depend on element placement, but the width of the attenuation band near each null depends on the ratio of the characteristic admittance of the side-branch pipe to that of the system piping. Many combinations of multiple sections are again possible, but the response function for filters with many sections may become confusingly complex. An example of the use of two closed tubes at the same point is also given.

Expansion chambers comprise the third class of filters covered. These filters provide broad attenuation bands with no infinities of transmission loss. The maximum transmission loss depends on the ratio of the characteristic admittance of the enlarged section to that of the system piping. For practical piping this admittance ratio is very nearly equal to the ratio of cross sectional areas.

The single section expansion chamber is simple to construct, but large size is required for large transmission loss at low frequencies. Much larger transmission losses are attainable with multiple sections; again, however, many combinations are possible. Only two sections are considered here, but several curves are required to indicate the effects of changing the various parameters.

Some of the advantages of the expansion chamber and the resonant side-branch filter may be obtained by combining the two types. The lumped element side-branch resonator combined with an expansion chamber produces a transmission loss with an infinite value at the resonator frequency, but it may degrade the broad band characteristic of the expansion chamber. A few of the possible arrangements are presented.

A combination of the closed-end side-branch tube and the expansion chamber can provide repeated infinities of transmission loss and retain the broad band character of the expansion chamber. A special case of this combination is called the re-entrant chamber; several variations of this type are presented. The single and double re-entrant chamber filters are rather easily constructed and provide attractive transmission loss characteristics.

September 1962
ELH:vh

The final type of filter presented is the Quincke tube. This arrangement of branched tubes has several transmission loss infinities that may be useful for some narrow band noise sources.

Following the filter response curves several nomographs are included to aid in the calculations necessary to acoustic filter design. The methods for determining values of the compliance, inertance, and parameter q for the lumped-element side-branch are presented. The characteristics of air-filled, side-branch elements depend on pressure; this dependence is presented in graphical form. Instructions for the calculation of wave velocity and characteristic admittance for system piping are also given; in addition, methods are shown for the calculation of expansion chamber m and length, closed-end, side-branch q and length, re-entrant chamber q and length, and Quincke tube pipe lengths.

Finally, example problems are presented to indicate the procedures used in designing filters for particular applications. Since no unique solution exists for a given noise source, several types of filters are considered for some of the noise reduction problems.

B. TRANSMISSION LOSS CURVES

It has been pointed out in Chapter II that of the many ways to characterize acoustic filter performance the transmission loss is the best for comparing one type of filter with others. Transmission loss is calculated for the filter terminated in the characteristic admittance of the system piping; and it gives, as a function of frequency, the reduction in noise level in dB produced by the filter when used under these conditions. The transmission loss curves to follow, then, give a good basis for comparing filters but not an accurate measure of the noise reduction to expect in an actual installation.

Several factors may prevent the actual noise reduction for a particular installation from being equal to the transmission loss. Terminating admittance may differ widely from Y_o and noise reduction may be enhanced at some frequencies and degraded at others. The metal pipe structure may provide another path to propagate noise past a filter. Flow noise in high volume systems can produce noise in the filter itself. For these several reasons, attempts to achieve very large transmission losses are not recommended. The filters included are thus rather simple and do not promise large noise reductions except at some very selected frequencies.

1. Lumped Element Side-Branch Filters

The first set of transmission loss curves (Fig. 22) are for a single section, resonant, side-branch filter. The branch element can be any type that provides a single admittance infinity at its resonant frequency. A very large loss is predicted for that frequency. The response does not depend on location of the side-branch element with respect to the noise source. A quantity that controls the bandwidth of the rejection band is a parameter, q, which is the ratio of the admittance of the compliance at the resonant frequency to the characteristic admittance of the pipe on which the element is placed.

This type of filter is quite simple and is useful in providing a large transmission loss at a single frequency. For large q it can also provide good noise reduction over a wide bandwidth. For a given size pipe, which

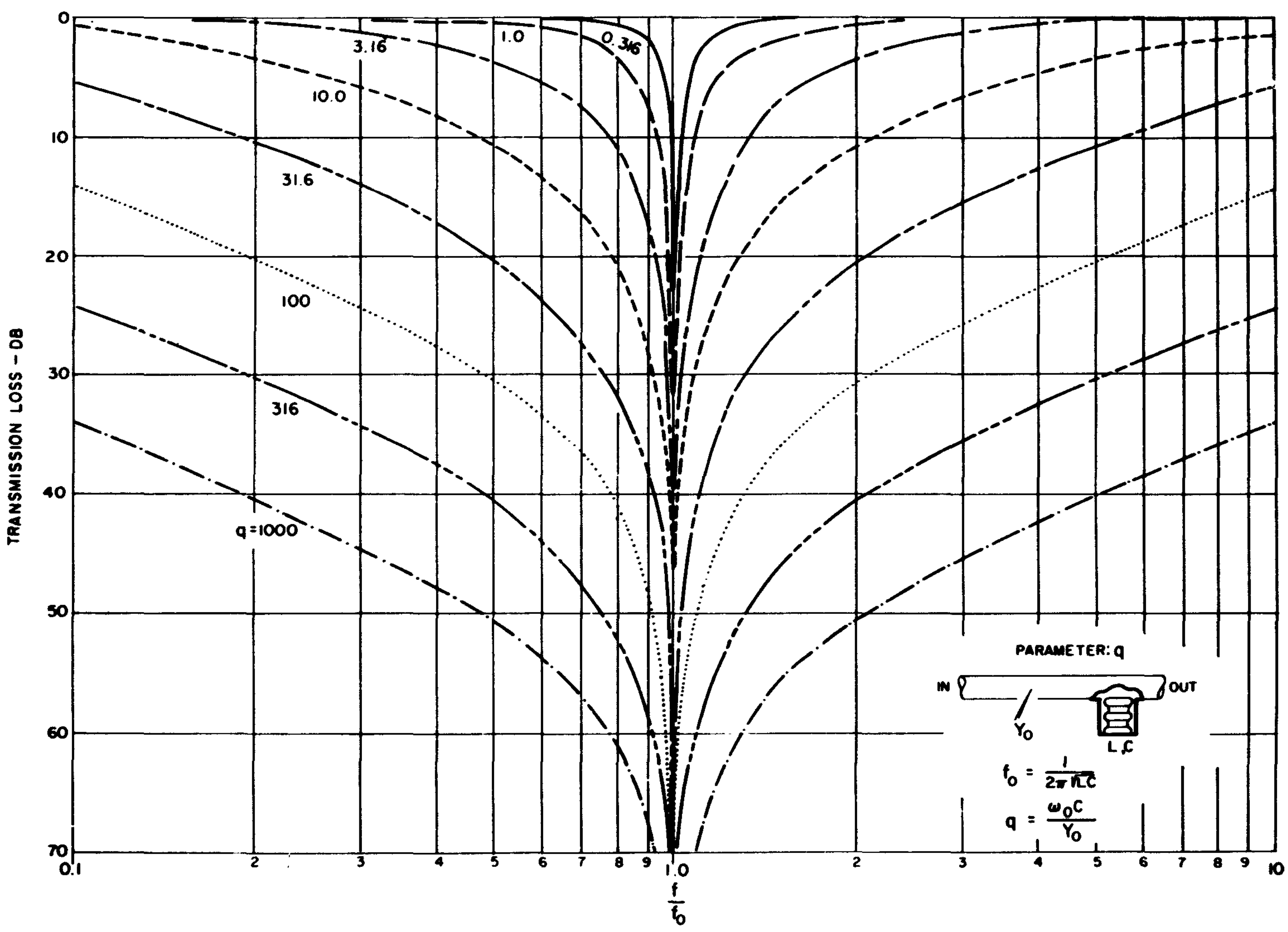

FIGURE 22
SIDE-BRANCH FILTER - SINGLE SECTION

DRL - UT
DWG BS6930
JVK - BEE
10 - 25 - 62

fixes Y_0, and a desired resonant frequency, f_0, the value of q depends directly on compliance. In practice there are limits on compliance that will be discussed later.

Greater transmission loss can be obtained by using two, identical, lumped parameter, resonant, side-branch elements as shown in Fig. 23. It is important that the two elements be separated by some length of pipe. If they are placed at the same position, the filter is still a single section filter with q increased by a factor of two. This predicts about 6 dB increase in transmission loss, while the two section filter of Fig. 23 gives approximately twice the transmission loss of the single section.

The curve shape has changed somewhat from that of the single section filter and depends on the length of the intervening pipe. This dependence will be discussed shortly. The overall noise reduction and bandwidth still depend on the q of the side-branch elements. Because of the limitations mentioned earlier it is unlikely that transmission losses of greater than 60-70 dB can be attained in practical systems. The higher values of q seem unnecessary then; however, they do result in filters with larger bandwidths than those obtained for low q's.

A variation on the two-section filter that is useful in suppressing the fundamental and second harmonic of a periodic noise source is shown in Fig. 24. Here the side-branch elements have identical values of q, but element No. 1 is resonant at the noise source fundamental, while element No. 2 is resonant at twice that frequency. The pipe length between elements is shorter than in Fig. 23 to move the first loss-of-attenuation peak to a higher frequency. This procedure gives less transmission loss at low frequencies, but a wider attenuation band is obtained.

The effect of the ratio of the resonant frequency of element No. 2 to that of No. 1 is shown in Fig. 25. Both side-branch elements have q = 100, but the separation between elements is greater than that for the filter of Fig. 24. The greater length gives greater transmission loss below the resonant frequencies.

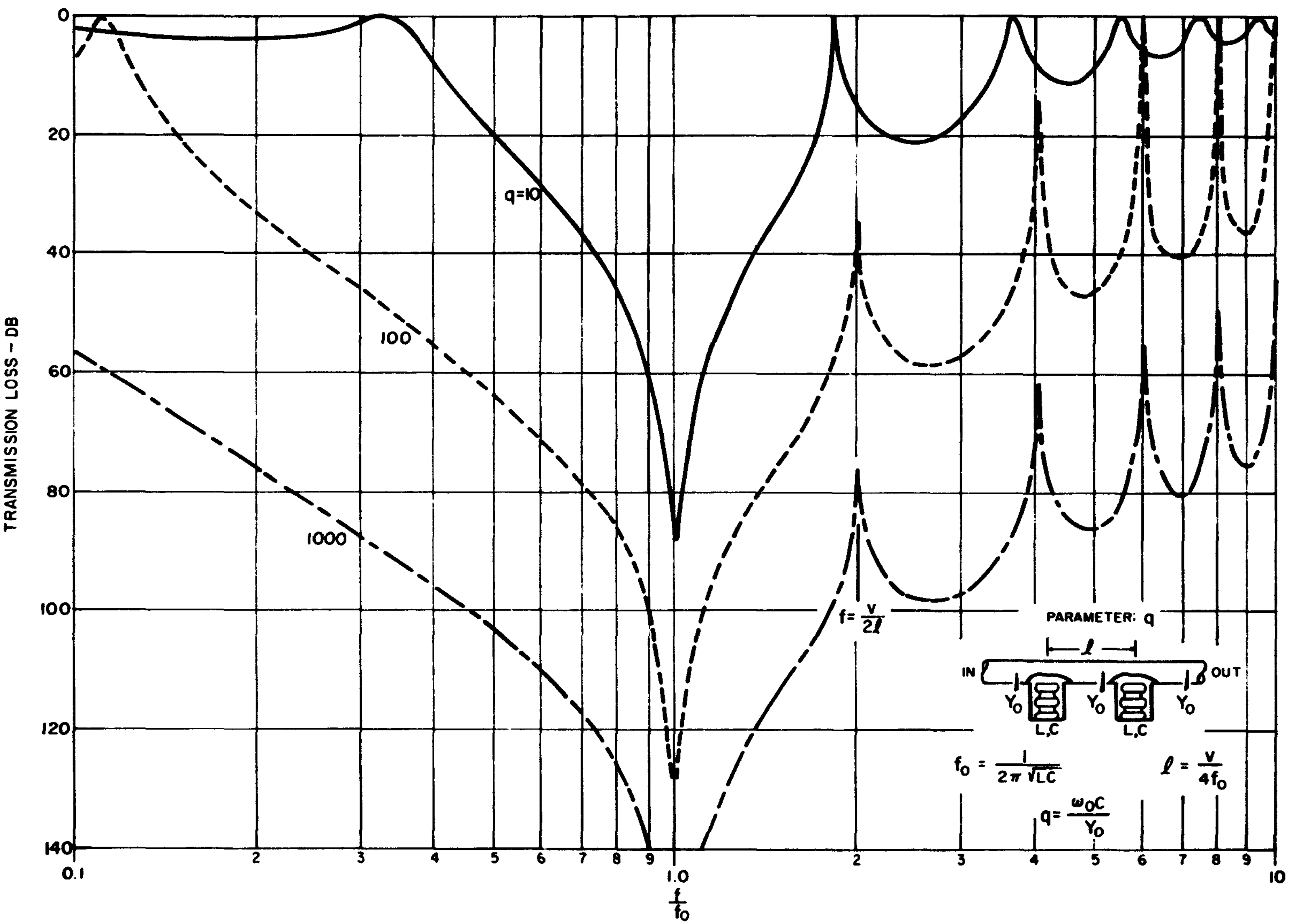

FIGURE 23
SIDE-BRANCH FILTER – TWO IDENTICAL SECTIONS

DRL-UT
DWG BS6931
JVK-BBB
9-7-62

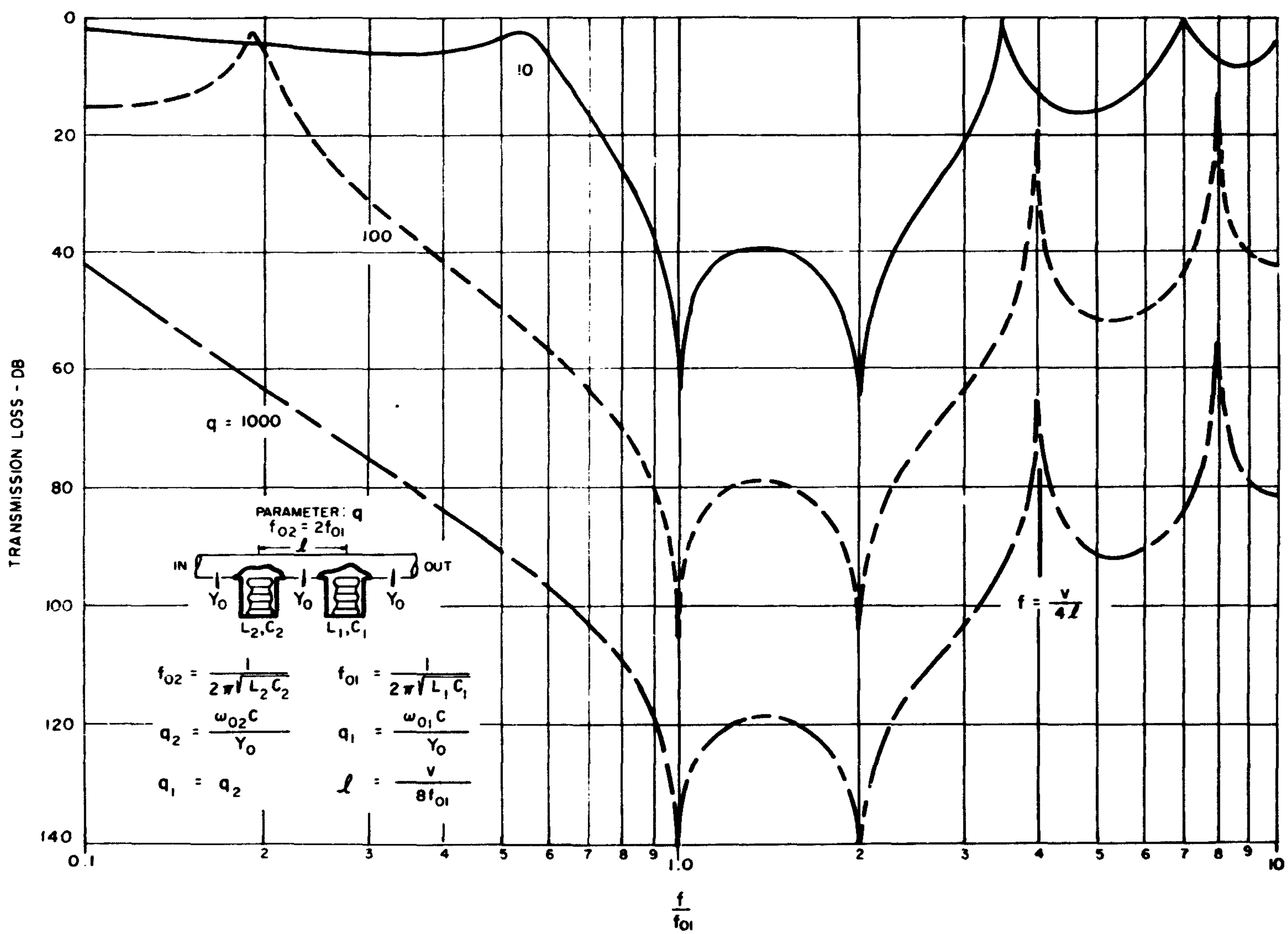

FIGURE 24
SIDE-BRANCH FILTER – TWO SECTICN

DRL - UT
DWG BS 6932
JVK - BEE
9 - 26 - 62

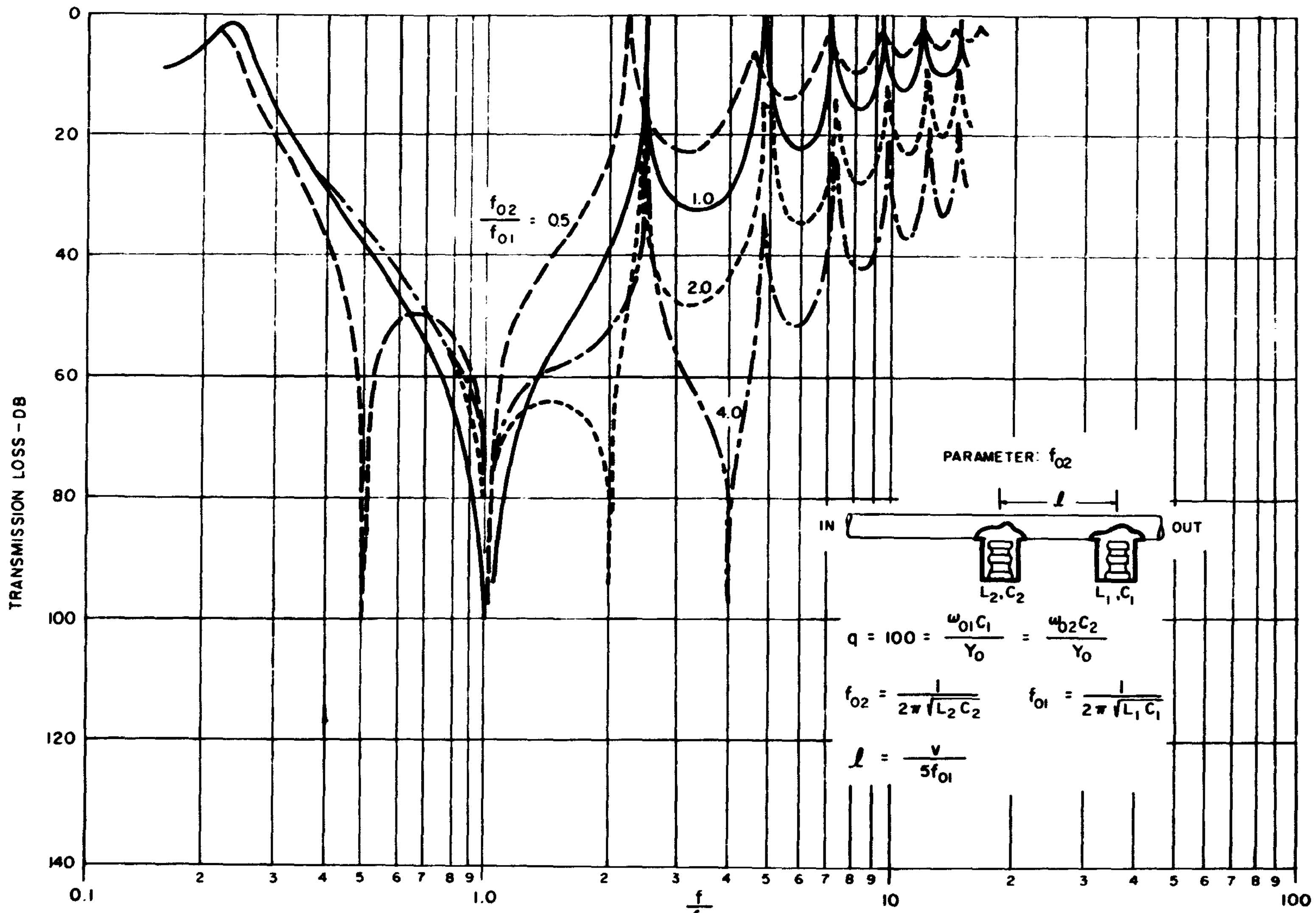

FIGURE 25
SIDE-BRANCH FILTER – TWO SECTION

DRL – UT
DWG BS 6933
JVK – BEE
9 – 27 – 62

The filter loses effectiveness near the frequency at which ℓ equals $\lambda/2$, but if f_{02} is above this frequency, an infinity does result.

The effect of the distance between elements on transmission loss for a two-section side-branch filter with identical elements is shown in Fig. 26. The resonant frequency of the side-branch elements with q = 100 is the same for each curve, but the frequency axis is normalized to the frequency at which ℓ equals $\lambda/2$. This is done because the shapes of the normalized curves are so nearly alike above $f/f_{\ell} = 1$. The parameter ℓ/ℓ_0 is the ratio of the actual length to the length that is $\lambda/2$ at f_0.

As further explanation of these curves the following example is presented:

Consider a piping system in which the sound velocity is 4000 fps, and $f_0 = 100$ cps is desired. It is desired to obtain the response for $\ell/\ell_0 = 0.5$, and the spacing between the elements, ℓ, must be calculated. Since $\ell_0 = v/2f_0 = 4000/2 \times 100 = 20$ ft, $\ell = 20 \times 0.5 = 10$ ft. These conditions make $f_{\ell} = f_0\ell_0/\ell = 100/0.5 = 200$ cps. The lowest frequency of 20 dB transmission loss is 0.072 times f_{ℓ}, or $f_1 = 0.072 \times 200 = 14.4$ cps. The first frequency at which the transmission loss curve crosses 20 dB again is 0.97 times f_{ℓ}, or $f_2 = 0.97 \times 200 = 194$ cps. The dimensionless frequencies 0.072 and 0.97 are taken from the $\ell/\ell_0 = 0.5$ curve. It can be seen from the curve that other attenuation bands exist at frequencies above $f/f_{\ell} = 1$.

The curve for $\ell/\ell_0 = 1.0$ appears to be most desirable. The use of this condition is not recommended, however, unless precise means for adjusting f_0 are provided. The lengths and resonant frequencies must be very accurately produced to obtain the desired condition. If the cancellation is not complete, a noise component near that frequency will pass through the filter with very little loss.

Three identical sections are cascaded to produce the lumped parameter side-branch filter shown in Fig. 27. The curve shapes are very much like those for the two-section filters of Fig. 23. Greater transmission loss is predicted here, but for practical filters it is doubtful that any improvement of a

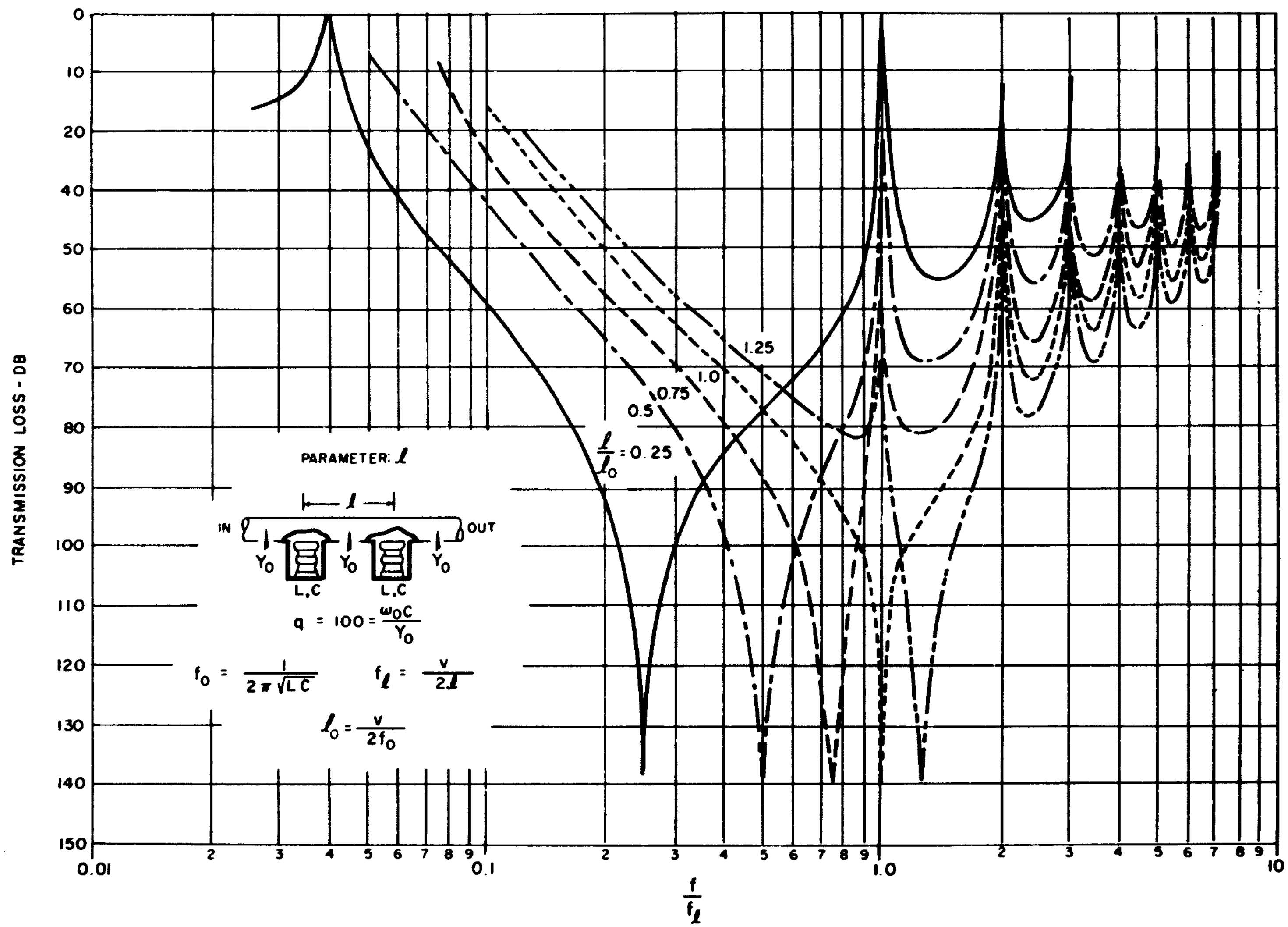

FIGURE 26
SIDE-BRANCH FILTER - TWO IDENTICAL SECTIONS

DRL - UT
DWG BS 6934
JVK - BEE
10 - 1 - 62

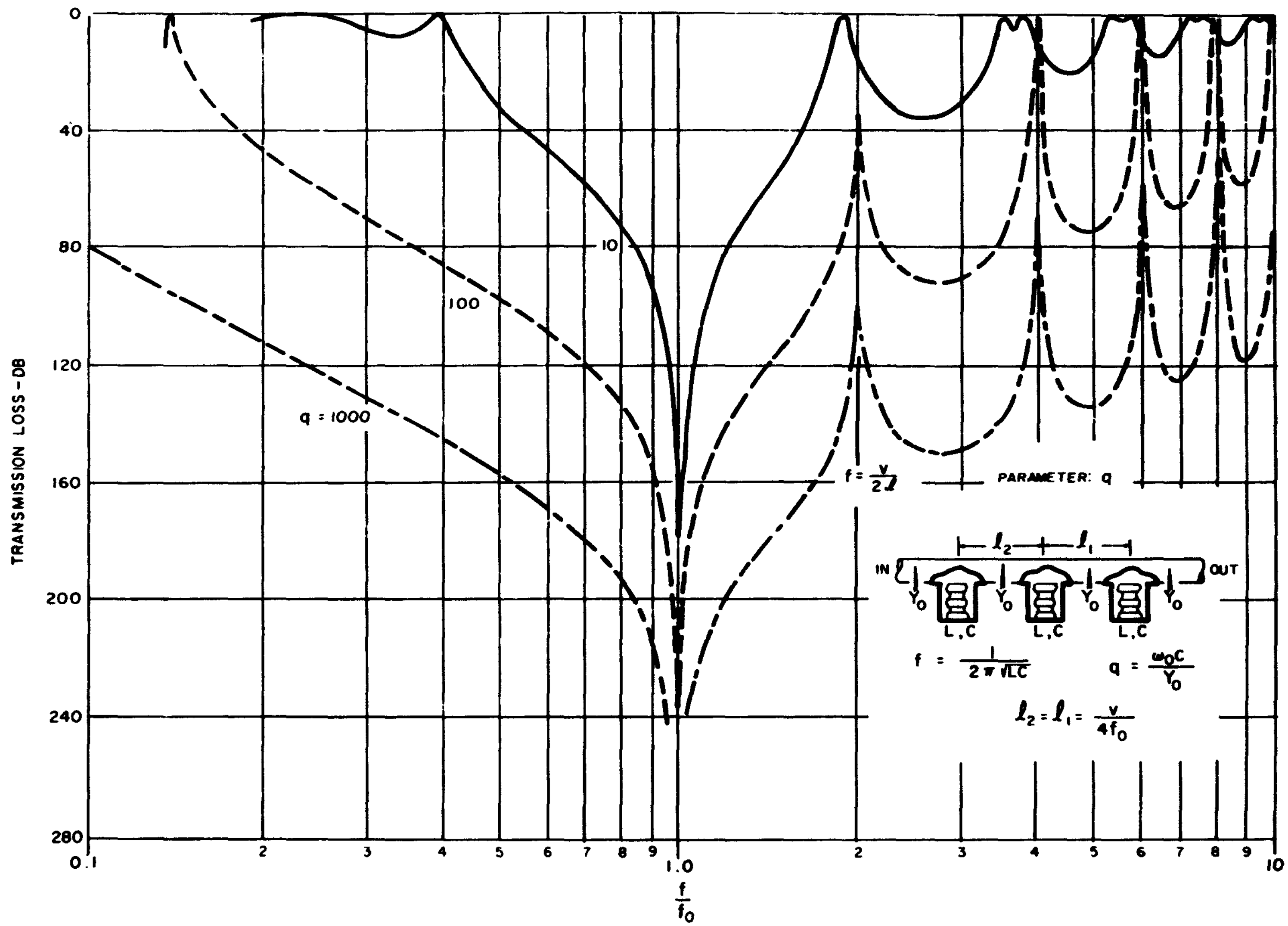

FIGURE 27
SIDE-BRANCH FILTER - THREE IDENTICAL SECTIONS

DRL - UT
DWG BS 6935
JVK - BEE
10 - 1 - 62

three-section over a two-section filter could be obtained without taking special pains to prevent mechanical coupling and noise regeneration.

A three-section filter can be used to suppress the fundamental and the second and third harmonics of a periodic source. Such an arrangement that also provides a wide rejection band is shown in Fig. 28.

As in the case of the two-section filter, the response of the three-section filter depends on element spacing. This dependence is shown in Fig. 29. The same calculations can be made as for the two-section filter, and the same precautions for the case of $l/l_o = 1$ should be noted.

2. Closed-End Tube, Side-Branch Filters

The side-branch element consisting of a closed-end, liquid-filled tube produces admittance infinities and thus infinities of transmission loss. These infinities occur at frequencies at which the tube length is an odd multiple of one-fourth wavelength. This repetitive nature is shown by the insert in Fig. 30. The transmission loss curves have repeated rejection bands with the bandwidth determined by a parameter, q'. This parameter is the ratio of the characteristic admittance of the side-branch tube to that of the system piping. In most cases, q' is approximately the ratio of the side-branch tube cross section area to pipe section area.

The transmission loss curves are drawn accurately only for a range of f/f_o from zero to two. The frequency scale can be simply changed to cover any higher ratio. Since the curves repeat, to go above $f/f_o = 2$, the scale can read 2, 3, 4, with the transmission loss infinity occurring at $f/f_o = 3$. This range is followed by 4, 5, 6, then 6, 7, 8, etc.

One of the many possible combinations of multiple, liquid-filled, side-branch elements is presented in Fig. 31. The arrangement is still a single-section filter, since both branches are at the same place on the pipe. The branch lengths are chosen to suppress the fundamental and harmonics of a periodic source. The longer branch tube is made one-quarter wavelength at the fundamental, f_o. Its

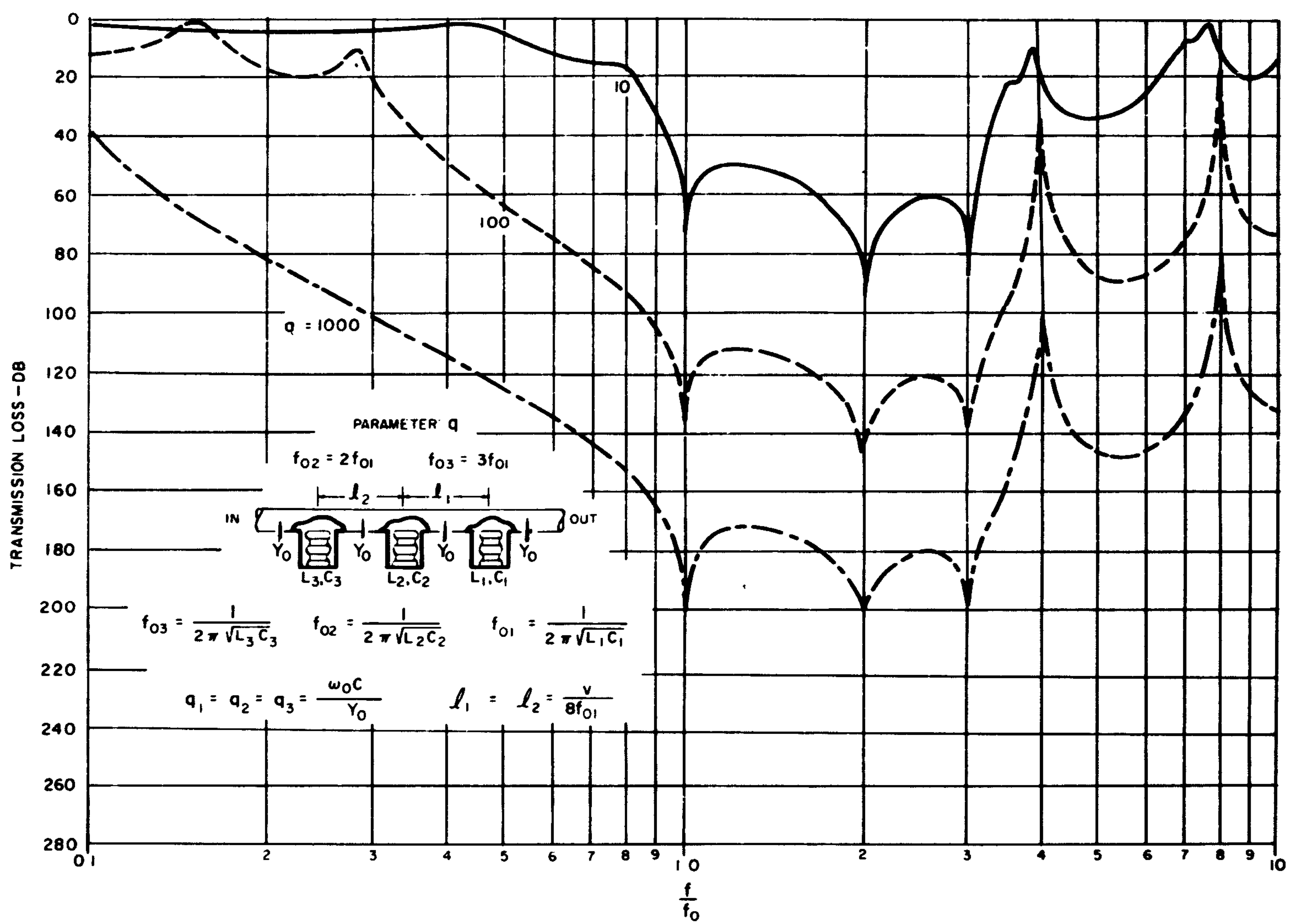

FIGURE 28
SIDE-BRANCH FILTER - THREE SECTIONS

DRL - UT
DWG BS 6936
JVK - BEE
9 - 28 - 62

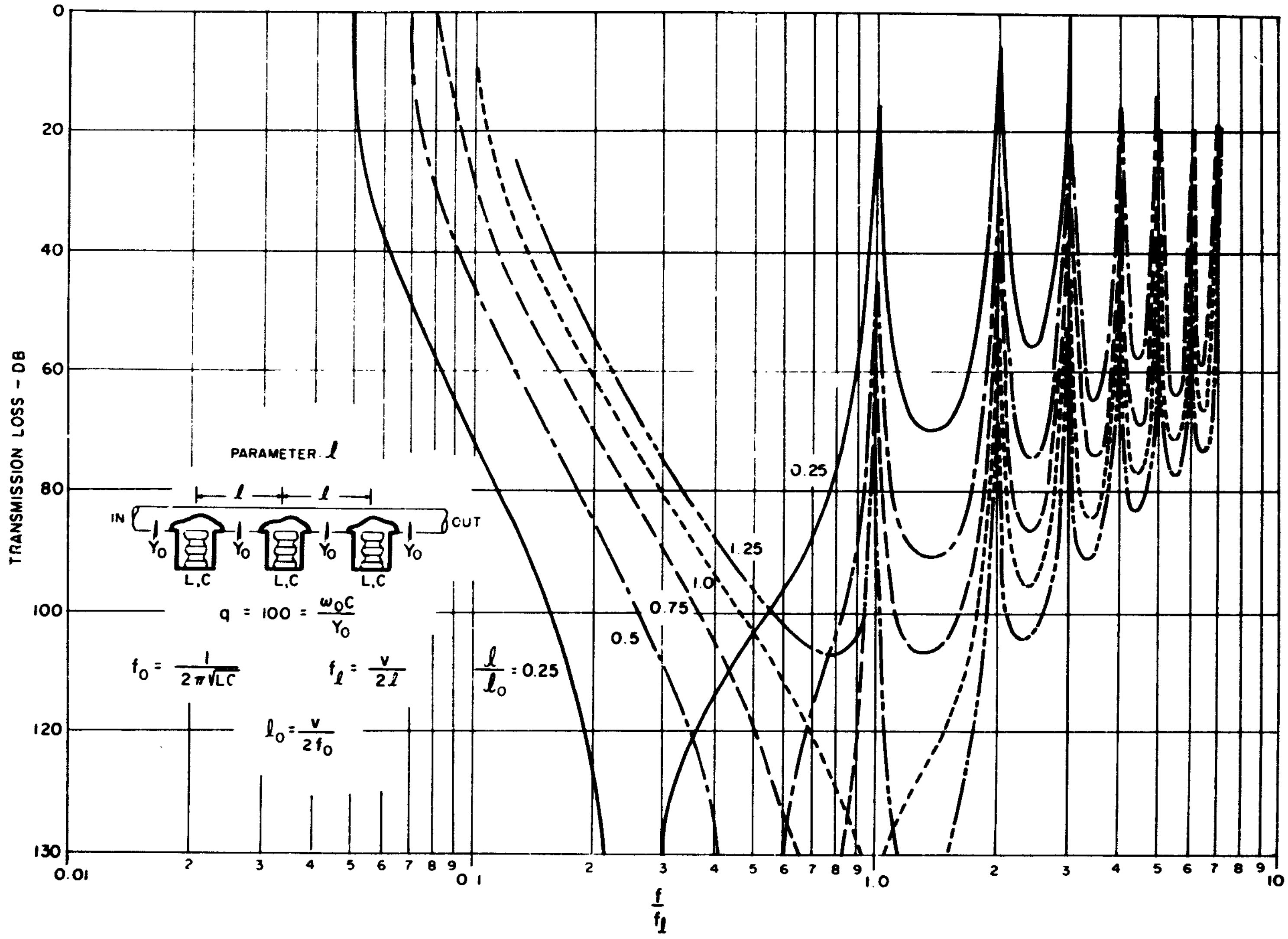

FIGURE 29
SIDE-BRANCH FILTER - THREE IDENTICAL SECTIONS

DRL - UT
DWG BS 6940
JVK - BEE
10 - 3 - 62

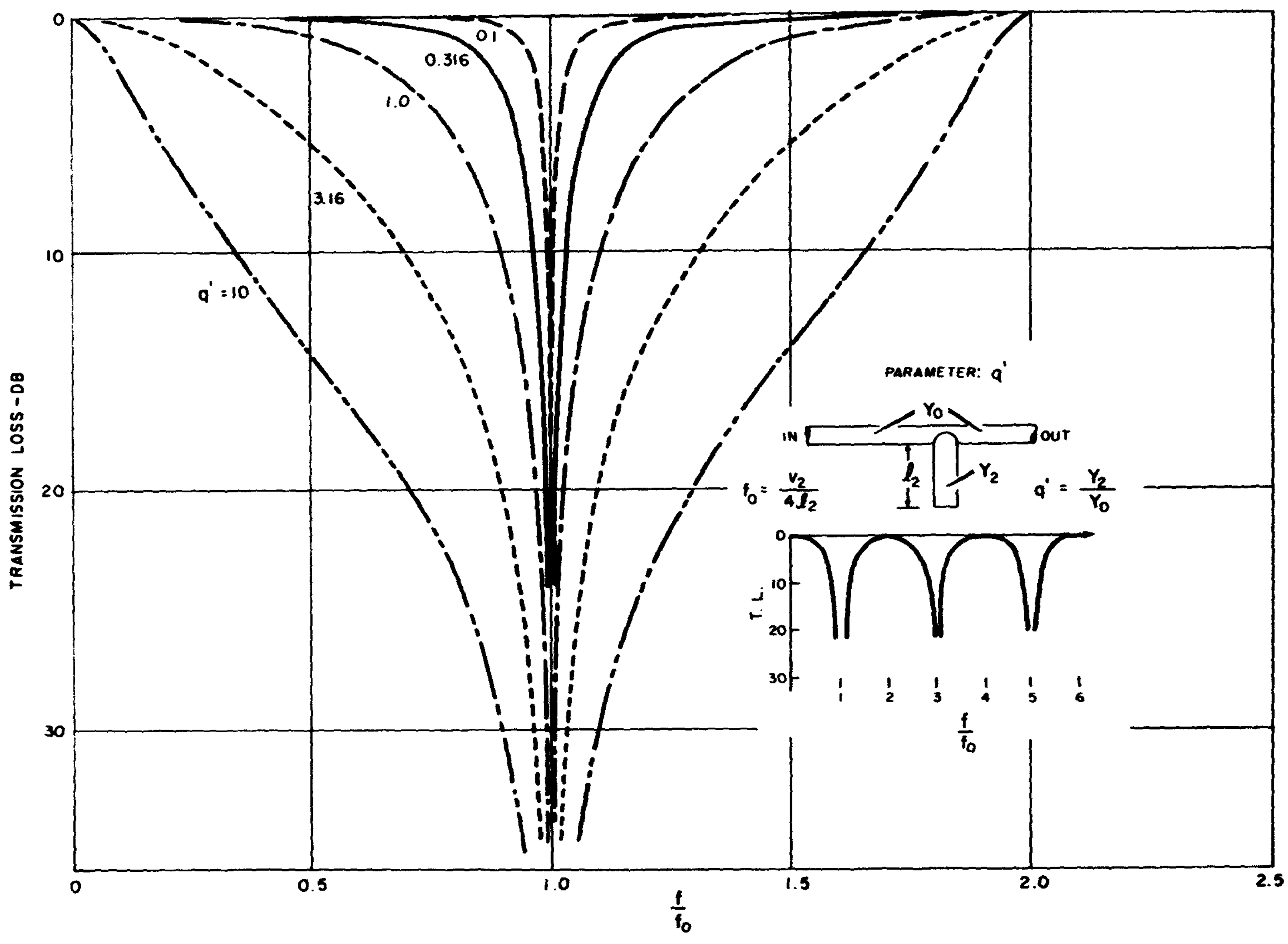

FIGURE 30
SINGLE SECTION LIQUID-FILLED SIDE-BRANCH FILTER

DRL - UT
DWG BS 6941
JVK - BEE
10 - 2 - 62

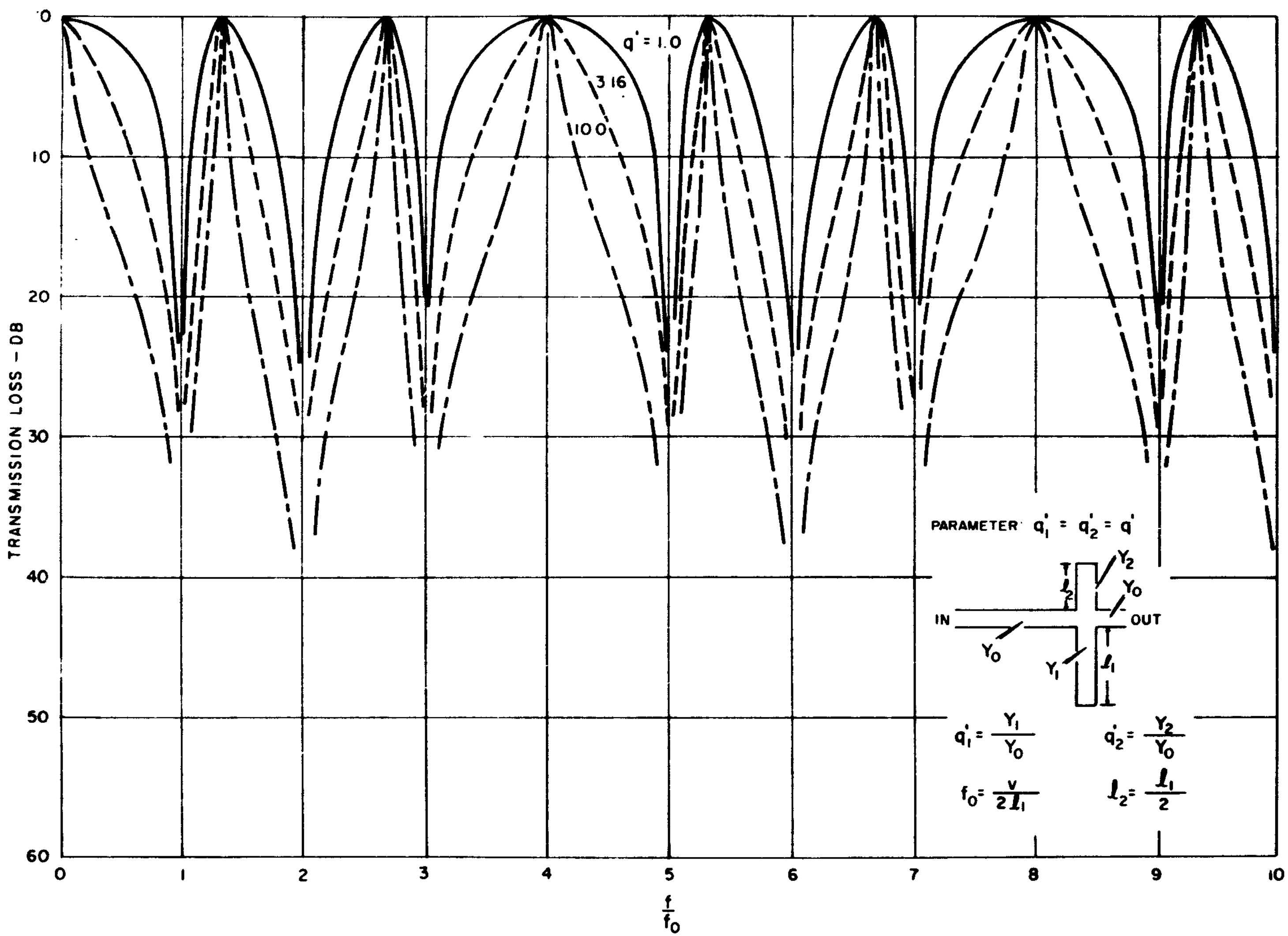

FIGURE 31
SINGLE SECTION LIQUID-FILLED DOUBLE SIDE-BRANCH FILTER

DRL - UT
DWG BS 6942
JVK - BEE
10 - 5 - 62

length, ℓ_1 is then

$$\ell_1 = v_1/4 f_o \quad .$$

This tube removes the fundamental and the odd harmonics: 3, 5, 7, ... The length of the second branch tube is chosen to be a quarter-wavelength at the second harmonic of the noise source, $2f_o$. Its length is then

$$\ell_2 = v_2/(4 \times 2f_o) \quad ,$$

and it eliminates the odd multiples of the second harmonic: 2, 6, 10, 14, ... The resulting transmission loss curves have infinities at the fundamental and all the harmonics except the 4th, 8th, 12th, etc.

A filter with improved broad band characteristics is obtained by separating the two side-branch tubes used in Fig. 31. It can be seen from Fig. 32 that transmission loss infinities occur at the same frequencies, but wide rejection bands are obtained for large q'.

3. Expansion Chamber Filters

Another simple filter configuration consists of an enlarged section of pipe, or expansion chamber, as shown in Fig. 33. A broad band transmission loss characteristic is produced with the magnitude related to a parameter, m. This quantity is the ratio of the characteristic admittance of the enlarged section to that of the rest of the piping in the system. The chosen values of m are related by $\sqrt{10}$, which makes the maximum transmission loss increase by 10 dB from one curve to the next.

Filtering action of the expansion chamber results from reflections at the ends of the chamber. This gives rise to the repetitive nature of the curves. The maxima of transmission loss occur at frequencies for which the chamber length is an odd multiple of a quarter wavelength, and the minima occur at frequencies for which the chamber length is a multiple of a half

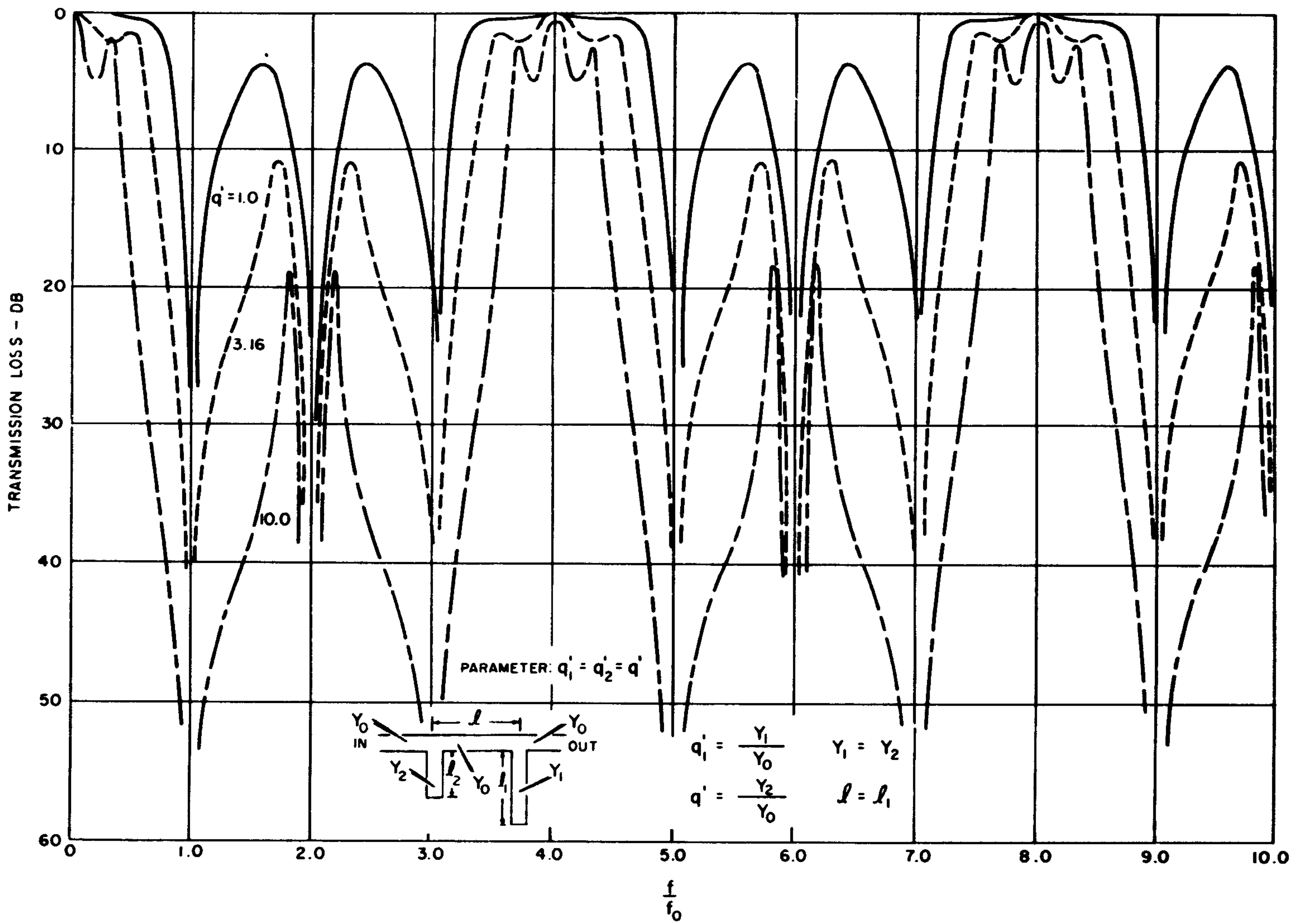

FIGURE 32
DOUBLE SECTION LIQUID-FILLED SIDE-BRANCH FILTER

DRL - UT
DWG BS 6943
JVK - BEE
10 - 11 - 62

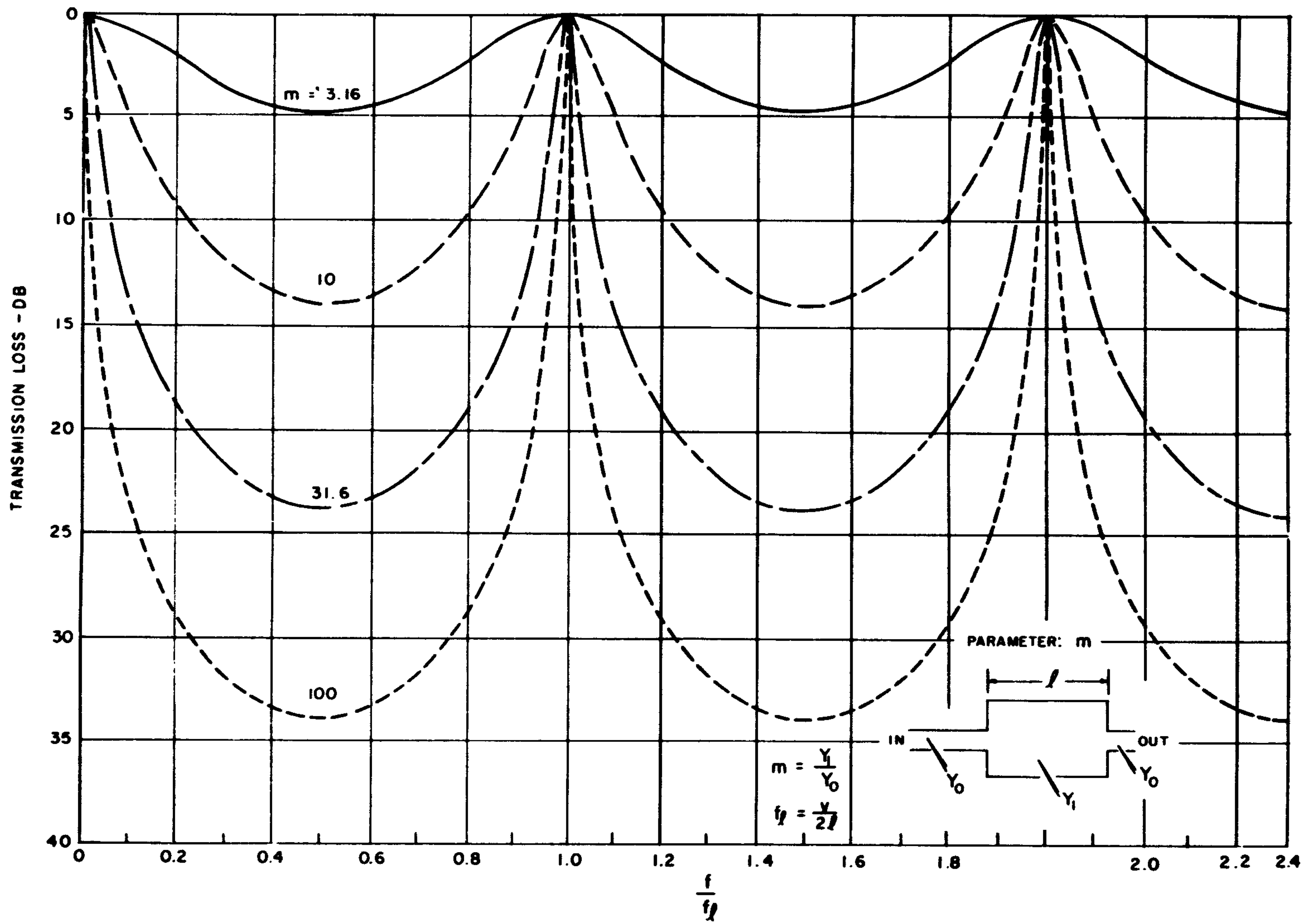

FIGURE 33
SINGLE EXPANSION CHAMBER FILTER

DRL - UT
DWG BS 6944
JVK - BEE
10 - 15 - 62

wavelength. For convenience, the frequency scale is normalized to the frequency at which the chamber is one-half wavelength long. If the maximum attenuation is desired at some frequency f_1, the length of the chamber that will produce the desired result is

$$\ell = \frac{v}{4f_1}(2n + 1) \quad , \qquad n = 0, 1, 2, \ldots \quad .$$

The wave velocity in the chamber is v, and the shortest chamber with the widest rejection band will be given by the value of ℓ for n = 0. The maximum transmission loss for large m is then given by the following:

$$\text{T.L. max} \approx 20 \log_{10}(m) - 6 \text{ dB} \quad , \qquad m \gtrapprox 10 \quad .$$

There are limitations on the size of m. The filter theory presented here is based on plane wave propagation of sound in pipes. This is referred to as the zero order propagation mode. There are other higher order modes that will be propagated at higher frequencies. The higher order modes will not be affected by the filter elements in the same way as the zero order mode and the filter effectiveness may be nullified. With each higher order mode there is a cutoff frequency below which it will not be propagated. The cutoff frequencies depend on pipe diameter and in general decrease as pipe diameter increases. Thus, in designing filter elements, particularly expansion chambers, care must be taken to keep chamber sizes small enough to prevent the propagation of higher order modes at frequencies in the desired noise reduction region. These limits on size are given in Chapter III, C, 1, Sound Velocity in Pipes.

In the case represented by Fig. 33, and in the following discussion of other expansion chambers, the lengths of chambers and connecting tubes are acoustical lengths. Filter calculations are based on the ratio of physical lengths to sound wavelength in the element. In the previous case, the chamber length was made equal to $\lambda/4$ at the frequency of interest. In the cases to be considered next, length ratios will be considered, and equal sound velocities will be assumed. When sound velocities differ, ratios of $\beta\ell$ must be considered. For example, the condition given as $\ell_1 = \ell_2$ implies $\beta_1\ell_1 = \beta_2\ell_2$, which leads to the relationship

$$\ell_1/v_1 = \ell_2/v_2 \quad .$$

Thus, to make two physical tube lengths, ℓ_1 and ℓ_2, with different sound velocities, v_1 and v_2, have equal acoustical length,

$$\ell_2 = \ell_1 \, v_2/v_1 \quad .$$

Two expansion chamber filters can be cascaded as in Fig. 34 to obtain greater transmission loss than that obtained with one chamber. The maximum transmission loss for this arrangement of two identical sections is given by

$$\text{T.L. max} \approx 40 \log_{10} (m) -6 \text{ dB} \quad , \quad m \geqq 10 \quad .$$

The shapes of the curves are modified from those of the single chamber to give a reduced rejection bandwidth.

Again the maximum transmission loss occurs at the frequencies that make the chamber odd quarter-wavelengths long, and zeros occur at frequencies that make the chamber length multiples of $\lambda/2$. The frequency is again normalized to the frequency of the first multiple of $\lambda/2$.

There are many physical dimensions of the two-section expansion chamber filter that could be varied. Each of these may have profound effects on the transmission loss curves. Several figures to follow will show the effects of length of connecting tube, the length of chamber No. 1 with respect to chamber No. 2, and of m for chamber No. 1 and connecting tube lengths different from those of Fig. 34.

Transmission loss curves are presented in Figs. 35, 36, and 37 for a two-section expansion chamber filter with identical chambers. In these figures, the ratio of the connecting tube length, ℓ_2, to the chamber length, ℓ_3, is varied from zero to 2.0. If a broad rejection band at low frequencies is

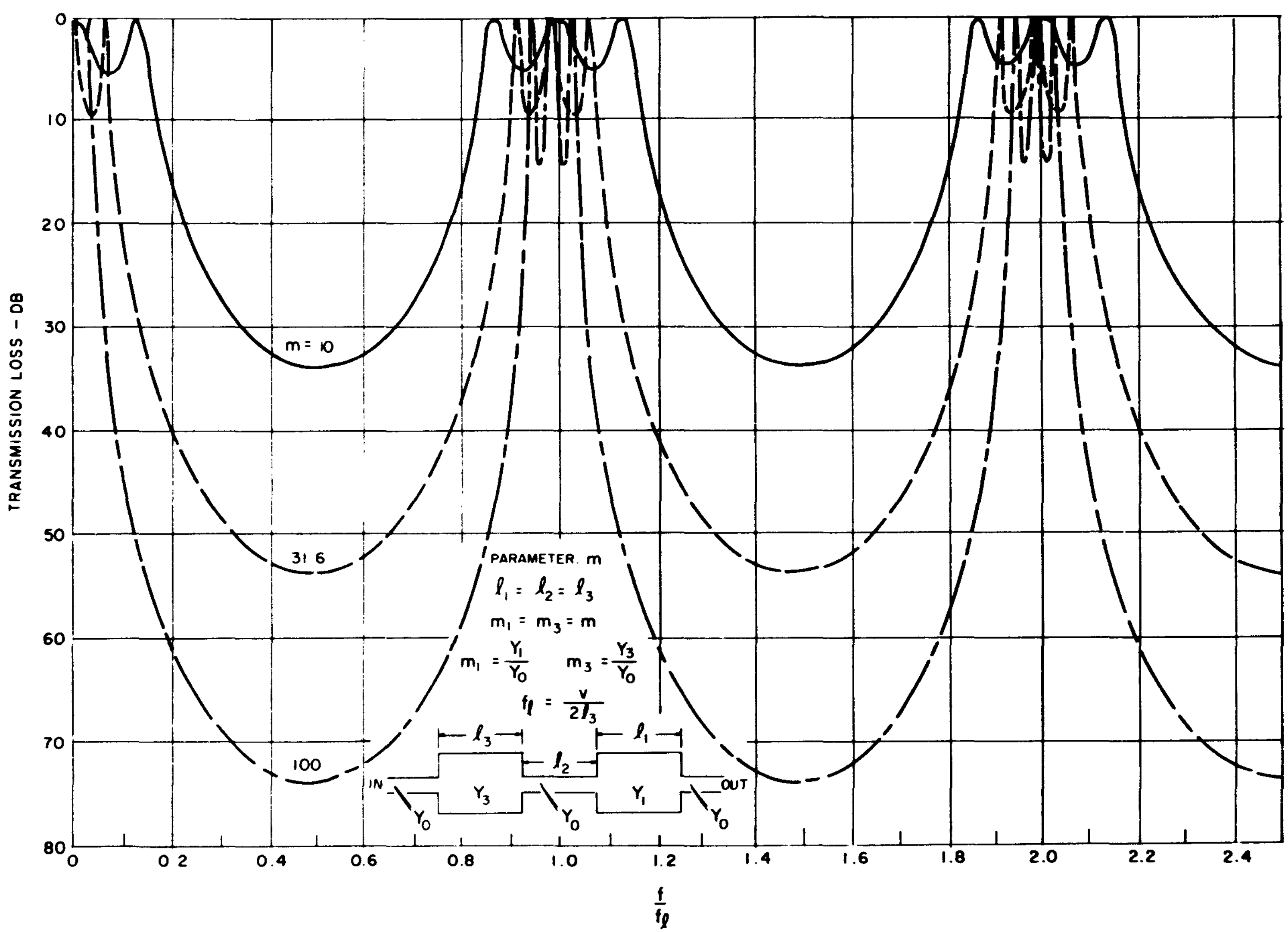

FIGURE 34
TWO SECTION EXPANSION CHAMBER FILTER

DRL – UT
DWG BS 6945
JVK – BEE
10 – 17 – 62

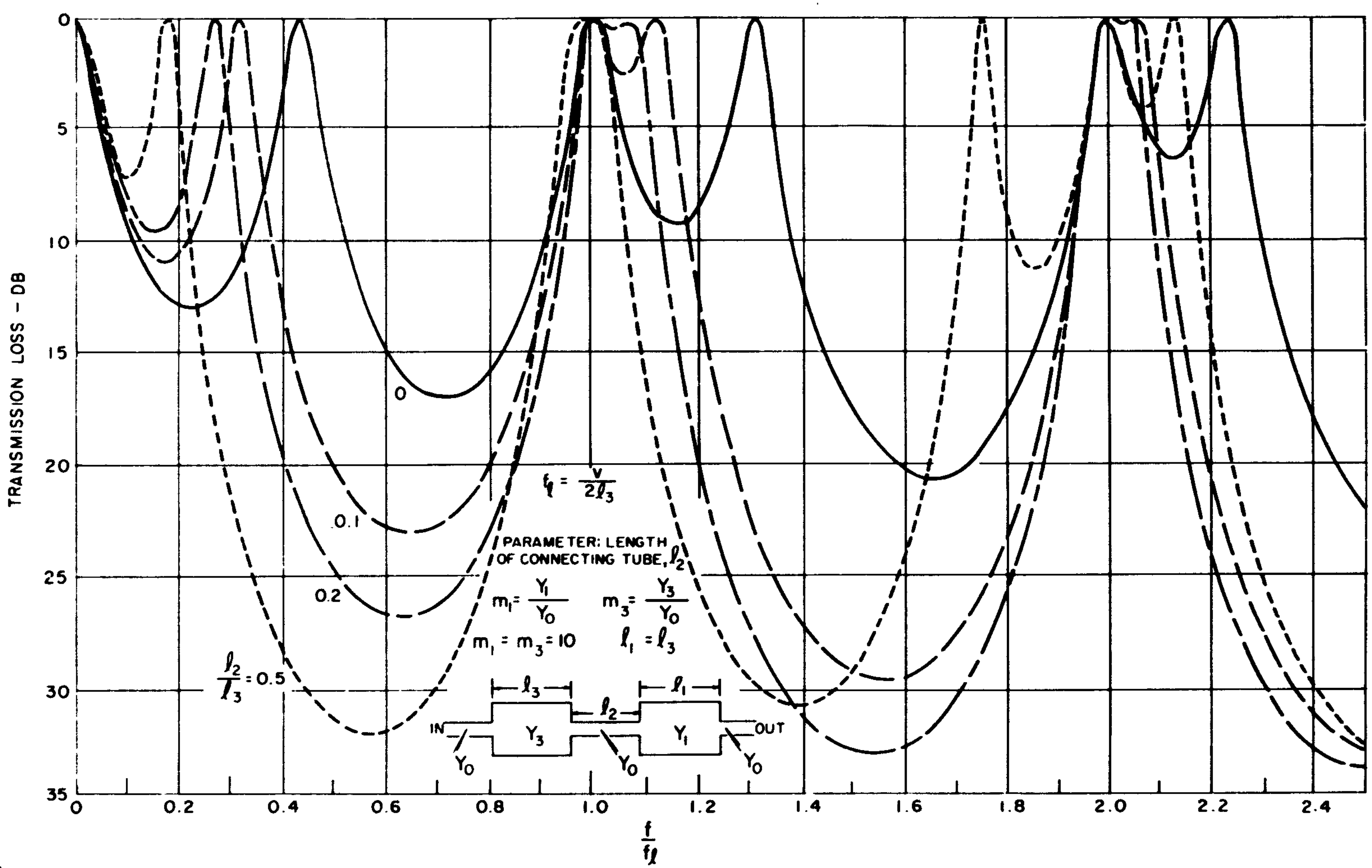

FIGURE 35
TWO SECTION EXPANSION CHAMBER FILTER

DRL - UT
DWG BS 6946
JVK - BEE
10 - 17 - 62

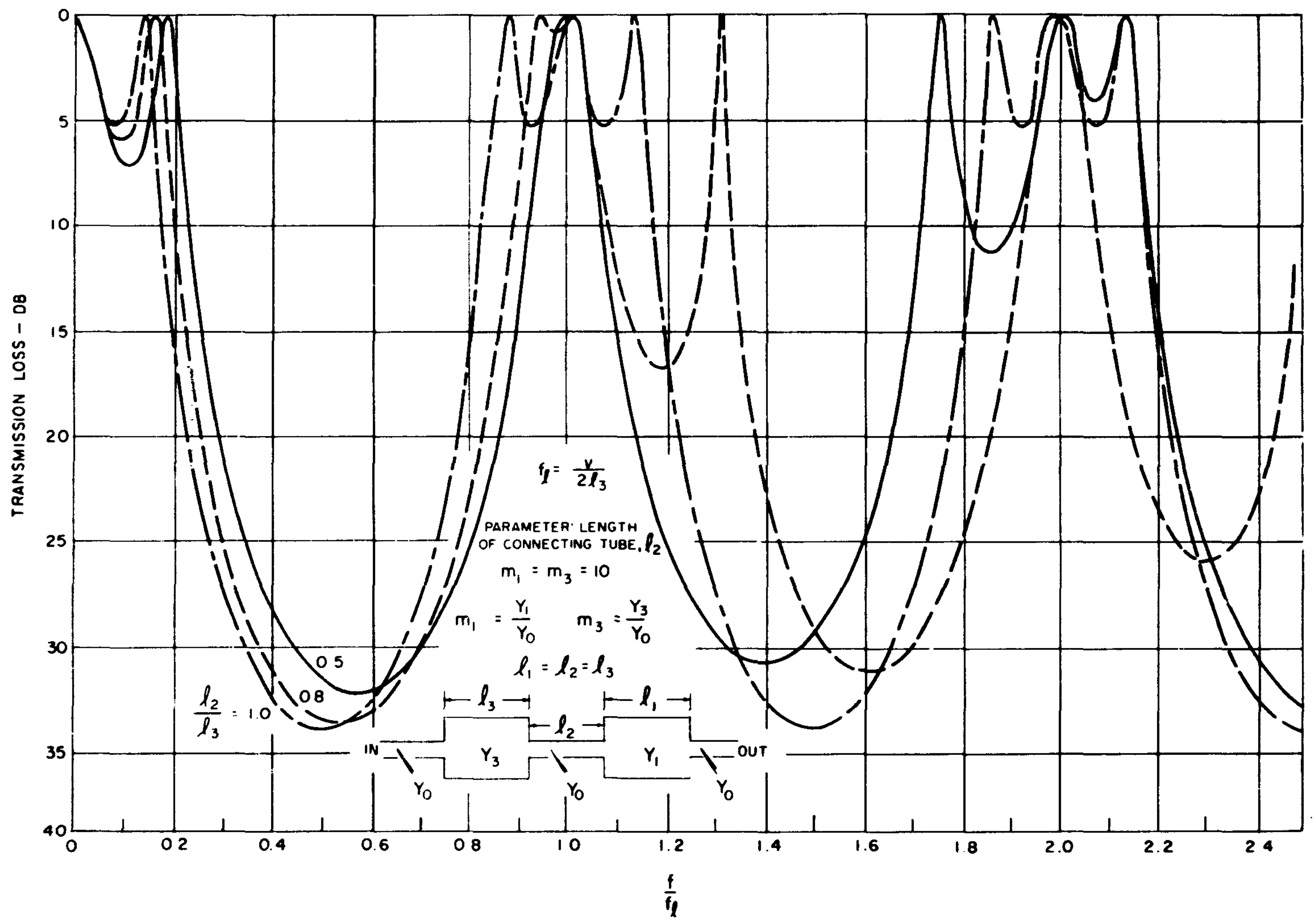

FIGURE 36
TWO SECTION EXPANSION CHAMBER FILTER

DRL – UT
DWG BS 6947
JVK – BEE
10 – 18 – 62

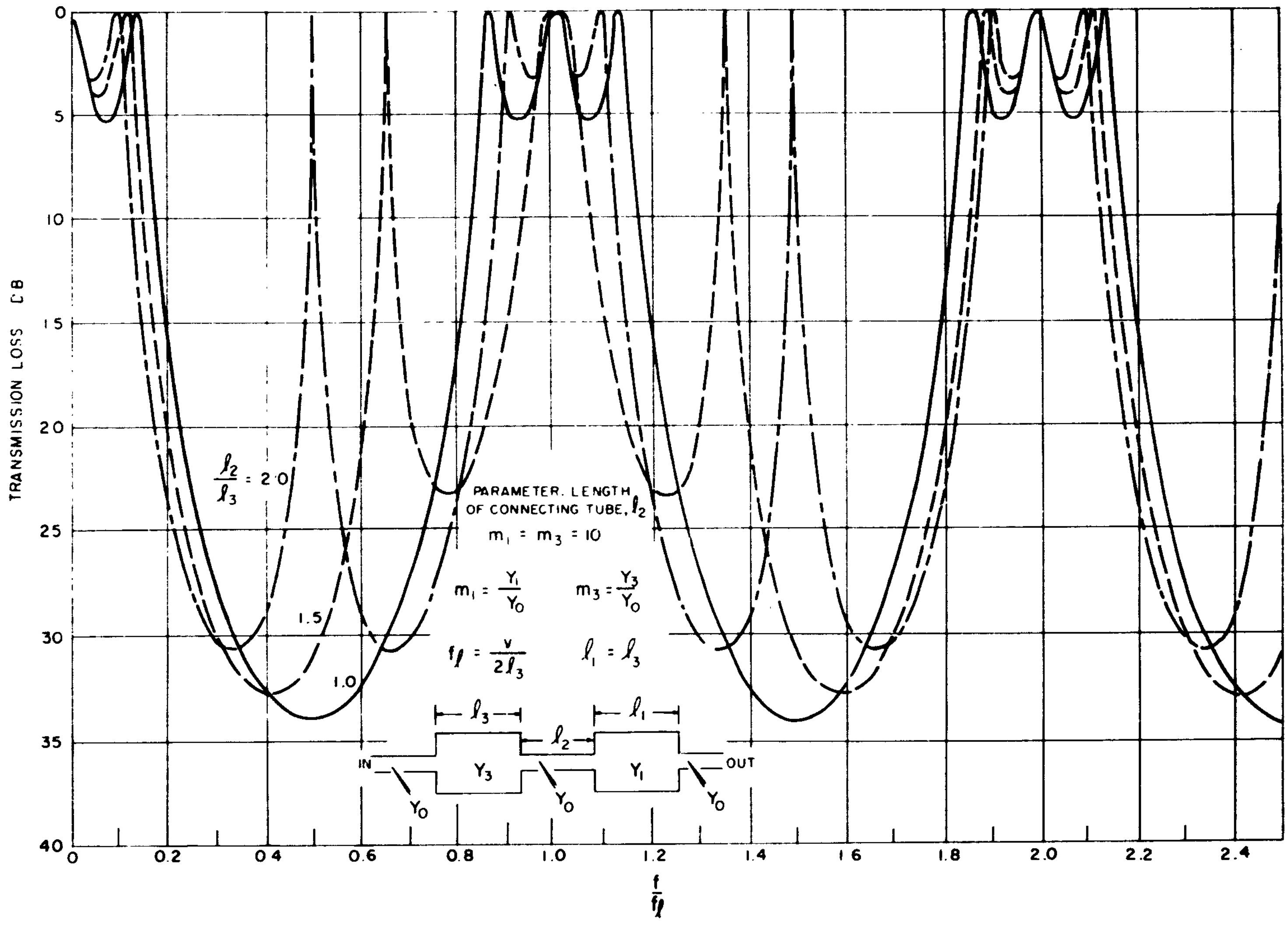

FIGURE 37
TWO SECTION EXPANSION CHAMBER FILTER

DRL - UT
DWG BS 6948
JVK - BEE
10 - 18 - 62

desired, it is evident from Fig. 36 that ℓ_2 should be between 0.5 and 1.0 times ℓ_1. For values lower than this (Fig. 35), the transmission loss bandwidth and magnitude are both reduced. For ratios greater than 1.0 the same effects are noted (Fig. 37). Another observation that can be made is that the length, ℓ_2, is not critical as long as it is approximately equal to the chamber length.

The improvement obtained over a single chamber by the addition of a second chamber is shown in Figs. 38 and 39. Even for the case in which the length of chamber No. 1 equals 0.1 of that of chamber No. 2, an increase in transmission loss is obtained. For this case, the response above $f/f_\ell = 1$ is almost as good as two equal length chambers. The curves are so lacking in symmetry that few general statements about the effects of the second chamber can be made. It is evident from the curves, however, that the transmission loss in the region of the maxima is increased and width of the rejection bands is reduced by the addition of a second chamber.

The effect on transmission loss caused by changing m for two unequal length chambers is shown in Figs. 40 and 41. In Fig. 40, the first chamber is 0.2 the length of the second chamber, and the connecting tube is the same length as the second chamber. The frequency is normalized to the value that makes chamber No. 2 a half-wavelength long. The maximum transmission loss is seen to increase directly with 20 $\log_{10}$ (m). In this case the rejection bandwidth also increases with m.

Figure 41 shows a case with the first chamber half as long as the second chamber and the connecting tube equal in length to the second chamber. Here the rejection bands are somewhat wider, but the maxima of transmission loss are a few dB less than for the equal length case shown in Fig. 34.

The value of m was varied for a double expansion chamber filter with a short connecting tube and the resulting transmission loss curves are plotted in Fig. 42. The two chambers are equal in length, and the connecting tube is 0.1 the chamber length. The rejection bandwidths are narrower than for the longer tube as shown in Fig. 34, but the transmission loss maxima increase directly with 20 $\log_{10}$ (m).

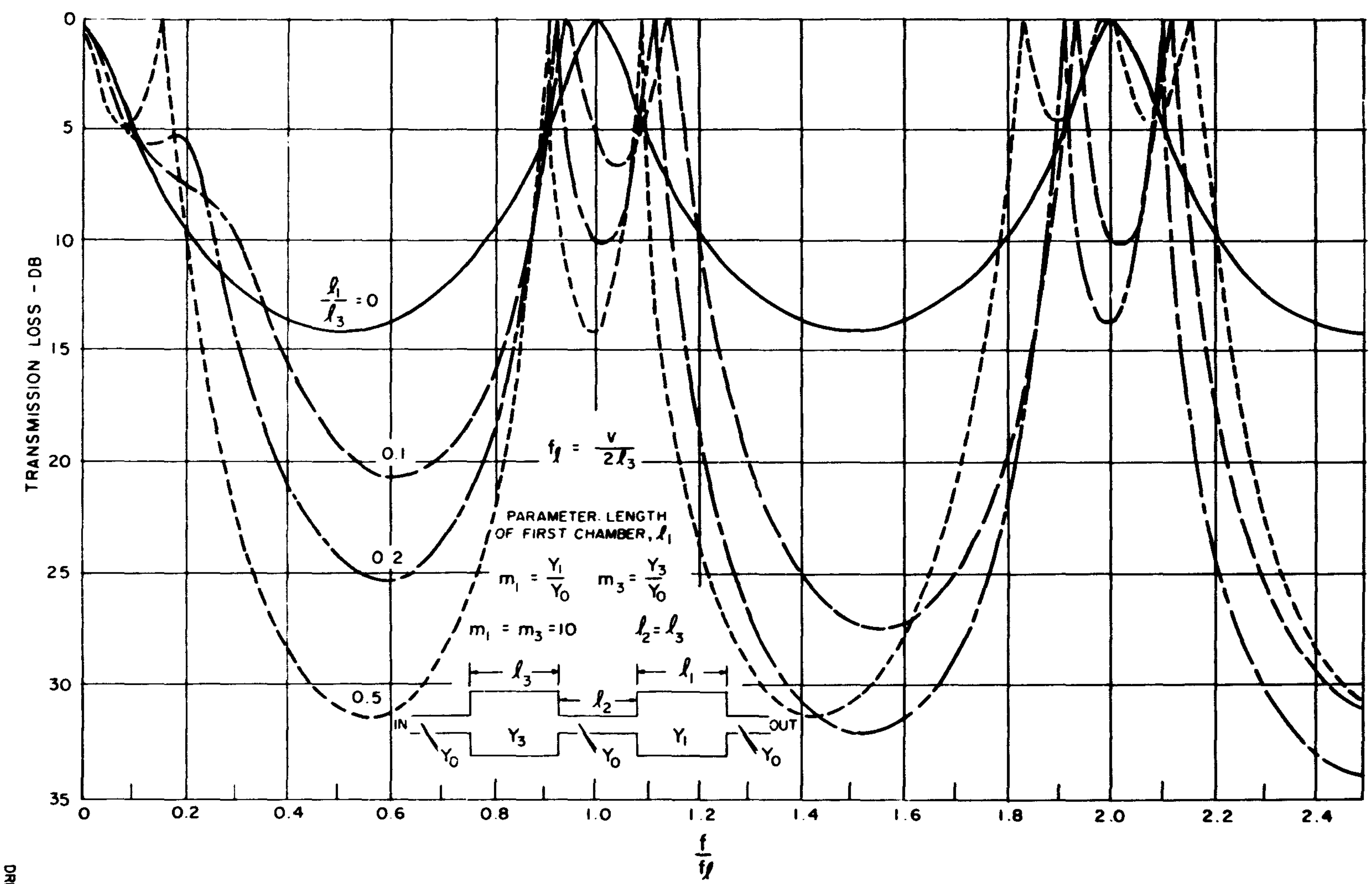

FIGURE 38
TWO SECTION EXPANSION CHAMBER FILTER

DRL - UT
DWG BS 6949
JVK - BEE
10 - 19 - 62

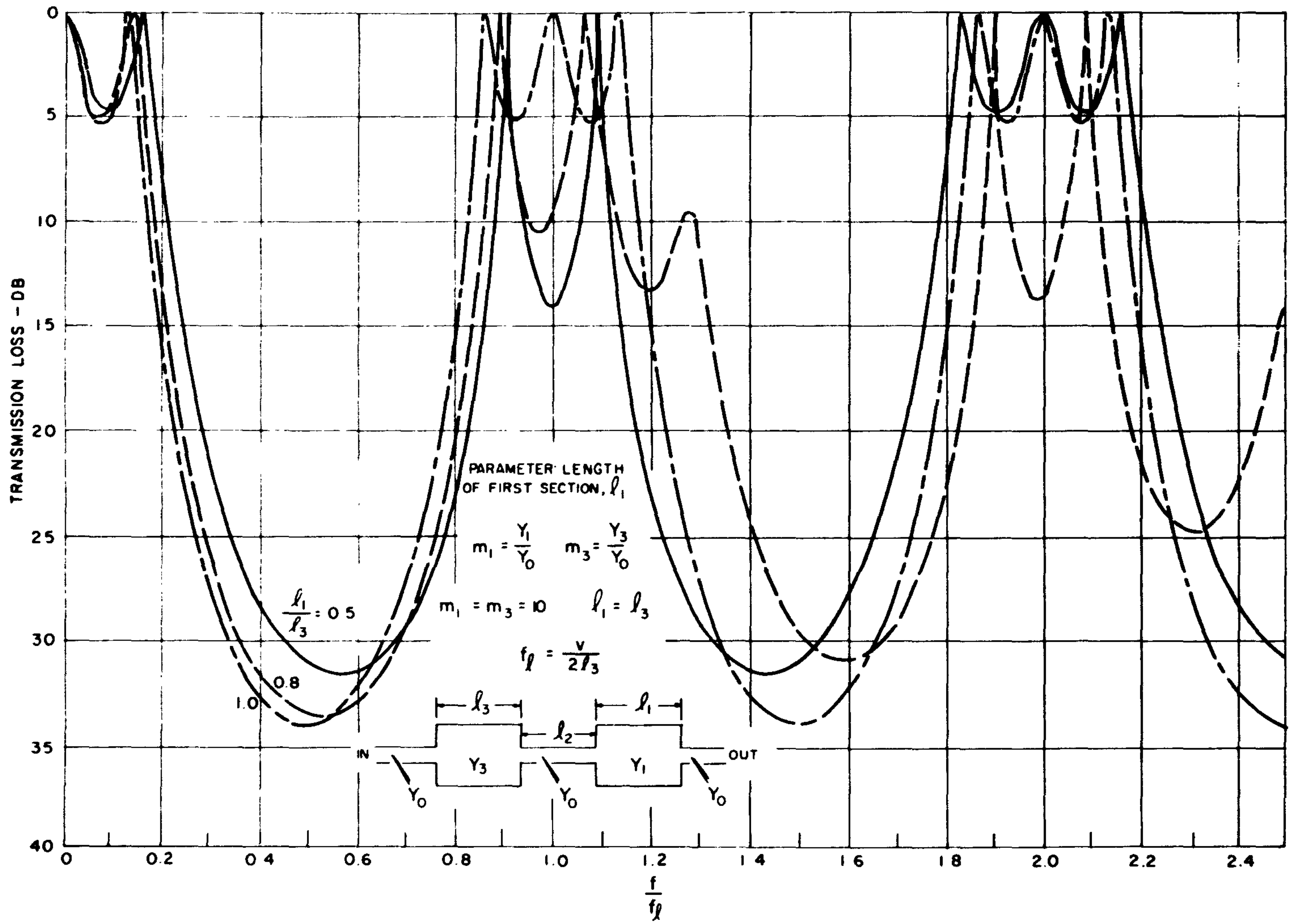

FIGURE 39
TWO SECTION EXPANSION CHAMBER FILTER

DRL - UT
DWG BS 6950
JVK - BEE
10 - 22 - 62

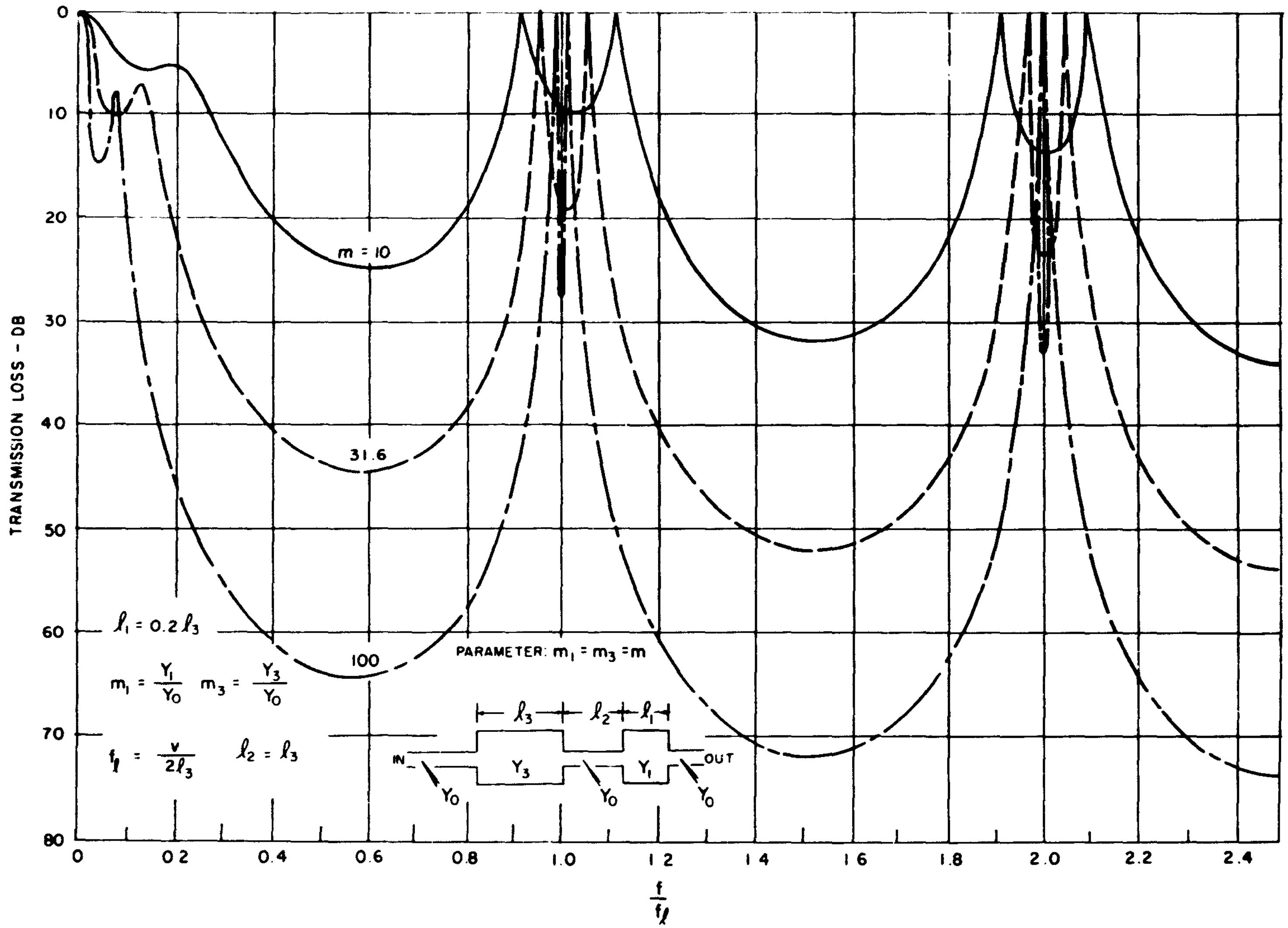

FIGURE 40
TWO SECTION EXPANSION CHAMBER FILTER

DRL - UT
DWG BS 6951
JVK - BEE
10 - 22 - 62

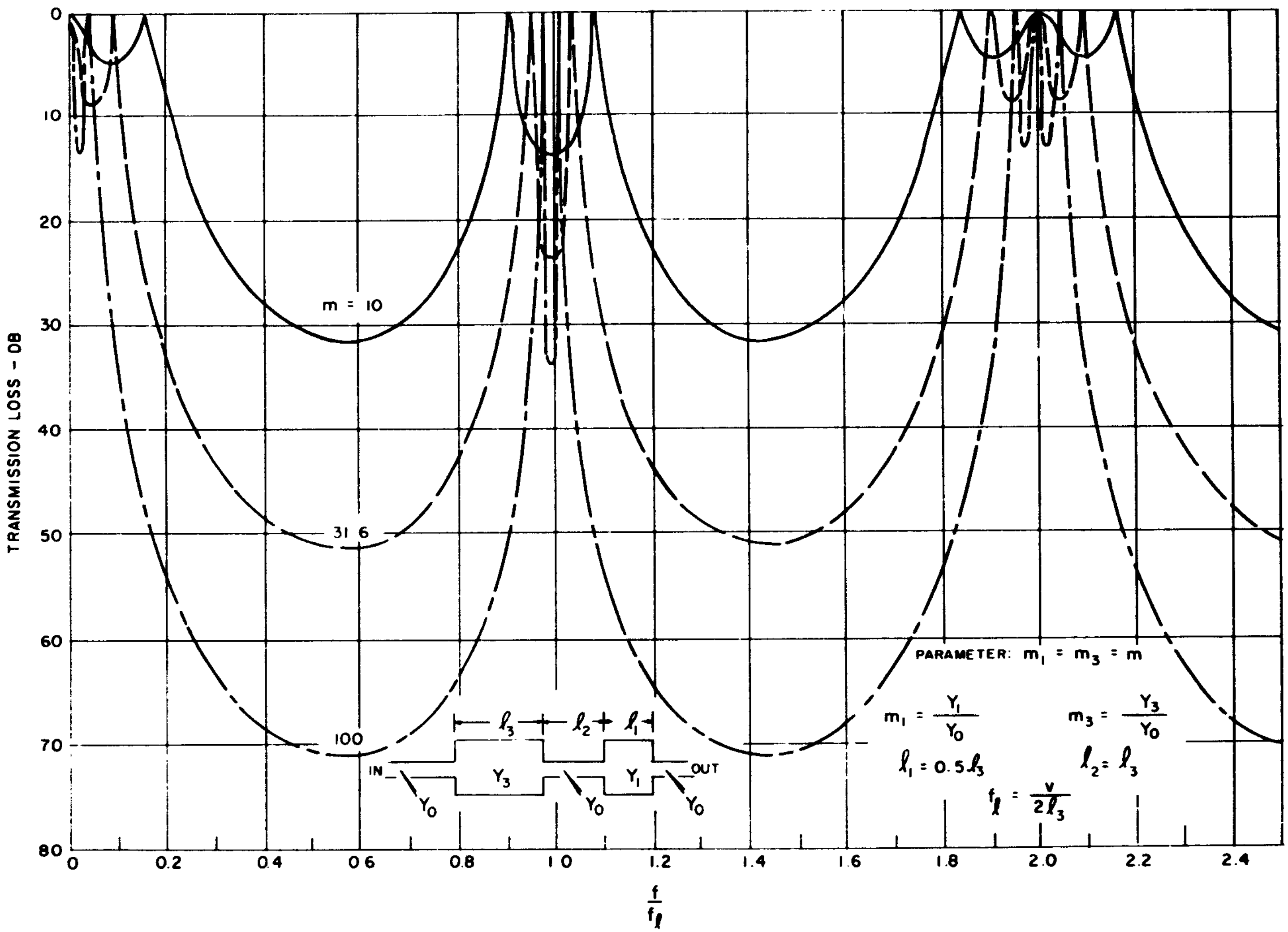

FIGURE 41
TWO SECTION EXPANSION CHAMBER FILTER

DRL - UT
DWG BS 6952
JVK - BEE
10 - 22 - 62

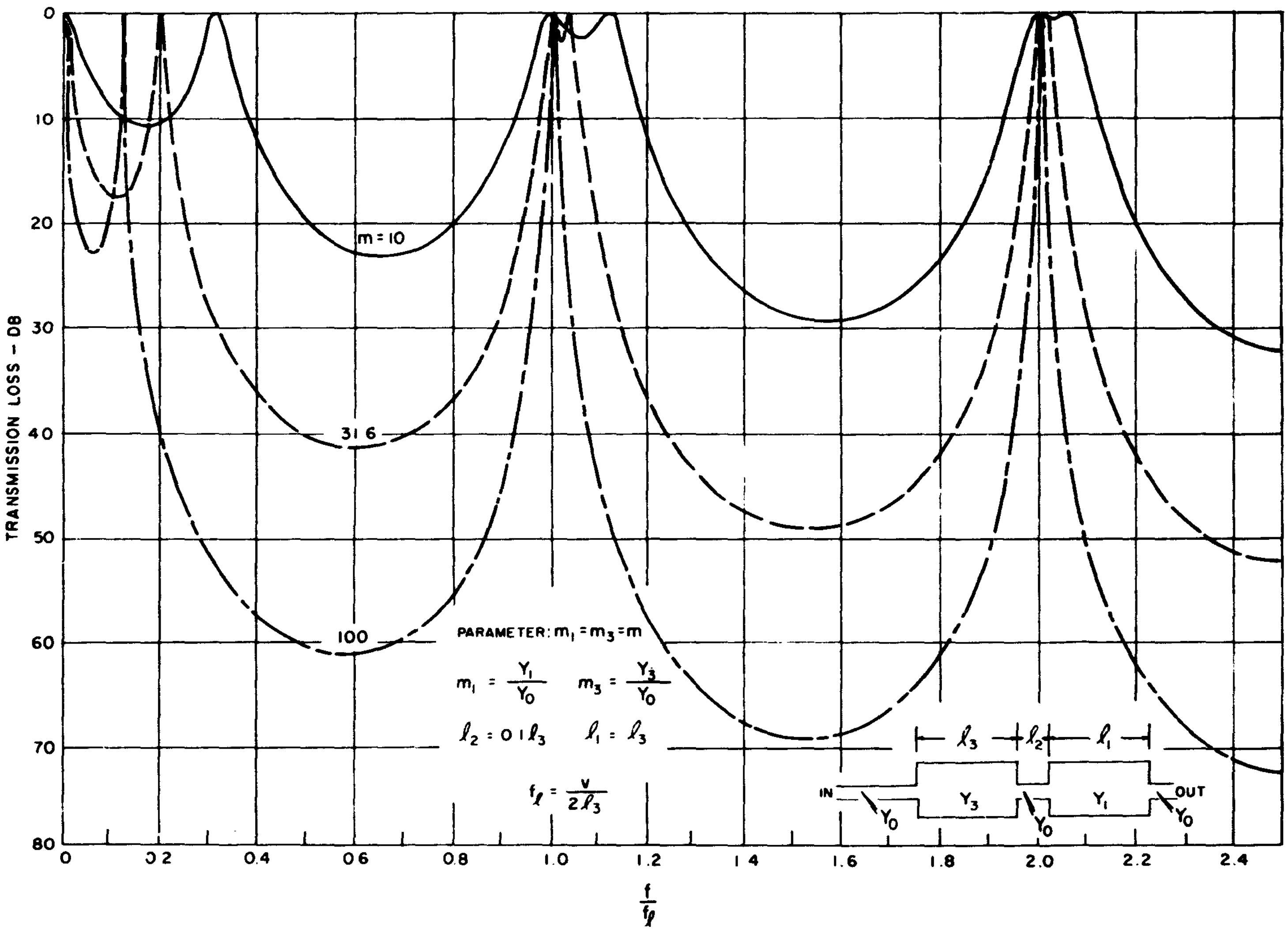

FIGURE 42
TWO SECTION EXPANSION CHAMBER FILTER

DRL - UT
DWG BS 6953
JVK - BEE
10 - 23 - 62

4. Combination of Expansion Chamber and Lumped Side-Branch Element

The combination of an expansion chamber filter with a resonant side-branch element can provide a transmission loss infinity as well as the broad band characteristic of the expansion chamber. Figure 43 shows such a combination with the chamber m = 10 and the side-branch element q = 100. The side-branch element can be placed on the pipe or the expansion chamber as long as it is near the pipe-chamber junction. The same transmission loss curve will result if the branch element is on either end of the chamber.

With the resonant frequency, f_0, within the first rejection band of the chamber, the transmission loss is greatly increased. An undesirable spike occurs except when f_ℓ is the frequency at which the chamber length equals $\lambda/4$. This condition for chamber length equal to $\lambda/4$ at f_0 is an advantageous one, since the transmission loss and rejection bandwidth are both greatly increased; however, it may be difficult to obtain and maintain in a physical system.

The effect of the value of m for the expansion chamber on the transmission loss curves is shown in Fig. 44. The side-branch resonant frequency is 0.5 f_ℓ and q = 100. It is seen that increasing m increases the transmission loss maxima, but the width of the first rejection band is considerably reduced. If most of the energy of the noise source lies in the region of the first rejection band, it would be advantageous to use a small m with the attendant saving in space.

The importance of large q for the branch element is shown by Fig. 45. The curves are computed for a chamber m = 10. The rejection bandwidth is increased; the transmission loss in the first rejection band is increased about 10 dB for each 10 dB increase in q.

Figures 44 and 45 consider only the case $f_0 = 0.5\, f_\ell$, but it is expected that variations of m and q will have similar effects on transmission loss for other ratios of f_0/f_ℓ. The undesirable spikes, as shown in Fig. 43, would still be expected, however.

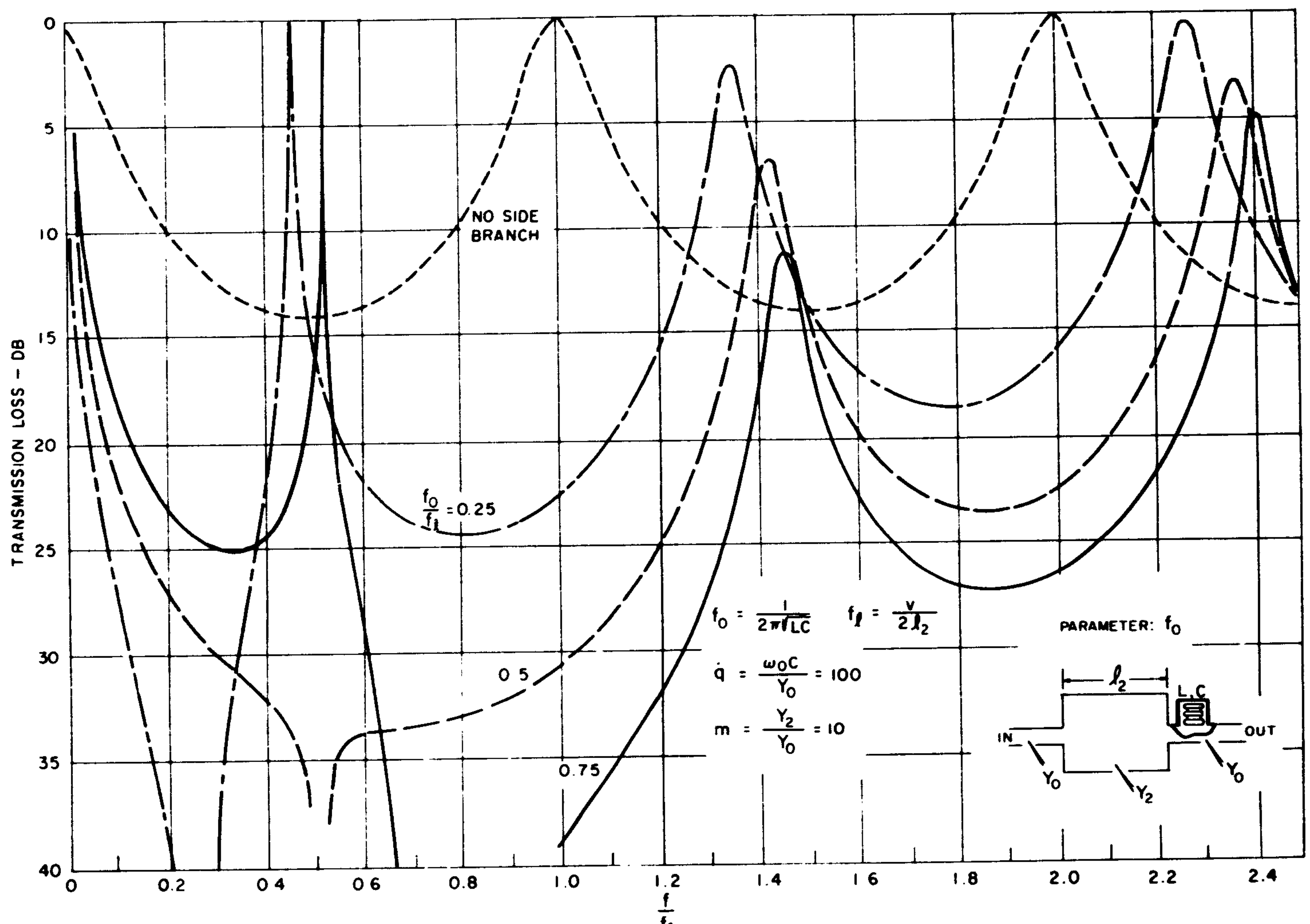

FIGURE 43
COMBINATION FILTER (EXPANSION CHAMBER AND LUMPED PARAMETER SIDE BRANCH)

DRL - UT
DWG BS 6954
JVK - BEE
10 - 23 - 62

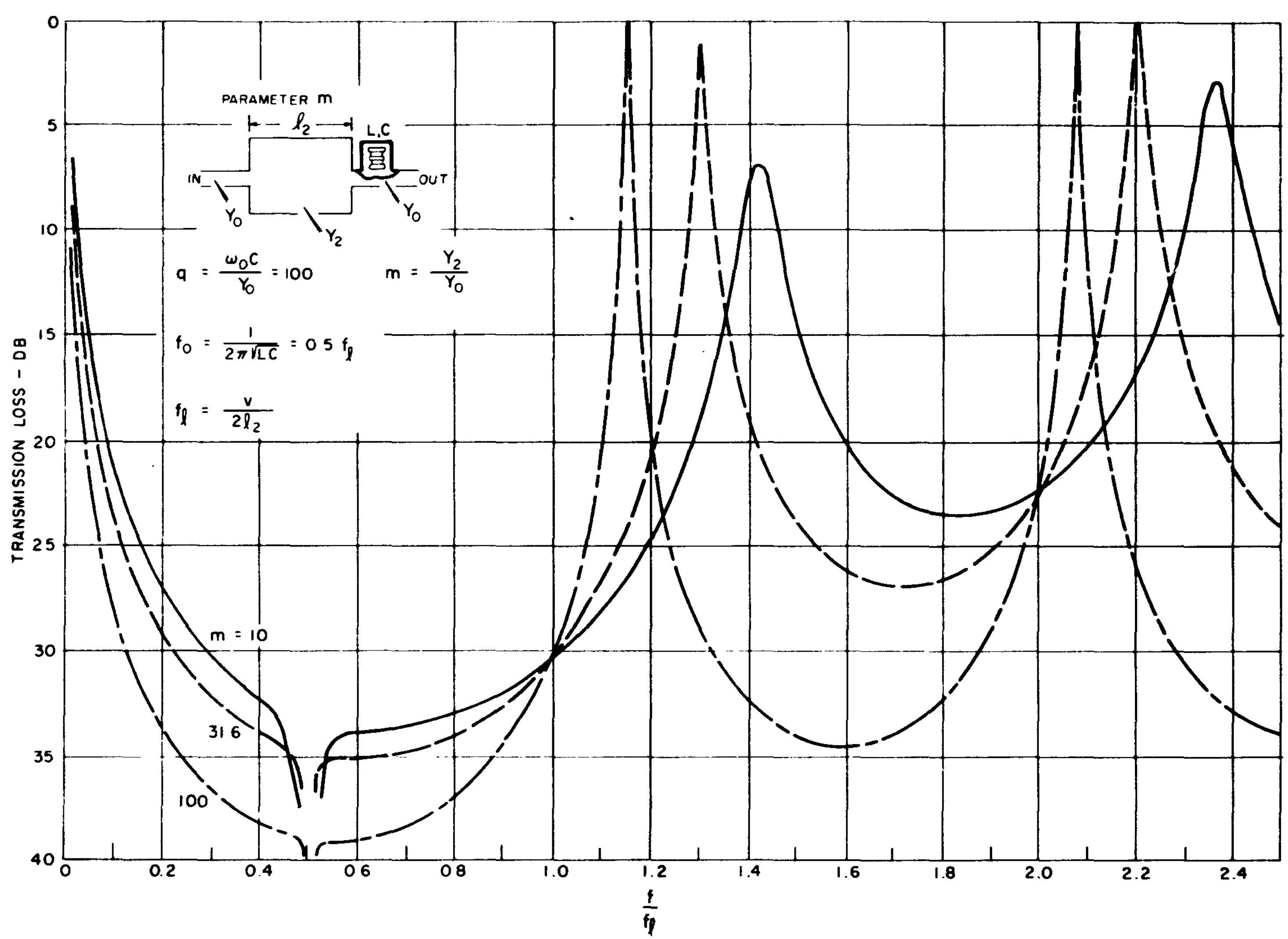

FIGURE 44
COMBINATION FILTER (EXPANSION CHAMBER AND LUMPED PARAMETER SIDE BRANCH)

DRL - UT
DWG BS 6955
JVK - BEE
10 - 24 - 62

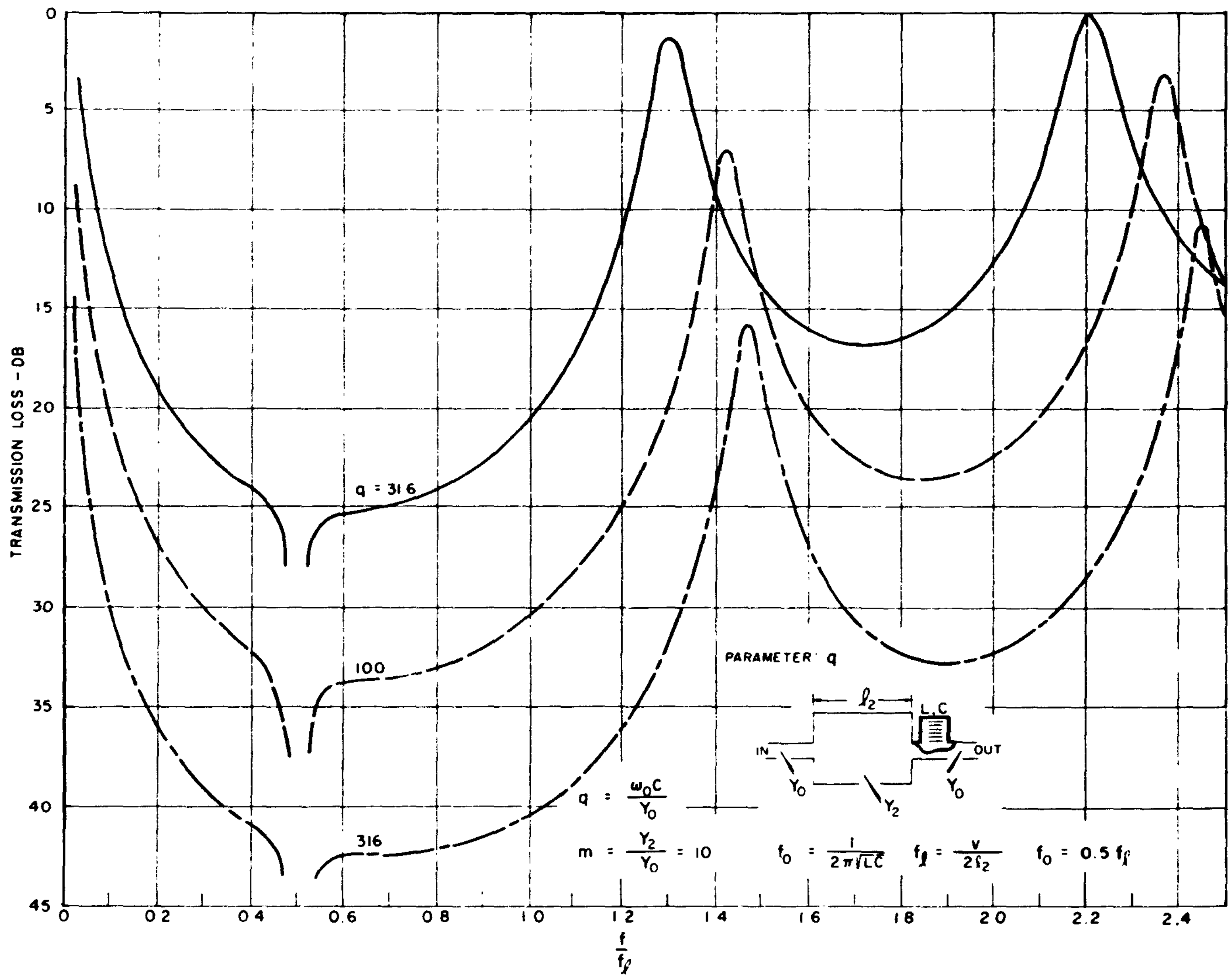

FIGURE 45
COMBINATION FILTER (EXPANSION CHAMBER AND LUMPED PARAMETER SIDE BRANCH)

DRL - UT
DWG BS 6956
JVK - BEE
10 - 24 - 62

5. Combination of Expansion Chamber and Closed-End Tube

When a closed-end, side-branch tube is combined with an expansion chamber, repeated rejection bands and repeated infinities of transmission loss are expected. The curves are drawn for a chamber m = 10 and the side-branch tube q' = 1. The side-branch tube may be placed on either end of the chamber, and it may communicate with the pipe or chamber as long as it is close to the junction of pipe and chamber.

As noted in the previous figures, the maxima of transmission loss for an expansion chamber occur at the frequency that makes the chamber length odd multiples of $\lambda/4$, and the closed-end side-branch tube produces an infinity when its length is also an odd multiple of $\lambda/4$. As shown in Fig. 46, for $\ell_1 = \ell_2$, this condition produces an infinity at each transmission loss maximum.

When the side-branch length is half the chamber length, the infinities of the closed tube coincide with odd numbered zeros of the chamber. This condition is shown as the curve for $\ell_1/\ell_2 = 0.5$. The infinity prevails, but the rest of the curve is little changed from the chamber alone. It will be shown later that larger q' results in a greater change in chamber characteristics.

When the side-branch tube length is 1/3 the chamber length, the first infinity occurs in the center of the second rejection band. The succeeding infinities occur at odd multiples of this frequency. Thus, they will occur in the center of the second, fifth, eighth, eleventh, etc., rejection bands.

The value of q' is varied for the case of equal chamber and side-branch lengths, and the resulting transmission loss curves are presented in Fig. 47. Some wide band improvement over the chamber alone is noted, and the transmission loss infinity is present even for q' = 1. However, the characteristics do not improve rapidly with q'. A filter of this type would be useful for attenuating the fundamental and odd harmonics of a periodic noise source. This filter would be undesirable for use with a source having strong, even harmonics since they would pass through the filter without attenuation.

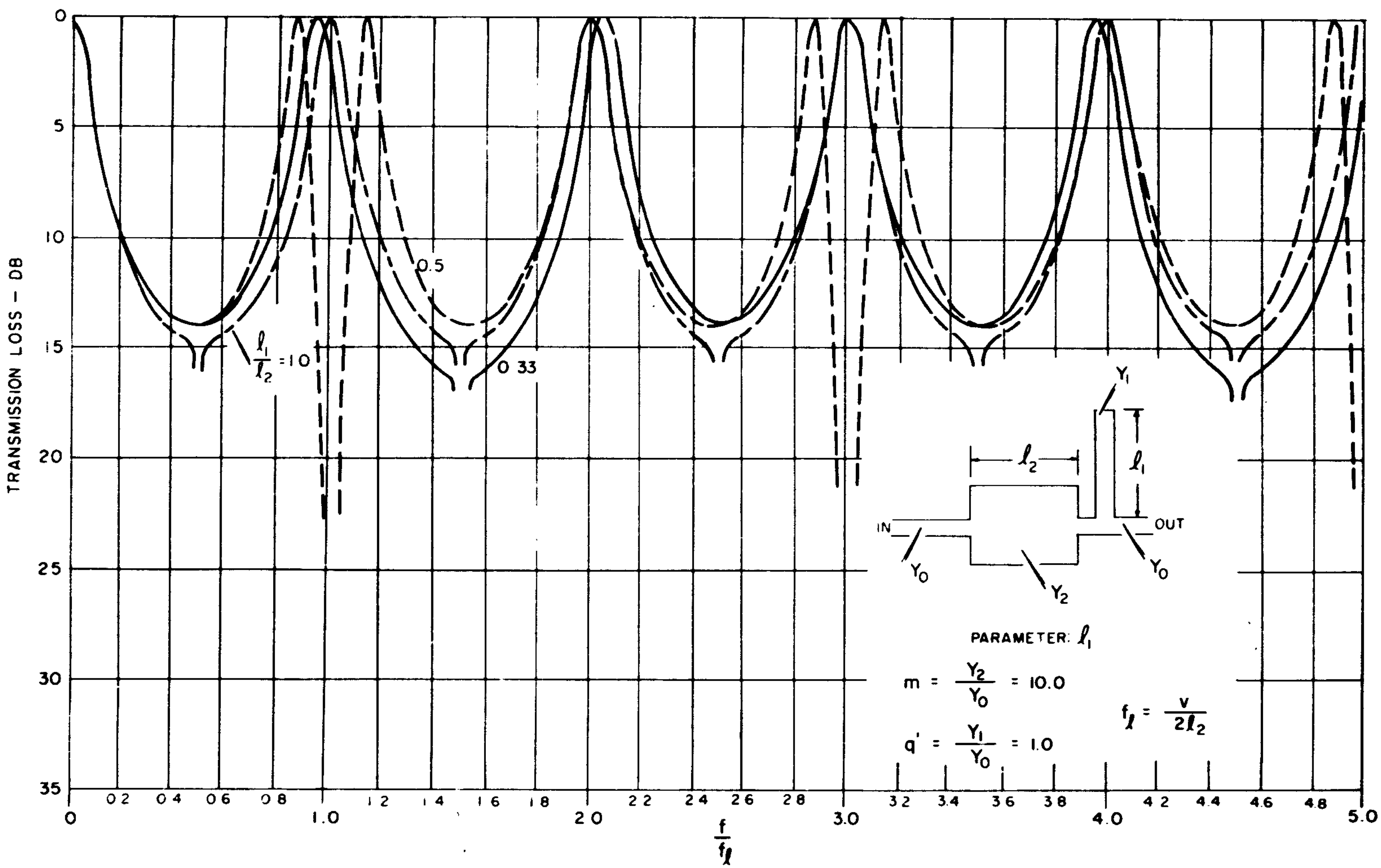

FIGURE 46
COMBINATION FILTER (EXPANSION CHAMBER AND LIQUID-FILLED SIDE BRANCH)

DRL - UT
DWG BS G957
JJK - BEE
10 - 16 - 62

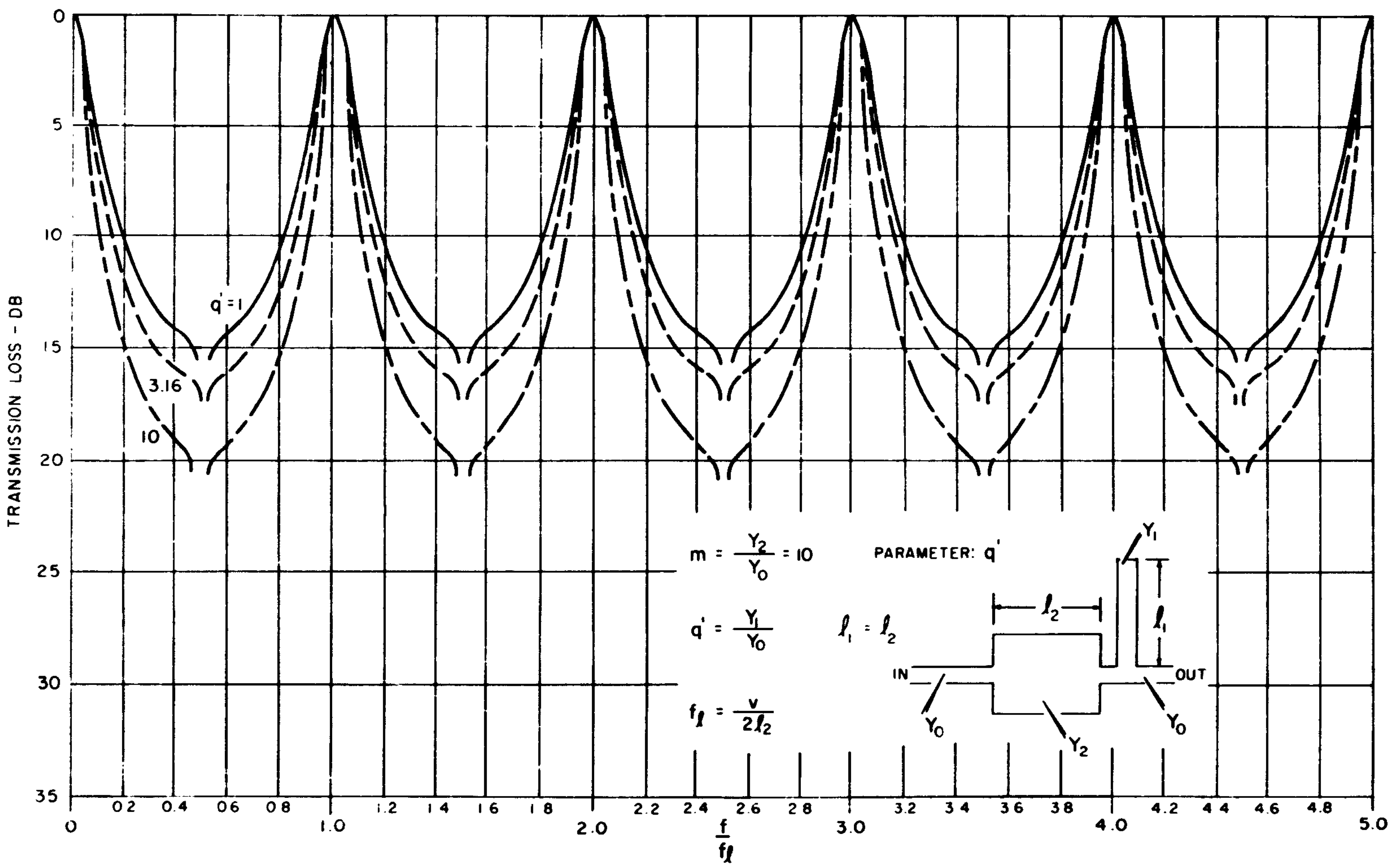

FIGURE 47
COMBINATION FILTER (EXPANSION CHAMBER AND LIQUID-FILLED SIDE BRANCH)

DRL - UT
DWG BS 6958
JVK - BEE
10 - 17 - 62

The value of m for the expansion chamber has a more pronounced effect on transmission loss than does q' for the side-branch tube. This dependence is shown in Fig. 48 for the same length conditions as in Fig. 47. The loss increases about 10 dB for each 10 dB increase in m.

A combination expansion chamber and closed-end tube filter, attractive because of its physical configuration, is shown in Fig. 49. Here the side-branch tube is placed coaxially about the pipe and the branch tube is just an extension of the chamber. This arrangement is usually called a "re-entrant tube expansion chamber filter." The length of the side-branch tube is determined by the protrusion of the pipe into the enlarged section, and the rest of the enlarged section is the chamber. When m is varied, as in this figure, the value of q' also varies. When the wave velocity in all parts of the system is the same, the values of m and q' are related as follows:

$$q' = m - 1 \quad .$$

The curves presented here are calculated for this condition with the tube length equal to chamber length.

Figure 50 presents the condition for the tube length equal to half the chamber length. Here the tube-produced infinity coincides with the chamber zero. Infinities occur at odd multiples of the tube resonant frequency; for large m, a fairly wide rejection band about these frequencies results.

Two sections of the re-entrant tube filters just discussed are cascaded in a special way to produce the double chamber re-entrant tube filters shown in Figs. 51, 52, 53, and 54. Two chambers are butted together and joined by a small connecting tube. The length of the closed-end, side-branch tube is then half the length of the connecting pipe. The acoustical length of the connecting pipe is modified by end effects. From the figures, the physical length of the connecting pipe, ℓ_3, is $\ell_2 + \ell_4$. The acoustical length is then

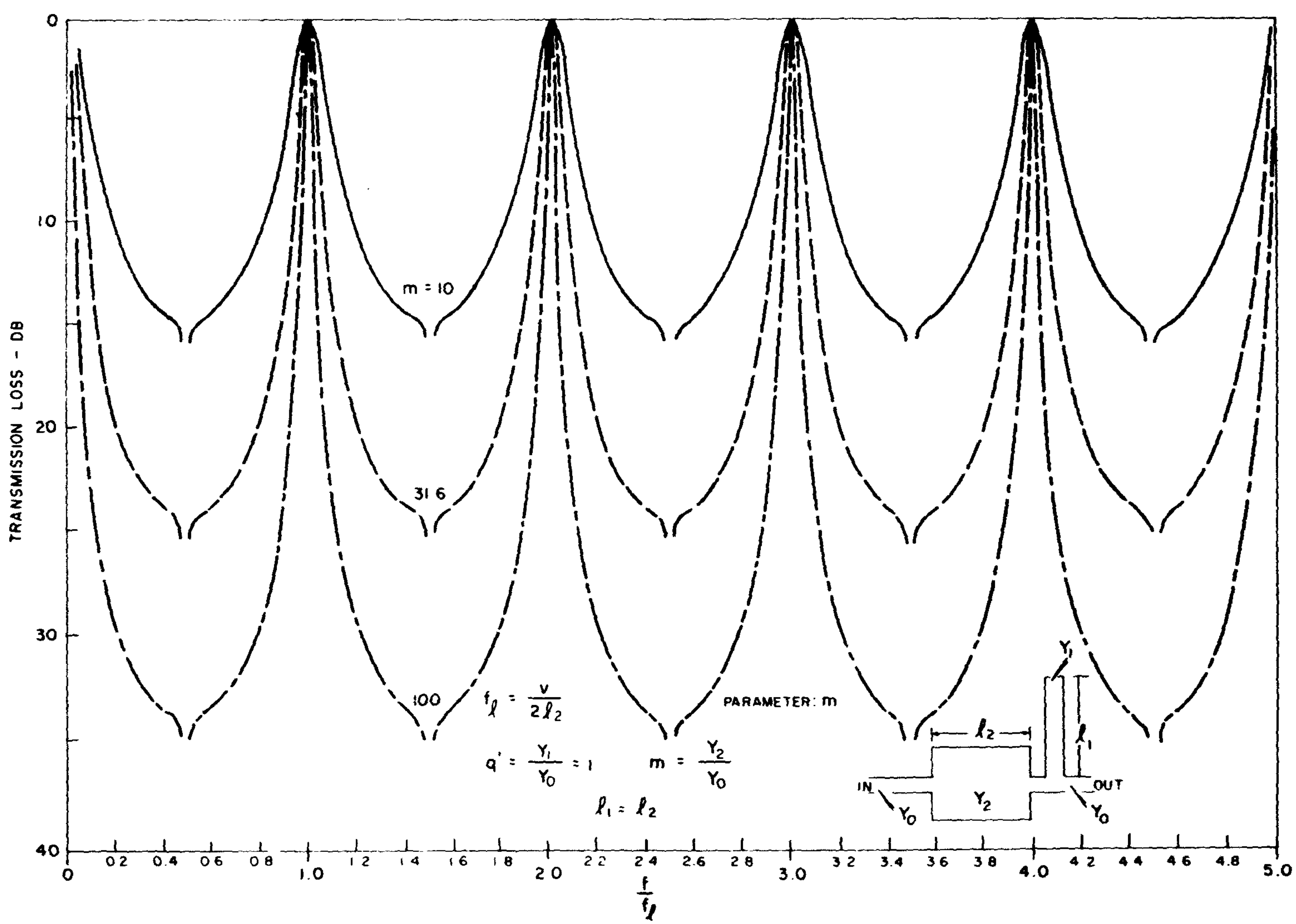

FIGURE 48
COMBINATION FILTER (EXPANSION CHAMBER AND LIQUID-FILLED SIDE BRANCH)

DRL - UT
DWG BS 6960
JVK - BEE
10 - 24 - 62

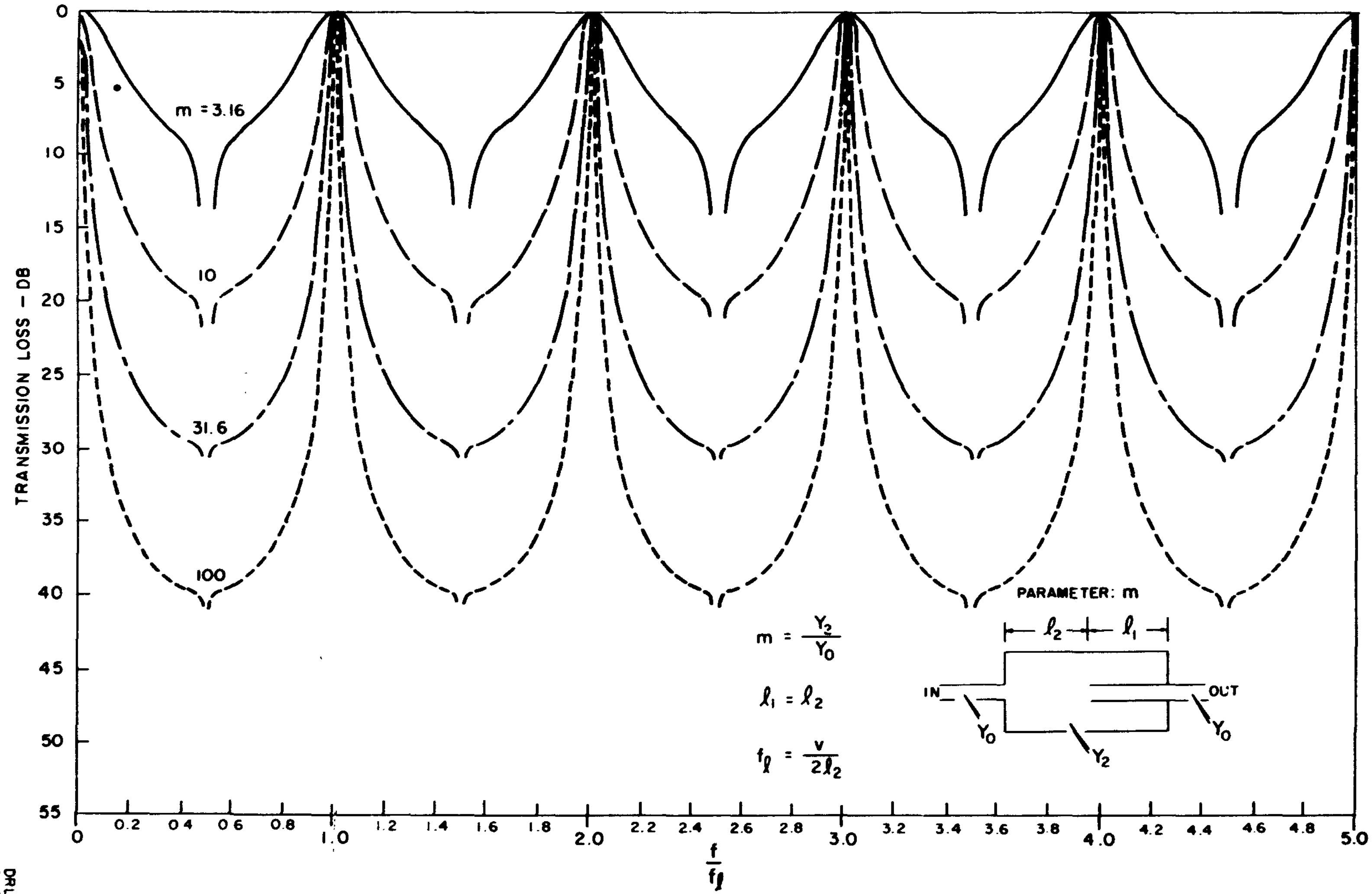

FIGURE 49
SINGLE CHAMBER RE-ENTRANT TUBE FILTER

DRL – UT
DWG BS 6959
JVK – BEE
10 – 24 – 62

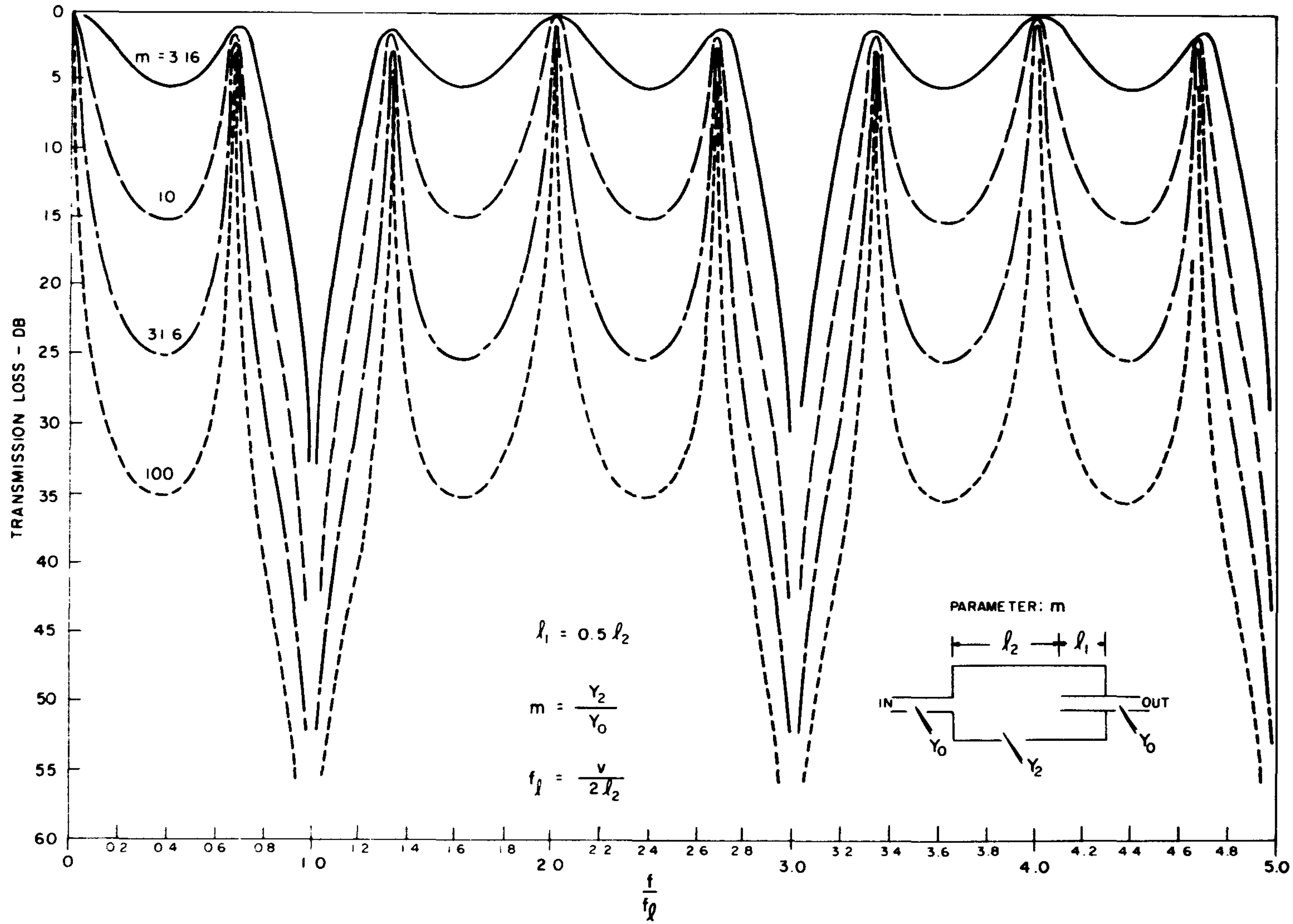

DRL - UT
DWG BS 6961
JVK - BEE
10 - 24 - 62

FIGURE 50
SINGLE CHAMBER RE-ENTRANT TUBE FILTER

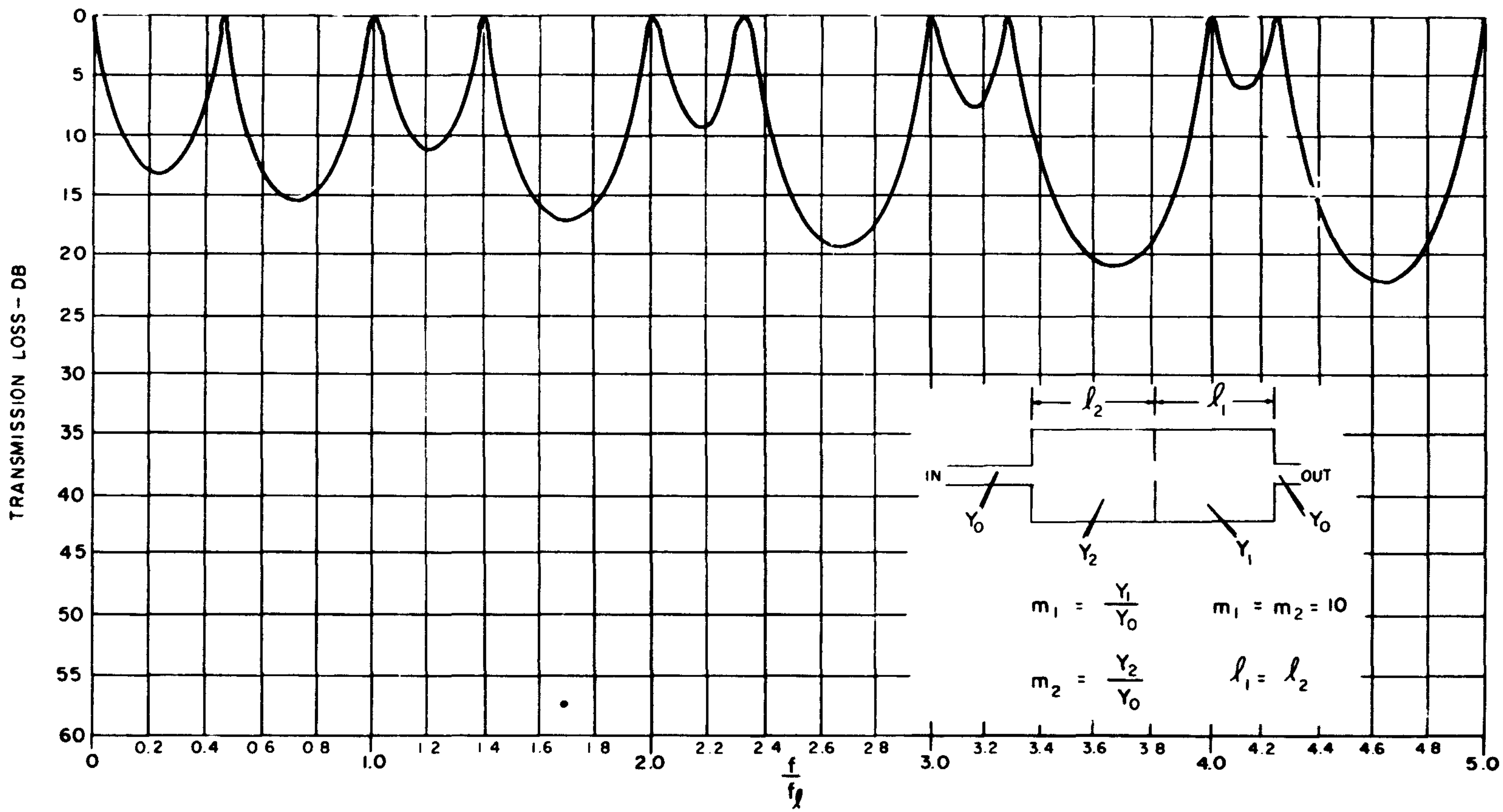

FIGURE 51
DOUBLE CHAMBER ORIFICE PLATE FILTER

DRL - UT
DWG BS 6965
JVK - BEE
12 - 10 - 62

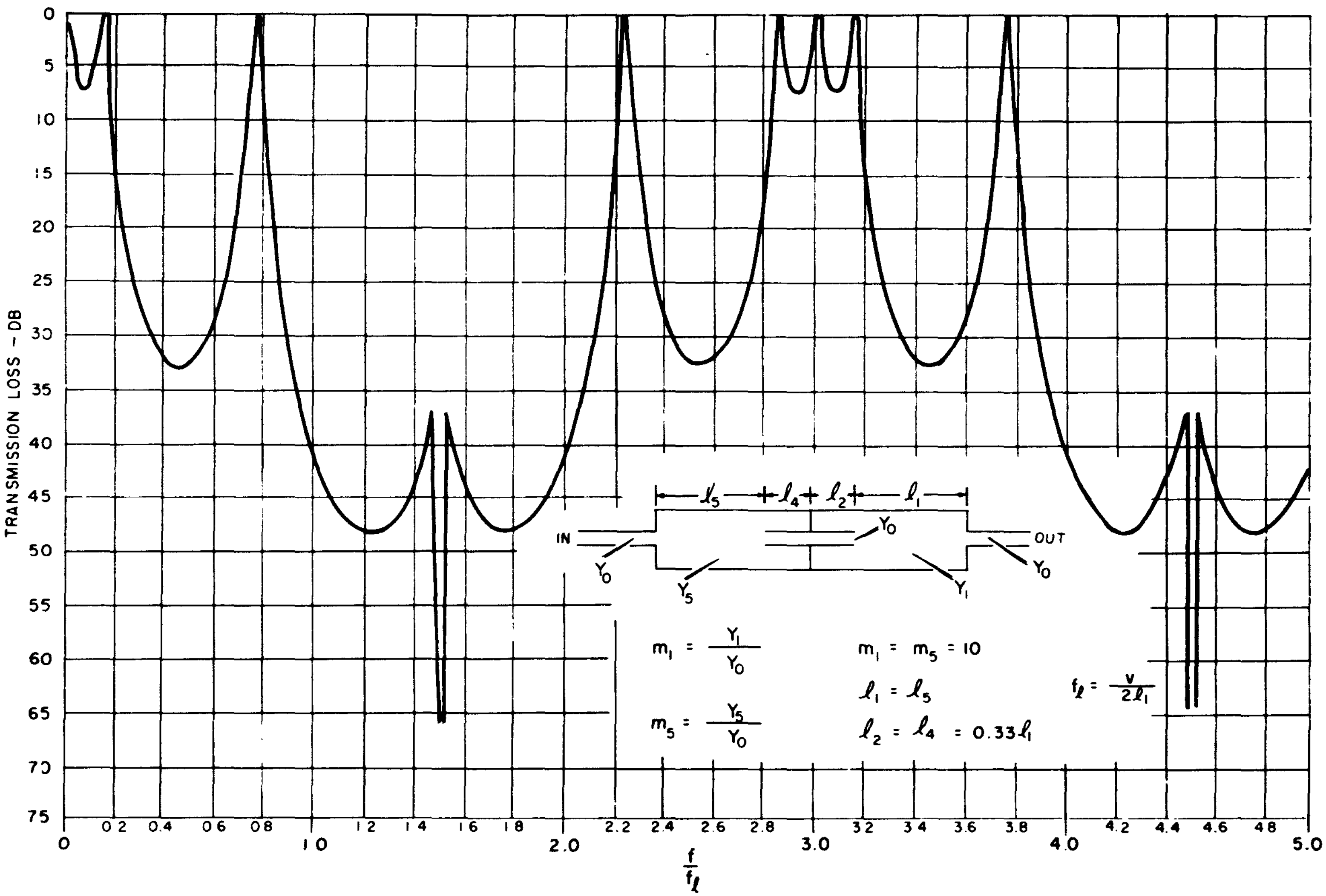

FIGURE 52
DOUBLE CHAMBER RE-ENTRANT TUBE FILTER

DRL - UT
DWG BS 6962
JVK - BEE
10 - 12 - 62

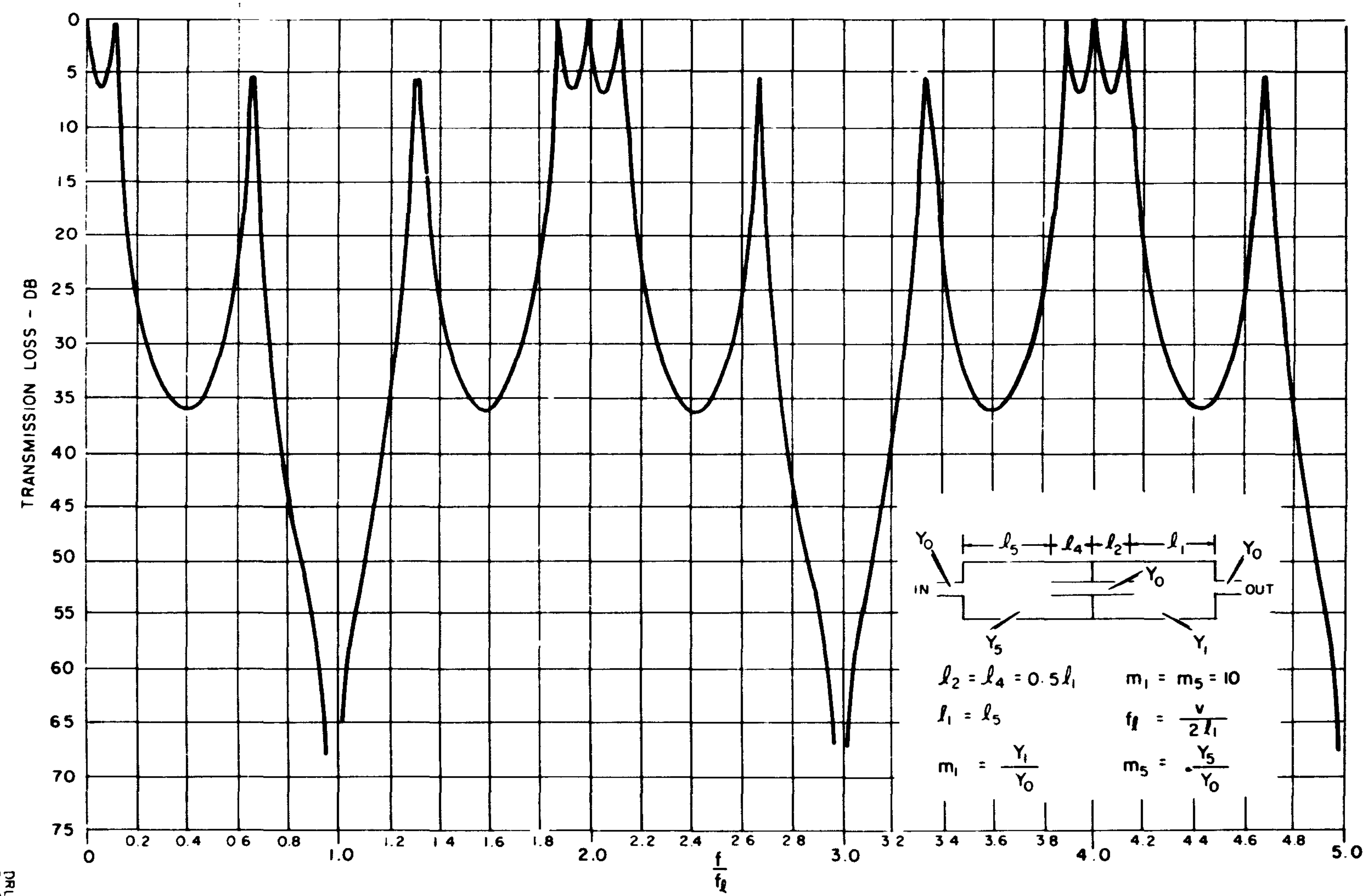

DRL - UT
DWG BS 6963
JVK - BFS
10 - 15 - 62

FIGURE 53
DOUBLE CHAMBER RE-ENTRANT TUBE FILTER

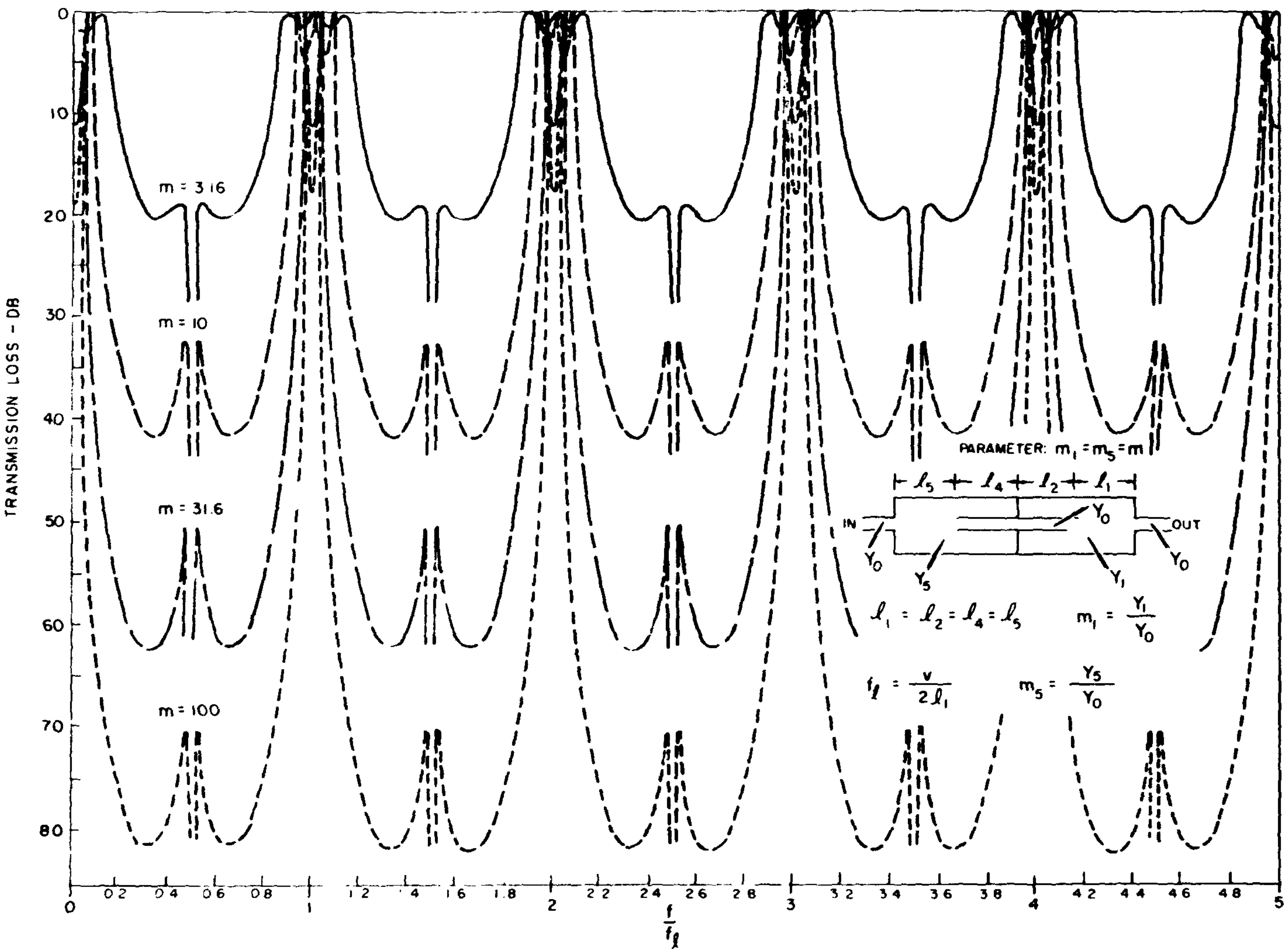

FIGURE 54
DOUBLE CHAMBER RE-ENTRANT TUBE FILTER

DRL - UT
DWG BS 6964
JVK - BEE
10 - 12 - 62

$$l_\alpha = l_3 + 0.8\sqrt{S} \quad ,$$

where S is the connecting pipe section area.

The filter in Fig. 51 is referred to as an orifice plate type. Calculations for it were made for a connecting tube length of $0.8\sqrt{S}$. Any resonant effect of a closed-end, side-branch of length $0.4\sqrt{S}$ was neglected since the resonant frequency would be very high, and it is doubtful that it would be observed in a physical system.

From the transmission loss curve it is noted that at low frequencies, the response is very nearly that for a single expansion chamber (Fig. 33) of length $l_1 + l_2$. At high frequencies, the response approaches the response of a two-section filter with short connecting tube (Fig. 35). Here, and in curves to follow, frequency is normalized to the half-wavelength frequency $f_l = \frac{v}{2l}$ for one chamber.

The case for a closed-end tube length of 1/3 the chamber length is shown in Fig. 52. A marked improvement over the single chamber of Fig. 47 is noted. Transmission loss infinities are produced along with wide rejection bands centered on these frequencies.

The double chamber re-entrant tube filter of Fig. 53 has a closed-end tube length of 1/2 the chamber length. This transmission loss characteristic is almost identical in shape to the single chamber filter of Fig. 50. In fact, the curve for m = 100 in Fig. 50 is almost identical to that of Fig. 53 which is drawn for m = 10. This gives the designer the choice of using the single section of Fig. 50 with a chamber diameter about 10 times the pipe diameter, or using the double chamber of Fig. 53 with about three times the pipe diameter but twice the length of the single chamber.

The double chamber re-entrant tube filter with the closed tube length equal to the chamber length is shown in Fig. 54. The curves are similar to those of the single section case of Fig. 49, but the rejection band transmission loss is approximately doubled here. The case for m = 3.16 is of some interest since it gives about 20 dB noise reduction as well as the repeated infinities.

This value of m implies a chamber diameter of only 1.78 times the piping diameter. Although it would be twice as long as a single section filter to provide the same general characteristics, it would be much smaller in diameter than the single chamber.

6. Quincke Tube Filter

The Quincke tube is a filter that can be made from standard piping system components. Only "tees," "els," and straight lengths of pipe are required. As shown in Fig. 55, the filter consists of two parallel paths of unequal length. The filter does not have any broad band characteristic when the pipes of the filter are the same size as the rest of the system piping. It does have transmission loss infinities which depend on the sum and difference of the pipe lengths. It has the ability to produce an infinity at harmonically related frequencies. Thus, the Quincke tube filter can be used to suppress the fundamental and all the harmonics of a periodic noise source.

The frequencies of the harmonically related infinities are determined by the sum of the tube lengths, and they occur when the sum of the lengths is any multiple of a wavelength. If, however, the difference of the pipe lengths is any multiple of a wavelength at the same frequency as one of the above infinities, the infinity is nullified and a zero is produced as in Fig. 56.

Independent infinities are produced at frequencies that make the length difference an odd multiple of a half-wavelength. In Fig. 55 the first infinity produced by the length differences, f_{20}, is 1.345 times f_{11}, the first infinity produced by the length sum. In Fig. 56, $f_{20} = 1.5 f_{11}$. This nullifies the infinities at $f/f_{11} = 3, 6, 9, \ldots$.

The Quincke tube produces infinities by virtue of phase cancellation of acoustic waves traveling different path lengths. If the pipes for the two paths do not have identical characteristic admittances, complete cancellation will not occur and finite transmission loss maxima will occur instead of infinities.

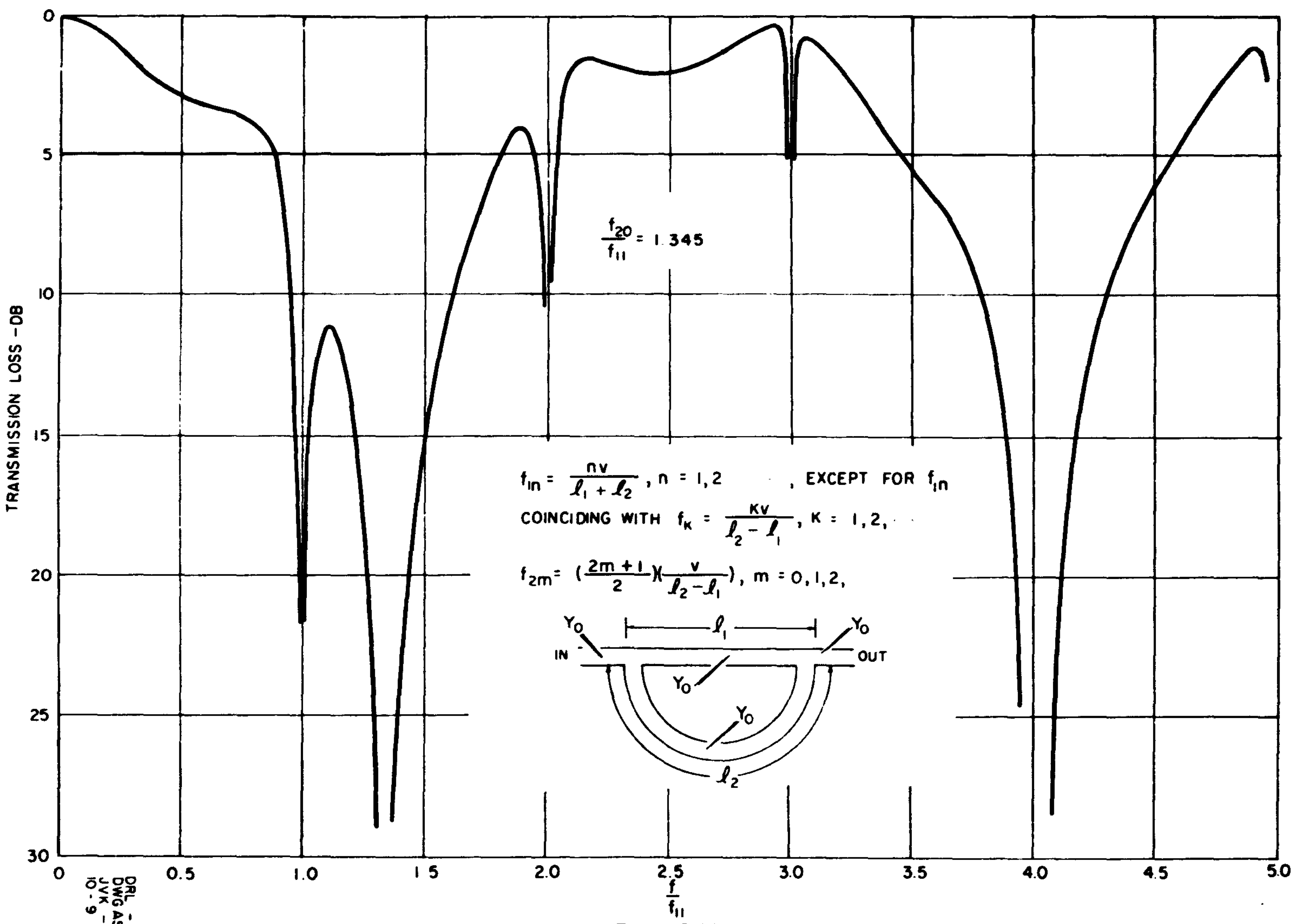

FIGURE 55
QUINCKE TUBE FILTER

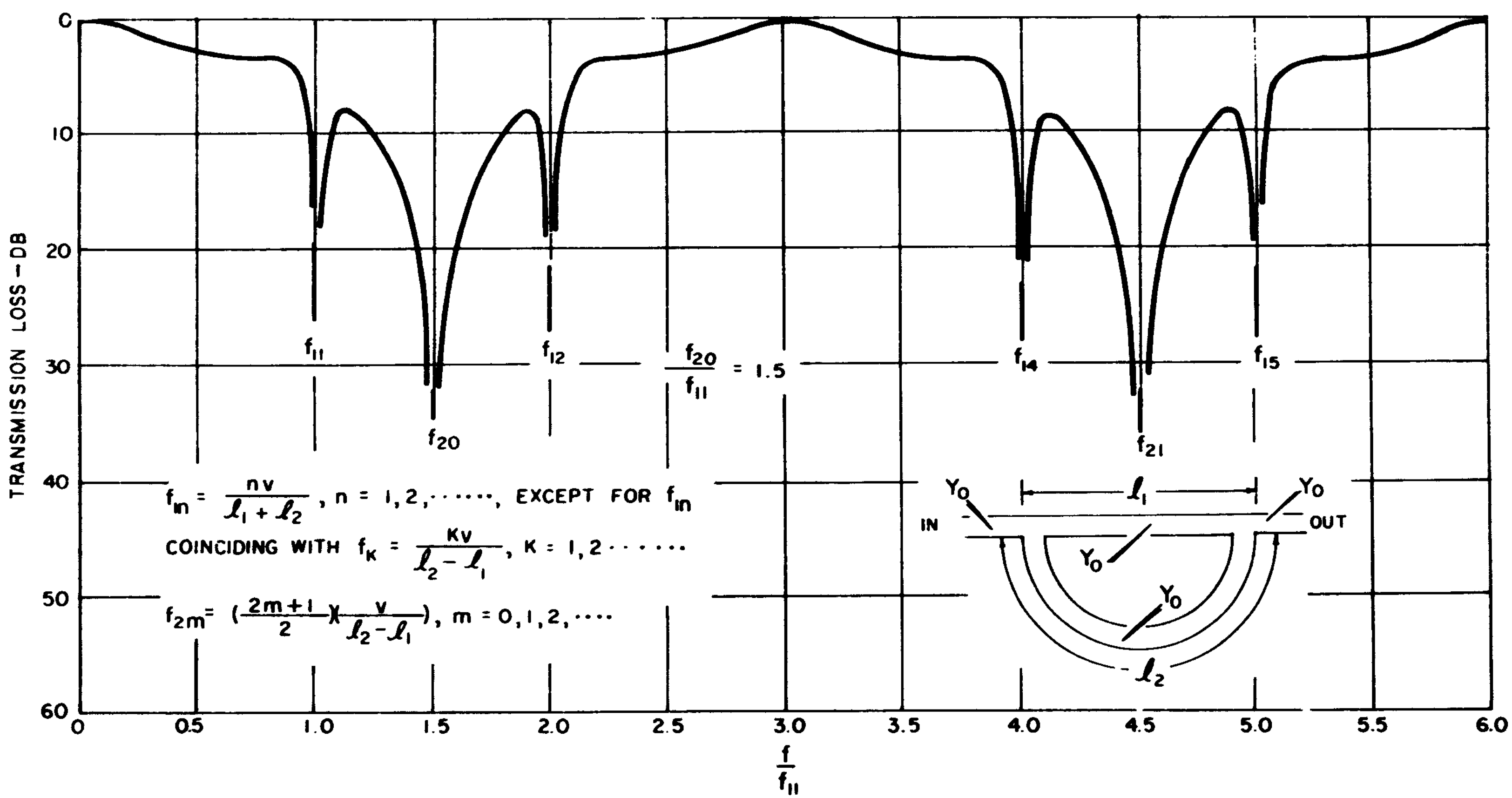

FIGURE 56
QUINCKE TUBE FILTER

DRL - U
DWG AS 69
JVK - BE
10 - 9 - 6

C. CALCULATION OF FILTER PARAMETERS

In order to be able to use the transmission loss curves just presented, in the design of acoustic filters, several acoustical quantities must be calculated from physical quantities of the piping system. The acoustical terms required for a particular filter must also be reduced to physical elements. This section will provide instruction and aids to these several computations.

1. Sound Velocity in Pipes

The velocity of sound waves in a liquid of infinite extent is determined by the liquid compressibility, κ, and its mass density, ρ:

$$v_o = \frac{1}{\sqrt{\rho\kappa}} \quad .$$

Liquid confined in a pipe will not propagate sound waves at this same velocity because of the mass and compliance of the pipe walls. The pipe wall material and thickness, and pipe inside diameter determine the mass and compliance. The resulting sound wave velocity can be calculated for particular liquids in particular pipes. This has been done for several liquids in several kinds of pipe, and the velocity has been plotted versus pipe diameter. Families of these curves with wall thickness as a parameter are presented in Appendix A (Figs. A-3 through A-17).

To determine the sound wave velocity in the liquid in a piping system, the curve for the liquid and pipe material should be located. Enter the curves at the pipe inside diameter and read the value of velocity in ft/sec from the curve for the pipe wall thickness. If the actual wall thickness falls between the values for which curves are drawn, linear interpolation will give adequate accuracy. The procedure to follow is given in an example:

Find the sound wave velocity in sea water contained in 3" brass tubing. The nominal outside diameter is 3" and the nominal wall thickness is 0.148".

The inside diameter is then

$$\text{i.d.} = 3 - 2 \times 0.148 = 2.704 \quad \text{in.}$$

The curves (Fig. A-7) are entered at i.d. = 2.7", but the thickness lies between 1/8" and 3/16". The velocity can be determined by reading the values for thicknesses of 1/8" and 3/16" and performing the following calculations:

$$v(0.148) = v(1/8) + [v(3/16) - v(1/8)] \times \frac{\alpha - 1/8}{3/16 - 1/8}$$

where α is wall thickness in inches. This becomes

$$v(0.148) = 4200 + (4400 - 4200) \times \frac{0.023}{0.0625} = 4274 \quad \text{fps} .$$

It has been mentioned previously that the propagation of higher order propagation modes should be prevented. This requirement places a limitation on piping or chamber diameter. The cutoff frequencies below which these modes will not propagate are given by

$$f_{mn} = \frac{v_o}{d} \alpha_{mn} ,$$

where v_o is the wave velocity in an infinite medium, d is inside pipe diameter, and α_{mn} is a quantity with a different value for each mode. Various values are given below:

Values of α_{mn}

m/n	0	1	2
0	0	1.22	2.23
1	0.586	1.697	----
2	0.972	-----	

The cutoff frequency of greatest concern is the lowest one. This will be given by the smallest value of α_{mn}, 0.586; all other values not shown are larger. The limits on pipe diameter can then be written in terms of the smallest value of α_{mn} and the highest frequency at which noise reduction is required. The maximum inside pipe diameter is then

$$d_{max} = 0.586\ v_o/f_{max} \quad ,$$

where d_{max} is in inches if v_o is in inches/sec.

For brass pipe in a sea water system and an upper frequency of interest equal to 1 kc, the maximum pipe inner diameter is found as follows:

The value of v_o is found on Fig. A-7 in Appendix A as 5030 fps. The maximum i.d. is then

$$d_{max} = 0.586 \times 5030 \times 12/1000 = 35.5 \quad \text{in.} \quad .$$

2. Characteristic Admittance of Pipes

The ratio of volume velocity to sound pressure in a sound wave traveling in the liquid in a pipe is the characteristic admittance of the pipe. This quantity, Y_o, is necessary for many calculations in acoustic filter design. In common pipe and liquids there is very little absorption of acoustic energy at the frequencies of interest here. In this case Y_o is a real number that is given by

$$Y_o = \frac{S}{\rho v} \quad \frac{\text{in.}^5}{\text{lb sec}} \quad ,$$

where S is pipe inside cross section area, ρ is the liquid density, and v is the wave velocity as found above. An aid to finding ρv is found on the velocity of sound curves in Appendix A. A constant (12 times the liquid density) is given; the velocity in ft/sec is multiplied by this constant to give ρv. The inside section area in square inches is divided by this number to obtain Y_o in

$\frac{in.^5}{lb\ sec}$. An alternative to the calculations just suggested is to use the nomograph of Fig. 57. With the nomograph, Y_o can be found by entering the graph with the value of ρv that was just found and reading the value of Y_o where the vertical ρv line intersects the particular inside diameter line. The procedure can be demonstrated by considering the 3" brass tubing of the previous section. The velocity was found to be 4274 fps. This value is multiplied by the number 1.15×10^{-3} as given in Fig. A-7, Appendix A. This gives

$$\rho v = 1.15 \times 10^{-3} \times 4274 = 4.92 \quad \frac{lb\ sec}{in.^3} .$$

Entering Fig. 57 with this value and reading Y_o for an inside diameter of 2.7" gives

$$Y_o = 1.2 \quad \frac{in.^5}{lb\ sec} .$$

This can be compared with the calculated value of 1.195 $\frac{in.^5}{lb\ sec}$

3. Side-Branch Elements

Two types of side-branch elements are used in the acoustic filters described here. One type consists of one of several kinds of lumped-element resonators, and the other is simply a closed-end tube. There are several properties of these elements based on their physical characteristics that are important to acoustic filter effectiveness. The calculation of these quantities will be presented here.

a. Compliance

The lumped side-branch element consists of a compliant element that communicates with the liquid in the piping system. An element such as this may consist of a sealed piston or membrane that is backed by a spring as

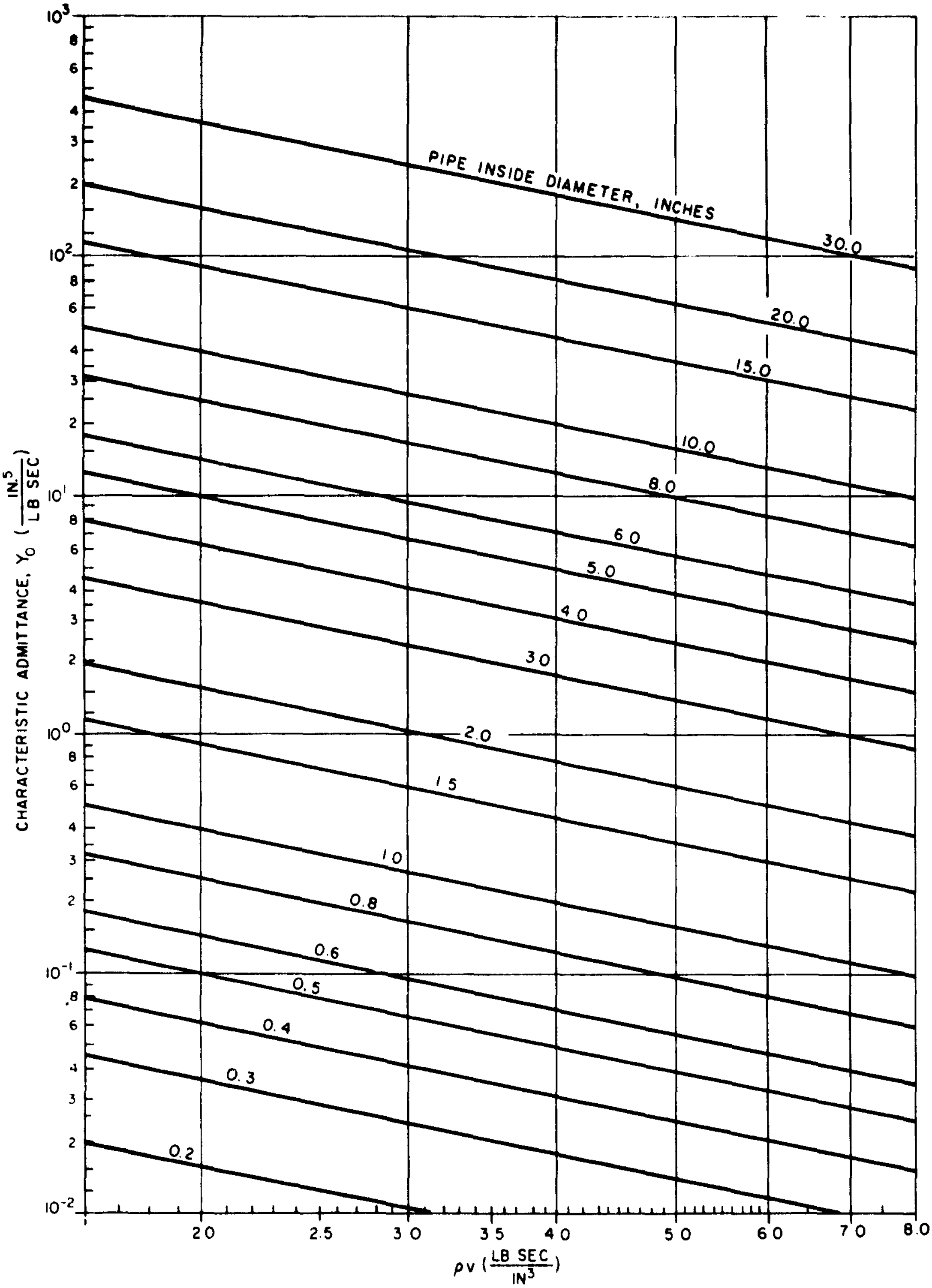

FIGURE 57
CHARACTERISTIC ADMITTANCE

DRL - UT
DWG BS 7123
JVK - BEE
10 - 10 - 62

shown in Fig. 58(a). The spring may be the usual helical type or any other that has a known force-deflection characteristic. An entrapped gas volume may provide a compliance in parallel with the spring. A bellows with sealed ends may provide the compliance as well as the liquid seal. Because of the mass inherent in all these elements, they will resonate at some frequency. This effect can be advantageously used and it will be discussed later.

For the simple spring-piston arrangement of Fig. 58, the acoustical property, compliance, is simply related to the mechanical stiffness of the spring:

$$C = \frac{S^2}{k} \quad \frac{\text{in.}^5}{\text{lb}} ,$$

where S is the piston area in sq in. and k is the spring stiffness in lb/in.. As an aid to computation, a nomograph of this equation is given in Fig. 59. For a known stiffness and piston diameter, the compliance can be read from the vertical scale. The curves may be entered with any two of the variables to find the third. The compliance can be found as above. For a known diameter and a desired compliance, the required spring stiffness may be found. For a given spring and desired compliance, the required area may be found.

A parallel combination of springs such as that shown in Fig. 58(b) may be used to obtain the required stiffness. A bellows that has a small stiffness may be used for the liquid seal then backed by a spring to obtain the required stiffness. In either case, the stiffness of the combination is as follows:

$$k = k_1 + k_2 \quad .$$

Then the compliance becomes

$$C = \frac{S^2}{(k_1 + k_2)} \quad .$$

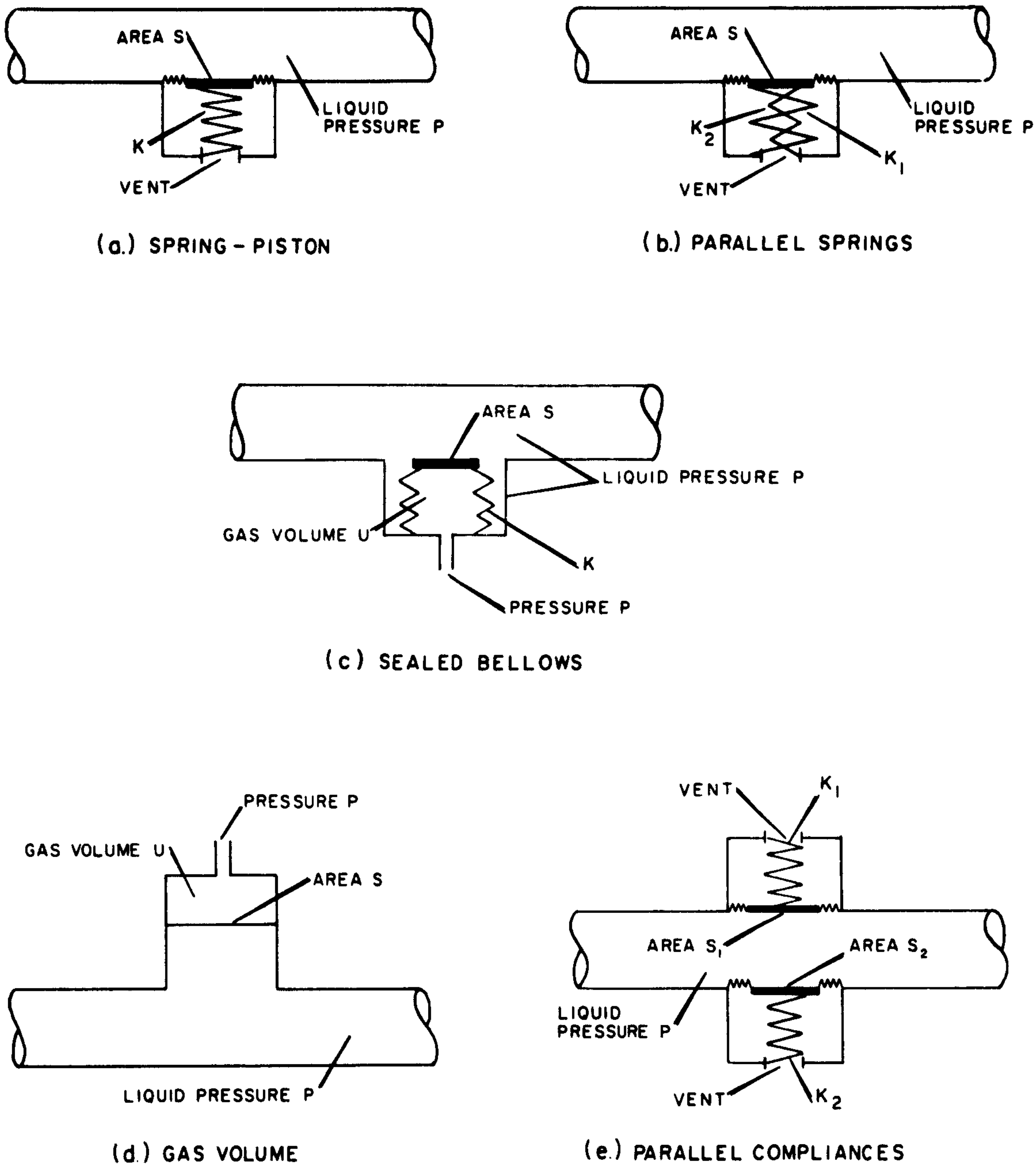

FIGURE 58
COMPLIANT ELEMENTS

DRL - UT
DWG AS 7124
JVK - BEE
9 - 14 - 62

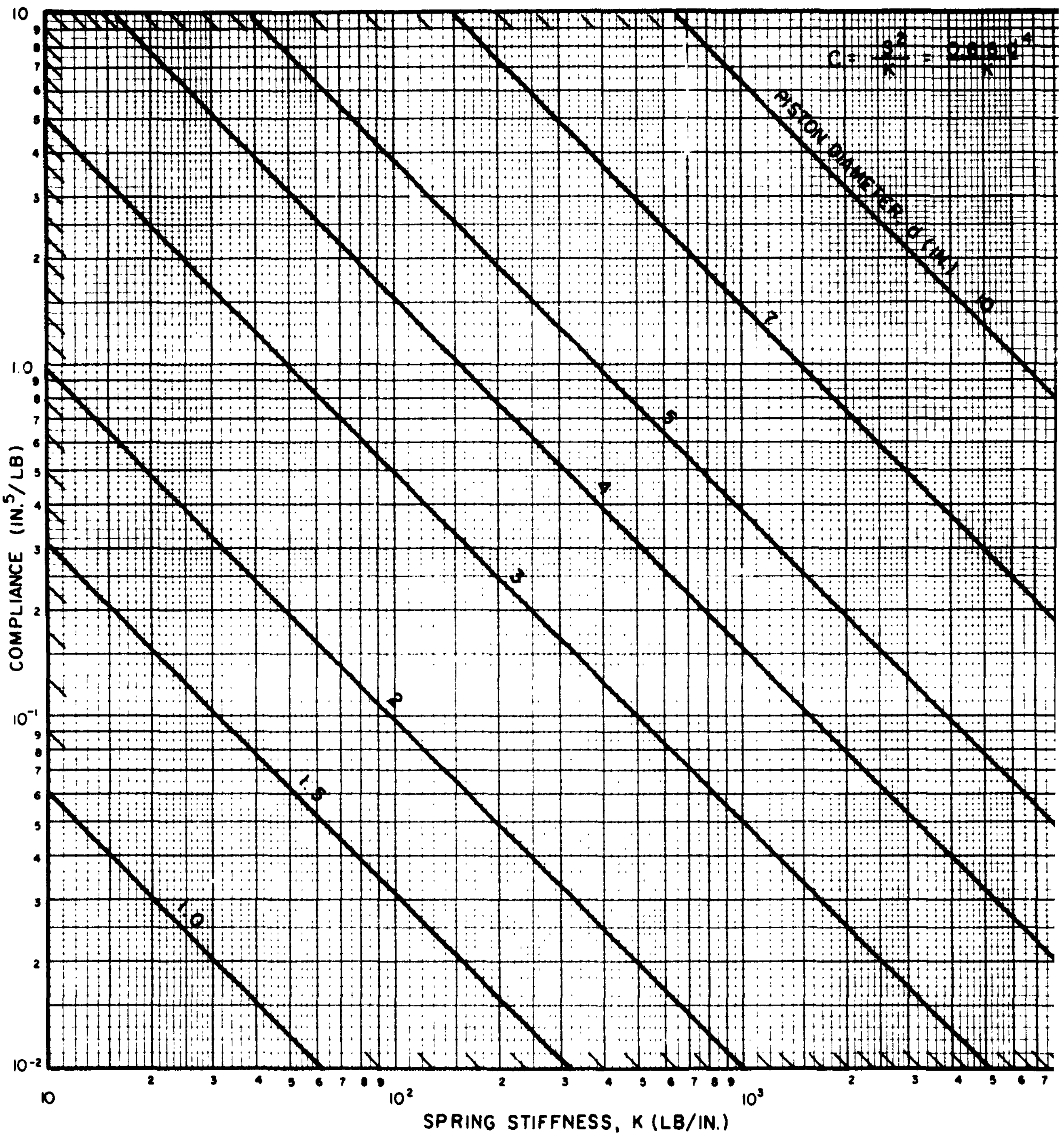

FIGURE 59
STIFFNESS VS COMPLIANCE

DRL - U
DWGAS
JVK - BI
2 - 22 -

For the bellows the <u>effective</u> area must be used. This is somewhat less than that calculated from the outside diameter of the bellows. Effective diameter or area information is usually supplied by the bellows manufacturer.

When a spring-piston or bellows is sealed or pressure compensated on the side away from the liquid, as in Fig. 58(c), the gas volume presents a stiffness in parallel with the spring or bellows. The compliance of such a gas volume is

$$C = \frac{U}{\gamma p}$$

which gives a stiffness of $k_2 = \frac{\gamma p S^2}{U}$ where γ is the ratio of specific heats for the gas, p is the gas pressure, and U is the gas volume. The compliance of the combination is then

$$C = \frac{S^2}{\left(k_1 + \frac{\gamma p S^2}{U}\right)} \quad .$$

Pressure compensation may be desired or even necessary in some situations. When there is a pressure differential across a compliant element, there will be a static deflection of the piston face. As later discussion will show, the static deflection will allow an increase of liquid mass on the piston which changes the characteristics of the element. The displacement will be

$$x = \frac{S\Delta p}{k} \quad ,$$

where Δp is the difference in the liquid pressure and the pressure back of the piston or bellows. For any combination of springs the effective stiffness may be found from Fig. 59 if the total compliance has been determined.

Fig. 58(d) shows a compliant element consisting of an entrapped gas volume. The compliance of the element is then

$$C = \frac{U}{\gamma p}$$

where p is the system pressure.

When more than one compliant element is placed on the pipe at the same place as in Fig. 58(e), the total compliance is the sum of each compliance:

$$C_t = C_1 + C_2 = \frac{S_1^2}{k_1} + \frac{S_2^2}{k_2} \quad .$$

This is derived on the basis that the two elements are acoustically in parallel and their admittances add. Thus, the admittance shunting the pipe at that point is

$$Y_s = Y_1 + Y_2 \quad .$$

b. <u>Inertance</u>

The pistons or bellows that seal the compliant elements just discussed have some mass. This mass gives rise to an acoustical inertance. Such an element is shown in Fig. 60(a). The inertance is given by

$$L = \frac{m}{S^2} = \frac{W}{S^2 g} \quad \frac{\text{lb sec}^2}{\text{in.}^5} \quad ,$$

where S is the piston area, and m is its mass which is also its weight W divided by the acceleration due to gravity. Here area is in square inches, W is in pounds, and g is 386.4 $\frac{\text{in.}}{\text{sec}^2}$. An aid to computation is provided by the nomograph of Fig. 61. The curve may be entered with any two of the quantities (weight, piston diameter, and inertance), and the third can then be found.

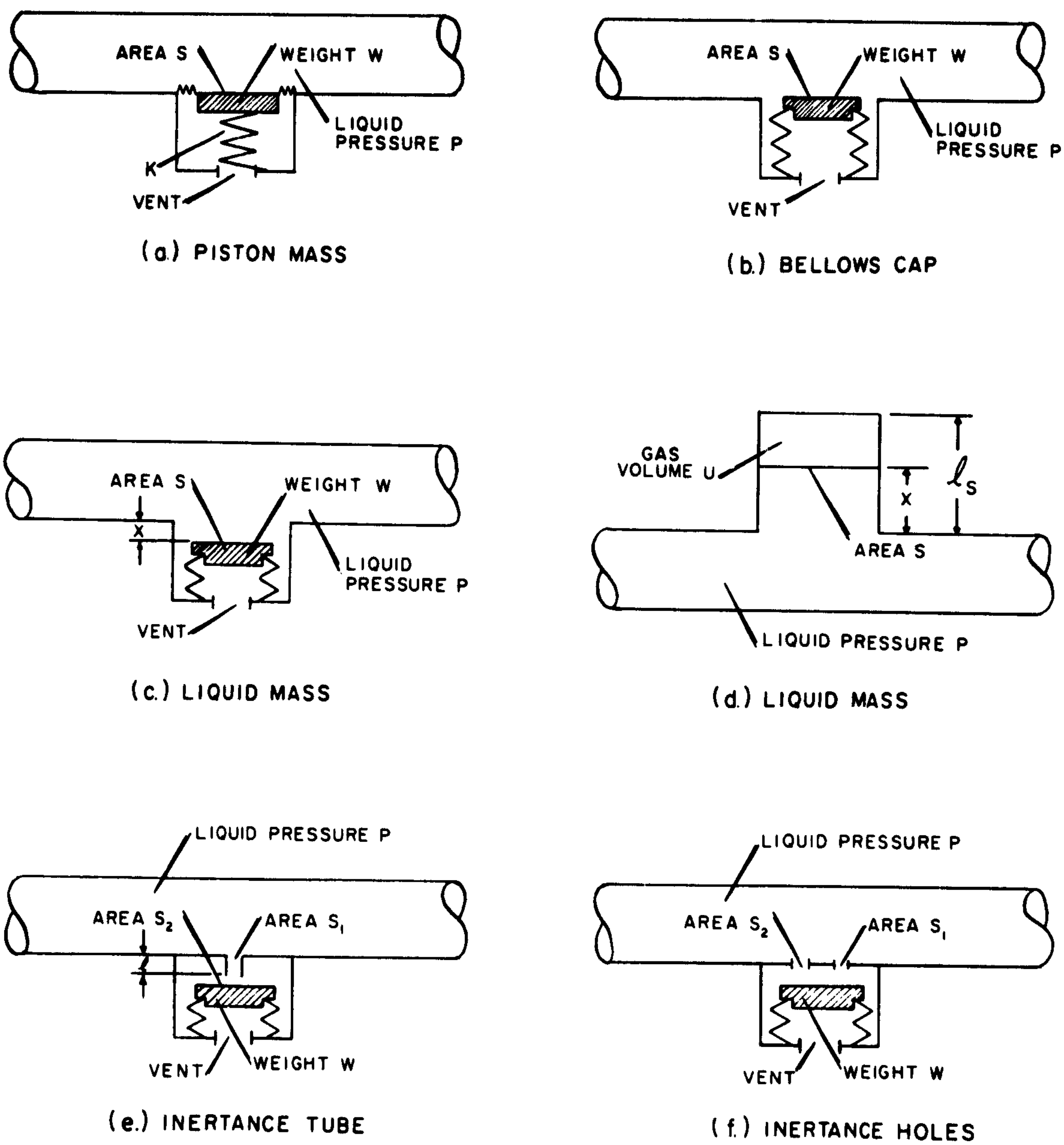

FIGURE 60
INERTANCE ELEMENTS

DRL - UT
DWG AS 7126
JVK - BEE
9 - 12 - 62

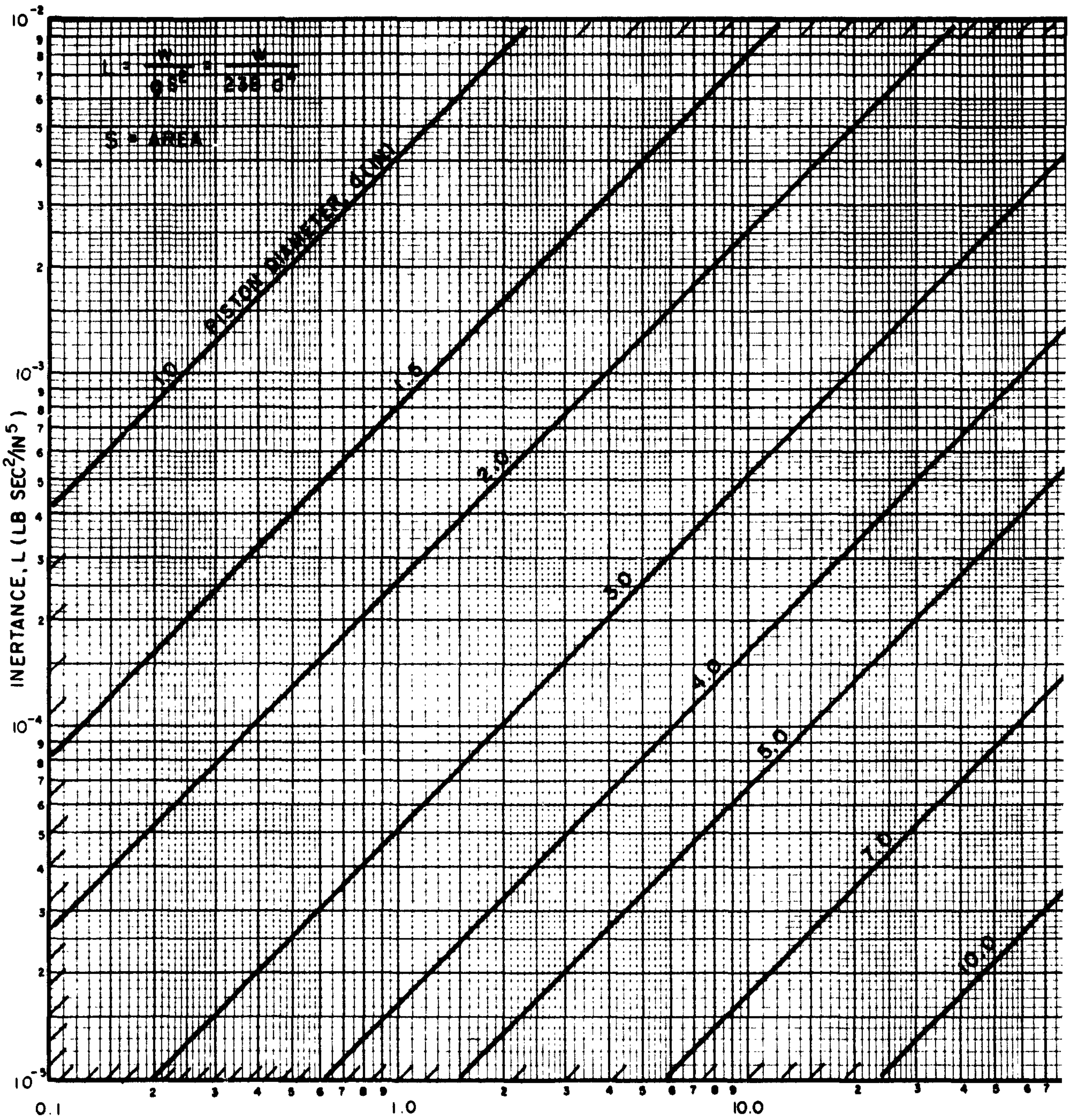

FIGURE 61
WEIGHT VS INERTANCE

DRL - UT
DWG AS 7127
JVK - BEE
2 - 22 - 63

For the physical arrangement of the side-branch elements, the mass is backed by a spring that also has mass. The total weight required to compute inertance is then the piston weight plus 1/3 the spring weight. This fraction of the spring weight is its effective vibrating weight.

The two elements here, spring and mass, have a common volume velocity and divide the force caused by the acoustic pressure. Thus, they are in series, and the acoustic impedances add. The impedance is then

$$Z_s = j\omega L + \frac{1}{j\omega C} \quad \frac{\text{lb sec}}{\text{in.}^5} ,$$

and the admittance shunting the pipe is then

$$Y_s = \frac{1}{j\omega L + \frac{1}{j\omega C}} \quad \frac{\text{in.}^5}{\text{lb sec}} .$$

The bellows that is provided with a cap to seal it, as in Fig 60(b), is completely analogous to the spring-piston of Fig. 60(a). The inertance is calculated in the same way by using the effective area of the bellows and the weight of the cap plus 1/3 the bellows weight.

As shown in Fig. 60(c), when the end of the bellows or piston is recessed a distance away from the pipe by placement or by compression of the spring by liquid pressure, a mass of liquid is added to the piston mass. The inertance of the liquid is

$$L_1 = \frac{\rho x}{S} = \frac{wx}{Sg} \quad \frac{\text{lb sec}^2}{\text{in.}^5} .$$

The weight of the liquid per cubic inch is w, x is in inches, S is the piston or bellows effective area in square inches, and g is 386.4 $\frac{\text{in.}}{\text{sec}^2}$. The inertance of the piston is in series with the inertance of the liquid, and the total value is

$$L_t = \frac{W}{S^2 g} + \frac{wx}{Sg} \quad \frac{\text{lb sec}^2}{\text{in.}^5} \ .$$

The inertance in the side-branch element may consist of liquid mass only as in Fig. 60(d). If the side-branch pipe was air- or gas-filled at some pressure p_o (say atmospheric pressure) before the addition of the liquid, then after the system is liquid-filled to some pressure p the distance x would become

$$x = \ell_s \left(1 - \frac{p_o}{p}\right) \quad \text{in.} \ ,$$

where ℓ_s is in inches and the pressures are psia. If the gas volume is regulated, the value of x may be determined by the regulator. In either case the inertance is given by

$$L = \frac{wx}{Sg} \quad \frac{\text{lb sec}^2}{\text{in.}^5} \ .$$

The gas volume is then

$$U = (\ell_s - x)S \ ,$$

and the compliance can be calculated as shown above.

The inertance produced by a side-branch element can be greatly increased by the addition of an inertance tube as in Fig. 60(e). This tube inertance can be expressed

$$L = \rho \frac{\ell_e}{S_1} = w \frac{\ell_e}{S_1 g} \quad \frac{\text{lb sec}^2}{\text{in.}^5} \ .$$

The effective length ℓ_e is given by

$$\ell_e = \ell + 0.8\sqrt{S_1} \quad \text{in.} \quad ,$$

where ℓ is the physical length and the second term is an end effect that results from the moving liquid beyond the ends of the tube. The inertance presented by the combination of the tube and piston mass is then

$$L_t = \frac{W}{S_2^{\,2} g} + w \frac{\ell_e}{S_1 g} \qquad \frac{\text{lb sec}^2}{\text{in.}^5} \quad .$$

The inertance that can be obtained by such a tube is limited by transmission line effects. For the preceding expressions to hold, the length of the tube must be very much less than a wavelength at the highest frequency of interest. A resistance effect also becomes important when the tube diameter is very much smaller than the tube length.

Inertance may be obtained from a small hole in the pipe wall as shown in Fig. 60(f). The hole becomes an inertance tube of almost zero physical length. The effective length is then just the end correction term. With reference to Fig. 60(f), the inertance of one hole is

$$L_1 = \frac{\rho \ell_e}{S_1} = 1.6 \frac{w}{g\sqrt{\pi d}} \qquad \frac{\text{lb sec}^2}{\text{in.}^5}$$

where w is again the specific weight of the liquid in $\frac{\text{lb}}{\text{in.}^3}$, d is the hole diameter in inches, and g is 386.4 $\frac{\text{in.}}{\text{sec}^2}$.

The two holes shown in the figure are acoustically in parallel, and their admittances add. The inertances then add as reciprocals

$$\frac{1}{L} = \frac{1}{L_1} + \frac{1}{L_2} \quad .$$

The effective diameter of the two holes is then

$$\frac{1}{d_e} = \frac{1}{d_1} + \frac{1}{d_2} \quad .$$

Finally the total inertance presented by the side-branch is

$$L_t = \frac{1.6w}{g\sqrt{\pi}d_e} + \frac{W}{S_3{}^2 g} \qquad \frac{\text{lb sec}^2}{\text{in.}^5} \quad .$$

c. Resonant Frequency

The total shunt admittance of the side-branch element was given above as

$$Y_s = \frac{1}{j\omega L + \frac{1}{j\omega C}} \quad .$$

When the denominator of this expression is zero, Y_s becomes infinite. It is this infinity that gives the transmission loss infinities for the filters discussed in the previous section. If the elements have any friction in the pressure seal or elsewhere, Y_s will not be zero, and the transmission loss will have a maximum but not an infinity. The zero of the denominator occurs at a frequency related to L and C:

$$\omega_o{}^2 = \frac{1}{LC} \qquad \text{sec}^{-2} \quad ,$$

or this resonant frequency is given by

$$f_o = \frac{1}{2\pi\sqrt{LC}} \qquad \text{cps} \quad .$$

When L and C are replaced by their corresponding values of k and W, f_o becomes

$$f_o = \frac{1}{2\pi}\sqrt{\frac{kg}{W}} \quad .$$

Figure 62 presents an aid to calculation for this expression. If the values of inertance and compliance have been determined instead of W and k, the effective weight can be determined from Fig. 61, and the effective stiffness can be determined from Fig. 59.

The resonant frequency is seen to depend on compliance and inertance. Thus, f_o will change if static pressure variations cause changes in x as in Fig. 60(c). In high pressure systems, the resonant frequency must be determined under operating conditions. It is possible to provide pressure regulation or preloading to keep f_o relatively constant. Even the pressure regulation does not maintain a completely constant f_o since the pressurizing gas presents a shunt compliance that varies with pressure.

d. Calculation of q

In the discussion of transmission loss curves for filters, a parameter q was used as a measure of side-branch filter performance. This quantity is defined as the ratio of the admittance of the compliant element to the characteristic admittance of the pipe upon which the side-branch element is placed:

$$q = \frac{\omega_o C}{Y_o} \quad .$$

This parameter is unitless. The curves of Fig. 63 graphically relate $\omega_o C$ and Y_o to q. These curves can be used in several ways. In designing a filter the values of Y_o will be determined by the system piping, and the desired value of q may be selected from the transmission loss curves. Entering Fig. 63 with Y_o and q gives the required product $\omega_o C$. If a certain value of ω_o is desired, the value of C is then fixed. In another possible case, the value of ω_o, C, and Y_o for a particular side-branch element and system piping has been determined.

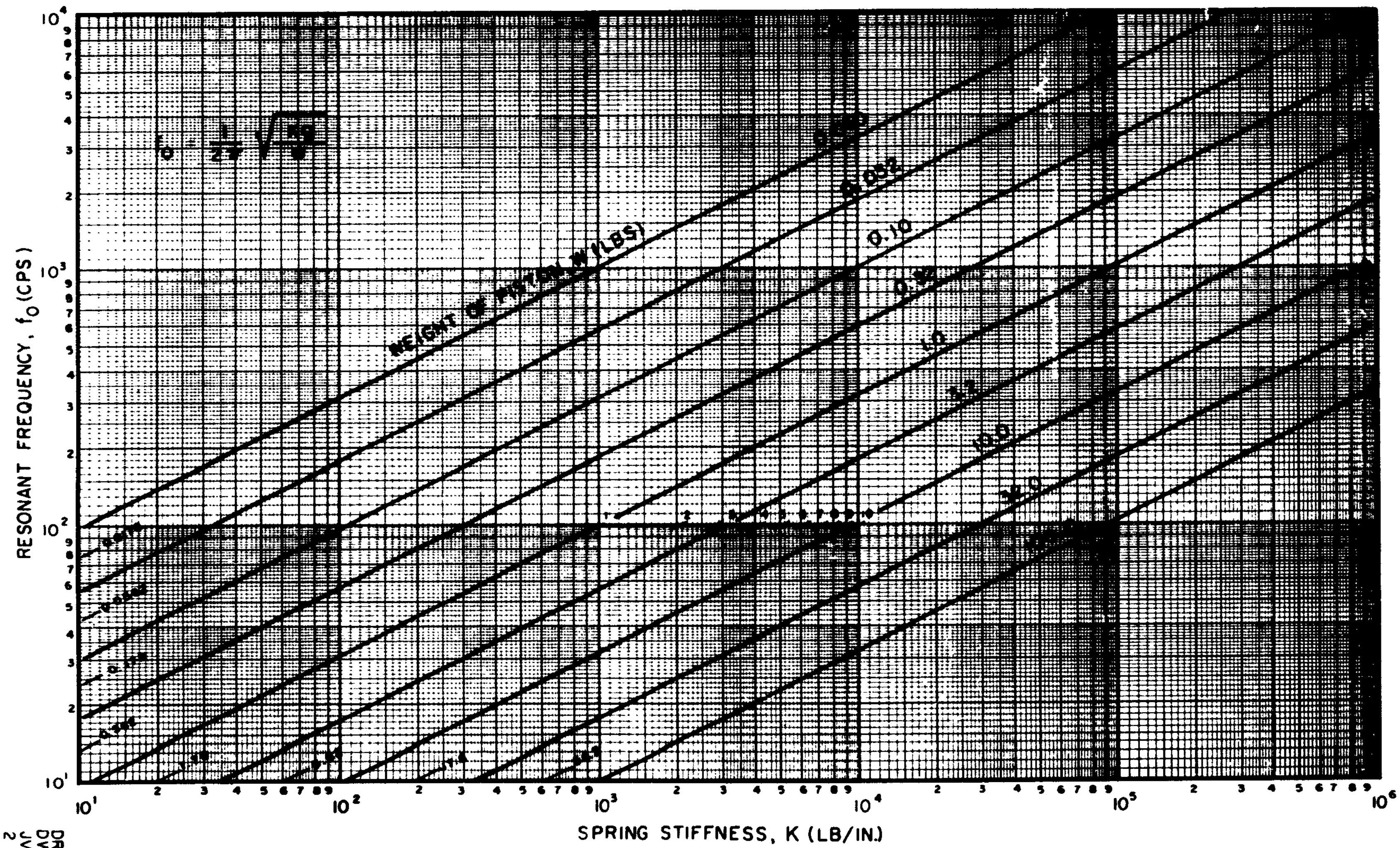

FIGURE 62
RESONANT FREQUENCY

DRL - UT
DWG AS7-
JVK - BE
2 - 22 -

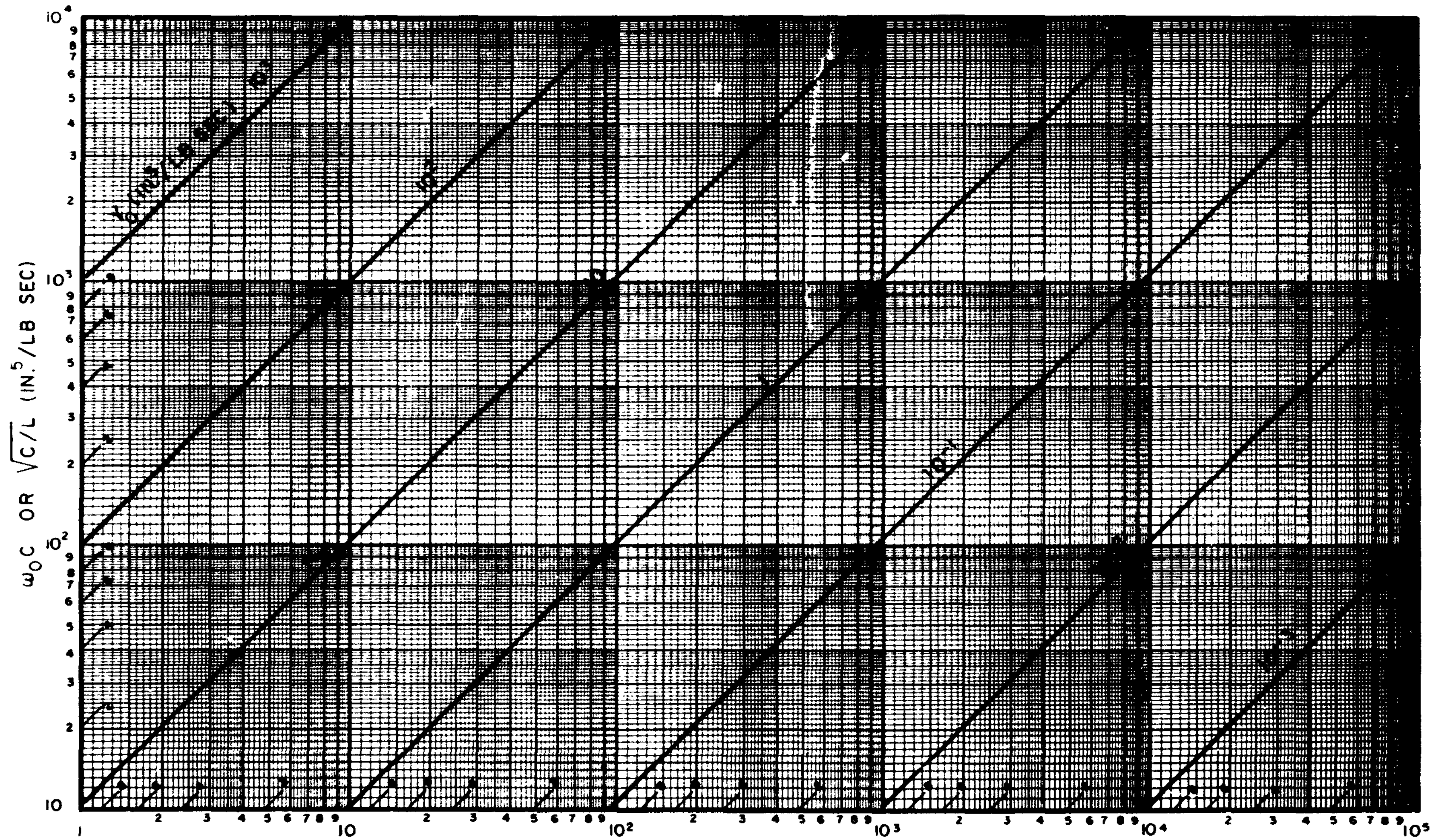

DRL - UT
DWG AS 71
JVK - BE
2 - 22 -

FIGURE 63
q OF A LUMPED ELEMENT SIDE-BRANCH

The value of q can then be determined from Fig. 63, and the calculated transmission loss characteristics may be found in the previous section.

e. Gas-Filled Side-Branch Element

The side-branch element consisting of a gas volume to provide the compliance and a liquid mass for the inertance is shown in Fig. 64. In the first case the closed-end side-branch is gas-filled at some pressure p_o before the liquid is added. Then the liquid is added and brought up to some pressure, p, greater than p_o. The liquid then partially fills the tube as the gas is compressed. The liquid height is then

$$x = \ell_s \left(1 - \frac{p_o}{p} \right).$$

In a second case, the gas volume is regulated to keep x fixed and independent of p. This case will be discussed later.

In the first case the inertance is given by

$$L = \rho \frac{x}{S} \quad \frac{\text{lb sec}^2}{\text{in.}^5} ,$$

and the compliance is

$$C = \frac{(\ell_s - x)S}{\gamma p} \quad \frac{\text{in.}^5}{\text{lb}} .$$

The resonant frequency of the system is then

$$f_o = \frac{p}{2\pi \ell_s} \sqrt{\frac{\gamma}{\rho \, p_o \left(1 - \frac{p_o}{p} \right)}} \quad \text{cps} .$$

To give this resonant frequency, the pipe length ℓ_s must be:

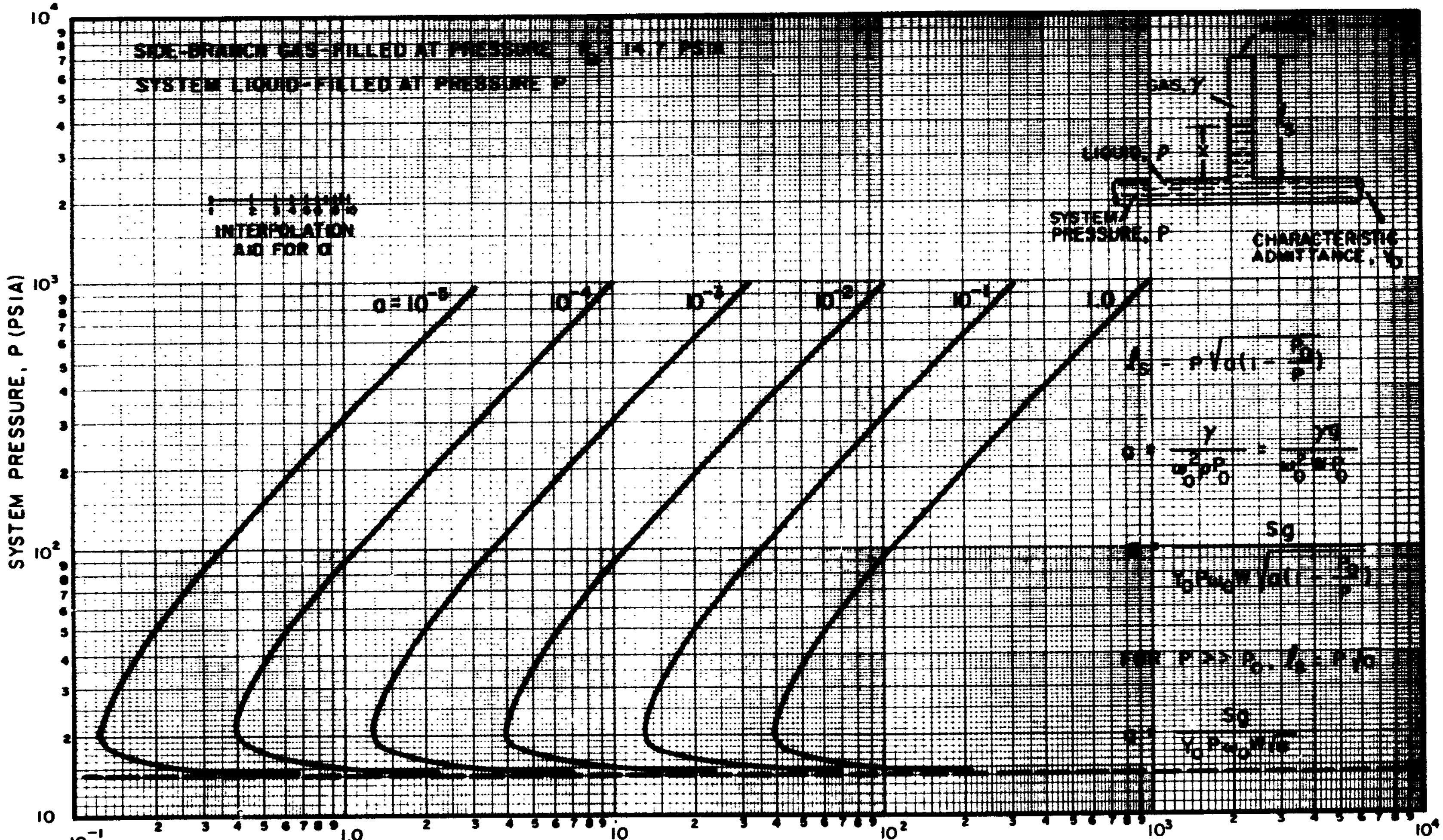

FIGURE 64
GAS-FILLED SIDE-BRANCH

$$\ell_s = \frac{p}{\omega_o}\sqrt{\frac{\gamma}{\rho\, p_o\left(1 - \frac{p_o}{p}\right)}} \ .$$

If a parameter, $a = \frac{\gamma}{\omega_o^2\, \rho\, p_o}$, is introduced, ℓ_s becomes:

$$\ell_s = p\sqrt{\frac{a}{1 - \frac{p_o}{p}}} \quad \text{in.} \ .$$

The quantity γ is the ratio of specific heats for the gas; ρ is the mass density of the liquid ($\rho = \frac{w}{g}$, w is weight in lb per cubic in., and $g = 386.4 \frac{\text{in.}}{\text{sec}^2}$); p and p_o are pressures in psia.

For a given value of p_o, a set of curves can be drawn, as in Fig. 64, relating ℓ_s and p with a as a parameter. These curves are drawn for p_o = 14.7 psia and are not valid for other p_o's. For a given gas, liquid, initial pressure p_o, and desired resonant frequency, the value of a is fixed. For the given system pressure p and a, the length of pipe ℓ_s is determined by the curves of Fig. 64. The interpolation aid may be used to measure in a direction parallel to the ℓ_s-axis for the determination of values of parameter a between and beyond the curves given.

The value of filter effectiveness parameter q is now of interest. This becomes

$$q = \frac{Sg}{Y_o p \omega_o w \sqrt{a\left(1 - \frac{p_o}{p}\right)}} \ .$$

From the previous paragraph, it can be seen that the resonant frequency does not depend on side-branch pipe area, S, but fortunately q does. The side-branch pipe length determines the system resonant frequency, and the area determines the q. Thus, the two quantities can be fixed independently.

Under operating conditions, the system pressure p may change, with the magnitude of change depending on the kind of pumping system involved. As p changes the gas volume changes, and there is a corresponding change in the liquid column height. Both the compliance and inertance are affected, and the side-branch resonant frequency and q are changed.

The change in resonant frequency is related to the change in system pressure as follows:

$$\frac{f_2}{f_1} = \frac{p_2}{p_1}\sqrt{\frac{1 - \frac{p_o}{p_1}}{1 - \frac{p_o}{p_2}}} \quad ,$$

where the resonant frequency was f_1 at the system pressure p_1, and the new frequency is f_2 at the new pressure p_2. As before, p_o was the initial pressure of the gas in the side-branch. This relationship is plotted for a few values of p_1 and p_o = 14.7 psia in Fig. 65.

The variation in q is given by

$$\frac{q_2}{q_1} = \sqrt{\frac{p_1(p_1 - p_o)}{p_2(p_2 - p_o)}} \quad .$$

The q at p_1 is q_1 and that at p_2 is q_2. This relationship is plotted for several values of p_1 with p_o = 14.7 psia in Fig. 66.

In the second type of gas-filled, side-branch element, a gas pressure regulator system is used to maintain the liquid level, x, constant as the pumping system pressure changes. Some type of level sensor is required for such a control system. In this case, the inertance will remain constant as pressure changes, but compliance will change. The net change in f_o and q is then less than that of the previous case. This improvement is the main advantage over the case for no regulation.

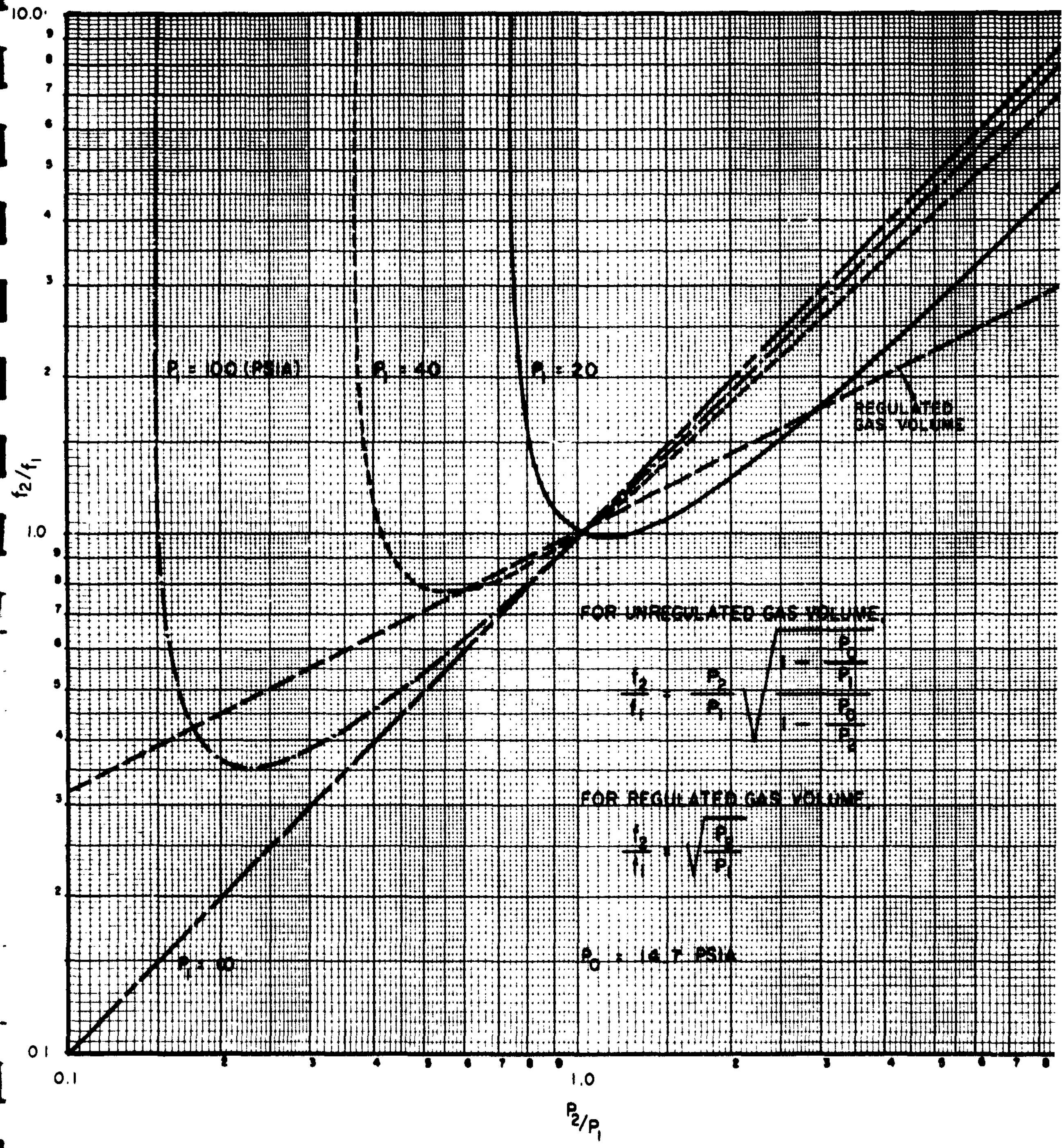

FIGURE 65
FREQUENCY VARIATION WITH PRESSURE FOR GAS-FILLED SIDE-BRANCH ELEMENTS

DRL - UT
DWG AS 713
JVK - BEI
10 - 31 - 6

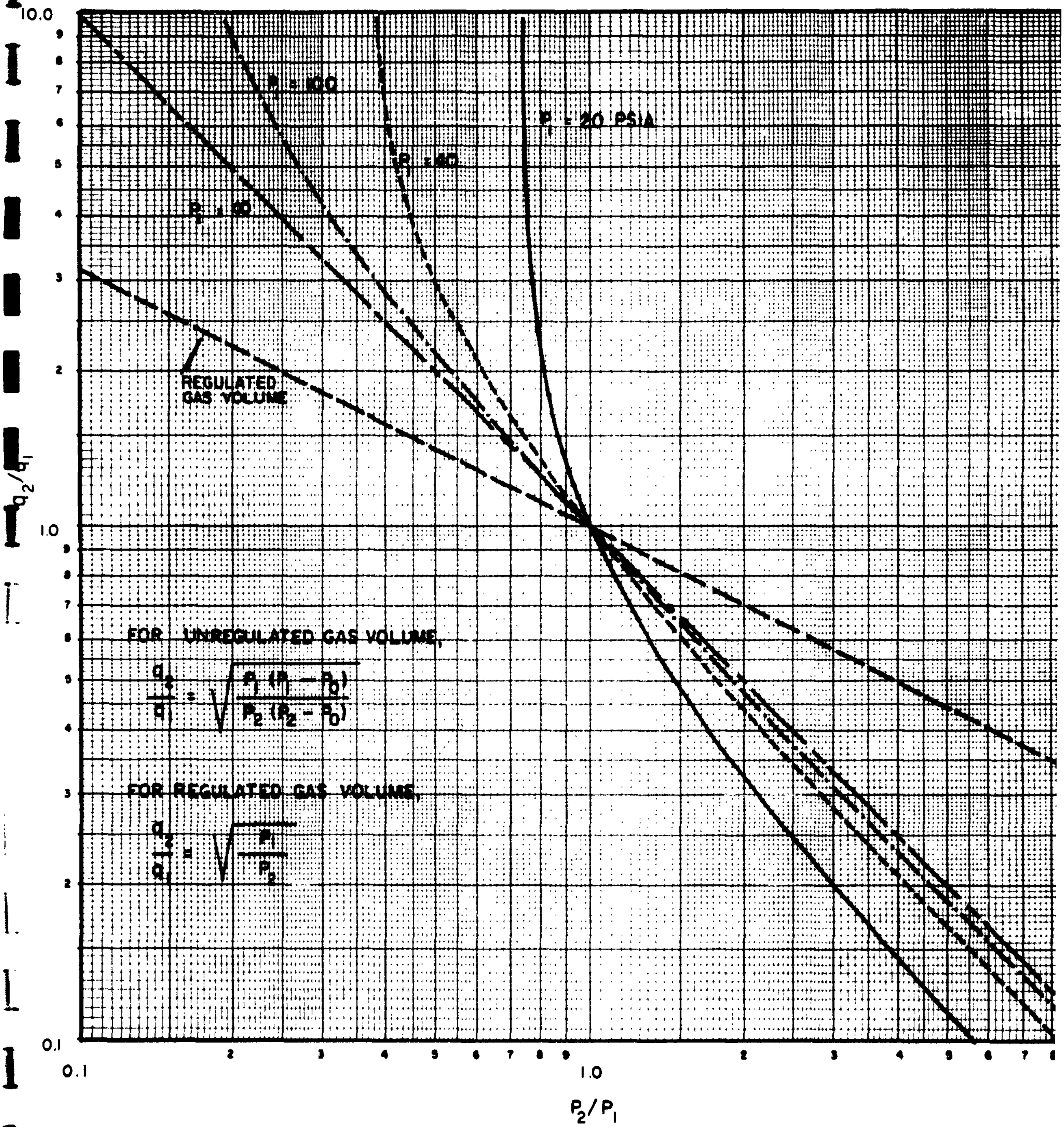

FIGURE 66
q VARIATION WITH PRESSURE FOR GAS-FILLED SIDE-BRANCH ELEMENTS

DRL -
DWG AS
JVK -
10 - 3

The regulated liquid height side-branch element is shown in Fig. 67. In terms of the symbols shown in the figure

$$C = \frac{\ell_a S}{\gamma p} \quad \frac{\text{in.}^5}{\text{lb}} \quad ,$$

$$L = \frac{\rho(\ell_s - \ell_a)}{S} \quad \frac{\text{lb sec}^2}{\text{in.}^5} \quad ,$$

and

$$f_o = \frac{1}{2\pi}\sqrt{\frac{\gamma p g}{w\ \ell_a(\ell_s - \ell_a)}} \quad \text{cps} \quad ,$$

where ℓ_s and ℓ_a are in inches, S is in square inches, p is pressure in psia, γ is the ratio of specific heats for the gas, and $\rho = \frac{w}{g}$ (w in $\frac{\text{lb}}{\text{in.}^3}$ and g = 386.4 $\frac{\text{in.}}{\text{sec}^2}$).

From the design standpoint the length of the pipe ℓ_s and the point at which to maintain ℓ_a by regulation to provide this resonant frequency are desired. In this case there is no unique value for ℓ_s, but ℓ_s and ℓ_a are related as follows:

$$(\ell_s - \ell_a)\ell_a = \frac{\gamma p g}{w\omega_o^2} \quad .$$

If a parameter $b = \frac{\gamma p g}{w\omega_o^2}$ is used, this relationship can be put in the form

$$\ell_s = \ell_a + \frac{b}{\ell_a} \quad .$$

If ℓ_s and ℓ_a satisfy this relationship, the resonant frequency will be f_o, ($f_o = \frac{\omega_o}{2\pi}$). This relation is plotted in Fig. 67, with b a parameter. For a

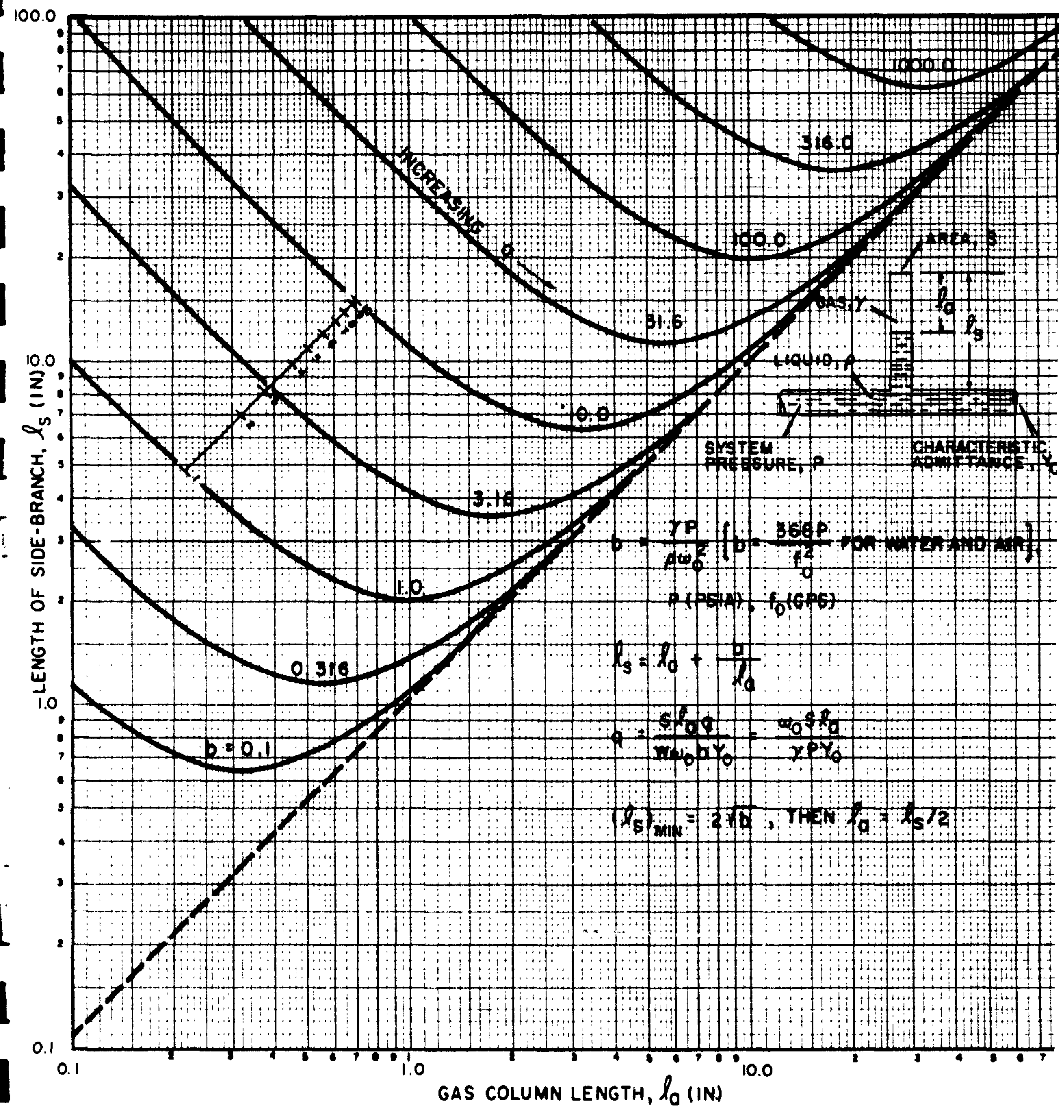

FIGURE 67
GAS-FILLED SIDE-BRANCH (REGULATED)

DRL - UT
DWG AS 7
JVK - BE
10 - 30 - 6

given system pressure p and desired resonant frequency f_o, the value of b is fixed; if ℓ_s is chosen, the value of ℓ_a may then be read from the abscissa. It can be noted that there are two values of ℓ_a given by the curves. Either value will give the correct f_o, but the value to the right will give the larger q for the filter.

There is a minimum value of ℓ_s given by

$$\ell_s(\min) = 2\sqrt{b} \quad .$$

Corresponding to this value of ℓ_s only one value of ℓ_a exists. It is given by

$$\ell_a = \frac{\ell_s}{2} \quad .$$

The filter effectiveness parameter q is found to be given by

$$q = \frac{\omega_o \ell_a S}{\gamma p Y_o} \quad , \text{ or}$$

$$q = \frac{\ell_a S g}{w \omega_o b Y_o} \quad .$$

As before, the resonant frequency is independent of the area of the side-branch pipe, but the value of q depends directly on S. In addition, q also depends directly on ℓ_a. Thus, the larger value of ℓ_a of the two possible should be chosen for a larger q.

For the minimum value of ℓ_s and ℓ_a, the q becomes

$$q_{(\min\ \ell_s)} = \frac{S}{Y_o} \sqrt{\frac{g}{w\gamma p}} \quad .$$

As mentioned earlier, the regulated side-branch has less dependence on system pressure variations than the other type. The variation in resonant frequency is given by

$$\frac{f_2}{f_1} = \sqrt{\frac{p_2}{p_1}} \quad .$$

This relationship is plotted in Fig. 65. It indicates that if the side-branch was designed to have a resonant frequency, f_1, at pressure p_1, when the pressure is raised to p_2 with the length ℓ_a held constant, the new resonant frequency is f_2.

The dependence of q on system pressure is given by

$$\frac{q_2}{q_1} = \sqrt{\frac{p_1}{p_2}} \quad .$$

This relationship is shown in Fig. 66 along with the curves for the case without regulation.

f. Liquid-Filled Side-Branch

The liquid-filled side-branch can have the configuration of a "tee" on the pipe or a coaxial arrangement as shown in Chapter III, B, Transmission Loss Curves. In either case, the element will have repeated infinities of admittance at frequencies for which the length of the tube is any odd multiple of $\lambda/4$. This is shown from the expression for admittance of a closed-end tube:

$$Y = j\, Y_{os} \tan \frac{2\pi \ell f}{v} \quad .$$

Y_{os} is the characteristic admittance of the side-branch pipe, ℓ is length in inches, v is wave velocity in in./sec, and f is frequency in cps. When the argument of the tangent function is any odd multiple of $\pi/2$, the value of the function is infinite:

$$\frac{2\pi \ell f}{v} = (2n + 1)\frac{\pi}{2} \quad , \qquad n = 0, 1, 2, \ldots \quad .$$

Then the frequencies for infinite shunt admittance and thus infinities of transmission loss are given by

$$f_n = \frac{v}{4\ell}(2n + 1) \quad , \qquad n = 0, 1, 2, \ldots \quad .$$

In designing such a side-branch element, the length must be determined. Lengt.. is fixed by the frequency for n = 0 in the above expression.

$$\ell = \frac{v}{4f_o} \quad \text{in.} \quad .$$

The velocity v in in./sec can be determined from the curves of Appendix A, and f_o, in cps, is the lowest frequency of infinite transmission loss.

The effectiveness parameter for such a filter is q' which is defined as the ratio of the side-branch tube characteristic admittance to that of the pipe in the system:

$$q' = \frac{Y_{os}}{Y_o} \quad .$$

These two admittances can be determined from the velocity, density, and pipe sizes as described in a previous section. In the usual system the liquid will be the same in both pipes and the sound velocities nearly identical. Then q' becomes

$$q' \approx \frac{S_s}{S_o} \quad ,$$

where S_s is the side-branch tube inside section area and S_o is the system piping section area. Thus,

$$q' \approx \left(\frac{d_s}{d_o}\right)^2 ,$$

where the d's are pipe inside diameters.

Precautions should be taken to prevent gas from collecting in these side-branch elements. If gas is present, the previous case with a gas-filled, side-branch element applies. The length equation and the transmission loss curves for the liquid-filled, side-branch tube no longer apply.

Care should be taken to close the side-branch tube with a very stiff cap. If the admittance at the closed end is not approximately zero, the above expressions do not apply. The closed end should not be attached to a structure that could conduct or radiate sound since that end can have large acoustic pressures acting on it at the resonant frequencies.

4. Expansion Chamber

The expansion chamber filter has a transmission loss characteristic that repeats for each frequency interval between successive values for which the chamber length is a multiple of $\lambda/2$. The maximum noise reduction occurs at odd multiples of $\lambda/4$. These maxima occur at

$$f_n = (2n + 1)\frac{v}{4\ell} , \qquad n = 0, 1, 2, \ldots ,$$

where v is the sound wave velocity in the chamber in in./sec and ℓ is the chamber length in inches, as shown in Fig. 68(a).

In designing a chamber, the length is determined by the lowest frequency for maximum transmission loss, f_o.

$$\ell = \frac{v}{4f_o} \quad \text{in.} ,$$

where f_o is in cps.

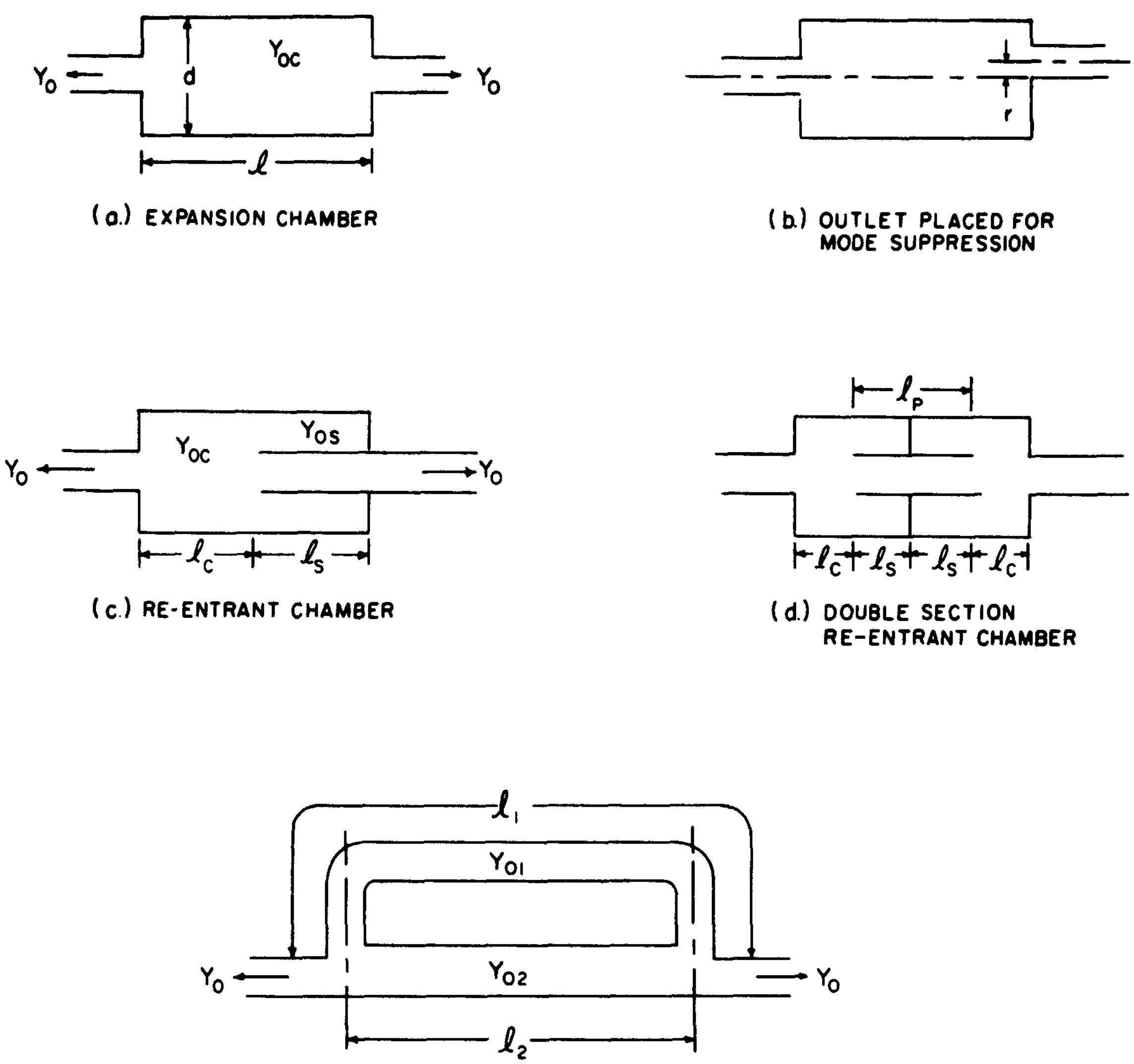

(a.) EXPANSION CHAMBER

(b.) OUTLET PLACED FOR MODE SUPPRESSION

(c.) RE-ENTRANT CHAMBER

(d.) DOUBLE SECTION RE-ENTRANT CHAMBER

(e.) QUINCKE TUBE

FIGURE 68

DRL - UT
DWG AS 7134
JVK - BEE
9 - 11 - 62

The effectiveness parameter, m, is defined as

$$m = \frac{Y_{oc}}{Y_o} \quad ,$$

where Y_{oc} is the characteristic admittance of the pipe comprising the chamber and Y_o is that of the system piping. These admittances and velocities can be determined as outlined previously.

To obtain a desired value of m, the chamber must have

$$Y_{oc} = mY_o \quad .$$

Or, in terms of chamber inside diameter, d,

$$d = \sqrt{\frac{4wmvY_o}{\pi g}} \quad \text{in.} \quad .$$

Here w is liquid weight in $\frac{\text{lbs}}{\text{in.}^3}$, $g = 386.4 \ \frac{\text{in.}}{\text{sec}^2}$, v is wave velocity in the chamber in $\frac{\text{in.}}{\text{sec}}$, and Y_o is characteristic admittance of the system piping in $\frac{\text{in.}^5}{\text{lb sec}}$.

Higher order propagation modes present a limitation to expansion chamber size. The cut-off frequencies for these modes are given by

$$f_{mn} = \frac{v_o}{d} \alpha_{mn} \quad .$$

The maximum diameter, d, is then

$$d_{max} = \frac{v_o}{f_{max}} \alpha_{mn} \quad .$$

Values of α_{mn} were given on page 125. The smallest α_{mn} corresponds to m = 1, n = 0. This gives a maximum diameter of

$$d_{max} = 0.586 \frac{v_o}{f_{max}} \quad .$$

This value can be considerably increased if the chamber is designed as shown in Fig. 68(b). If the inlet to the chamber is exactly on the center line, the asymmetric modes (n = 0) will not be excited. Then, if the outlet pipe is placed at a pressure zero for any one of the axially symmetric modes (m = 0), that mode will not pass through the chamber. If the outlet is placed as shown in Fig. 68(b) at an offset from the center line,

$$r = 0.314d \quad ,$$

the 0,1 mode is eliminated. Thus, this design eliminates the m,0 and 0,1 modes which leaves $\alpha_{11} = 1.697$ as the smallest value of α_{mn}. The maximum diameter is now

$$d_{max} = 1.697 \frac{v_o}{f_{max}} \quad .$$

In practice, these modes cannot be entirely eliminated because of the finite inlet and outlet size, but a considerable reduction in transmission can be acheived.

5. Re-entrant Tube

The filter consisting of an expansion chamber and a closed-end tube, as shown in Fig. 68(c), is commonly called a "re-entrant tube expansion chamber filter." This filter can be simply made by extending the inlet or outlet pipe into the chamber. The chamber effectiveness parameter, m, was given in the previous section and its length is ℓ_c as shown in the figure. The closed-end tube produces transmission loss infinities and has an effectiveness parameter previously defined as $q' = Y_{os}/Y_o$.

The closed-end tube of length ℓ_s is now a hollow cylinder with an area $S_s = S_c - S_o$, where S_c is the chamber section area and S_o is the pipe outside cross section area. The characteristic admittance is then

$$Y_{os} = \frac{S_c - S_o}{\rho v_s} \quad ,$$

where ρ is the liquid mass density and v_s is the wave velocity in the closed-end tube. For the case in which the wave velocities in the chamber, tube, and pipe are equal (usually very nearly true),

$$Y_{os} = Y_o \ (m - 1) \quad .$$

Then q' becomes

$$q' = m - 1 \quad .$$

The frequencies for infinite transmission loss occur for ℓ_s equal to an odd number of quarter-wavelengths. This gives

$$f_{ns} = \frac{(2n + 1) \ v_s}{4\ell_s} \quad , \qquad n = 0, 1, 2 \ldots \quad .$$

The length required for such a tube is given for the lowest frequency of infinite transmission loss ($n = 0$). Thus,

$$\ell_s = \frac{v_s}{4f_{os}} \quad \text{in.} \quad ,$$

for v_s in $\frac{\text{in.}}{\text{sec}}$.

The expansion chamber length is related to the frequency of the first transmission loss maximum:

$$\ell_c = \frac{v_c}{4f_{oc}} \quad .$$

The same precautions as for the expansion chamber should be observed here.

A two-section, re-entrant chamber filter is shown in Fig. 68(d). Only the case of identical sections (mirror symmetry about the center) has been considered here. The parameters m and q' are calculated as before, and the filter characteristics depend on the closed tube length ℓ_s and the chamber length ℓ_c. For calculating the transmission loss, the acoustical length of the connecting tube must be used. This gives connecting tube length

$$\ell_\alpha = \ell_p + 0.8\sqrt{S_p} = \ell_p \left(1 + 0.71 \frac{d_p}{\ell_p} \right) ,$$

where S_p is tube section area and d_p is tube inside diameter.

The end correction of the connecting tube has little effect on chamber and closed-end pipe characteristics; it affects the connecting tube length only when the length is comparable in size to the tube diameter.

6. Quincke Tube

The arrangement of two parallel acoustic paths shown in Fig. 68(e) produces transmission loss infinities at frequencies related to the path lengths. For true infinities to occur, the characteristic admittances of the pipes in the two paths must be identical; $Y_{01} = Y_{02}$. The most practical arrangement would use the same piping as that of the rest of the system. Then $Y_{01} = Y_{02} = Y_0$.

September 1962
ELH:vh

Repeated infinities are given for the condition that the sum of the pipe lengths, $(\ell_1 + \ell_2)$, is an integral number of wavelengths. This gives a series of infinities at

$$f_{1n} = \frac{nv}{\ell_1 + \ell_2} \quad \text{cps} \quad , \quad n = 1, 2, 3, \ldots \quad .$$

Another series of infinities occurs at frequencies that make the difference in lengths, $(\ell_1 - \ell_2)$, an odd multiple of a half-wavelength:

$$f_{2m} = \frac{(2m + 1)\, v}{2(\ell_1 - \ell_2)} \quad , \qquad m = 1, 2, 3, \ldots \quad , \qquad (\ell_1 > \ell_2) \quad .$$

The infinities of f_{1n} can be nullified if the difference in length is any multiple of a wavelength at any of the frequencies f_{1n}. If f_k is defined as

$$f_k = \frac{kv}{\ell_1 - \ell_2} \quad , \qquad k = 1, 2, \ldots \quad ,$$

then infinities of transmission loss will occur at f_{1n}, unless

$$f_{1n} = f_k$$

for any n or k. This relation leads to the condition on ℓ_1 and ℓ_2 which will result in the coincidence of f_{1n} and f_k.

$$\ell_2 = \ell_1 \frac{n - k}{n + k} \qquad n = 1, 2, 3, \ldots \quad , \qquad k = 1, 2, 3, \ldots \quad , \qquad (n > k) \quad .$$

To avoid nullification of the infinities at f_{1n}, ℓ_1 and ℓ_2 should not be related as above. For all allowed values of n and k, n - k and n + k will be integers. Thus, ℓ_2 should not be related to ℓ_1 by a rational number but by some fraction of an irrational number such as $\sqrt{2}$, $\sqrt{3}$, π, or e.

September 1962
ELH:vh

D. FILTER DESIGN EXAMPLES

This section includes the design of acoustic filters for several hypothetical noise reduction problems. The examples chosen are not necessarily typical. They were chosen to include a wide range of system characteristics and to involve the calculations of most of the possible filter parameters. Only the engineering considerations that effect the acoustical characteristics are considered. Important problems such as choice of materials, strength of materials, and types of pressure seals are not discussed. It should be noted, however, that any engineering decisions that involve the weight, stiffness, or friction of the filter elements also involve the acoustical characteristics of the filter.

The first phase of filter design is a consideration of the noise source and piping system characteristics. The frequency spectrum of the noise will give an indication of the frequency region where noise reduction is needed. This information will lead to a choice of the type of transmission loss characteristic required of an acoustic filter. The size of the system piping and the system pressure will affect the choice of type of filter.

Some general considerations of the types of filters presented earlier may be of some help to the designer and will be presented before the examples are given:

(a) Lumped-element side-branch filters--this type of filter provides an infinite transmission loss at one or more selected frequencies, and the broad band noise reduction characteristics are good. Good low frequency characteristics can be attained with rather small physical size.

The characteristics of these filters change with system pressure, and large pressures require added complications. Pressure compensation and liquid level regulation allow improved operation at high pressures, but at high pressures it is difficult to provide any appreciable compliance.

Lumped-element, side-branch filters with moving parts might require more maintenance than filters of other types, since seal aging, mechanical spring fatigue, and pressure regulator adjustment could be important considerations.

(b) Closed-end side-branch tube--this type of filter provides repeated infinities of transmission loss that can be placed at a desired frequency and its odd harmonics. The length of the tube is large for low frequency infinities, and the section area required to provide broad band characteristics becomes large.

The liquid-filled tube is simple to construct and can be designed for service at high pressures. The acoustical characteristics do not change with pressure. The tube volume required may be large, but the tube can be run in any convenient direction.

(c) Expansion chamber filters--the expansion chamber filter does not provide transmission loss infinities, but it has the best broad band noise reduction characteristics of any filter considered here. It has the further advantage of being simple to construct and usable at high pressures. The acoustical characteristics do not change with pressure.

Expansion chamber filters must be long and large to produce large transmission losses at low frequencies. For large chamber diameters, the filter effectiveness may be nullified by higher order modes of sound propagation through the chamber.

(d) Combination filters--the combination of an expansion chamber and a lumped side-branch element will incur the disadvantages of both types, but a transmission loss infinity is provided and the broad band characteristics may even be improved over those of only a chamber.

A liquid-filled, side-branch tube combined with an expansion chamber provides repeated infinities and good broad band characteristics. This combination is suitable for high pressure applications, and in the form of a re-entrant chamber the construction is simple.

(e) Quincke tube--the use of two parallel acoustic paths provides a filter characteristic with infinities of transmission loss at harmonically related frequencies. The Quincke tube is ineffective, however, for the reduction of broad band noise. The design and construction of such a filter is simple, the space requirements are not severe, and high pressure operation is feasible.

1. Fresh Water System, 6 in. Piping
(Single-Section, Lumped-Element, Side-Branch Filter; Pressure Compensation; Two Parallel Elements)

It is desired to provide a simple filter for a piping system that carries fresh water in 6", schedule 40, steel pipe at a pressure of 50 psig. The pump produces a strong 30 cps component in its noise spectrum. An inspection of the transmission loss curves for various filters reveals that a single-section, lumped-element, side-branch filter with q = 100 would give an infinite transmission loss at 30 cps if the resonator were tuned there. In addition, at least 20 dB of transmission loss is predicted from $f/f_o = 0.2$ (6cps here) to $f/f_o = 5$ (150 cps here). An actual installation with nonideal terminations would probably not be as good as predicted, but appreciable noise reduction should be expected over this band. The calculation of the physical quantities required for such a filter will follow.

a. Characteristic Admittance of the Piping

For schedule 40 6" steel pipe:

o.d. = 6.625"

Wall thickness = 0.280"

i.d. = 6.625 - (2 × 0.280) = 6.065"

Entering the velocity curve of Fig. A-3 in Appendix A for i.d. = 6" and wall thickness = 1/4", the sound velocity is found to be

$$v = 4380 \quad \text{fps} \ .$$

From the same figure, the density of water which may be needed for inertance calculation is

$$\rho = 9.35 \times 10^{-5} \quad \frac{\text{lb sec}^2}{\text{in.}^4} \ ,$$

$$\text{or } w = \rho g = 0.0356 \quad \frac{\text{lb}}{\text{in.}^3} \ .$$

The value of ρv, required for the calculation of Y_o, is given as 1.12×10^{-3} times the sound velocity just found.

$$\rho v = 1.12 \times 10^{-3} \times 4380 = 4.9 \quad \frac{\text{lb sec}}{\text{in.}^3} \ .$$

Entering Fig. 57 with this value and a pipe i.d. of 6 in. gives

$$Y_o = 6.0 \quad \frac{\text{in.}^5}{\text{lb sec}} \ .$$

b. <u>Spring Stiffness</u>

For q = 100, the product $\omega_o C$ is found from Fig. 63 to be 600. Then the compliance required is

$$C = \frac{600}{2\pi \times 30} = 3.18 \quad \frac{\text{in.}^5}{\text{lb}} \ .$$

A piston diameter of 5 in. is assumed, and the required stiffness for a spring to back the piston is found from Fig. 59:

$$k = 120 \quad \frac{\text{lb}}{\text{in.}} \ .$$

Before continuing, the static deflection of the spring is calculated.

$$x = \frac{F}{k} = \frac{pS}{k} = \frac{50 \times \pi(5)^2}{4 \times 120} = 8.2 \quad \text{in.} \quad ,$$

where p is the system pressure of 50 psig. Such a large static displacement suggests that pressure compensation be employed to reduce it or that an alternate design be used.

Pressure compensation will require a different spring, since the pressurized gas also presents a compliance. The compliance due to the spring and gas volume are acoustically in parallel; hence, their complicance add as reciprocals:

$$\frac{1}{C} = \frac{k}{S^2} + \frac{\gamma p}{U} \quad .$$

The required stiffness is then

$$k = S^2 \left(\frac{1}{C} - \frac{\gamma p}{U} \right) \quad .$$

By finding the compliance required of the spring,

$$\frac{S^2}{k} = \frac{1}{\frac{1}{C} - \frac{\gamma p}{U}} \quad ,$$

Fig. 59 may be entered to obtain k. Assuming that pressurized air in a cylindrical volume of 6 in. i.d. by 10 in. long is used, S^2/k becomes

$$C_{ef} = \frac{S^2}{k} = \frac{1}{\frac{1}{3.18} - \frac{1.4 \times 50}{\pi(6/2)^2 \times 10}} = 15 \quad \frac{\text{in.}^5}{\text{lb}} \quad .$$

Entering Fig. 59 for a 5 in. piston diameter and a compliance of 15 in.^{5}/lb determines a point which is off the graph. Thus, k will have to be calculated.

$$k = \frac{S^2}{C_{ef}} = \frac{[(\pi)(25/4)]^2}{15} = 25.7 \quad \frac{\text{lb}}{\text{in.}}$$

A smaller air volume would produce a smaller compliance and require a spring with even smaller k. A larger volume would thus require a larger value for k.

To reduce the static deflection without pressure compensation, the spring constant, k, must be increased, but the compliance must remain unchanged. Since the deflection is $x = pS/k$ and $k = S^2/C$,

$$x = \frac{pC}{S} \quad .$$

Thus, for a given pressure p and compliance C the deflection x can be reduced by using a larger piston area S.

Another approach to this problem involves multiple side-branch elements at the same place on the pipe. Since these elements are in parallel, their compliances are additive, and the compliance for each element is less than the total compliance required.

Both these methods will be applied to the problem at hand. Two identical elements will be used, and the piston diameter will be increased to 6 in. The required compliance for each element is then

$$C' = \frac{C}{2} = \frac{3.18}{2} = 1.59 \quad \frac{\text{in.}^5}{\text{lb}} \quad .$$

For this value of compliance and a piston diameter of 6 in., Fig. 59 gives

$$k = 510 \quad \frac{\text{lb}}{\text{in.}} \quad .$$

The static deflection is then

$$x = \frac{pS}{k} = \frac{50 \times \pi(6)^2}{4 \times 510} = 2.77 \quad \text{in.} \quad .$$

This is a more reasonable figure. When the spring is compressed under the pressure p, there will be a mass of liquid above the piston as in Fig. 60(c) which may be used to tune the compliance to the resonant frequency of 30 cps.

c. Piston Weight

The piston weight required to tune the compliance is found from Fig. 62. For k = 510 lb/in. and f_o = 30 cps,

$$W = 5.6 \quad \text{lb} \quad .$$

This weight is divided between the piston that seals the unit, 1/3 of the mechanical spring, and the liquid between the piston face and the side of the pipe.

Considering the spring first, one possible spring made of stainless steel has a 3 in. outside diameter, 0.48 in. wire diameter, 10 turns, and weight of 4.02 lb. It must be at least 8 in. long to accommodate the 2.77 in. static deflection. A third of the spring weight is 1.34 lb, which leaves 5.6 - 1.34 = 4.26 lb for the piston and liquid.

If a 3/8 in. thick by 6 in. diameter stainless steel piston is used, the piston weight will be

$$\frac{(0.280)(\pi)(6)^2\ (3)}{(4)(8)} = 2.96 \quad \text{lb}$$

where 0.280 is the weight per cubic inch for stainless steel. This leaves only

$$4.26 - 2.96 = 1.3 \quad \text{lb}$$

for the liquid above the piston.

The height of the water column is then

$$x = \frac{U}{S} = \frac{W}{wS} = \frac{(1.3)(4)}{(0.0356)(\pi)(6)^2} = 1.29 \quad \text{in.}\ .$$

Since the static deflection under a pressure of 50 psig was 2.77", the spring can be compressed a distance of

$$2.77 - 1.29 = 1.48 \quad \text{in.}$$

at a system pressure of zero. The spring will then be clamped and the element ineffective until the system pressure gets up to

$$p = 50 \left(\frac{1.48}{2.77}\right) = 26.7 \quad \text{psig}\ .$$

At this pressure the resonant frequency will be higher than 30 cps because the water mass is zero. At 50 psig, then, the resonant frequency will be correct. With no water mass the resonant frequency is

$$f_o = \frac{1}{2\pi}\sqrt{\frac{510 \times 386.4}{4.3}} = 34.3 \quad \text{cps}$$

since the total mass is then 4.3 lb. When the static pressure goes up to 75 psi, the deflection is increased to 2.67 in., which gives a total weight of 8.28 lb. The resonant frequency is then

$$f_o = \frac{1}{2\pi}\sqrt{\frac{510 \times 386.4}{8.28}} = 24.5 \quad \text{cps}\ .$$

The physical arrangement of this filter and the predicted transmission loss for three system pressures are shown in Fig. 69. The element should be

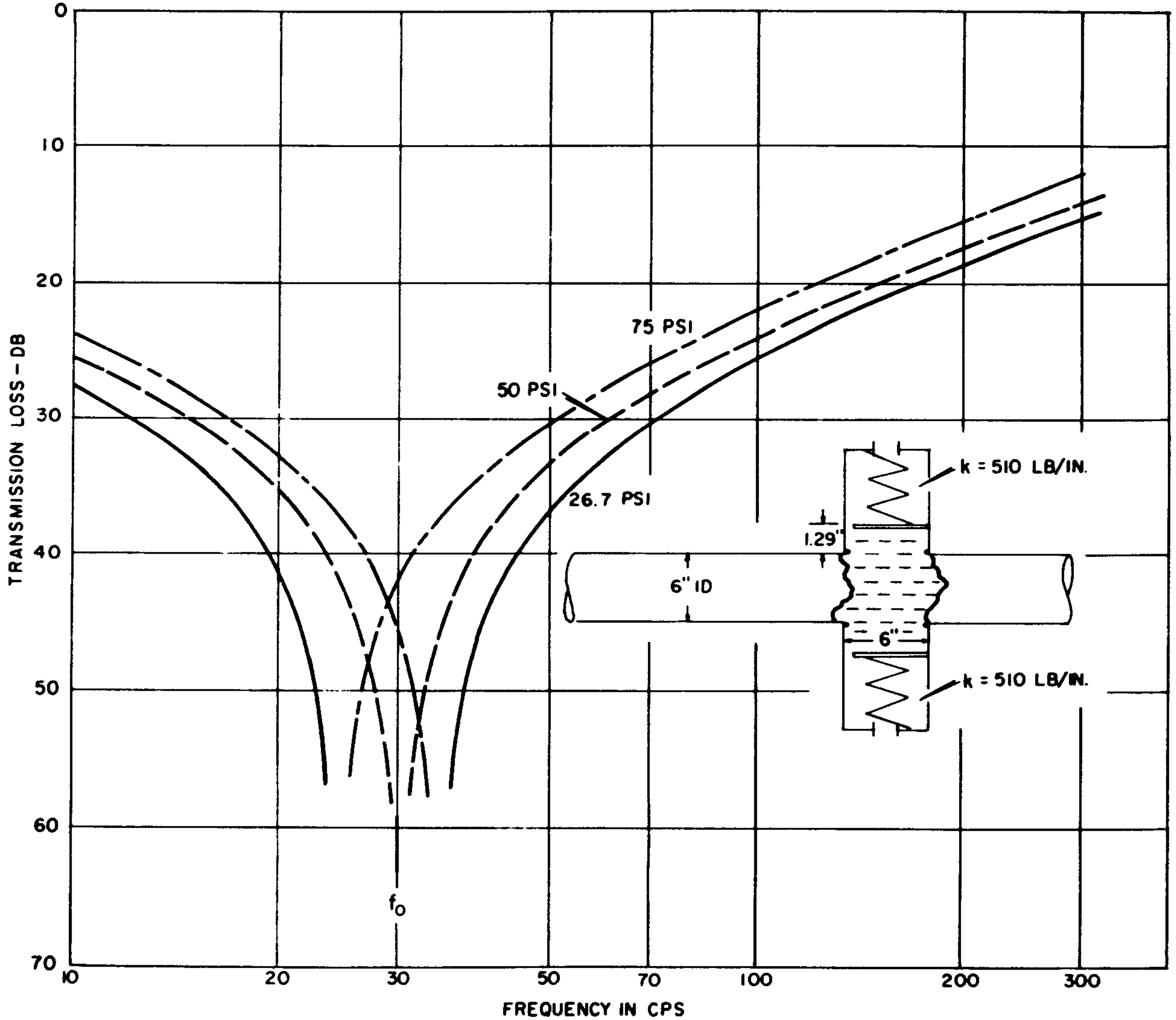

FIGURE 69
LUMPED ELEMENT SIDE-BRANCH FILTER

DRL - UT
DWG BS 7135
JVK - BEE
10 - 26 - 62

placed an appreciable distance from the noise source. The distance should be some reasonable fraction of a wavelength at 30 cps to prevent large acoustic pressures in the input section. Here a length of 6-10 ft should suffice. There are many possible arrangements that may be much better than the simple filter used here. The use of bellows instead of spring-piston combinations would greatly simplify the seal problem. A compromise to a lower value of q may greatly simplify the design requirements.

2. Low Pressure Lubricating Oil System
(Single-Section Filter; Lumped, Side-Branch Element; Gas-Filled, Side-Branch Element; Regulated, Gas-Filled, Side-Branch Element; and Expansion Chamber)

A simple filter is desired for a low pressure lubricating oil system with the following characteristics:

Pipe: 1 in. i.d., 1/8 in. wall thickness

Material: brass

System pressure: 100 psia

Pump Noise Characteristics: Strong component at pump blade frequency of 240 cps. Appreciable energy at rotational frequency of 30 cps and at second, third, and fourth harmonics of the blade frequency (480, 720, 960 cps). A broad band noise with a spectrum extending from 30 cps to above 1 kc with a broad peak at 500 cps is present.

Several types of simple, single-section filters will be designed, and their transmission loss curves will be compared. The sound wave velocities in the liquid and the characteristic admittance for the pipe will be required.

From Fig. A-11 in Appendix A, the value of sound wave velocity and several other quantities are found:

$$v = 4330 \quad \text{fps}$$

$$v_0 = 4600 \quad \text{fps}$$

$$\rho = 8.23 \times 10^{-5} \quad \frac{\text{lb sec}^2}{\text{in.}^4}$$

$$\rho v = 9.88 \times 10^{-4} \times 4330 = 4.28 \quad \frac{\text{lb sec}}{\text{in.}^3} \ .$$

The characteristic admittance is found from Fig. 57 to be

$$Y_o = 1.8 \times 10^{-1} \quad \frac{\text{in.}^5}{\text{lb sec}} \ .$$

a. Lumped-Element, Side-Branch Filter

Resonate the element at 240 cps to give large transmission loss at the pump blade frequency, and design for q = 100 for broad band noise reduction. Use capped bellows for the compliant element.

For $Y_o = 0.18 \ \frac{\text{in.}^5}{\text{lb sec}}$ and q = 100, enter Fig. 63 to obtain

$$\omega_o C = 18 \quad \frac{\text{in.}^5}{\text{lb sec}} \ .$$

Then for $\omega_o = 2\pi \times 240$, find the required compliance C:

$$C = \frac{18}{2\pi \times 240} = 1.19 \times 10^{-2} \quad \frac{\text{in.}^5}{\text{lb}} \ .$$

The effective diameter for a bellows is given approximately by the average of the outside and inside diameter of the bellows convolutions. For an effective diameter of 1 in., Fig. 59 gives a required stiffness of

$$k = 52 \quad \frac{\text{lb}}{\text{in.}} \ .$$

The deflection of such a bellows under the static system pressure of 100 psia will be

$$x = \frac{pS}{k} = (100 - 14.7) \frac{\pi}{4 \times 52} = 1.29 \quad \text{in.} \quad .$$

This is an unreasonable figure, and a redesign is indicated. Larger bellows area, multiple elements, pressure compensation, or smaller q are suggested. This type element will not be considered further except that the weight to resonate the bellows will be calculated as an example.

For a stiffness of 52 lb/in., Fig. 62 indicates a weight of a little less than 0.01 lb to resonate the bellows at 240 cps. Since this must include 1/3 the bellows weight and the cap weight, 0.01 lb is much too small. A much stiffer bellows is thus indicated for this element.

b. Air-Filled, Side-Branch Element (Not Regulated)

An unregulated, air-filled, side-branch element consists of a vertical length of pipe that communicates freely with the main system piping. It will be simply free to the air (air-filled) before the oil is pumped into the system. System pressure will then compress the air, allowing oil to partially fill the pipe. For filter design it is then necessary to find the pipe length to resonate the element at 240 cps and the pipe diameter to give the required q. Figure 64 gives the methods for determining both these quantities.

The parameter a is required first.

$$a = \frac{\gamma}{\rho p_o \omega_o^2} = \frac{1.4}{8.23 \times 10^{-5} \times 14.7 \times (2\pi \times 240)^2} = 5.03 \times 10^{-4}$$

Here $\gamma = 1.4$ for air, ρ for oil was given above as 8.23×10^{-5} $\frac{\text{lb sec}^2}{\text{in.}^4}$, and

p_o is atmospheric pressure of 14.7 psia. At p = 100 psia and this value for a, Fig. 64 gives the side-branch pipe length as

$$\ell_s = 2.5 \quad \text{in.} \quad .$$

From the expression for q the side-branch pipe inside diameter may be found. Since

$$q = \frac{S_s}{Y_o \omega_o \rho \ell_s} \quad , \qquad S_s = Y_o \omega_o \rho \ell_s q \quad , \text{ and}$$

$$d_s = 2\sqrt{\frac{Y_o \omega_o \rho \ell_s q}{\pi}} \quad .$$

Then d_s in this case is

$$d_s = 2\sqrt{\frac{0.18 \times 2\pi \times 240 \times 8.23 \times 10^{-5} \times 2.5 \times 100}{\pi}} = 2.744 \quad \text{in.} \quad .$$

The physical arrangement and the transmission loss for this filter are shown in Fig. 70. The curve shown is valid for any lumped-element, side-branch resonator element, such as the one just described or the bellows discussed earlier with q = 100 and f_o = 240 cps.

c. Regulated, Air-Filled, Side-Branch Element

Since the resonant frequency for the air-filled, side-branch element without regulation varies almost directly with system pressure (as shown in Fig. 65 for p = 100 psia), the regulated case is considered. When the liquid level is maintained constant, only the compliance of the air volume varies, and the resonant frequency varies as the square root of the pressure change.

The lengths of the side-branch pipe and gas column and diameter of the pipe may be determined by referring to Fig. 67. The parameter b for this case is then

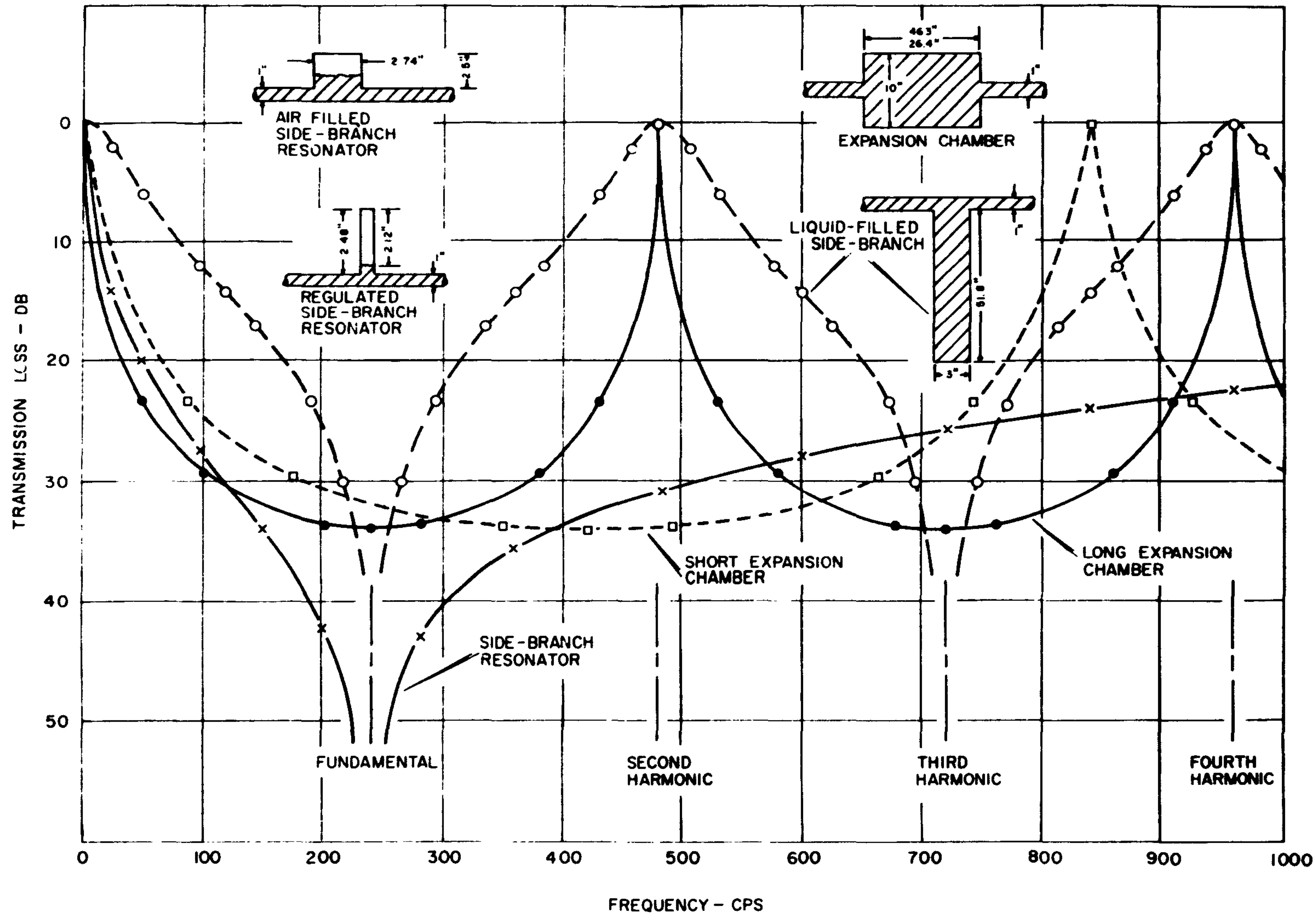

DRI - UT
DWG B57136
JVK - PVW
10 - 9 - 62

FIGURE 70
FILTERS FOR LUBRICATING-OIL SYSTEMS

$$b = \frac{\gamma p}{\rho \omega_o^2} = \frac{1.4 \times 100}{8.23 \times 10^{-5} \times 4\pi^2 \, (240)^2} = 0.75 \quad .$$

If the minimum length side-branch pipe is used, the length becomes

$$\ell_s = 2\sqrt{b} = 2\sqrt{0.75} = 1.124 \quad \text{in.} \quad .$$

The length of the air column is then

$$\ell_a = \frac{\ell_s}{2} = 0.562 \quad \text{in.} \quad .$$

Since q is given by

$$q = \frac{\omega_o S \ell_a}{\gamma p Y_o} \quad ,$$

$$S = \frac{\gamma p Y_o q}{\omega_o \ell_a} \quad .$$

Then the side-branch pipe diameter is given by

$$d_s = 2\sqrt{\frac{\gamma p Y_o q}{\pi \omega_o \ell_a}} \quad .$$

In this case

$$d_s = 2\sqrt{\frac{1.4 \times 100 \times 0.18 \times 100}{\pi \times 2\pi \times 240 \times 0.562}} = 1.945 \quad \text{in.} \quad .$$

A side-branch pipe that is almost 2 in. in diameter and about 1-1/8 in. high with the liquid level held at 0.562 in. is indicated.

One might desire to make the side-branch tube of the same pipe as the rest of the system. For q and b fixed, l_a and S are inversely related. If the pipe diameter is reduced to 1 in., then the new l_a is

$$l_a = 0.562 \left(\frac{1.945}{1.0}\right)^2 = 2.12 \quad \text{in.} \quad .$$

The new pipe length is then given by

$$l_s = l_a + \frac{b}{l_a} = 2.12 + \frac{0.75}{2.12} = 2.475 \quad \text{in.} \quad .$$

For this side-branch pipe, the i.d. is 1 in., the length inside is 2.75 in., and the air column length is 2.12 in. The liquid level is then regulated at a height of 0.355 in. from the edge of the system piping.

The transmission loss curve for this filter is the same as for the previous case without regulation, but the variation of f_0 with system pressure is reduced. An infinity is provided at the pump blade frequency fundamental and at least 15 dB transmission loss is predicted from 30 cps to above 1 kc, to reduce the broad band noise.

d. Liquid-Filled, Side-Branch Pipe

Transmission loss infinities can be provided at the pump blade frequency fundamental and its odd harmonics with a liquid-filled, side-branch pipe.

The required pipe length has been given previously as

$$l = \frac{v}{4f_0} \quad ,$$

where f_0 is the lowest frequency at which an infinity is desired, and v is velocity in in./sec. The length cannot be calculated until the sound wave velocity in the oil is known for the pipe to be used for the side-branch tube. Inspection of Fig. 30 reveals that q' must be large to obtain any appreciable bandwidth in the transmission loss rejection bands. If a value of q' = 10 is chosen, the characteristic admittance for the pipe becomes

$$Y_{os} = q'\ Y_o = 10 \times 0.18 = 1.8 \quad \frac{\text{in.}^5}{\text{lb sec}} \ .$$

If the velocity in the side-branch pipe is the same as that in the system piping, the admittance ratio q' is also the area ratio, since $Y_o = \frac{S}{\rho v}$. This will be approximately true, so a pipe size of

$$d_s = d_o\sqrt{10} = 1 \times 3.16 \approx 3 \quad \text{in.}$$

will be used. For a wall thickness of 3/16 in., Fig. A-11 gives $v = 4150\ \frac{\text{ft}}{\text{sec}}$ and $\rho v = 4.1\ \frac{\text{lb sec}}{\text{in.}^3}$. Then, from Fig. 57, $Y_{os} = 1.7\ \frac{\text{in.}^5}{\text{lb sec}}$ and

$$q' = \frac{1.7}{0.18} = 9.45 \ .$$

The required length of the closed-end pipe is then

$$l = \frac{v}{4f_o} = 4150 \times \frac{12}{4} \times 240 = 51.8 \quad \text{in.} \ .$$

The transmission loss curve for q' = 10 is shown in Fig. 70. The fundamental and odd harmonics are eliminated, but the even harmonics are not attenuated at all, and there is very little attenuation at 30 cps.

e. Expansion Chamber

Broad band rejection characteristics can be obtained by use of expansion chamber filters. If the maximum transmission loss is set at 240 cps, the odd harmonics are also attenuated by this same amount. The length is then given by

$$l = \frac{v}{4f_o} \quad .$$

As in the case of the liquid-filled, side-branch pipe, the length cannot be determined until v is found. Referring to Fig. 33, a value of m = 100 gives 34 dB maximum transmission loss. Since the percentage change in sound velocity with pipe diameter is small, the parameter m is very nearly equal to the area ratio of the pipes. Thus the expansion chamber diameter should be

$$d_c = \sqrt{100} = 10 \quad \text{in. i.d.} \quad .$$

Reference to Fig. A-13 of Appendix A reveals that this value of i.d. for an assumed wall thickness of 1/4 in. gives a velocity of 3700 ft/sec. The product ρv is then 3.66 and from Fig. 57, $Y_{oc} = 22 \ \frac{\text{in.}^5}{\text{lb sec}}$. The actual value of m is thus

$$m = \frac{22}{0.18} = 122 \quad .$$

The predicted maximum transmission loss is then

$$\text{T.L.} = 20 \log (122) - 6 = 35.7 \quad \text{dB} \quad .$$

The length can now be calculated.

$$l = \frac{3700 \times 12}{4 \times 240} = 46.3 \quad \text{in.}$$

The transmission loss curve for this filter with m = 100 is shown in Fig. 70. Again the fundamental and odd harmonics are attenuated the most, but the even harmonics are unaffected. The loss at 30 cps is almost 20 dB.

If some reduction of transmission loss at the fundamental is allowed, a shorter length chamber will give a broader rejection band and good attenuation at all the narrow band components. In this case, the first peak in the curve is placed between the third and fourth harmonic. The length is then

$$\ell = \frac{v}{2f} = \frac{3700 \times 12}{2 \times 840} = 26.4 \quad \text{in.} \quad .$$

The curve for this case is also shown in Fig. 70. At least 25 dB of transmission loss is predicted up through the sixth harmonic. The value at 30 cps is about 15 dB, and this filter would be expected to give the best attenuation of the broad band noise.

3. Sea Water System, 4 in. Piping
(Two-Section, Lumped-Element, Side-Branch Element; Inertance Tube; Inertance Holes)

Consider a sea water pumping system using 4 in. i.d., 1/8 in. wall thickness, copper-nickel pipe. It is desired to provide a transmission loss infinity at 30 cps and 60 cps with a two-section, lumped-element, side-branch filter. A response as shown in Fig. 24 is desired, and bellows are available with a 4 in. effective diameter and a convolution stiffness of 4000 lb/in.

From Fig. 24 it is seen that here, $f_{01} = 30$ cps, $f_{02} = 60$ cps, and q_1 must equal q_2. The length between elements is then

$$\ell = \frac{v}{8f_{01}} \quad .$$

Before proceeding, v and Y_o must be found.

From Fig. A-9 in Appendix A for salt water in Cu-Ni pipe with d = 4 in. and wall thickness = 1/8 in.,

$$v = 4170 \quad \text{fps} \quad ,$$

$$\rho v = 4170 \times 1.15 \times 10^{-3} = 4.80 \quad \frac{\text{lb sec}}{\text{in.}^3} \ ,$$

$$\rho = 9.56 \times 10^{-5} \quad \frac{\text{lb sec}^2}{\text{in.}^4} \ .$$

Y_o is then given by Fig. 57, for 4 in. i.d.,

$$Y_o = 2.6 \quad \frac{\text{in.}^5}{\text{lb sec}} \ .$$

Now the length between side-branch elements is

$$l = \frac{4170 \times 12}{8 \times 30} = 208 \quad \text{in.} \quad (17.4\ \text{ft}) \ .$$

The second element should be placed at about this distance from the noise source.

For element No. 1 a four convolution bellows is used. This bellows then has a stiffness of

$$k = \frac{4000}{4} = 1000 \quad \frac{\text{lb}}{\text{in.}} \ .$$

Entering Fig. 59 with this value of k and a 4 in. effective diameter gives

$$C = 0.16 \quad \frac{\text{in.}^5}{\text{lb}} \ .$$

The q of the element can then be found from Fig. 63 by calculating $\omega_{01}C = 2\pi \times 30 \times 0.16 = 30.1$, and entering with $Y_o = 2.6$,

$$q = 11 \ .$$

The weight required to tune this bellows to 30 cps is found from Fig. 62;

$$W = 11 \quad \text{lb} \quad .$$

The weight of 1/3 the bellows and the cap to seal it is 2 lb, leaving 9 lb to be added. Instead of adding this weight, an inertance tube or hole will be used. Fig. 61 gives the inertance equivalent to 9 lb for a 4 in. effective piston diameter as

$$L = 1.46 \times 10^{-4} \quad \frac{\text{lb sec}^2}{\text{in.}^5} \quad .$$

The inertance of a tube is given by

$$L = \frac{\rho \ell_e}{S} \quad ,$$

where S is the tube section area and ℓ_e is the effective length for a physical length ℓ given by $\ell_e = \ell + 0.8\sqrt{S}$. For an inertance hole $\ell_e = 0.8\sqrt{S}$ and $L = 0.8\ \rho\sqrt{S}/S$. The hole diamter required to give a certain inertance is then

$$d = \frac{1.6\rho}{L\sqrt{\pi}} = 0.902\,\frac{\rho}{L} \quad \text{in.} \quad .$$

The inertance hole diameter in this case is then

$$d = \frac{0.902 \times 9.56 \times 10^{-5}}{1.46 \times 10^{-4}} = 0.59 \quad \text{in.} \quad .$$

The bellows cap should be placed a distance of about $\ell_e/2$ away from the inertance hole. In this case that distance is 0.21 in.

If more than one identical hole is used, the required inertance for each hole is

$$L_n = nL \quad ,$$

where n is the number of identical holes. In this example, if two holes are used, the diameter of each hole should be

$$d = \frac{0.902 \times 9.56 \times 10^{-5}}{2 \times 1.46 \times 10^{-4}} = 0.295 \quad \text{in.} \quad .$$

These two holes should be placed at least 1 in. apart to prevent interaction between them.

Next consider the use of a 1 in. i.d. inertance tube. Its inertance must be $1.46 \times 10^{-4} \ \frac{\text{lb sec}^2}{\text{in.}^5}$. The effective length is then

$$\ell_e = \frac{LS}{\rho} = \frac{\pi d^2 L}{4\rho}$$

$$= \frac{1.46 \times 10^{-4} \times \pi \times (1)^2}{4 \times 9.56 \times 10^{-5}} = 1.2 \quad \text{in.} \quad .$$

The physical length is then

$$\ell = \ell_e - 0.8\sqrt{S} = \ell_e - 0.4d\sqrt{\pi}$$

$$= 1.2 - 0.4 \times 1\sqrt{\pi} = 0.49 \quad \text{in.} \quad .$$

The bellows cap should be placed at a distance of about one end correction from the end of the tube. In this case that distance is $0.2d\sqrt{\pi} = 0.355$ in.

The second side-branch is to be resonant at 60 cps and have a q = 11. Then the compliance required is

$$C = \frac{q_2 Y_o}{\omega_{02}} = \frac{11 \times 2.6}{2\pi \times 60} = 7.57 \times 10^{-2} \quad \frac{\text{in.}^5}{\text{lb}} \quad .$$

For a piston diameter of 4 in., Fig. 59 gives a stiffness of

$$k = 2100 \quad \frac{\text{lb}}{\text{in.}}$$

for bellows No. 2. A two convolution bellows can then be used for the compliant element to give a $k = 2000$ lb/in., but the q of the element will be slightly different from 11.

The weight required to resonate this bellows at 60 cps is given by Fig. 62:

$$W = 5.62 \quad \text{lb} \quad .$$

The weight of the cap and 1/3 the bellows is taken as 1.5 lb here, which leaves a weight of 5.62 - 1.5 = 4.12 lb to be added. The inertance equivalent to this weight from Fig. 61 is

$$L = 6.5 \times 10^{-5} \quad \frac{\text{lb sec}^2}{\text{in.}^5} \quad .$$

This inertance is then obtained by an inertance hole of diameter

$$d = \frac{0.902 \times 9.65 \times 10^{-5}}{6.7 \times 10^{-5}} = 1.3 \quad \text{in.} \quad .$$

The bellows cap should be placed about 0.46 in. from the hole.

This filter with the inertance tube used to tune the first element and an inertance hole tuning the second element is shown in Fig. 71. The transmission loss characteristics will be very much like those shown in Fig. 24 for $q = 10$. The infinities will occur at 30 and 60 cps, and the zeroes will be at 105, 210, 315, etc., cps.

4. High Pressure Hydraulic System
(Two-Section Expansion Chamber Filter)

The fluid lines of 1000 psia hydraulic system have pump noise and gear noise that extends from about 180 cps up to about 20 kc. Most of the noise energy lies in the range of 1 to 3 kc. For system pressures of the order of 1000 psia, compliant elements are probably impractical. The liquid-filled, side-branch tube or expansion chamber should be considered. Here a two-section expansion chamber with identical sections will be used to provide large transmission loss characteristics and wide rejection bands (Fig. 34). The first maximum of transmission loss will be set at 2.5 kc which makes $f_\ell = 5$ kc. The chamber length is then

$$\ell = \frac{v}{2f_\ell} \quad .$$

An m value of about 31.6 will be used. Before proceeding, v and Y_0 must be calculated.

The system piping has 1/2 in. i.d., and 0.147 in. wall thickness; the material is steel. From Appendix A, Fig. A-14,

$$v = 3590 \quad \text{fps} \quad ,$$

$$v_0 = 3635 \quad \text{fps} \quad ,$$

$$\rho v = 3590 \times 1.08 \times 10^{-3} = 3.88 \quad \frac{\text{lb sec}}{\text{in.}^3} \quad .$$

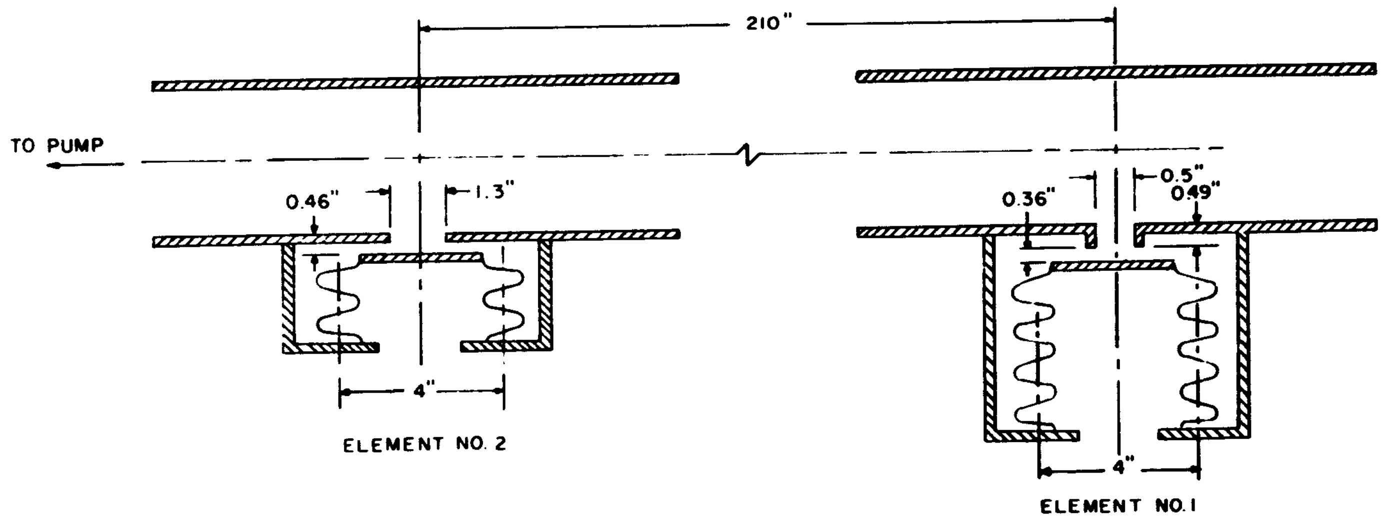

(a.) TWO-SECTION LUMPED-ELEMENT SIDE - BRANCH FILTER

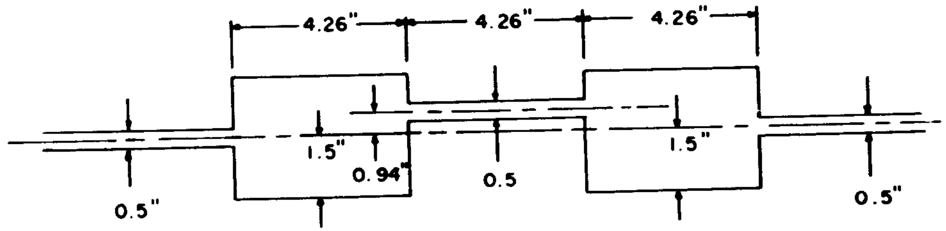

(b.) TWO SECTION EXPANSION CHAMBER FILTER

FIGURE 71

DRL - UT
DWG AS 7137
JVK - BEE
9 - 14 - 62

From Fig. 57 for 1/2 in. i.d., the characteristic admittance is given as

$$Y_o = 5.2 \times 10^{-2} \quad \frac{\text{in.}^5}{\text{lb sec}} \quad .$$

The value of m is nearly equal to the ratio of the chamber area to the pipe area. Or,

$$\frac{d_c}{d_o} \approx \sqrt{m} = \sqrt{31.6} = 5.62 \quad ,$$

where d_c is the chamber i.d. and d_o is the pipe i.d. Here d_c should be

$$d_c = 0.5 \times 5.62 = 2.81 \quad \text{in.} \quad ,$$

but a standard 3 in. i.d. pipe with 0.3 in. wall thickness will be used for the chamber. Fig. A-14 in Appendix A does not cover the region for a wall thickness of 0.3 in. and i.d. = 3 in. A rough extrapolation gives v = 3550 fps for the velocity in the large pipe. An error in this number can affect the value of m and the length of the chamber slightly.

Figure 57 gives the characteristic admittance for the chamber. For $\rho v = 1.08 \times 10^{-3} \times 3550 = 3.83$,

$$Y_{oc} = 1.8 \quad \frac{\text{in.}^5}{\text{lb sec}} \quad .$$

The value of m for the chamber is thus,

$$m = \frac{Y_{oc}}{Y_o} = \frac{1.8}{0.052} = 34.6 \quad .$$

The predicted maximum transmission loss is then

$$\text{T.L.} = 40 \log_{10} (34.6) - 6 = 55.6 \quad \text{dB} \ .$$

The required length of each chamber and connecting tube is found to be

$$l = \frac{3550 \times 12}{2 \times 5000} = 4.26 \quad \text{in.} \ .$$

Unless the inlet and outlet of each chamber are properly placed, the first higher order mode will be propagated by the chamber at

$$f_{01} = \frac{\alpha_{10} v_0}{d} = \frac{0.586 \times 3635 \times 12}{3} = 8.5 \quad \text{kc} \ ..$$

If the inlet to a chamber is placed exactly on the chamber center line, the first two modes will not be excited. Then, by placing the outlet tube at a distance

$$r = 0.314 \ d = 0.314 \times 3 = 0.94 \quad \text{in.}$$

off the center line, the next higher mode will not escape the chamber. This arrangement allows only the modes above a frequency of

$$f = 1.697 \times 3635 \times \frac{12}{3} = 24.6 \quad \text{kc}$$

to be propagated through the filter.

When the connecting tube is placed as shown in Fig. 71(b), the second chamber inlet is offset, and the third mode will not be excited. With the outlet on the centerline, the first two modes have a pressure zero at the outlet and do not leave the chamber.

September 1962
ELH:vh

The transmission loss curve will be very nearly that shown in Fig. 34 for m = 31.6. No more than 10 dB loss will occur below f = 0.07 × 5000 cps = 350 cps. Between 350 cps and 0.91 × 5 kc = 4.6 kc, the transmission loss goes to a maximum of 55.6 dB and back to zero. There are regions of low transmission loss approximately 700 cps wide centered at 5, 10, 15, ... kc. The shape of the curve should be preserved up to nearly 25 kc, since the first undesired mode is at 24.6 kc.

September 1962
ELH:vh

CHAPTER IV: SUMMARY OF LABORATORY MEASUREMENTS OF FILTER PERFORMANCE

A. INTRODUCTION

During the filter investigation program at DRL, sound measurements were made on experimental filters. With the exception of side-branch filters with gas volume type lumped-parameter branch elements, one or more of each of the types of filters described in Chapter III were built and tested in the Laboratory. It is the purpose of this chapter (1) to describe the filter test conditions, (2) to specify what kind of sound measurements were made, and (3) to present representative test results for each of the filters tested.

September 1962
ELH/JVK:vh

B. FILTER TEST CONDITIONS

Although there was considerable variation in the details of tests on the various filters, most of the tests had certain features in common. Each filter tested was installed between a sound source and some form of acoustic termination in a water-filled system. Hydrophones at the filter input and output ports sensed pressure inside the lines at those points. Signals from these transducers were analyzed. The resultant noise spectra were either individually plotted against frequency or expressed in decibels relative to a common reference, differenced, and then plotted.

Sound sources used were (1) an electromagnetic shaker unit fitted with a compliantly-mounted, pressure-sealed piston, (2) submarine water pumps of the multistage, centrifugal type, and (3) a partially closed valve producing flow-generated noise in a water line.

The magnetic shaker unit, Fig. 72, was used in so-called no-flow tests; the test filters were water-filled, but there was no net circulation of water through them. Character of the sound produced by the shaker unit was of course governed by the electrical signal applied to it. Either sine wave or random noise signals were used in no-flow tests.

Two different submarine pumps were used for filter test noise sources. One was a six stage, series connected, centrifugal drain pump. Figure 73 shows a sketch of it and gives some information on its size and rating. The other pump was also a six stage, centrifugal pump but was of somewhat larger capacity and had provision for connecting the six stages in two parallel groups of three each. This pump is shown in Fig. 74. When either of these pumps was used in filter tests, water was pumped through the filter. These flow tests simulated conditions in a practical system. The pumps produced noise having a broad spectrum with peaks at the pump rotation and impeller blade frequencies. Pump noise spectra varied with speed, system static pressure, and stage connections. In interpreting results of flow tests made with either of the submarine pumps as a sound source, it should be kept in mind that under flow conditions noise is generated by fluid turbulence inside the filters and connecting lines.

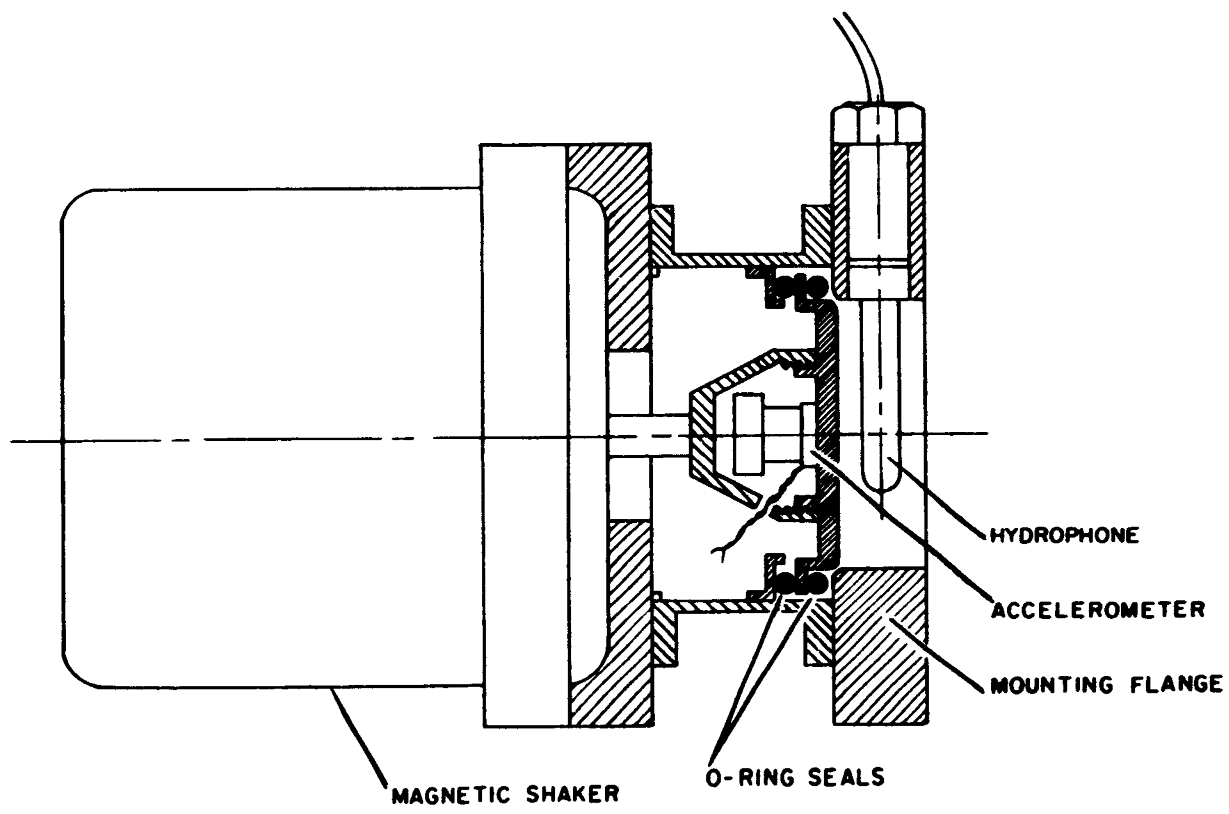

FIGURE 72
MAGNETIC SHAKER TYPE SOUND SOURCE AND ACOUSTIC IMPEDANCE MEASURING HEAD

DRL - UT
DWG AS 7392
JVK - BEE
9 - 14 - 62

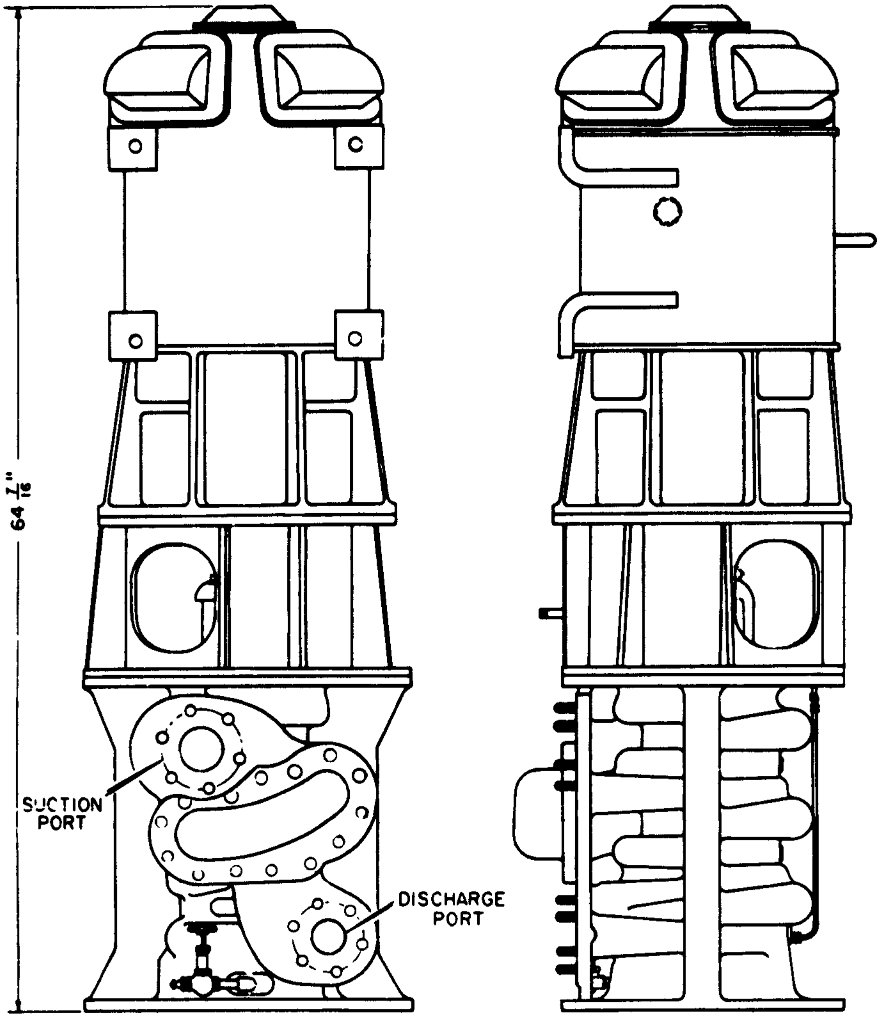

RATING

80 GPM (SEA WATER) AT 50 FT TOTAL DYNAMIC HEAD

50 GPM (SEA WATER) AT 500 FT TOTAL DYNAMIC HEAD

FIGURE 73
OUTLINE DRAWING - DRAIN PUMP - GOULDS PUMPS, INC.
FIGURE 3375 2" 6 STAGE

DRL - UT
DWG AS 7393
JVK - BEE
9 - 25 - 62

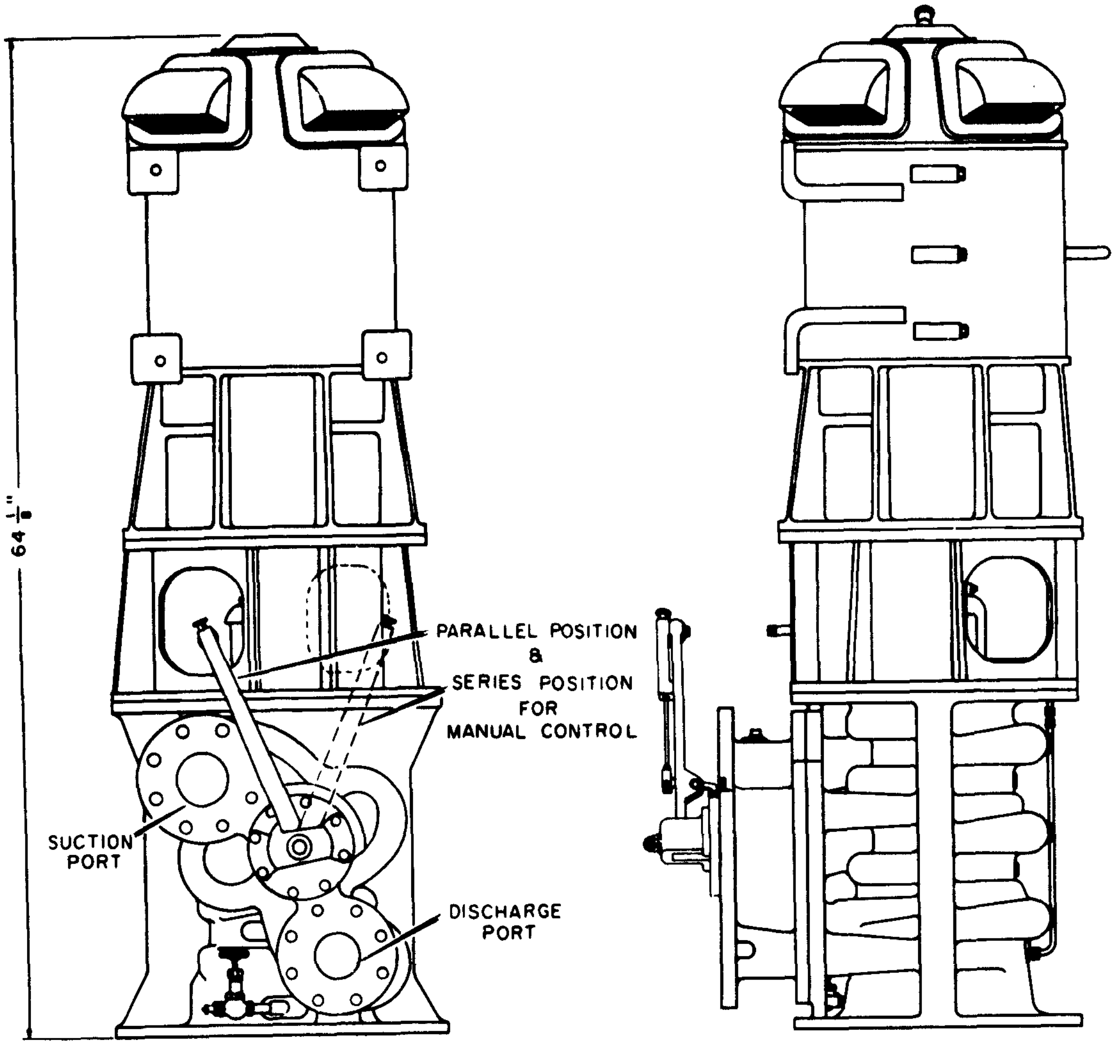

RATING

70 GPM (SEA WATER) AT 600 FT TOTAL DYNAMIC HEAD

250 GPM (SEA WATER) AT 240 FT TOTAL DYNAMIC HEAD

FIGURE 74
OUTLINE DRAWING - TRIM PUMP - GOULDS PUMPS, INC.
FIGURE 3374 2" 6 STAGE

DRL - UT
DWG AS 7394
JVK - BEE
9 - 26 - 62

The partly closed valve was used as a noise source in flow tests at much lower flow velocities than those produced by the pumps. The valve, connected to the municipal water supply lines, was adjusted to produce broad band noise. The noise spectrum was very sensitive to changes in the valve setting.

A wide variety of acoustic terminations were used on the filters. In no-flow tests, open-ended water columns contained in metal pipes or fire hoses or both were used. In some cases, filter output ports were connected to pipe or hose lines leading to water storage tanks. For some tests, a submarine trim system manifold was included in the system between the filter output port and the storage tanks.

In flow tests in which either pump was used, water was circulated in a closed path including the filter. Either pipe or hose connected the filter output port to storage tanks. Metal pipe lines returned water from the tanks to the pump suction port. The submarine trim manifold was used in some of these flow tests also.

In the few tests in which the hissing valve was used as a sound source, flow rates were very low; water flowed through the filter, through a length of pipe, and into a steel barrel from which it overflowed onto the ground.

September 1962
JVK:vh

C. SOUND MEASUREMENTS

In all the laboratory tests for which results are presented, the filter output and input ports were determined by the location of hydrophones used to measure sound pressures inside the lines at those points.

Several different hydrophones were used in the course of the filter program. They are specified in the following list.

	Name	Serial No.	Nominal Sensitivity dB ref 1 V/μbar
(1)	Massa H-11	13	- 88.5
(2)	Chesapeake I 6P 330/T	8	-104
(3)	Chesapeake II 6P 330/T	9	-104
(4)	ARC BC-32	51	-109.5
(5)	ARC BC-32	53	-109.8
(6)	ARC LC-32	149	-103.5
(7)	ARC BC-10	230	-117
(8)	ARC BC-10	237	-117

In a majority of the no-flow tests, and in all the flow tests, fixed hydrophones, those not on movable probes, were mounted in small side cavities separated from the inside of the pipe by rubber fairings. Figure 75(a) and (b) shows the usual hydrophone arrangements. In some cases the membrane between the hydrophone space and the inside of the pipe was omitted. Fig. 75(c).

Figure 76 is a block diagram indicating electronic instruments in an arrangement typical of those used for measuring and analyzing hydrophone signal voltages. The instruments that were available for making these measurements are listed below.

Vacuum Tube Voltmeters

(1)	True RMS VTVM	Ballantine Labs	Model 320
(2)	AC Voltmeter	Ballantine Labs	Model 310A

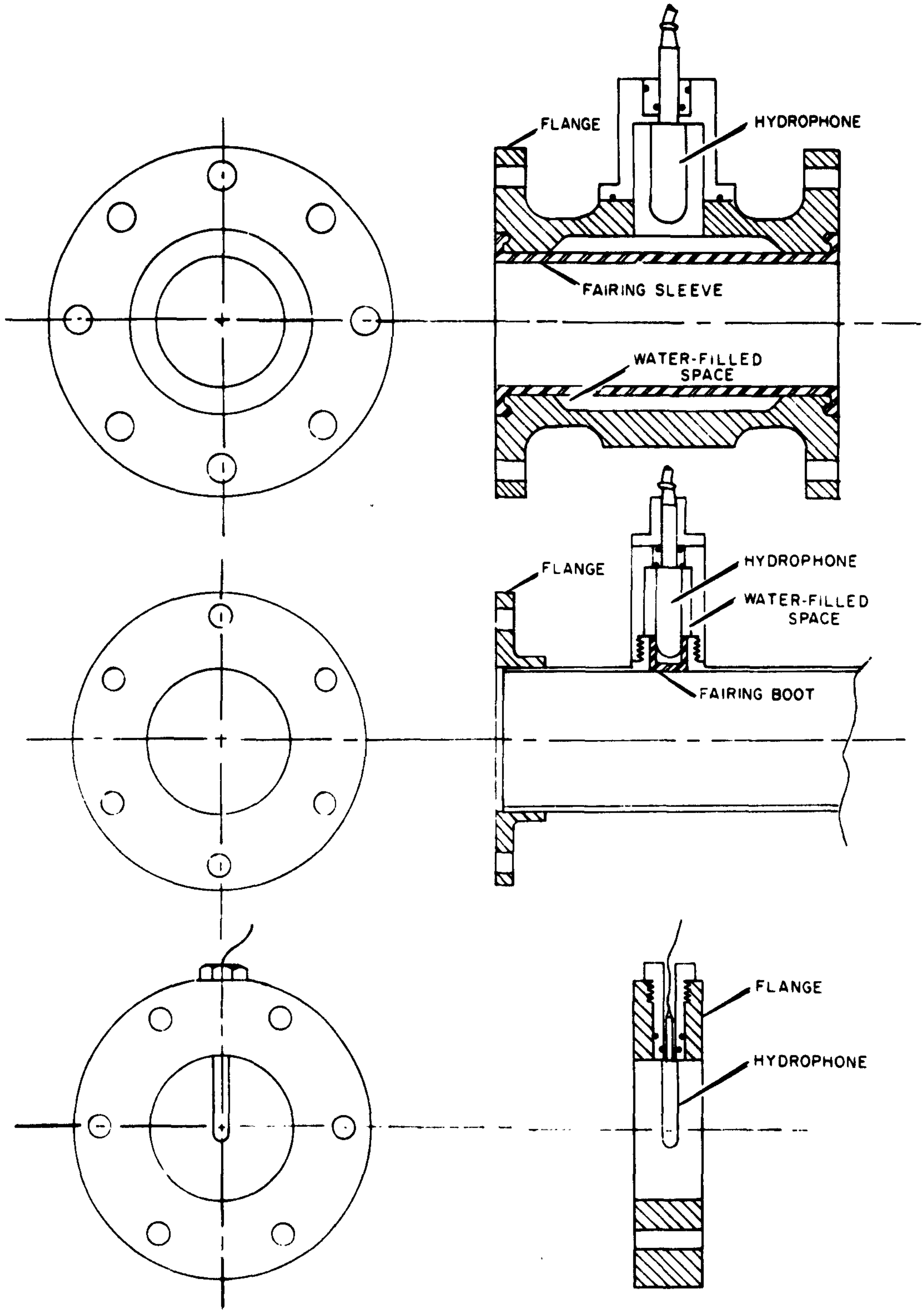

FIGURE 75
HYDROPHONE PORTS

DRL - UT
DWG AS 7405
JVK - BEE
9 - 21 - 62

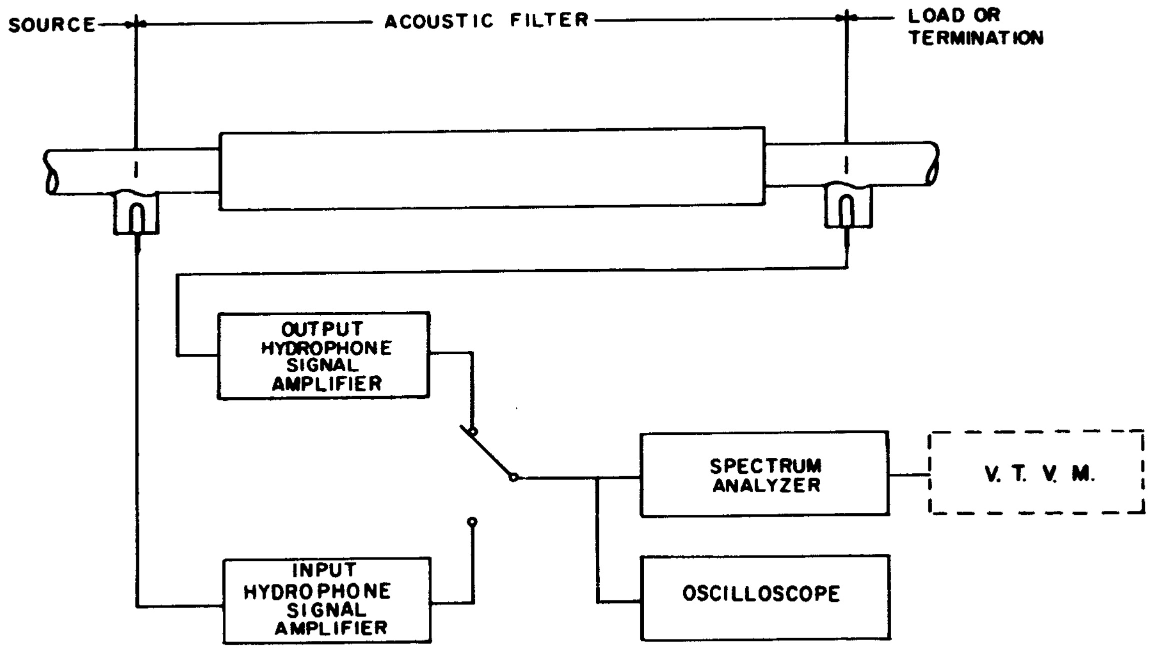

FIGURE 76
INSTRUMENTATION FOR SOUND MEASUREMENTS ON ACOUSTIC FILTERS

DRL - UT
DWG AS 7396
JVK - BEE
9 - 14 - 62

September 1962
JVK:vh

Oscilloscopes

(1)	Single Trace	Hewlett Packard	Model 130A
(2)	Dual Trace	Hewlett Packard	Model 122A

Spectrum Analyzers

(1) Sound analyzer--General Radio--Model 760-A (2% proportional bandwidth, 25 cps to 7500 cps)

(2) Octave band analyzer--General Radio--Model 1550-A, 20 cps to 10,000 cps

(3) Half-octave band analyzer--H. H. Scott--Model 420-A, 20 cps to 9600 cps (used with additional filters)

(4) Half-octave band analyzer--White Instrument Labs--Model 1410, 8 cps to 10 kc

(5) Sound and vibration analyzer--General Radio--Type 1554-A, One-third octave, narrow band and all pass, 2.5 cps to 25,000 cps

D. INTERPRETATION OF TEST DATA

For several reasons, the test data of this section are subject to interpretation different from that for predictions based on transmission loss curves of Chapter III. The ratio of output sound pressure magnitude to input sound pressure magnitude expressed as sound pressure level differences or sound pressure band level differences in decibels in this section is different from the transmission loss. Transmission loss, it will be recalled, expresses for a single frequency the ratio of the output sound pressure magnitude to the magnitude of the incident wave contribution to sound pressure at the input under the imposed condition that the filter is terminated by a load having an input admittance equal to the characteristic admittance of the liquid line in which the filter is used. Also, some of the measured data given apply to bands of frequencies rather than single frequencies as do the transmission loss values. Another fundamental difference between conditions for measured and calculated filter performance is the presence of standing waves in the lines at the ends of the filter in the actual tests. Finally, flow noise distributed continuously throughout the filter and its connecting lines was present in the flow tests, but it was not considered in the calculation of transmission loss.

September 1962
JVK:vh

E. TEST RESULTS

Curves showing results of tests on the various filters are arranged according to the following outline:

I. Side-Branch-Element Filters

A. Filters with One Branch Element

1. Spring-Piston Type Branch Elements

Figures 77 through 78.

2. Metal Bellows Type Branch Element

Figures 79 through 84.

3. Closed-end Stub Type Branch Element

Figures 85 through 87.

B. Filters with Two Branch Elements

1. Spring-Piston Type Branch Elements

Figures 88 through 94.

2. Disk Spring Type Branch Elements

Figures 95 through 99.

3. Metal Bellows Type Branch Elements

Figures 100 through 105.

C. Filters with Three Side-Branch Elements

1. Spring-Piston Type Branch Elements

Figures 106 through 123.

2. Metal Bellows Type Branch Elements

Figures 124 through 127.

II. Expansion Chamber Filters

A. Single Chamber Filters

1. Chamber 2 ft Long; Area Ratio 14.1

Figures 128 through 130.

2. Chamber 5 ft Long; Area Ratio 14.1

Figures 131 through 135.

3. Chamber 7 ft Long; Area Ratio 14.1

Figures 136 through 138.

4. Chamber 10 ft Long; Area Ratio 14.1

Figures 139 through 141.

B. Double Chamber Filters

1. Chambers 2 ft Long and 5 ft Long; Area Ratio 14.1

Figures 142 through 143.

2. Chambers 5 ft Long; Area Ratio 14.1

Figures 144 through 147.

3. Chambers 5 ft Long and 7 ft Long; Area Ratio 14.1

Figures 148 through 151.

III. Combination Filters

A. Single-Chamber and Lumped-Parameter, Side-Branch Element

Figures 152 through 154.

B. Double-Chamber and Closed-End Stubs

Figures 155 through 156.

IV. Quincke Tube Filter

Lengths 55 in. and 133 in.: Figure 157.

On each sheet of curves showing filter test results there is drawn a sketch of the physical layout of the filter to which the curves pertain. Below the layout sketch is the transmission line acoustical circuit of the filter with the significant information given. Units are not written for all numerical values of acoustical parameters listed on the curves, but the same units are used consistently throughout. These are as follows:

Quantity	Symbol	Unit IPS
Length	ℓ	in.
Wave Velocity	v	$\frac{\text{ft}}{\text{sec}}$
Acoustic Admittance	Y	$\frac{\text{in.}^5}{\text{lb sec}}$
Inertance	L	$\frac{\text{lb sec}^2}{\text{in.}^5}$
Compliance	C	$\frac{\text{in.}^5}{\text{lb}}$

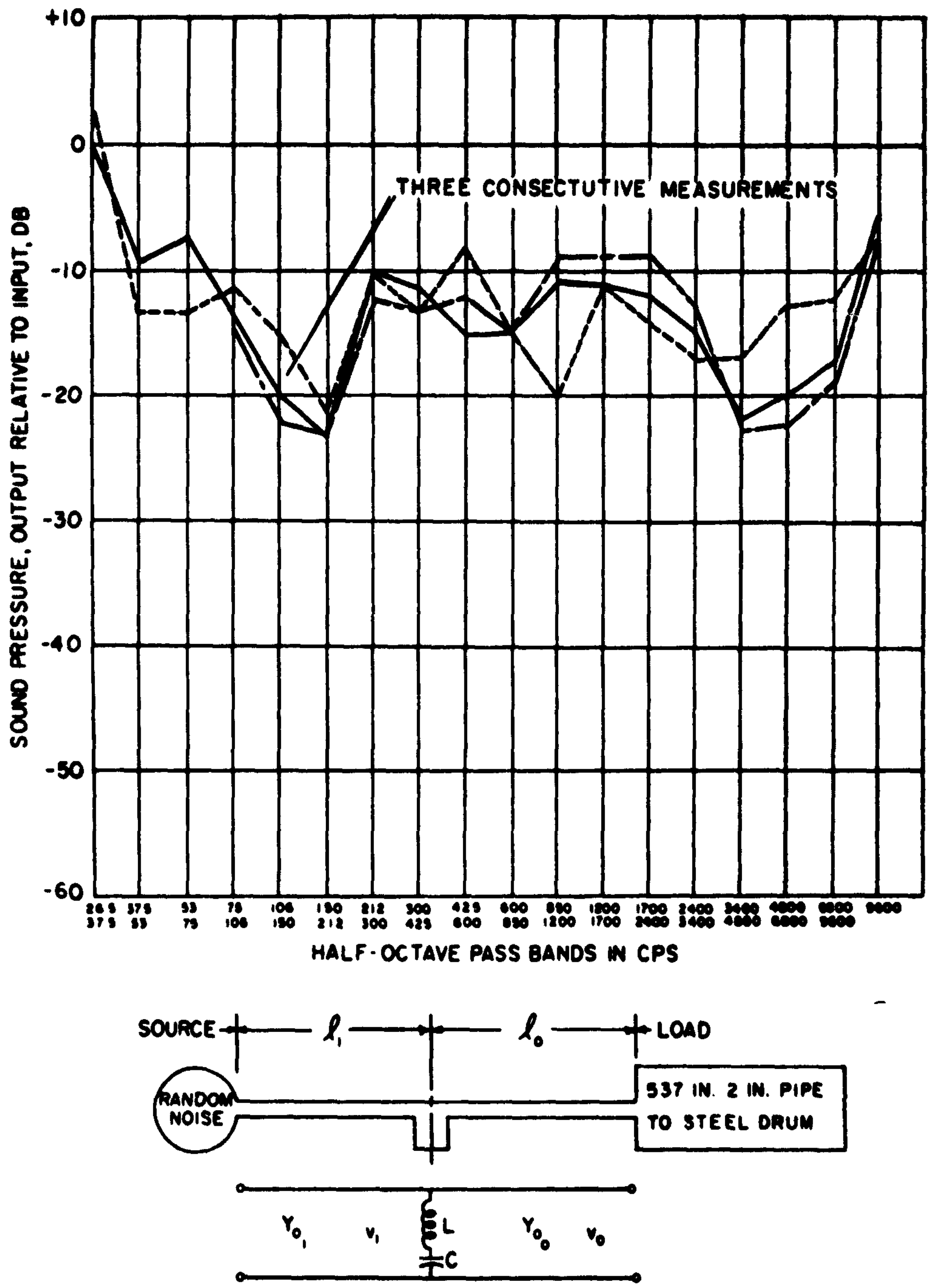

l_0 = 198 IN. $\quad Y_{0_0}$ = .657 $\quad v_0$ = 4280 $\quad L = 1.32 \times 10^{-4}$

l_1 = 198 IN. $\quad Y_{0_1}$ = .657 $\quad v_1$ = 4280 $\quad C = 5.26 \times 10^{-2}$

FIGURE 77
ONE ELEMENT SIDE-BRANCH FILTER WITH SPRING-PISTON BRANCH ELEMENT

DRL - UT
DWG AS 6981
JVK - BEE
11 - 13 - 62

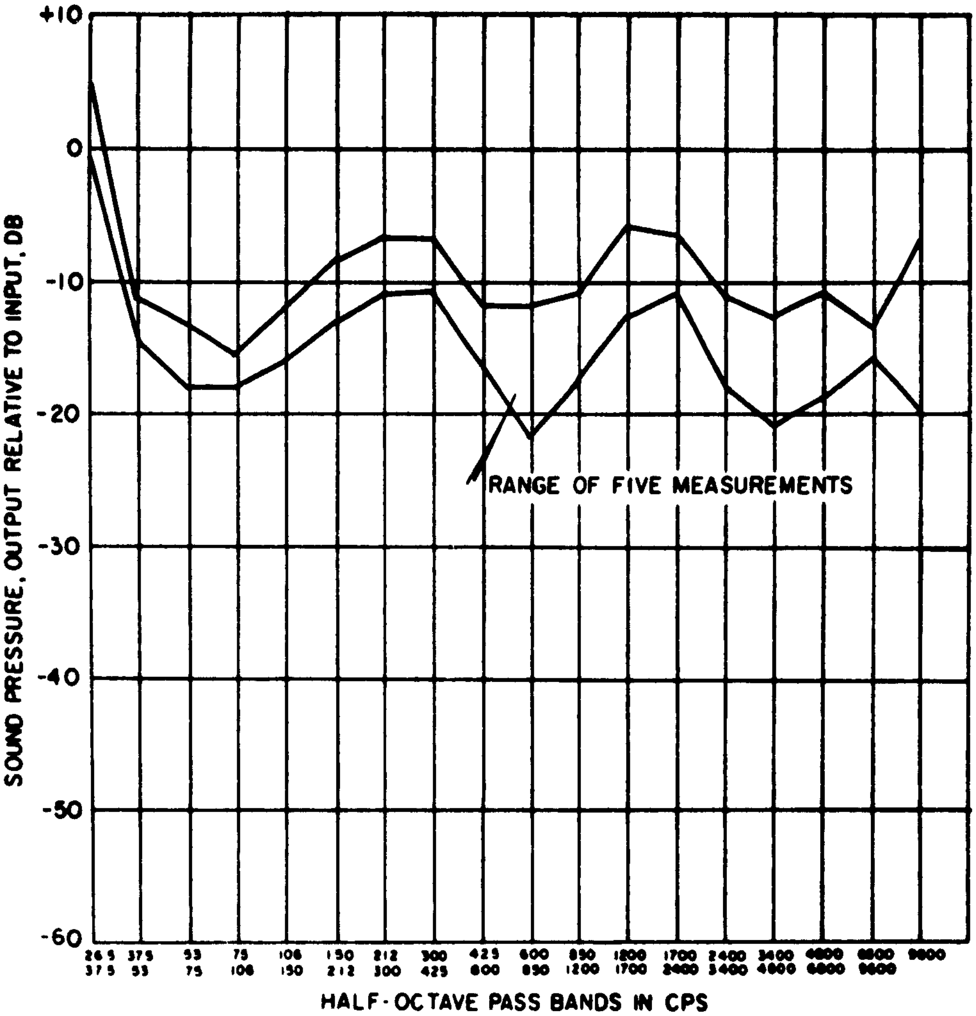

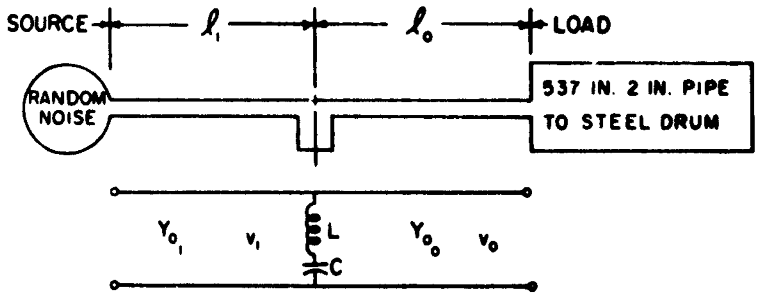

ℓ_0 = 198 IN. Y_{0_0} = .657 v_0 = 4280 L = 4.5 $\times 10^{-5}$

ℓ_1 = 198 IN. Y_{0_1} = .354 v_1 = 4430 C = 11.05 $\times 10^{-8}$

FIGURE 78
ONE ELEMENT SIDE-BRANCH FILTER WITH SPRING-PISTON BRANCH ELEMENT

DRL - UT
DWG AS 6983
JVK - BEE
11 - 13 - 62

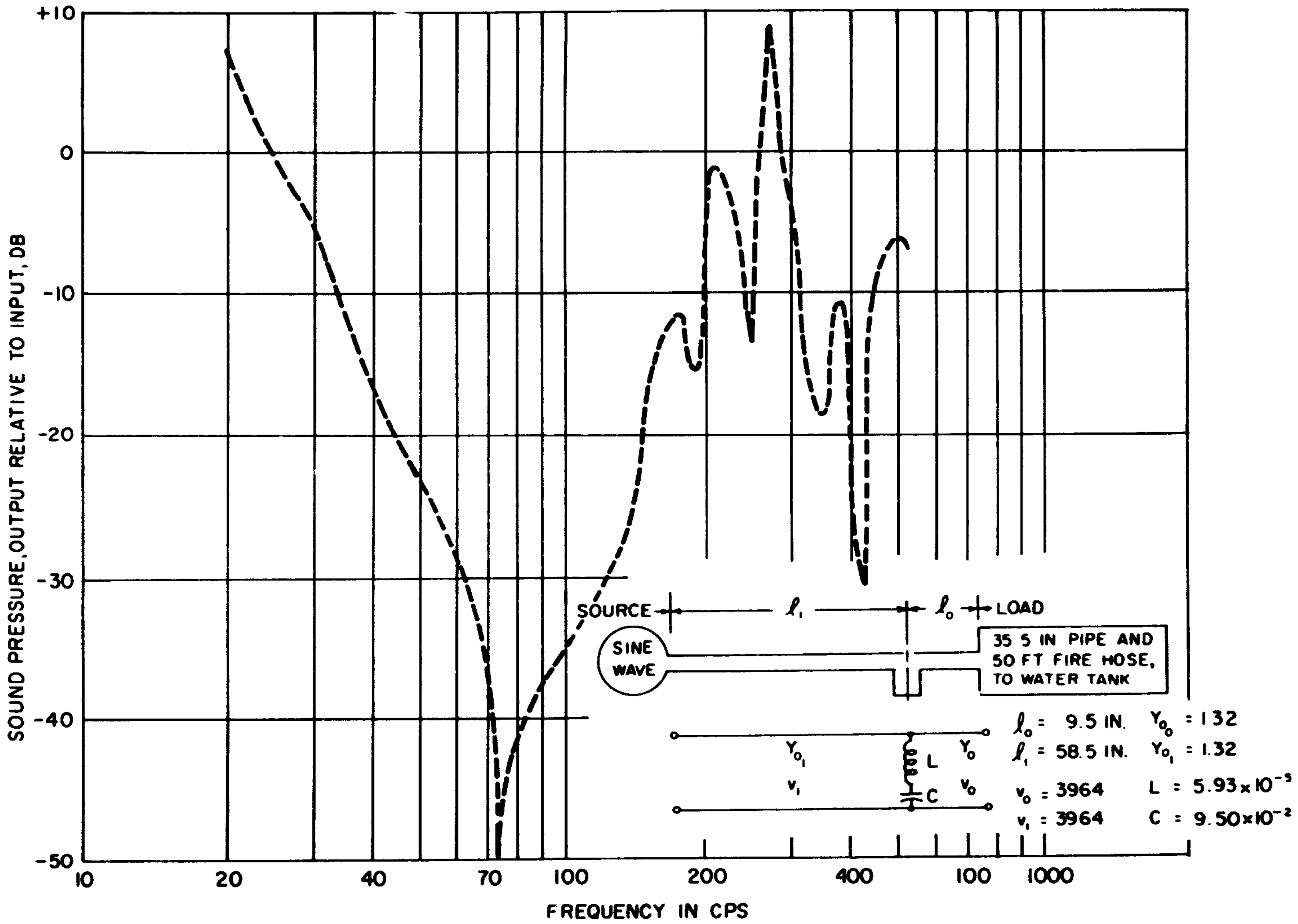

FIGURE 79
ONE ELEMENT SIDE-BRANCH FILTER WITH METAL BELLOWS BRANCH ELEMENT

DRL - UT
DWG AS 6985
JVK - BEE
11 - 12 - 62

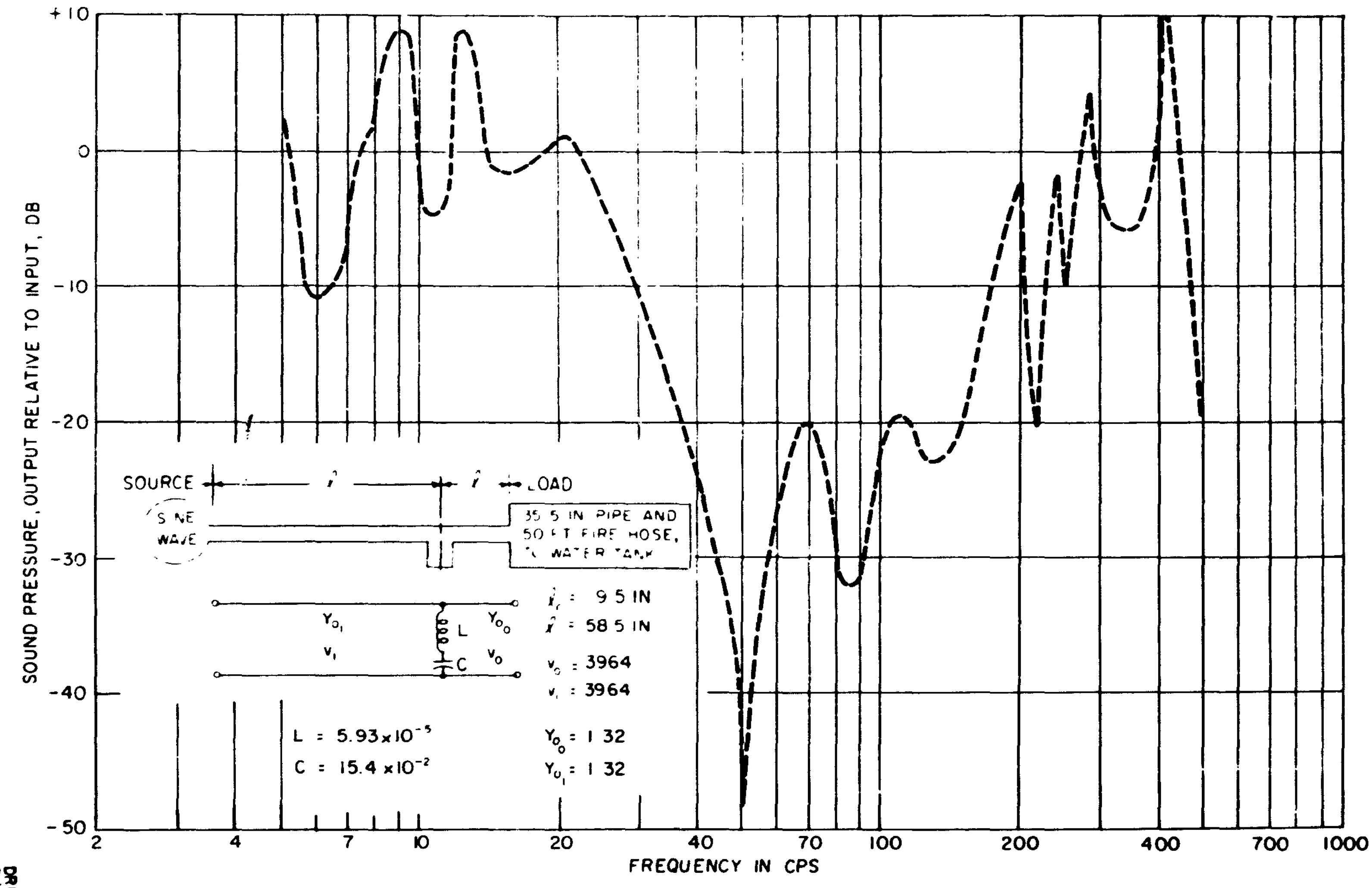

FIGURE 80
ONE ELEMENT SIDE-BRANCH FILTER WITH METAL BELLOWS BRANCH ELEMENT

DRL - UT
DWG AS 6987
JVK - BEE
11 - 12 - 62

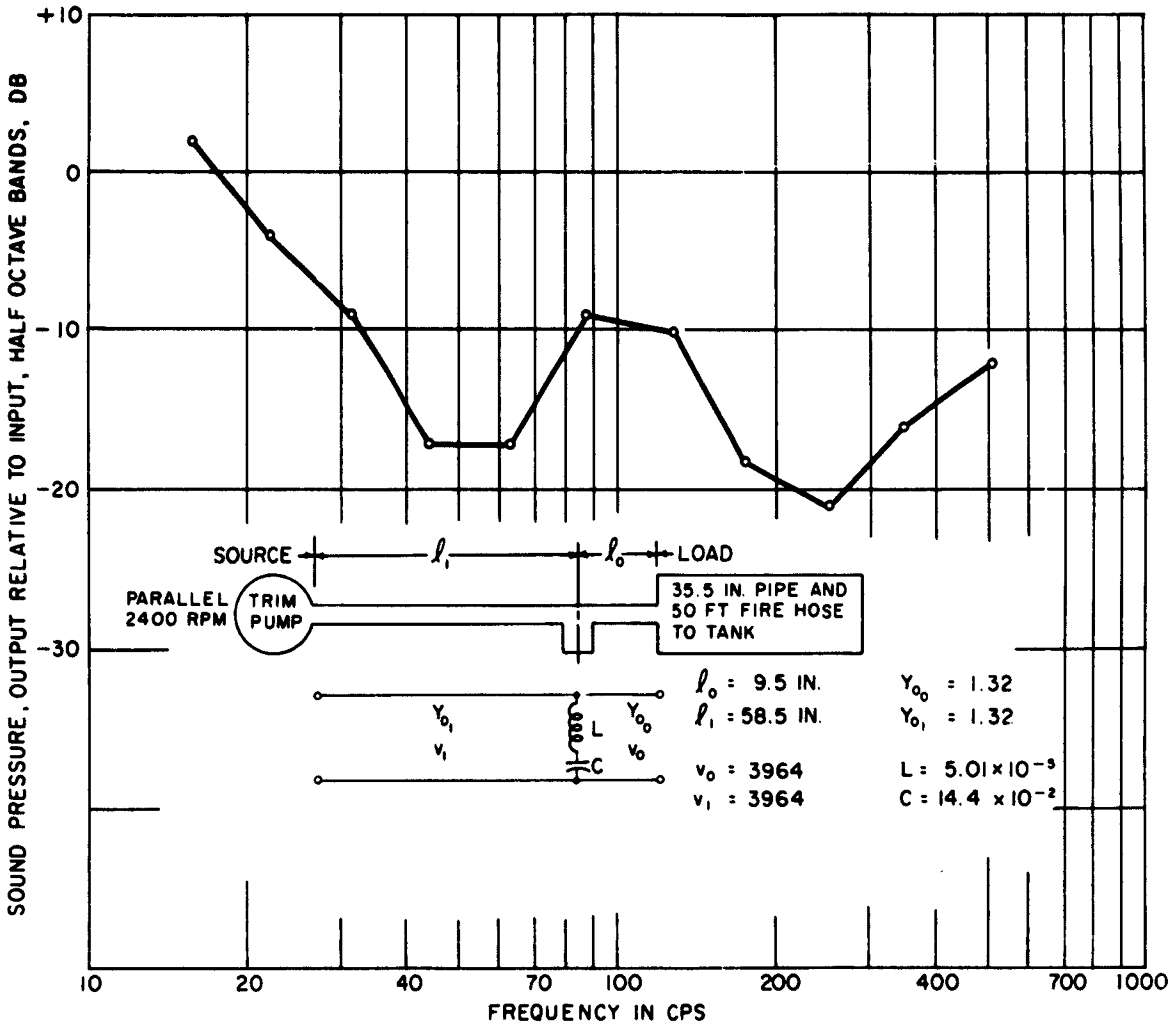

FIGURE 81
ONE ELEMENT SIDE-BRANCH FILTER WITH METAL BELLOWS
BRANCH ELEMENT

DRL - UT
DWG AS 6988
JVK - BEE
11 - 8 - 62

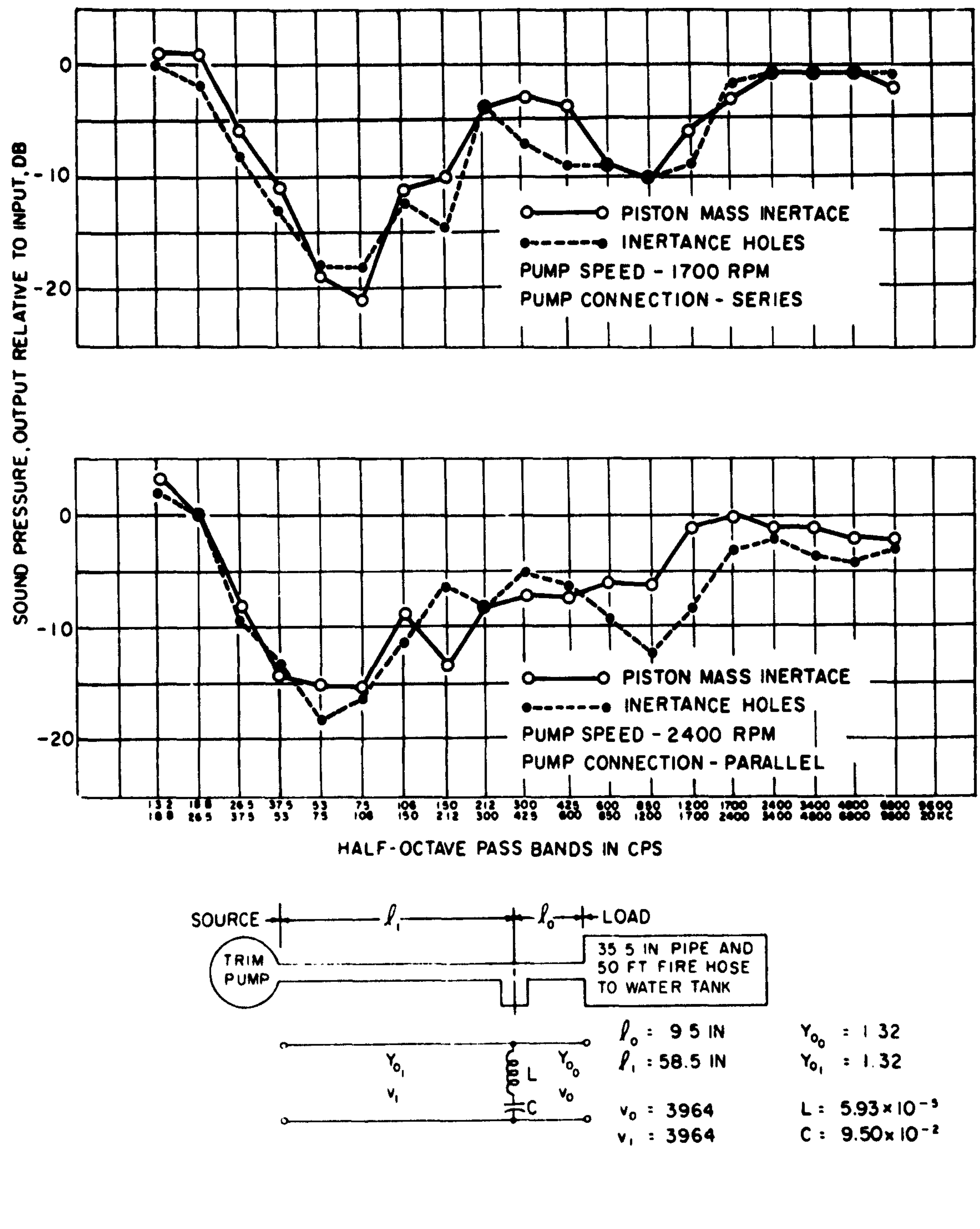

FIGURE 82
ONE ELEMENT SIDE-BRANCH FILTER WITH METAL BELLOWS BRANCH ELEMENT

DRL - UT
DWG AS 6990
JVK - BEE
11 - 8 - 62

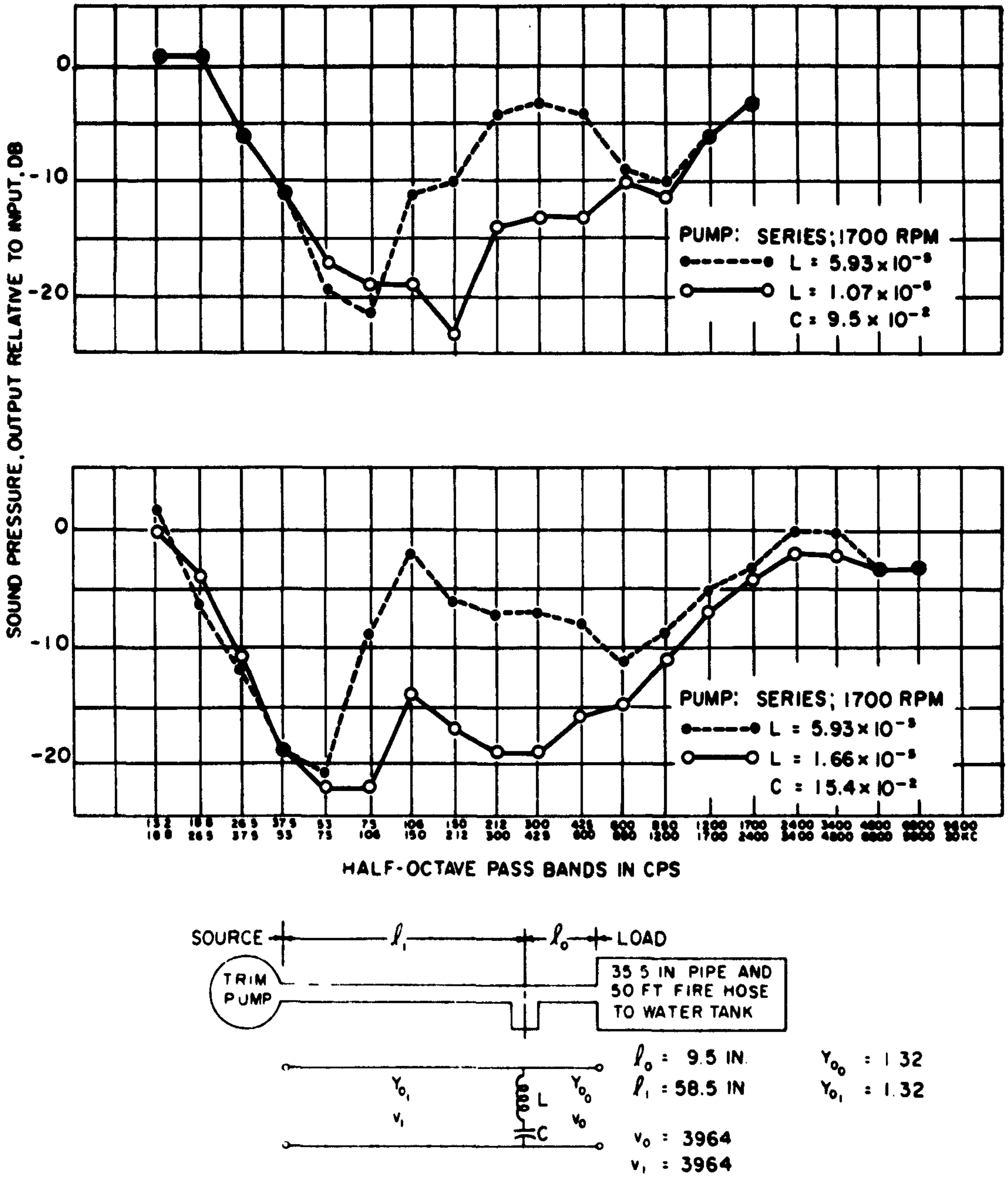

FIGURE 83
ONE ELEMENT SIDE-BRANCH FILTER WITH METAL BELLOWS
BRANCH ELEMENT

DRL - UT
DWG AS 6991
JVK - BEE
11 - 8 - 62

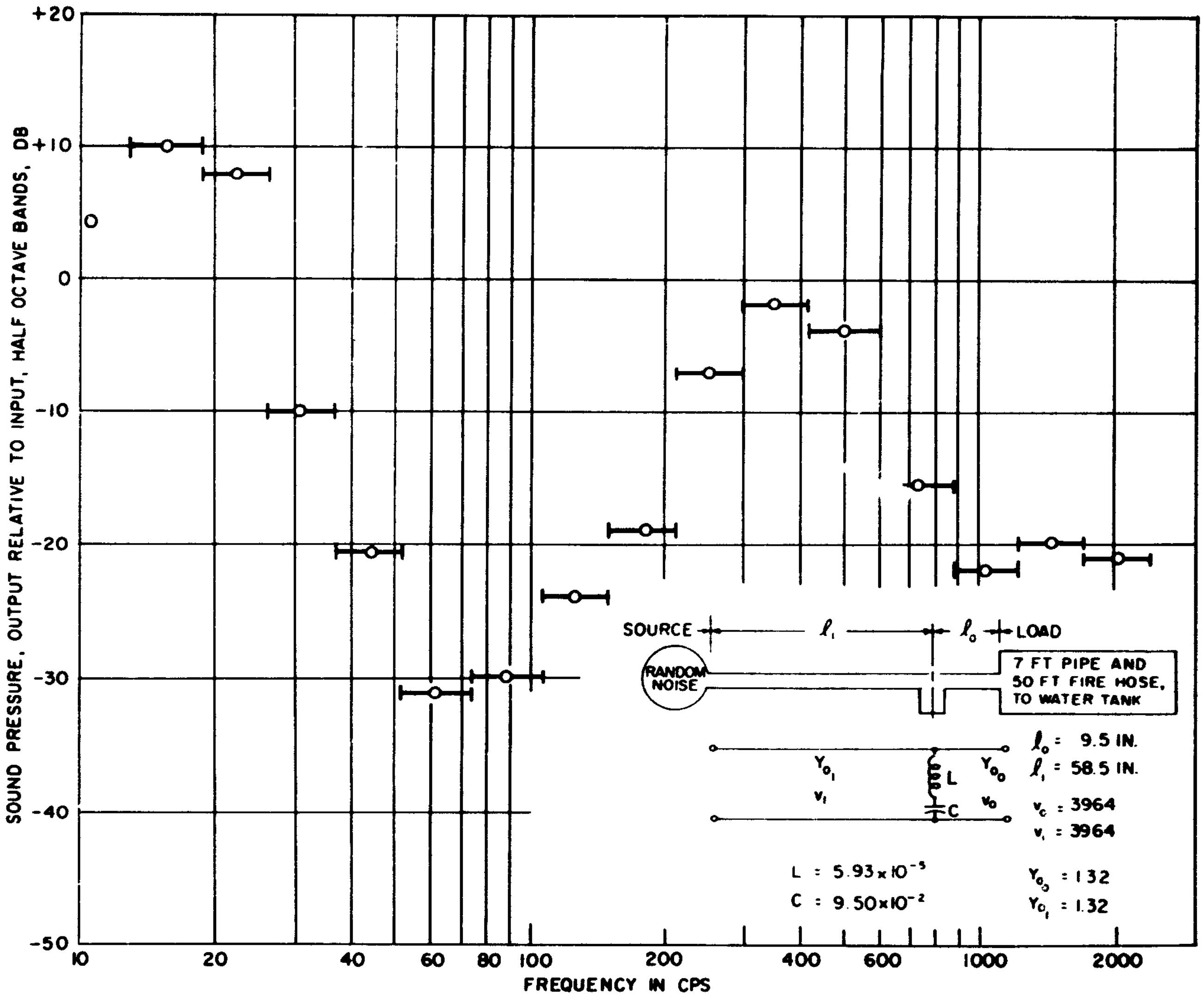

DRL - UT
DWG AS 6993
JVK - BEE
11 - 12 - 62

FIGURE 84
ONE ELEMENT SIDE-BRANCH FILTER WITH METAL BELLOWS BRANCH ELEMENT

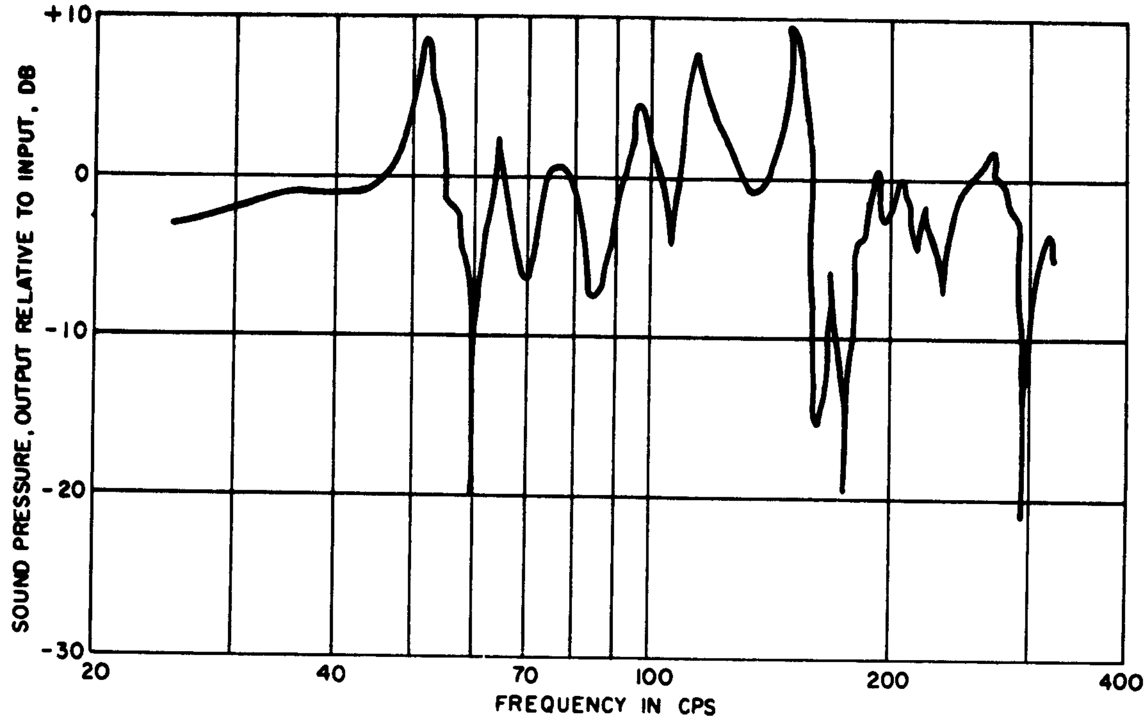

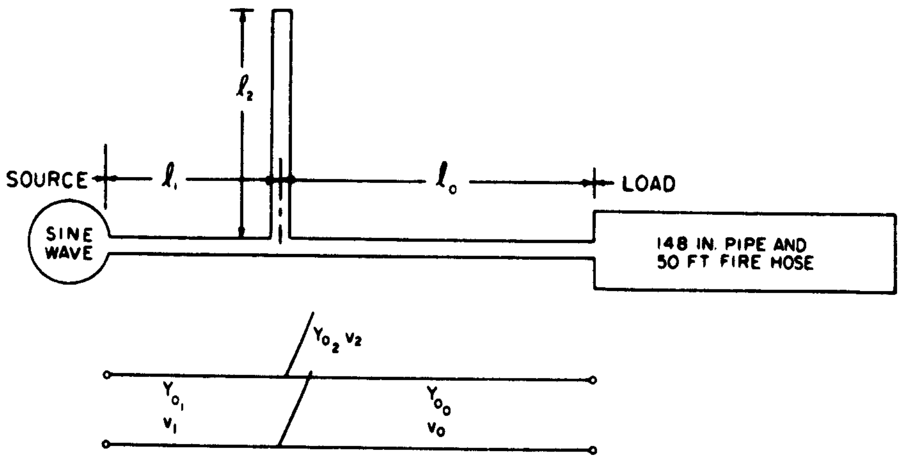

ℓ_0 : 57 IN.	Y_{0_0} : 1.32	v_0 : 3964
ℓ_1 : 32 IN.	Y_{0_1} : 1.32	v_1 : 3964
ℓ_2 : 173 IN.	Y_{0_2} : 1.32	v_2 : 3964

FIGURE 85
ONE ELEMENT SIDE-BRANCH FILTER WITH CLOSED END STUB BRANCH ELEMENT

DRL - UT
DWG AS 6996
JVK - BEE
11 - 7 - 62

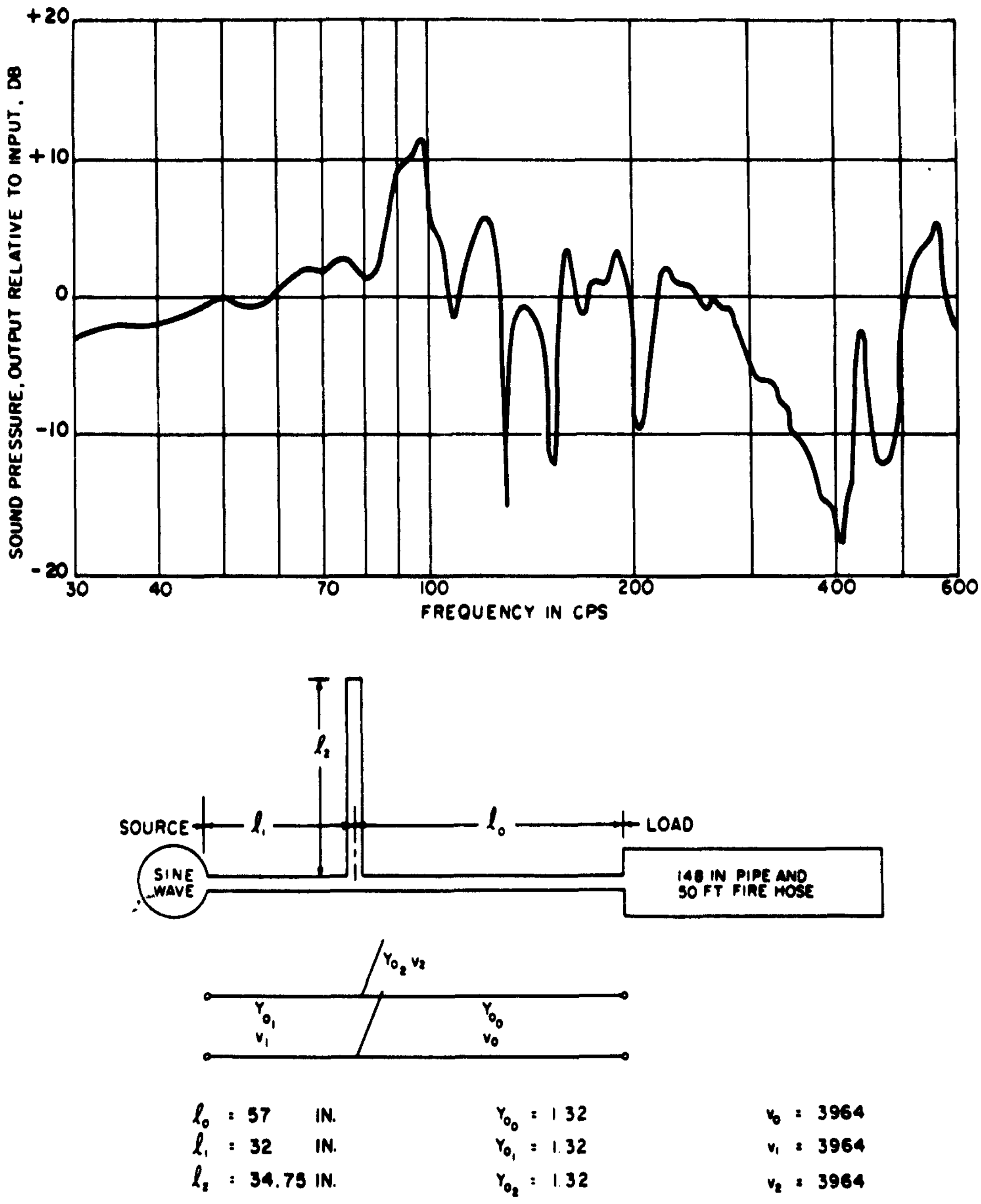

FIGURE 86
ONE ELEMENT SIDE-BRANCH FILTER WITH CLOSED END STUB BRANCH ELEMENT

DRL - UT
DWG AS 6997
JVK - BEE
11 - 7 - 62

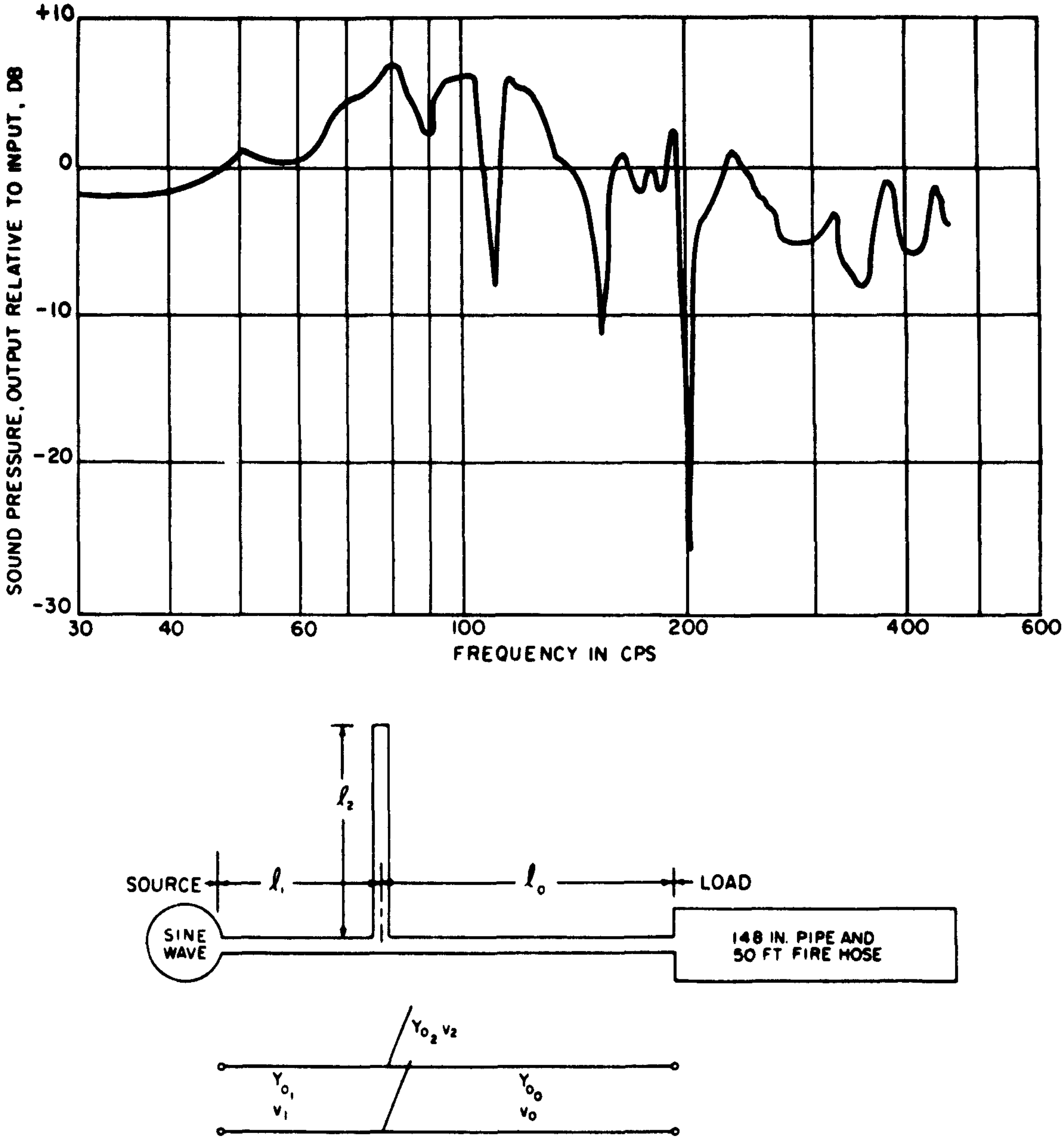

ℓ_0 : 57 IN. Y_{0_0} : 1 32 v_0 : 3964

ℓ_1 : 32 IN. Y_{0_1} : 1 32 v_1 : 3964

ℓ_2 : 58 IN. Y_{0_2} : 1 32 v_2 : 3964

FIGURE 87

ONE ELEMENT SIDE-BRANCH FILTER WITH CLOSED END STUB BRANCH ELEMENT

DRL - UT
DWG AS 6998
JVK - BEE
11 - 7 - 62

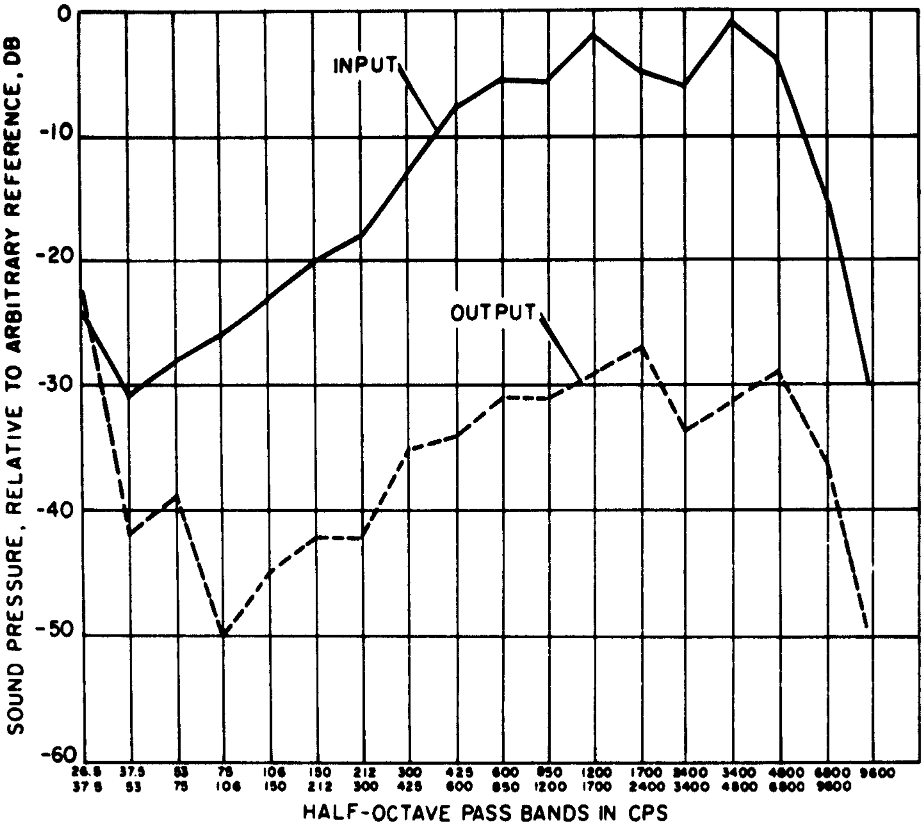

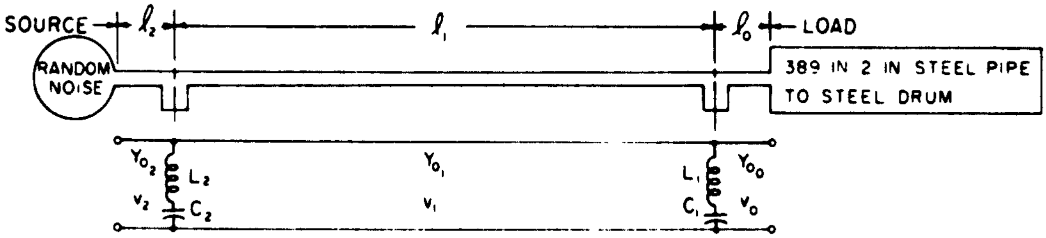

ℓ_0 : 7.5 IN. $\quad Y_{0_0}$: 657 $\quad v_0$: 4280 $\quad L_1 : 1.32 \times 10^{-4}$

ℓ_1 : 5.5 IN. $\quad Y_{0_1}$: 657 $\quad v_1$: 4280 $\quad L_2 : 4.50 \times 10^{-5}$

ℓ_2 : 7.5 IN $\quad Y_{0_2}$: 657 $\quad v_2$: 4280 $\quad C_1 : 5.27 \times 10^{-2}$

$C_2 : 11.05 \times 10^{-2}$

FIGURE 88
TWO ELEMENT SIDE-BRANCH FILTER WITH SPRING-PISTON BRANCH ELEMENTS

DRL - UT
DWG AS 6999
JVK - BEE
11 - 14 - 62

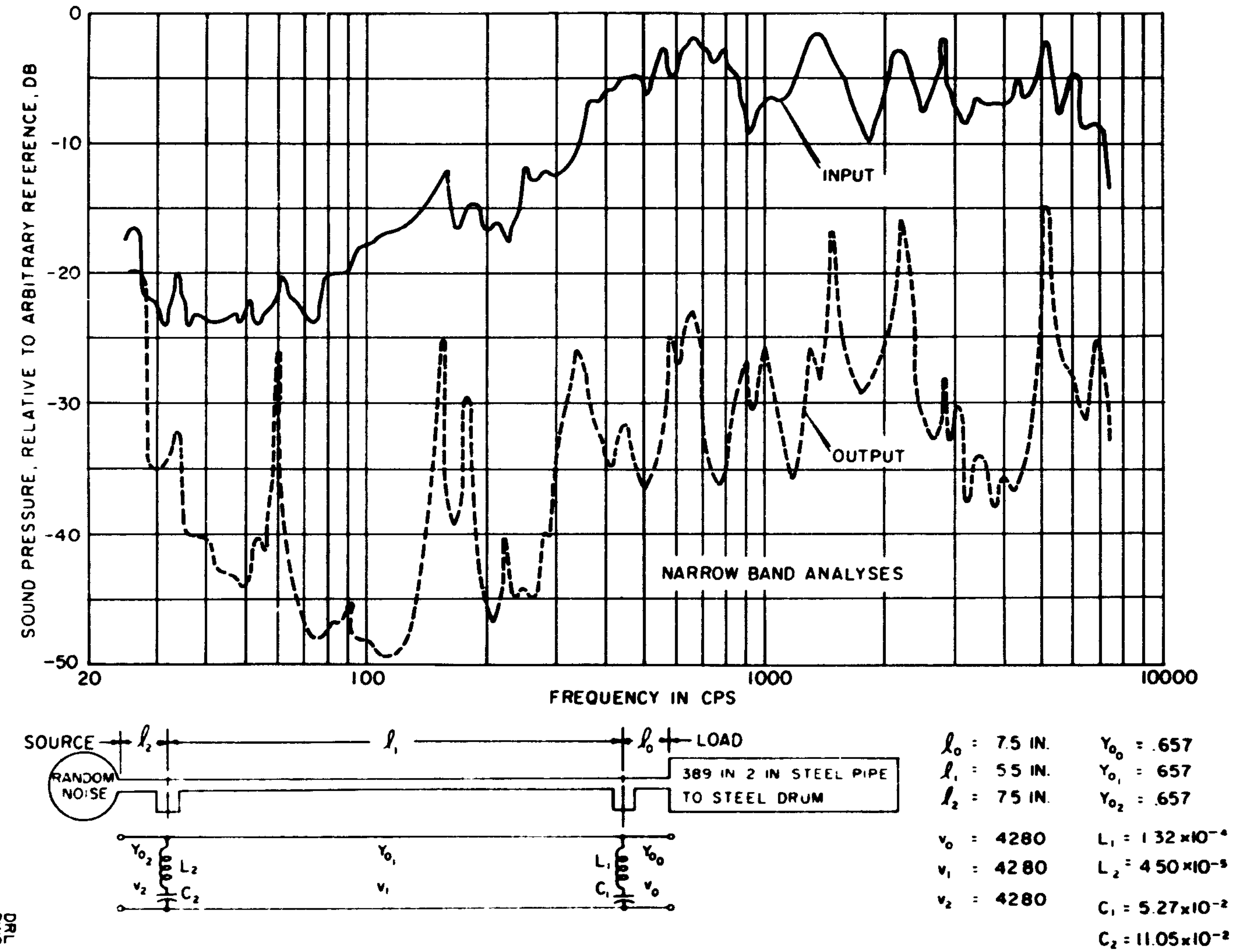

DRL - UT
DWG AS 7000
JVK - BEE
11 - 14 - 62

FIGURE 89
TWO ELEMENT SIDE-BRANCH FILTER WITH SPRING-PISTON BRANCH ELEMENTS

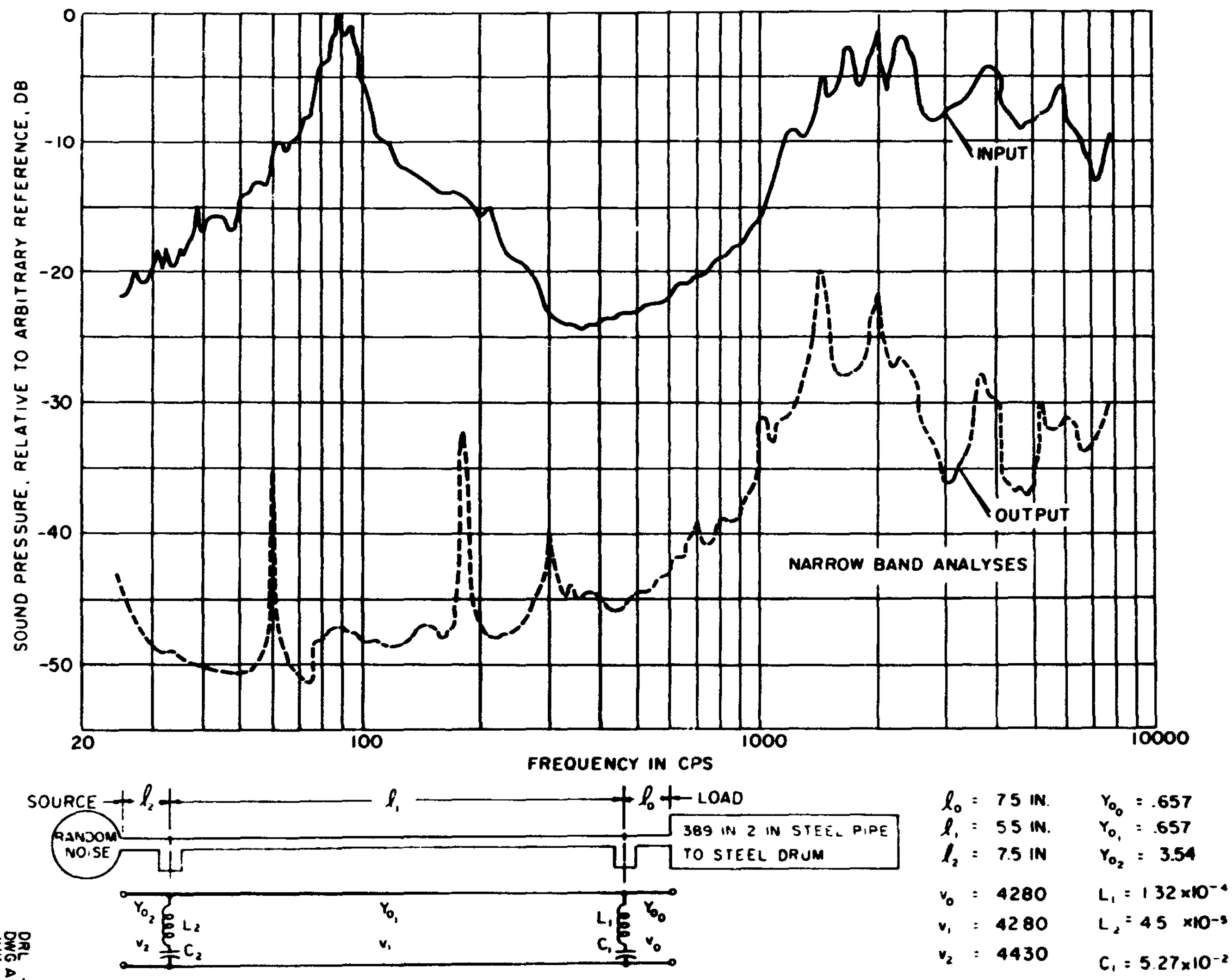

DRL - UT
DWG AS7002
JVK - BEE
11 - 13 - 62

FIGURE 90
TWO ELEMENT SIDE-BRANCH FILTER WITH SPRING-PISTON BRANCH ELEMENTS

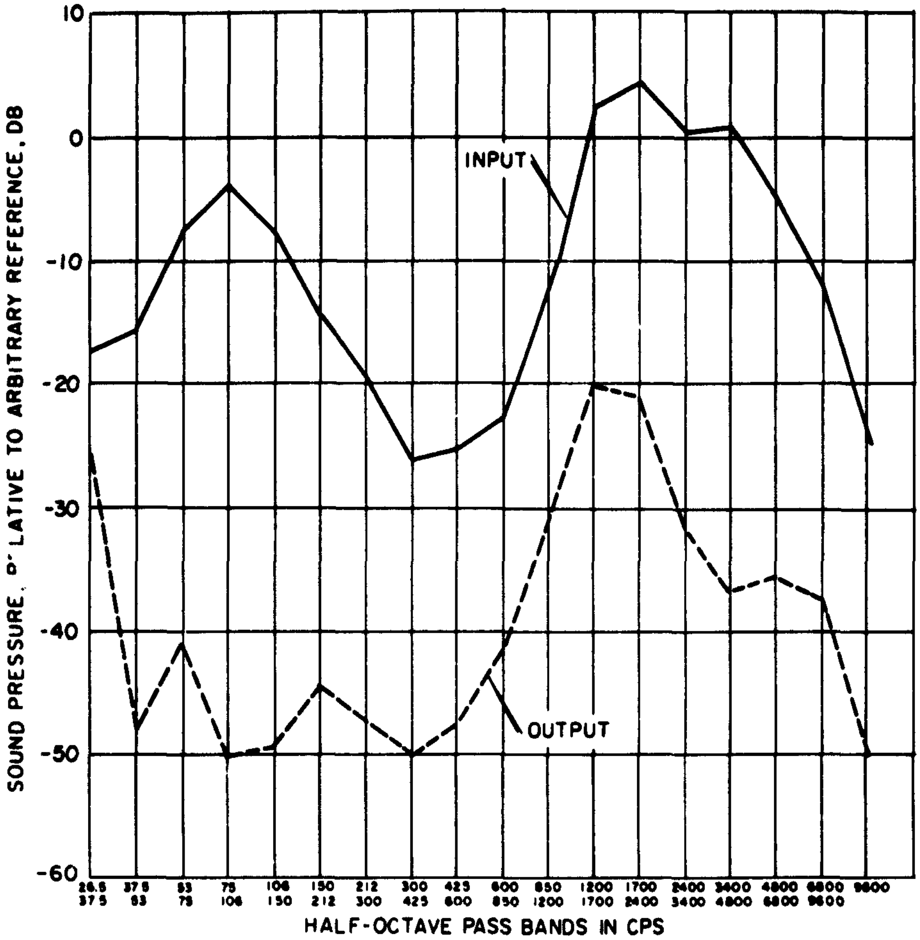

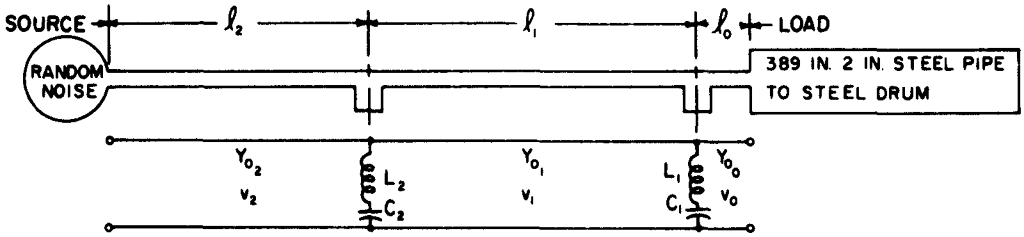

$L_1 = 1.32 \times 10^{-4}$

$L_2 = 4.50 \times 10^{-5}$

ℓ_0 = 7.5 IN.	Y_{o_0} = .657	v_0 = 4280	$C_1 = 5.27 \times 10^{-2}$
ℓ_1 = 55 IN.	Y_{o_1} = .657	v_1 = 4280	$C_2 = 11.05 \times 10^{-2}$
ℓ_2 = 41.5 IN.	Y_{o_2} = 3.54	v_2 = 4430	

FIGURE 91
TWO ELEMENT SIDE-BRANCH FILTER WITH SPRING-PISTON BRANCH ELEMENTS

DRL - UT
DWG AS 7001
JVK - BEE
11 - 14 - 62

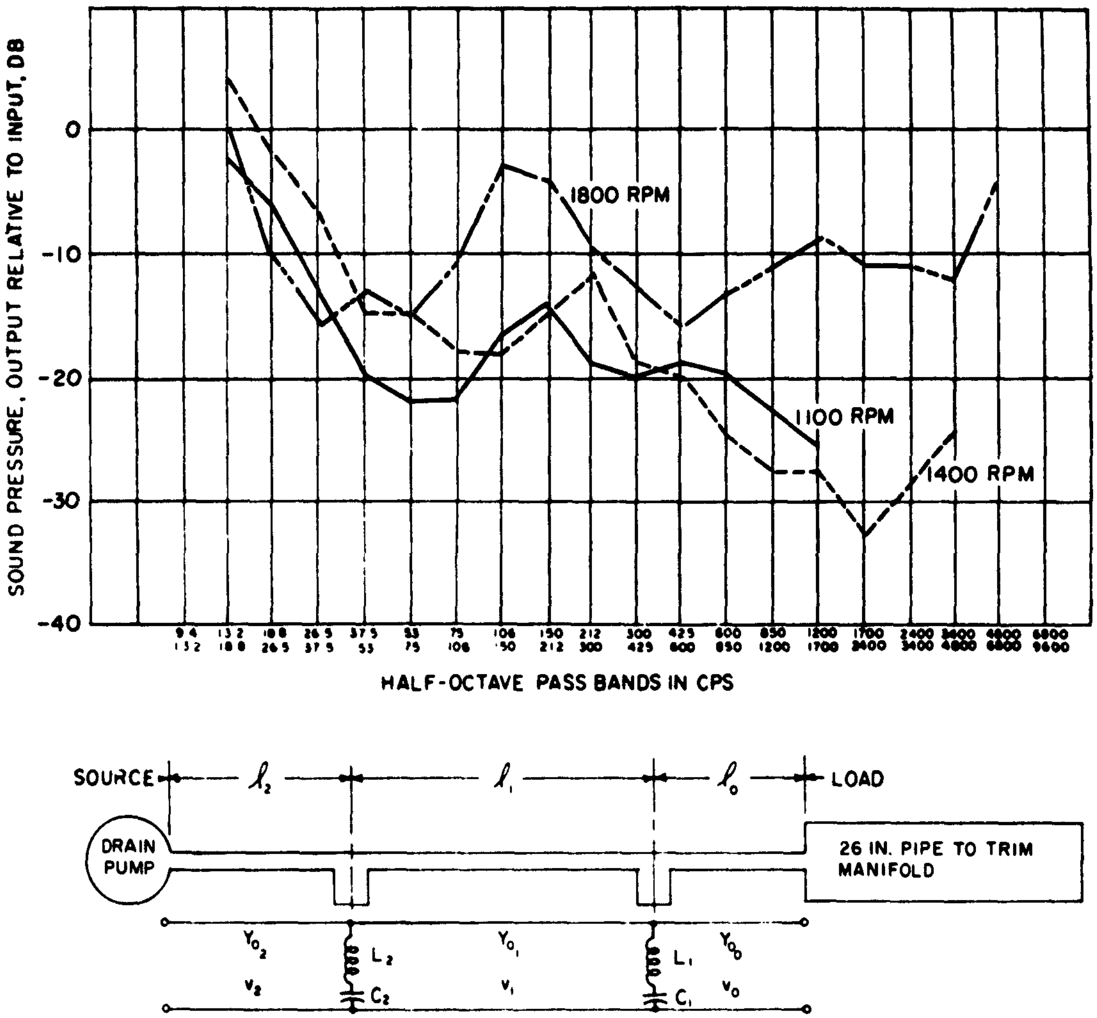

$L_1 = 2.84 \times 10^{-4}$

$L_2 = 5.92 \times 10^{-4}$

$l_0 = 50$ IN.	$Y_{0_0} = 1.32$	$v_0 = 3964$	$C_1 = 5.26 \times 10^{-2}$
$l_1 = 32.5$ IN.	$Y_{0_1} = 1.32$	$v_1 = 3964$	$C_2 = 5.55 \times 10^{-2}$
$l_2 = 92.25$ IN.	$Y_{0_2} = 1.32$	$v_2 = 3964$	

FIGURE 92
TWO ELEMENT SIDE-BRANCH FILTER WITH SPRING-PISTON BRANCH ELEMENTS

DRL - UT
DWG AS 7003
JVK - BEE
11 - 16 - 62

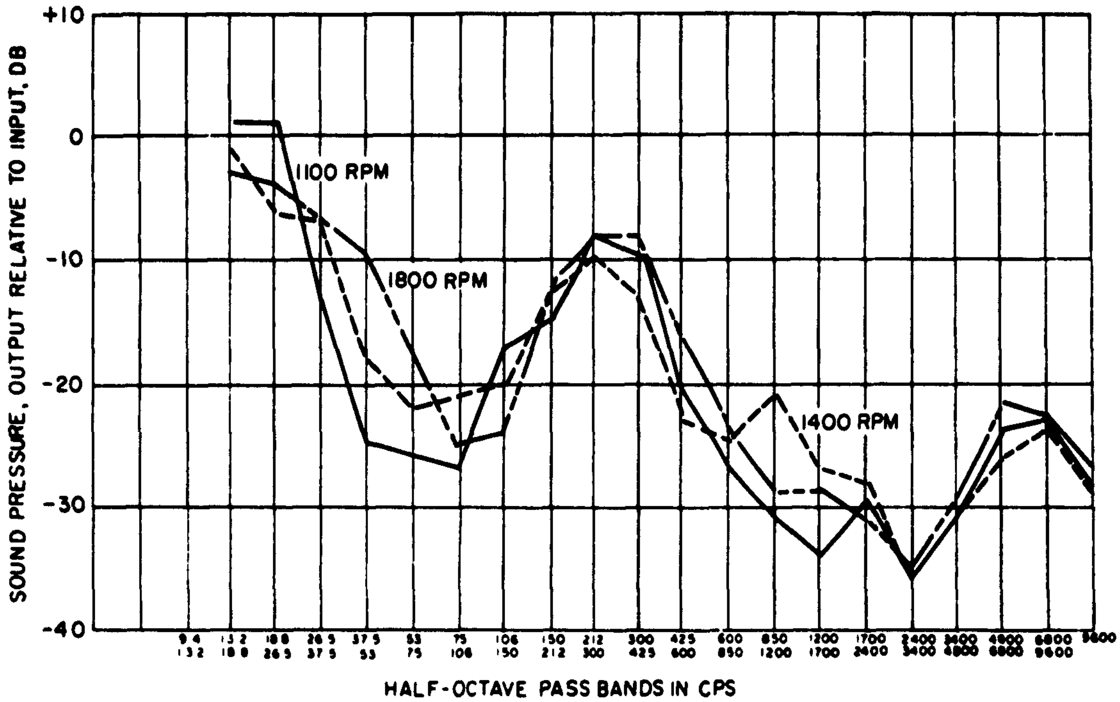

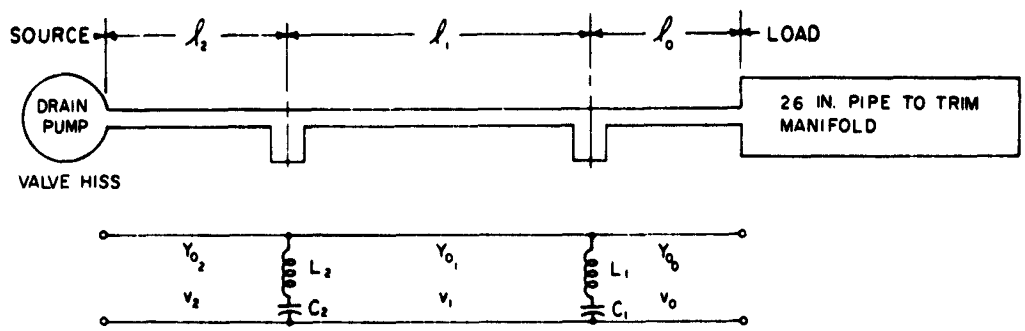

$L_1 = 2.84 \times 10^{-4}$

$L_2 = 5.92 \times 10^{-4}$

ℓ_0 = 50 IN.	Y_{o_0} : 1.32	v_0 : 3964
ℓ_1 = 32.5 IN.	Y_{o_1} : 1.32	v_1 : 3964
ℓ_2 = 92.25 IN.	Y_{o_2} : 1.32	v_2 : 3964

$C_1 = 5.26 \times 10^{-2}$

$C_2 = 5.55 \times 10^{-2}$

FIGURE 93
TWO ELEMENT SIDE - BRANCH FILTER WITH SPRING-PISTON BRANCH ELEMENTS

DRL - UT
DWG AS7004
JVK - BEE
11 - 16 - 62

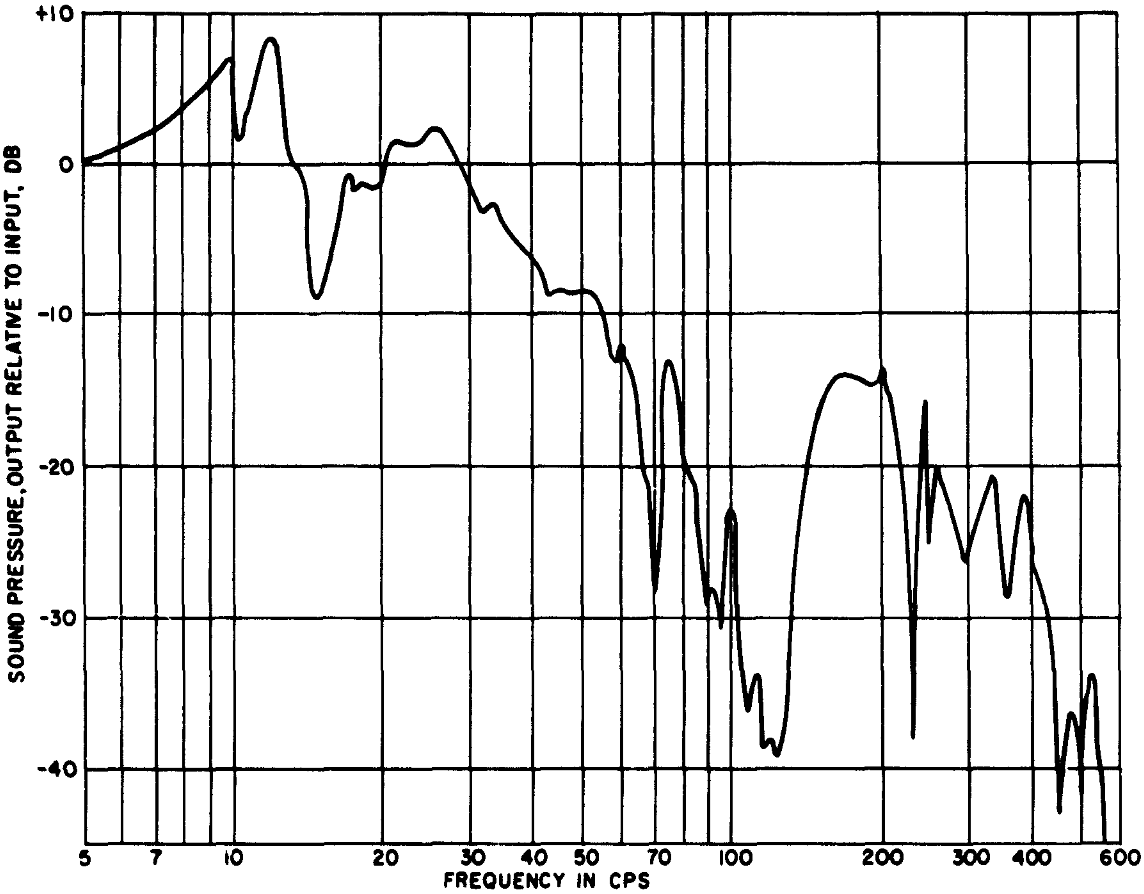

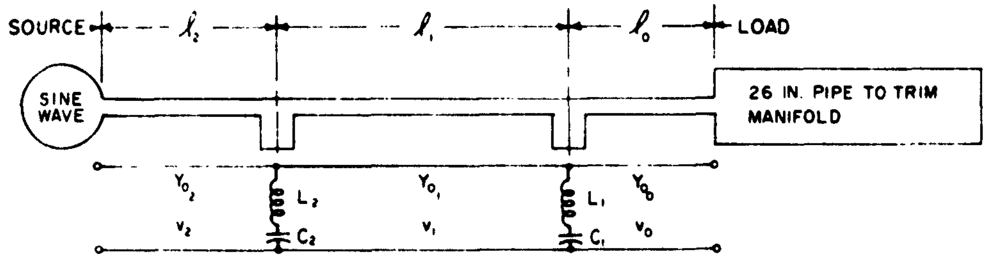

$L_1 = 2.84 \times 10^{-4}$

$L_2 = 5.92 \times 10^{-4}$

ℓ_0 : 50 IN.	Y_{0_0} : 1.32	v_0 : 3964	C_1 : 5.26×10^{-2}
ℓ_1 : 32.5 IN.	Y_{0_1} : 1.32	v_1 : 3964	C_2 : 5.55×10^{-2}
ℓ_2 : 92.25 IN.	Y_{0_2} : 1.32	v_2 : 3964	

FIGURE 94
TWO ELEMENT SIDE - BRANCH FILTER WITH SPRING-PISTON BRANCH ELEMENTS

DRL - UT
DWG AS 7005
JVK - BEE
11 - 28 - 62

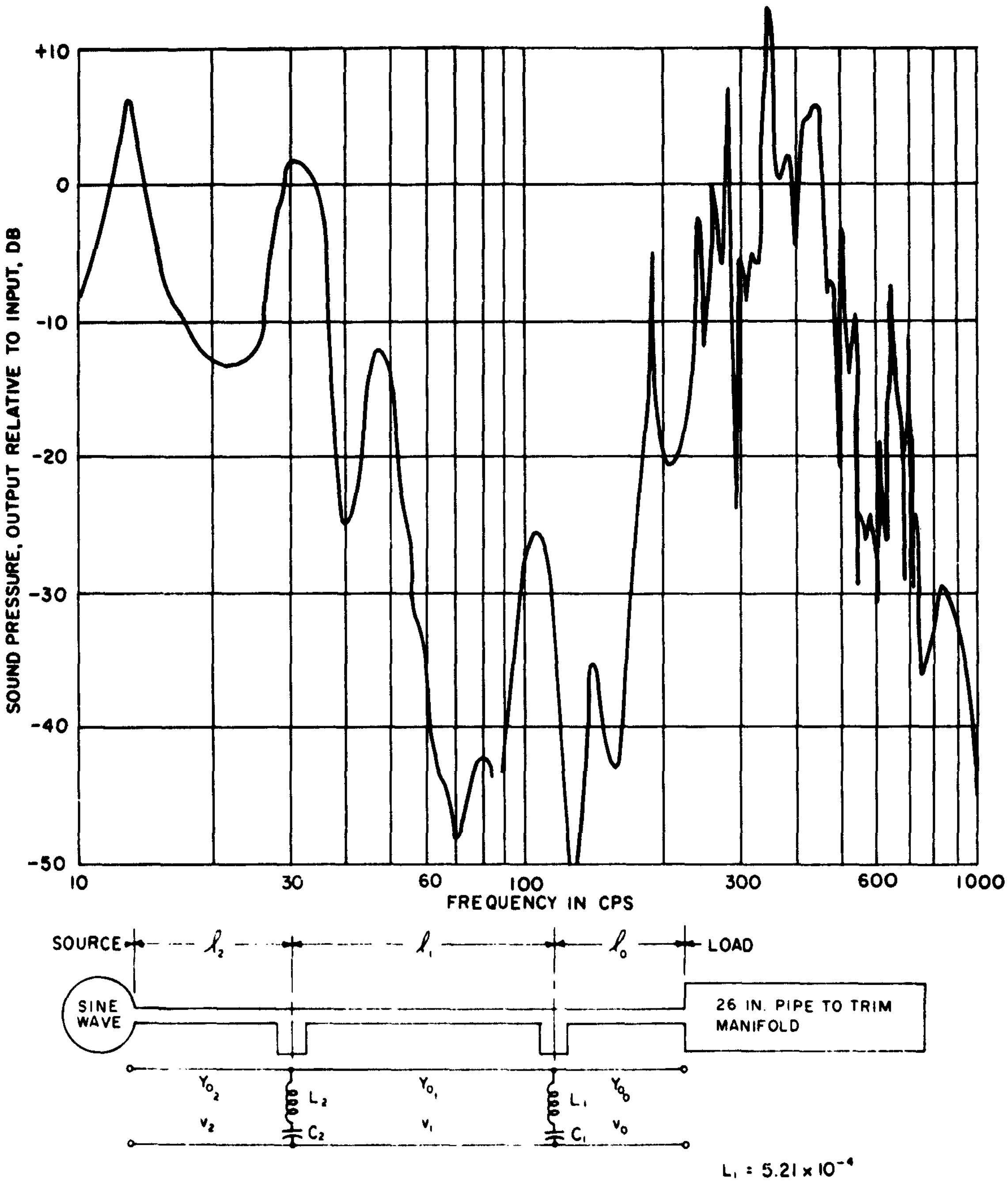

$L_1 = 5.21 \times 10^{-4}$

$L_2 = 1.23 \times 10^{-4}$

ℓ_0 : 28.5 IN.	Y_{0_0} : 1.32	v_0 : 3964	$C_1 = 4.12 \times 10^{-2}$
ℓ_1 : 126 IN.	Y_{0_1} : 1.32	v_1 : 3964	
ℓ_2 : 20 IN.	Y_{0_2} : 1.32	v_2 : 3964	$C_2 = 3.99 \times 10^{-2}$

DRL - UT
DWG AS 7006
JVK - BEE
11 - 28 - 62

FIGURE 95
TWO ELEMENT SIDE-BRANCH FILTER WITH DISK SPRING BRANCH ELEMENTS

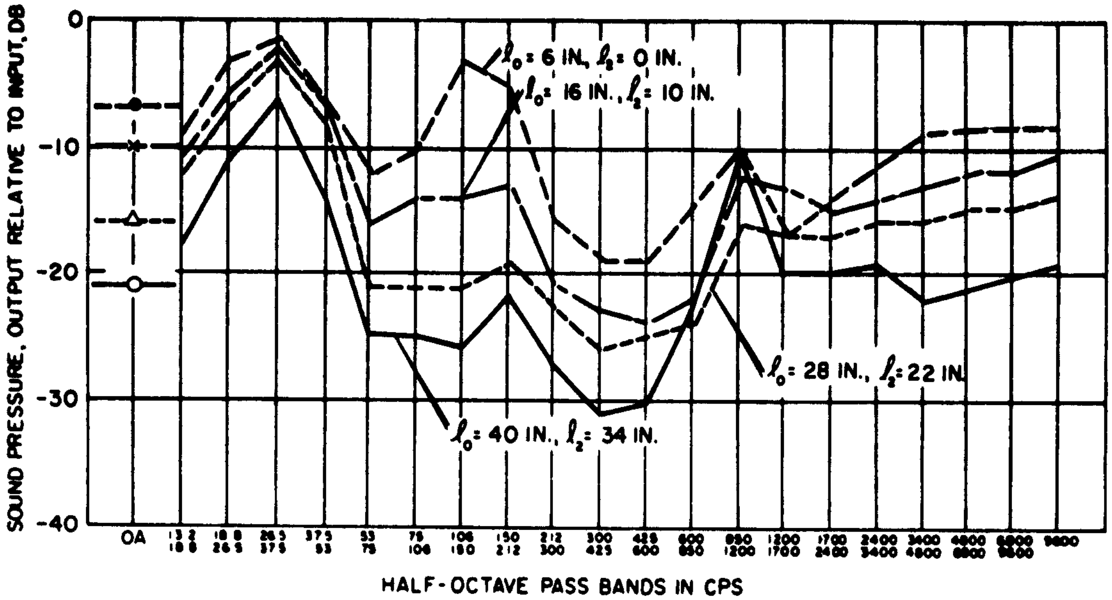

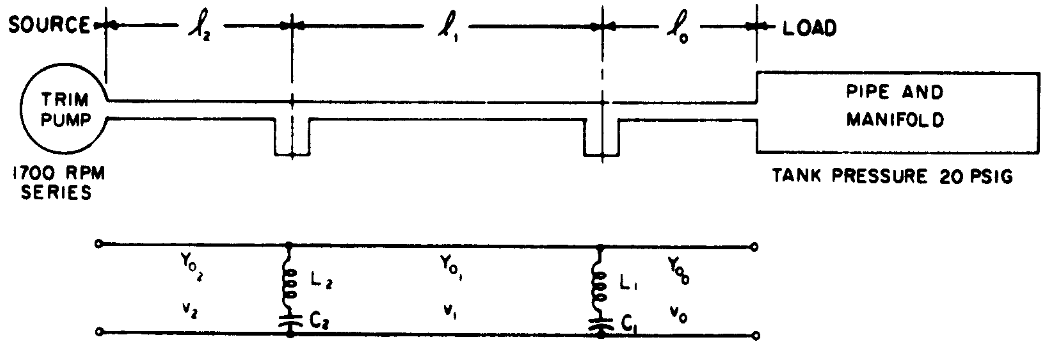

$L_1 = 5.21 \times 10^{-4}$
$L_2 = 1.23 \times 10^{-4}$

ℓ_0 : (SEE CURVES)	Y_{0_0} : 1.32	v_0 : 3964
ℓ_1 : 126 IN.	Y_{0_1} : 1.32	v_1 : 3964
ℓ_2 : (SEE CURVES)	Y_{0_2} : 1.32	v_2 : 3964

$C_1 = 4.12 \times 10^{-2}$
$C_2 = 3.99 \times 10^{-2}$

FIGURE 96
TWO ELEMENT SIDE-BRANCH FILTER WITH DISK SPRING BRANCH ELEMENTS

DRL - UT
DWG AS7007
JVK - BEE
11 - 15 - 62

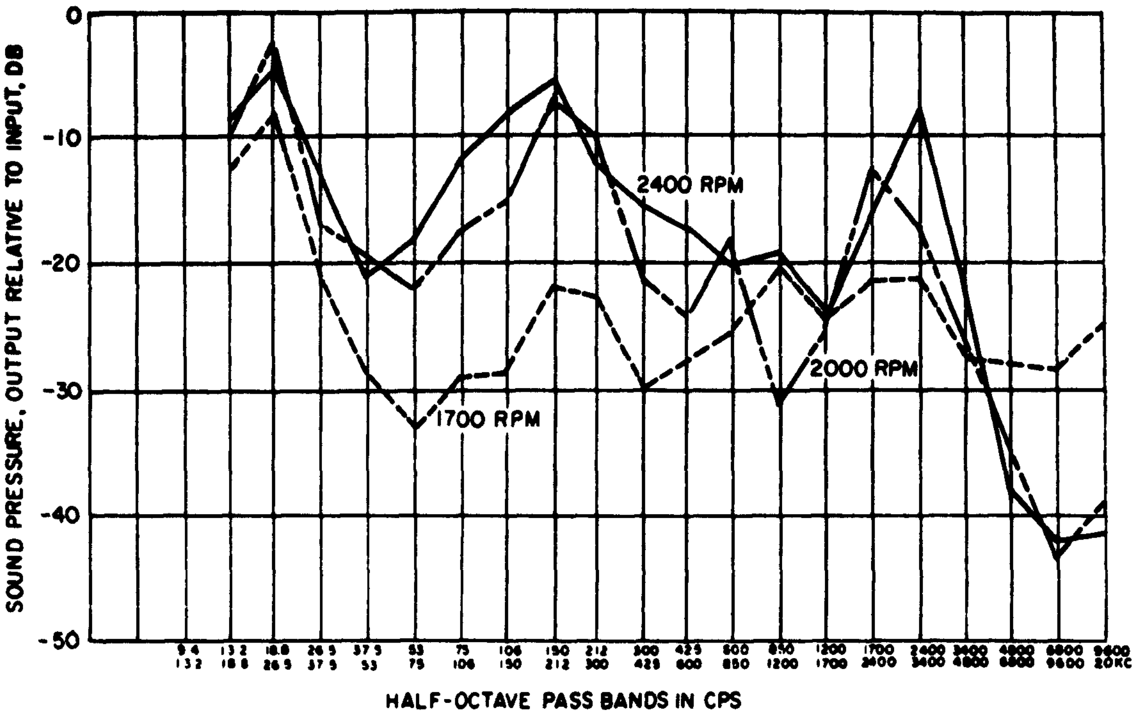

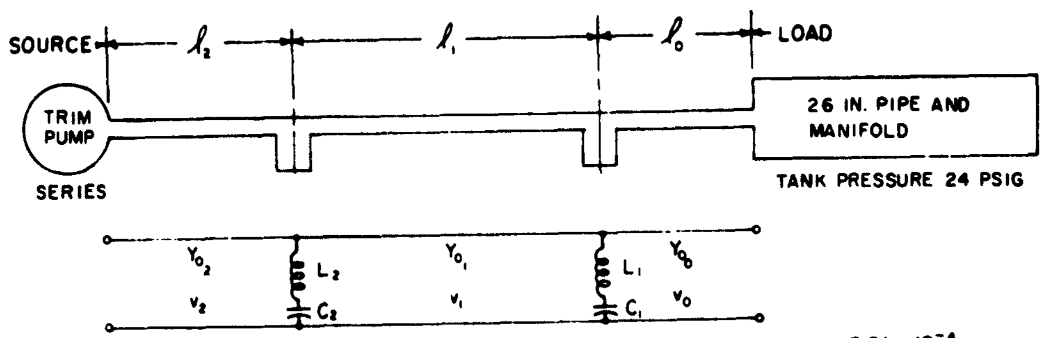

			$L_1 = 5.21 \times 10^{-4}$
ℓ_0 = 25 IN.	Y_{0_0} = 1.32	v_0 = 3964	$L_2 = 1.23 \times 10^{-4}$
ℓ_1 = 126 IN.	Y_{0_1} = 1.32	v_1 = 3964	$C_1 = 4.12 \times 10^{-2}$
ℓ_2 = 146 IN.	Y_{0_2} = 1.32	v_2 = 3964	$C_2 = 3.99 \times 10^{-2}$

FIGURE 97
TWO ELEMENT SIDE-BRANCH FILTER WITH DISK SPRING BRANCH ELEMENTS

DRL - UT
DWG AS 7010
JVK - BEE
11 - 16 - 62

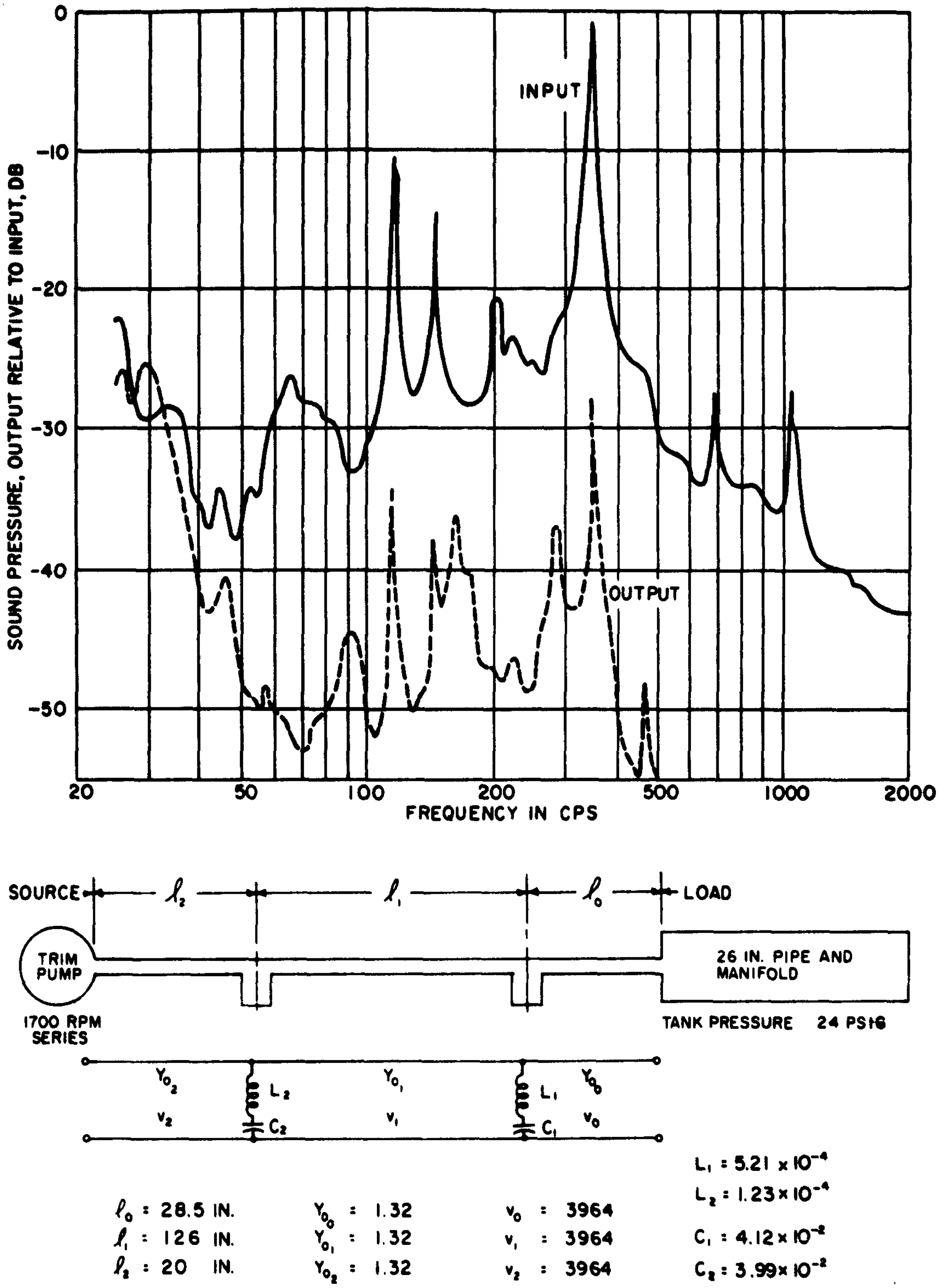

FIGURE 98
TWO ELEMENT SIDE-BRANCH FILTER WITH DISK SPRING BRANCH ELEMENTS

DRL - UT
DWG AS 7008
JVK - BEE
11 - 28 - 62

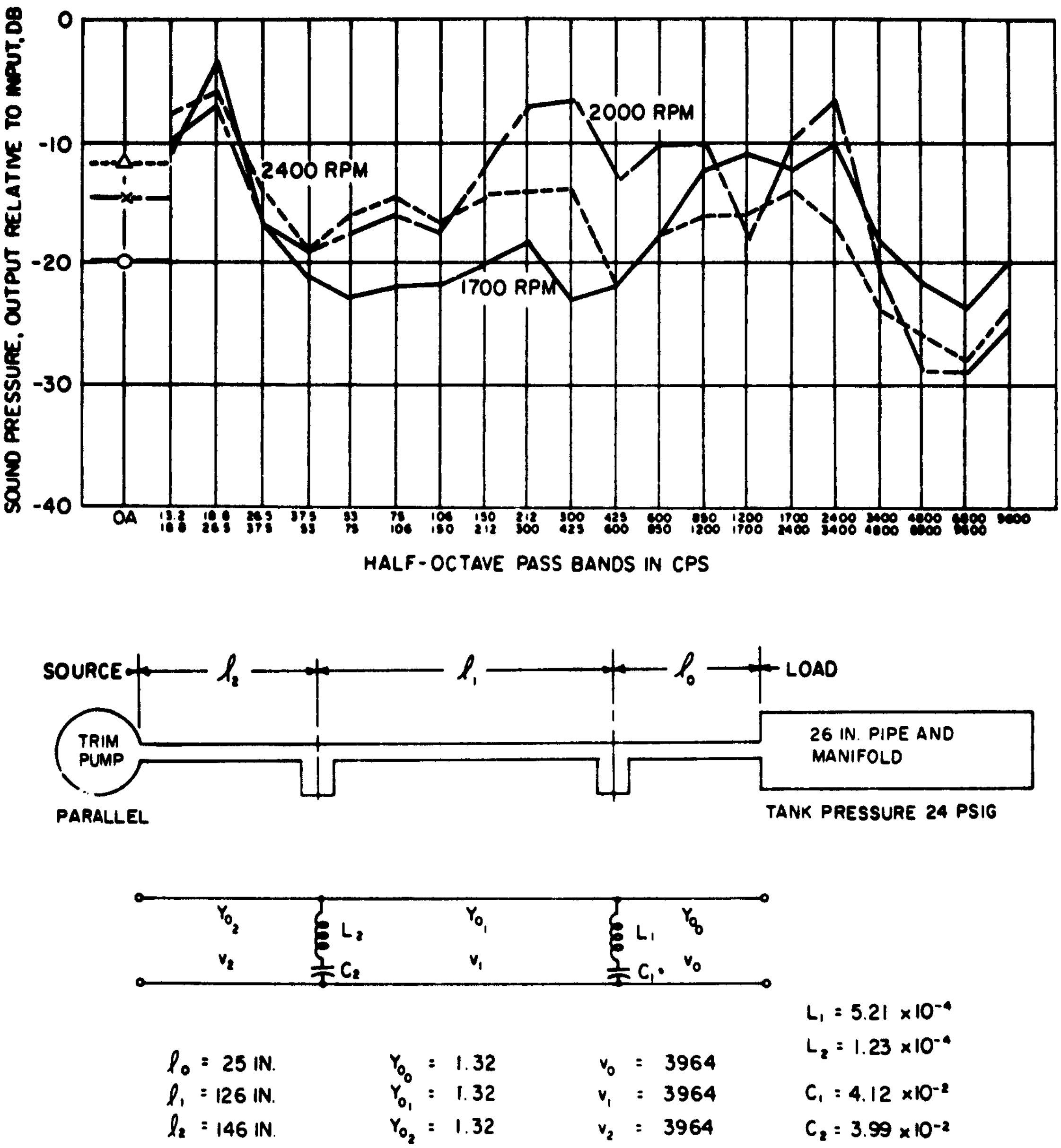

FIGURE 99
TWO ELEMENT SIDE-BRANCH FILTER WITH DISK SPRING BRANCH ELEMENTS

DRL - UT
DWG AS 7009
JVK - BEE
11 - 15 - 62

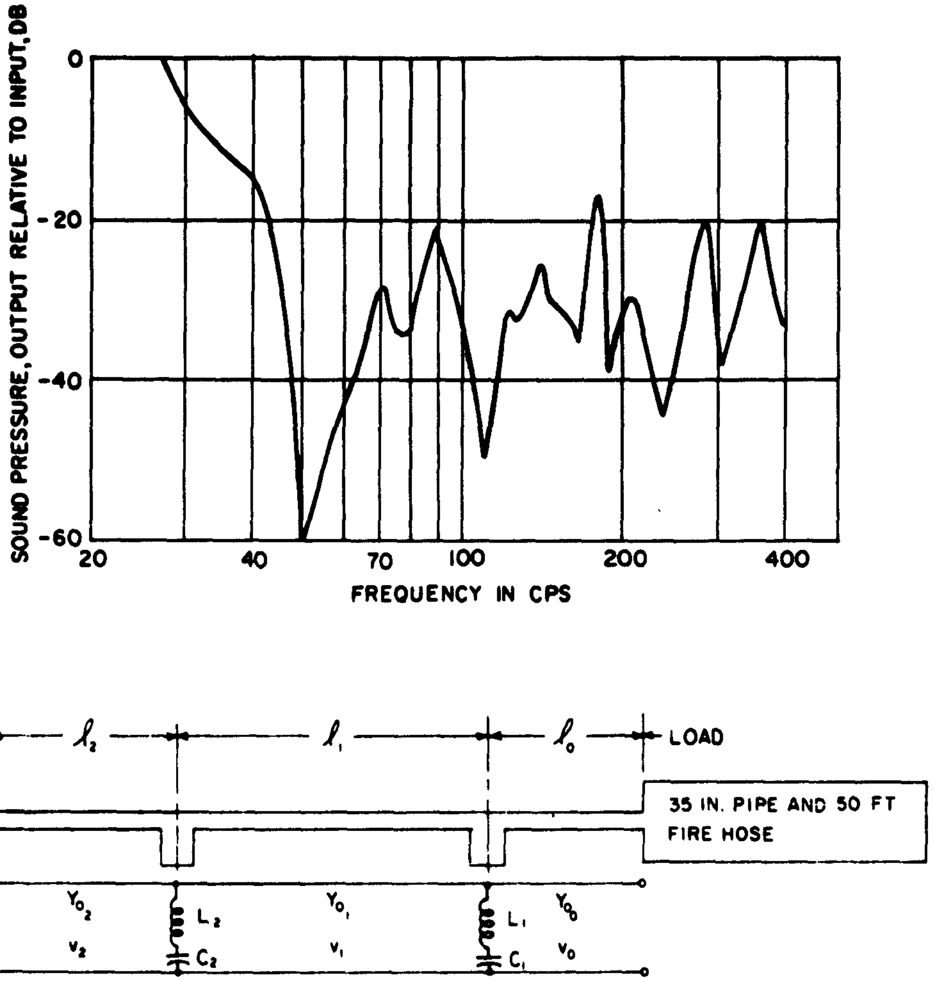

$L_1 = 1.07 \times 10^{-5}$
$L_2 = 5.92 \times 10^{-5}$

ℓ_0 = 9.5 IN.	Y_{0_0} = 1.32	v_0 : 3964	$C_1 = 9.50 \times 10^{-2}$
ℓ_1 = 44 IN.	Y_{0_1} = 1.32	v_1 : 3964	$C_2 = 15.4 \times 10^{-2}$
ℓ_2 = 58.5 IN.	Y_{0_2} = 1.32	v_2 : 3964	

FIGURE 100
TWO ELEMENT SIDE-BRANCH FILTER WITH METAL BELLOWS BRANCH ELEMENTS

DRL - UT
DWG AS 7012
JVK - BEE
11 - 26 - 62

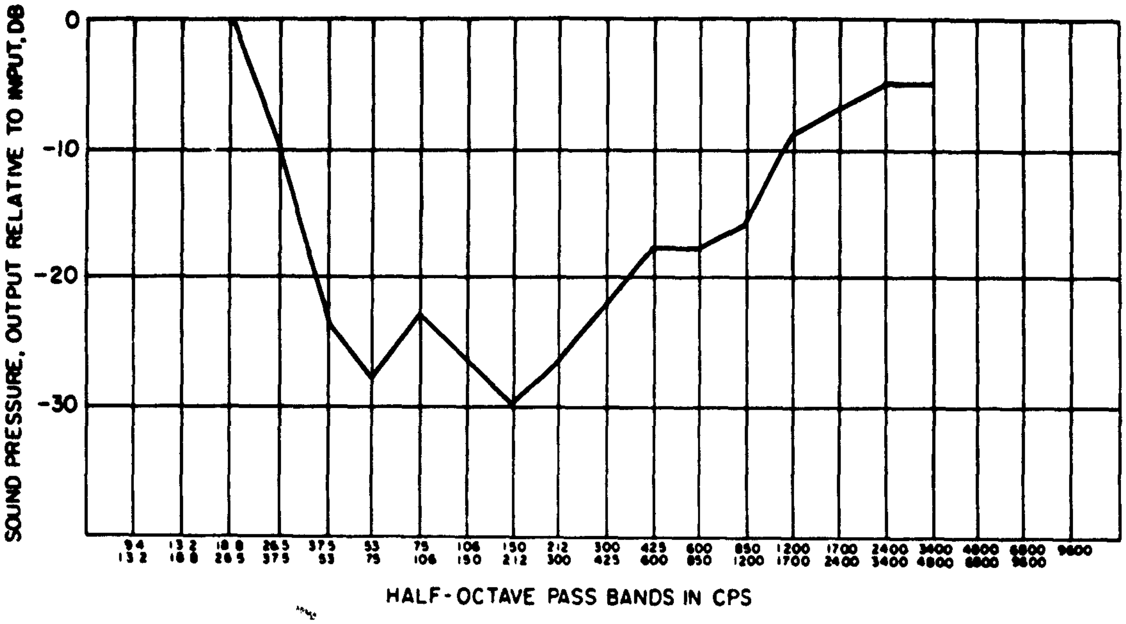

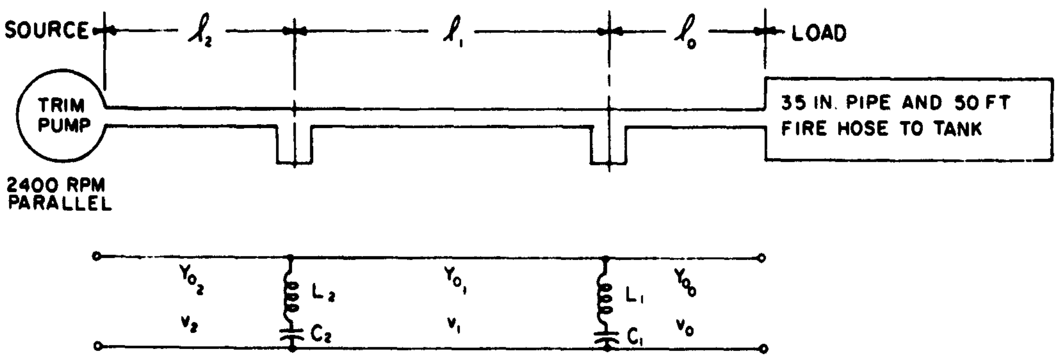

$L_1 = 1.07 \times 10^{-5}$
$L_2 = 5.92 \times 10^{-5}$

ℓ_0 = 10 IN.	Y_{0_0} = 1.32	v_0 : 3964	$C_1 = 9.50 \times 10^{-2}$
ℓ_1 = 44 IN.	Y_{0_1} = 1.32	v_1 : 3964	
ℓ_2 = 58.5 IN.	Y_{0_2} = 1.32	v_2 : 3964	$C_2 = 15.4 \times 10^{-2}$

FIGURE 101
TWO ELEMENT SIDE-BRANCH FILTER WITH METAL BELLOWS BRANCH ELEMENTS

DRL - UT
DWG AS 7015
JVK - BEE
11 - 15 - 62

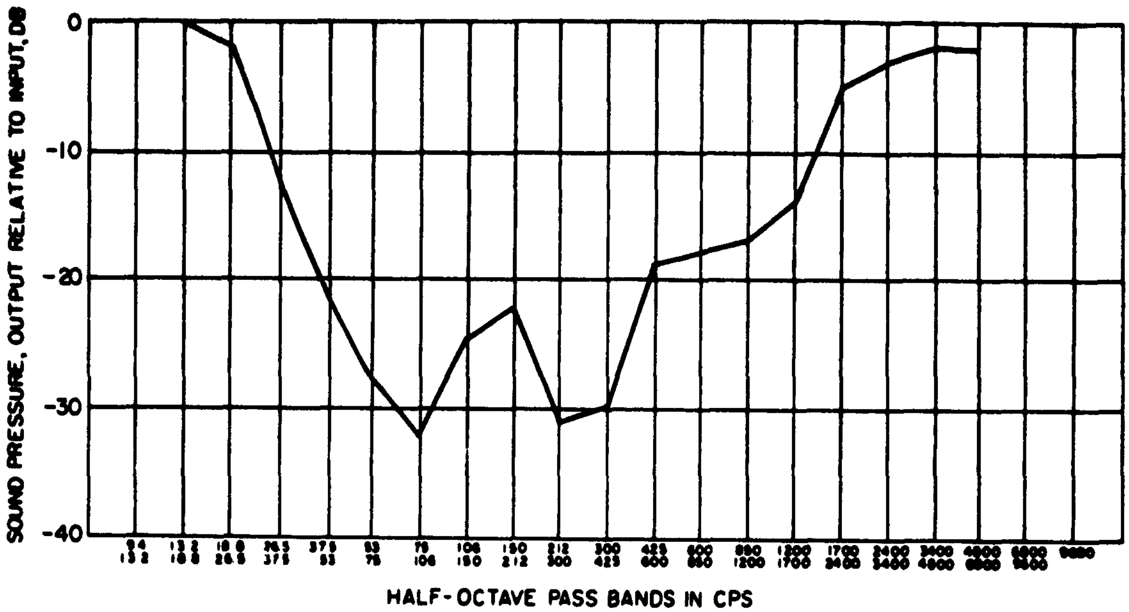

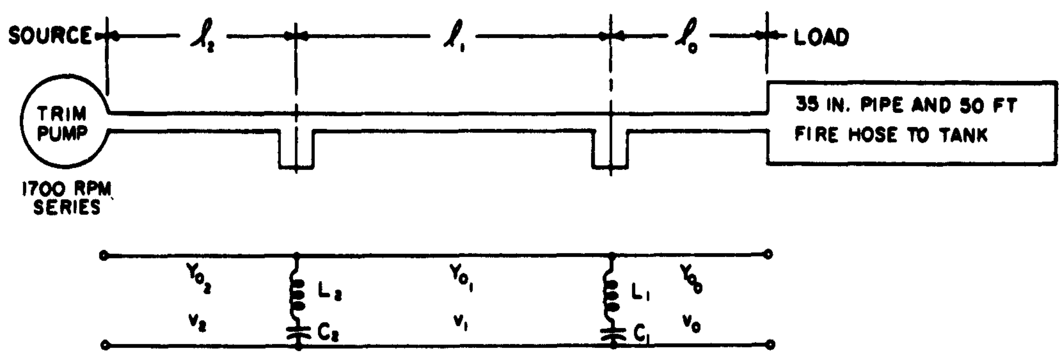

$L_1 = 1.07 \times 10^{-5}$

$L_2 = 5.92 \times 10^{-5}$

l_0 = 9.5 IN.	Y_{0_0} = 1.32	v_0 = 3964	$C_1 = 9.50 \times 10^{-2}$
l_1 = 44 IN.	Y_{0_1} = 1.32	v_1 = 3964	
l_2 = 58.5 IN.	Y_{0_2} = 1.32	v_2 = 3964	$C_2 = 15.4 \times 10^{-2}$

FIGURE 102
TWO ELEMENT SIDE-BRANCH FILTER WITH METAL BELLOWS BRANCH ELEMENTS

DR. -
DWG AS7
JVK -
11 - 15

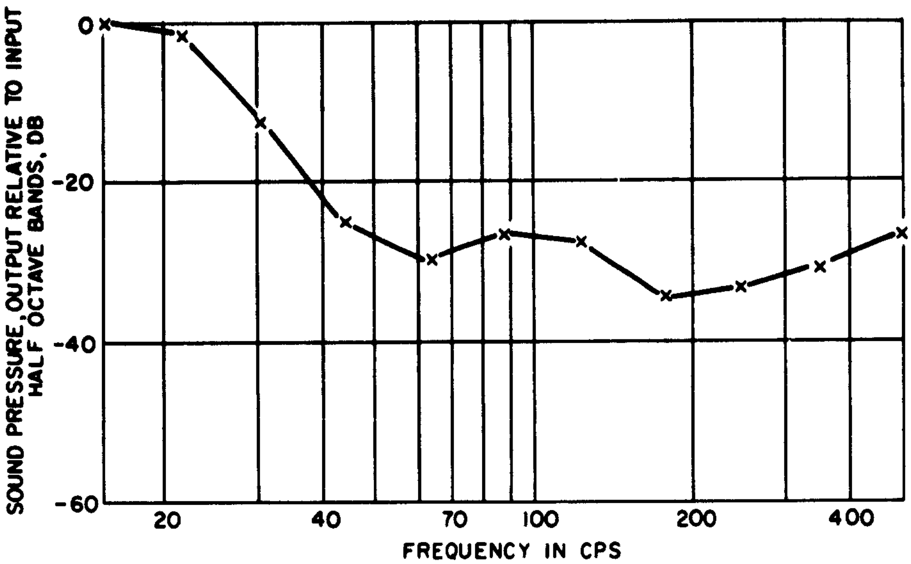

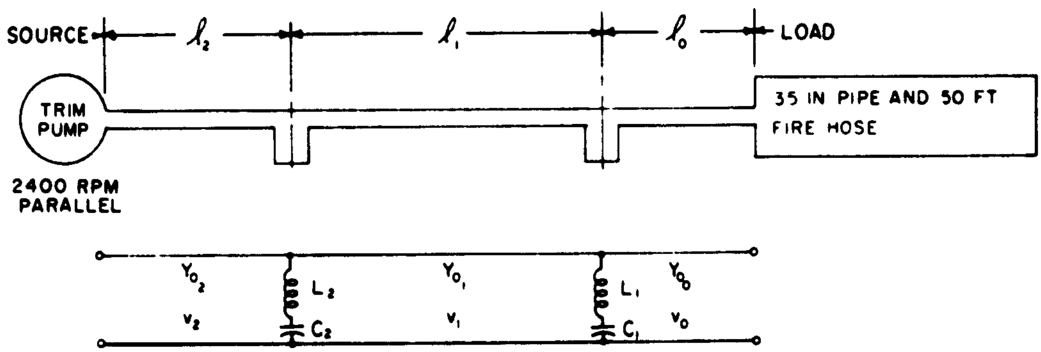

$L_1 = 5.02 \times 10^{-5}$

$L_2 = 1.66 \times 10^{-5}$

ℓ_0 : 9.5 IN	Y_{0_0} : 1.32	v_0 : 3964	$C_1 = 14.4 \times 10^{-2}$
ℓ_1 : 51 IN	Y_{0_1} : 1.32	v_1 : 3964	$C_2 = 15.4 \times 10^{-2}$
ℓ_2 : 58.5 IN	Y_{0_2} : 1.32	v_2 : 3964	

FIGURE 103
TWO ELEMENT SIDE-BRANCH FILTER WITH METAL BELLOWS BRANCH ELEMENTS

DRL - UT
DWG AS 7013
JVK - BEE
11 - 27 - 62

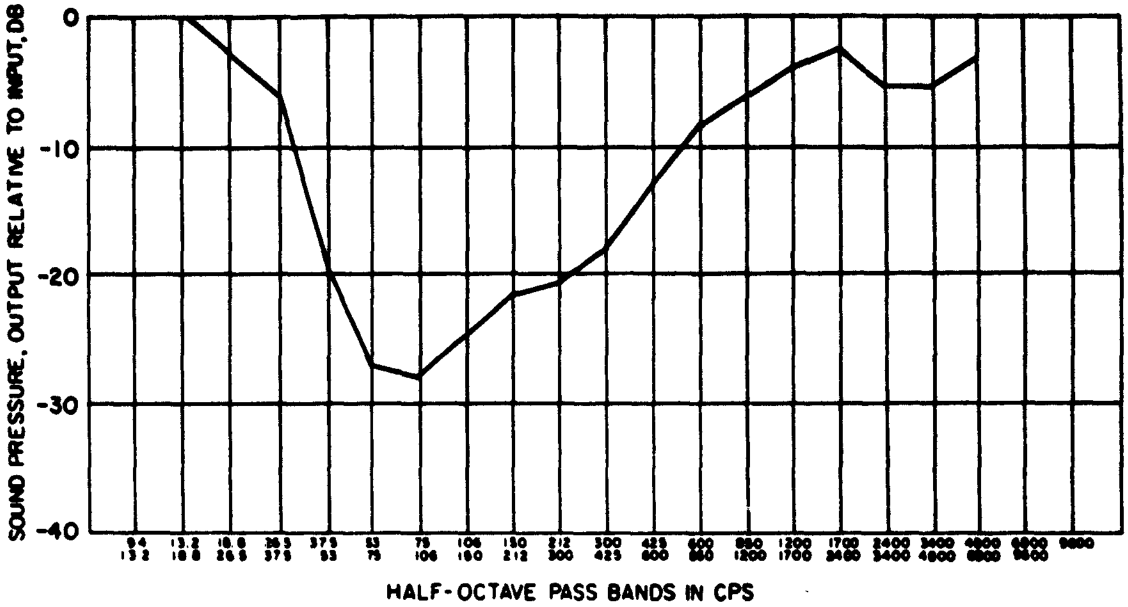

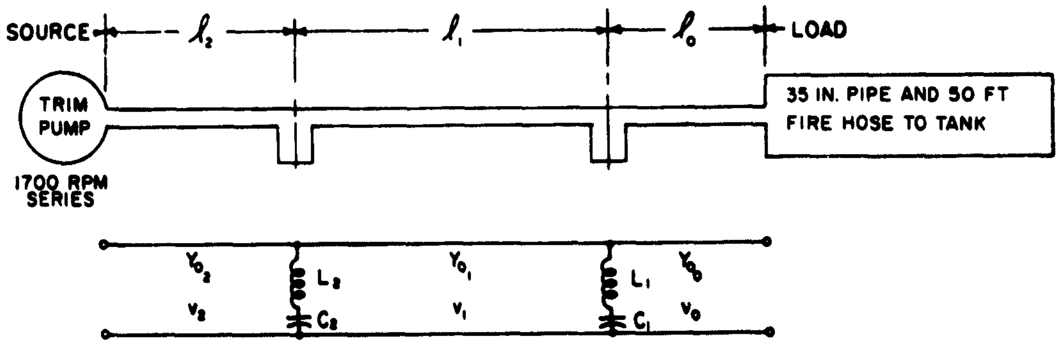

$L_1 = 5.01 \times 10^{-5}$

$L_2 = 1.66 \times 10^{-5}$

$l_0 = 10$ IN.	$Y_{0_0} = 1.32$	$v_0 = 3964$
$l_1 = 51$ IN.	$Y_{0_1} = 1.32$	$v_1 = 3964$
$l_2 = 58.5$ IN.	$Y_{0_2} = 1.32$	$v_2 = 3964$

$C_1 = 14.4 \times 10^{-2}$

$C_2 = 15.4 \times 10^{-2}$

FIGURE 104
TWO ELEMENT SIDE-BRANCH FILTER WITH METAL BELLOWS BRANCH ELEMENTS

DRL - UT
DWG AS 7016
JVK - BEE
11 - 15 - 62

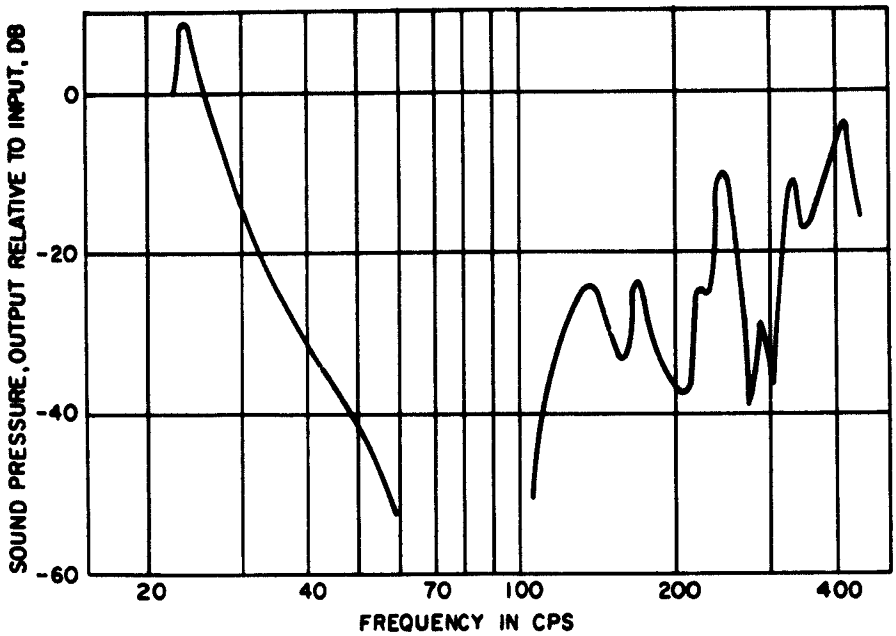

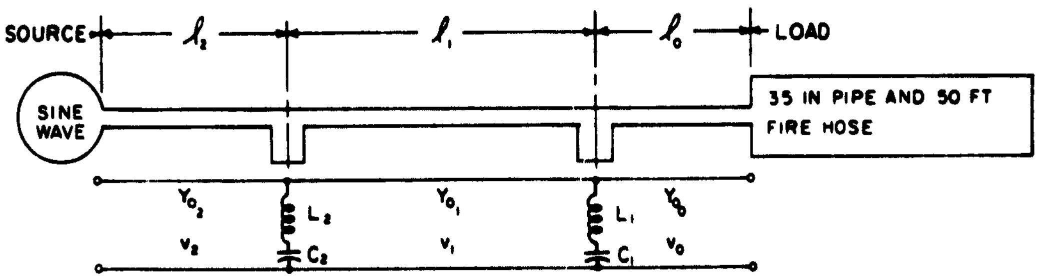

$L_1 = 5.02 \times 10^{-5}$

ℓ_0 = 9.5 IN	Y_{0_0} = 1.32	v_0 = 3964	$L_2 = 1.66 \times 10^{-5}$
ℓ_1 = 51 IN	Y_{0_1} = 1.32	v_1 = 3964	$C_1 = 14.4 \times 10^{-2}$
ℓ_2 = 58.5 IN.	Y_{0_2} = 1.32	v_2 = 3964	$C_2 = 15.4 \times 10^{-2}$

FIGURE 105
TWO ELEMENT SIDE-BRANCH FILTER WITH METAL BELLOWS BRANCH ELEMENTS

DRL - UT
DWG AS 7014
JVK - BEE
11 - 27 - 62

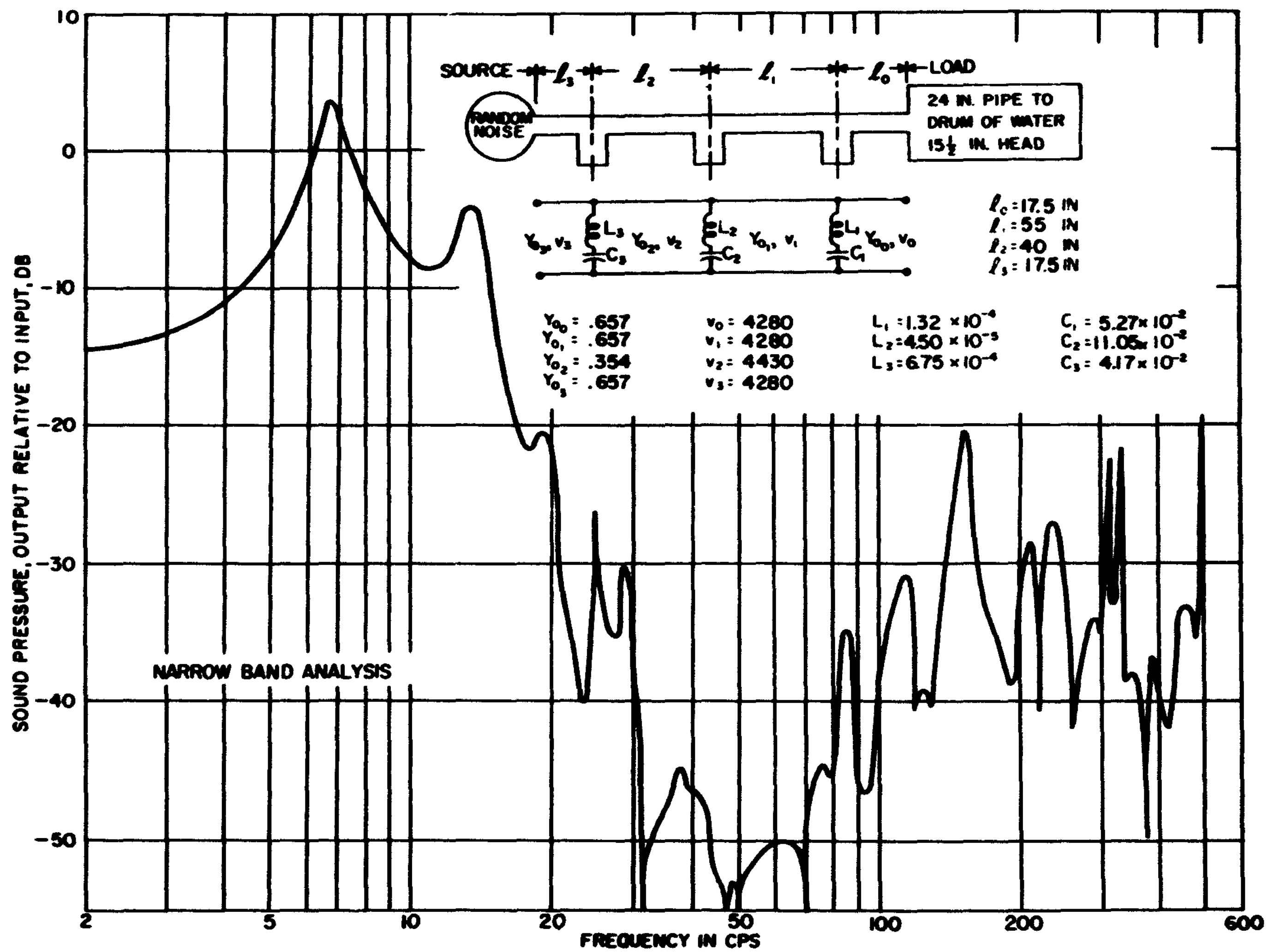

FIGURE 106
THREE ELEMENT SIDE-BRANCH FILTER WITH SPRING-PISTON BRANCH ELEMENTS

DRL - UT
DWG AS 7018
JVK - BEE
11 - 30 - 62

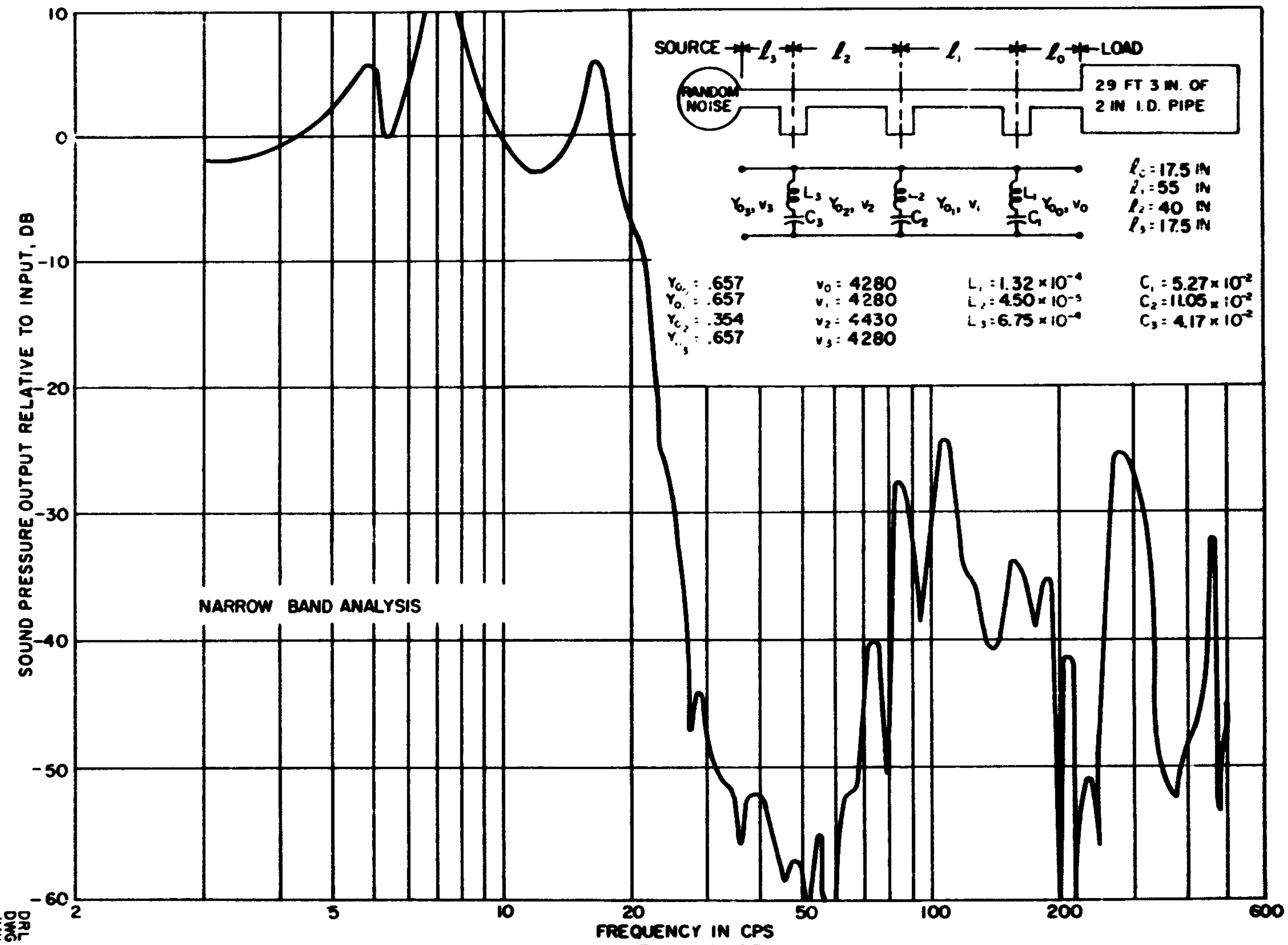

FIGURE 107

THREE ELEMENT SIDE-BRANCH FILTER WITH SPRING-PISTON BRANCH ELEMENTS

DRL - UT
DWG AS 7019
JVK - BEE
12 - 3 - 62

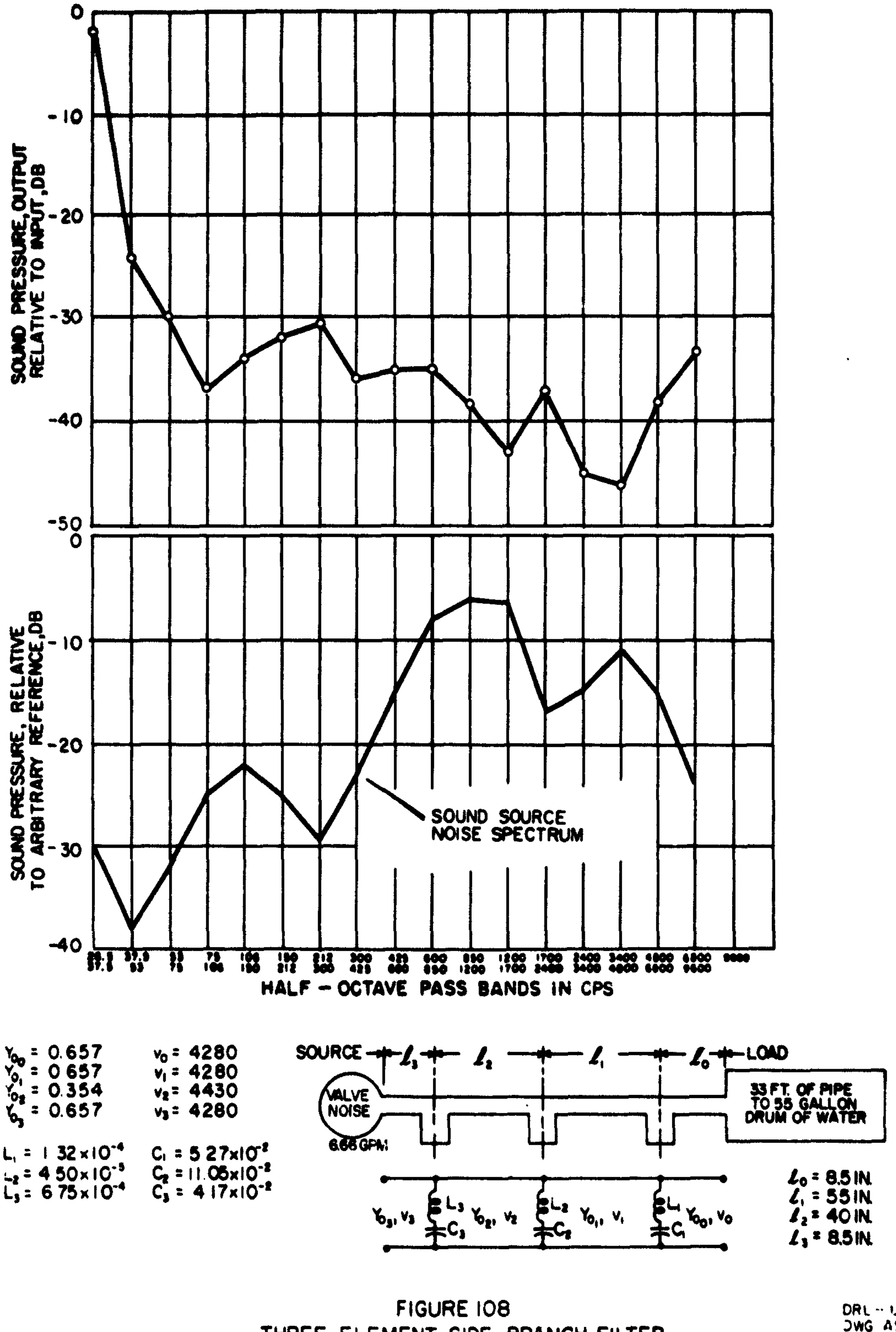

FIGURE 108
THREE ELEMENT SIDE-BRANCH FILTER
WITH SPRING-PISTON BRANCH ELEMENTS

DRL – UT
DWG AS7020
JVK – MJV
10-15-62

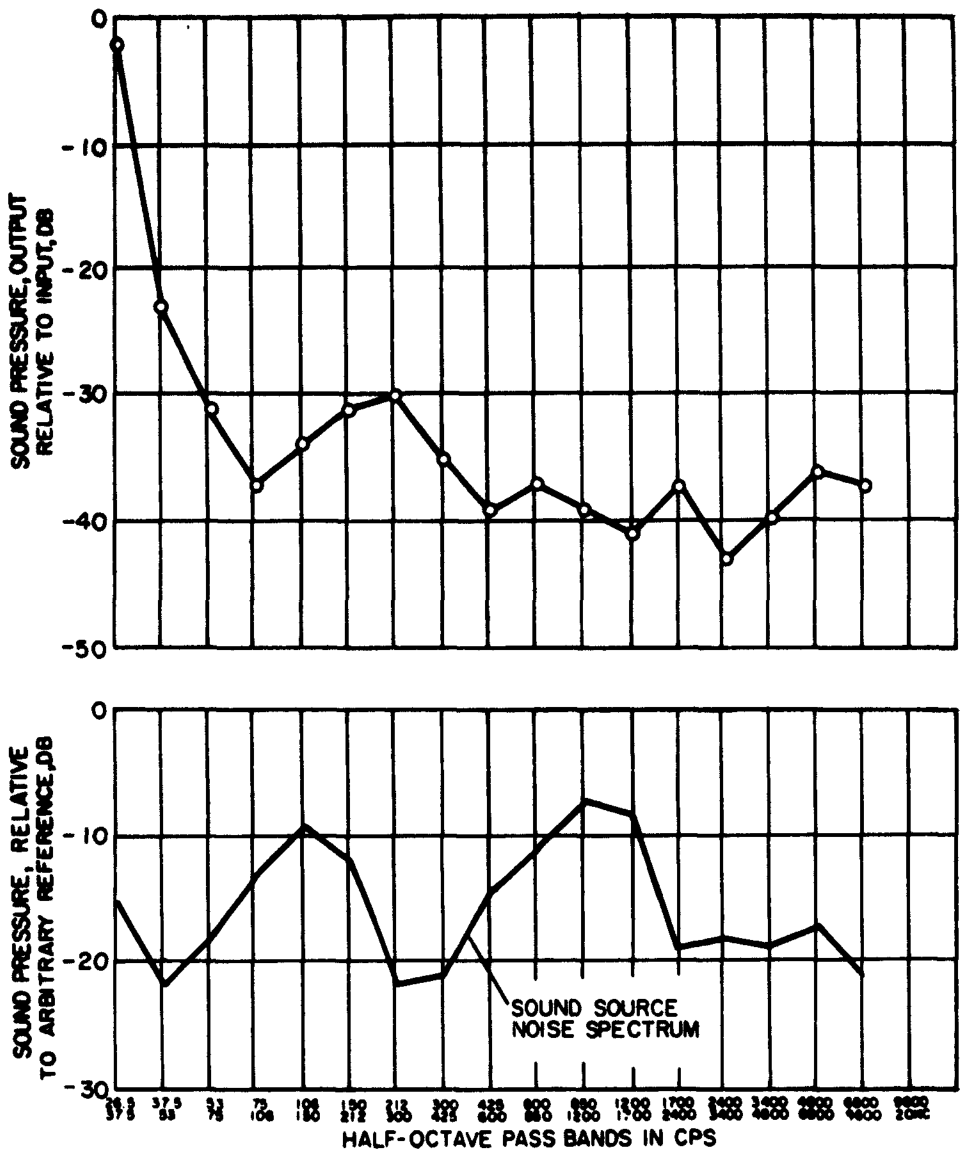

$Y_{0_0} = 0.657$ $v_0 = 4280$
$Y_{0_1} = 0.657$ $v_0 = 4280$
$Y_{0_2} = 0.354$ $v_0 = 4430$
$Y_{0_3} = 0.657$ $v_0 = 4280$

$L_1 = 1.32 \times 10^{-4}$ $C_1 = 5.27 \times 10^{-2}$
$L_2 = 4.50 \times 10^{-5}$ $C_2 = 11.05 \times 10^{-2}$
$L_3 = 6.75 \times 10^{-4}$ $C_3 = 4.17 \times 10^{-2}$

$\ell_0 = 8.5$ IN.
$\ell_1 = 55$ IN.
$\ell_2 = 40$ IN.
$\ell_3 = 8.5$ IN.

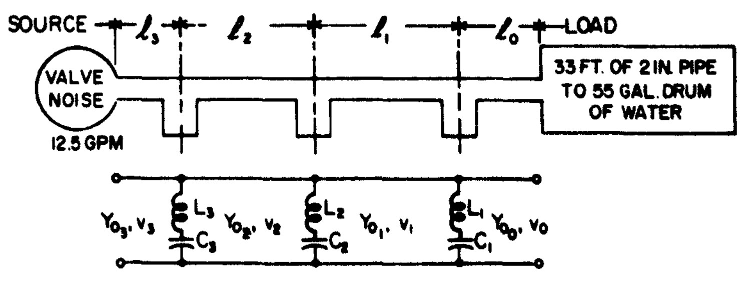

FIGURE 109
THREE ELEMENT SIDE-BRANCH FILTER
WITH SPRING-PISTON BRANCH ELEMENTS

DRL – UT
DWG AS7021
JVK – MJM
10-4-62

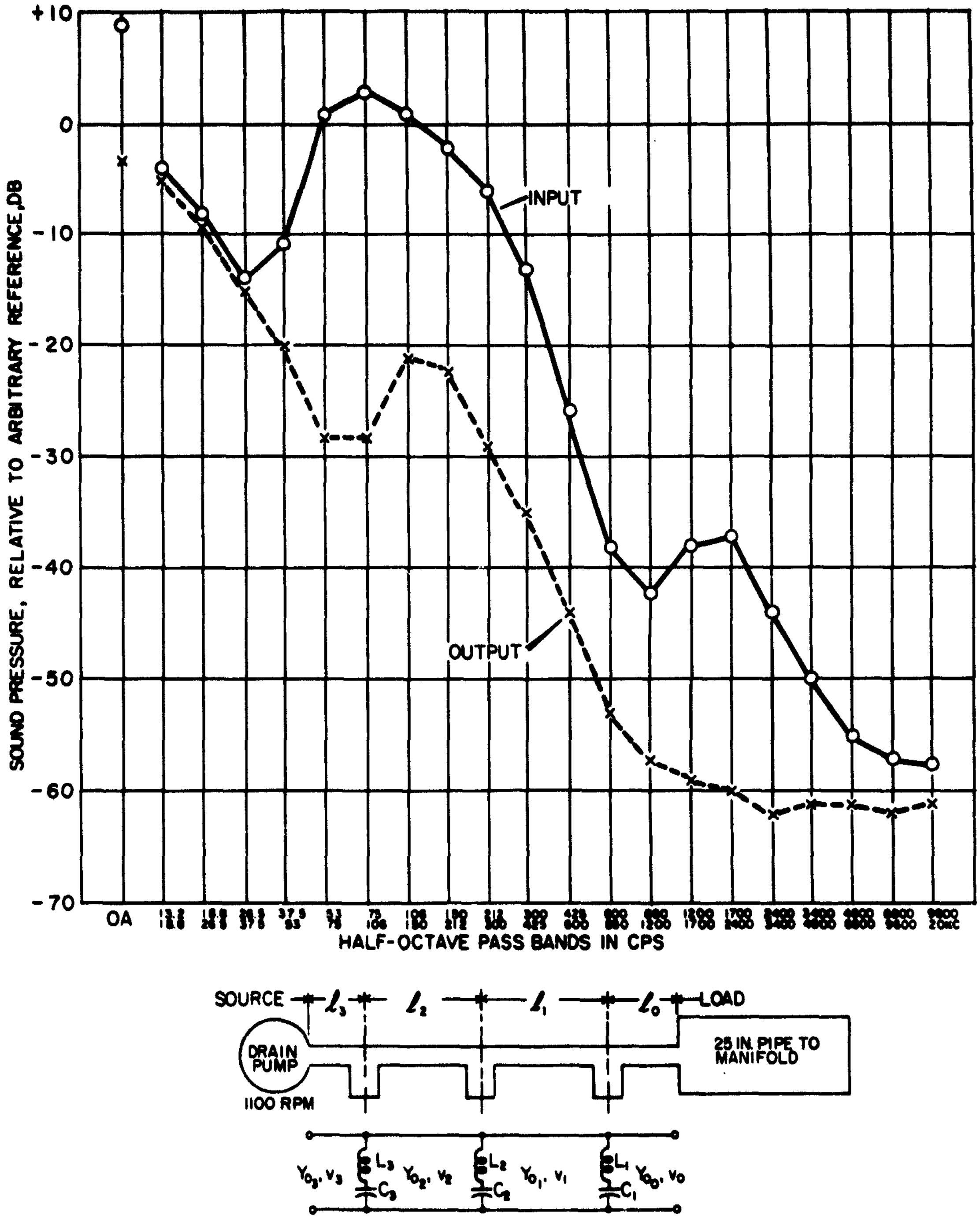

$Y_{0_0} = 1.32$	$v_0 = 3964$	$L_1 = 1.32 \times 10^{-4}$	$C_1 = 5.27 \times 10^{-2}$	$l_0 = 41$ IN
$Y_{0_1} = 0.657$	$v_1 = 4280$	$L_2 = 4.50 \times 10^{-5}$	$C_2 = 11.05 \times 10^{-2}$	$l_1 = 55$ IN
$Y_{0_2} = 0.354$	$v_2 = 4430$	$L_3 = 6.75 \times 10^{-4}$	$C_3 = 4.17 \times 10^{-2}$	$l_2 = 40$ IN
$Y_{0_3} = 1.32$	$v_3 = 3964$			$l_3 = 41$ IN

FIGURE 110

THREE ELEMENT SIDE-BRANCH FILTER
WITH SPRING-PISTON BRANCH ELEMENTS

DRL - UT
DWG AS7025
JVK MJM
10-27-62

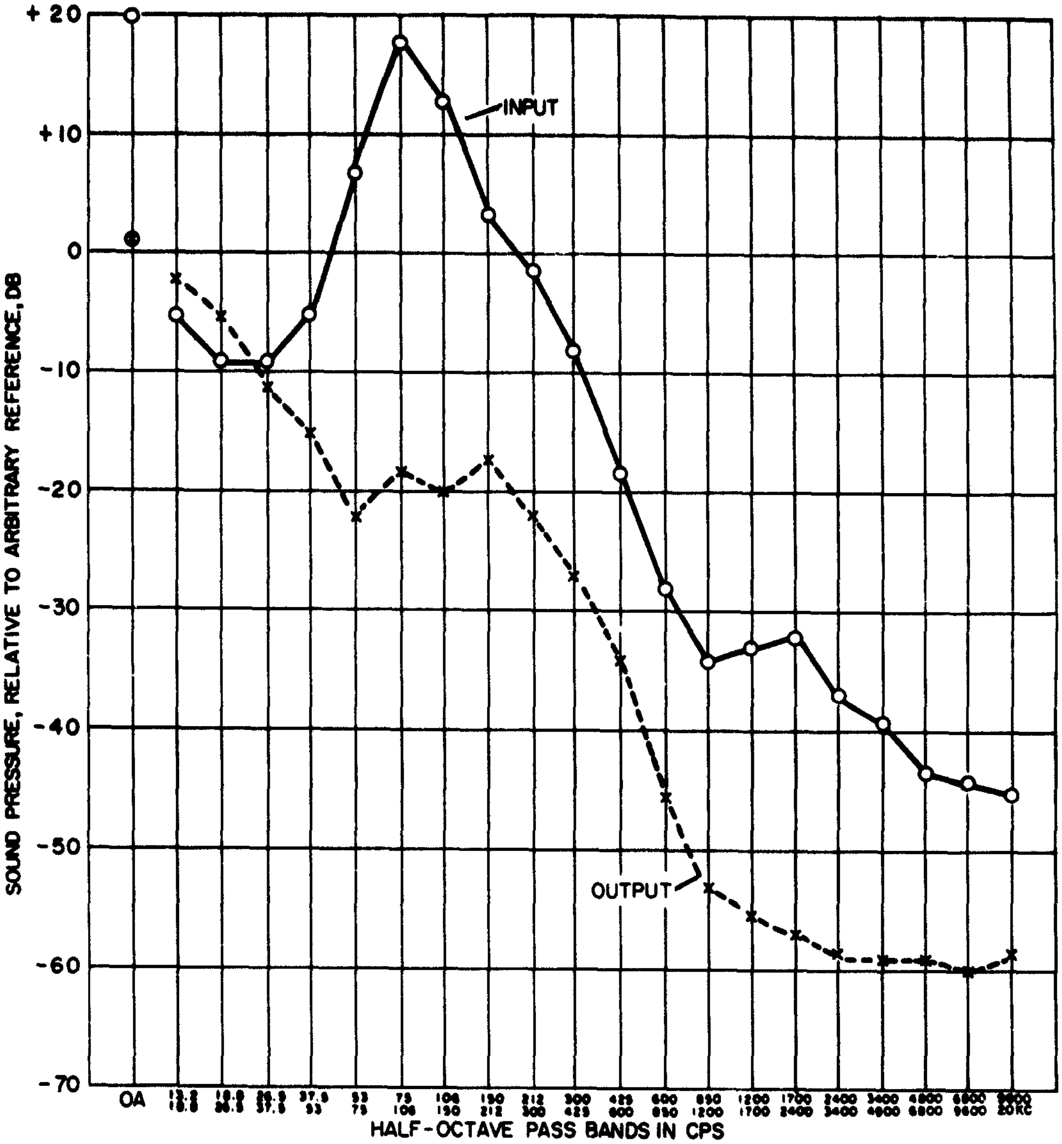

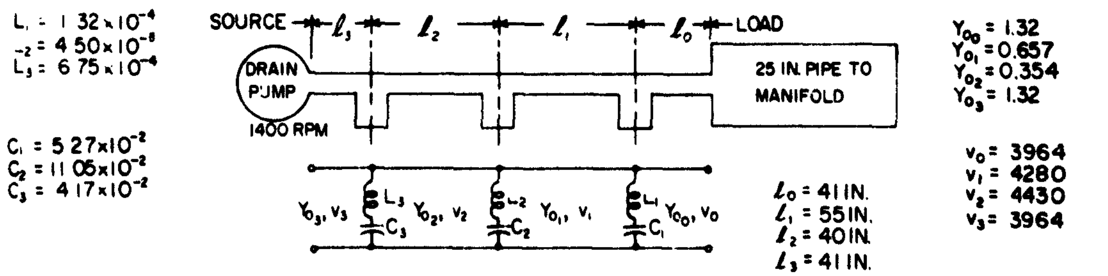

FIGURE III

THREE ELEMENT SIDE-BRANCH FILTER
WITH SPRING-PISTON BRANCH ELEMENTS

DRL - UT
DWG AS7026
JVK - MJM
10-13-62

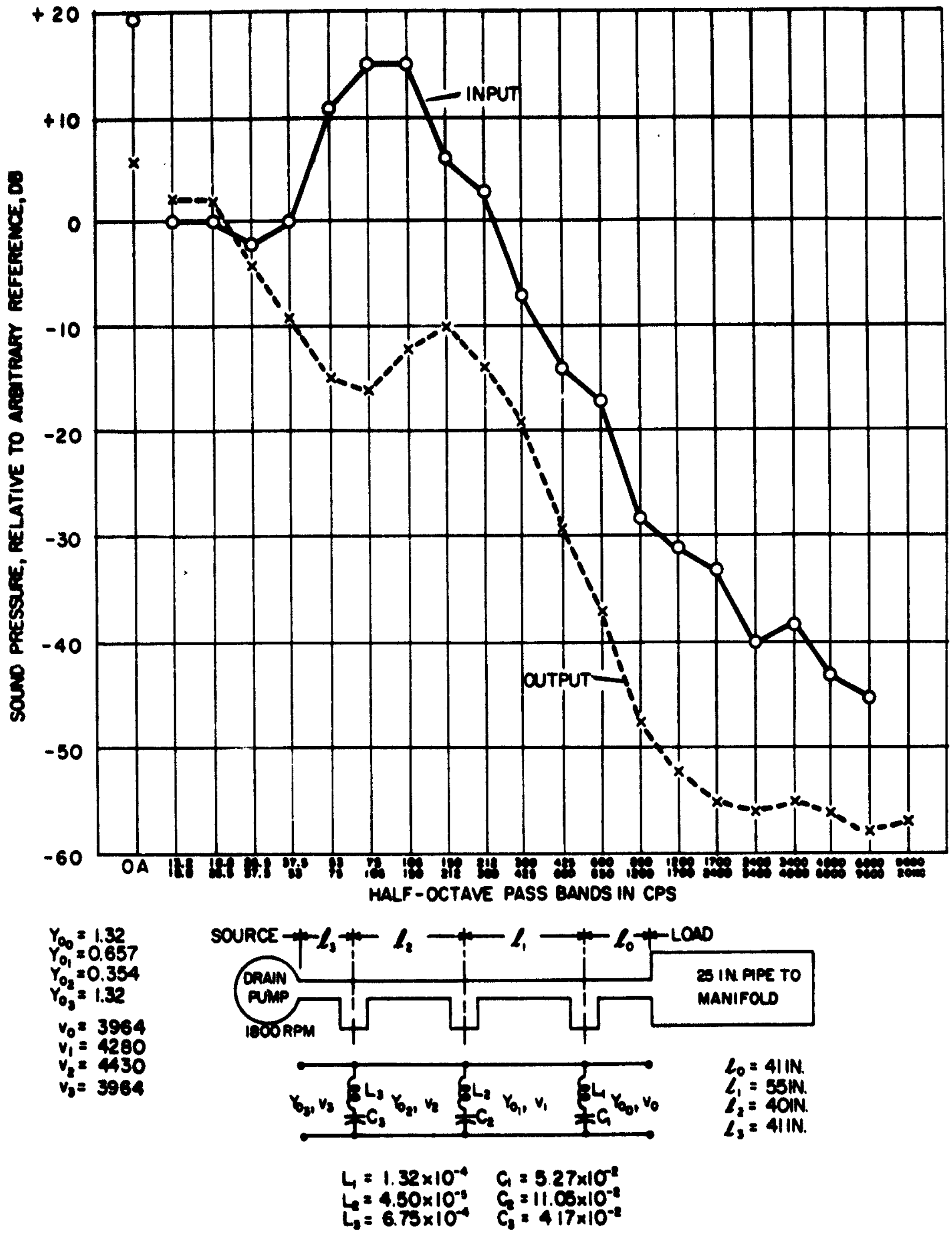

FIGURE 112
THREE ELEMENT SIDE-BRANCH FILTER
WITH SPRING-PISTON BRANCH ELEMENT

DRL-UT
DWG AS7027
JVK - MJM
10-14-62

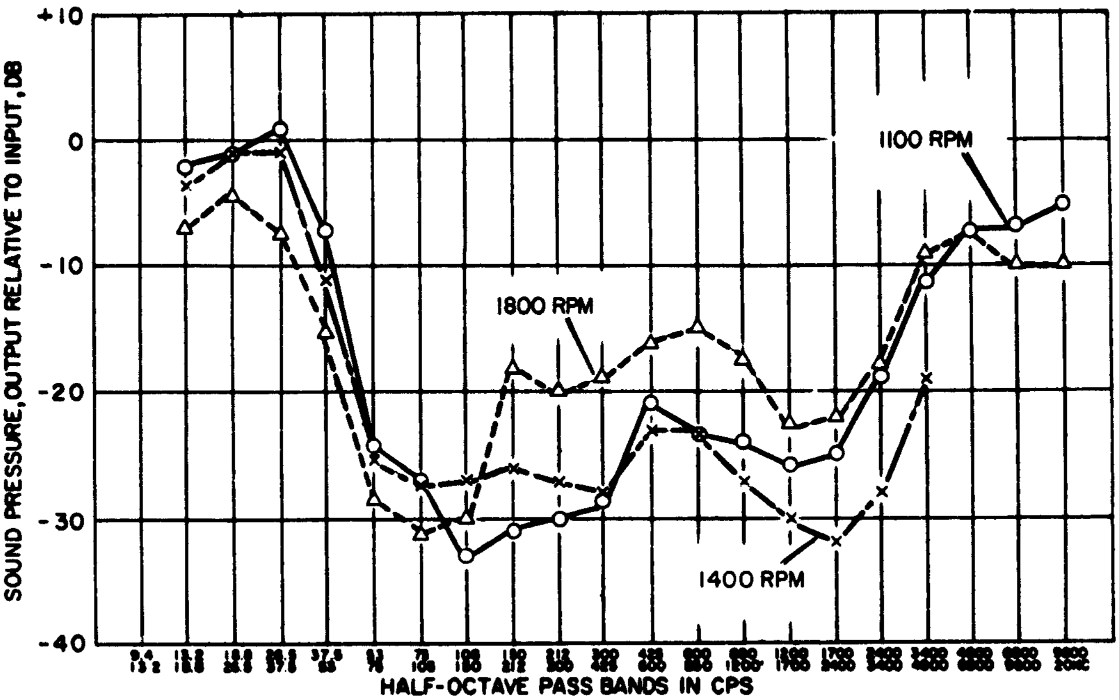

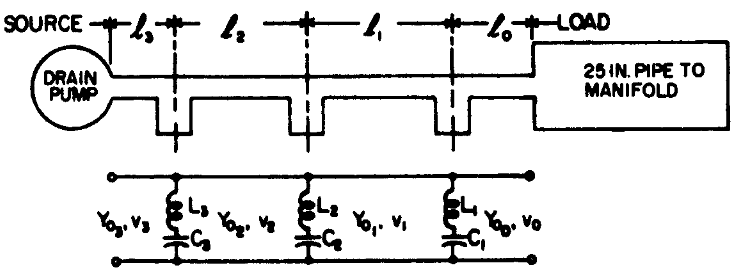

$Y_{o_0} = 1.32$ $v_0 = 3964$ $L_1 = 1.32 \times 10^{-4}$ $C_1 = 5.27 \times 10^{-2}$ $l_0 = 41$ IN.

$Y_{o_1} = 0.657$ $v_1 = 4280$ $L_2 = 4.50 \times 10^{-5}$ $C_2 = 11.05 \times 10^{-2}$ $l_1 = 55$ IN

$Y_{o_2} = 0.354$ $v_2 = 4430$ $L_3 = 6.75 \times 10^{-4}$ $C_3 = 4.17 \times 10^{-2}$ $l_2 = 40$ IN

$Y_{o_3} = 1.32$ $v_3 = 3964$ $l_3 = 41$ IN.

FIGURE 113
THREE ELEMENT SIDE-BRANCH FILTER
WITH SPRING-PISTON BRANCH ELEMENTS

DRL - UT
DWG AS7028
JVK - MJM
10-21-62

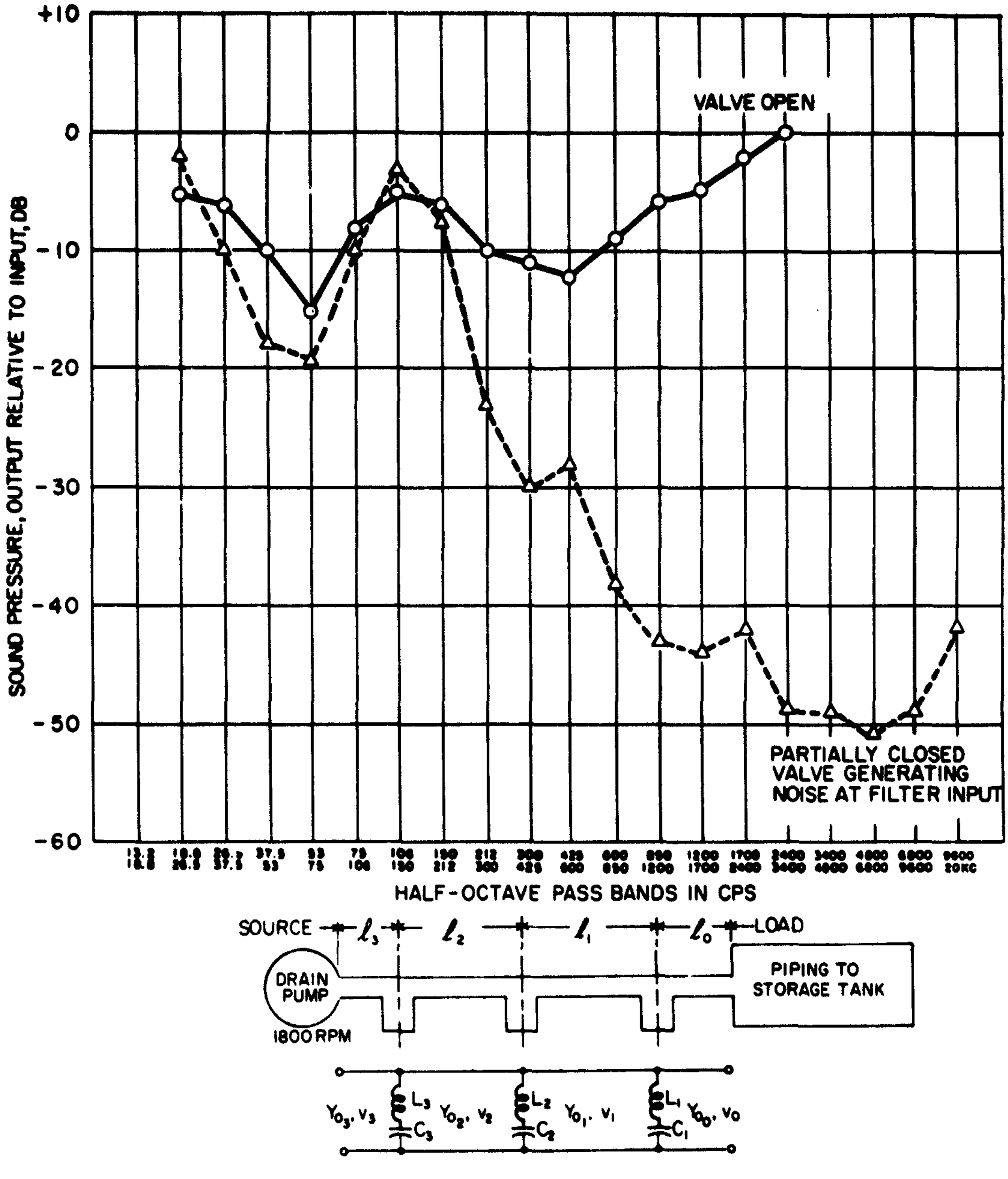

$Y_{0_0} = 1.32$ $v_0 = 3964$ $L_1 = 1.32 \times 10^{-4}$ $C_1 = 5.27 \times 10^{-2}$ $\ell_0 = 41$ IN.

$Y_{0_1} = 0.657$ $v_1 = 4280$ $L_2 = 4.50 \times 10^{-5}$ $C_2 = 11.05 \times 10^{-2}$ $\ell_1 = 55$ IN

$Y_{0_2} = 0.354$ $v_2 = 4430$ $L_3 = 6.75 \times 10^{-4}$ $C_3 = 4.17 \times 10^{-2}$ $\ell_2 = 40$ IN

$Y_{0_3} = 1.32$ $v_3 = 3964$ $\ell_3 = 41$ IN.

FIGURE 114
THREE ELEMENT SIDE-BRANCH FILTER
WITH SPRING-PISTON BRANCH ELEMENTS

DRL - UT
DWG AS7030
JVK - MJM
12 - 3 - 62

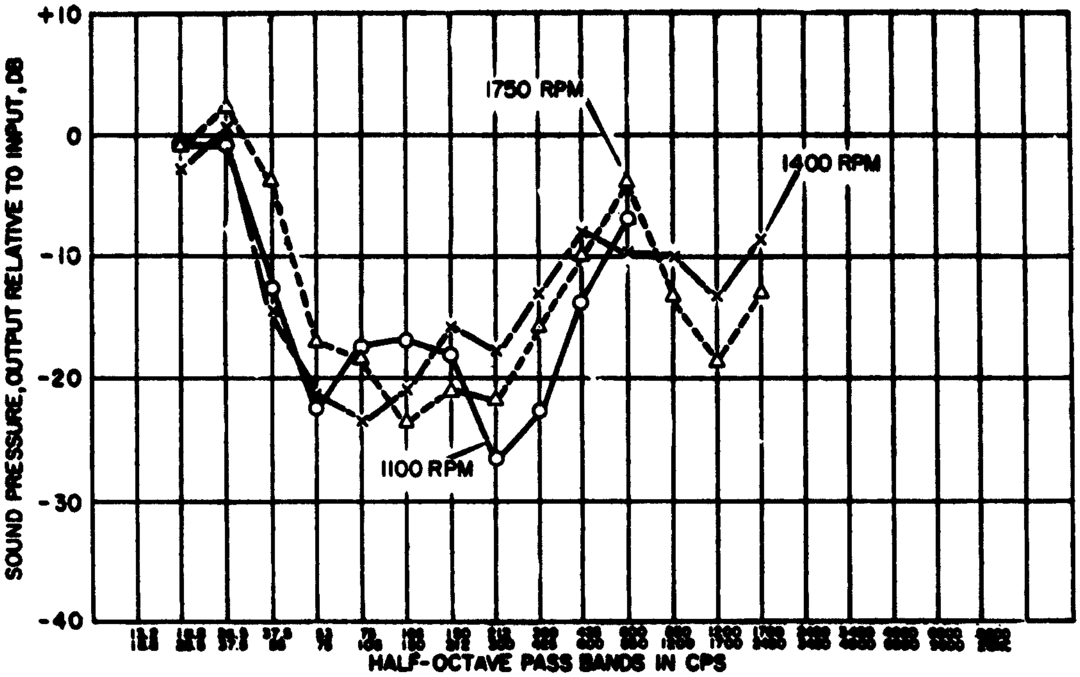

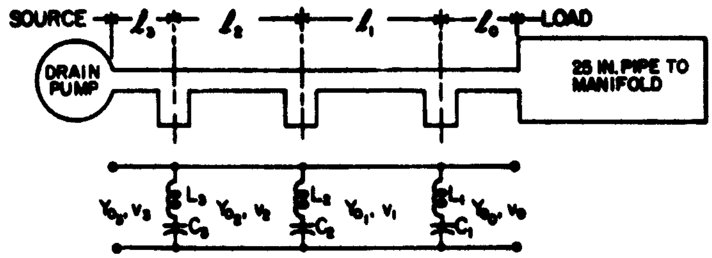

Y_{0_0} = (UNKNOWN)	v_0 = (UNKNOWN)	$L_1 = 1.32 \times 10^{-4}$	$C_1 = 5.27 \times 10^{-8}$	ℓ_0 = 7 IN.
Y_{0_1} = 0.657	v_1 = 4280	$L_2 = 4.50 \times 10^{-4}$	$C_2 = 11.06 \times 10^{-8}$	ℓ_1 = 55 IN.
Y_{0_2} = 0.354	v_2 = 4430	$L_3 = 6.75 \times 10^{-4}$	$C_3 = 4.17 \times 10^{-8}$	ℓ_2 = 40 IN.
Y_{0_3} = (UNKNOWN)	v_3 = (UNKNOWN)			ℓ_3 = 7 IN.

FIGURE 115
THREE ELEMENT SIDE-BRANCH FILTER
WITH SPRING-PISTON BRANCH ELEMENTS

DRL - UT
DWG AS7089
JVK - MJM
10-26-62

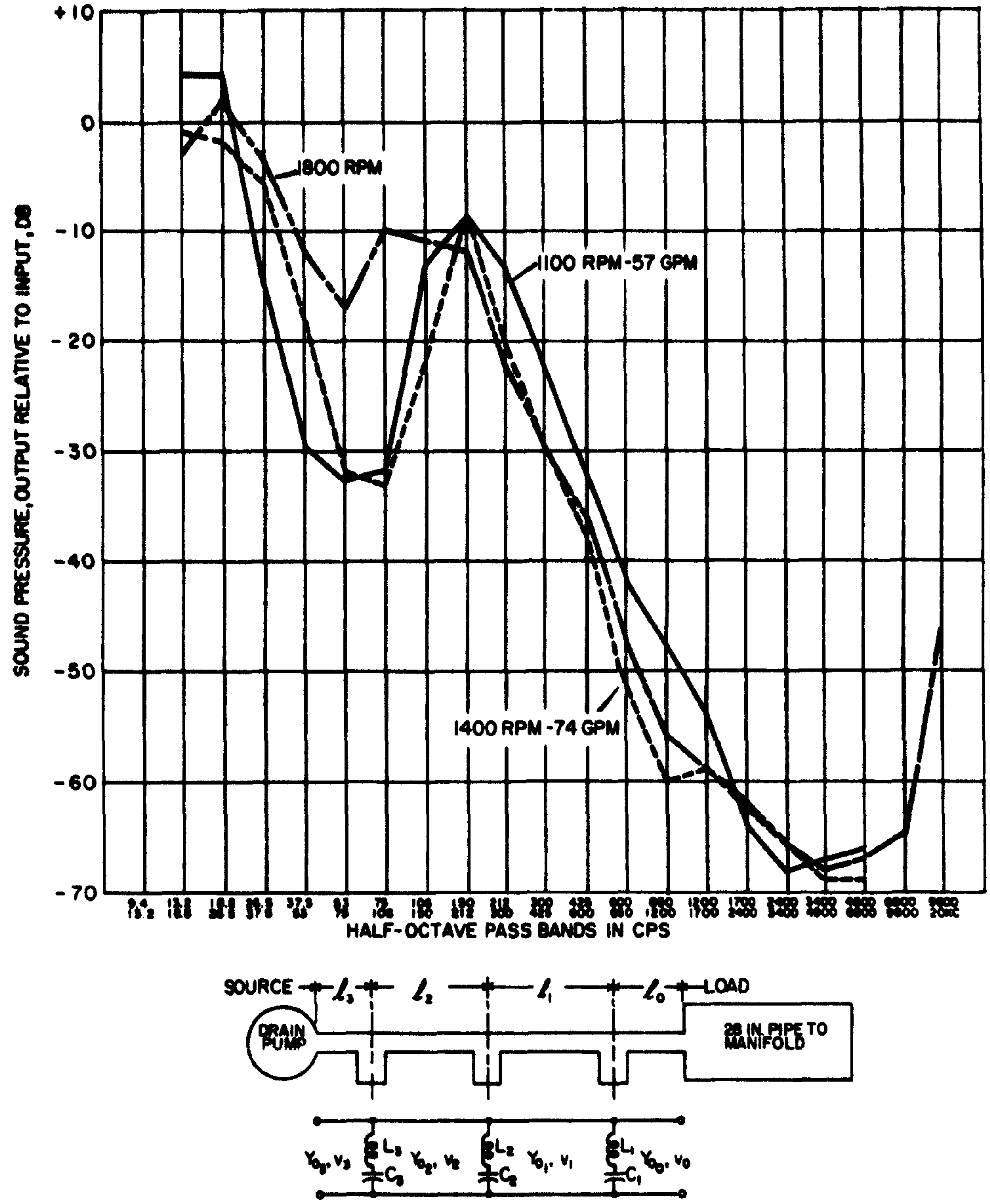

$Y_{0_0} = 1.32$	$v_0 = 3964$	$L_1 = 1.32 \times 10^{-4}$	$C_1 = 5.27 \times 10^{-2}$	$\ell_0 = 35$ IN
$Y_{0_1} = 0.657$	$v_1 = 4280$	$L_2 = 4.50 \times 10^{-5}$	$C_2 = 11.05 \times 10^{-2}$	$\ell_1 = 55$ IN
$Y_{0_2} = 0.354$	$v_2 = 4430$	$L_3 = 6.75 \times 10^{-4}$	$C_3 = 4.17 \times 10^{-2}$	$\ell_2 = 40$ IN
$Y_{0_3} = 1.32$	$v_3 = 3964$			$\ell_3 = 35$ IN

FIGURE 116

THREE ELEMENT SIDE-BRANCH FILTER
WITH SPRING-PISTON BRANCH ELEMENTS

DRL - UT
DWG AS7032
JVK MJM
10-27-62

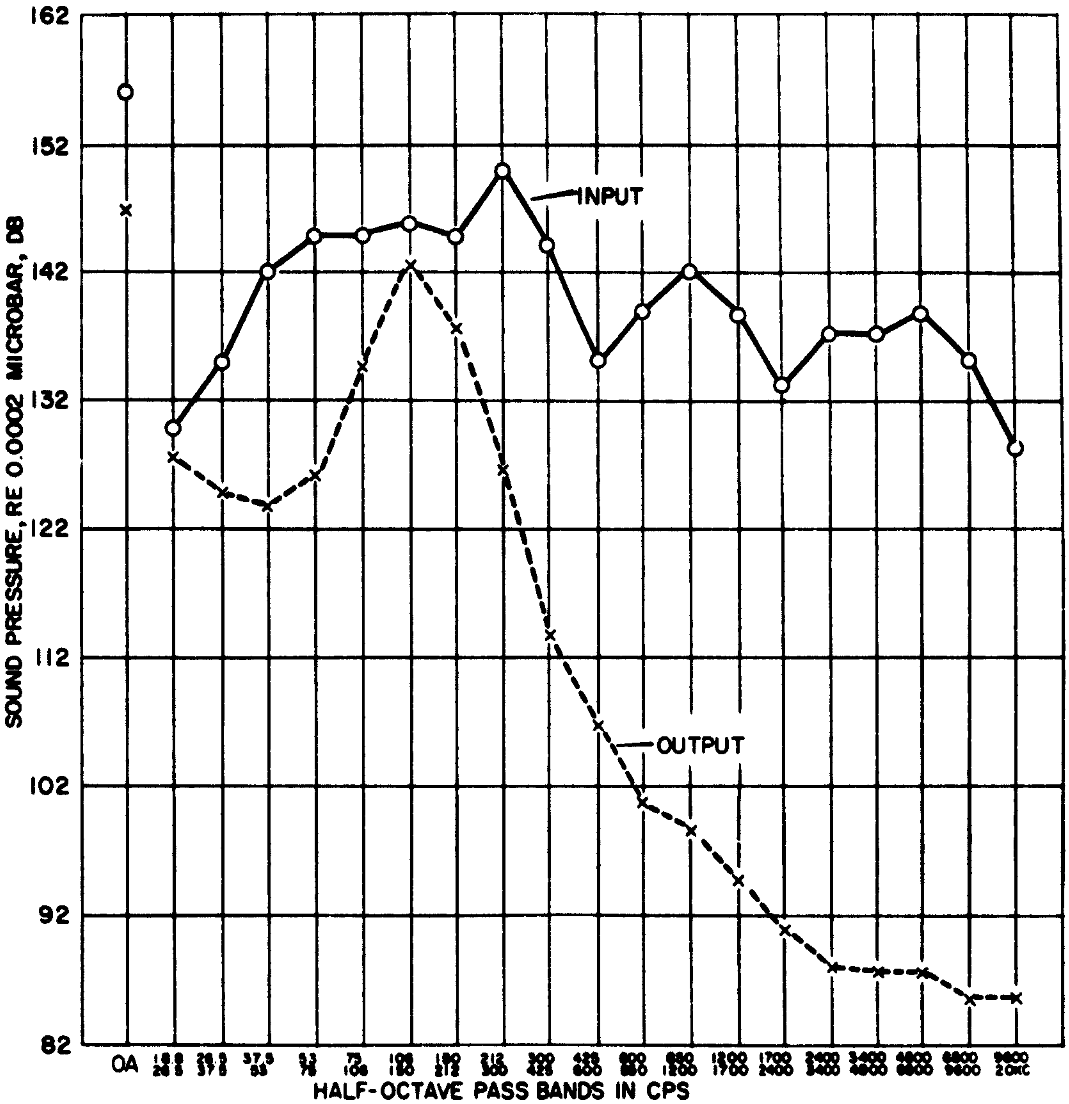

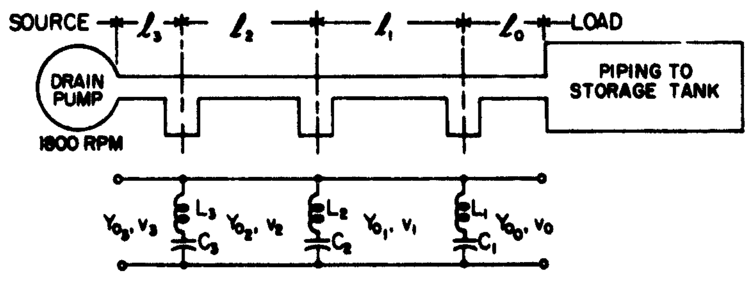

$Y_{0_0} = 1.32$	$v_0 = 3964$	$L_1 = 1.32 \times 10^{-4}$	$C_1 = 5.27 \times 10^{-2}$	$\ell_0 = 41$ IN.
$Y_{0_1} = 0.657$	$v_1 = 4280$	$L_2 = 4.50 \times 10^{-5}$	$C_2 = 11.05 \times 10^{-2}$	$\ell_1 = 55$ IN
$Y_{0_2} = 0.354$	$v_2 = 4430$	$L_3 = 6.75 \times 10^{-4}$	$C_3 = 4.17 \times 10^{-2}$	$\ell_2 = 40$ IN
$Y_{0_3} = 1.32$	$v_3 = 3964$			$\ell_3 = 41$ IN.

FIGURE 117
THREE ELEMENT SIDE-BRANCH FILTER
WITH SPRING-PISTON BRANCH ELEMENTS

DRL - UT
DWG AS7031
JVK - MJM
10-29-62

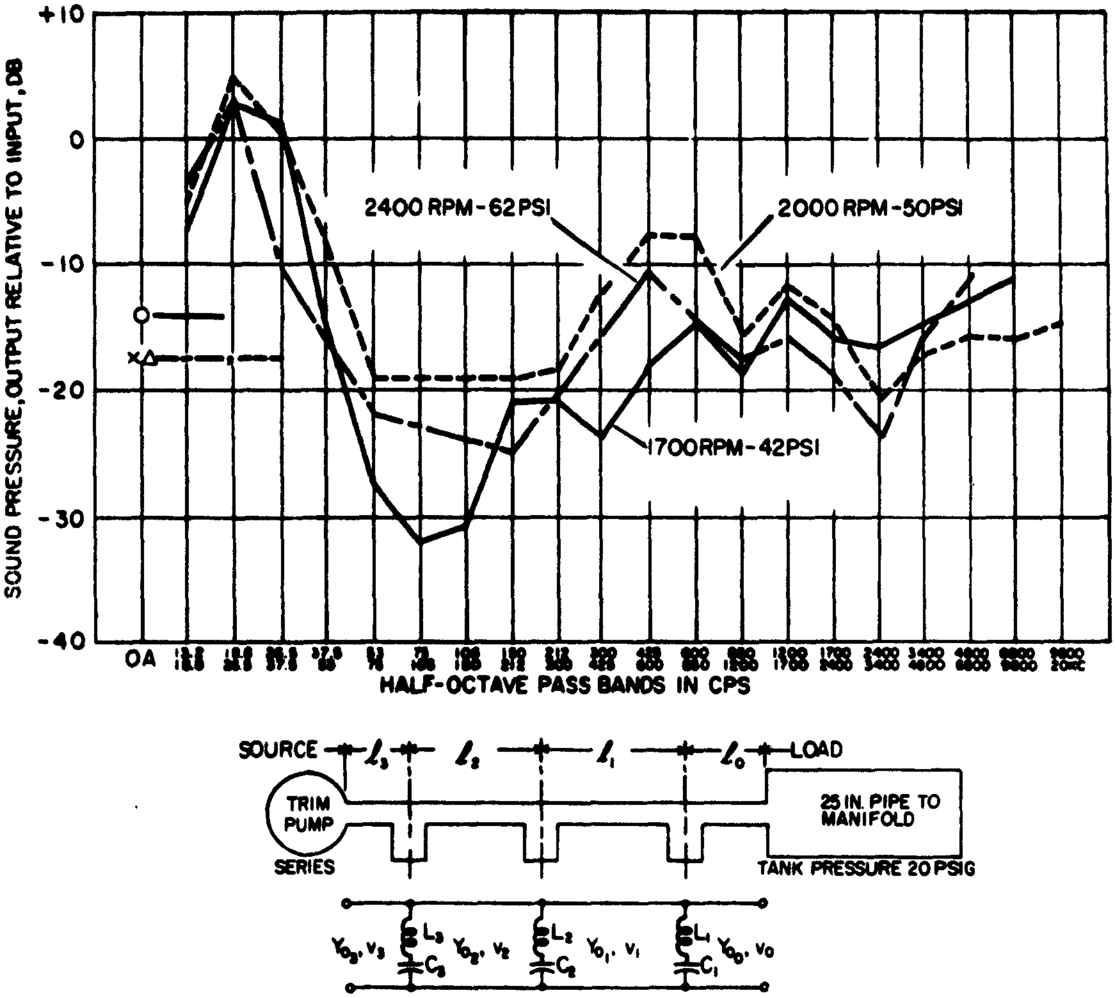

$Y_{0_0} = 1.32$	$v_0 = 3964$	$L_1 = 1.32 \times 10^{-4}$	$C_1 = 5.27 \times 10^{-2}$	$\ell_0 = 41$ IN
$Y_{0_1} = 0.657$	$v_1 = 4280$	$L_2 = 4.50 \times 10^{-5}$	$C_2 = 11.05 \times 10^{-2}$	$\ell_1 = 55$ IN
$Y_{0_2} = 0.354$	$v_2 = 4430$	$L_3 = 6.75 \times 10^{-4}$	$C_3 = 4.17 \times 10^{-2}$	$\ell_2 = 40$ IN
$Y_{0_3} = 1.32$	$v_3 = 3964$			$\ell_3 = 41$ IN

FIGURE 118
THREE ELEMENT SIDE-BRANCH FILTER
WITH SPRING-PISTON BRANCH ELEMENTS

DRL - UT
DWG AS7033
IVK MJM
10-20-62

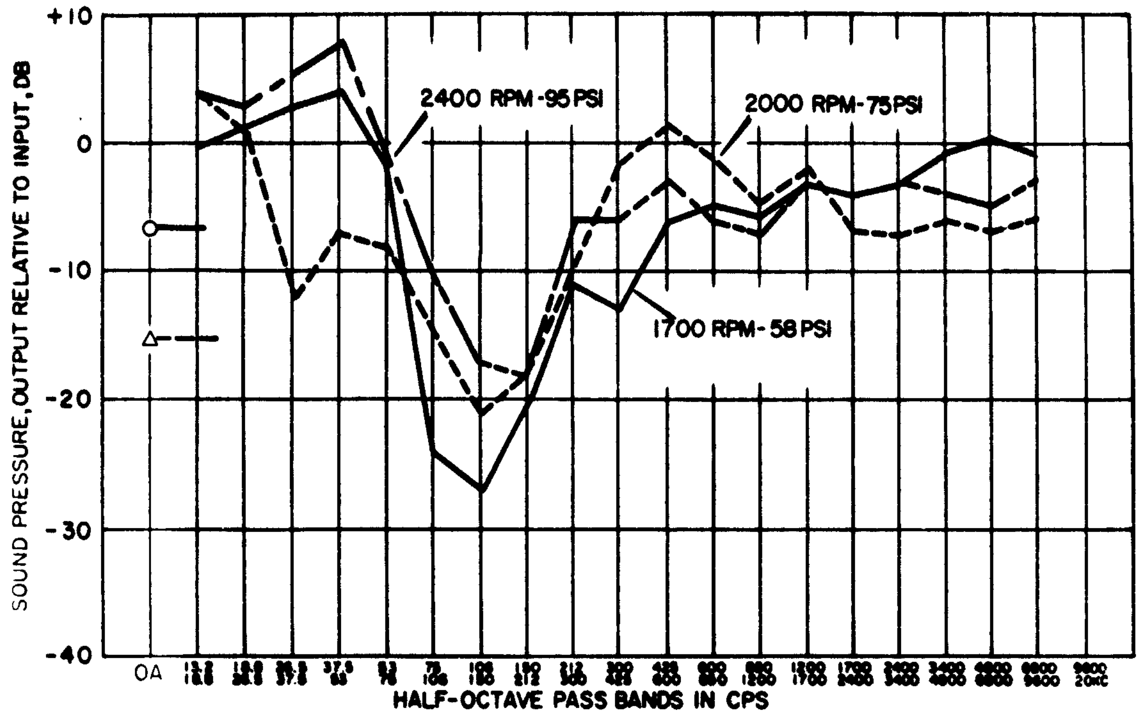

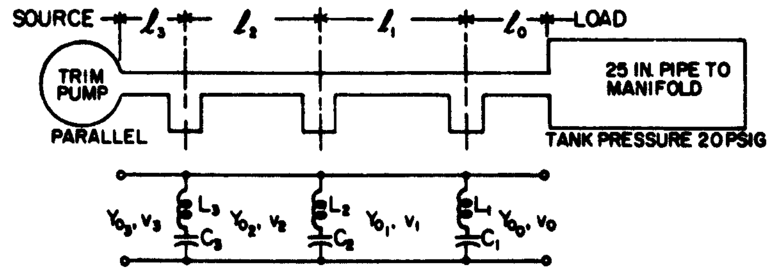

$Y_{0_0} = 1.32$	$v_0 = 3964$	$L_1 = 1.32 \times 10^{-4}$	$C_1 = 5.27 \times 10^{-2}$	$\ell_0 = 41$ IN.
$Y_{0_1} = 0.657$	$v_1 = 4280$	$L_2 = 4.50 \times 10^{-5}$	$C_2 = 11.05 \times 10^{-2}$	$\ell_1 = 55$ IN.
$Y_{0_2} = 0.354$	$v_2 = 4430$	$L_3 = 6.75 \times 10^{-4}$	$C_3 = 4.17 \times 10^{-2}$	$\ell_2 = 40$ IN
$Y_{0_3} = 1.32$	$v_3 = 3964$			$\ell_3 = 41$ IN

FIGURE 119
THREE ELEMENT SIDE-BRANCH FILTER
WITH SPRING-PISTON BRANCH ELEMENTS

DRL - UT
DWG A57034
JVK - MJM
10-20-62

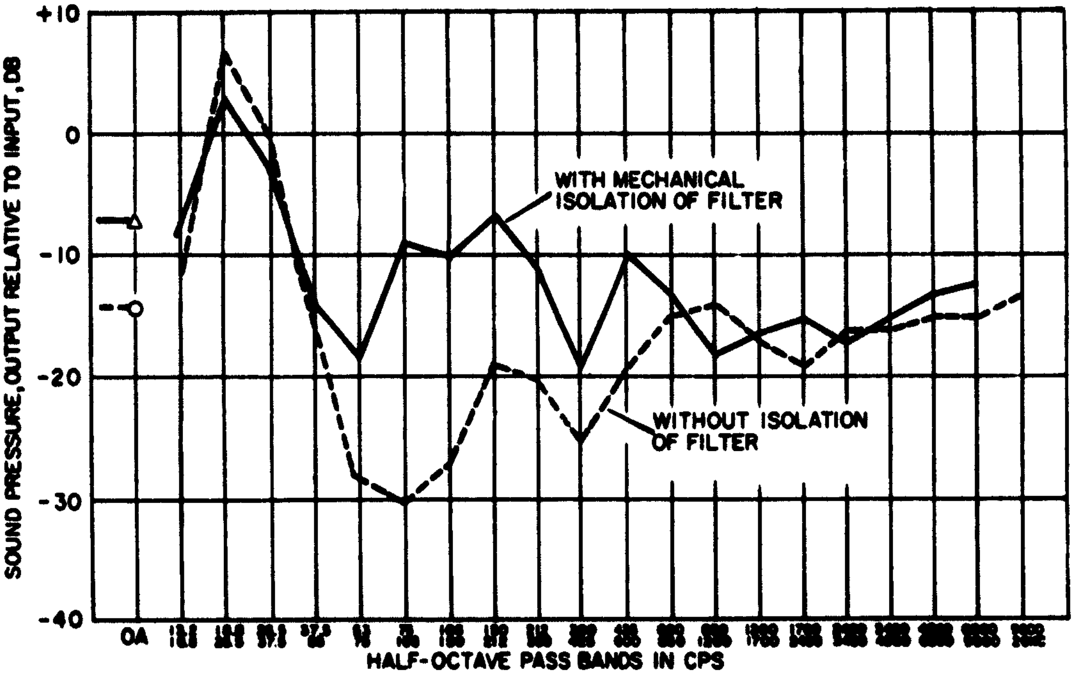

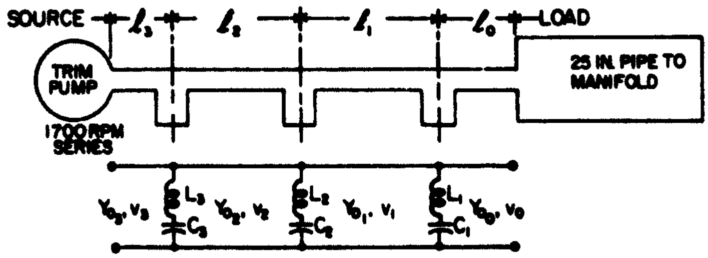

$Y_{0_0} = 1.32$	$v_0 = 3964$	$L_1 = 1.32 \times 10^{-4}$	$C_1 = 5.27 \times 10^{-2}$	$\ell_0 = 41$ IN.
$Y_{0_1} = 0.657$	$v_1 = 4280$	$L_2 = 4.50 \times 10^{-5}$	$C_2 = 11.05 \times 10^{-2}$	$\ell_1 = 55$ IN.
$Y_{0_2} = 0.354$	$v_2 = 4430$	$L_3 = 6.75 \times 10^{-4}$	$C_3 = 4.17 \times 10^{-2}$	$\ell_2 = 40$ IN.
$Y_{0_3} = 1.32$	$v_3 = 3964$			$\ell_3 = 41$ IN.

FIGURE 120
THREE ELEMENT SIDE-BRANCH FILTER
WITH SPRING-PISTON BRANCH ELEMENTS

DRL - UT
DWG AS7036
JVK - MJM
10-19-62

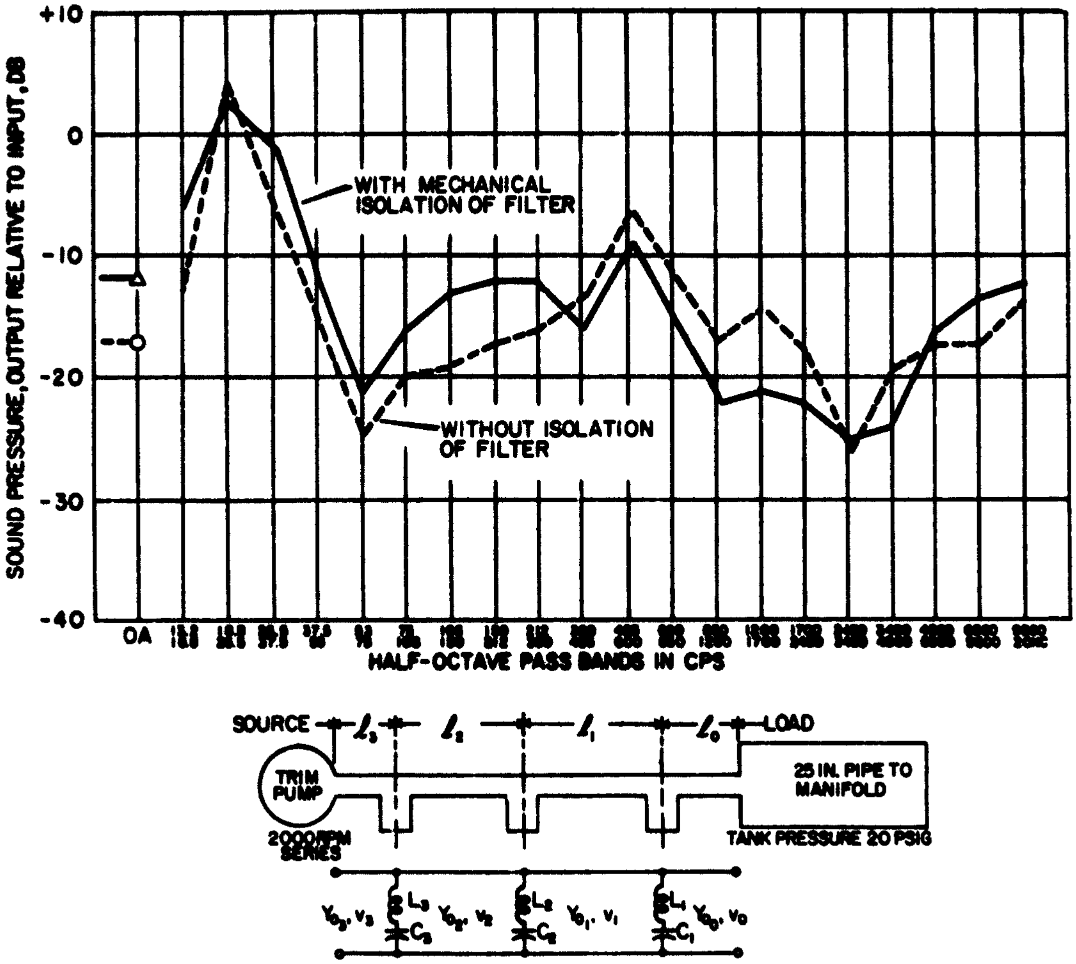

$Y_{0_0} = 1.32$	$v_0 = 3964$	$L_1 = 1.32 \times 10^{-4}$	$C_1 = 5.27 \times 10^{-2}$	$\ell_0 = 41$ IN.
$Y_{0_1} = 0.657$	$v_1 = 4280$	$L_2 = 4.50 \times 10^{-5}$	$C_2 = 11.05 \times 10^{-2}$	$\ell_1 = 55$ IN.
$Y_{0_2} = 0.354$	$v_2 = 4430$	$L_3 = 6.75 \times 10^{-4}$	$C_3 = 4.17 \times 10^{-2}$	$\ell_2 = 40$ IN
$Y_{0_3} = 1.32$	$v_3 = 3964$			$\ell_3 = 41$ IN.

FIGURE 121
THREE ELEMENT SIDE-BRANCH FILTER
WITH SPRING-PISTON BRANCH ELEMENTS

DRL - UT
DWG A57036
JVK - MJM
10-19-62

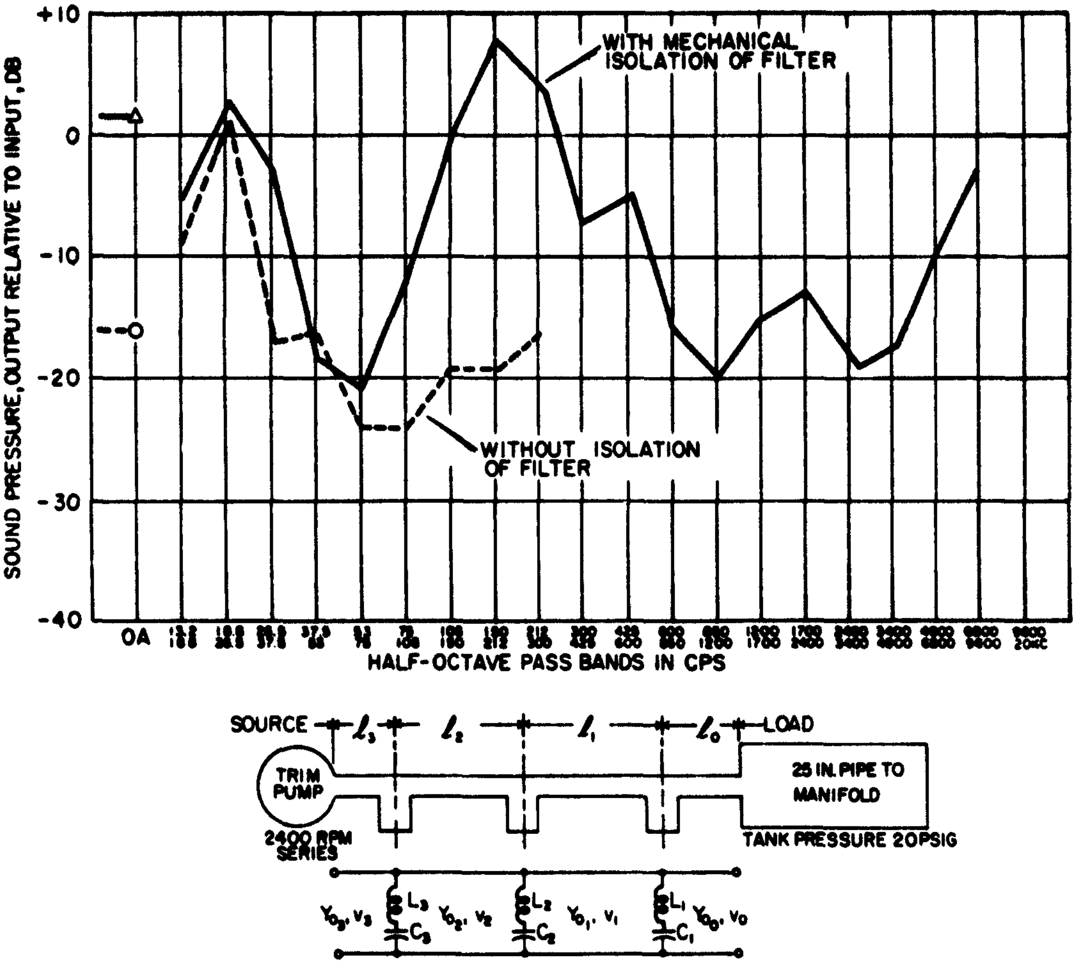

$Y_{o_0} = 1.32$	$v_0 = 3964$	$L_1 = 1.32 \times 10^{-4}$	$C_1 = 5.27 \times 10^{-2}$	$\ell_0 = 41$ IN
$Y_{o_1} = 0.657$	$v_1 = 4280$	$L_2 = 4.50 \times 10^{-5}$	$C_2 = 11.05 \times 10^{-2}$	$\ell_1 = 55$ IN
$Y_{o_2} = 0.354$	$v_2 = 4430$	$L_3 = 6.75 \times 10^{-4}$	$C_3 = 4.17 \times 10^{-2}$	$\ell_2 = 40$ IN
$Y_{o_3} = 1.32$	$v_3 = 3964$			$\ell_3 = 41$ IN

FIGURE 122
THREE ELEMENT SIDE-BRANCH FILTER
WITH SPRING-PISTON BRANCH ELEMENTS

DRL - UT
DWG AS7037
JVK - MJM
10-16-62

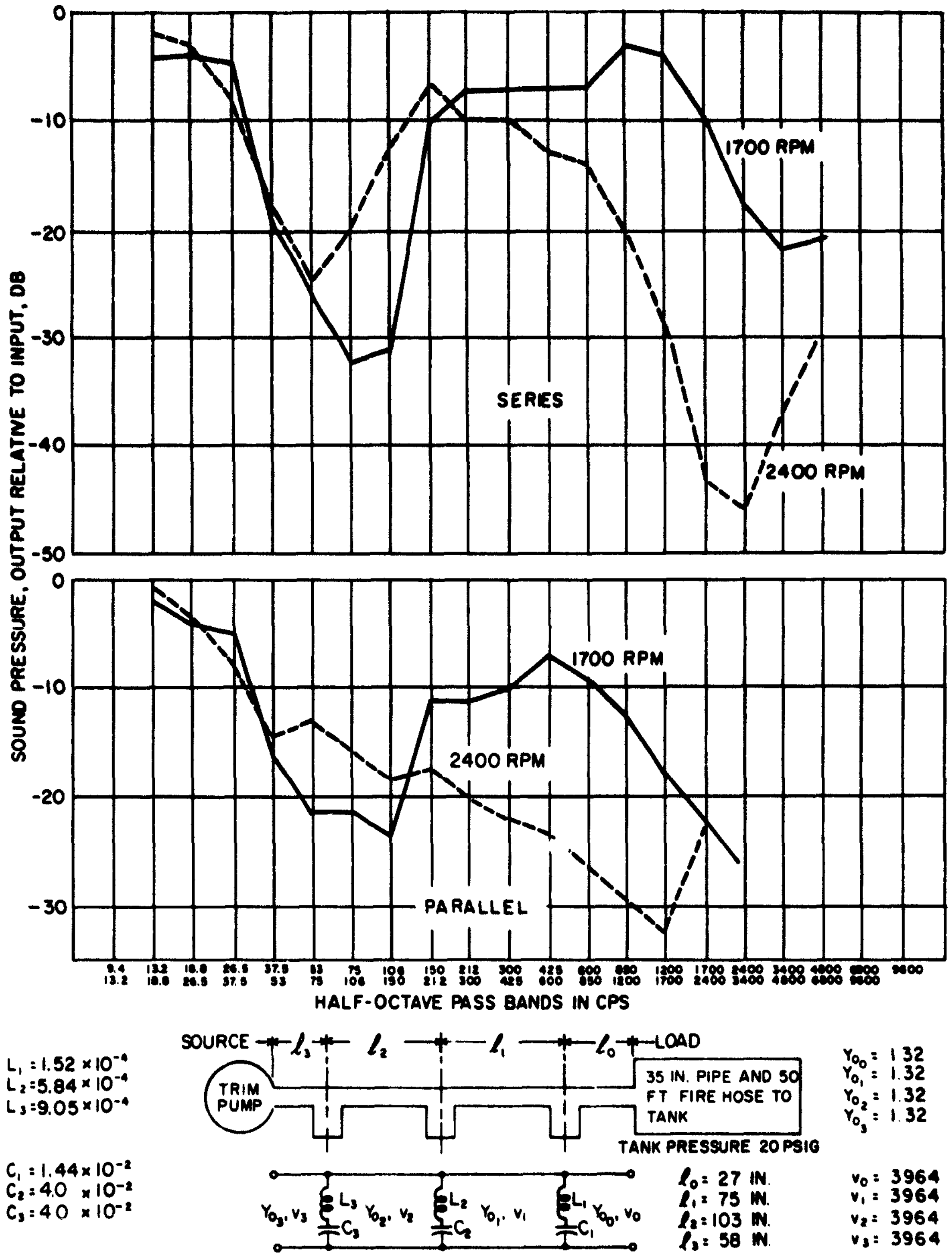

FIGURE 123
THREE ELEMENT SIDE-BRANCH FILTER WITH SPRING-PISTON BRANCH ELEMENTS

DRL - UT
DWG AS 7040
JVK - BEE
11 - 30 - 62

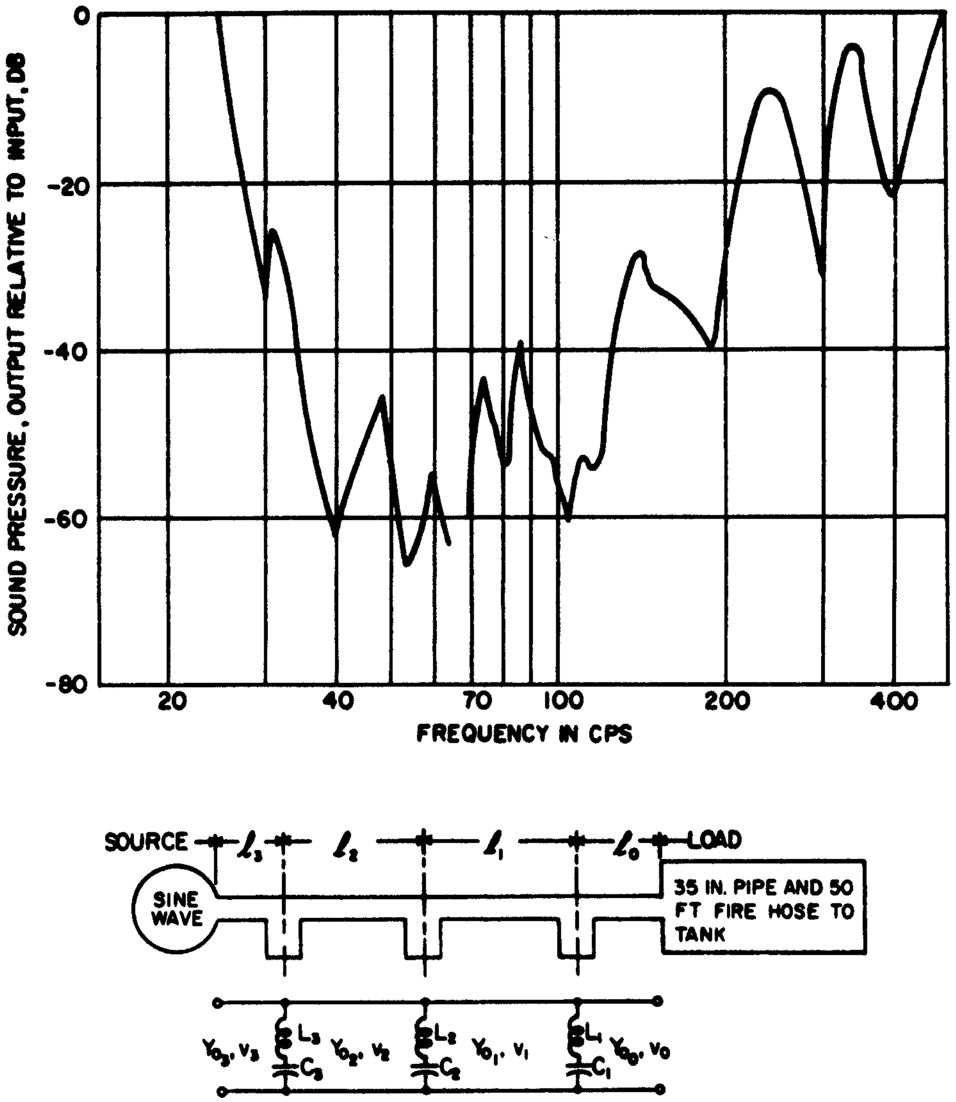

Y_{o_0} = 1.32	v_0 = 3964	L_1 = 2.37×10^{-5}	C_1 = 9.5×10^{-2}	ℓ_0 = 10 IN.
Y_{o_1} = 1.32	v_1 = 3964	L_2 = 4.50×10^{-5}	C_2 = 15.4×10^{-2}	ℓ_1 = 85.5 IN.
Y_{o_2} = 1.32	v_2 = 3964	L_3 = 8.72×10^{-5}	C_3 = 14.4×10^{-2}	ℓ_2 = 51 IN.
Y_{o_3} = 1.32	v_3 = 3964			ℓ_3 = 51 IN.

FIGURE 124
THREE ELEMENT SIDE-BRANCH FILTER WITH METAL BELLOWS BRANCH ELEMENTS

DRL - UT
DWG AS 7050
JVK - BEE
11 - 30 - 62

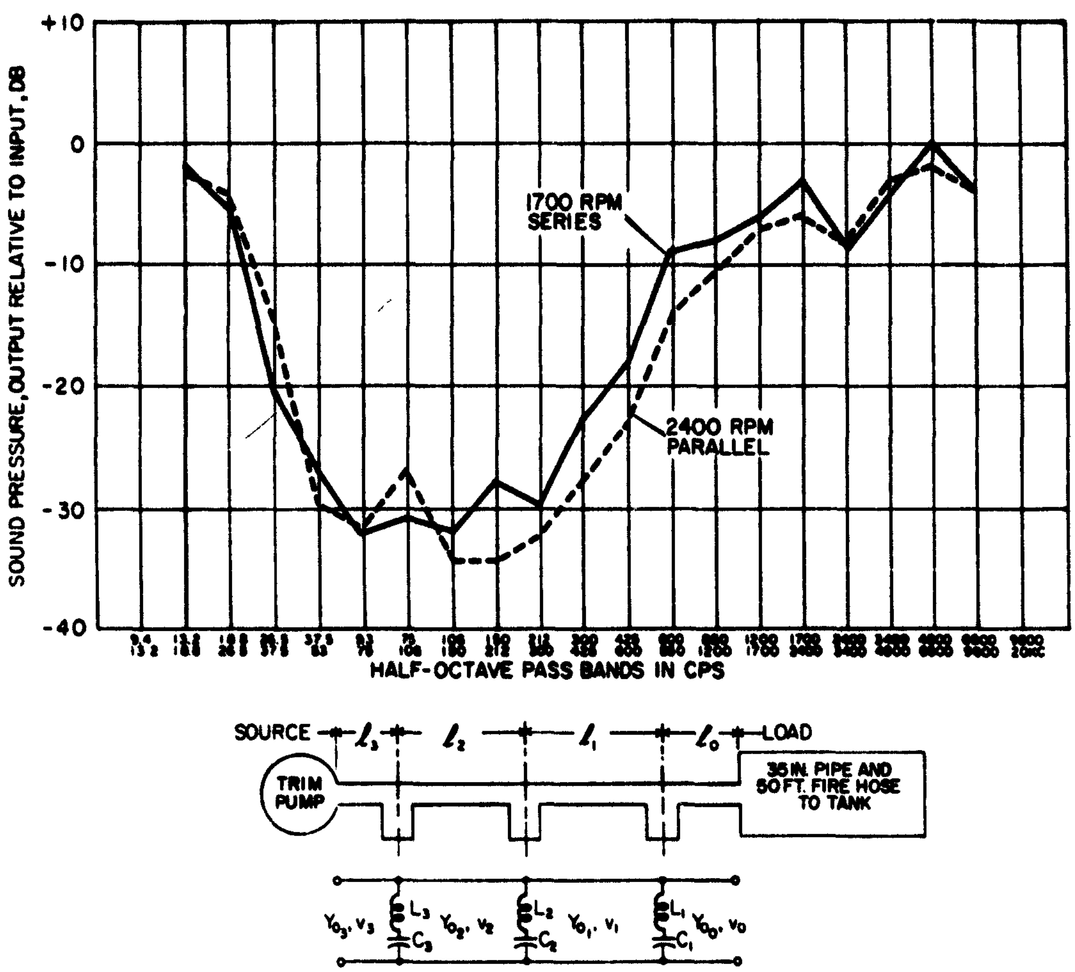

Y_{0_0} = 1.32	v_0 = 3964	L_1 = 2.37×10^{-8}	C_1 = 9.5×10^{-2}	ℓ_0 = 10 IN
Y_{0_1} = 1.32	v_1 = 3964	L_2 = 4.50×10^{-8}	C_2 = 15.4×10^{-2}	ℓ_1 = 85 IN
Y_{0_2} = 1.32	v_2 = 3964	L_3 = 8.72×10^{-8}	C_3 = 14.4×10^{-2}	ℓ_2 = 51 IN
Y_{0_3} = 1.32	v_3 = 3964			ℓ_3 = 51 IN

FIGURE 125
THREE ELEMENT SIDE-BRANCH FILTER
WITH METAL BELLOWS BRANCH ELEMENTS

DRL - UT
DWG AS7061
JVK - MJM
10-16-62

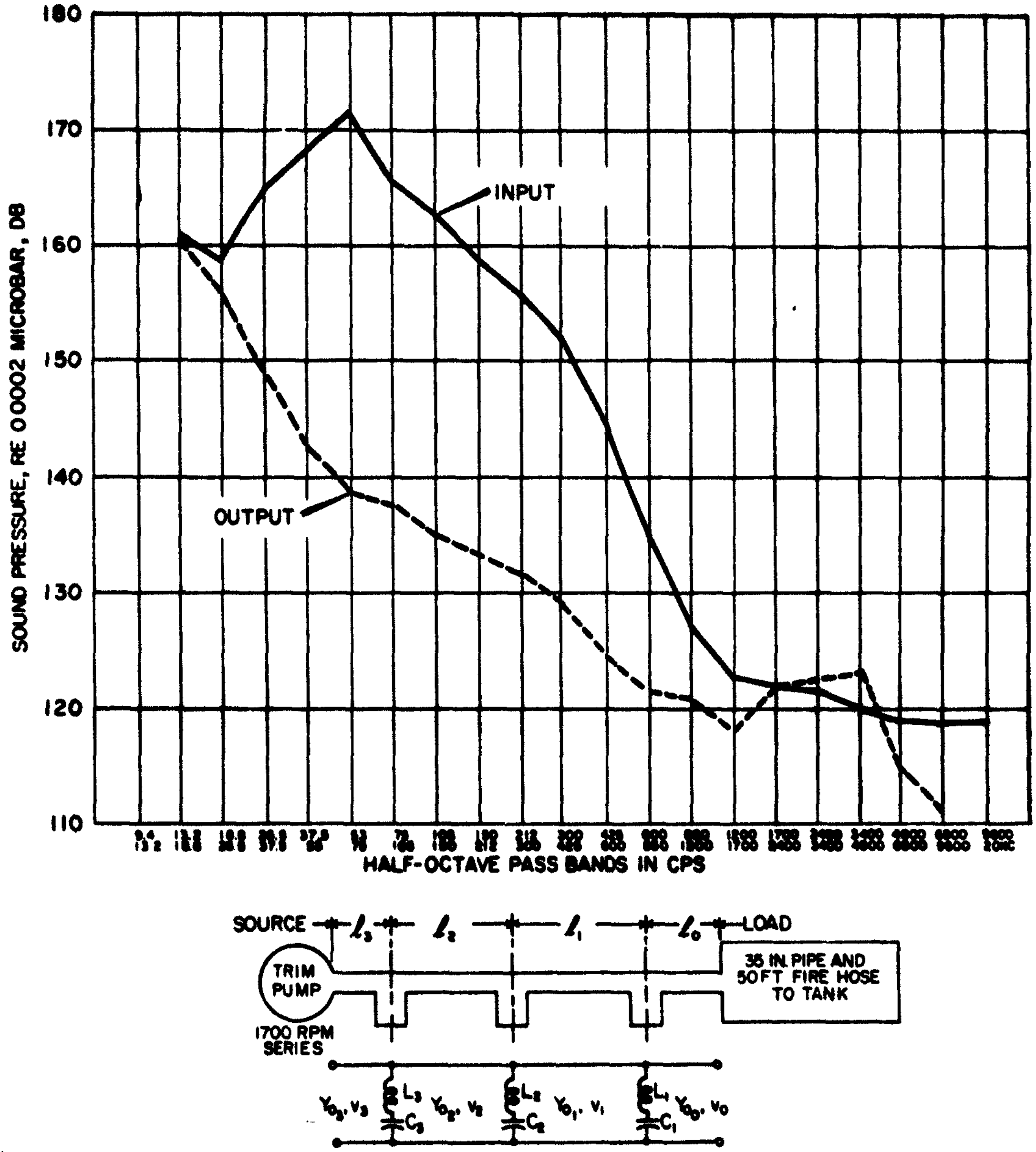

Y_{0_0} = 1.32	v_0 = 3964	L_1 = 2.37 × 10^{-8}	C_1 = 9.5 × 10^{-2}	ℓ_0 = 9.5 IN.
Y_{0_1} = 1.32	v_1 = 3964	L_2 = 4.5 × 10^{-8}	C_2 = 15.4 × 10^{-2}	ℓ_1 = 84.5 IN.
Y_{0_2} = 1.32	v_2 = 3964	L_3 = 8.72 × 10^{-8}	C_3 = 14.4 × 10^{-2}	ℓ_2 = 50.75 IN.
Y_{0_3} = 1.32	v_3 = 3964			ℓ_3 = 50.75 IN.

FIGURE 126

THREE ELEMENT SIDE-BRANCH FILTER WITH METAL BELLOWS BRANCH ELEMENT

DRL - UT
DWG AS7053
JVK · MJM
10·30·62

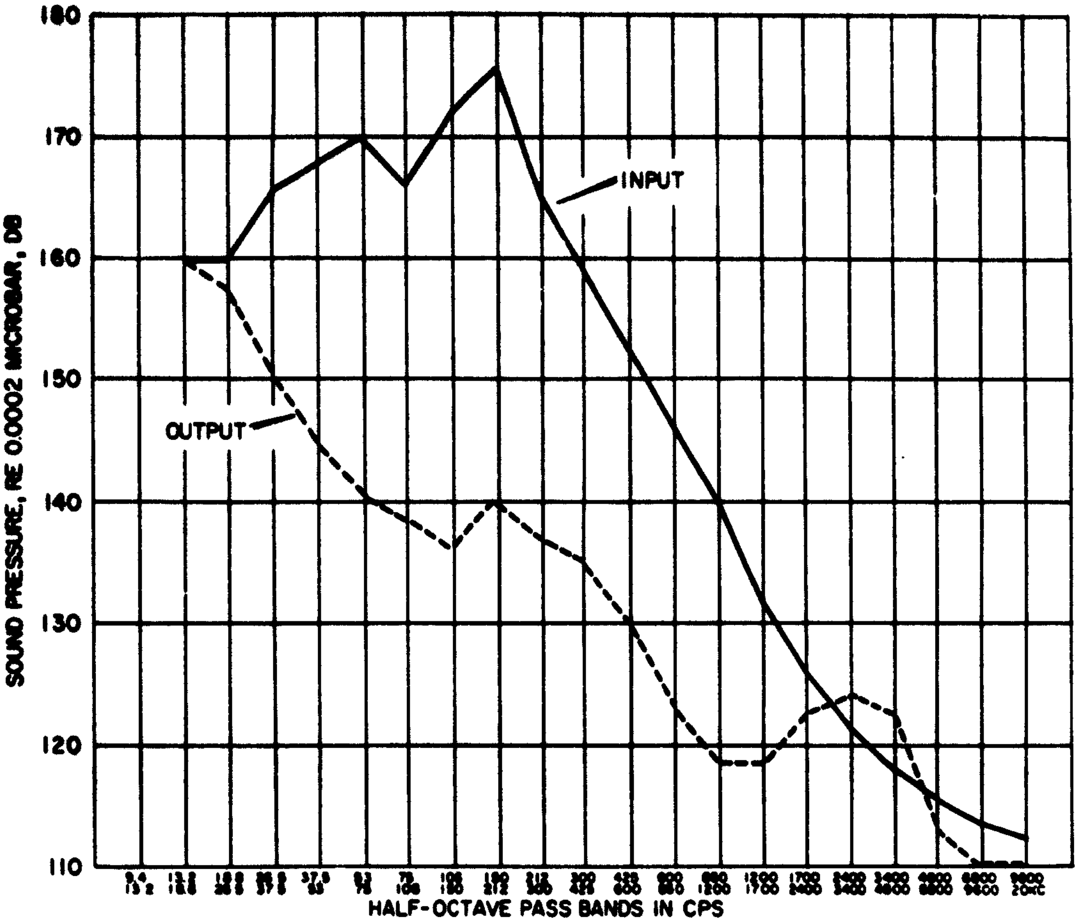

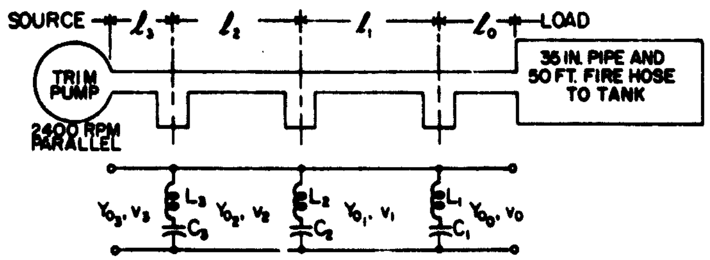

Y_{o_0} = 1.32	v_0 = 3964	L_1 = 2.37×10^{-6}	C_1 = 9.5×10^{-2}	ℓ_0 = 10 IN.
Y_{o_1} = 1.32	v_1 = 3964	L_2 = 4.5×10^{-6}	C_2 = 15.4×10^{-2}	ℓ_1 = 85 IN.
Y_{o_2} = 1.32	v_2 = 3964	L_3 = 8.72×10^{-6}	C_3 = 14.4×10^{-2}	ℓ_2 = 51 IN.
Y_{o_3} = 1.32	v_3 = 3964			ℓ_3 = 51 IN

FIGURE 127

THREE ELEMENT SIDE-BRANCH FILTER
WITH METAL BELLOWS BRANCH ELEMENT

DRL - UT
DWG AS7064
JVK - MJM
10-30-62

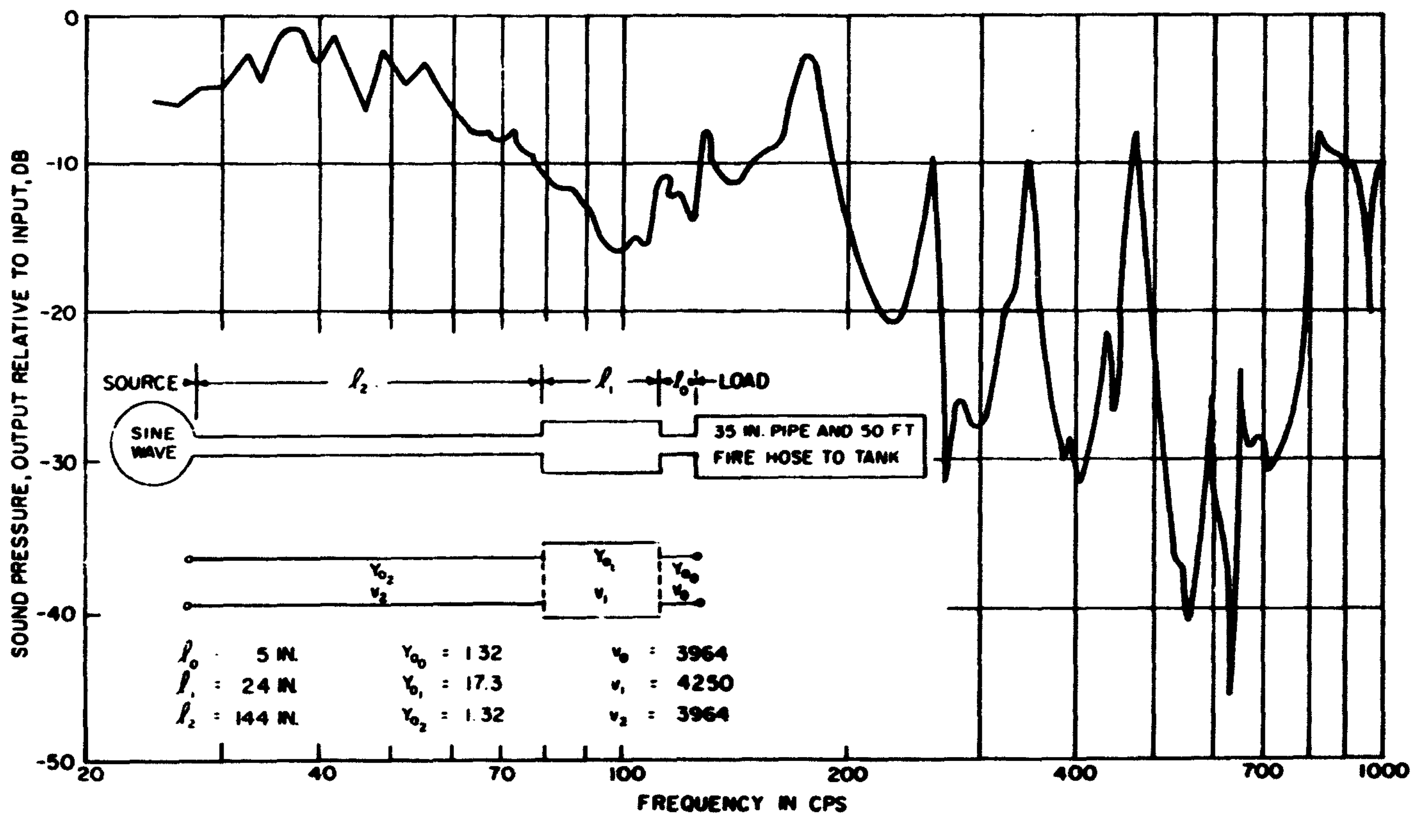

FIGURE 128
SINGLE CHAMBER EXPANSION CHAMBER FILTER

DRL - UT
DWG AS 7055
JVK - BEE
11 - 16 - 62

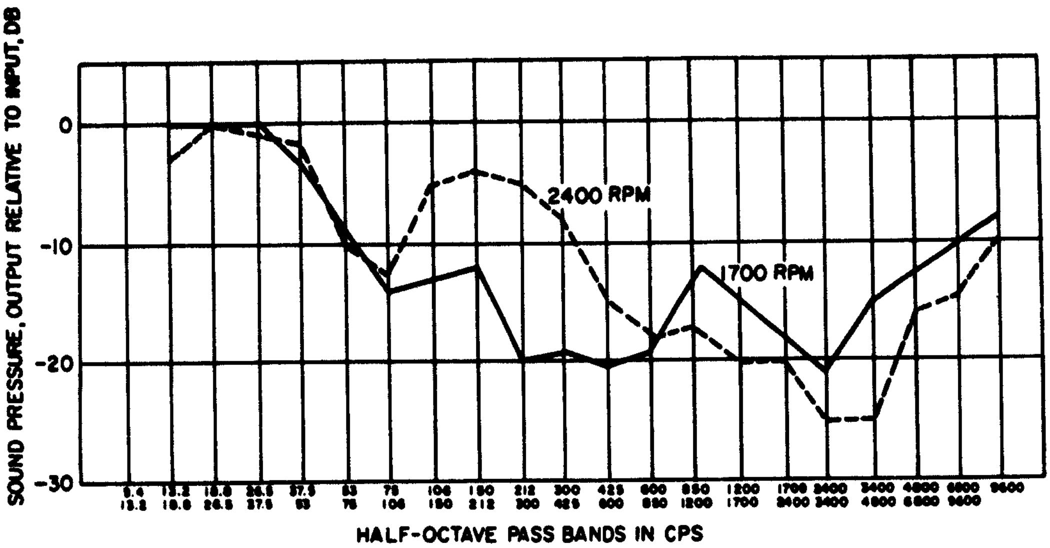

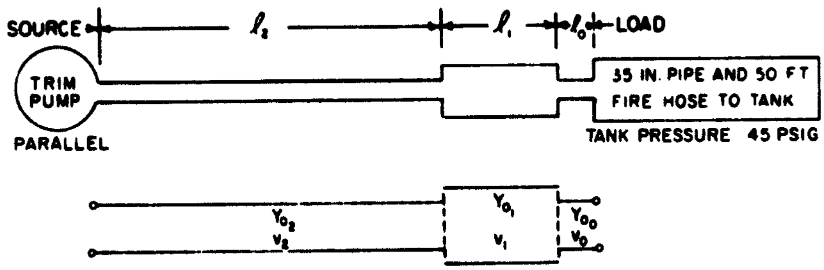

ℓ_0	:	5 IN.	Y_{0_0}	:	1.32	v_0	:	3964
ℓ_1	:	24 IN.	Y_{0_1}	:	17.3	v_1	:	4250
ℓ_2	:	144 IN.	Y_{0_2}	:	1.32	v_2	:	3964

FIGURE 129
SINGLE CHAMBER EXPANSION CHAMBER FILTER

DRL – UT
DWG AS 7059
JVK – BEE
11 - 16 - 62

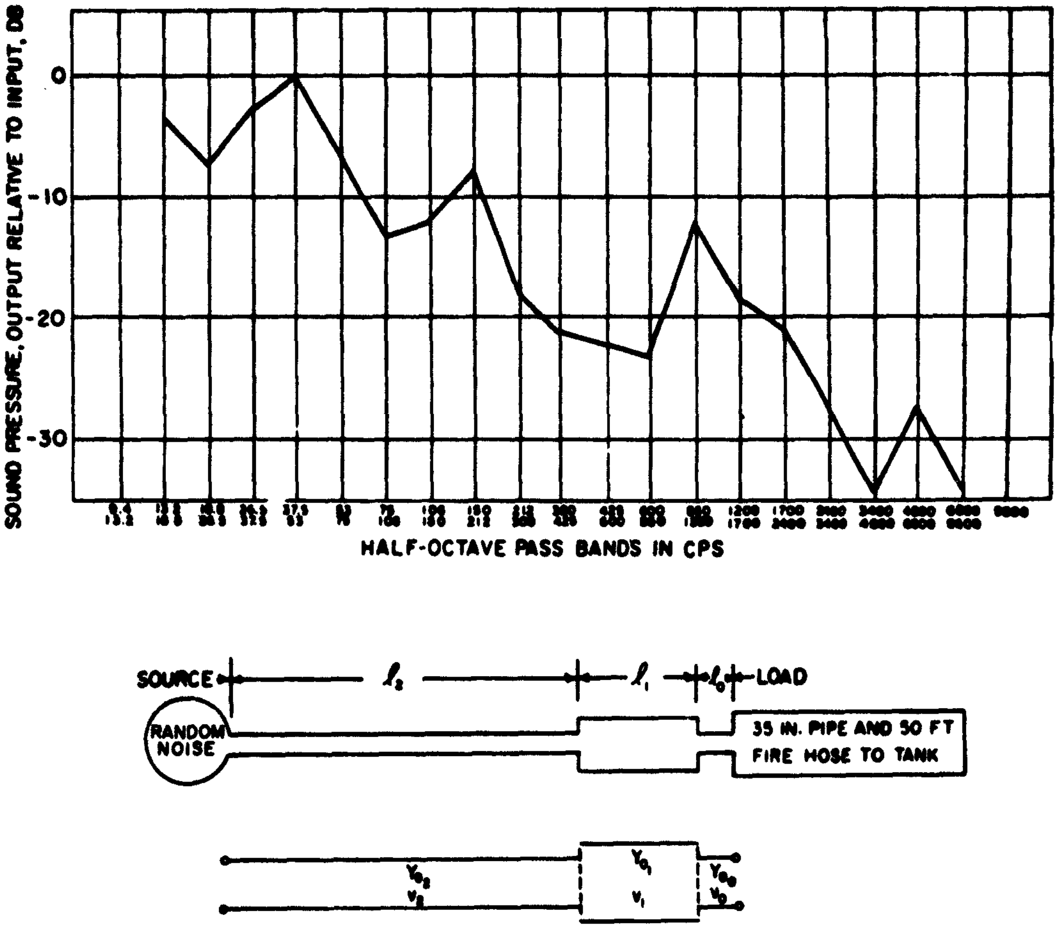

l_0 : 5 IN. $\quad Y_{0_0}$ = 1.32 $\quad v_0$ = 3964

l_1 = 24 IN. $\quad Y_{0_1}$ = 17.3 $\quad v_1$ = 4250

l_2 = 144 IN. $\quad Y_{0_2}$ = 1.32 $\quad v_2$ = 3964

FIGURE 130
SINGLE CHAMBER EXPANSION CHAMBER FILTER

DRL - UT
DWG AS 7060
JVK - BEE
11 - 16 - 62

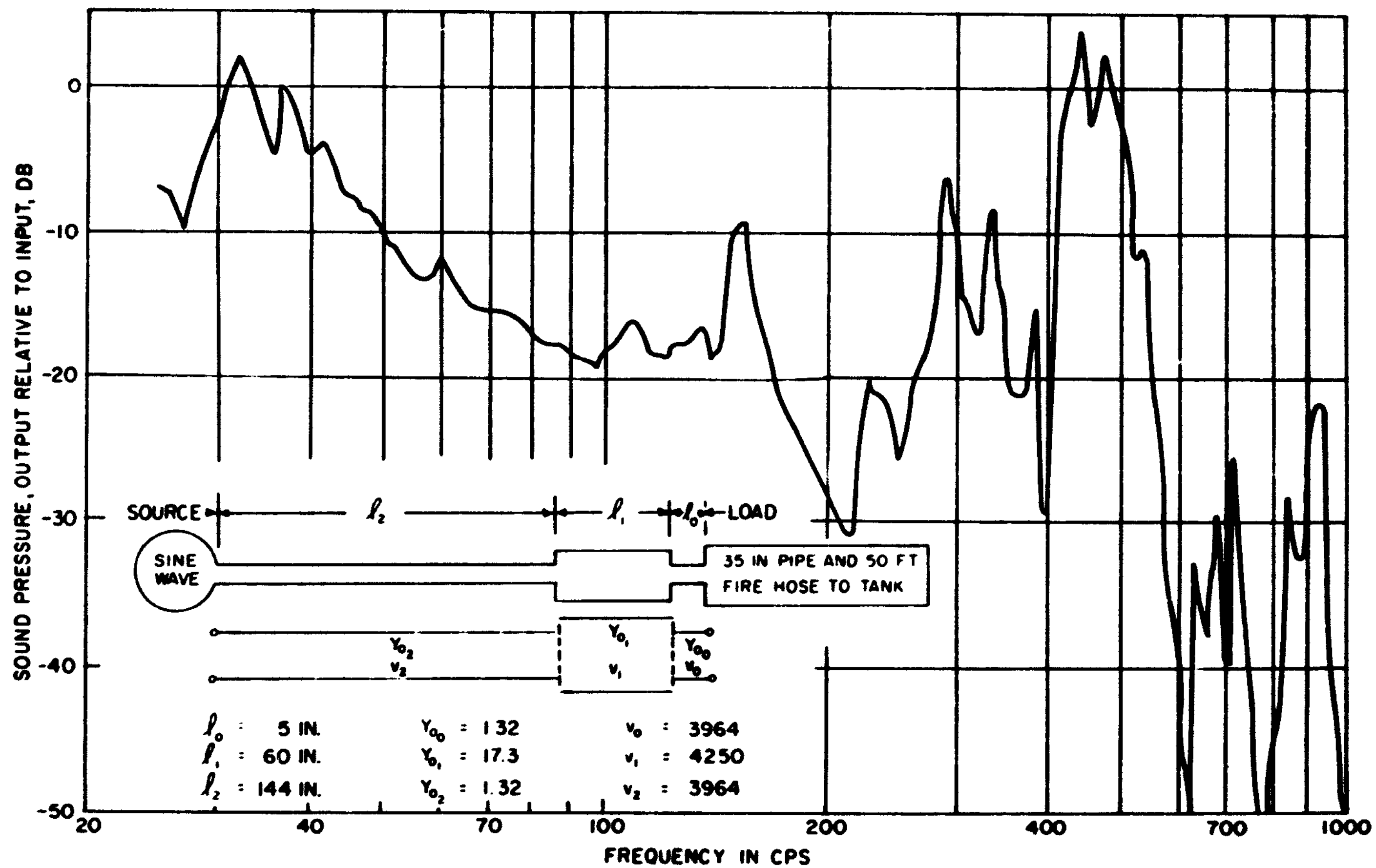

FIGURE 131
SINGLE CHAMBER EXPANSION CHAMBER FILTER

DRL - UT
DWG AS 7056
JVK - BEE
11 - 20 - 62

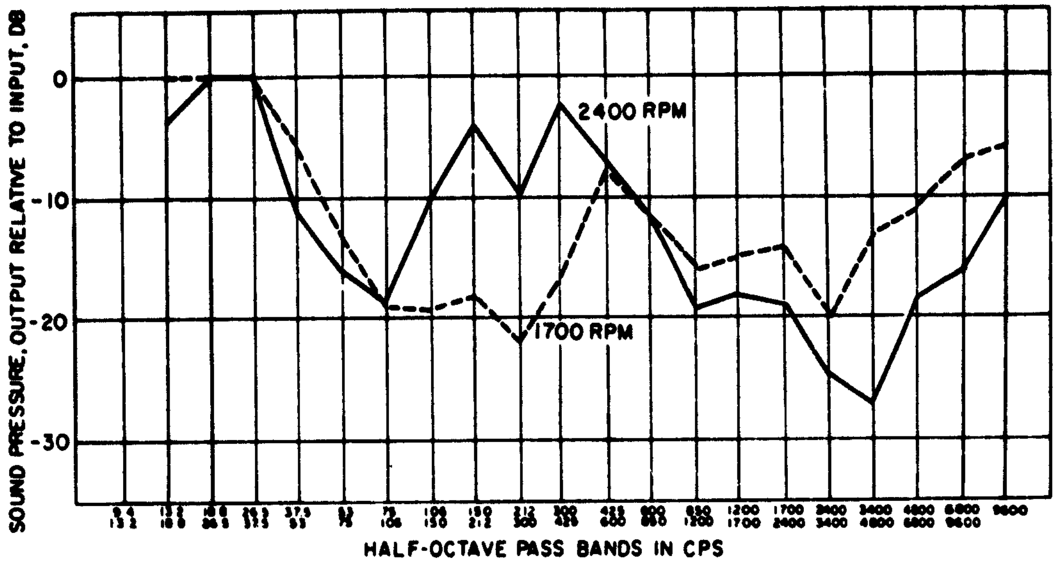

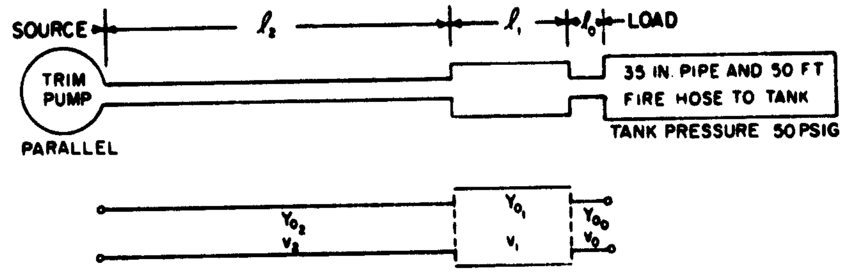

ℓ_0 : 5 IN.	Y_{0_0} : 1.32	v_0 : 3964
ℓ_1 : 60 IN.	Y_{0_1} : 17.3	v_1 : 4250
ℓ_2 : 144 IN.	Y_{0_2} : 1.32	v_2 : 3964

FIGURE 132
SINGLE CHAMBER EXPANSION CHAMBER FILTER

DRL - UT
DWG AS 7064
JVK - BEE
11 - 16 - 62

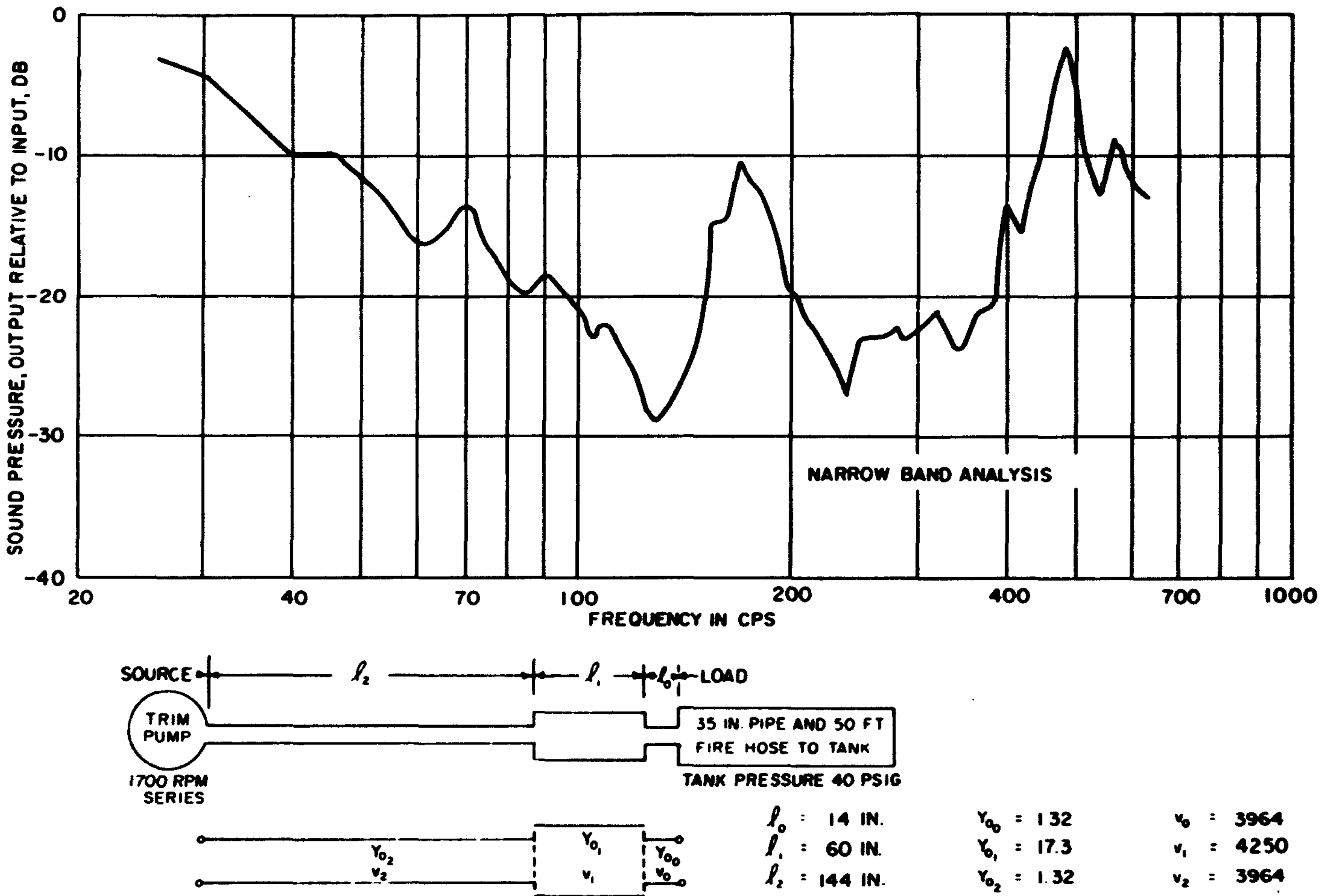

FIGURE 133
SINGLE CHAMBER EXPANSION CHAMBER FILTER

DRL - UT
DWG AS 7069
JVK - BEE
11 - 28 - 62

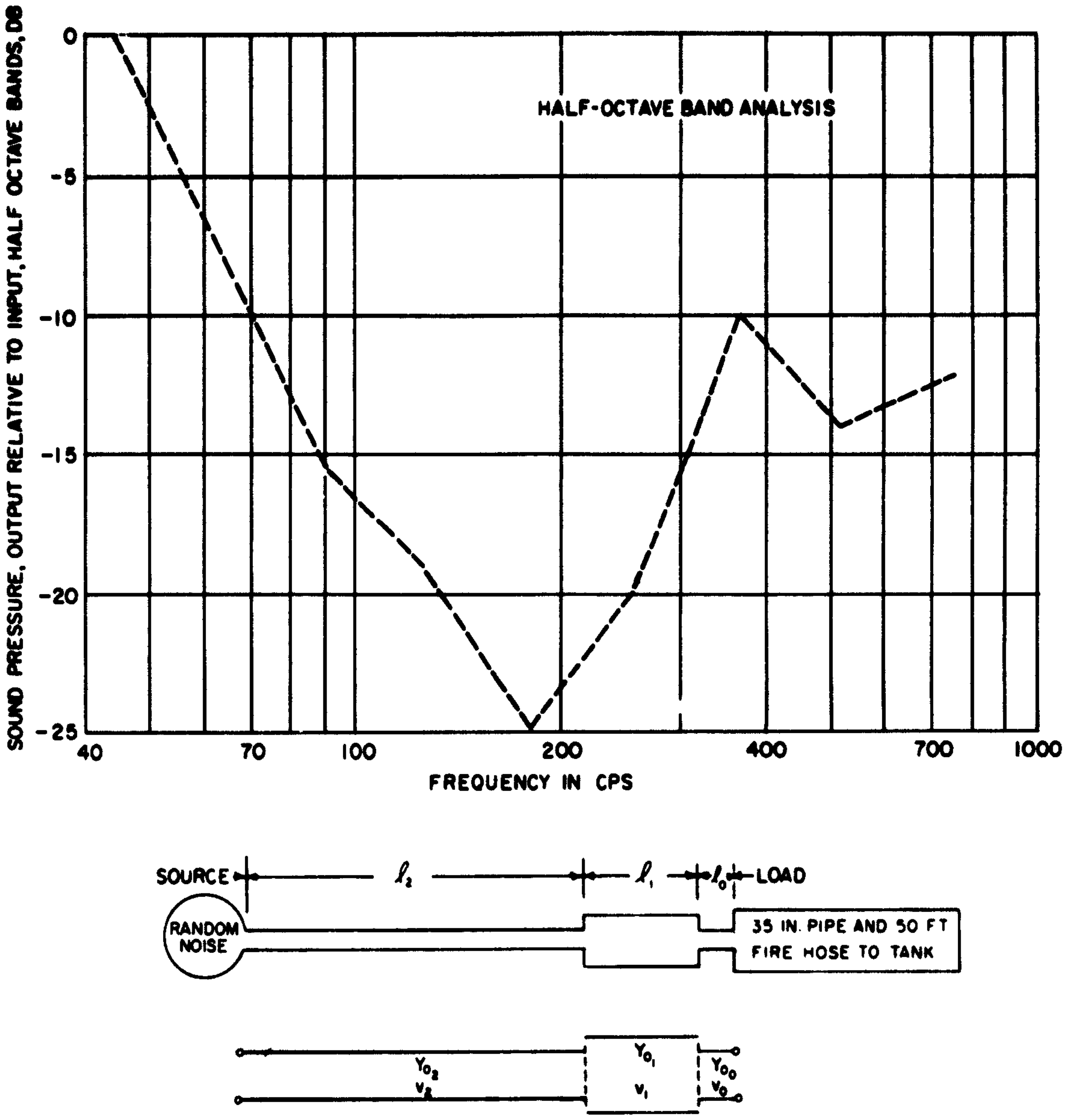

l_0 : 12 IN. $\quad Y_{0_0}$: 1.32 $\quad v_0$: 3964

l_1 : 60 IN. $\quad Y_{0_1}$: 17.3 $\quad v_1$: 4250

l_2 : 46 IN. $\quad Y_{0_2}$: 1.32 $\quad v_2$: 3964

FIGURE 134
SINGLE CHAMBER EXPANSION CHAMBER FILTER

DRL - UT
DWG AS 7070
JVK - BEE
11 - 26 - 62

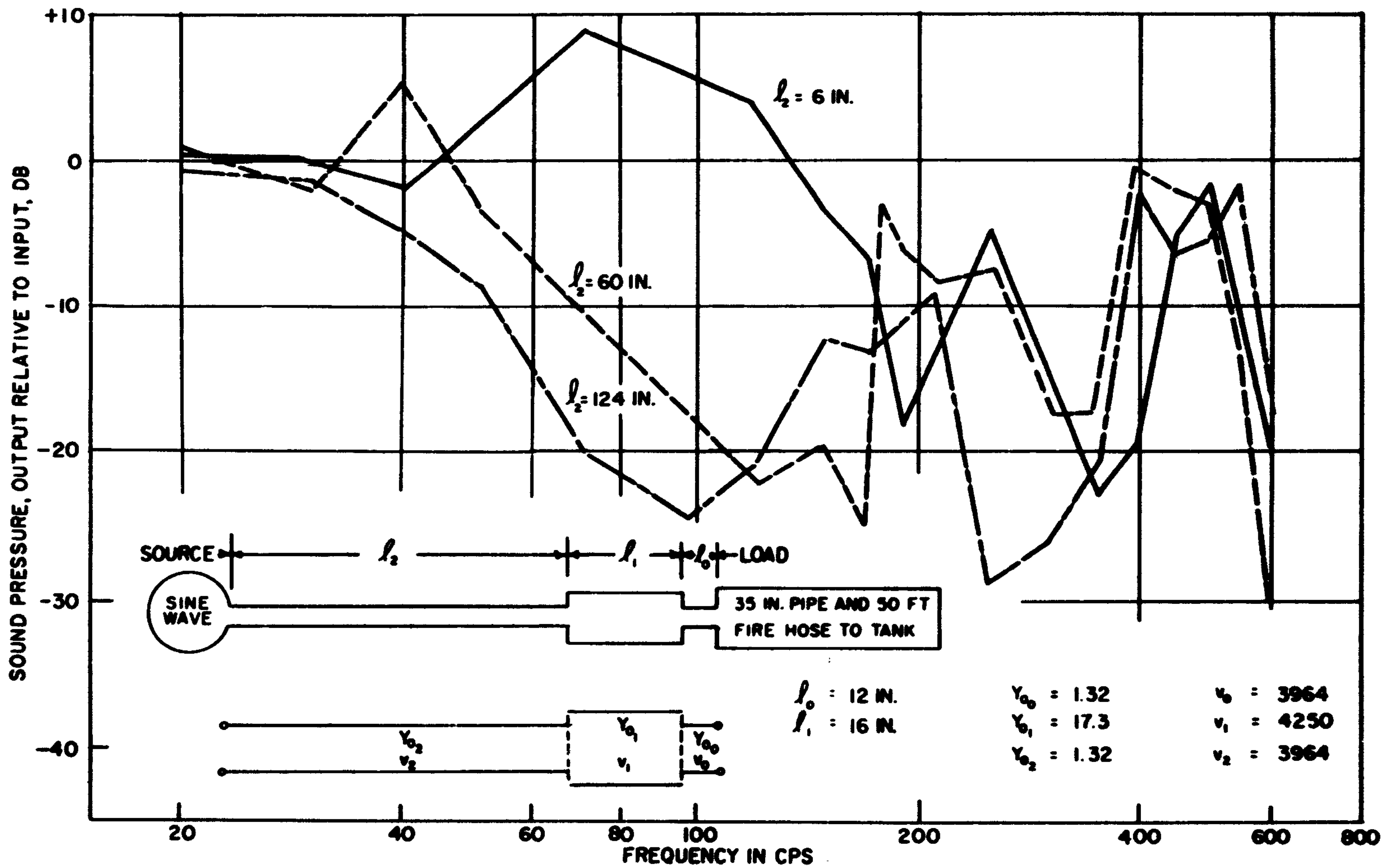

DRL - UT
DWG AS 7071
JVK - BEE
11 - 28 - 62

FIGURE 135
SINGLE CHAMBER EXPANSION CHAMBER FILTER

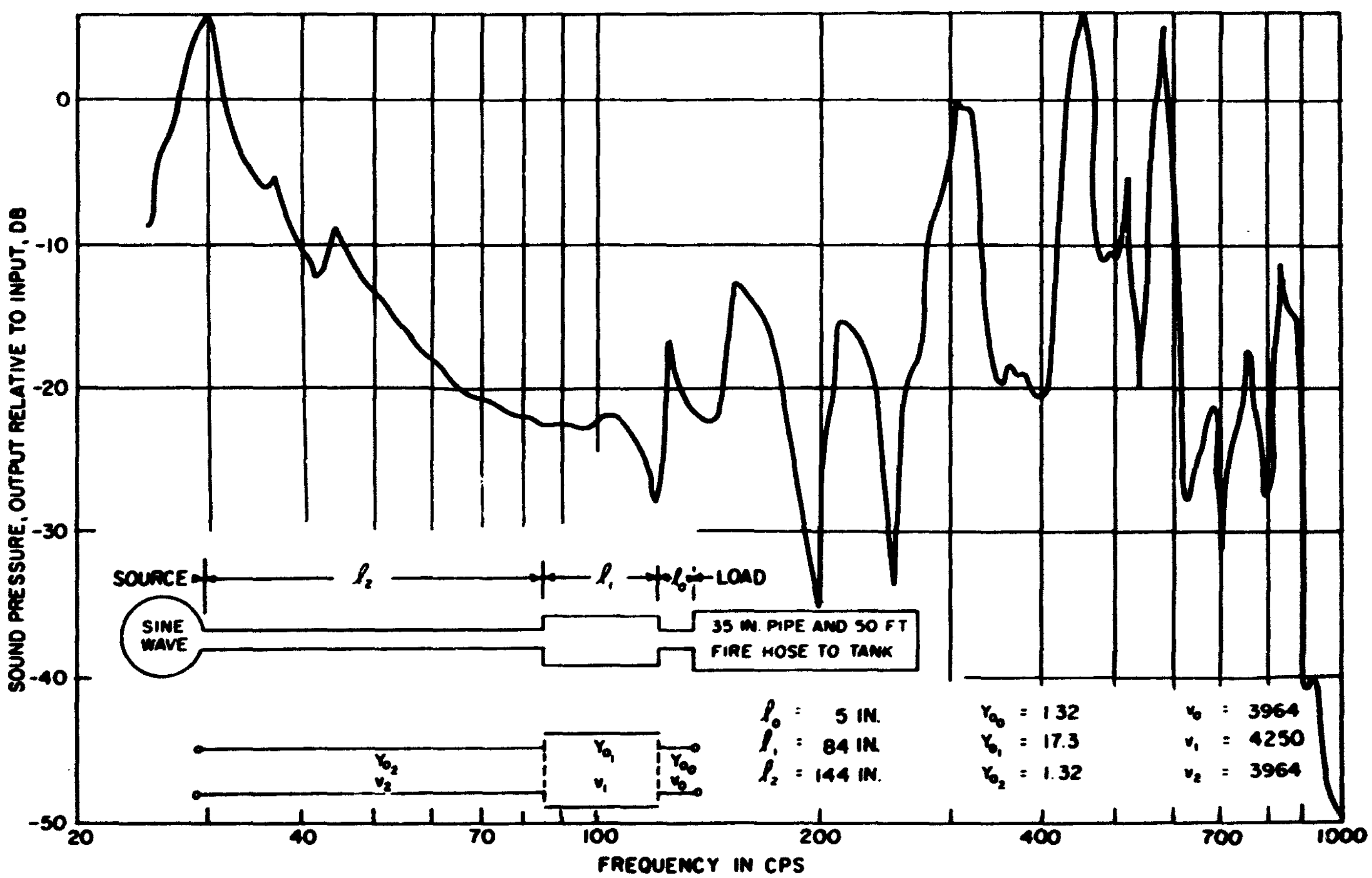

FIGURE 136
SINGLE CHAMBER EXPANSION CHAMBER FILTER

DRL - UT
DWG AS 7057
JVK - BEE
11 - 20 - 62

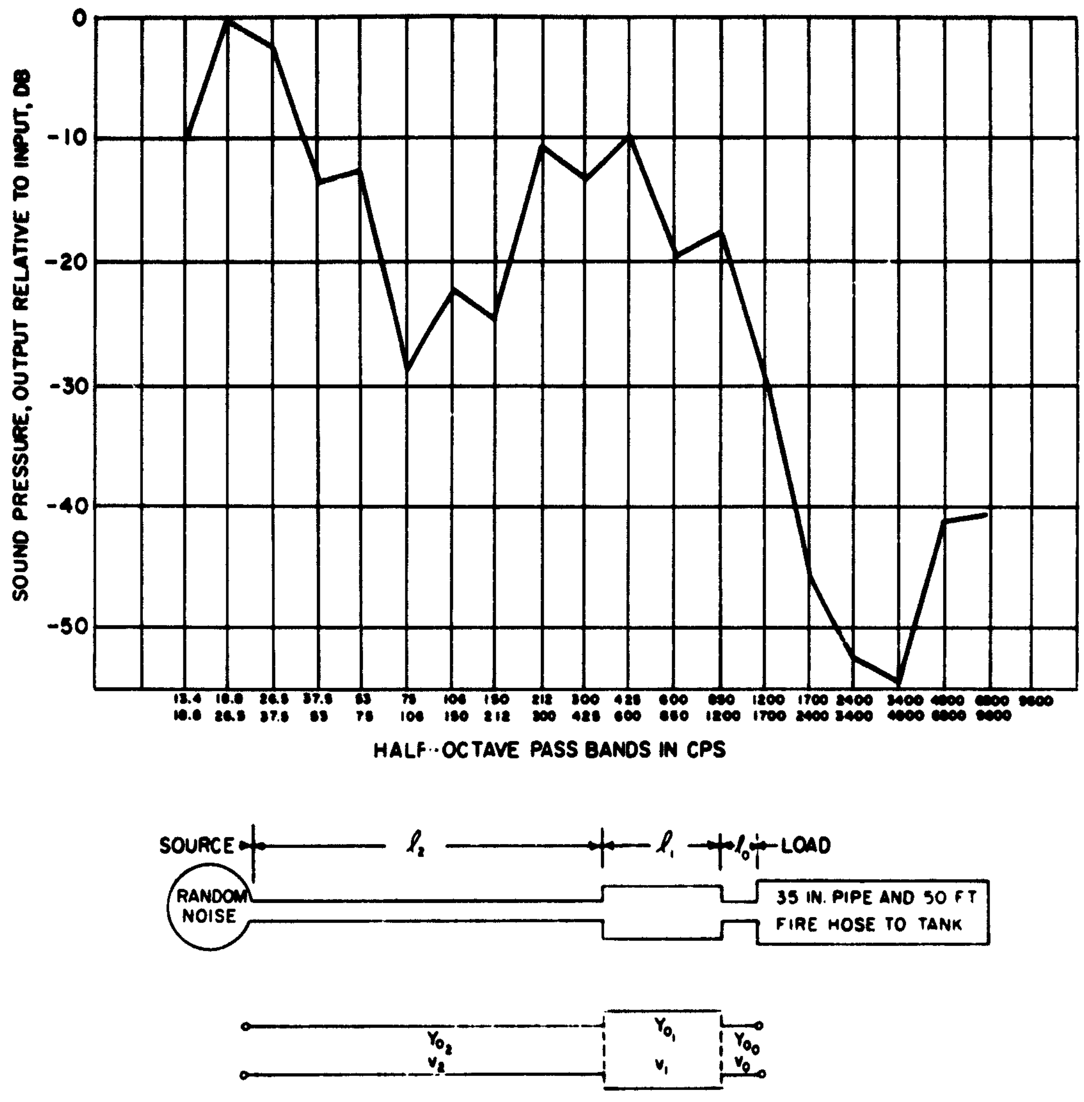

ℓ_0 : 5 IN.	Y_{0_0} : 1 32	v_0 : 3964
ℓ_1 : 84 IN.	Y_{0_1} : 17 3	v_1 : 4250
ℓ_2 : 144 IN.	Y_{0_2} : 1 32	v_2 : 3964

FIGURE 137
SINGLE CHAMBER EXPANSION CHAMBER FILTER

DRL - UT
DWG AS 7063
JVK - BEE
11 - 26 - 62

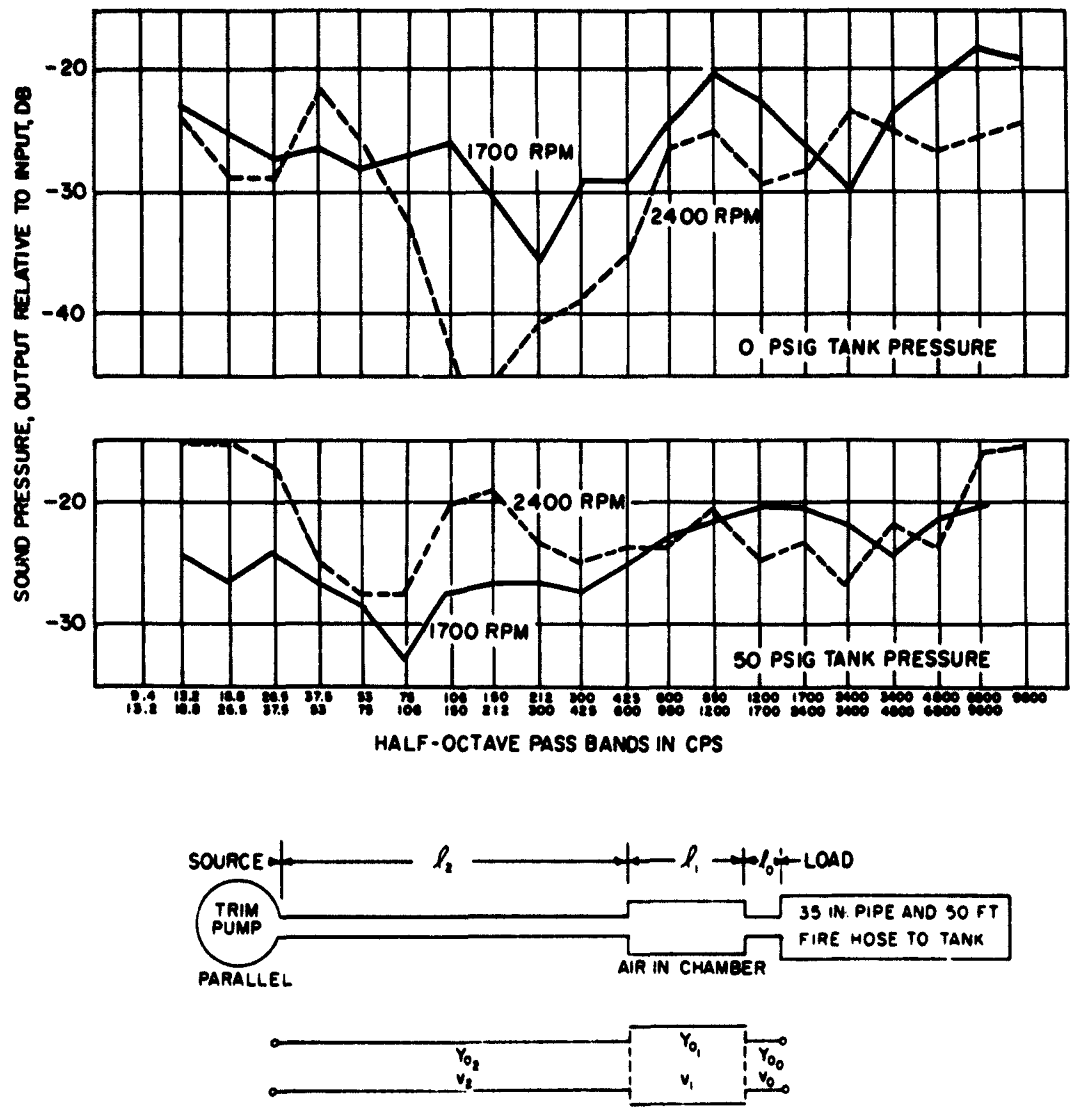

l_0 : 5 IN. Y_{0_0} : 1.32 v_0 : 3964

l_1 : 84 IN. Y_{0_1} : 17.3 v_1 : 4250

l_2 : 144 IN. Y_{0_2} : 1.32 v_2 : 3964

FIGURE 138
SINGLE CHAMBER EXPANSION CHAMBER FILTER

DRL - UT
DWG AS 7068
JVK - BEE
11 - 16 - 62

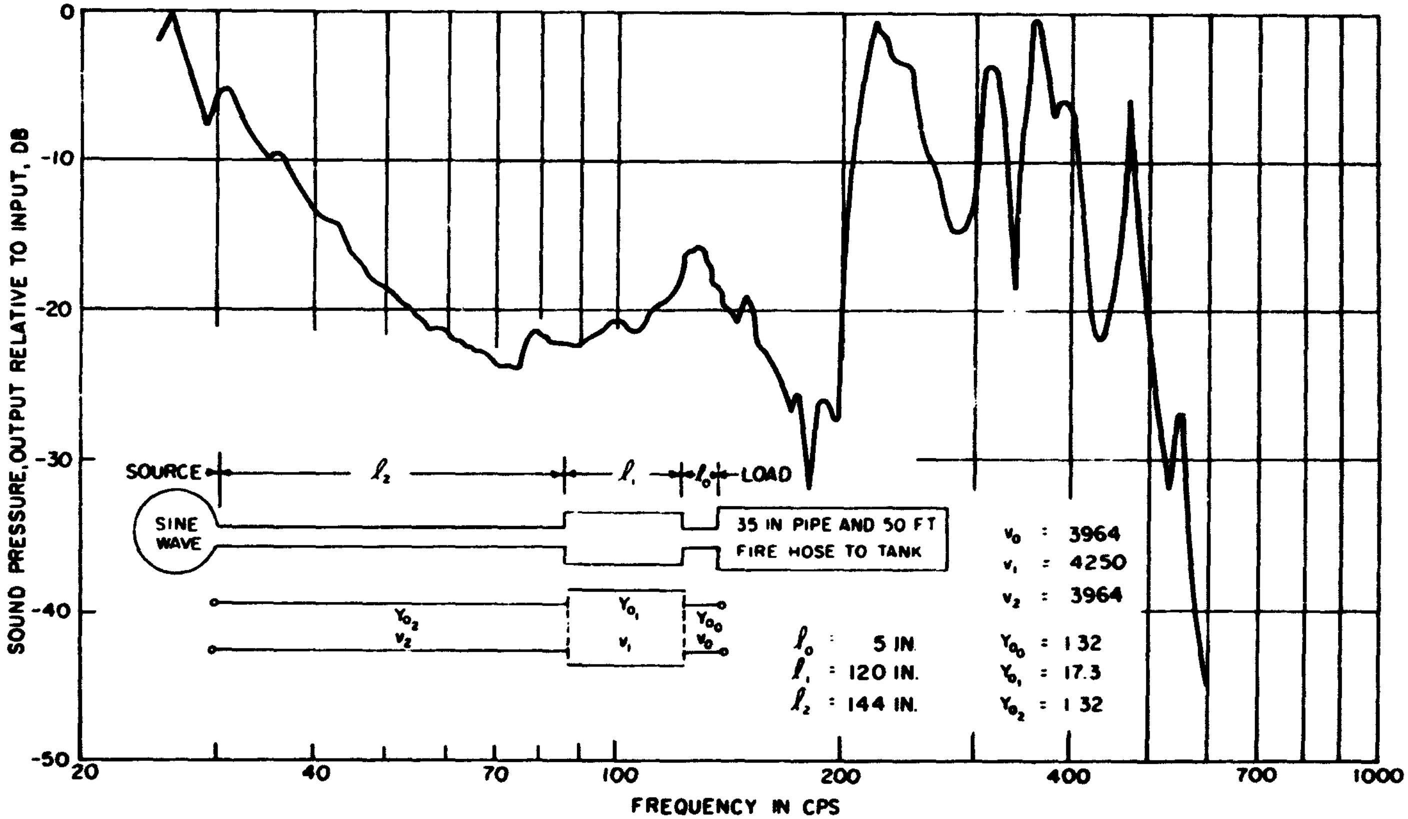

FIGURE 139
SINGLE CHAMBER EXPANSION CHAMBER FILTER

DRL - UT
DWG AS7058
JVK - BEE
11 - 16 - 62

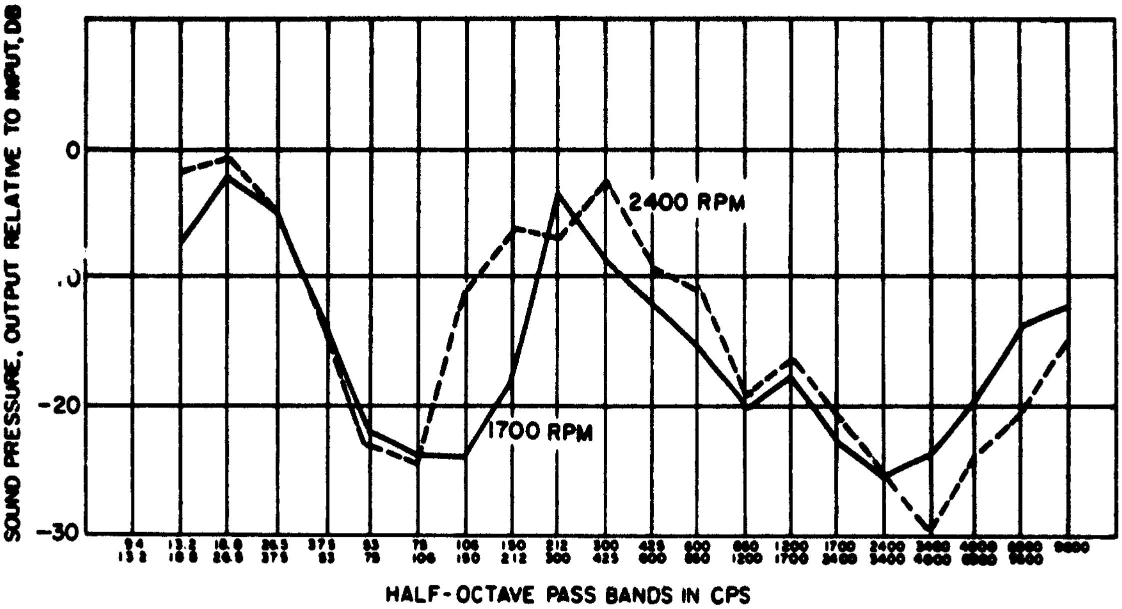

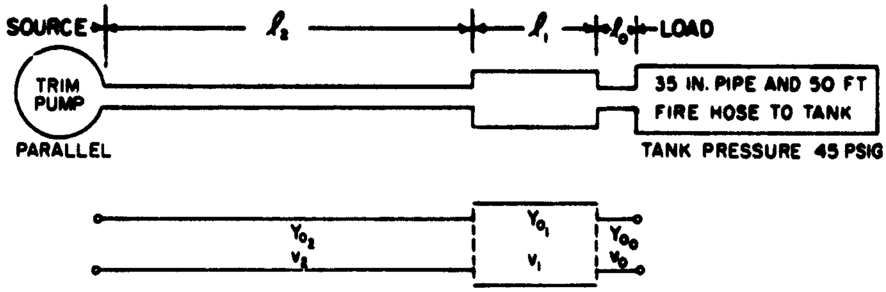

l_0 : 5 IN.	Y_{O_0} : 1.32	v_0 : 3964
l_1 : 120 IN.	Y_{O_1} : 17.3	v_1 : 4250
l_2 : 144 IN.	Y_{O_2} : 1.32	v_2 : 3964

FIGURE 140
SINGLE CHAMBER EXPANSION CHAMBER FILTER

DRL - UT
DWG AS 7061
JVK - BEE
11 - 15 - 62

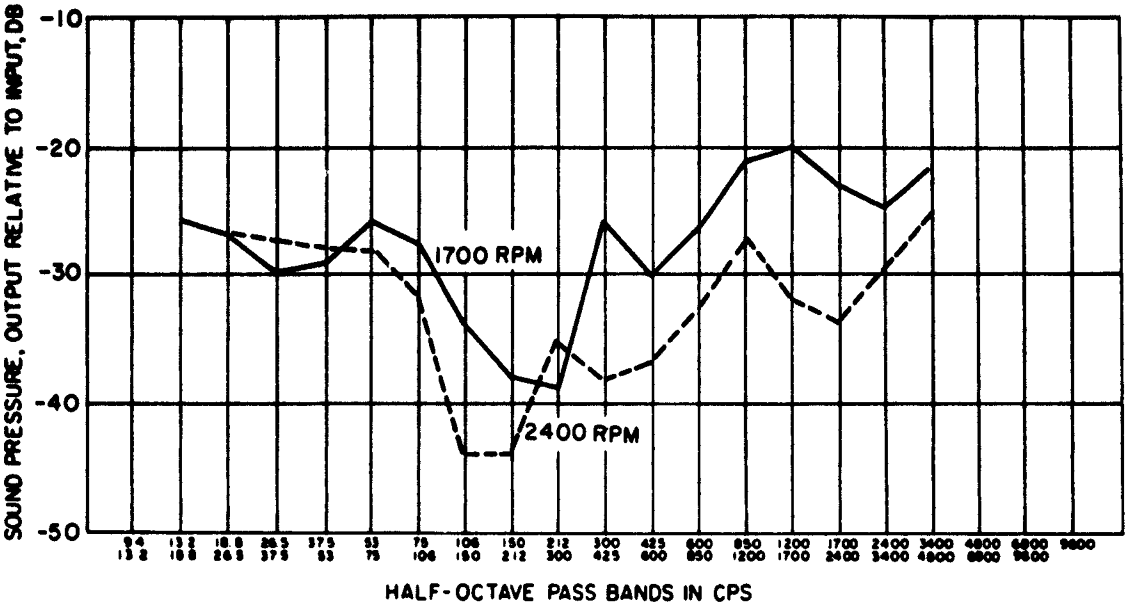

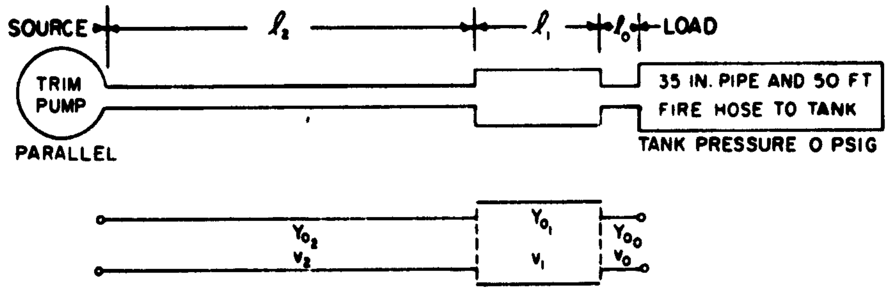

ℓ_0 : 5 IN.	Y_{0_0} : 1.32	v_0 : 3964
ℓ_1 : 120 IN.	Y_{0_1} : 17.3	v_1 : 4250
ℓ_2 : 144 IN.	Y_{0_2} : 1.32	v_2 : 3964

FIGURE 141
SINGLE CHAMBER EXPANSION CHAMBER FILTER

DRL - UT
DWG AS 7067
JVK - BEE
11 - 15 - 62

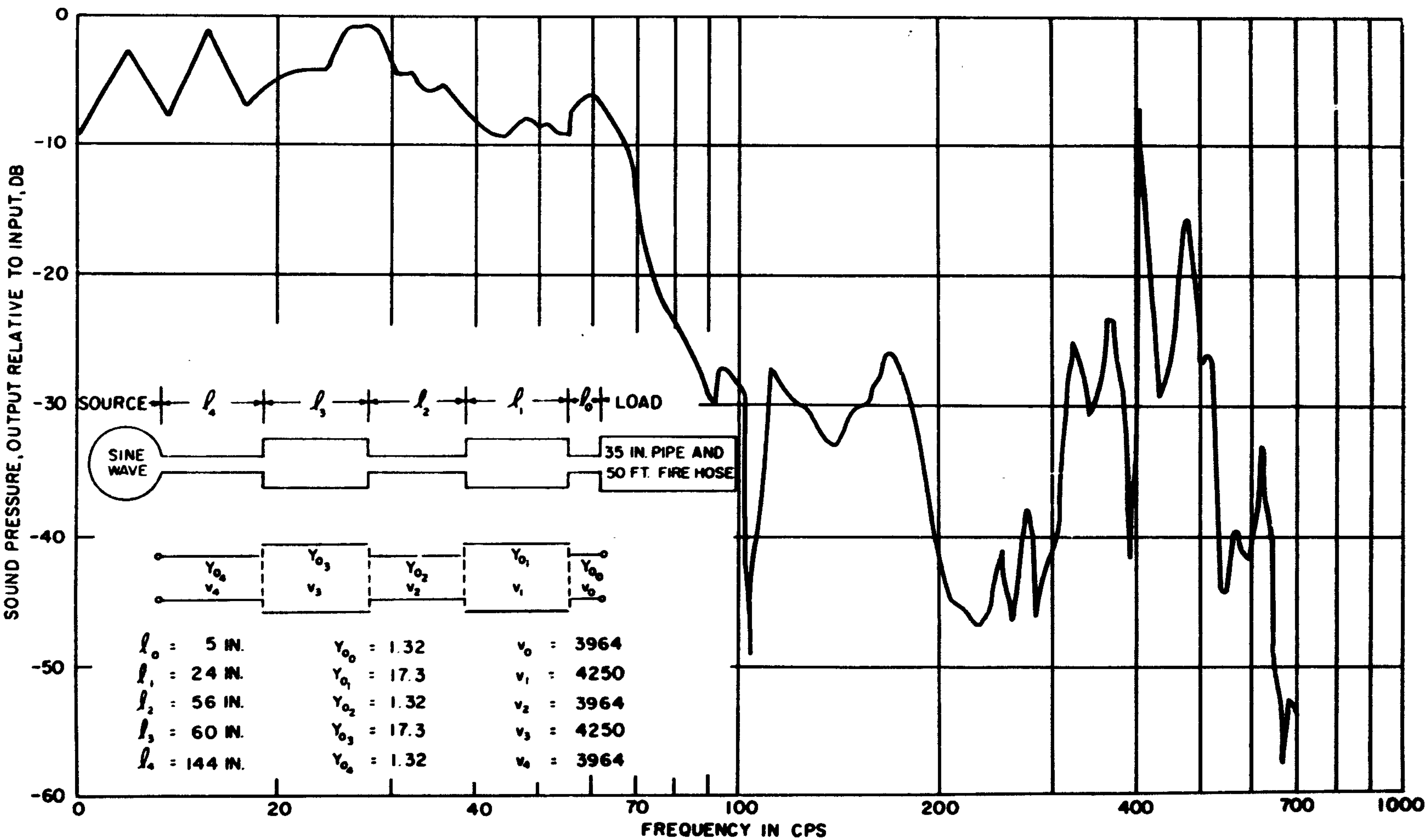

FIGURE 142
TWO CHAMBER EXPANSION CHAMBER FILTER

DRL - UT
DWG AS 7079
JVK - BEE
11 - 28 - 62

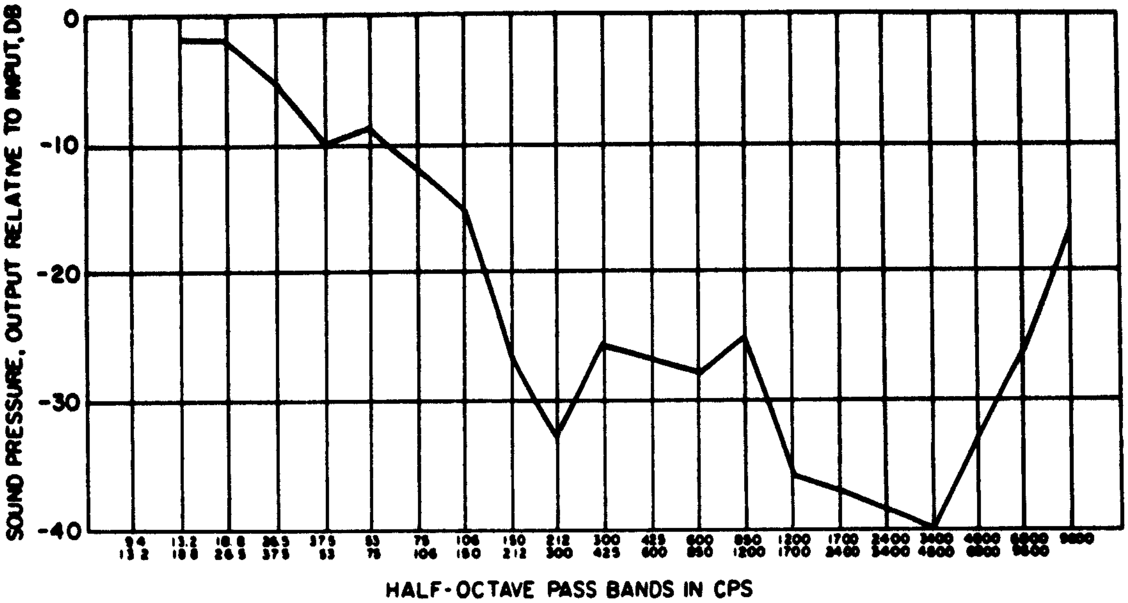

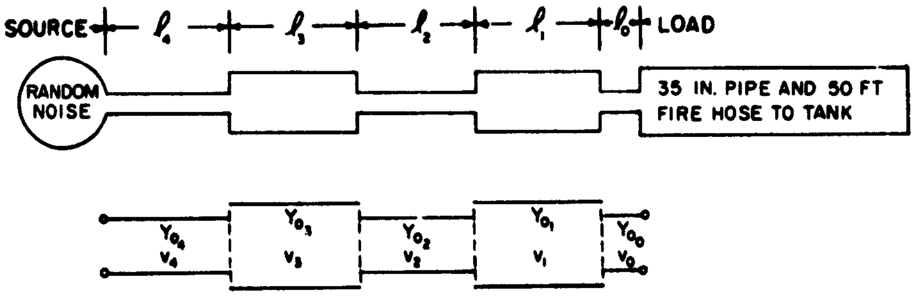

ℓ_0 : 5 IN.	Y_{0_0} : 1.32	v_0 : 3964
ℓ_1 : 24 IN.	Y_{0_1} : 17.3	v_1 : 4250
ℓ_2 : 56 IN.	Y_{0_2} : 1.32	v_2 : 3964
ℓ_3 : 60 IN.	Y_{0_3} : 17.3	v_3 : 4250
ℓ_4 : 3 IN.	Y_{0_4} : 1.32	v_4 : 3964

FIGURE 143
TWO CHAMBER EXPANSION CHAMBER FILTER

DRL - UT
DWG AS 7083
JVK - BEE
11 - 15 - 62

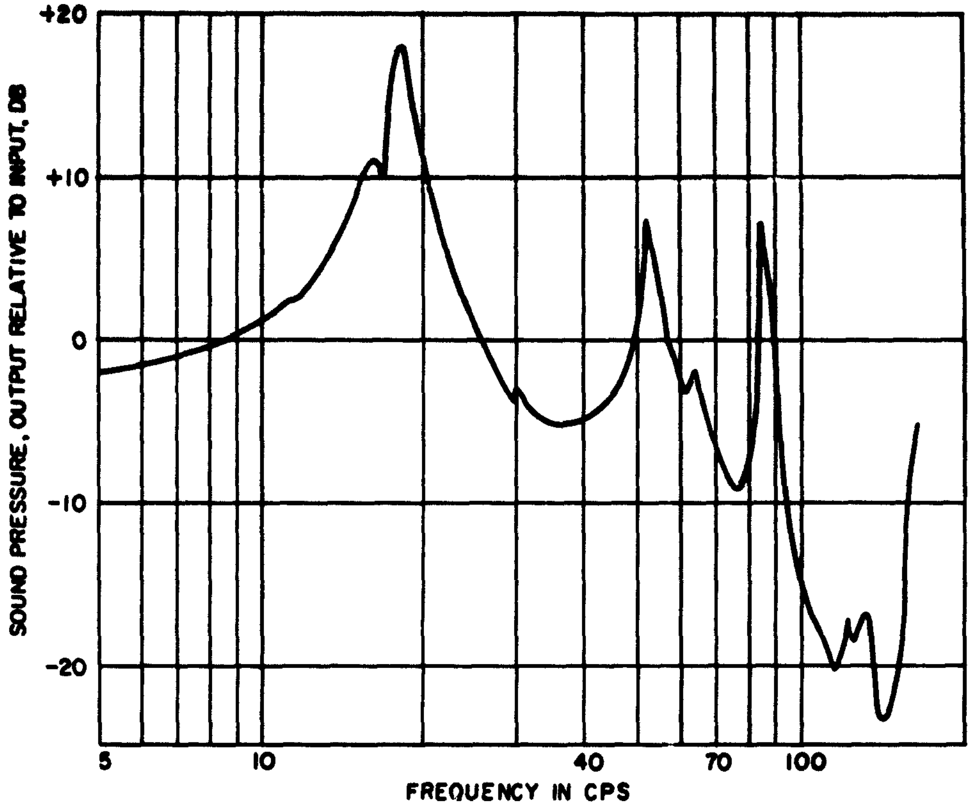

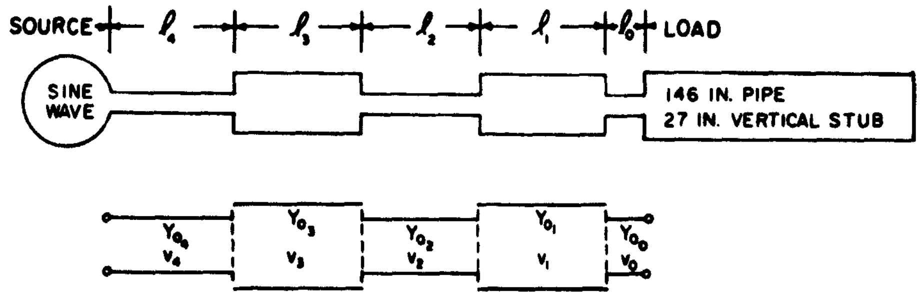

ℓ_0 : 3 IN.	Y_{0_0} : 1.32	v_0 : 3964
ℓ_1 : 60 IN.	Y_{0_1} : 17.3	v_1 : 4250
ℓ_2 : 60 IN.	Y_{0_2} : 1.32	v_2 : 3964
ℓ_3 : 60 IN.	Y_{0_3} : 17.3	v_3 : 4250
ℓ_4 : 3 IN.	Y_{0_4} : 1.32	v_4 : 3964

FIGURE 144
TWO CHAMBER EXPANSION CHAMBER FILTER

DRL - UT
DWG AS 7074
JVK - BEE
11 - 27 - 62

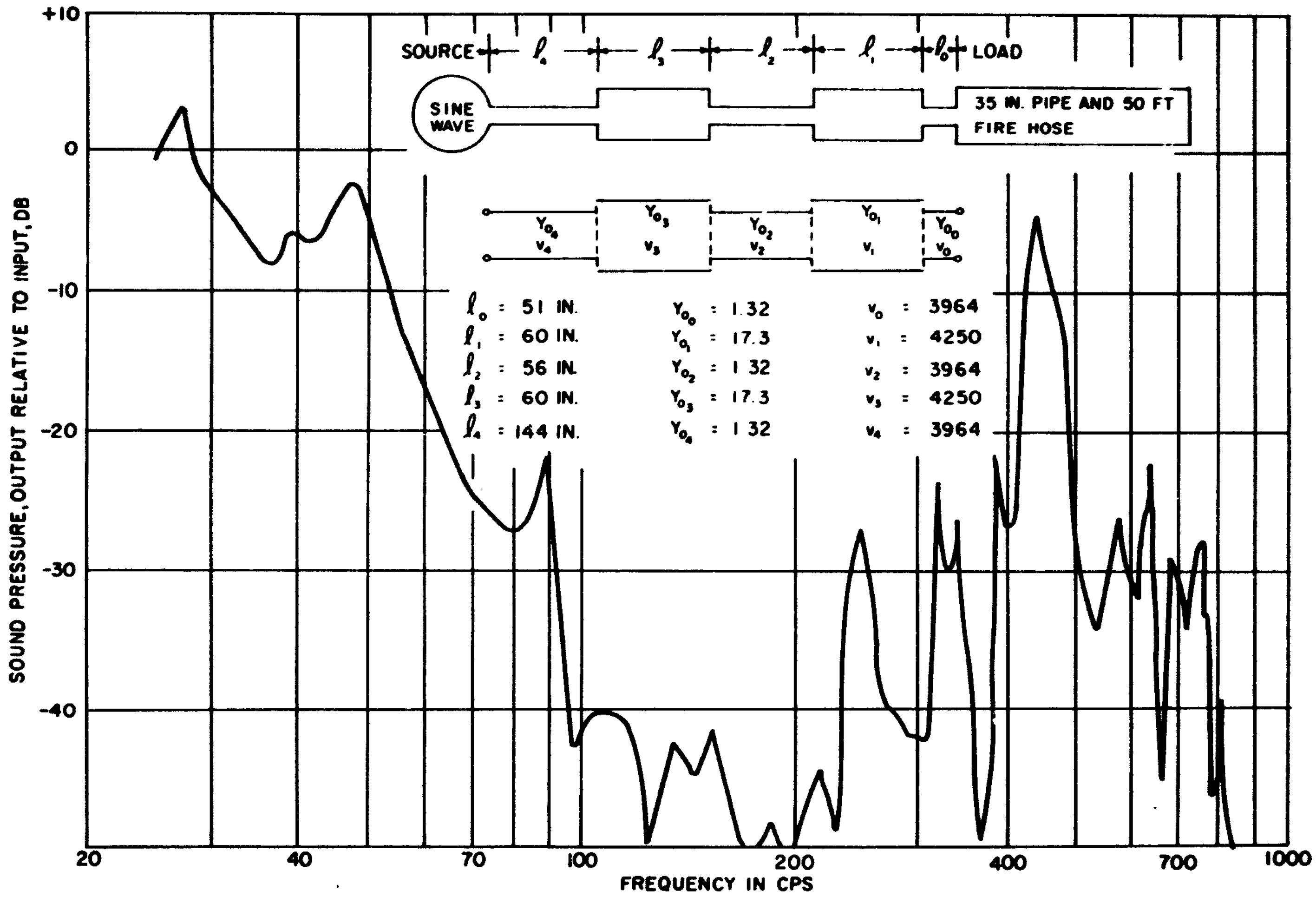

FIGURE 145
TWO CHAMBER EXPANSION CHAMBER FILTER

DRL - UT
DWG AS 7078
JVK - BEE
11 - 27 - 62

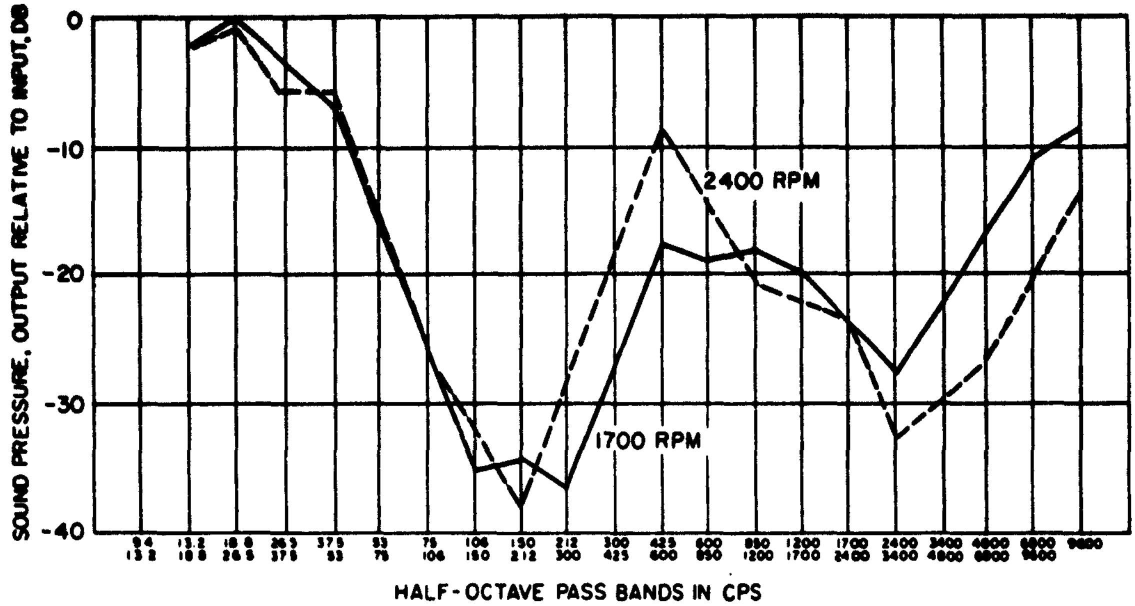

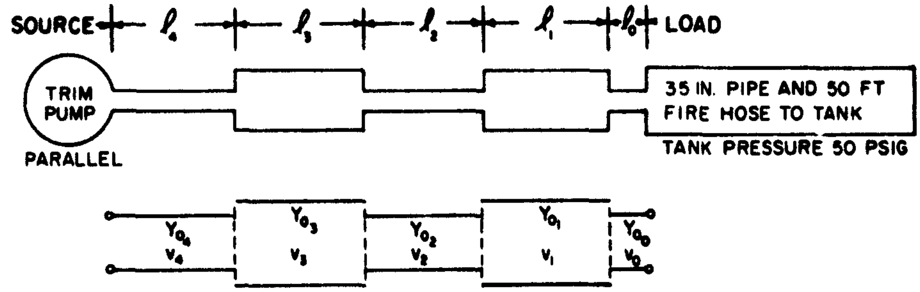

ℓ_0 : 5 IN.	Y_{0_0} : 1.32	v_0 : 3964
ℓ_1 : 60 IN.	Y_{0_1} : 17.3	v_1 : 4250
ℓ_2 : 56 IN.	Y_{0_2} : 1.32	v_2 : 3964
ℓ_3 : 60 IN.	Y_{0_3} : 17.3	v_3 : 4250
ℓ_4 : 144 IN.	Y_{0_4} : 1.32	v_4 : 3964

FIGURE 146
TWO CHAMBER EXPANSION CHAMBER FILTER

DRL - UT
DWG AS 7081
JVK - BEE
11 - 15 - 62

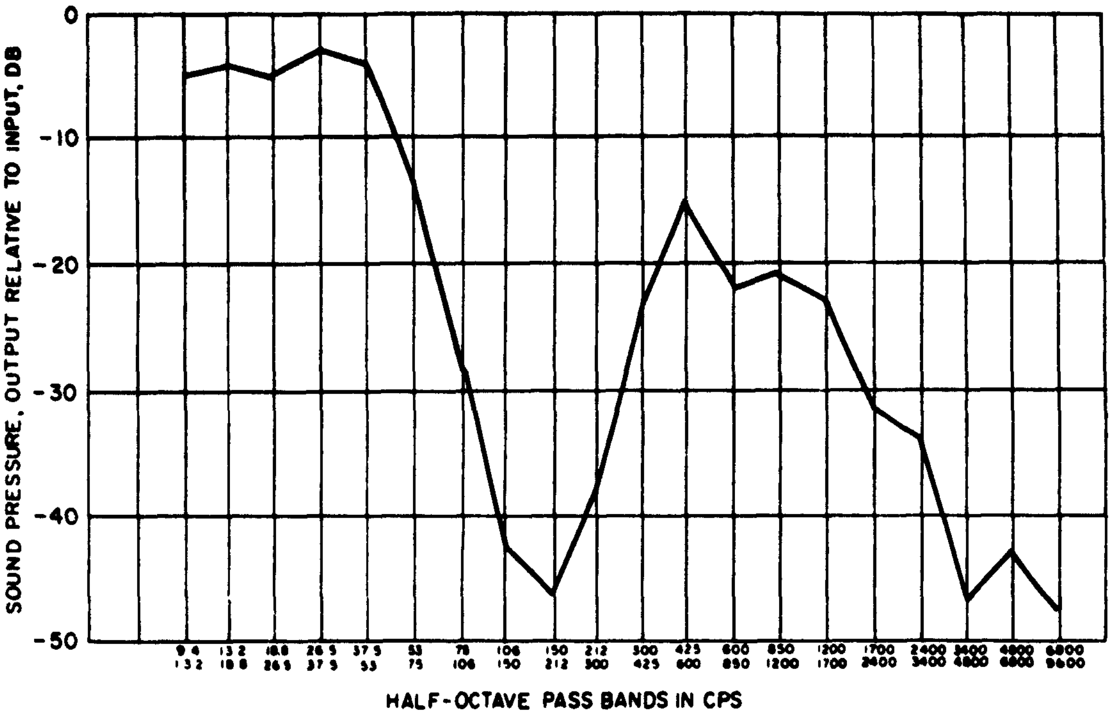

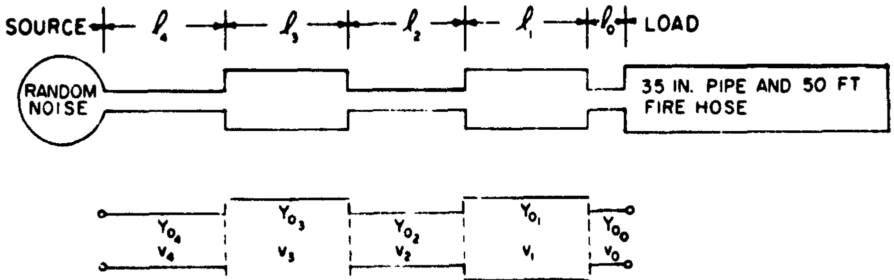

ℓ_0 : 5 IN.	Y_{0_0} : 1.32	v_0 : 3964
ℓ_1 : 60 IN.	Y_{0_1} : 17.3	v_1 : 4250
ℓ_2 : 56 IN.	Y_{0_2} : 1.32	v_2 : 3964
ℓ_3 : 60 IN.	Y_{0_3} : 17.3	v_3 : 4250
ℓ_4 : 144 IN.	Y_{0_4} : 1.32	v_4 : 3964

FIGURE 147
TWO CHAMBER EXPANSION CHAMBER FILTER

DRL - UT
DWG AS 7082
JVK - BEE
11 - 16 - 62

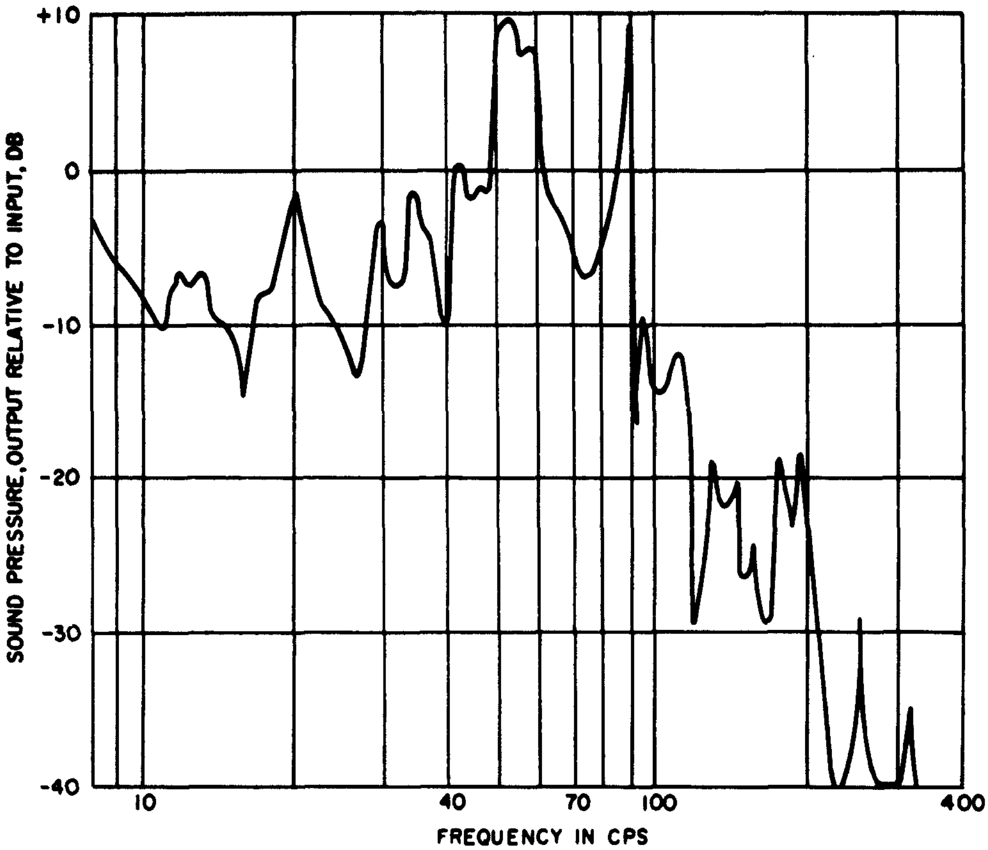

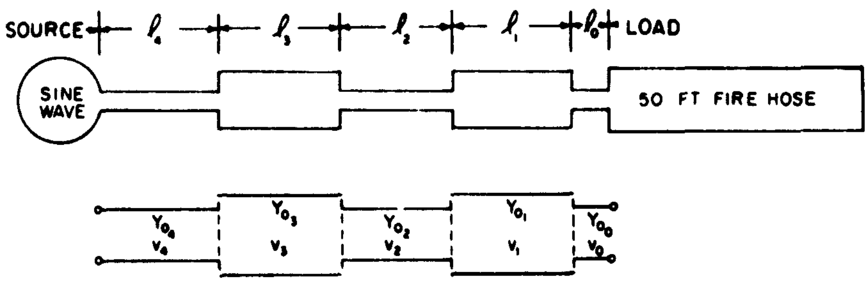

ℓ_0	: 3 IN.	Y_{0_0}	: 1.32	v_0	: 3964
ℓ_1	: 60 IN.	Y_{0_1}	: 17.3	v_1	: 4250
ℓ_2	: 60 IN.	Y_{0_2}	: 1.32	v_2	: 3964
ℓ_3	: 84 IN.	Y_{0_3}	: 17.3	v_3	: 4250
ℓ_4	: 3 IN.	Y_{0_4}	: 1.32	v_4	: 3964

FIGURE 148
TWO CHAMBER EXPANSION CHAMBER FILTER

DRL - UT
DWG AS 7075
JVK - BEE
11 - 27 - 62

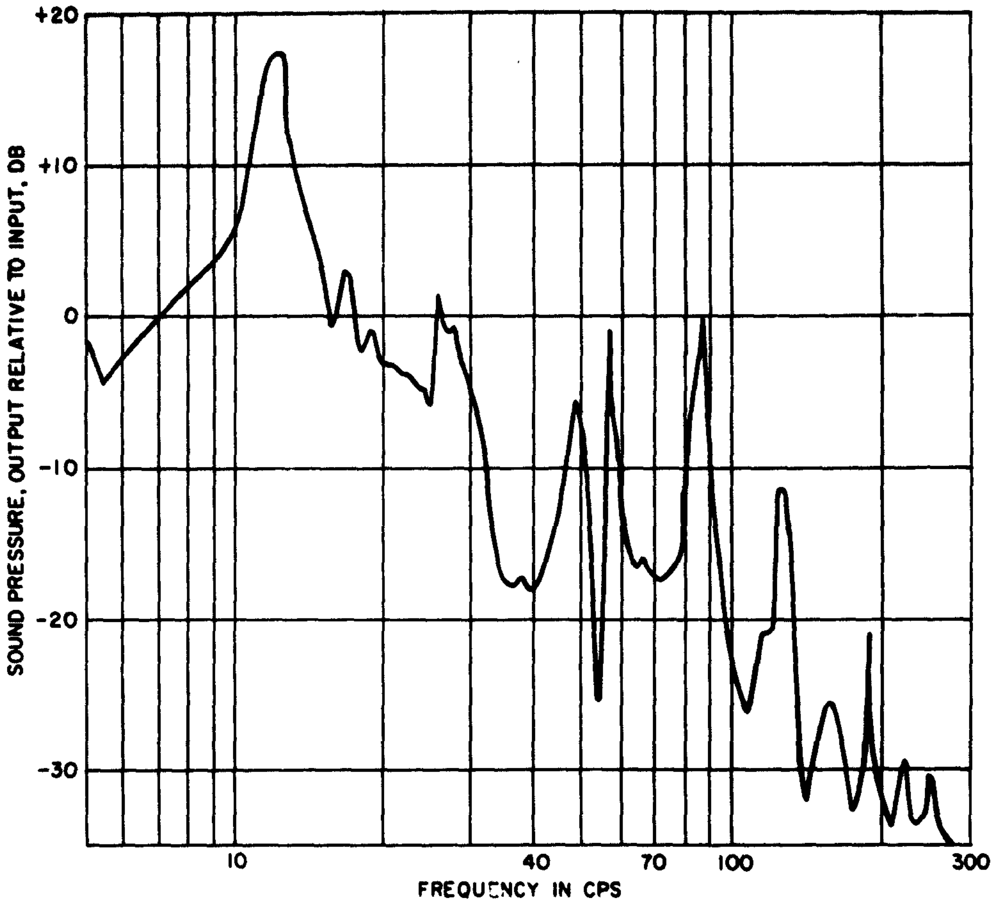

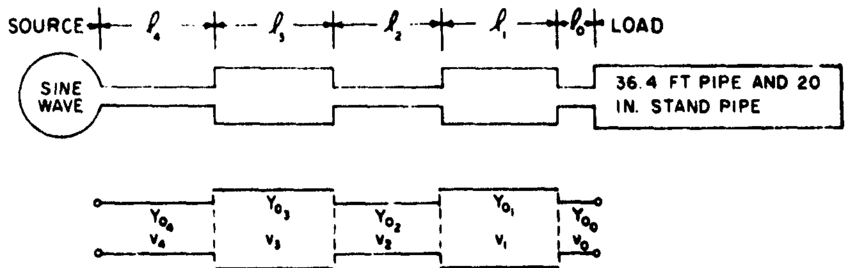

ℓ_0 : 3 IN.	Y_{0_0} : 1.32	v_0 : 3964
ℓ_1 : 60 IN.	Y_{0_1} : 17.3	v_1 : 4250
ℓ_2 : 60 IN.	Y_{0_2} : 1.32	v_2 : 3964
ℓ_3 : 84 IN.	Y_{0_3} : 17.3	v_3 : 4250
ℓ_4 : 3 IN.	Y_{0_4} : 1.32	v_4 : 3964

FIGURE 149
TWO CHAMBER EXPANSION CHAMBER FILTER

DRL - UT
DWG AS 7076
JVK - BEE
11 - 27 - 62

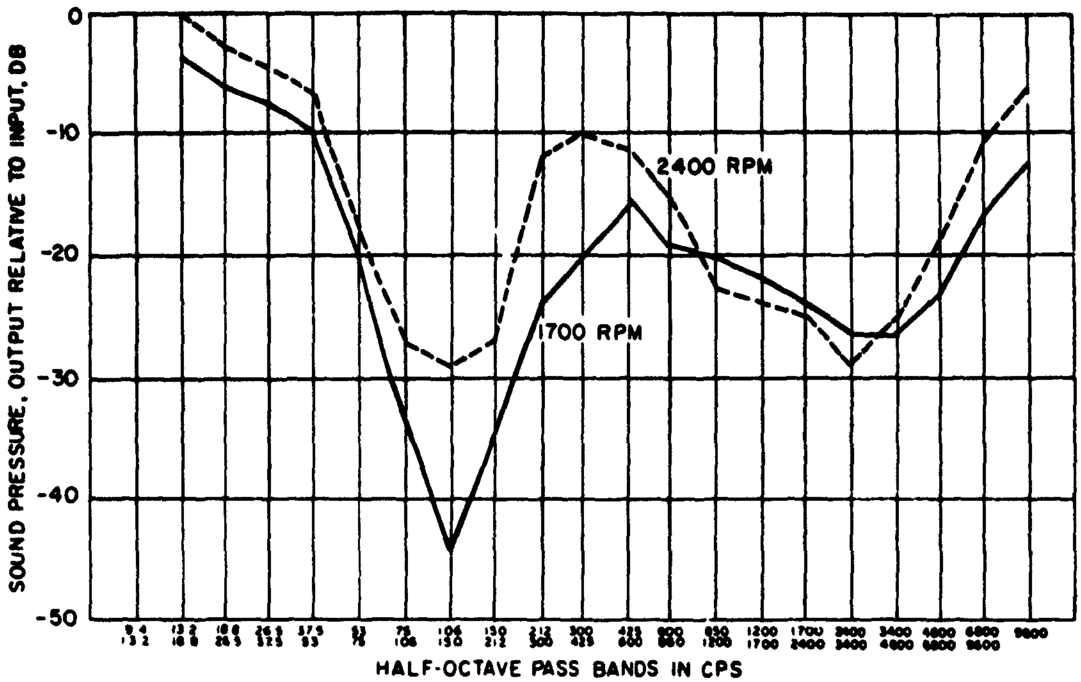

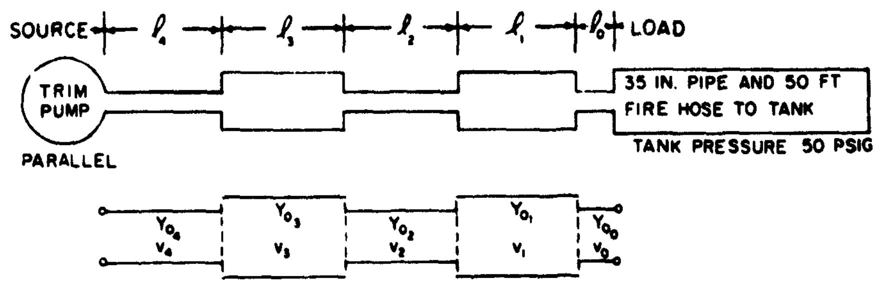

ℓ_0 : 5 IN.	Y_{0_0} : 1.32	v_0 : 3964
ℓ_1 : 60 IN.	Y_{0_1} : 17.3	v_1 : 4250
ℓ_2 : 56 IN.	Y_{0_2} : 1.32	v_2 : 3964
ℓ_3 : 84 IN.	Y_{0_3} : 17.3	v_3 : 4250
ℓ_4 : 144 IN.	Y_{0_4} : 1.32	v_4 : 3964

FIGURE 150
TWO CHAMBER EXPANSION CHAMBER FILTER

DRL - UT
DWG AS7080
JVK - BEE
11 - 16 - 62

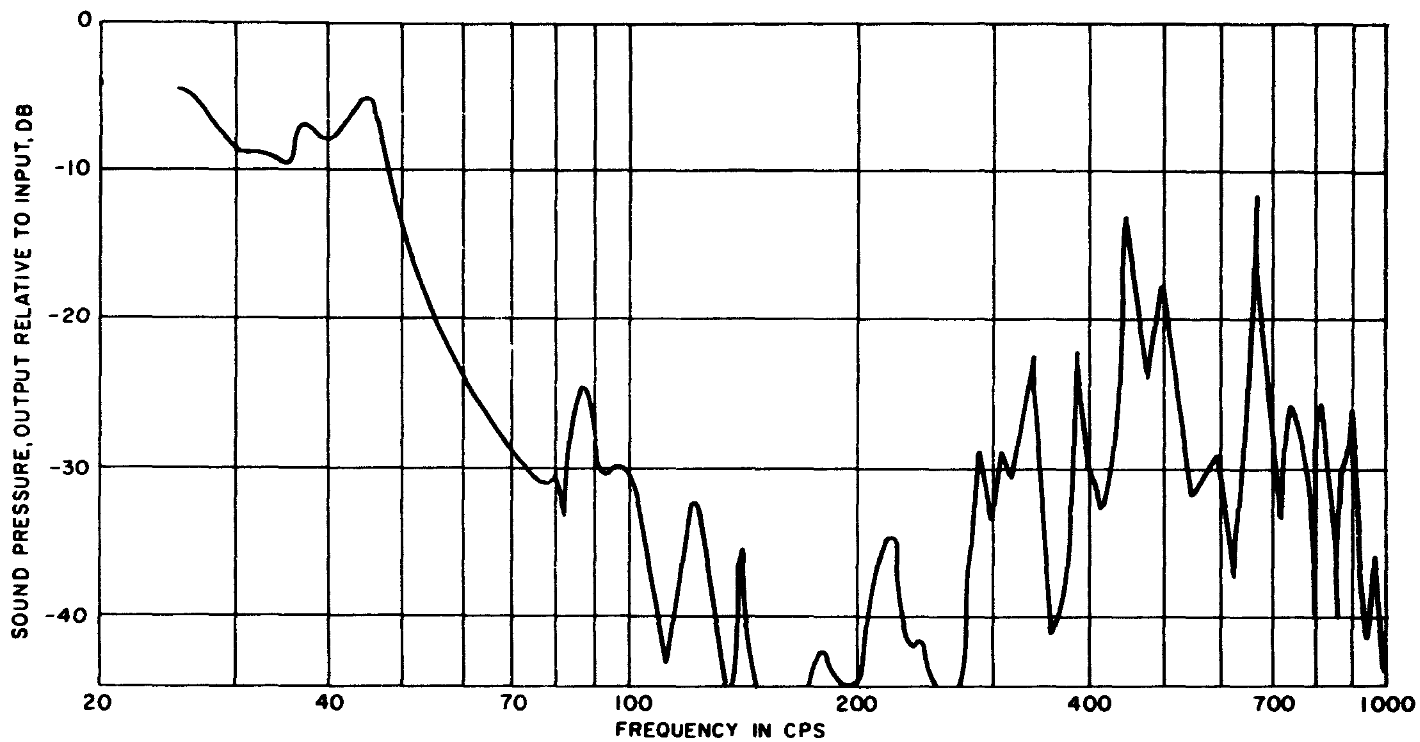

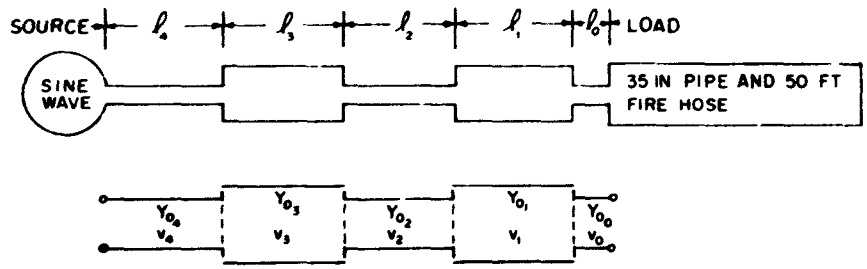

ℓ_0 : 5 IN.	Y_{0_0} : 1.32	v_0 : 3964
ℓ_1 : 84 IN.	Y_{0_1} : 17.3	v_1 : 4250
ℓ_2 : 56 IN.	Y_{0_2} : 1.32	v_2 : 3964
ℓ_3 : 60 IN.	Y_{0_3} : 17.3	v_3 : 4250
ℓ_4 : 144 IN.	Y_{0_4} : 1.32	v_4 : 3964

DRL - UT
DWG AS 7077
JVK - BEE
11 - 28 - 62

FIGURE 151
TWO CHAMBER EXPANSION CHAMBER FILTER

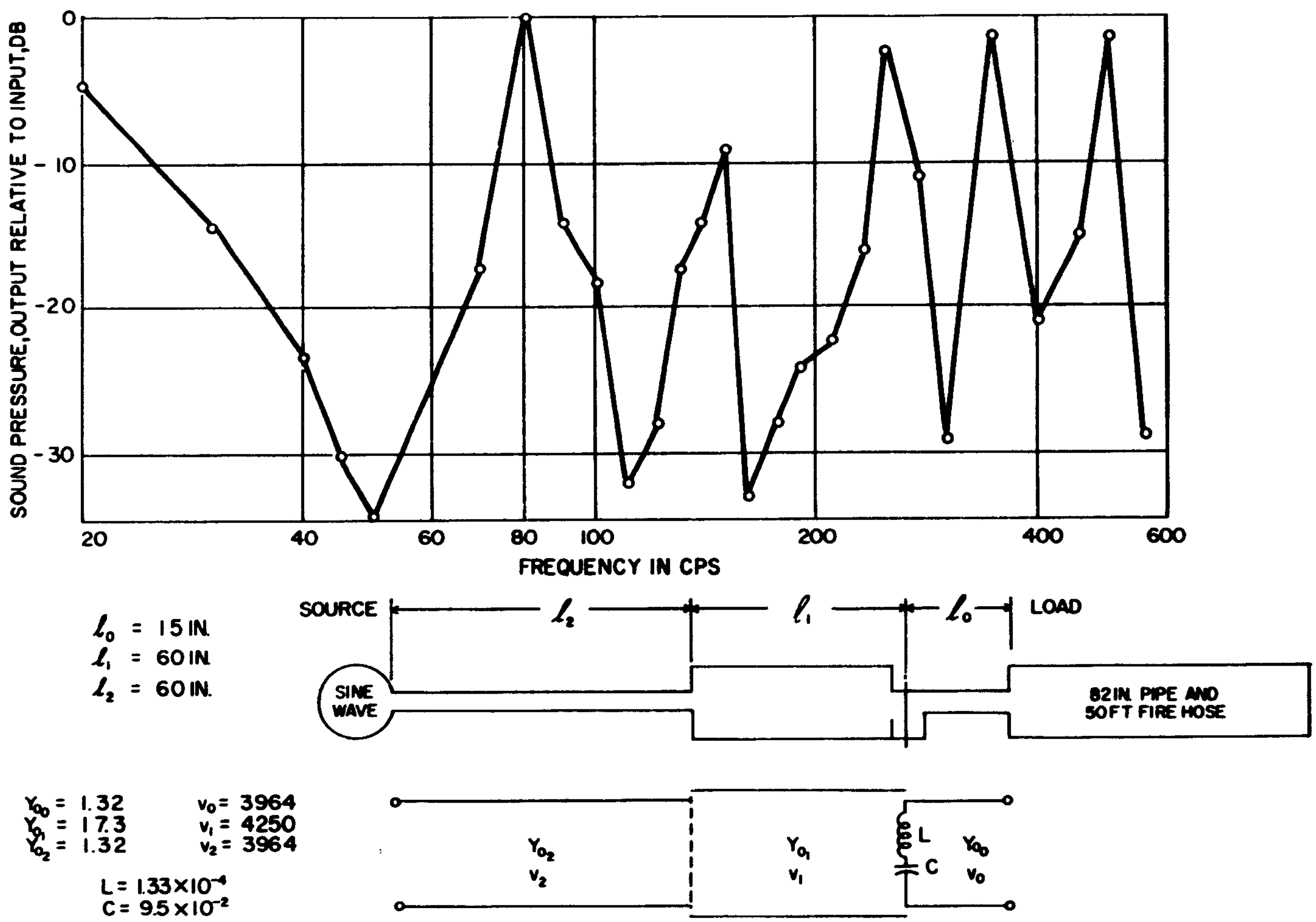

FIGURE 152

COMBINATION SINGLE EXPANSION CHAMBER AND ONE SIDE-BRANCH ELEMENT FILTER WITH METAL BELLOWS BRANCH ELEMENT

DRL-UT
DWG AS7085
JVK- MJM
10-10-62

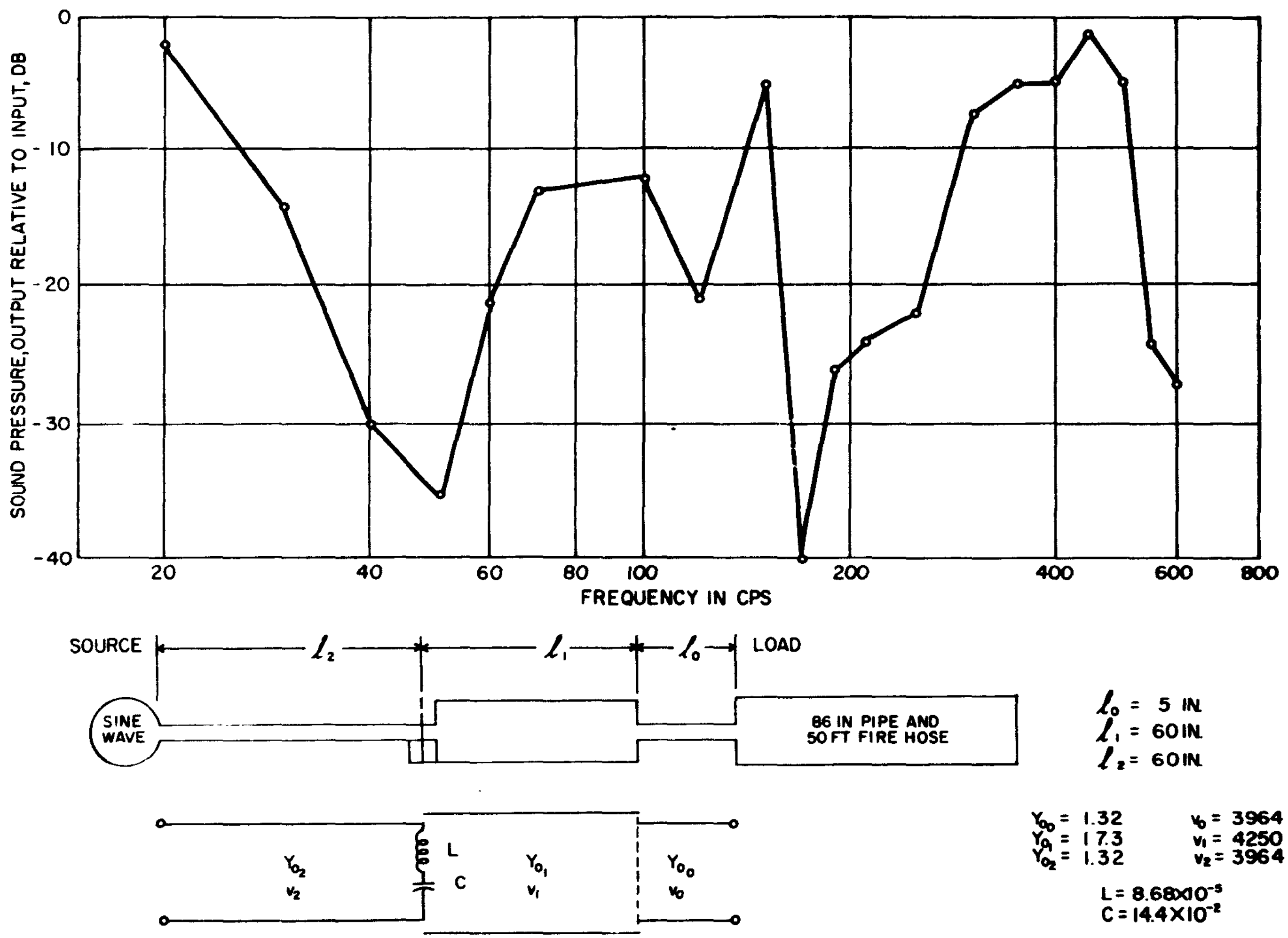

ℓ_0 = 5 IN.
ℓ_1 = 60 IN.
ℓ_2 = 60 IN.

Y_{0_0} = 1.32 v_0 = 3964
Y_{0_1} = 17.3 v_1 = 4250
Y_{0_2} = 1.32 v_2 = 3964

L = 8.68×10^{-5}
C = 14.4×10^{-2}

FIGURE 153

COMBINATION SINGLE EXPANSION CHAMBER AND ONE SIDE-BRANCH ELEMENT FILTER WITH METAL BELLOWS BRANCH ELEMENT

DRL - UT
DWG AS7086
JVK - MJM
10-15-62

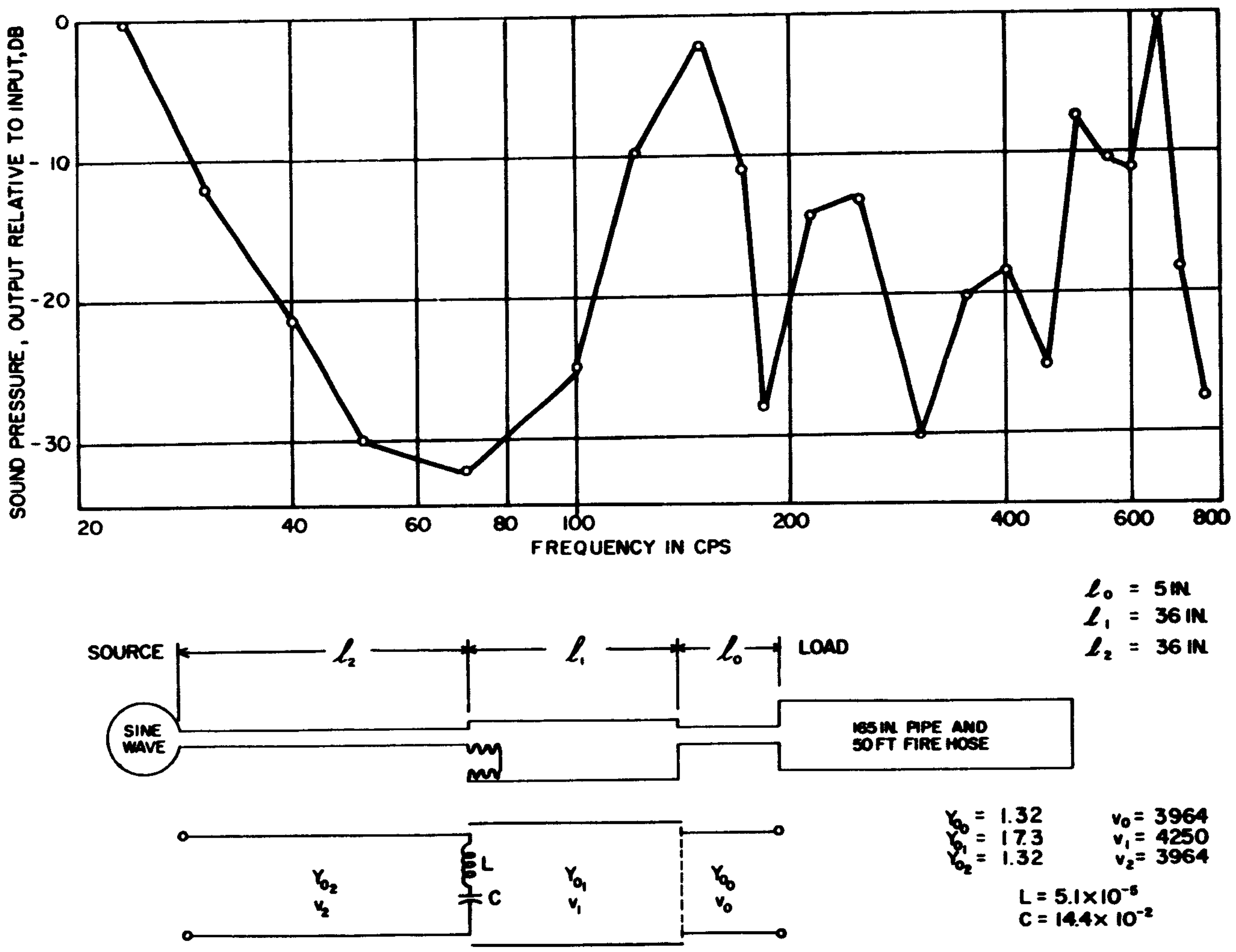

FIGURE 154

COMBINATION SINGLE EXPANSION CHAMBER AND ONE SIDE-BRANCH ELEMENT FILTER WITH METAL BELLOWS BRANCH ELEMENT

DRL - UT
DWG AS7087
JVK - MJM
10-9-62

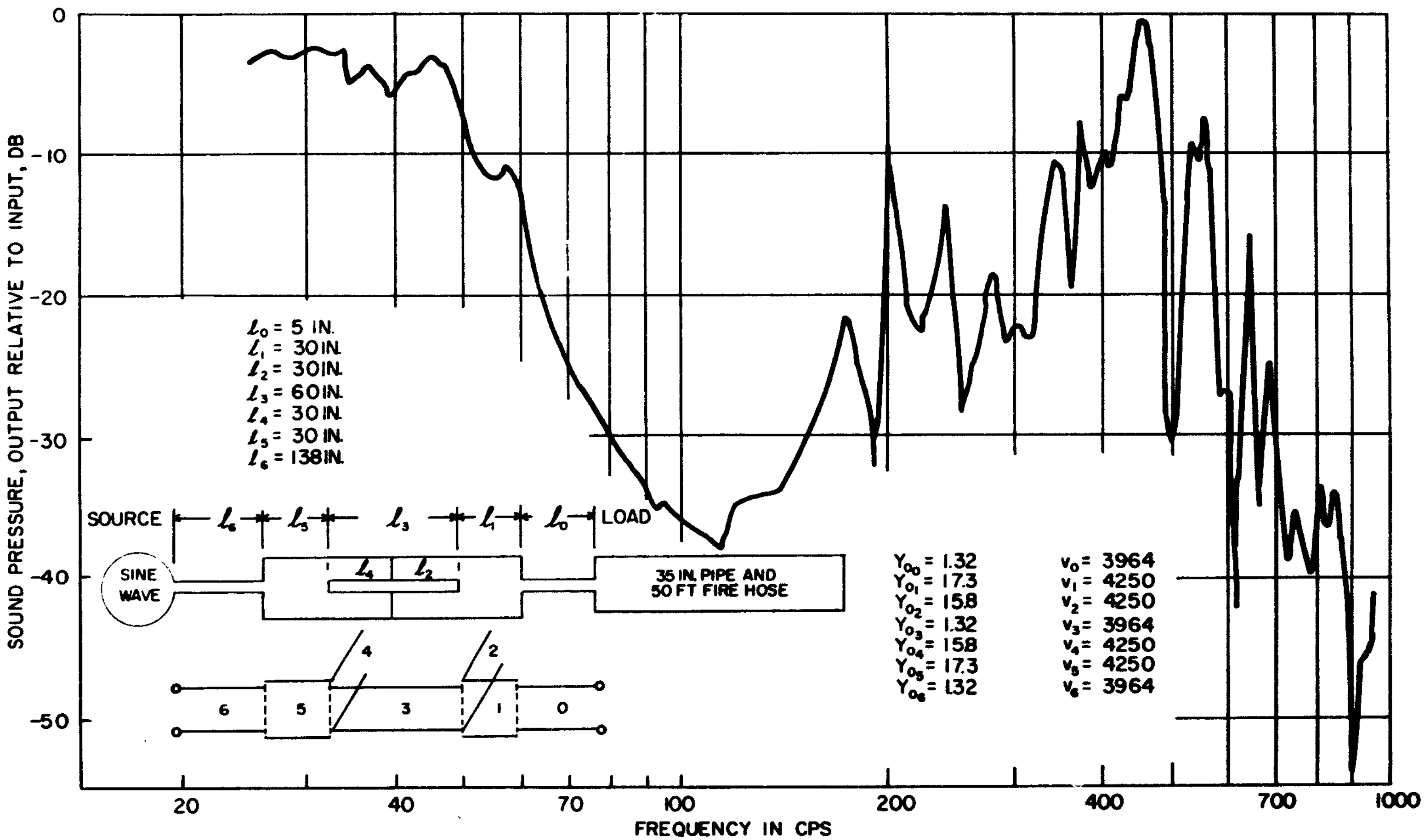

DRL - UT
DWG AS7088
JVK - MJM
10 - 5 - 62

FIGURE 155

COMBINATION EXPANSION CHAMBER AND SIDE-BRANCH FILTER WITH CLOSED END STUB BRANCH ELEMENTS

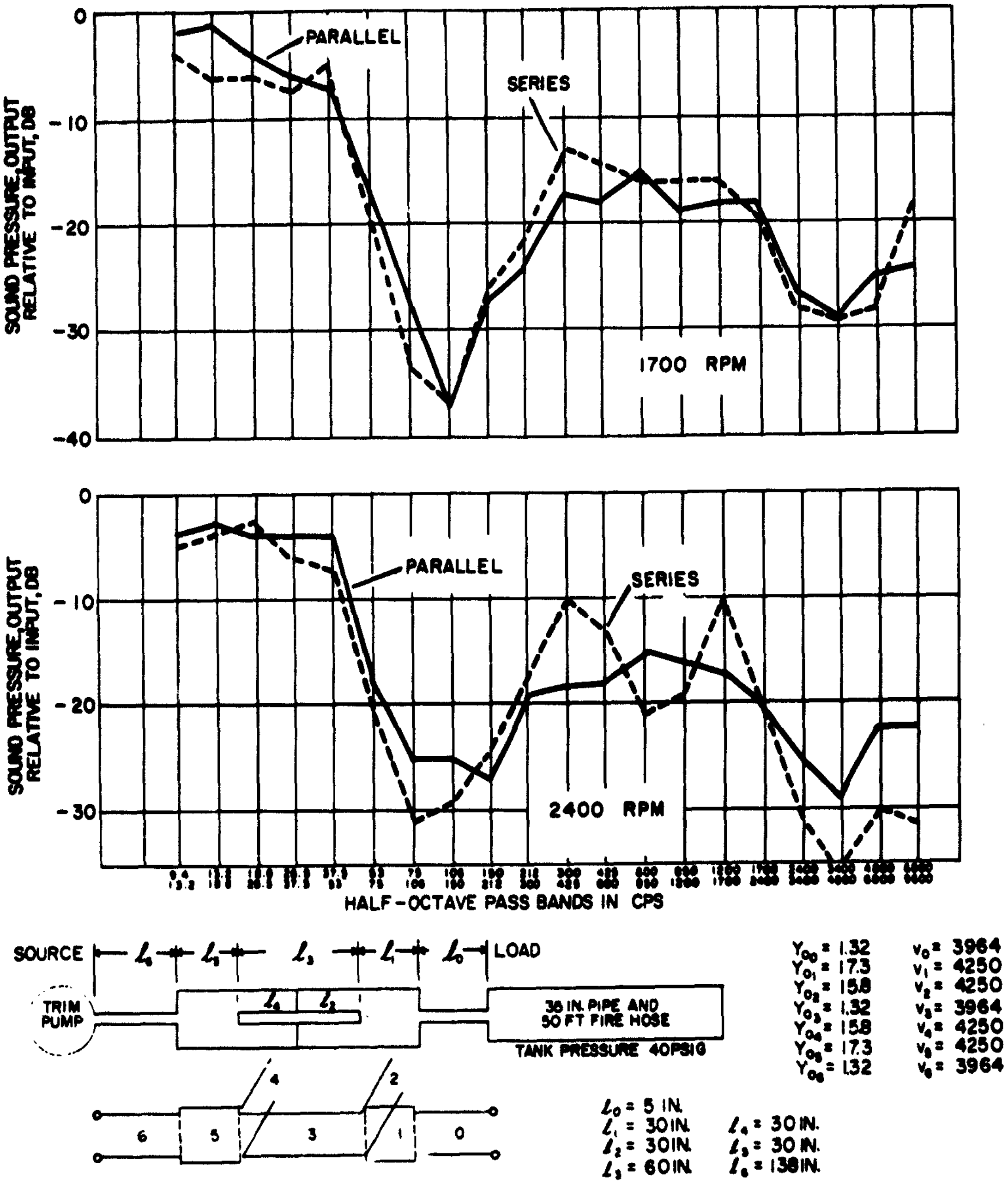

FIGURE 156

COMBINATION EXPANSION CHAMBER AND SIDE-BRANCH FILTER WITH CLOSED END STUB BRANCH ELEMENTS

DRL - UT
DWG AS7069
JVK - MJM
10-12-62

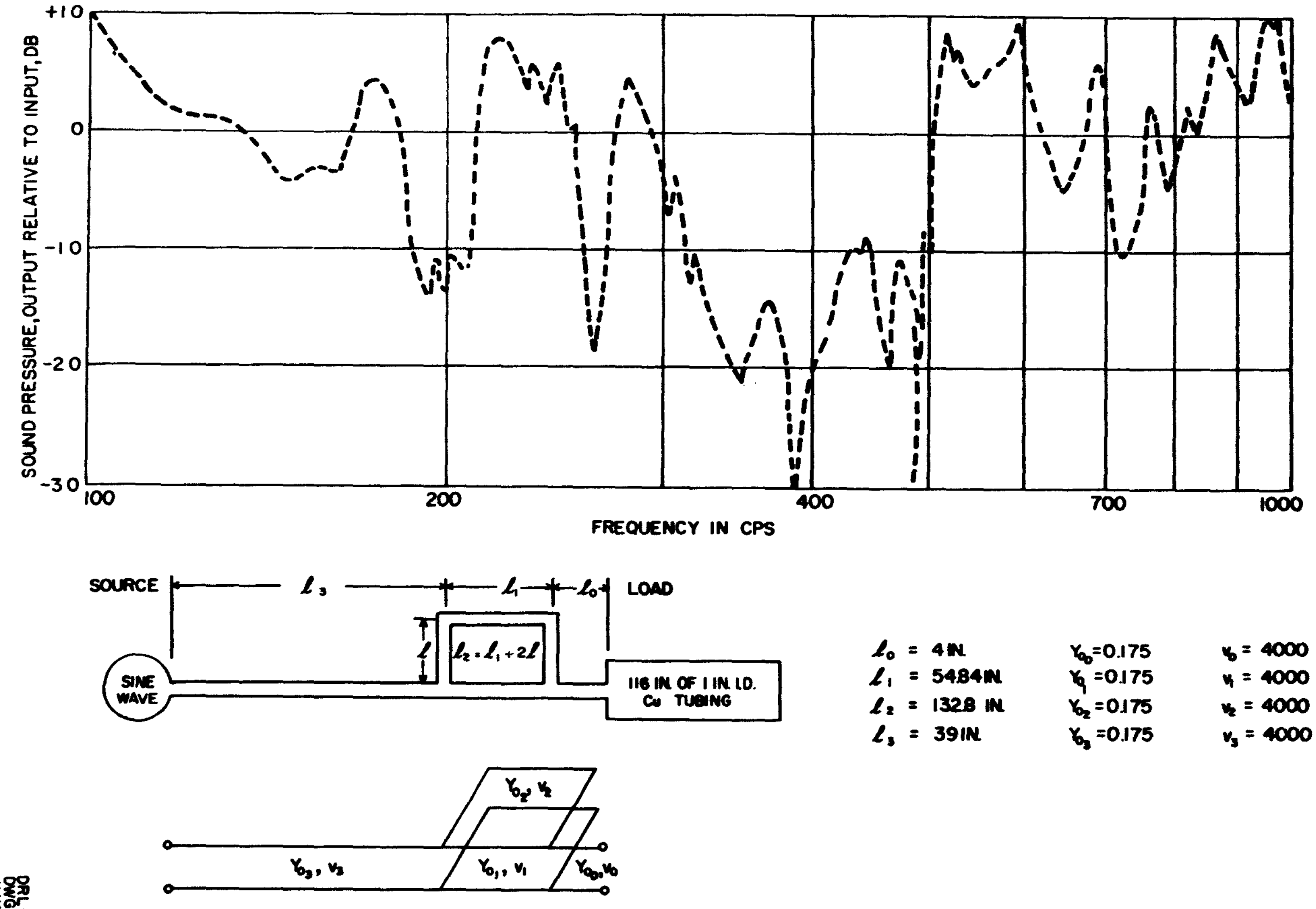

FIGURE 157
QUINKE TUBE FILTER

DRL - UT
DWG AS7091
JVK - MJM
10-12-62

It must be remembered that the ratios of sound pressures at the filter output ports to those at the input ports are not the same as transmission loss, so exact agreement between these data and theoretical predictions for the filter transmission loss could not be expected, even if the filters were ideally terminated.

These curves have been plotted from test data collected since 1955. When the tests were run it was recognized that acoustic terminations of the filters influenced test results; but since resistive, matched terminations were not available, choice of the piping arrangement was governed by pumping system requirements and availability of piping components.

These curves furnish a record of acoustic filter test results obtained during the filter investigation program at Defense Research Laboratory. They show performances typical of those that were measured during the experimental filter program. It is probable that filter behavior of the same general character would be found in actual practice.

September 1962
JVK:vh

CHAPTER V: CLOSING REMARKS

The computer program used for calculating filter transmission loss as a function of frequency, Appendix B, requires filter branch element admittances at certain stages of the computation. For a particular filter, the program will either calculate these admittance values from parameters of the branch elements, accept values of branch admittance as input data, or even operate on a mixed basis with some admittances calculated and others supplied. This flexibility permits calculation of transmission loss for multi-element filters from measured values of input admittance. Deviation from ideal characteristics for the branch elements can thereby be taken into account.

Actual measurements of acoustic admittance of metal bellows type filter branch elements have shown that the characteristics of such units may depart considerably from those of simple spring-piston resonators.

It cannot be expected that filter performances in actual practice will exactly duplicate those predicted by the methods of Chapter III. The principal reasons are that in obtaining the design curves it was assumed that in any particular case (1) there was a single liquid column sound transmission path, (2) the admittance of the filter load was purely resistive and equal to the characteristic admittance of the system piping, and (3) only one noise source was present. Nevertheless, it is believed that the analytical approach to filter design given here is considerably more powerful than guesswork or methods based on lumped-parameter approximation of filter behavior.

September 1962
DGG:vh

APPENDIX A

Calculated Velocities of Sound Waves in Liquid Inside Metal Pipes

The sound velocity values presented in this appendix were computed using a formula developed from an acoustical circuit representation of the pipe-liquid system. The distributed reactance of an acoustic transmission system can be represented by a cascaded length of lumped-element sections. Each section consists of an arrangement of compliance and inertance which represents the distributed series and shunting acoustic impedance found per unit length. Since such a liquid system is very nearly lossless, no resistances need be included in this representation.

The expression for the velocity of sound waves through such a system is

$$v = \frac{1}{\sqrt{LC}} ,$$

where L = series inertance per unit length of the line, and
C = shunt compliance per unit length of line.

The compliance C is defined as the change in volume per unit change in pressure for the system under consideration. Two compliance effects are present in pipe-liquid systems: (1) the pipe itself can expand radially, thus allowing a change in overall system volume, and (2) the liquid has elastic properties, independent of its means of confinement. These two effects add, as will be seen, to produce an overall compliance.

The inertance is defined as the ratio of mass moved by the changing pressure to the square of the area (normal to the direction of mass movement) over which the mass is distributed. Two inertance effects are found in pipe-liquid systems: (1) the pipe mass moves radially, and (2) the liquid mass moves axially. Only the latter of these motions has any appreciable effect on the sound velocity at the low frequencies of interest ($f < 2000$ cps).

The acoustical circuit for a unit length of the pipe is given in Fig. A-1,

where L_ℓ = inertance per unit length due to liquid,
L_p = inertance per unit length due to pipe,
C_ℓ = compliance per unit length due to liquid, and
C_p = compliance per unit length due to pipe.

The liquid inertance per unit length is

$$L_\ell = \frac{m_\ell}{S_\ell^2} = \frac{4\rho_\ell}{\pi d_i^2} \quad ,$$

where m_ℓ = mass of liquid per unit length,
S_ℓ = cross-sectional area of liquid,
ρ_ℓ = mass density of liquid, and
d_i = inside diameter of pipe.

The pipe inertance per unit length is

$$L_p = \frac{m_p}{S_p^2} = \frac{\rho_p d_m a}{\pi d_i^2} \quad ,$$

where m_p = mass of pipe per unit length,
S_p = inside surface area of pipe per unit length
ρ_p = mass density of pipe,
d_m = mean diameter of the pipe, and
a = thickness of pipe wall.

The liquid compliance per unit length is

$$C_\ell = \frac{\Delta U_\ell}{\Delta p} = \kappa U_\ell = \frac{\pi d_i^2 \kappa}{4} \quad ,$$

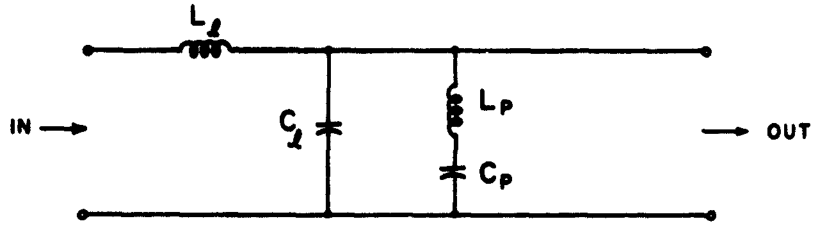

FIGURE A-1

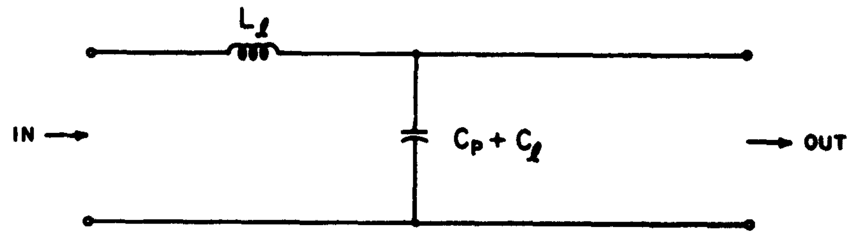

FIGURE A-2

PIPE-LIQUID ACOUSTICAL CIRCUITS

DRL - UT
DWG AS 7138
JVK - BEE
9 - 21 - 62

where U_ℓ = volume of liquid per unit length,
p = system pressure, and
κ = compressibility of liquid.

The pipe compliance calculation is somewhat more involved. An expression for the inner radial expansion Δx of a pipe for a pressure change Δp is (page 264 of Ref. 27)

$$\Delta x = \frac{\Delta p\, r_i}{E}\left[\frac{r_o^2 + r_i^2}{r_o^2 - r_i^2} - \nu\left(\frac{r_i^2}{r_o^2 - r_i^2} - 1\right)\right]$$

where E = Young's modulus of elasticity,
r_o = inside pipe radius,
r_i = outside pipe radius, and
ν = Poisson's Ratio.

The associated volume change per unit length of pipe is

$$\Delta U_p \approx 2\pi r_i \Delta x \quad .$$

Therefore, the pipe compliance per unit length reduces to

$$C_p = \frac{\Delta U_p}{\Delta p} = \frac{\pi d_i^2}{2E}\left[1 + \nu + \frac{d_i^2\,(2 - \nu)}{4a\,(d_i + a)}\right]$$

where d_i = inside diameter.

To show that the pipe inertance is negligible for the frequencies of interest, note that for a series compliance-inertance branch an equivalent compliance is given by

$$C_{eq} = \frac{C_1}{1 - \omega^2 L_1 C_1} \quad ,$$

where $\omega = 2\pi f$, and L_1 and C_1 are the series elements. If this expression is applied to the series L_p and C_p branch of Fig. A-1, it is seen that $\omega^2 L_p C_p \ll 1$ for normal values of inertance and compliance and for low values of $\omega = 2\pi f$. The circuit reduces to that shown in Fig. A-2. Therefore, using the velocity expression already mentioned,

$$v = \frac{1}{\sqrt{L_\ell (C_\ell + C_p)}} .$$

The velocities computed using these relationships compare favorably with measured values. Agreement to within 5-10% was found in all cases. The computed velocities are plotted versus pipe inside diameter for various pipe materials and wall thicknesses in Figs. A-3 through A-17.

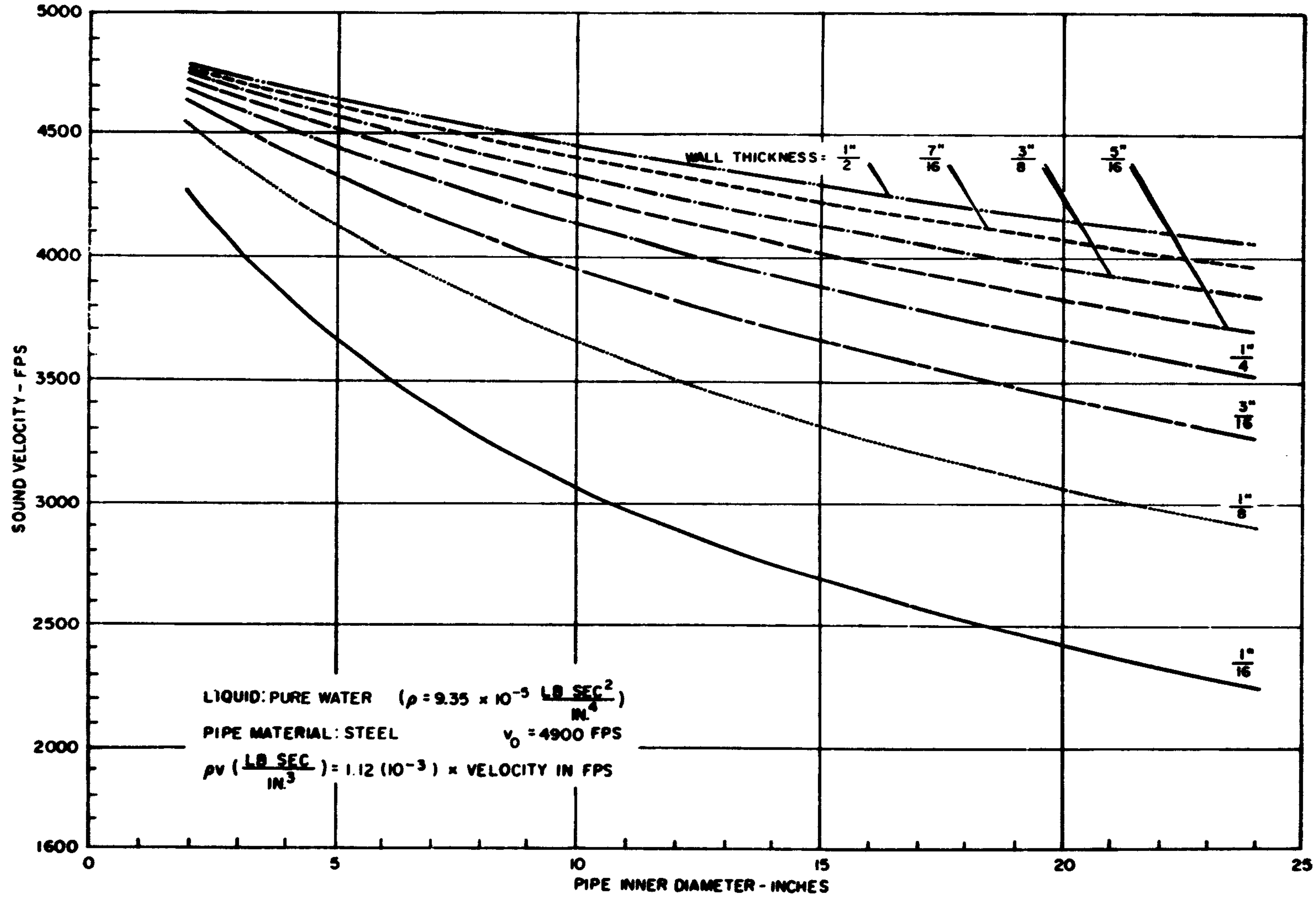

FIGURE A-3
CALCULATED VELOCITIES OF SOUND WAVES IN LIQUID
INSIDE METAL PIPES

DRL - UT
DWG AS 7260
JVK - BEE
11 - 5 - 62

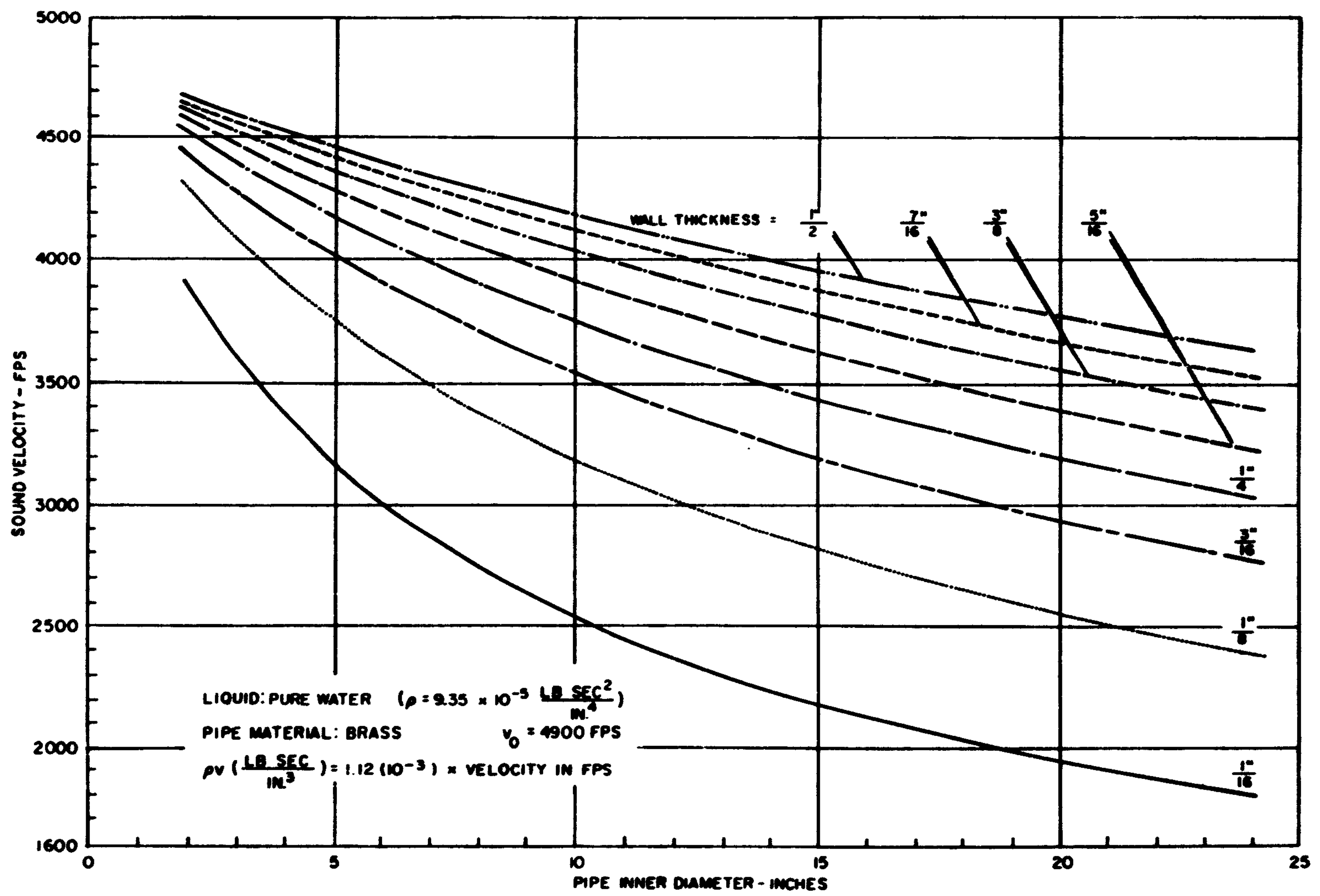

FIGURE A-4
CALCULATED VELOCITIES OF SOUND WAVES IN LIQUID
INSIDE METAL PIPES

DRL - UT
DWG AS7261
JVK - BEE
11 - 5 - 62

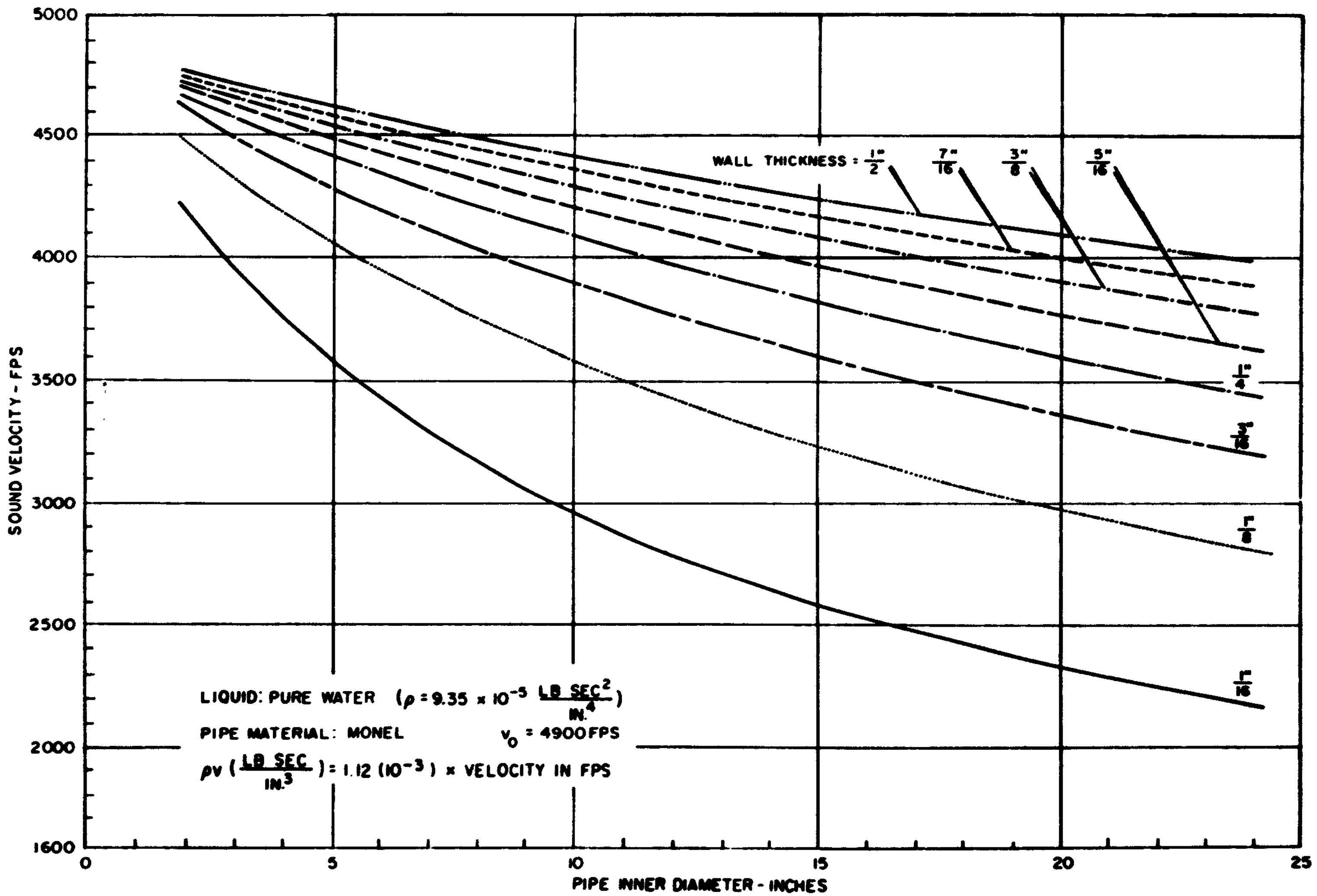

FIGURE A-5
CALCULATED VELOCITIES OF SOUND WAVES IN LIQUID
INSIDE METAL PIPES

DRL - UT
DWG AS7262
JVK - BEE
11 - 5 - 62

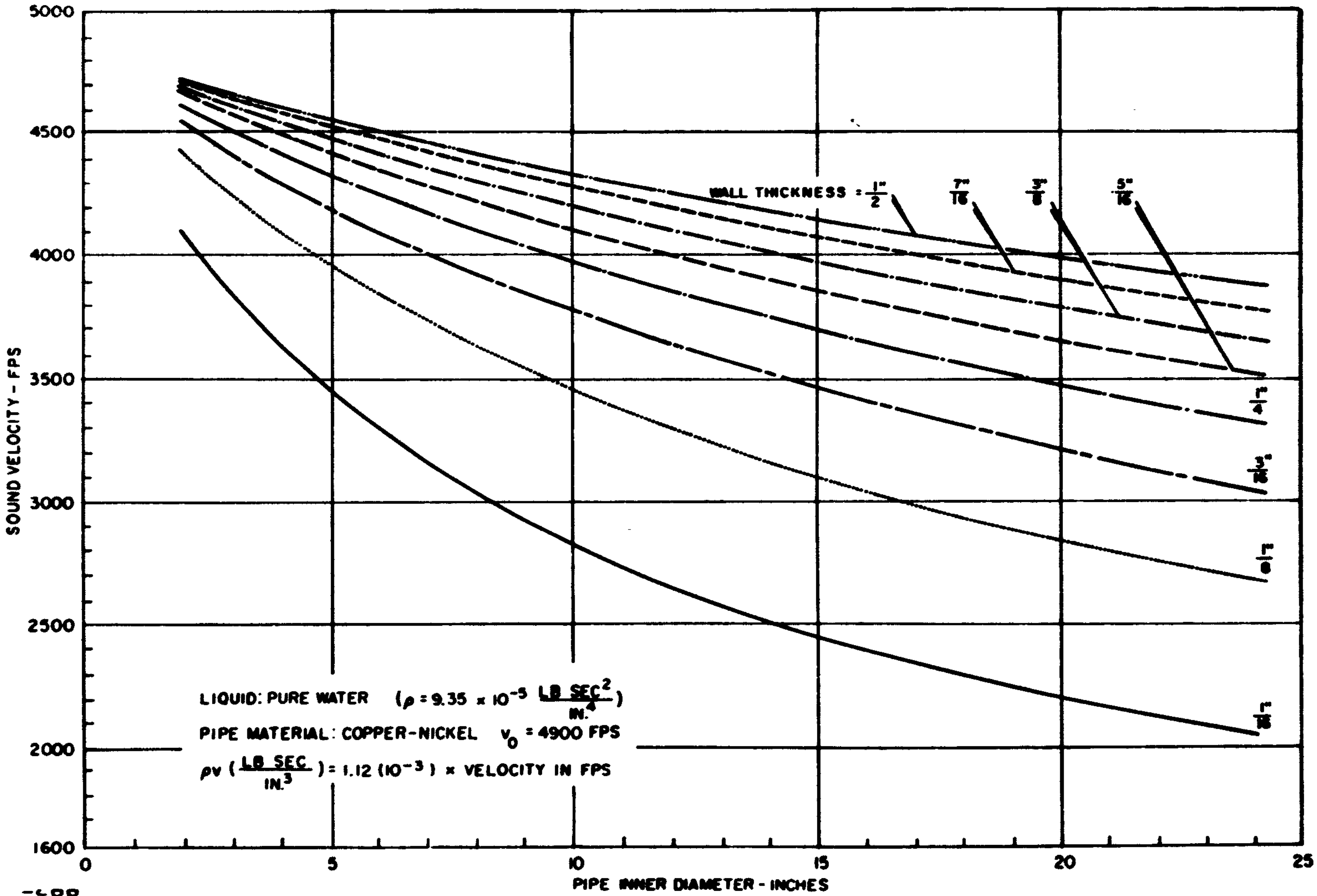

DRL - UT
DWG AS7263
JVK - BEE
11 - 5 - 62

FIGURE A-6
CALCULATED VELOCITIES OF SOUND WAVES IN LIQUID
INSIDE METAL PIPES

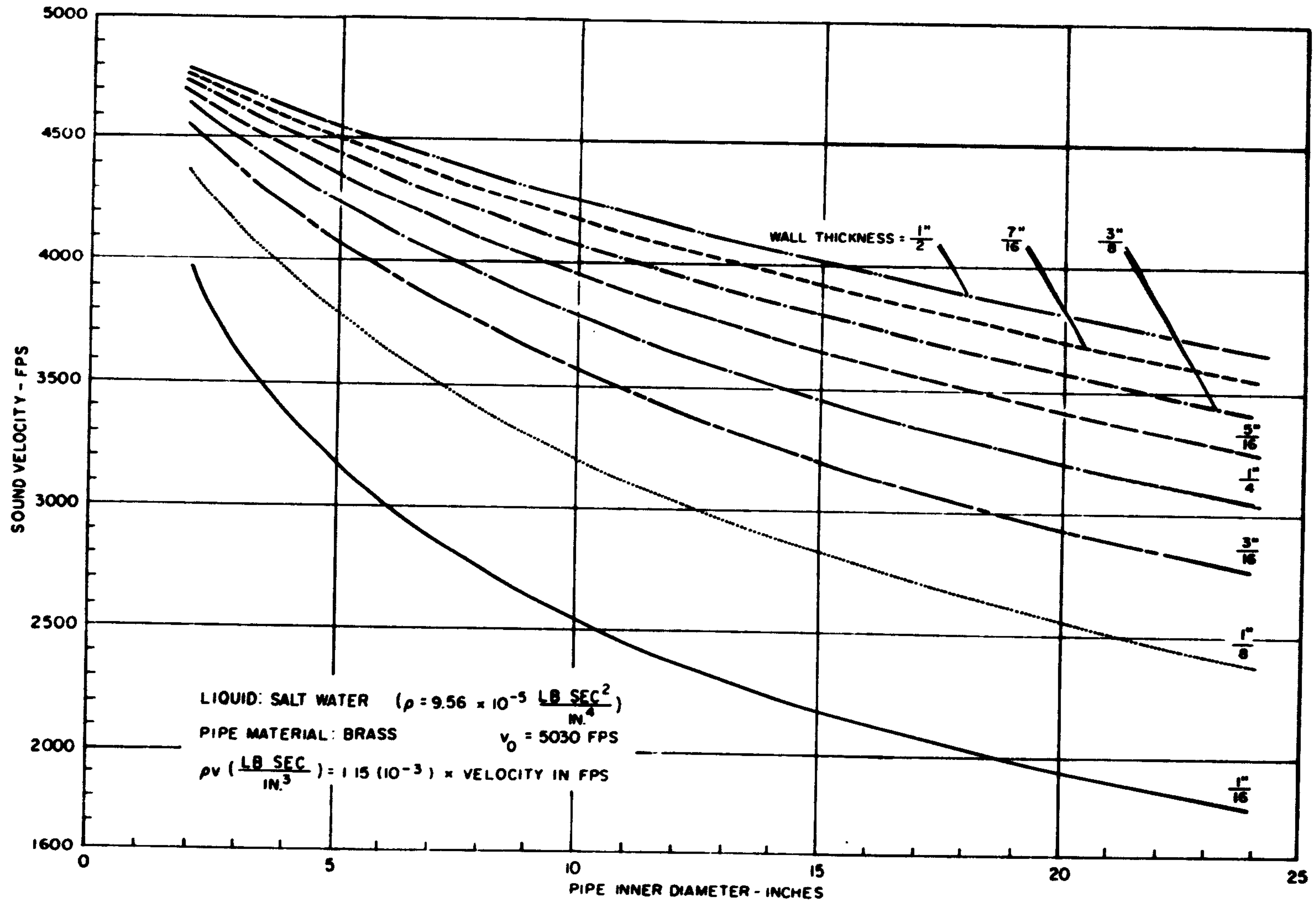

FIGURE A-7
CALCULATED VELOCITIES OF SOUND WAVES IN LIQUID
INSIDE METAL PIPES

DRL - UT
DWG AS7264
JVK - BEE
11 - 5 - 62

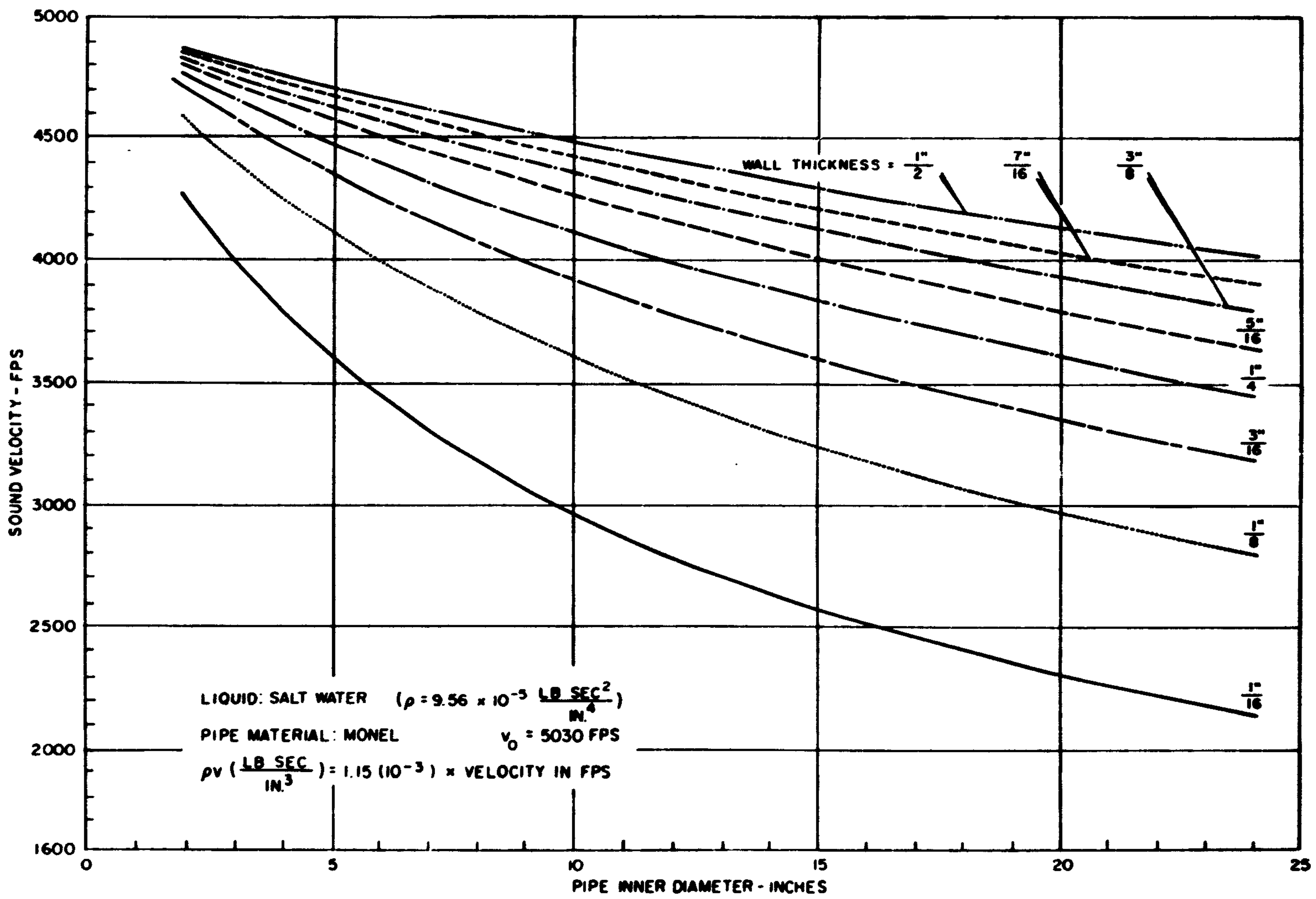

FIGURE A-8
CALCULATED VELOCITIES OF SOUND WAVES IN LIQUID
INSIDE METAL PIPES

DRL - UT
DWG AS 7265
JVK - BEE
11 - 5 - 62

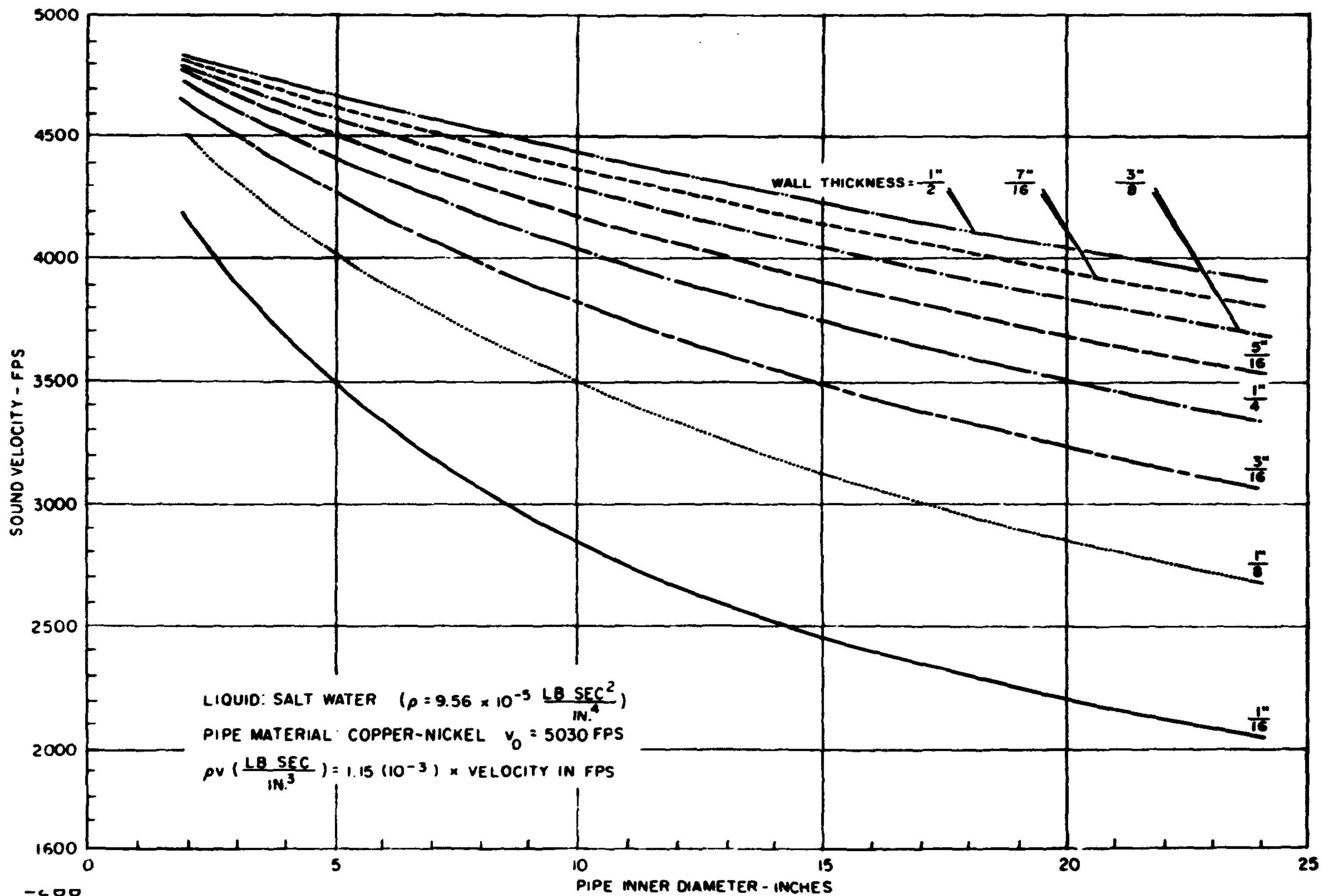

DRL - UT
DWG AS7266
JVK - BEE
11 - 5 - 62

FIGURE A-9
CALCULATED VELOCITIES OF SOUND WAVES IN LIQUID
INSIDE METAL PIPES

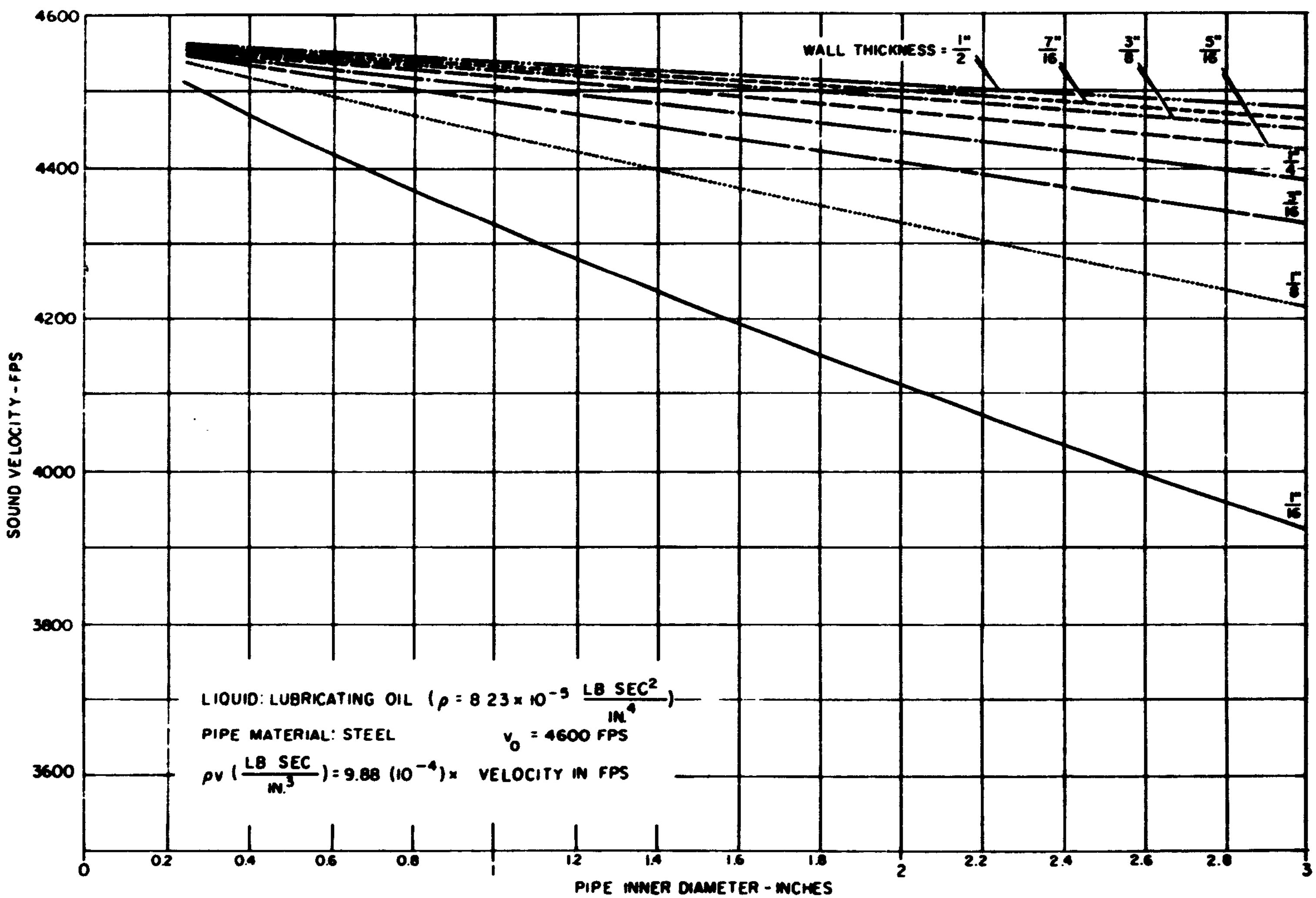

FIGURE A-10
CALCULATED VELOCITIES OF SOUND WAVES IN LIQUID
INSIDE METAL PIPES

DRL - UT
DWG AS7267
JVK - BEE
11 - 2 - 62

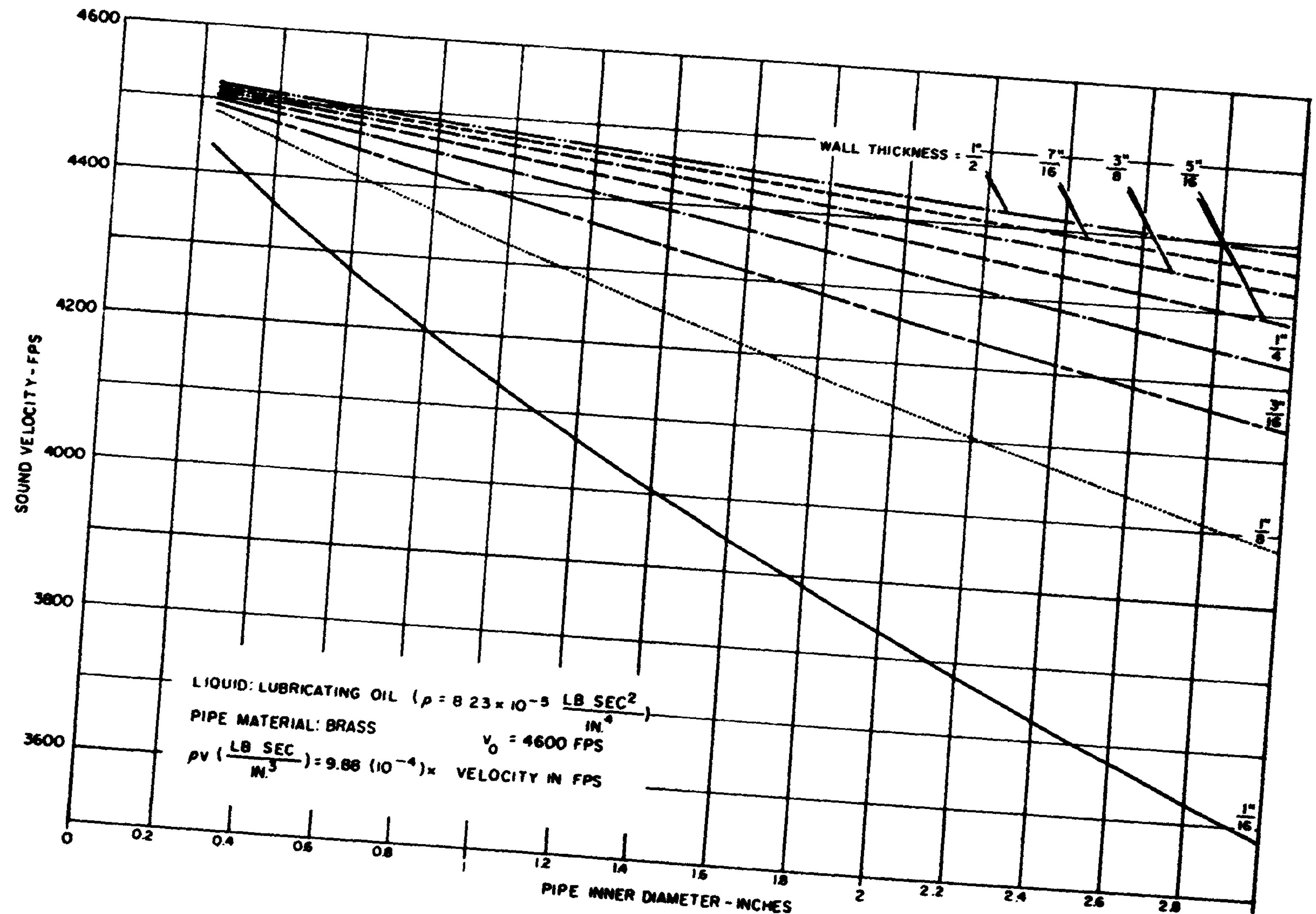

FIGURE A-11
CALCULATED VELOCITIES OF SOUND WAVES IN LIQUID
INSIDE METAL PIPES

DRL - UT
DWG AS 7268
JVX - BEE
11 - 2 - 62

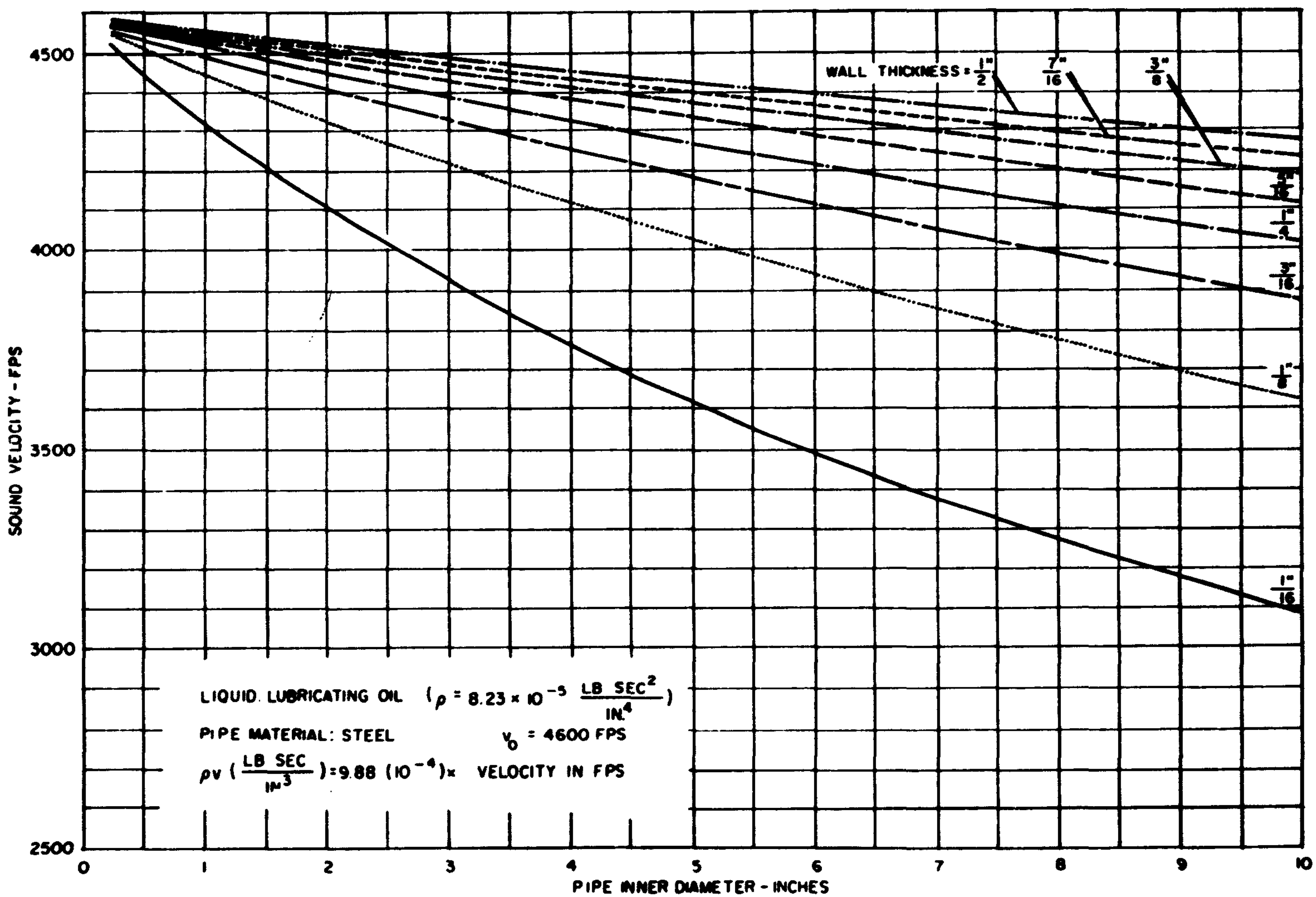

FIGURE A-12
CALCULATED VELOCITIES OF SOUND WAVES IN LIQUID
INSIDE METAL PIPES

DRL - UT
DWG AS7269
JVK - BEE
11 - 2 - 62

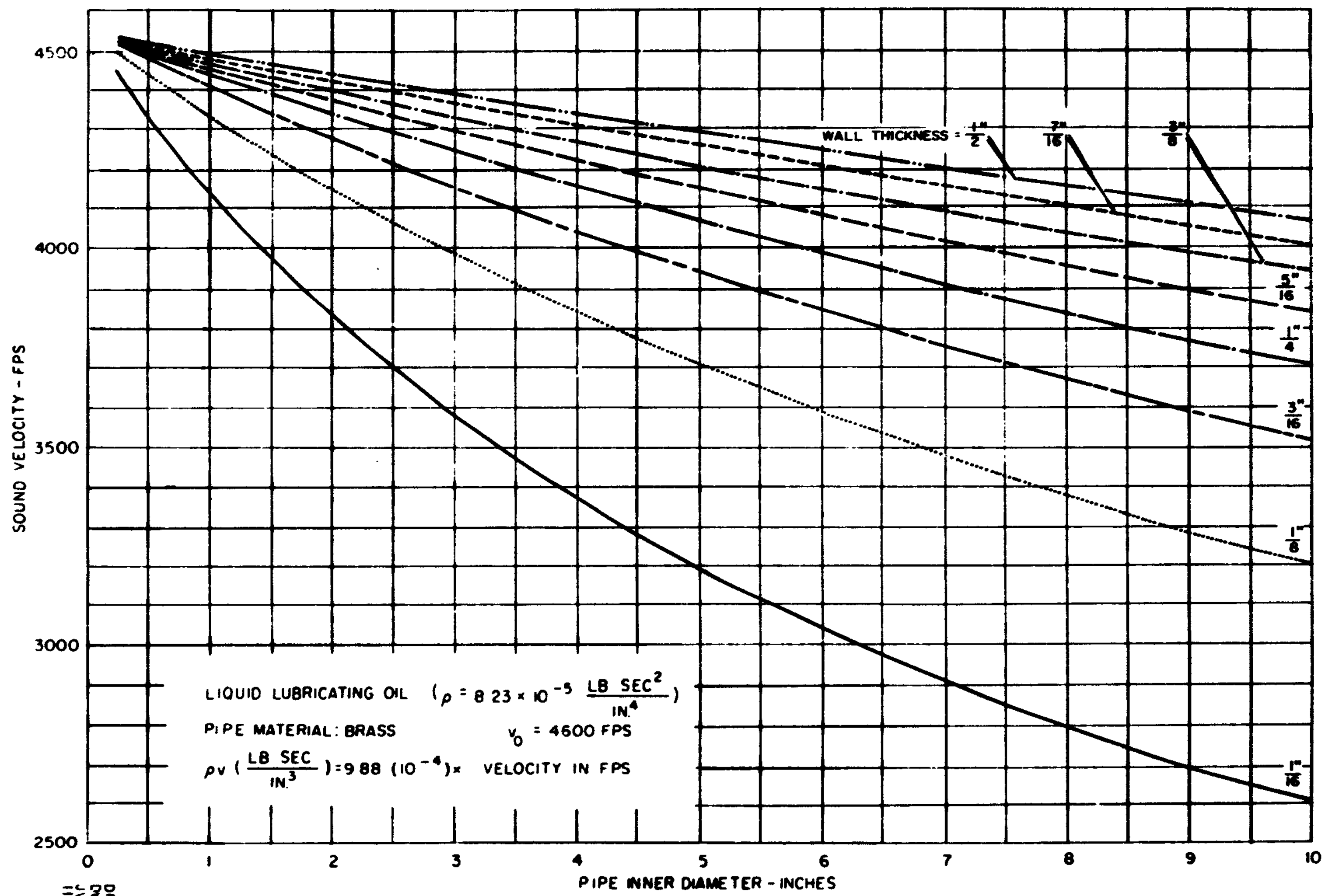

DRL - UT
DWG AS7270
JVK - BEE
11 - 2 - 62

FIGURE A-13
CALCULATED VELOCITIES OF SOUND WAVES IN LIQUID
INSIDE METAL PIPES

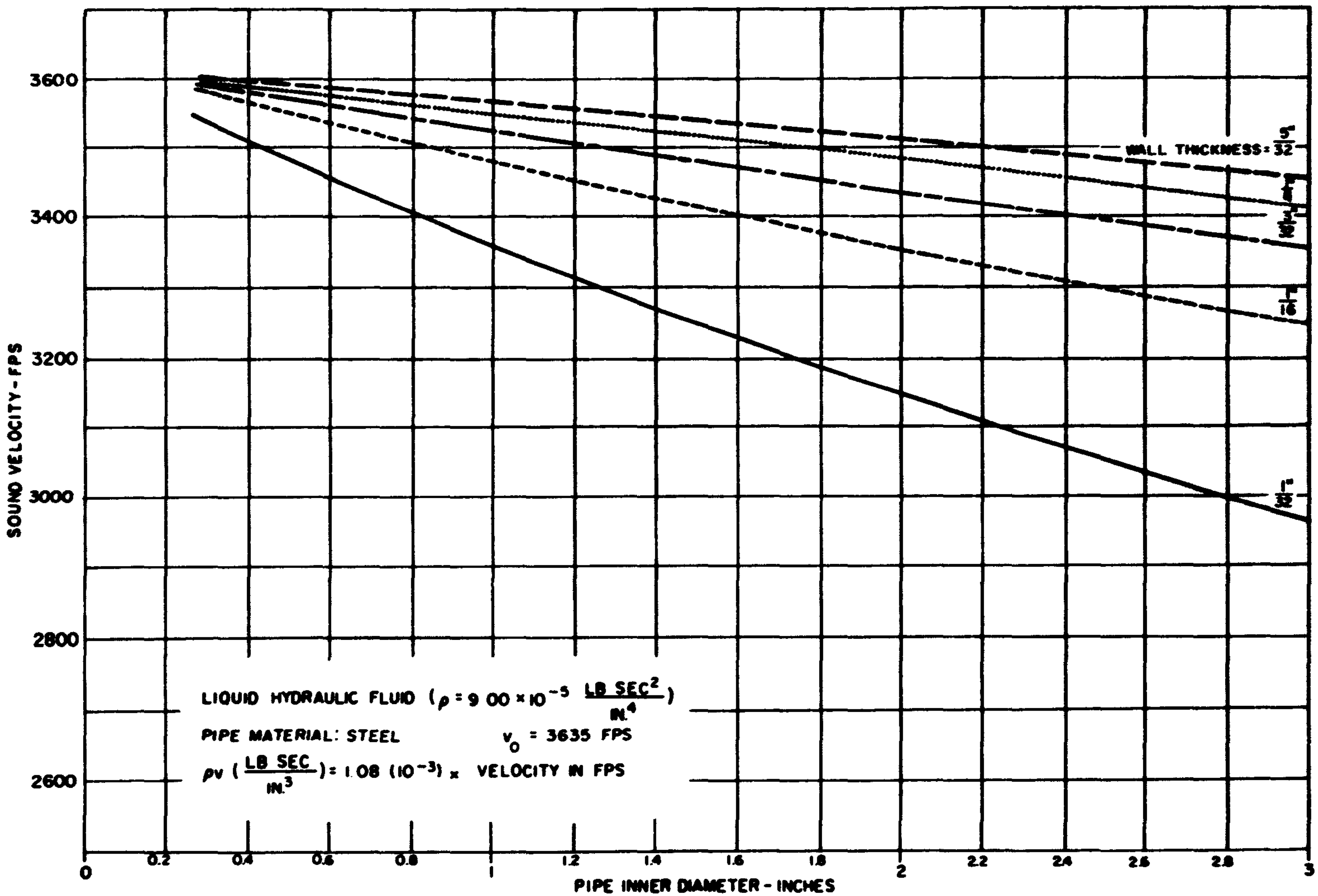

FIGURE A-14
CALCULATED VELOCITIES OF SOUND WAVES IN LIQUID
INSIDE METAL PIPES

DRL - UT
DWG AS 7271
JVK - BEE
11 - 2 - 62

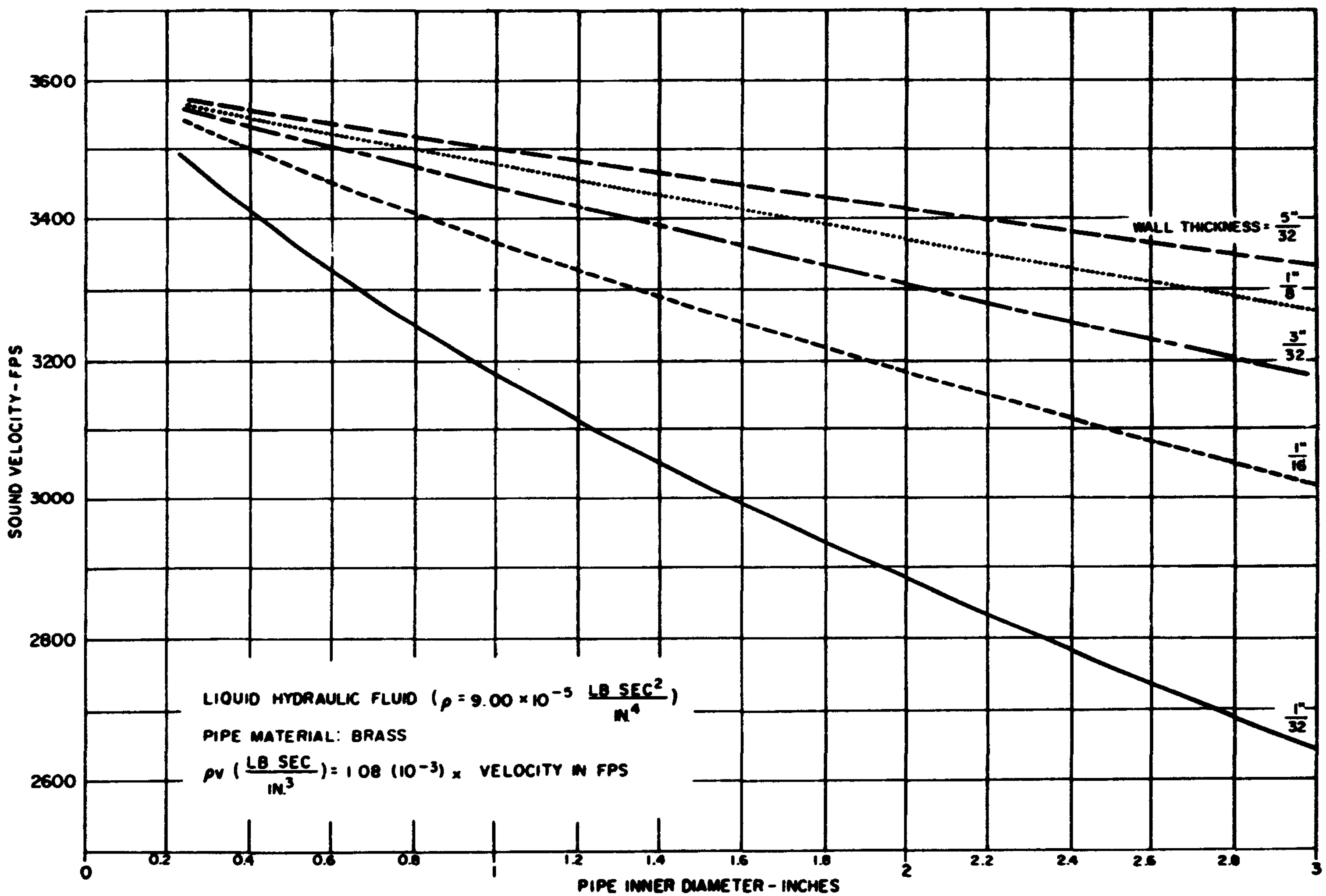

FIGURE A-15
CALCULATED VELOCITIES OF SOUND WAVES IN LIQUID
INSIDE METAL PIPES

DRL - UT
DWG AS 7272
JVK - BEE
11 - 2 - 62

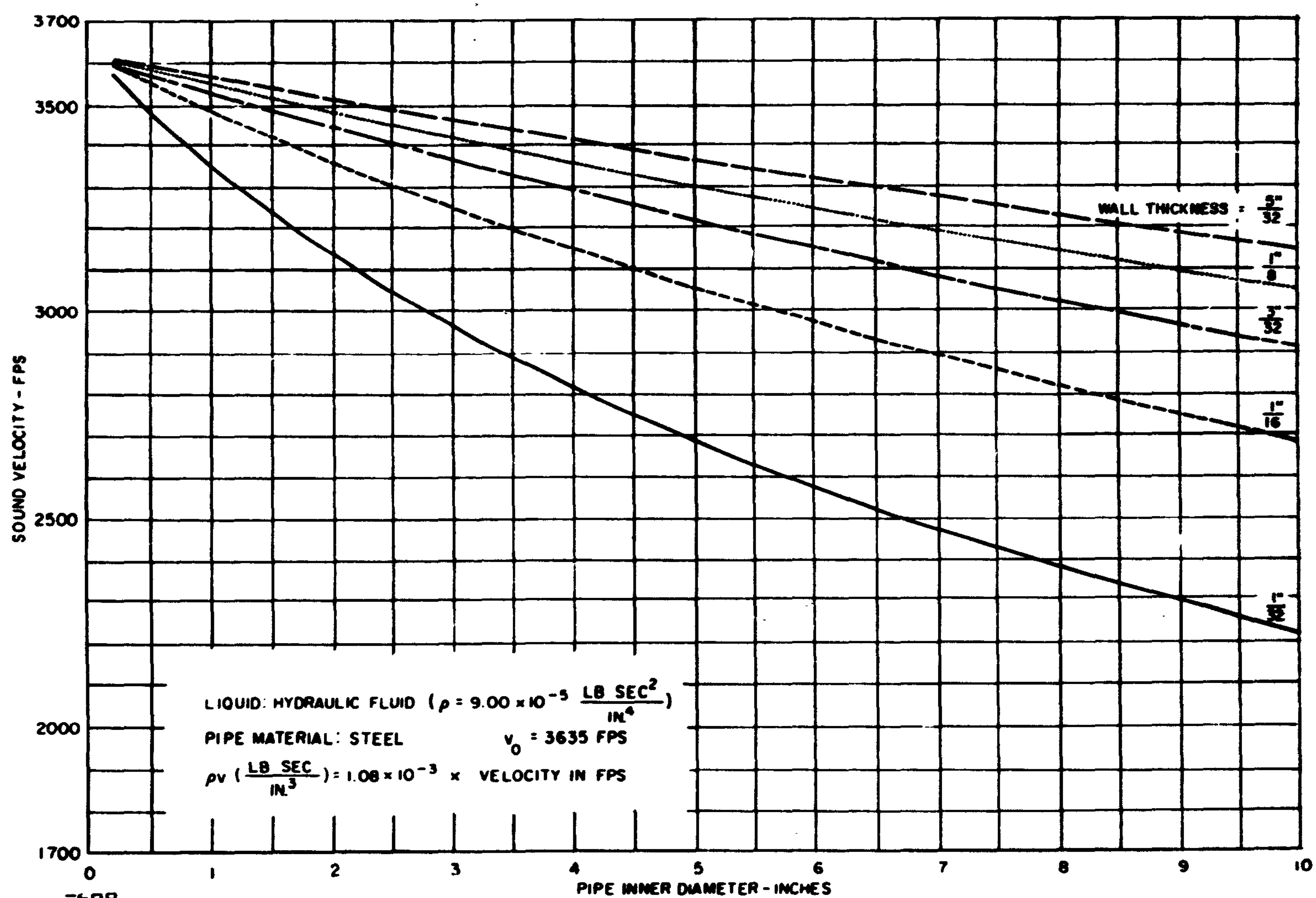

DRL - UT
DWG AS7273
JVK - BEE
11 - 8 - 62

FIGURE A-16
CALCULATED VELOCITIES OF SOUND WAVES IN LIQUID
INSIDE METAL PIPES

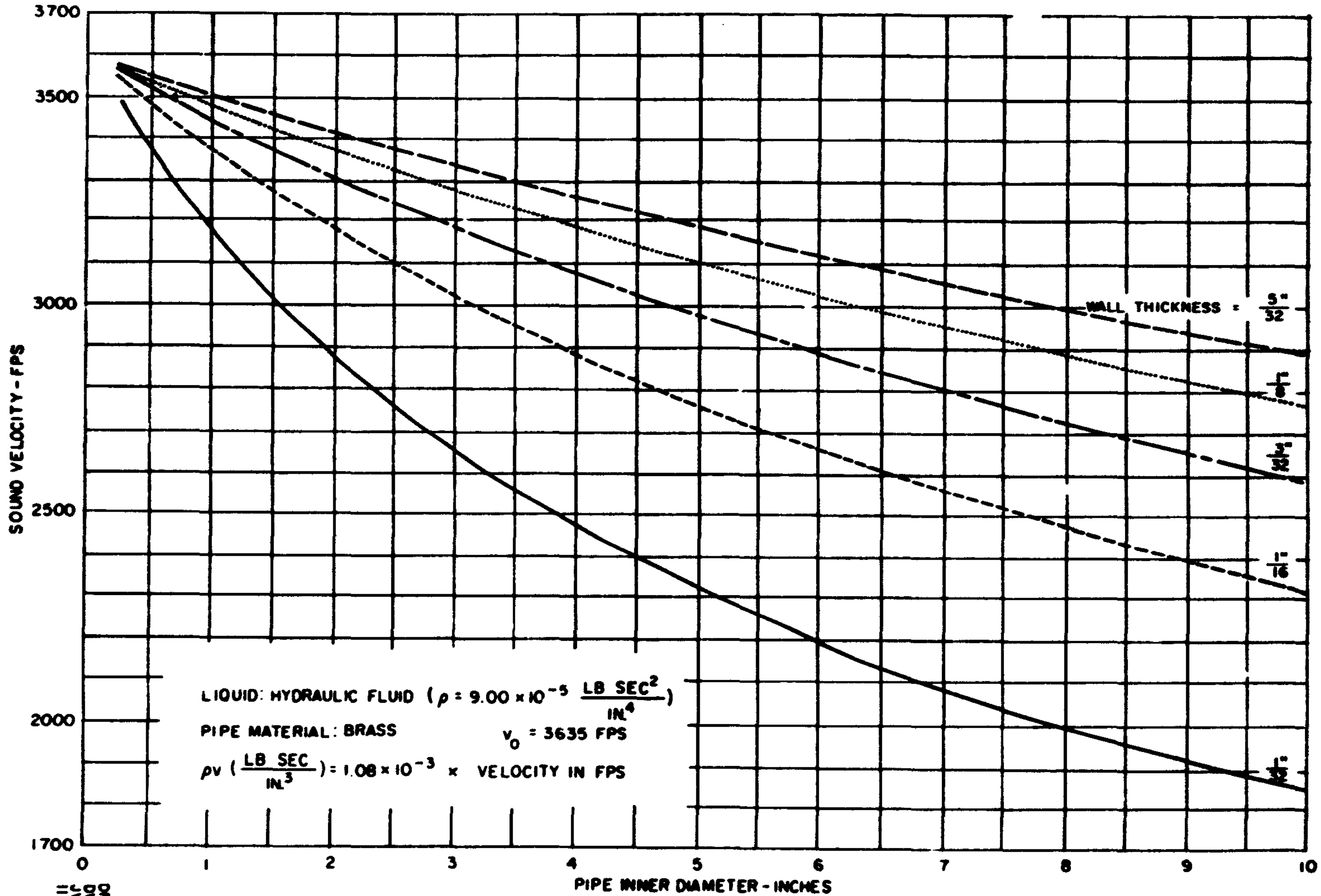

DRL - UT
DWG AS7274
JVK - BEE
11 - 5 - 62

FIGURE A-17
CALCULATED VELOCITIES OF SOUND WAVES IN LIQUID
INSIDE METAL PIPES

September 1962
DGG:vh

APPENDIX B

Digital Computer Program for Analyzing Acoustic Filters in a Pipe-Liquid System

The purpose of this program is to compute, as a function of frequency, a transmission loss which indicates the amount of sound attenuation caused by several types of acoustic filters. A transfer function and a system input admittance are also available for print-out. These computations pertain to pipe-contained liquid systems.

Computations can be performed for the following types of filters: (1) side-branch, both lumped- and distributed-element types, (2) expansion chamber and (3) combination. To clarify what is to follow, it should be noted that the phrase "filter section" is applied to the side-branch (or expansion chamber) and the length of pipe which follows before the next admittance discontinuity. Progressing along the line from load to source a "discontinuity" results from one of two things: (1) appearance of a side-branch, or (2) change in main pipe characteristic admittance. In expansion chambers this latter discontinuity is caused by ends of the chamber.

Any number of the same type or of mixed types of these filter sections may be connected in series along the system piping. Further, more than one side-branch element may be connected at the same position on the pipe. The program will begin at the end opposite the noise source input and proceed past each discontinuity, finally arriving at the noise source with a transmission loss solution for the frequency under consideration. Any frequency range may be chosen for computations.

There is one further extension of the program. Since side-branch filter computations involve the admittances presented to a piping system by the side-branch element, it may sometimes be desirable to skip the theoretical computation at the discontinuity and for it substitute experimentally determined admittance values. This may be done at one or more side-branch positions as desired; theoretical calculations are still carried out at any remaining discontinuities. Measured admittance values can also be put in at the termination of the pipe system (opposite the noise source end); this latter alternative is in lieu of considering the terminal admittance constant.

Five mathematical expressions are used in this program; three deal with admittance calculation or transformation, and two express the sound attenuation caused by the filter system. Each expression is briefly discussed below.

The program is based primarily on the admittance transformation equation. This expression is presented in the text in a form different from the trigonometric version given below:

$$Y_{i+1} = Y_c \left(\frac{Y_i + jY_c \tan\beta \ell}{Y_c + jY_i \tan\beta \ell} \right) ,$$

where Y_c = characteristic admittance of pipe,
Y_i = admittance "seen" at previous discontinuity,
Y_{i+1} = transformed admittance after moving down the pipe a length ℓ,
$\beta = \frac{2\pi f}{v}$ = phase constant of main pipe system,
f = frequency of sound source, and
v = velocity of sound in system.

This expression ties together the admittance discontinuities which occur at positions along the main pipe.

A second expression, used for finding the admittance presented to the main pipe by a closed-end side-branch, is simply a special case of the admittance transformation equation. Since the Y_i "seen" at the closed end of the side-branch is zero, the expression reduces to

$$Y_b = jY_c \tan\beta \ell ,$$

where Y_b = admittance added in parallel with main pipe,
Y_c = characteristic admittance of side-branch pipe length ℓ, and
β = phase constant of side-branch pipe.

The other admittance calculation involves the lumped element side-branch. Such a side-branch can be represented by a series inertance-compliance combination connected in parallel with the main pipe. The total admittance of the series elements is given by

$$Y_b = \frac{-j2\pi f_o C}{\frac{f}{f_o} - \frac{f_o}{f}} ,$$

where Y_b = admittance in parallel with main pipe,

f_o = desired resonant frequency of the series inertance-compliance combination, and

C = compliance element value.

The other two mathematical expressions are shown below:

$$\text{Transfer Function (dB)} = -20 \log_{10} \left| \frac{P_o}{P_s} \right| , \text{ and}$$

$$\text{Transmission Loss (dB)} = -20 \log_{10} \left| \frac{P_o}{P_i} \right| ,$$

where P_o = output (opposite source end) sound pressure,

P_s = source sound pressure, and

P_i = sound pressure incident at filter input.

These pressure ratios appear in the program as functions of admittance; the necessary expressions are given in the main text.

The accompanying flow diagram, Fig. B-1, is mostly self-explanatory. A list of the required input parameters is given below along with several clarifying comments.

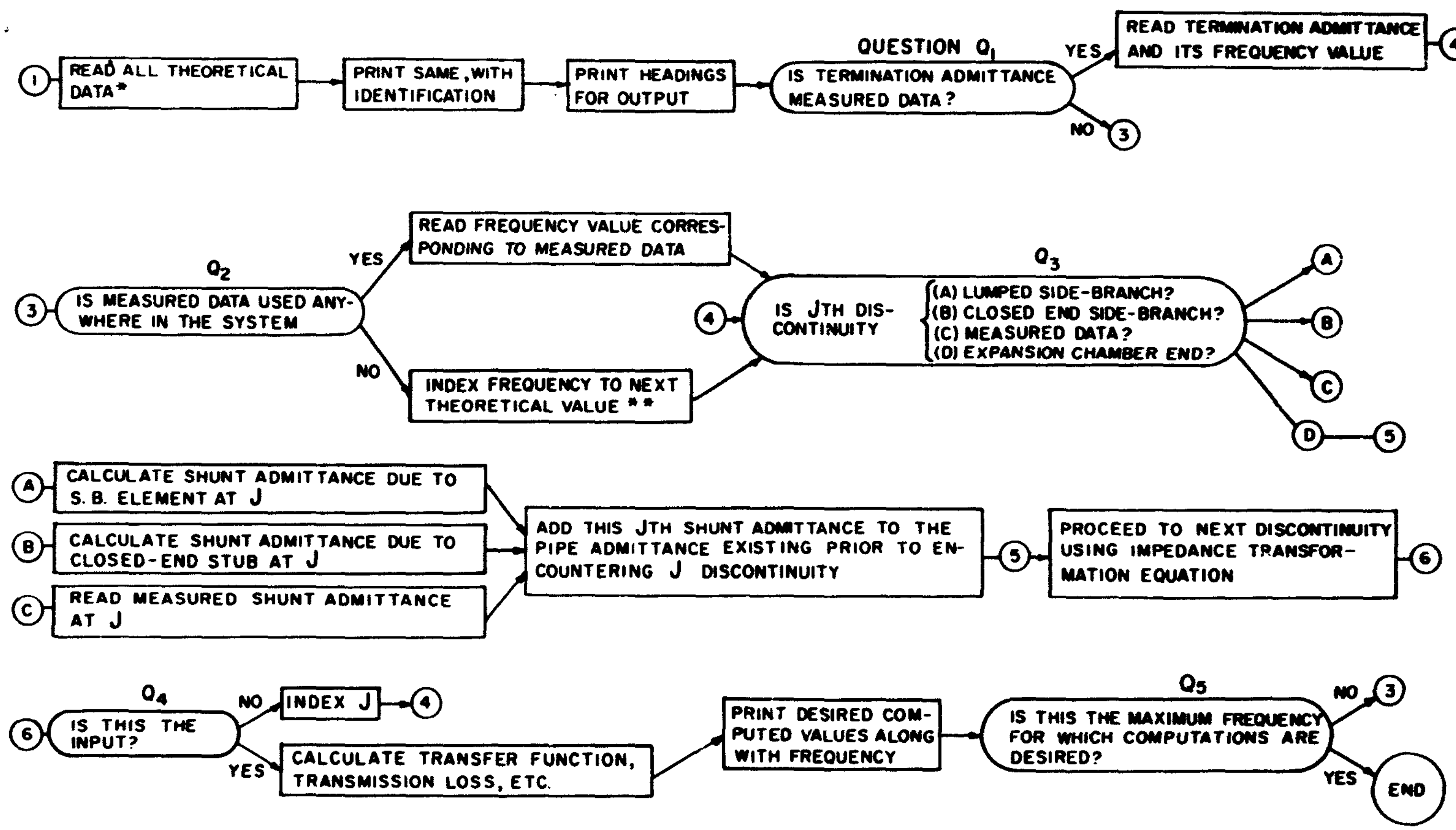

* THIS INCLUDES ALL EXCEPT MEASURED ADMITTANCE VALUES. THE DATA FOR COMPUTATION OF THE SHUNT ADMITTANCE AT THE JTH DISCONTINUITY MUST BE SUBSCRIPTED ACCORDINGLY.

** THE BEGINNING FREQUENCY WILL BE IDENTICAL WITH THE Δf OF THE INDEXING STEP IF AN INPUT STATEMENT INITIALLY EQUATES THE FREQUENCY SYMBOL TO ZERO.

DRL - UT
DWG AS 7113
JVK - BEE
10 - 4 - 62

FIGURE B-1
COMPUTER FLOW DIAGRAM

Each filter section represents a value of J as indicated on the diagram. Hence, one set of parameters has the property that each parameter has not only its physical value but also a value of J associated with it. A second set of inputs is common to the whole system, e.g., frequency limits, etc. Those inputs in this latter class are as follows:

(1) initial frequency,
(2) frequency index,
(3) final frequency,
(4) control parameter for Q_1,
(5) control parameter for Q_2,
(6) control parameter for Q_4 (i.e., max value for J), and
(7) termination admittance value (used if Q_1 answer is NO).

The inputs which must possess a J subscript are as follows:

lumped element side-branch parameters	(1)	control parameter for Q_3,
	(2)	resonant frequency of lumped-element side-branch,
	(3)	compliance of lumped-element side-branch,
distributed element side-branch parameters	(4)	length of closed-end side-branch,
	(5)	characteristic admittance of closed-end side-branch,
	(6)	velocity of sound in closed-end side-branch,
main pipe parameters	(7)	length of main pipe before next discontinuity is reached,
	(8)	characteristic admittance of this length of pipe, and
	(9)	velocity of sound in this length of pipe.

Note that re-entrant tube expansion chamber calculations are carried out using alternative B of question Q_3, Fig. B-1. That is, since re-entrant tubes result in closed-end, side-branch effects, the same mathematics applies to both cases (See Chapter III, C, 5.).

Question Q_2 exists to prevent unnecessary theoretical calculations at frequencies other than those at which measured data were taken. For example, if measured data are to be inserted at, say, J = 3 discontinuity, while theoretical computations are to be carried out at the J = 1 and 2 discontinuities, Q_2 causes these theoretical computations to be performed only at those frequencies which correspond to measured data points.

Alternative D of Q_3 bypasses any addition of lumped admittance in parallel with the system because no such admittance is added when an expansion chamber end is encountered. The characteristic admittance and velocity are changed due to an entrance or exit of the chamber, and then the admittance transformation process continues as if no discontinuity were present.

Finally, the arithmetic of the program must, of necessity, contain complex numbers. The programmer must therefore carefully arrange the steps so that the operations on real and imaginary quantities are appropriately separated.

September 1962
JVK:vh

APPENDIX C

References

Listed below are reports, technical journal articles, and books that should be helpful as sources of additional information on acoustic filters and related subjects.

DRL Reports

1. DRL Progress Reports No. 1 through 9, Phase II, Contract NObs-66932

Report No.	Date
1	1 December 1956
2	1 April 1957
3	1 July 1957
4	21 November 1957
5	7 February 1958
6	14 May 1958
7	13 August 1958
8	22 October 1958
9	28 January 1959

2. DRL Progress Reports No. 10 through 20, Phase II, Contract NObs-77033

Report No.	Date
10	21 April 1959
11	11 August 1959
12	29 October 1959
13	28 January 1960
14	28 April 1960
15	15 August 1960
16	29 November 1960
17	8 February 1961
18	23 May 1961
19	28 July 1961
20	31 October 1961

3. J. D. Gavenda, "A Study of the Feasibility of a Hydroacoustic Filter to Attenuate Liquid-Borne Noise in Piping Systems," Defense Research Laboratory Acoustical Report No. 97, 30 November 1955.
4. E. E. Mikeska, "Final Report on Contract NObs-66932," 7 January 1960.
5. E. L. Hixson, "The Design of Acoustic Filters for Piping Systems Using Cascaded Half Sections," Defense Research Laboratory Acoustical Report No. 152, April, 1959.
6. J. V. Kahlbau, "Barge Tests of Fluid Acoustic Filters and Experimental Study of Noise Transmission Paths," Defense Research Laboratory Acoustical Report No. 195, 12 February 1962.
7. J. V. Kahlbau, "Summary Report on Contract NObs-77033," Defense Research Laboratory Acoustical Report No. 199, September, 1961.

Other Reports

8. Don D. Davis, Jr., George M. Stokes, Dewey Moore, and George L. Stevens, Jr., "Theoretical and Experimental Investigation of Mufflers with Comments on Engine Exhaust Muffler Design," NACA Report No. 1192, 1954.
9. O. M. Phillips, "Generation and Transmission of Sound in Liquid-filled Pipe Systems," Hydromatics, Inc. Technical Report No. 125-1, February, 1962.
10. M. Hirschorn, "General Notes on the Development of a Noise Attenuating Coupling for Liquid Lines," T. R. Finn and Company, Inc. Technical Report on U.S. Navy Contract No. 53569.
11. E. J. Waller, "Fundamental Analysis of Unsteady Pressure Variations in Pipeline Systems," Publication No. 92 of Oklahoma Engineering Experiment Station, Stillwater, Oklahoma, 21, 4, May, 1954.

Papers Published in Technical Journals and Magazines

12. Eugen Ganitta, "Untersuchunger uber die Schalleitung in Wassergefullten Rohren," Akustische Zeitschrift, V 5, pp. 87-102, September, 1940.
13. R. B. Lindsay, "The Filtration of Sound, I," J. App. Phy., 9, pp. 612-622, October, 1938.
14. R. B. Lindsay, "The Filtration of Sound, II," J. App. Phy., 10, pp. 680-687, October, 1939.

15. W. L. Rogers, "Experimental Approaches to the Study of Noise and Noise Transmission in Piping Systems," ASHVE Transactions, 59, p. 347, 1953.

16. W. L. Rogers, "Sound Pressure Levels and Frequencies Produced by Flow of Water Through Pipe and Fittings," ASHVE Transactions, 60, p. 411, 1954.

17. W. L. Rogers, "Noise Production and Damping in Water Piping," Journal Section, Heating, Piping, and Air Conditioning, January, 1956.

18. J. H. Dawson, "Through-Flow Desurger Minimizes Line Shock," Pipe Line Section, World Oil, December, 1949.

19. E. L. Hixson, J. V. Kahlbau, and E. E. Mikeska, "Resonant Side-Branch Acoustic Filters for Liquid Piping Systems," J. Acoust. Soc. Am. 34, 594, May, 1962.

Books

20. G. W. Stewart and R. B. Lindsay, Acoustics, D. Van Nostrand Company, New York, 1930.

21. L. L. Beranek, Noise Reduction, McGraw-Hill Book Co., Inc., New York, 1960.

22. T. E. Shea, Transmission Networks and Wave Filters, D. Van Nostrand Company, New York, 1930.

23. L. E. Kinsler and A. R. Frey, Fundamentals of Acoustics, John Wiley and Sons, New York, 1950.

24. P. M. Morse, Vibration and Sound, McGraw-Hill Book Co., Inc., New York, 1948.

25. Cyril M. Harris, Handbook of Noise Control, McGraw-Hill Book Co., Inc., New York, 1957.

26. H. F. Olson, Elements of Acoustical Engineering, D. Van Nostrand Co., Inc., New York, 1940.

27. R. J. Roark, Formulas for Stress and Strain, McGraw-Hill Book Co., New York, 1943.

28. Theodore Baumeister, Marks Mechanical Engineers' Handbook, 6th Edition, McGraw-Hill Book Co., Inc., New York, 1958.

September 1962
JVK:vh

APPENDIX D

Glossary of Symbols

Upper Case Letters

C - acoustic compliance

E - modulus of elasticity

K - pressure reflection coefficient

P - phasor sound pressure

P_+ - phasor sound pressure of a forward traveling wave

P_- - phasor sound pressure of a backward traveling wave

R - acoustic resistance

S - area

T.L. - transmission loss

U - volume

V - phasor particle velocity

$\overline{V}$ - phasor volume velocity

W - total weight, acoustic power

Y - acoustic admittance

Y_o - characteristic acoustic admittance

Z - acoustic impedance

Z_o - characteristic acoustic impedance

Lower Case Letters

a - gas-filled side-branch filter element parameter, pipe wall thickness

b - regulated gas-filled, side-branch element parameter

d - diameter

f - frequency

g - acceleration due to gravity

i - subscript for input; index number

$j = \sqrt{-1}$

k - spring stiffness

ℓ - length

September 1962
JVK:vh

m - mass, index number

n - index number

p - static pressure

p(t) - instantaneous sound pressure

p_o - initial static pressure

p_{max} - amplitude of sound pressure

q - lumped, side-branch element effectiveness parameter or closed-end tube side-branch element parameter

r - mechanical damping constant

t - time

v_o - wave velocity in an infinite medium

v - wave velocity

v(t) - instantaneous particle velocity

v_{max} - amplitude of particle velocity

w - weight per unit volume

x - displacement

Greek Letters

α - wave propagation normal mode coefficients

β - phase constant

γ - ratio of specific heats for a gas

κ - compressibility

λ - wavelength

ν - Poisson's ratio

ρ - mass density

φ_p - pressure phase angle

φ_v - particle velocity phase angle

ω - angular frequency

DISTRIBUTION LIST

Copy No.	
1 - 3	Chief, Bureau of Ships, U. S. Navy Department, Washington 25, D. C., Attn: Code 335
4 - 25	Chief, Bureau of Ships, U. S. Navy Department, Washington 25, D. C., Attn: Code 345
26	Chief, Bureau of Ships, U. S. Navy Department, Washington 25, D. C., Attn: Code 420
27	Chief, Bureau of Ships, U. S. Navy Department, Washington 25, D. C., Attn: Code 430
28	Chief, Bureau of Ships, U. S. Navy Department, Washington 25, D. C., Attn: Code 434
29	Chief, Bureau of Ships, U. S. Navy Department, Washington 25, D. C., Attn: Code 436
30	Chief, Bureau of Ships, U. S. Navy Department, Washington 25, D. C., Attn: Code 440
31	Chief, Bureau of Ships, U. S. Navy Department, Washington 25, D. C., Attn: Code 648
32	Chief, Bureau of Ships, U. S. Navy Department, Washington 25, D. C., Attn: Code 649
33	Commanding Officer, U. S. Naval Shipyard, Boston, Mass.
34	Commanding Officer, U. S. Naval Shipyard, Charleston, S. C.
35	Commanding Officer, U. S. Naval Shipyard, Long Beach, Calif.
36	Commanding Officer, U. S. Naval Shipyard, Mare Island, Vallejo, Calif.
37	Commanding Officer, U. S. Naval Shipyard, New York, Brooklyn, N. Y.
38	Commanding Officer, U. S. Naval Shipyard, Norfolk, Portsmouth, Va.
39	Commanding Officer, U. S. Naval Shipyard, Pearl Harbor, Oahu, Hawaii
40	Commanding Officer, U. S. Naval Shipyard, Philadelphia, Pa.
41	Commanding Officer, U. S. Naval Shipyard, Portsmouth, N. H.
42	Commanding Officer, U. S. Naval Shipyard, Puget Sound, Bremerton, Wash.
43	Commanding Officer, U. S. Naval Shipyard, San Francisco, Calif.

DISTRIBUTION LIST (Cont'd)

Copy No.	
44	U. S. Naval Repair Facility, San Diego, Calif.
45	U. S. Naval Submarine Base, New London, Conn.
46	U. S. Naval Boiler and Turbine Laboratory, Philadelphia, Pa.
47	David Taylor Model Basin, Carderock, Md.
48	U. S. Navy Electronics Laboratory, San Diego 52, Calif.
49	U. S. Naval Engineering Experiment Station, Annapolis, Md.
50	Material Laboratory, New York Naval Shipyard, Brooklyn 1, N. Y.
51	Rubber Laboratory, Mare Island Naval Shipyard, Vallejo, Calif.
52	U. S. Naval Mine Defense Laboratory, Panama City, Fla.
53	U. S. Navy Underwater Sound Laboratory, Fort Trumbull, New London, Conn.
54	U. S. Navy Radiological Defense Laboratory, San Francisco, Calif.
55	Supervisor of Shipbuilding, U. S. Navy, Bath, Maine
56	Supervisor of Shipbuilding, U. S. Navy, Bay City, Mich.
57	Supervisor of Shipbuilding, U. S. Navy, Camden, N. J.
58	Supervisor of Shipbuilding, U. S. Navy, Long Beach, Calif.
59	Supervisor of Shipbuilding, U. S. Navy, Newport News, Va.
60	Supervisor of Shipbuilding, U. S. Navy, New York, New York
61	Supervisor of Shipbuilding, U. S. Navy, Pascagoula, Miss.
62	Supervisor of Shipbuilding, U. S. Navy, Quincy, Mass.
63	Supervisor of Shipbuilding, U. S. Navy, San Francisco, Calif.
64	Supervisor of Shipbuilding, U. S. Navy, Seattle, Wash.
65	Supervisor of Shipbuilding, U. S. Navy, Westwego, La.
66 - 75	Armed Services Technical Information Agency, Arlington Hall, Arlington 12, Va.
76	U. S. Naval Underwater Sound Reference Laboratory, Orlando, Fla.

DISTRIBUTION LIST (Cont'd)

Copy No.	
77	Chief, Bureau of Yards and Docks, U. S. Navy Dept., Washington 25, D. C.
78	U. S. Naval Academy, Annapolis, Md.
79	U. S. Naval Postgraduate School, Monterey, Calif.
80	Air Force Office of Scientific Research, Washington 25, D. C.
81	Army Office of Research and Development, Washington 25, D. C.
82	Director of Research, National Aeronautics and Space Adminstration, 1512 H Street N.W., Washington 25, D. C.
83	National Bureau of Standards, Washington, D. C.
84	Electric Boat Division, General Dynamics Corp., Groton, Conn.
85	Newport News Shipbuilding and Drydock Co., Newport News, Va.
86	Bethlehem Steel Corp., Shipbuilding Division, Quincy, Mass.
87	Bath Iron Works Corp., Bath, Maine
88	New York Shipbuilding Corp., Camden, N. J.
89	Ingalls Shipbuilding Corp., Pascagoula, Miss.
90	Gibbs and Cox Inc., New York, N. Y.
91	Ordnance Research Laboratory, Pennsylvania State University, University Park, Pa.
92	Armour Research Foundation, Chicago, Ill.
93	University of Michigan, Engineering and Research Institute, Ann Arbor, Mich.
94	Oklahoma State University, School of Civil Engineering, Stillwater, Okla.
95	Westinghouse Electric Corp., Research Laboratories, Pittsburgh, Pa.
96	General Engineering Laboratory, General Electric Co., Schenectady, N. Y.
97	Bolt, Beranek and Newman, Inc., 50 Moulton St., Cambridge, Mass.
98	Hydronautics, Inc., 200 Monroe St., Rockville, Md.

DISTRIBUTION LIST (Cont'd)

Copy No.	
99	Cambridge Acoustical Associates Inc., 1278 Mass. Ave., Cambridge, Mass.
100	Conesco Inc., 205 Sixth Street, Cambridge, Mass.
101	Robert Taggart Inc., 400 Arlington Blvd., Falls Church, Va.
102	Mr. F. M. Lucas, Special Representative, Office of Naval Research, 2506 Main Building, The University of Texas, Austin 12, Texas
103	Director, DRL/UT
104	C. M. McKinney, DRL/UT
105	J. V. Kahlbau, DRL/UT
106	E. L. Hixson, DRL/UT
107	M. V. Mechler, DRL/UT
108	F. O. Bohls, DRL/UT
109-110	Library, DRL/UT
111-800	DRL Reserve

Defense Research Laboratory, The University of Texas, Austin, Texas.
GUIDE TO THE SELECTION OF ACOUSTIC FILTERS FOR LIQUID-FILLED SYSTEMS, by E. L. Hixson, J. V. Mahlbau, and D. G. Galloway. September 1962. x, 328 p. incl. illus. (Acoustical rept. no. DRL-A-202)
(Contract NObs-86165) Unclassified report

Passive, dissipationless acoustic filters for attenuating noise in liquid-filled piping systems are analyzed as irregular transmission lines. Equations for calculating a theoretical transmission loss for filters are developed. These equations are then applied to a variety of filters of the following types: (1) side branch filters, (2) expansion chamber filters, (3) combination filters, and (4) Quincke tube filters. Graphical aids for use in finding filter parameter values are given along with filter design examples. Principal results obtained during the program of experimental investigation of acoustic filters at Defense Research Laboratory are summarized.

UNCLASSIFIED

1. Acoustic filters
2. Acoustic impedance
3. Acoustic transmission lines

I. Title
II. Hixson, E. L.
III. Mahlbau, J. V.
IV. Galloway, D. G.
V. DRL-A-202
VI. Contract NObs-86165

UNCLASSIFIED

Defense Research Laboratory, The University of Texas, Austin, Texas.
GUIDE TO THE SELECTION OF ACOUSTIC FILTERS FOR LIQUID-FILLED SYSTEMS, by E. L. Hixson, J. V. Mahlbau, and D. G. Galloway. September 1962. x, 328 p. incl. illus. (Acoustical rept. no. DRL-A-202)
(Contract NObs-86165) Unclassified report

Passive, dissipationless acoustic filters for attenuating noise in liquid-filled piping systems are analyzed as irregular transmission lines. Equations for calculating a theoretical transmission loss for filters are developed. These equations are then applied to a variety of filters of the following types: (1) side branch filters, (2) expansion chamber filters, (3) combination filters, and (4) Quincke tube filters. Graphical aids for use in finding filter parameter values are given along with filter design examples. Principal results obtained during the program of experimental investigation of acoustic filters at Defense Research Laboratory are summarized.

UNCLASSIFIED

1. Acoustic filters
2. Acoustic impedance
3. Acoustic transmission lines

I. Title
II. Hixson, E. L.
III. Mahlbau, J. V.
IV. Galloway, D. G.
V. DRL-A-202
VI. Contract NObs-86165

UNCLASSIFIED

Defense Research Laboratory, The University of Texas, Austin, Texas.
GUIDE TO THE SELECTION OF ACOUSTIC FILTERS FOR LIQUID-FILLED SYSTEMS, by E. L. Hixson, J. V. Mahlbau, and D. G. Galloway. September 1962. x, 328 p. incl. illus. (Acoustical rept. no. DRL-A-202)
(Contract NObs-86165) Unclassified report

Passive, dissipationless acoustic filters for attenuating noise in liquid-filled piping systems are analyzed as irregular transmission lines. Equations for calculating a theoretical transmission loss for filters are developed. These equations are then applied to a variety of filters of the following types: (1) side branch filters, (2) expansion chamber filters, (3) combination filters, and (4) Quincke tube filters. Graphical aids for use in finding filter parameter values are given along with filter design examples. Principal results obtained during the program of experimental investigation of acoustic filters at Defense Research Laboratory are summarized.

UNCLASSIFIED

1. Acoustic filters
2. Acoustic impedance
3. Acoustic transmission lines

I. Title
II. Hixson, E. L.
III. Kahlbau, J. V.
IV. Galloway, D. G.
V. DRL-A-202
VI. Contract NObs-86165

UNCLASSIFIED

Defense Research Laboratory, The University of Texas, Austin, Texas.
GUIDE TO THE SELECTION OF ACOUSTIC FILTERS FOR LIQUID-FILLED SYSTEMS, by E. L. Hixson, J. V. Mahlbau, and D. G. Galloway. September 1962. x, 328 p. incl. illus. (Acoustical rept. no. DRL-A-202)
(Contract NObs-86165) Unclassified report

Passive, dissipationless acoustic filters for attenuating noise in liquid-filled piping systems are analyzed as irregular transmission lines. Equations for calculating a theoretical transmission loss for filters are developed. These equations are then applied to a variety of filters of the following types: (1) side branch filters, (2) expansion chamber filters, (3) combination filters, and (4) Quincke tube filters. Graphical aids for use in finding filter parameter values are given along with filter design examples. Principal results obtained during the program of experimental investigation of acoustic filters at Defense Research Laboratory are summarized.

UNCLASSIFIED

1. Acoustic filters
2. Acoustic impedance
3. Acoustic transmission lines

I. Title
II. Hixson, E. L.
III. Mahlbau, J. V.
IV. Galloway, D. G.
V. DRL-A-202
VI. Contract NObs-86165

UNCLASSIFIED